frontiers | Research Topics

Women in experimental pharmacology and drug discovery pharmacology 2023

Edited by
Patricia Rijo, Emel Timucin, Valeria Bruno and Maria M. M. Santos

Published in
Frontiers in Pharmacology

ISSN 1664-8714
ISBN 978-2-8325-5208-7
DOI 10.3389/978-2-8325-5208-7

About Frontiers

Frontiers is more than just an open access publisher of scholarly articles: it is a pioneering approach to the world of academia, radically improving the way scholarly research is managed. The grand vision of Frontiers is a world where all people have an equal opportunity to seek, share and generate knowledge. Frontiers provides immediate and permanent online open access to all its publications, but this alone is not enough to realize our grand goals.

Frontiers journal series

The Frontiers journal series is a multi-tier and interdisciplinary set of open-access, online journals, promising a paradigm shift from the current review, selection and dissemination processes in academic publishing. All Frontiers journals are driven by researchers for researchers; therefore, they constitute a service to the scholarly community. At the same time, the *Frontiers journal series* operates on a revolutionary invention, the tiered publishing system, initially addressing specific communities of scholars, and gradually climbing up to broader public understanding, thus serving the interests of the lay society, too.

Dedication to quality

Each Frontiers article is a landmark of the highest quality, thanks to genuinely collaborative interactions between authors and review editors, who include some of the world's best academicians. Research must be certified by peers before entering a stream of knowledge that may eventually reach the public - and shape society; therefore, Frontiers only applies the most rigorous and unbiased reviews. Frontiers revolutionizes research publishing by freely delivering the most outstanding research, evaluated with no bias from both the academic and social point of view. By applying the most advanced information technologies, Frontiers is catapulting scholarly publishing into a new generation.

What are Frontiers Research Topics?

Frontiers Research Topics are very popular trademarks of the *Frontiers journals series*: they are collections of at least ten articles, all centered on a particular subject. With their unique mix of varied contributions from Original Research to Review Articles, Frontiers Research Topics unify the most influential researchers, the latest key findings and historical advances in a hot research area.

Find out more on how to host your own Frontiers Research Topic or contribute to one as an author by contacting the Frontiers editorial office: frontiersin.org/about/contact

Women in experimental pharmacology and drug discovery pharmacology 2023

Topic editors

Patricia Rijo — Lusofona University, Portugal
Emel Timucin — Acıbadem University, Türkiye
Valeria Bruno — Sapienza University of Rome, Italy
Maria M. M. Santos — University of Lisbon, Portugal

Citation

Rijo, P., Timucin, E., Bruno, V., Santos, M. M. M., eds. (2024). *Women in experimental pharmacology and drug discovery pharmacology 2023*. Lausanne: Frontiers Media SA. doi: 10.3389/978-2-8325-5208-7

Table of contents

05 Editorial: Women in experimental pharmacology and drug discovery 2023
Patricia Rijo, Emel Timucin, Maria M. M. Santos and Valeria Bruno

07 The *in vitro* effects of black soldier fly larvae (*Hermitia illucens*) oil as a high-functional active ingredient for inhibiting hyaluronidase, anti-oxidation benefits, whitening, and UVB protection
Rungsinee Phongpradist, Warathit Semmarath, Kanokwan Kiattisin, Jutamas Jiaranaikulwanitch, Wantida Chaiyana, Siripat Chaichit, Yuthana Phimolsiripol, Pornngarm Dejkriengkraikul and Chadarat Ampasavate

21 Hepatoprotective effects of bioactive compounds from traditional herb Tulsi (*Ocimum sanctum* Linn) against galactosamine-induced hepatotoxicity in rats
Fatemah O. Kamel, Shahid Karim, Duaa Abdullah Omer Bafail, Hibah Mubarak Aldawsari, Sabna Kotta and U. K. Ilyas

34 Potential antioxidative and anti-hyperuricemic components in *Rodgersia podophylla* A. Gray revealed by bio-affinity ultrafiltration with SOD and XOD
Can Liang, Yongbing Xu, Minxia Fan, Felix Wambua Muema, Guilin Chen, Mingquan Guo and Guangwan Hu

46 Antisense oligonucleotides: a novel Frontier in pharmacological strategy
D. Collotta, I. Bertocchi, E. Chiapello and M. Collino

64 Analysis of anti-rheumatic activity of *Nyctanthes arbor-tristis* via *in vivo* and pharmacovigilance approaches
Ayushi Sharma, Anjana Goel and Zhijian Lin

79 Overexpression of CXCL17 increases migration and invasion of A549 lung adenocarcinoma cells
Ekin Koni, Irem Congur and Zeynep Tokcaer Keskin

88 Relationships between trace elements and cognitive and depressive behaviors in sprague dawley and wistar albino rats
Melis Yavuz, Ekin Dongel Dayanc, Fatma Merve Antmen, Elif Keskinöz, Esra Altuntaş, Gökçen Dolu, Berkcan Koç, Emre Tunçcan, Damla Şakar, Ufuk Canözer, Ceyda Büyüker, Ece Polat, Metincan Erkaya, Rui Azevedo, Devrim Öz Arslan, Agostinho Almeida and Güldal Süyen

98 The effect of black cohosh extract and risedronate coadministration on bone health in an ovariectomized rat model
Amy L. Inselman, Elysia A. Masters, Jalina N. Moore, Rajiv Agarwal, Audrey Gassman, Gemma Kuijpers, Richard D. Beger, Kenneth B. Delclos, Sybil Swift, Luísa Camacho, Michelle M. Vanlandingham, Daniel Sloper, Noriko Nakamura, Gonçalo Gamboa da Costa, Kellie Woodling, Matthew Bryant, Raul Trbojevich, Qiangen Wu, Florence McLellen and Donna Christner

108 The mysterious association between adiponectin and endometriosis
Yong-Qing Zhao, Yi-Fan Ren, Bing-Bing Li, Chao Wei and Bin Yu

130 Exploring orphan GPCRs in neurodegenerative diseases
Devrim Öz-Arslan, Melis Yavuz and Beki Kan

frontiers | Frontiers in Pharmacology

TYPE Editorial
PUBLISHED 12 July 2024
DOI 10.3389/fphar.2024.1439405

OPEN ACCESS

EDITED AND REVIEWED BY
Filippo Drago,
University of Catania, Italy

*CORRESPONDENCE
Patricia Rijo,
patricia.rijo@ulusofona.pt

RECEIVED 27 May 2024
ACCEPTED 24 June 2024
PUBLISHED 12 July 2024

CITATION
Rijo P, Timucin E, Santos MMM and Bruno V (2024), Editorial: Women in experimental pharmacology and drug discovery 2023. *Front. Pharmacol.* 15:1439405. doi: 10.3389/fphar.2024.1439405

Editorial: Women in experimental pharmacology and drug discovery 2023

Patricia Rijo[1,2]*, Emel Timucin[3], Maria M. M. Santos[2] and Valeria Bruno[4,5]

[1]CBIOS—Lusófona University's Research Center for Biosciences and Health Technologies, Lisbon, Portugal, [2]Instituto de Investigação do Medicamento (iMed.ULisboa), Faculdade de Farmácia, Universidade de Lisboa, Lisbon, Portugal, [3]Department of Biostatistics and Medical Informatics, School of Medicine, Acibadem University, Istanbul, Türkiye, [4]IRCCS Neuromed, Pozzilli, Italy, [5]Department of Physiology and Pharmacology, University Sapienza, Rome, Italy

KEYWORDS

natural products, sustainable ingredients, therapeutic potential, antioxidative components, pharmacology

Editorial on the Research Topic
Women in experimental pharmacology and drug discovery 2023

As editors of Frontiers in Pharmacology, we are thrilled to introduce the Research Topic "*Women in Experimental Pharmacology and Drug Discovery 2023*," marking a significant part of our series commemorating International Women's Day on 8 March 2023. This Research Topic serves as a testament to the remarkable achievements of women scientists in pharmacology, spotlighting their diverse and impactful research endeavors. From pioneering advancements in theory and experimentation to developing innovative methodologies, these contributions address pressing challenges and propel the field forward.

According to UNESCO, less than 30% of researchers worldwide are women. Persistent biases and gender stereotypes deter many girls and women from pursuing careers in science-related fields, particularly in STEM. However, science and gender equality are essential for sustainable development. To change traditional mindsets, it is crucial to promote gender equality, defeat stereotypes, and encourage girls and women to pursue STEM careers.

Frontiers in Pharmacology is proud to offer this platform to highlight the outstanding work of women scientists. Here are some key studies featured:

The study, led by Kamel et al., investigates the hepatoprotective potential of Ocimum sanctum L. (Tulsi) against galactosamine-induced toxicity in rats, identifying and quantifying bioactive compounds such as rutin, ellagic acid, and quercetin, which demonstrate significant protective effects.

The study, led by Phongpradist et al., examines the *in vitro* effects of black soldier fly larvae (BSFL) oil, highlighting its potential as a sustainable, high-functional ingredient for inhibiting hyaluronidase, providing antioxidant benefits, promoting skin whitening, and offering UVB protection, with significant findings showing its efficacy comparable to well-known cosmetic ingredients.

The study, led by Liang et al., explores the antioxidative and anti-hyperuricemic components of Rodgersia podophylla A. Gray, identifying potent bioactive compounds such as norbergenin, catechin, procyanidin B2, and gallic acid through bio-affinity

ultrafiltration with superoxide dismutase (SOD) and xanthine oxidase (XOD), demonstrating significant antioxidant and enzyme inhibition activities.

In their review, Collotta et al. delve into antisense oligonucleotides (ASOs), synthetic RNA or DNA molecules that target disease-causing genes. ASOs offer a novel therapeutic strategy, particularly for orphan genetic disorders. The review outlines advancements addressing pharmacological challenges and provides a comparative analysis of ASOs approved by regulatory agencies, showcasing their clinical potential.

The study by Koni et al. investigates the role of CXCL17 in lung adenocarcinoma, showing that overexpression of CXCL17 in A549 cells significantly enhances their migration and invasion capabilities without affecting cell proliferation, suggesting a potential role of CXCL17 in promoting tumor metastasis.

Sharma et al. explored the anti-rheumatic potential of Nyctanthes arbor-tristis (NAT) extracts. Their study demonstrated the safety and efficacy of a 500 mg/kg dose of NAT leaf extract in rats, with significant reductions in inflammation and improvements in arthritis symptoms. NAT shows promise as a therapeutic option for inflammatory arthritis.

Inselman et al. investigated how black cohosh extract and risedronate interact in improving bone health in ovariectomized rats. They found that while high-dose risedronate significantly increased bone mineral density (BMD) in the femur and vertebrae, black cohosh extract had minimal effect alone and did not interfere with risedronate's BMD-enhancing properties when co-administered.

Yavuz et al. examined the effects of social isolation on mental health and cognition in Sprague Dawley (SD) and Wistar Albino (WIS) rats, amid the COVID-19 pandemic. They found that while SD rats learned faster, they were more prone to depression after isolation compared to WIS rats. Elevated levels of certain trace elements in isolated SD rats hint at their role in stress responses, offering insights for future preventive treatments against stress-related neurobehavioral issues.

Öz Arslan et al. reviewed the potential of orphan G protein-coupled receptors (GPCRs) in treating neurodegenerative diseases like Alzheimer's, Parkinson's, Huntington's, and multiple sclerosis. Despite limited therapies, orphan receptors offer promising targets due to their roles in critical cellular processes. The review discusses their therapeutic potential, recent advances in drug discovery, and outlines future research directions and challenges.

Zhao et al. reviewed the link between adiponectin and endometriosis. Adiponectin, primarily from adipose tissue, influences energy regulation and estrogen-related diseases. Despite evidence suggesting lower adiponectin levels in endometriosis patients, its exact role remains unclear. The review highlights adiponectin's involvement in key biological processes related to endometriosis and emphasizes the need for further research to identify therapeutic targets and understand the condition better.

Promoting gender equality in pharmacology is essential for scientific advancement and sustainable development. The diverse research presented here underscores the vital contributions of women scientists. By supporting and celebrating their work, we foster a more inclusive and innovative scientific community.

Frontiers in Pharmacology remains dedicated to this mission, showcasing the remarkable work of women in the field and inspiring future generations.

Author contributions

PR: Conceptualization, Supervision, Validation, Writing–original draft. ET: Visualization, Writing–review and editing. MS: Visualization, Writing–review and editing. VB: Visualization, Writing–review and editing.

Funding

The author(s) declare that no financial support was received for the research, authorship, and/or publication of this article.

Conflict of interest

The authors declare that the research was conducted in the absence of any commercial or financial relationships that could be construed as a potential conflict of interest.

The author(s) declared that they were an editorial board member of Frontiers, at the time of submission. This had no impact on the peer review process and the final decision.

Publisher's note

frontiers | Frontiers in Pharmacology

TYPE Original Research
PUBLISHED 20 September 2023
DOI 10.3389/fphar.2023.1243961

OPEN ACCESS

EDITED BY
Patrícia Mendonça Rijo,
Lusofona University, Portugal

REVIEWED BY
Catarina Rosado,
CBIOS, Universidade Lusófona Research Center for Biosciences and Health Technologies, Portugal
Giovanni Messina,
University of Foggia, Italy
André Rolim Baby,
University of São Paulo, Brazil

*CORRESPONDENCE
Pornngarm Dejkriengkraikul,
pornngarm.d@cmu.ac.th
Chadarat Ampasavate,
chadarat.a@cmu.ac.th

†These authors have contributed equally to this work and share first authorship

RECEIVED 21 June 2023
ACCEPTED 28 August 2023
PUBLISHED 20 September 2023

CITATION
Phongpradist R, Semmarath W, Kiattisin K, Jiaranaikulwanitch J, Chaiyana W, Chaichit S, Phimolsiripol Y, Dejkriengkraikul P and Ampasavate C (2023), The *in vitro* effects of black soldier fly larvae (*Hermitia illucens*) oil as a high-functional active ingredient for inhibiting hyaluronidase, anti-oxidation benefits, whitening, and UVB protection. *Front. Pharmacol.* 14:1243961. doi: 10.3389/fphar.2023.1243961

The *in vitro* effects of black soldier fly larvae (*Hermitia illucens*) oil as a high-functional active ingredient for inhibiting hyaluronidase, anti-oxidation benefits, whitening, and UVB protection

Rungsinee Phongpradist[1†], Warathit Semmarath[2,3†], Kanokwan Kiattisin[1], Jutamas Jiaranaikulwanitch[1], Wantida Chaiyana[1,4], Siripat Chaichit[1,4], Yuthana Phimolsiripol[5], Pornngarm Dejkriengkraikul[6,7,8]* and Chadarat Ampasavate[1,4,6]*

[1]Department of Pharmaceutical Sciences, Faculty of Pharmacy, Chiang Mai University, Chiang Mai, Thailand, [2]Akkhraratchakumari Veterinary College, Walailak University, Nakhon Si Thammarat, Thailand, [3]Centre for One Health, Walailak University, Nakhon Si Thammarat, Thailand, [4]Center of Excellence in Pharmaceutical Nanotechnology, Faculty of Pharmacy, Chiang Mai University, Chiang Mai, Thailand, [5]Division of Product Development Technology, Faculty of Agro-Industry, Chiang Mai University, Chiang Mai, Thailand, [6]Center for Research and Development of Natural Products for Health, Chiang Mai University, Chiang Mai, Thailand, [7]Department of Biochemistry, Faculty of Medicine, Chiang Mai University, Chiang Mai, Thailand, [8]Anticarcinogenesis and Apoptosis Research Cluster, Faculty of Medicine, Chiang Mai University, Chiang Mai, Thailand

Objective: Larvae of *Hermitia illucens*, or black soldier fly larvae (BSFL), have been recognized for their high lipid yield with a remarkable fatty acid profile. BSFL oil (SFO) offers the added value of a low environmental footprint and a sustainable product. In this study, the characteristics and cosmetic-related activities of SFO were investigated and compared with rice bran oil, olive oil and krill oil which are commonly used in cosmetics and supplements.

Methods: The physicochemical characteristics were determined including acid value, saponification value, unsaponifiable matter and water content of SFO. The fatty acid composition was determined using GC-MS equipped with TR-FAME. The *in vitro* antioxidant properties were determined using DPPH, FRAP and lipid peroxidation inhibition assays. Antihyaluronidase (anti-HAase) activity was measured by detecting enzyme activity and molecular docking of candidate compounds toward the HAase enzyme. The safety assessment towards normal human cells was determined using the MTT assay and the UVB protection upon UVB-irradiated fibroblasts was determined using the DCF-DA assay. The whitening effect of SFO was determined using melanin content inhibition.

Results: SFO contains more than 60% polyunsaturated fatty acids followed by saturated fatty acids (up to 37%). The most abundant component found in SFO was linoleic acid (C18:2 n-6 cis). Multiple anti-oxidant mechanisms of SFO were discovered. In addition, SFO and krill oil prevented hyaluronic acid (HA) degradation via strong HAase inhibition comparable with the positive control, oleanolic acid. The molecular docking confirmed the binding interactions and molecular recognition of major free fatty acids toward HAase. Furthermore, SFO exhibited no cytotoxicity on primary human skin fibroblasts, HaCaT keratinocytes

and PBMCs (IC_{50} values > 200 μg/mL). SFO possessed significant *in-situ* anti-oxidant activity in UVB-irradiated fibroblasts and the melanin inhibition activity as effective as well-known anti-pigmenting compounds (kojic acid and arbutin, $p < 0.05$).

Conclusion: This study provides scientific support for various aspects of SFO. SFO can be considered an alternative oil ingredient in cosmetic products with potential implications for anti-skin aging, whitening and UVB protection properties, making it a potential candidate oil in the cosmetic industry.

KEYWORDS

***Hermitia illucens*, black soldier fly, oil, anti-oxidation, whitening, hyaluronidase inhibition, UV protection, cosmetic application**

Introduction

With a focus on energy conservation and sustainability, a growing demand has arisen for cost-effective sources of nutrients. The black soldier fly (*Hermitia illucens*) is a versatile insect that can thrive in various environments, particularly in hot and humid climates. Its larvae, also known as black soldier fly larvae (BSFL), are efficient decomposers of organic waste and can produce soil or frass as fertilizer and animal feed (Schmitt and de Vries, 2020). The farmed larvae, when at optimal age, can be used as an alternative source of lipid and protein in the animal nutrition industry (Driemeyer, 2016). Unlike houseflies, adult black soldier flies have no records of natural infections caused by entomopathogens in BSF (Joosten et al., 2020). Due to their unique properties and abilities, black soldier flies (BSFs) are now being used in various industries. They are considered a sustainable alternative to traditional protein sources for animal feed and an effective way to reduce food waste by converting organic waste to useful products (Kim et al., 2021). From a waste management perspective, the larvae can consume a variety of organic waste, including food scraps, fertilizer and agricultural waste and convert it to high-quality protein and oil (Wang and Shelomi, 2017). Moreover, as more people seek to ban nonbiodegradable products, BSFL can feed on organic waste and produce chitin-based bioplastics that are both biodegradable and compostable (Caligiani et al., 2018).

Insects have a significant amount of lipids in their biomass, and the highest concentration is found during the larval stage, ranging from 10% to 50% on a dry basis (da Silva Lucas et al., 2020; Franco et al., 2021). Interestingly, the oil derived from BSFL is currently being used in various cosmetic products, including soaps, lotions and shampoos (Verheyen et al., 2018; Almeida et al., 2020). The lipid composition of this oil is a combination of saturated and unsaturated fatty acids and triglycerides. Among all the lipid components, fatty acids and their derivatives are the most valuable for their beneficial properties. The larvae of BSFs are rich in fatty acids such as lauric acid, oleic acid and linoleic acid, possessing antibacterial, antifungal, and anti-inflammatory properties. They also nourish and moisturize the skin and hair, making them useful for treating various skin and scalp conditions (Xu et al., 2020; dos Santos Aguilar, 2021). Insect lipid and fatty acid profiles are influenced by several factors, including species, life stage, diet, environmental conditions, migratory flight and sex (Downer and Matthews, 1976; Franco et al., 2021). Recent studies have revealed that the composition of fatty acids in oils from BSFL is diverse. Some studies have reported that the primary fatty acids in *H. illucens* larvae are lauric acid, followed by palmitic, oleic, myristic and linoleic acids (Ushakova et al., 2016; Caligiani et al., 2019; Rabani et al., 2019). Additionally, another study has identified that the fatty acid content in the oil extracted from BSFL includes 28.8% lauric acid, 11.1% linoleic acid and 0.4% linolenic acid, which were extracted and purified from the larvae (Mai et al., 2019).

Cosmetics often incorporate fatty acids, and other components of *H. illucens* larvae oil can be applied, either isolated or as a lipidic structural complex (Almeida et al., 2020). Key components of the human epidermis, including palmitic, oleic and linoleic acid, are present in this oil (Botinestean et al., 2012). Linoleic acid plays a crucial physiologic role in maintaining the water permeability barrier of the skin (Lin et al., 2017). A deficiency in linoleic acid has been linked to dermatitis development among adults and children (Horrobin, 2000). Lauric acid is biologically active and can be transformed into monolaurin, which has antiviral, antibacterial, and antiprotozoal properties (Lieberman et al., 2006). It has also been used to treat severe antibiotic-resistant bacterial infections (Dayrit, 2015). Oleic acid activates lipid metabolism, restores the skin barrier, and helps retain moisture in the stratum corneum (Feingold and Elias, 2014). Palmitic acid and its derivatives are used as emulsifiers and emollients in creams and lotions (Mawazi et al., 2022). Fatty acids are vital components of the skin barrier and their application as formulation ingredients has increased due to their functional effects, biological activities and high biocompatibility (Duffy et al., 2017).

Several studies related to the use of BSFs in the cosmetic industry have been conducted, particularly regarding the properties and benefits of the oil produced from their larvae (Verheyen et al., 2018; Franco et al., 2021). With a lipid content ranging from 15% to 49% of total dry weight, BSFs have been found to have a high lipid yield compared with other insects (Almeida et al., 2020; dos Santos et al., 2021). Additionally, BSFs are a rich source of fatty acid derivatives that can be used as natural cosmetic ingredients, considering the high quality and quantity of fatty acids identified in their lipid composition (Müller et al., 2017; Ravi et al., 2019; Almeida et al., 2020; Franco et al., 2021). Currently, many cosmetics use palm oil, rice bran oil, olive oil, krill oil, coconut oil and lecithin as active ingredients. However, these products have become relatively expensive and palm oil in particular leaves a high environmental footprint and is non-sustainable (Huang et al., 2009). BSFs oil, on the other hand, has a fatty acid profile similar to that of palm or coconut oil, with high levels of beneficial fatty acids and anti-oxidant activity. This makes it a promising ingredient in cosmetic products (Verheyen et al., 2020). Verheyen and others have

demonstrated that SFO could be a suitable alternative to palm or coconut oil to synthesize glycine-acyl surfactants, which can be used for technical applications (Verheyen et al., 2018). Overall, the potential benefits of BSFs in the cosmetic industry are significant and merit further research and exploration.

Nevertheless, information on the cosmetic-related activities of the SFO remains scarce. This study explored the potential use of BSFL in a closed farming system to generate a continuous supply of larvae, which can then be used to extract oil within 2 weeks. The resulting oil was evaluated for its potential as a new ingredient in cosmetics or functional foods, but scientific data were necessary to support its use. To this end, we conducted an evaluation of SFO as a potential oil for cosmetic application, comparing it with other commonly used oils in cosmetic production such as rice bran oil, olive oil, krill oil and lecithin. The study also discussed various aspects of the SFO preparation process, quality control, chemical composition and its cosmetic properties, compared with other oils frequently used in cosmetic applications.

Materials and methods

SFO oil and chemicals

SFO was supplied by Food Innovation and Packaging Center (Chiang Mai University, Chiang Mai, Thailand). Briefly, the 12-day BSFL were collected and kept frozen at −18°C before extraction. Frozen BSFL were thawed and dried in a hot air oven (FD 115, BINDER, Germany) at 80°C for 5 h and then further dried at 60°C for 3 h until moisture content achieved lower than 8%. The dried BSFL were subjected to screw pressing using a pressing machine (AS 700 W, Alangkarn Siam, Thailand) at 65–70 rpm. The obtained oil was further centrifuged using a centrifuge and filtered before filling in aluminum bags with N_2 flushed and kept at room temperature before subjecting to further studies. The 1,1-diphenyl-2-picrylhydrazine (DPPH), 2,4,6-tris (2-pyridyl)-s-triazine (TPTZ), 2,2′-azobis (2-amidinopropane) dihydrochloride (AAPH), 6-hydroxy-2,5,7,8-tetramethylchromane-2-carboxylic acid (Trolox), and linoleic acid were purchased from Sigma Chemical Co. (St. Louis, MO, United States). Rice bran oil (5,000 ppm oryzanol, King, Thailand) and olive oil (Bertolli, extra virgin, Italy) were purchased from a local gourmet store. Krill oil and lecithin (food grade) were purchased from Xi'an Natural Field Bio-Technique, China. Methanol, dichloromethane, ethanol, acetonitrile and other solvents were purchased from RCI Labscan, Bangkok, Thailand. Dulbecco's modified Eagle medium (DMEM), trypsin, and penicillin-streptomycin were supplied by Gibco (Grand Island, NY, United States). Fetal bovine serum (FBS) was supplied by GE Healthcare (Little Chalfont, United Kingdom). The 3-(4,5-dimethylthiazol-2-yl)-2,5-diphenyltetrazolium bromide (MTT) dye, 2′,7′-dichlorofluorescin diacetate (DCF-DA), kojic acid, and arbutin were purchased from Sigma-Aldrich (St. Louis, MO, United States).

Physicochemical characterization of SFO

The pH value of SFO was determined at 25°C using a pH meter (Metrohm, Herisau, Switzerland), which was calibrated using pH 4 and 7 buffers. Viscosity of SFO was measured at 25°C with a Brookfield R/S-CC rheometer using a Bob and Cup format (Brookfield, MA, United States). The measuring system was the CC48 DIN with a controlled shear rate. The values of acids, saponification and unsaponification were examined according to the method of <401> USP 40 (Pharmacopeia, 2017). The water content was determined by the well-established methods of Karl Fischer titration using Karl Fischer V20 Titrator (Mettler Toledo, OH, United States). All measurements were carried out in triplicate.

Fatty acid composition analysis

Lipids were extracted using a modified version of the method described by Lepage and Roy, (1986). Three grams of sample were homogenized for 4 min × 15 min with 12 mL of dichloromethane: methanol (2:1 v/v). The sample was filtered, and potassium chloride was added. A biphasic separation was obtained by centrifugation (2000 rpm, 10 min). After that, the supernatant was collected and methanolic solution of 0.5 mM NaOH was then added for incubating at 100°C, 15 min. Methylation was catalyzed by 2 mL 14% BF_3-methanol complex in methanol. To extract the fatty acid methyl esters, 5 mL 20% NaCl and 0.5 mL hexane were added, followed by centrifugation for 5 min at 1,000 rpm. The upper phase (containing the fatty acid methyl esters; FAME) was collected for the analysis for fatty acid profile using GC-MS (Trace GCultra, Italy/Polaris Q, United States), equipped with a TR-FAME (60 m × 0.25 mm, film thickness 0.25 μm). The carrier gas was helium, and the detector temperature was 230°C with a split ratio (20:1), and 1 μL was injected (split ratio 1:20). Fatty acid composition was calculated using the fatty acid methyl ester internal standard and expressed as percentage of total detected fatty acids. All measurements were performed by the Research and Service Laboratory, The Halal Science Center, Chulalongkorn University, Bangkok, Thailand under the Halal GMP/HACCP and Halal-QHS/ISO 22000.

Determination of anti-oxidant activities

Anti-oxidation potential of SFO was determined in comparison with other oils and a positive control, Trolox (5 mM), using different methods including DPPH, FRAP and lipid peroxidation inhibition assays. The free radical scavenging property of samples was evaluated using the DPPH assay (Kiattisin et al., 2019). DPPH solution at a concentration of 167 μM was prepared in absolute ethanol. In brief, DPPH solution was added in a 96-well plate and mixed with an oil sample (20 μL), mixed well. Following that, the sample was incubated in the dark at 25°C for 30 min. The absorbance was then measured at 520 nm using a microplate reader (SPECTROstar Nano, Offenburg, Germany). The percentage of inhibition was determined using the equation below.

$$\%\ Inhibition = \left[\frac{C - S}{C}\right] x\ 100$$

where C is the absorbance of control, and S is the absorbance of sample. The experiments were performed in triplicate.

The reducing capacity of samples was investigated using the ferric reducing anti-oxidant power (FRAP) assay (Kiattisin et al., 2019). The FRAP reagent was prepared by mixing 300 mM acetate buffer, 20 mM ferric chloride solution and 10 mM TPTZ. Then FRAP reagent was

mixed with each undiluted sample in a 96-well plate and incubated at room temperature for 5 min. The sample was then measured for absorbance at 595 nm using a microplate reader (SPECTROstar Nano, Germany). The experiments were performed in triplicate, and the results were expressed as a FRAP value or ferrous sulfate ($FeSO_4$) equivalent per Gram of sample.

The lipid peroxidation inhibition property of samples was determined using the linoleic acid thiocyanate method (Poomanee et al., 2021). Each sample was mixed with linoleic acid in methanol, phosphate buffer pH 7.0, DI water and AAPH in a test tube. The sample was then incubated in a water bath at 45°C for 4 h. After, the reaction mixtures were mixed with 75%v/v methanol, 10% ammonium thiocyanate solution and 2 mM ferrous chloride in a 96-well plate. After precisely 3 min, the absorbance was measured at 500 nm using a microplate reader (SPECTROstar Nano, Germany). The experiments were performed in triplicate. The percentage of lipid peroxidation inhibition was determined using the equation below.

$$\%\ Inhibition = \left[\frac{C - S}{C}\right] x\ 100$$

where C is the absorbance of the control, and S is the absorbance of the sample.

Determination of hyaluronidase (HAase) inhibitory activity

The inhibition of HAase was determined by measuring *N*-acetyl-glucosamine level, which was produced by the interaction of sodium hyaluronate with HAase (Laothaweerungsawat et al., 2020). Before each experiment, the HAase enzyme activity was measured, and only enzyme activity more than 90% was employed. In brief, the oil samples were incubated for 10 min with 15 unit/mL HAase at 37°C. Following that, 0.03% w/v hyaluronic acid (HA) in phosphate buffer pH 5.35 was added and incubated for 45 min at 37°C. HA was then precipitated using acid bovine serum albumin, produced from sodium acetate, acetic acid and bovine serum albumin. Using a multimode detector, the absorbance of the resultant combination was measured at 600 nm (BMG Labtech, Offenburg, Germany). Every experiment was carried out in triplicate. The HAase inhibition was determined using the equation below.

$$\%\ Inhibition = \left[1 - \left(\frac{a}{b}\right)\right] x\ 100$$

where a is the absorbance of the mixtures comprising oil sample, HAase, HA and bovine serum albumin solution, and b is the absorbance of the mixtures comprising HAase, HA and bovine serum albumin solution without oil samples. As a positive control, oleanolic acid, an anti-inflammatory and anti-oxidative triterpenoid compound was employed.

Molecular docking of promising compounds toward the HAase enzyme

In this study, a crystal structure of human HAase was retrieved from Protein Data Bank (PDB ID: 2PE4) (Chao et al., 2007). All the hetero-atoms and water molecules were removed from the protein structure. The 3D structures of free fatty acids and oleanolic acid were obtained in the PubChem database (https://pubchem.ncbi.nlm.nih.gov/) and further geometry optimized using Gaussian09w with the B3LYP/6-311G (d,p) basis set (Hehre et al., 1970). The hydrogen atoms and Gasteiger's charges were assigned using AutoDockTools 1.5.6 (Morris et al., 2009) The docking simulation was performed using AutoDock Vina (Trott and Olson, 2010). A grid box ($25 \times 25 \times 25$ Å^3) was created from the center of the catalytic site (X: 41.945, Y: -21.787 and Z: -16.336). The structures with the lowest binding energies were selected for analysis, and the molecular recognition was identified using LigandScout 4.4.8 (Wolber and Langer, 2005). Structural figures were generated using PyMOL (PyMOL Molecular Graphics System, Version 2.0 Schrödinger, LLC).

Cell culture

Primary human skin fibroblasts were aseptically isolated from an abdominal scar after a surgical procedure involving a cesarean delivery at the surgical ward of CM Maharaj Hospital, Chiang Mai University, Chiang Mai, Thailand (Study code: BIO-2558-03541 approved by Medical Research Ethics Committee, Chiang Mai University). The protocol of isolating and preparing the primary fibroblasts were followed according to a described protocol (Limtrakul et al., 2016).

HaCaT cells (human keratinocytes) and B16-F10 melanoma cells were purchased from ATCC (VA, United States). All cell types were cultured in DMEM with 10% FBS and supplemented with 100 U/mL penicillin and 100 µg/mL streptomycin. The cells were maintained in a 5% CO_2 humidified incubator at 37°C.

Human blood samples were obtained from the Blood Bank Laboratory, Maharaj Hospital, Chiang Mai, Thailand which remained in the laboratory and could not be identified by hosts. Human Peripheral Blood Mononuclear Cells (PBMC) were prepared using Ficoll-hypaque density gradient centrifugation. Cells were rested in RPMI 1640 medium supplemented with 10% fetal bovine serum, 2 mM L-glutamine, 100 IU/mL penicillin and 100 µg/mL streptomycin, overnight before the experiment.

Cytotoxicity effects using the MTT assay

The effects of SFO on cell viability were determined using the MTT assay as described. Briefly, the cells were treated with increasing concentrations of SFO (0–200 µg/mL) in culture medium or culture medium alone (vehicle control) for 24 and 48 h. Following the SFO treatment, the cells were incubated with 10 µL of 0.5 mg/mL MTT in PBS for 4 h. The culture supernatant was then removed, and the culture was re-suspended with 200 µL of DMSO to dissolve the MTT formazan crystals. The absorbance was measured at 540 and 630 nm using a UV-visible spectrophotometer, and the assay was performed in triplicate.

Determination of *in situ* intracellular ROS inhibitory effects

Intracellular ROS after UVB irradiation was determined using a DCF-DA assay, as described (Eruslanov and Kusmartsev, 2010;

TABLE 1 Chemical properties of SFO.

Chemical property	Result
pH	6.00 ± 0.15
Viscosity (cPa.s)	52.0 ± 0.3
Unsaponifiable matter (%)	0.72 + 0.17
Acid value (mg KOH/g)	3.00 ± 0.81
Saponification value (mg KOH/g)	197.1 ± 9.5
Water content (%w/w)	0.13 ± 0.02

He et al., 2017). The fibroblasts (8.0×10^5 cells/well) were seeded in a 96-well plate for 24 h. After that, the cells were exposed to UVB (15 mJ/cm^2) using a ultraviolet crosslinker machine. The cells were then treated with or without SFO (0–200 μg/mL) for 24 h. After that, the cells were washed with PBS, 10 μM of DCF-DA was added and the cells were incubated for a further 30 min. The fluorescent intensity was measured at an excitation wavelength of 485 nm and an emission wavelength of 525 nm. The inhibitory effects of SFO on intracellular ROS production at 24-h post UVB exposure was calculated and compared with the control of UVB-irradiated fibroblast cells.

Determination of melanin content inhibition

B16-F10 cells (1×10^5 cells/dish) were seeded in a 60×15 mm^2 dish and incubated for 24 h at 37°C, 5% CO_2. After that, the cells were treated with 50 μg/mL of kojic acid or arbutin (positive controls) or SFO, olive oil and linoleic acid at the concentrations of 50 μg/mL. The cells were incubated for 48 h and then collected and washed with PBS. NaOH was added and the cells were incubated at 80°C for 30 min. The absorbance was determined using a microplate reader at 405 nm.

Statistical analysis

Data were collected from three independent experiments and are shown as mean ± SD. Statistical analysis was performed using t-tests, ANOVA and Tukey's multiple comparison test, using SPSS, Version 19.0 (IBM® SPSS Statistics, Armonk, NY, United States). A *p-value* less than 0.05 was considered statistically significant.

Results

Physicochemical characterization and fatty acid composition analysis of SFO

The oil obtained from SFO was subjected to physicochemical and fatty acid composition analysis to validate its quality. SFO was found to possess a brownish color and oily texture. Table 1 summarizes the physicochemical characteristics of SFO, including pH (6.0), viscosity (52 cPa.s), unsaponifiable matter (0.72 + 0.17%), acid value (3.00 ± 0.81 mg KOH/g) and water content (0.13%w/w).

In addition to the physiochemical evaluation of SFO, the fatty acid composition of SFO was analyzed using GC-MS. The lipid extracts of SFO were displayed as a chromatogram, and the percentage of fatty acid composition was calculated and is presented in Figure 1 and Table 2. Linoleic acid was found to be the predominant fatty acid, with a content of 34.19%, followed by oleic acid (15.95%), palmitic acid (15.93%) and lauric acid (13.25%). The remaining fatty acids, including capric acid, myristic acid, palmitoleic acid, margaric acid, steric acid and linolenic acid, were all found present in amounts less than 10%. SFO contained high percentages of polyunsaturated fatty acids (PUFA) of up to 60%, followed by saturated fatty acids of up to 37%.

Determination of anti-oxidant activities of SFO

The use of natural oils in pharmaceutical and cosmetic products for their anti-oxidant properties has been well established. Therefore, our study aimed to examine the anti-oxidant activities of SFO compared with Trolox and commonly used oils in the cosmetic and nutraceutical industries. We evaluated the anti-oxidant activity of SFO using different assays including DPPH, radical scavenging, FRAP, and lipid peroxidation inhibition tests, and compared it with rice bran oil, olive oil, krill oil, lecithin and linoleic acid.

The results of the anti-oxidant activity tests of SFO, rice bran oil, olive oil, krill oil, lecithin and linoleic acid are shown in Figures 2A–C. According to the results, SFO exhibited multiple mechanisms to interrupt the oxidation processes compared with the other oils. The DPPH assay is a well-known method for assessing stable free radical scavenging activity (Rahman et al., 2015). Neat SFO showed the highest DPPH radical scavenging activity (96.61% inhibition) which was significantly higher than that of the other oils and even linoleic acid (24.93%–92.69%, $p < 0.05$), except for rice bran oil, which was higher but did not differ significantly (Figure 2A). The free radical scavenging activity of SFO is comparable to the activity of 5 mM Trolox, a positive control.

The FRAP assay directly measures anti-oxidants (or reductants) in a sample and represents the corresponding concentration of electron-donating anti-oxidants with reduced ferric iron (Fe^{3+}) compared with the ferrous ion (Fe^{2+}) (Kiattisin et al., 2019). In our study, the FRAP assay showed that krill oil exhibited the highest reducing power (110.59 ± 3.99 mM $FeSO_4$/g sample), followed by SFO (51.61 ± 2.08 mM $FeSO_4$/g sample), while the common oils exhibited significantly lower reducing power. Interestingly, the positive control, Trolox (5 mM) exhibited significantly higher FRAP value of 28,724 mM $FeSO_4$/g sample that is significantly high and could not be plotted with the oils' FRAP values. Contrastingly, linoleic acid was inactive, implying that it could not be responsible for the reducing ability of SFO (Figure 2B). Lipid peroxidation in cells leads to degrading the lipid bilayer composing cell membranes, and the end-products can further promote mutagenesis or protein oxidation, disturbing cellular homeostasis (Ali et al.,

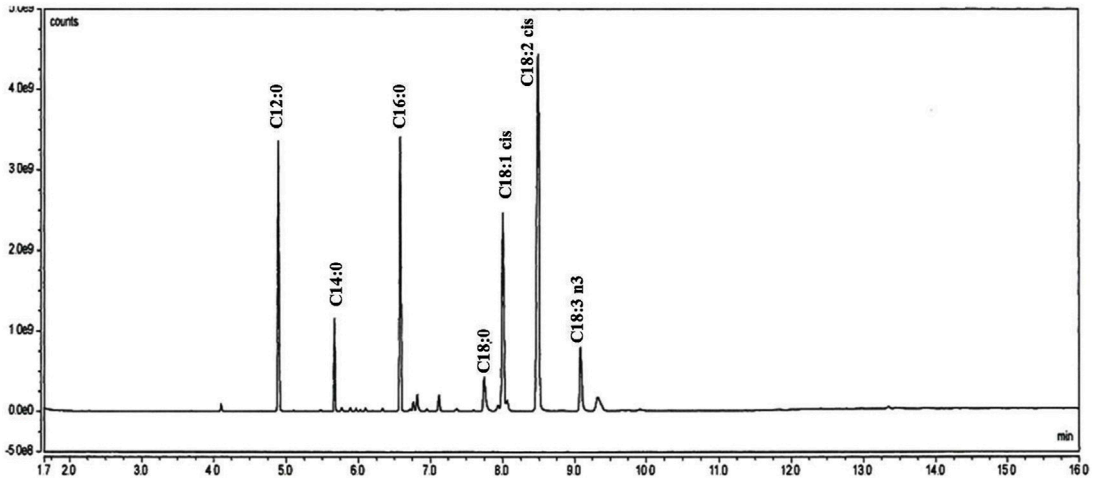

FIGURE 1
GC/MS analysis of fatty acids in black soldier fly oil.

TABLE 2 Fatty acid profile of black soldier fly oil.

Fatty acid	Percentage (%)
Capric acid (C10:0)	0.33 ± 0.02
Lauric acid (C12:0)	13.25 ± 1.81
Myristic acid (C14:0)	3.82 ± 0.19
Palmitic acid (C16:0)	15.93 ± 0.56
Palmitoleic acid (C16:1)	0.95 ± 0.16
Margaric acid (17:0)	0.99 ± 0.03
Steric acid (C18:0)	3.43 ± 0.32
Oleic acid (C18:1 n-9 cis)	15.95 ± 0.64
Linoleic acid (C18:2 n-6 cis)	34.19 ± 0.44
Linolenic acid (C18:3 n-3)	5.68 ± 0.33

2022). Inhibition of chain reactions of lipid peroxidation is promoted in anti-aging discovery. Similar to the FRAP assay, the lipid peroxidation inhibition assay showed that SFO (69.03%) had significantly higher activity than that of the other oils (18.05%–53.17%) except for krill oil and the positive control, Trolox (5 mM), exhibiting the highest lipid peroxidation inhibition activity (84.71% and 87.12%, respectively) (Figure 2C).

HAase inhibitory activity of SFO and molecular docking of its major fatty acids toward the HA enzyme

The study investigated whether SFO and its potential fatty acids could inhibit the activity of HAase, which primarily degrades HA in the skin. The disappearance of HA in the skin can result in significant histochemical changes associated with aging (Farage et al., 2008). In this

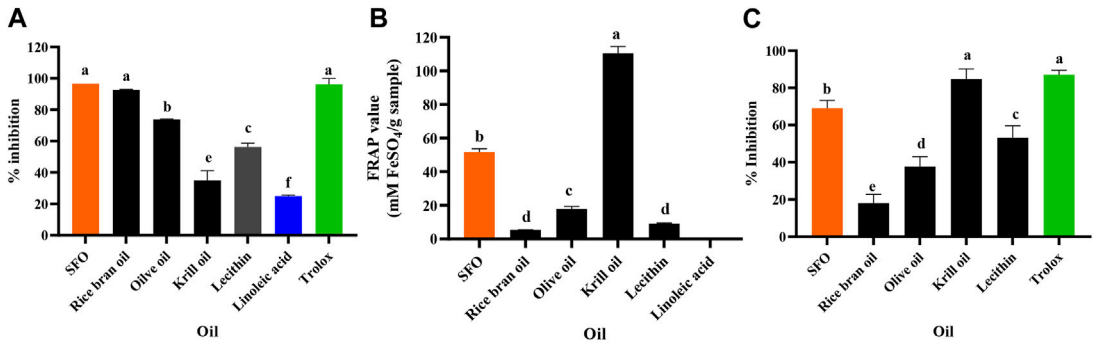

FIGURE 2
Anti-oxidant activity evaluated with **(A)** DPPH, **(B)** FRAP and **(C)** Lipid peroxidation inhibition assays of SFO, rice bran oil, olive oil, lecithin, linoleic acid, and Trolox (a, b, c, d, e and f denote significant differences among samples at $p < 0.05$).

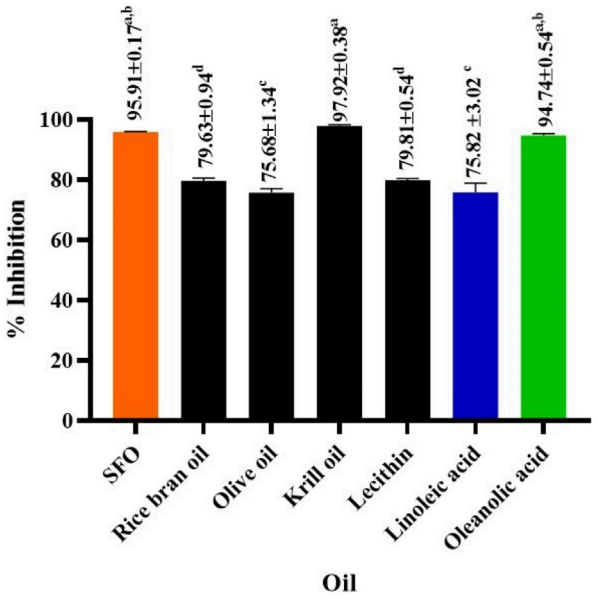

FIGURE 3
Effect of SFO, rice bran oil, olive oil, krill oil, lecithin, linoleic acid and oleanolic acid (a positive control) on hyaluronidase inhibitory activity., (a, b, c and d denote significant differences among samples at $p < 0.05$).

study, we investigated whether SFO and its potential fatty acid could possess inhibitory effects on HAase activity. The HAase inhibitory activity of SFO, rice bran oil, olive oil, krill oil, lecithin, linoleic acid as well as the positive control, oleanolic acid, are shown as the %inhibition in Figure 3. SFO (95.91%) and krill oil (97.92%) exhibited strong HAase inhibition comparable with the positive control, oleanolic acid (94.74%). Linoleic acid, a major fatty acid in SFO, also showed HAase inhibitory activity, but to a lesser extent than the crude oil (75.82%).

To further understand the mechanism of enzyme inhibition, molecular docking studies were conducted on major fatty acid components of SFO including linoleic acid, oleic acid and palmitic acid, as well as the positive control, oleanolic acid. Molecular docking was carried out to investigate the binding interactions and molecular recognition of selected free fatty acids toward HAase (PDB: 2PE4). The molecular interactions of the docked complexes are depicted in Figures 4A–D. Linoleic acid, oleic acid and palmitic acid were positioned at the binding pocket of the HAase enzyme. The fatty acid-binding pocket was mostly hydrophobic with residues including M71, I73 and Y75, where the tail of fatty acids fits well (Figures 4A–C). The positive compound was well accommodated within the active site of the enzyme by forming a hydrogen bond with S245 and hydrophobic interaction with residues Y202, F204, T293 and W321 (Figure 4D). The docking results showed that linoleic acid exhibited the highest binding affinity to HAase at −6.5 kcal/mol, followed by oleic acid and palmitic acid with binding energies of −6.0 and −5.8 kcal/mol, respectively. The positive control, oleanolic acid, showed a strong binding score of −8.5 kcal/mol, which was consistent with the *in vitro* experiment.

Effects of SFO on cells viability

To examine the potential use of SFO in cosmetic preparation, we conducted a safety assessment by determining its cytotoxicity effects on human skin cells (keratinocytes and fibroblasts) as well as human white blood cells (PBMC), using the MTT assay. Primary human skin fibroblasts, HaCaT keratinocyte cell line and PBMCs were treated with increasing concentrations of SFO for 24 and 48 h. Our results, as shown in Figures 5A–C, indicated that even at a high concentration of 200 μg/mL, SFO did not display cytotoxicity effects on human dermal fibroblasts (Figure 5A), HaCaT keratinocytes (Figure 5B) or PBMCs (Figure 5C) after 24 and 48 h of incubation. The IC_{50} value for all types of cells was greater than 200 μg/mL of SFO. Therefore, our findings suggested that SFO is safe for use in

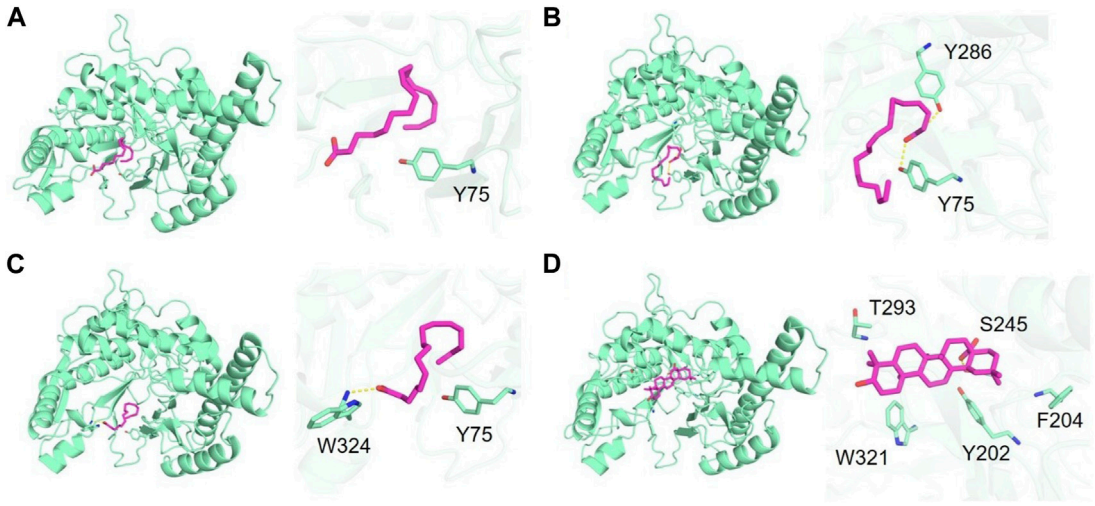

FIGURE 4
Binding of hyaluronidase (green) interacting with free fatty acids (magenta) including **(A)** linoleic acid, **(B)** oleic acid, **(C)** palmitic acid and **(D)** positive control (oleanolic acid).

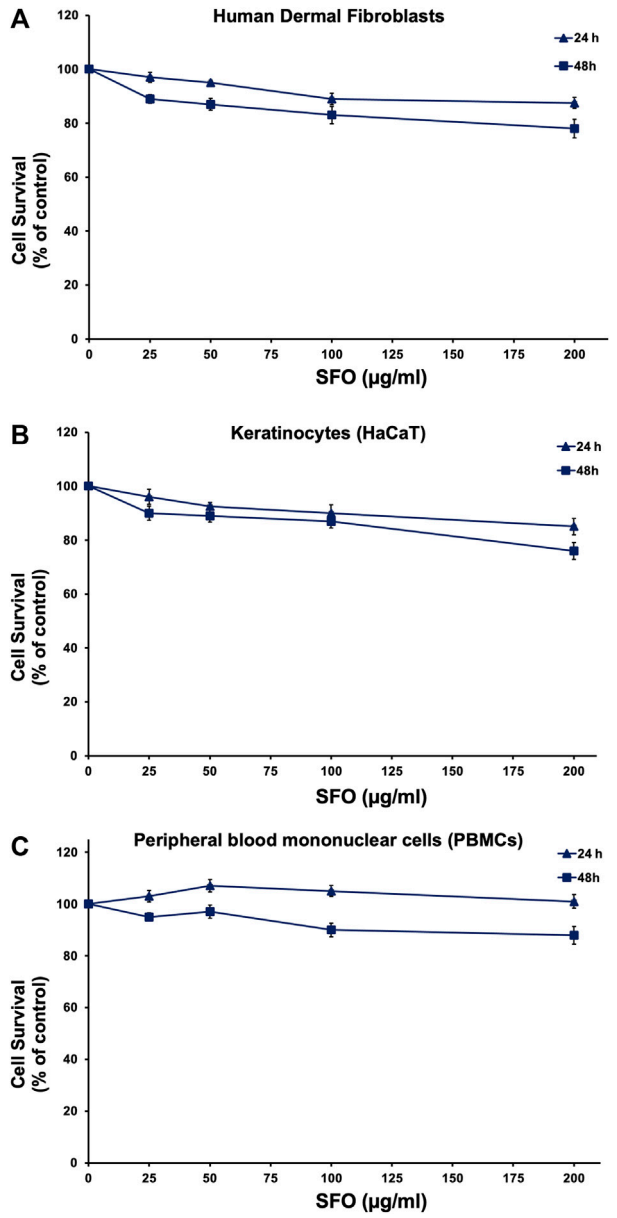

FIGURE 5
Effect of SFO on human normal cells viability, Human dermal fibroblasts **(A)**, HaCaT human keratinocytes **(B)** and human PBMCs **(C)** were treated with varying concentrations of SFO for 24 h and 48 h. The viability of cells was assessed using the MTT assay, and the results are presented as mean ± S.D. of three independent experiments.

cosmetic applications as it did not show any cytotoxicity effects on human normal cells.

In-situ ROS scavenging effects of SFO on UVB-irradiated human dermal fibroblasts

We initially evaluated the *in vitro* anti-oxidant properties of SFO and found it exhibited strong anti-oxidant effects. To further confirm its anti-oxidant capacity *in-situ*, we conducted DCF-DA assays to determine the intracellular ROS scavenging properties in UVB-irradiated dermal fibroblasts. The results are shown in Figure 6. The findings indicated that UVB radiation increased ROS generation in human dermal fibroblasts by approximately 60% when compared with nonirradiated fibroblasts. Interestingly, when the cells were pretreated with SFO, increasing concentrations of SFO significantly reduced intracellular ROS production in UVB-irradiated fibroblasts in a dose-dependent manner at post-24 h of UVB exposure ($p < 0.05$). At this exposure time, SFO at the concentration of 200 µg/mL inhibited the intracellular ROS production to less than 20% when compared with the irradiated fibroblasts group. These findings demonstrated that SFO has the potential capacity to reduce the generation of ROS through its ROS scavenging ability. Thus, SFO exhibited antioxidant properties in both *in vitro* and *in situ*.

The effects of SFO on the inhibition of melanin content

As of today, in addition to anti-oxidant compounds, many cosmetic products contain antipigmenting active ingredients, such as kojic acid and arbutin, exhibiting skin whitening effects. To investigate whether SFO possesses antipigmenting properties, we assessed its ability to inhibit melanin content in B16F10 melanoma cells. As is shown in Figure 7, pretreating the cells with SFO led to reduced melanin content (78% inhibition). Furthermore, the level of melanin content inhibition achieved by SFO at the same concentration was comparable with that of well-known positive control agents, kojic acid and arbutin (75% and 77% inhibition, respectively). Conversely, olive oil at 50 µg/mL had little to no effect on melanin inhibition (5% inhibition). Meanwhile, linoleic acid, the major fatty acid present in SFO, exhibited similar inhibitory effects on melanin levels (74% inhibition). Our findings suggest that SFO, at a concentration of 50 µg/mL, can inhibit melanin content as effectively as well-known melanin pigment inhibitors. Therefore, SFO may be considered as a potent new antipigmenting agent.

Discussion

This study provides scientific data on the SFO obtained from *Hermetia illucens* larvae. The physiochemical characteristics and lipid composition of the oil were determined and compared with other oils commonly used in cosmetic and supplement applications. Compared with another study, the acid value, saponification value and unsaponifiable matter of SFO revealed less than those reported in a related study (Mai et al., 2019). Briefly, the study reported the acid value of SFO at 11.8 mg KOH/g while its saponification value and unsaponifiable matter were 213 and 86 mg KOH/g, respectively. An increase or rise in acid value indicates the rancidification tendency of the oil. Taken together with the acid value, a measurement of potassium hydroxide (mg), required to neutralize the free fatty acid contained in unit mass (g) of chemical substance, the lower the acid value of oil, the fewer free fatty acids it contains making it less exposed to rancidification (Kardash and Tur'yan, 2005). Therefore, SFO in our study

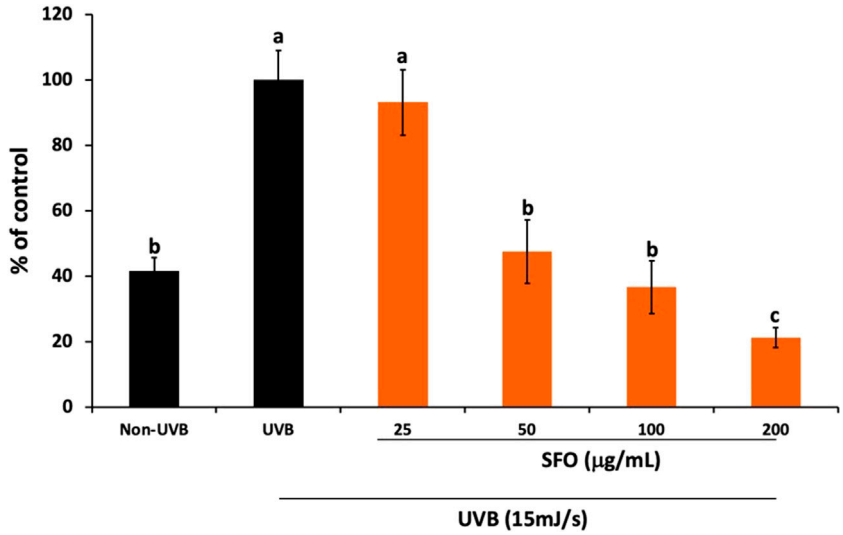

FIGURE 6
In-situ anti-oxidant activity of SFO. The inhibition of intracellular ROS upon UVB irradiation in human dermal fibroblasts was determined using the DCF-DA fluorescent assay. The data is presented as mean ± S.D. of 3 independent experiments (a, b and c denote significant differences among samples at p <0.05).

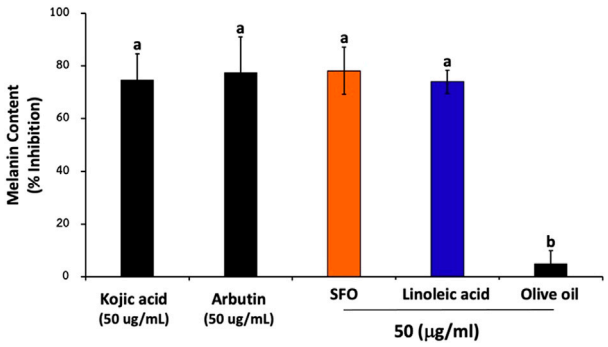

FIGURE 7
Effects of SFO on melanin content inhibition, B16F10 melanoma cells were treated with SFO, linoleic acid, olive oil, kojic acid or arbutin at a concentration of 50 μg/mL for 48 h at 37°C. After treatment, the cells were collected and washed with PBS. Then NaOH was added to the cells and incubated at 80°C for 30 min. The absorbance was measured at 405 nm using a microplate reader; (a and b denote significant differences among samples at p < 0.05).

possessed a lower acid value and was less likely to generate the rancidity. A high saponification value suggested the presence of a fair amount of fatty acids but their acid values were low pointing to the fact that these fatty acids were not free but in an esterified form (Ekpo et al., 2009).

The fatty acid composition of SFO was compared with that of olive oil (*Olea europaea* L.), krill oil (*Euphausia superba*) and rice bran oil (*Oryza sativa*) from related studies (Orthoefer and Eastman, 2005; Ivanova et al., 2016). The data showed that olive oil contained a high amount of oleic acid (73.6%) followed by palmitic acid (14.11%) and linoleic acid (8.35%). Krill oil contained a high amount of palmitic acid (20.43%) followed by oleic acid (9.49%) and myristic acid (8.76%), while the highest fatty acid in rice bran oil was oleic acid (38.4%) followed by linoleic acid (34.4%) and palmitic acid (21.5%). In contrast, the most abundant component found in SFO was linoleic acid (C18:2 n-6 cis), which was consistent with related research (Barroso et al., 2017; Ewald et al., 2020). Linoleic acid has been shown to exhibit several pharmaceutical activities, especially regarding skin function (Huang et al., 2018). For example, it has been demonstrated to downregulate melanin synthesis, and clinical trials have reported the effectiveness of liposome containing 0.1% linoleic acid to treat melasma and lightening UVB-induced hyperpigmentation of the skin (Shigeta et al., 2004). Interestingly, linoleic acid was reported to positively correlate between amounts of linolenic acid and anti-oxidant activity (Saffaryazdi et al., 2020). Nevertheless, linoleic acid exhibited the ability to decrease in the epidermis with age causing skin sensitivity and roughness (Ahmad and Ahsan, 2020). Therefore, oils enriched with linoleic acid could be an interesting source for skin cosmetics. However, the lipid composition of BSFL significantly vary with their diets (Kim et al., 2020; Li et al., 2022). A higher percentage of omega-6 and 3 was obtained when the larvae were given the diet riches in polyunsaturated fatty acids from agricultural by-products (rape and flax cakes) (Hoc et al., 2021). Together with the work of Almeida et al. reported that the extraction technique significantly affects fatty acids profile of BSFL biomass (Almeida et al., 2022). Thus, it should be noted that consistency of batch-to-batch production should be highly considered to lessen variation of SFO lipid composition.

Several vegetable oils including rose hip, flax, hemp, thistle, safflower and camelina, have been chosen for cosmetic use due to their composition and high anti-oxidant activity. Anti-oxidants play a crucial role in preventing or reducing oxidative stress, leading to numerous health problems such as cancer, cardiovascular diseases, neurodegenerative disorders and skin aging. Natural anti-oxidants can inhibit or decrease the damage caused by oxidative stress

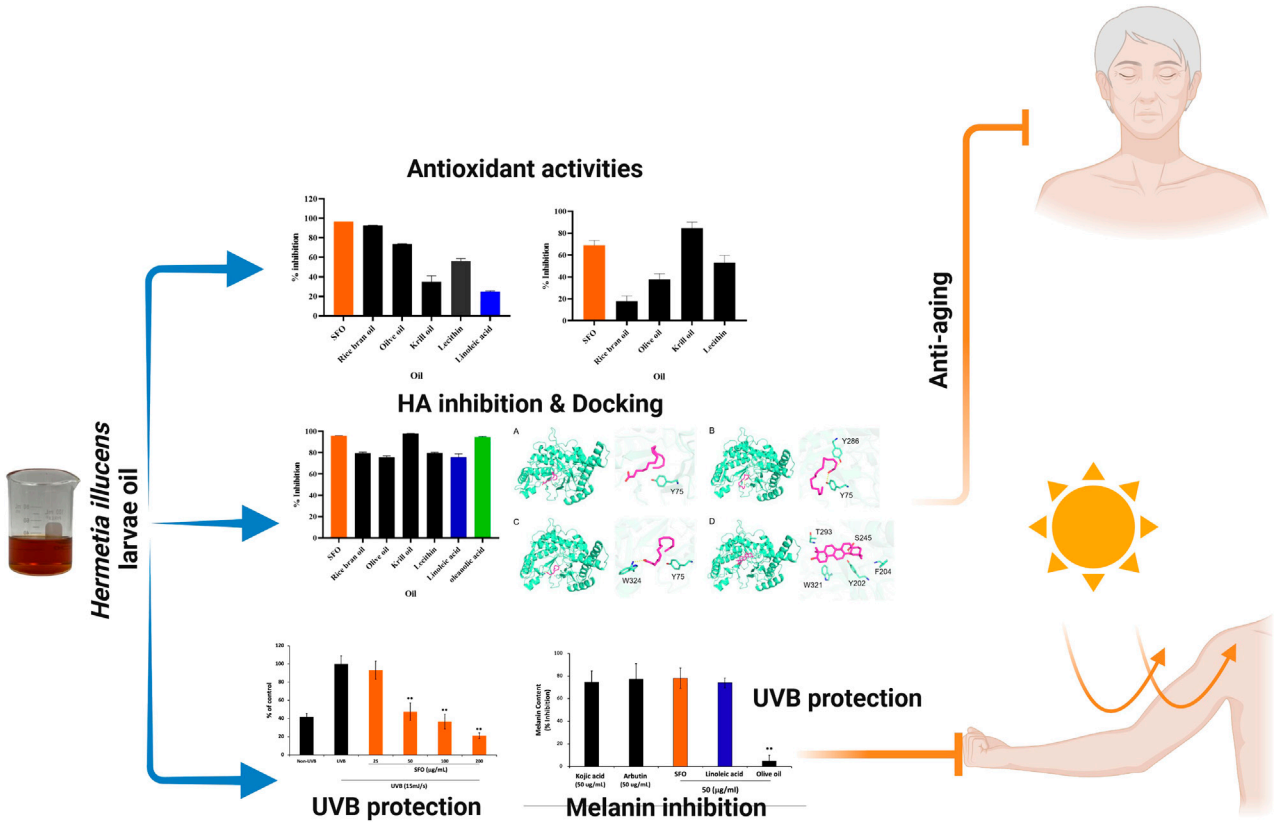

FIGURE 8
Pictorial summary illustrates the pharmacologic and cosmetic-related activities of black soldier fly oil. Figure was created with Biorender.com.

through different mechanisms of action (Ionescu et al., 2015). Long term exposure to oxidative stress leads to redox imbalance, various biomolecules damage and abnormal gene expression, including those involved in aging pathways (Rungratanawanich et al., 2018). *In vitro* assays have demonstrated that SFO has higher radical scavenging, reducing power, and lipid peroxidation inhibition properties compared with rice bran oil, olive oil and lecithin. The anti-oxidant capacity of SFO was comparable with 5 mM Trolox (positive control) in the lipid peroxidation inhibition and slightly lower in the DPPH assays. However, the reducing capacity of SFO was much lesser than that of Trolox. Although linoleic acid, a major fatty acid in SFO did not exhibit strong anti-oxidant activity, SFO's anti-oxidant activity may be due to other phenolic compounds, flavonoids, α-tocopherol and various fatty acids (Elagbar et al., 2016; El-Agbar et al., 2018). Studies have also shown that sterols and tocopherols/tocotrienols in insects' larvae oil may contribute to anti-oxidant capacity by acting as a chain-breaking activity (Mariod, 2013; dos Santos et al., 2021). Furthermore, PUFA, specifically alpha-linolenic acid and linoleic acid, have been found to be related to anti-oxidant activity (Alves et al., 2016). Phospholipids such as phosphatidylethanolamine and phosphatidylcholine can increase the ability of tocopherol to suppress lipid peroxidation (Bandarra et al., 1999; Judde et al., 2003; Takenaka et al., 2007). The polyunsaturated fatty acid moieties and amine groups in phospholipids can regenerate tocopheroxyl radicals to tocopherol (Henna Lu et al., 2011; Doert et al., 2012; Huang et al., 2020). These compounds have been shown to scavenge free radicals and prevent lipid oxidation, contributing to the overall anti-oxidant activity of SFO.

HA is a natural polysaccharide found in the extracellular matrix of vertebrate tissues, particularly soft connective tissues. It has a high molecular weight and consists of repeating disaccharide units of D-glucuronic acid and N-acetyl-D-glucosamine linked through (β-1,3 and β-1,4) glycosidic linkages. HA is naturally found in synovial fluid of joints, epidermis and dermis, where it serves as a lubricant for joints and a natural moisturizing factor that maintains skin moisture (Farage et al., 2008; Girish et al., 2009). HA degradation was attenuated when SFO was added to the HA-HAase system in hyaluronidase (HAase) inhibitory activity assay. HAase is a class of glycosidase that predominantly degrades HA, which is an extracellular matrix with a critical role in skin hydration and plumpness. Inhibition of this enzyme has received considerable attention in biological, pharmaceutical and cosmetic application (Girish et al., 2009). Since HAase is over activated and excessively breaks down HA, leading to the destruction of the proteoglycan network under chronic inflammation and/or oxidative stress (Hwang, 2010).

Linoleic acid, a representative major compound in SFO, was found to potentially be responsible for HAase inhibition activity, and other lipids such as oleanolic acid, eicosatrienoic acid and nervonic acid were reported for their HAase inhibitory activity (Girish et al., 2009). Suzuki et al. reported the inability of saturated fatty acid to inhibit the HA enzyme, whereas the cis-

unsaturated fatty acids having double bonds are essential for inhibition (Suzuki et al., 2002). Molecular docking of the major components in SFO including linoleic acid, oleic acid and palmitic acid was carried out to investigate the binding interactions and molecular recognition of selected free fatty acids toward HAase. Interestingly, linoleic acid displayed the highest binding affinity to HAase when compared with other major fatty acids in SFO. The residue Y75 was found to be a crucial amino acid for binding HAase (Chao et al., 2007; Papaemmanouil et al., 2022). Reduction of HA degradation could lead to regulation of skin homeostasis, mitigates inflammatory and allergic states and diminish the aged appearance of skin (Hwang, 2010).

Based on our testing using MTT cell viability assay on HaCaT keratinocytes, primary human dermal fibroblasts, and peripheral blood mononuclear cells, we have found no cytotoxicity effects of SFO with the IC_{50} values exceeding 200 μg/mL. Other studies have also shown no cytotoxicity effects of oils derived from BSFL when tested on L-929 fibroblasts or using the *Artemia salina* model (Almeida et al., 2020; Franco et al., 2021; Riolo et al., 2023). Given these findings, we consider SFO to be safe for use in pharmaceutical and cosmetic products. To assess the *in vitro* biological effects of SFO in cell line models, we first tested its anti-oxidant activity by assessing its effects on UVB irradiation induced intracellular ROS in human dermal fibroblasts. The UVB-irradiation model in human dermal fibroblasts established in this study was modified from our described protocol (Mapoung et al., 2020). UV radiation can increase intracellular ROS levels and cause damage to the skin. Although the skin has a defense mechanism to prevent radical damage, this innate system can be overwhelmed, leading to aging and photo-aging. SFO's strong anti-oxidant properties could potentially delay the skin's aging process by counteracting the photo-aging process by reducing inflammatory responses (Jadoon et al., 2015; Xu et al., 2015). Although in this study we did not examine the anti-inflammation properties of SFO, previous studies have reported on the potential anti-inflammation properties of the major fatty acid of SFO, linoleic acid. Briefly, fatty acids, particularly, n-3 and n-6 essential fatty acids and conjugated linoleic acid (CLA), have been shown to modulate inflammation. Linoleic acid, an n-6 polyunsaturated fatty acid present in SFO, has been acknowledged for its potential anti-inflammatory properties (Saiki et al., 2017). Related studies have demonstrated that linoleic acid inhibits inflammatory responses in human THP-1 monocytes stimulated with LPS, leading to a decrease in the secretion of interleukin (IL)-6, IL-1β, and tumor necrosis factor-α (TNF-α) (Zhao et al., 2005). CLA isomers have also been found to possess anti-inflammatory effects by inhibiting ROS production and reducing the expression of inflammatory genes such as IL-6, IL-1beta and TNF-α in LPS-induced inflammation in bovine mammary epithelial cells (Dipasquale et al., 2018). Moreover, a Southern European nested case-control study (De Pablo et al., 2018) showed a significant inverse association (protective effects) between n-6 PUFA linoleic acid levels and pre-rheumatoid arthritis, indicating a lower risk of subsequent rheumatoid arthritis. Taken together, these findings suggest that the radical scavenging properties of SFO might be due to the presence of linoleic acid and that SFO may have anti-inflammatory effects potentially delaying the skin aging process. Nevertheless, the inhibitory effects of SFO and its major fatty acid (linoleic acid) on the cytokine production from skin cells should be confirmed.

In this study, we found that SFO and linoleic acid could promote the skin whitening effects not only through the removal of free radicals and the chelation of metal ions (antioxidant properties), but also through the depigmenting properties as evidence by the inhibition of melanin synthesis in B16F10 cells. Hyperpigmentation is a common skin condition that is particularly noticeable in individuals with darker skin tones and can be challenging to treat effectively. Numerous studies have been conducted by cosmetic scientists to identify skin-whitening agents that can address this issue, both through *in vivo* and *in vitro* research (Binic et al., 2013; Burger et al., 2016). One of the primary causes of hyperpigmentation is the overproduction of melanin by melanocytes, resulting in the formation of dark spots on the skin, particularly among older individuals and those with sun-exposed skin (Yodkeeree et al., 2018). To prevent or treat skin aging and hyperpigmentation, skincare products often utilize compounds that can protect the skin in various ways. These compounds may scavenge ROS, suppress ECM degradation enzymes, or inhibit melanogenesis. According to our results, SFO demonstrated a significant reduction in melanin synthesis by inhibiting melanin content in B16F10 melanoma cells, similar to well-known anti-pigmenting agents like kojic acid and arbutin. This suggests that SFO possesses potential whitening effects. Additionally, the major fatty acid found in SFO, linoleic acid, also exhibited inhibitory effects on melanin content. Linoleic acid has been previously associated with the modulation of melanogenesis and the inhibition of melanin synthesis in skin cells. Furthermore, other sources of linoleic acid, such as Chia seed extract (*Salvia hispanica*) and Passiflora edulis oil, have demonstrated the ability to inhibit melanin biosynthesis and reduce tyrosinase activity *in vitro* (Jorge et al., 2012; Diwakar et al., 2014). These findings suggested that compounds containing linoleic acid, like SFO, could be valuable in the prevention and treatment of hyperpigmentation and other signs of skin aging. Thus, our study supports the potential of SFO as a skin-whitening agent by inhibiting melanin synthesis. The presence of linoleic acid in SFO, along with previous research on mother sources of linoleic acid, indicates its involvement in the inhibition of melanin biogenesis. These findings contribute to the understanding of the mechanism of action behind the whitening effect of SFO and highlight the potential use of linoleic acid-containing compounds in combating hyperpigmentation and skin aging. Regarding the anti-skin aging properties, the strong antioxidant properties of the SFO could delay the aging process of the skin by counteracting the photo-aging process upon UV penetration. In addition, possible protective action of the SFO on the skin against ROS provoked and inhibition of HA degradation might serve as an anti-aging agent, mechanistically through reducing the inflammatory responses and oxidative stress, or by influencing specific survival signaling pathways, including MAPK and PI3K/Akt pathways. However, confirmation of the anti-skin aging effects of SFO and linoleic acid at the molecular level should be further investigated. The modulation of aged skin markers such as collagen type I/III ratio, fibroblast senescent markers (SA-β -gal activity, PTEN, and p53), and cell cycle regulator molecules ($p16^{INK4a}$, p53) upon SFO treatment should be further identified.

Conclusion

As of today, the search for novel compounds as sustainable active ingredients in cosmetic formulations has been an ongoing

task in the industry. In our study, we have introduced and investigated the environmental-friendly and sustainable oil from *Hermetia illucens* larvae (SFO). SFO displayed its potential use in cosmetic applications as an alternative oil incorporated into the cosmetic formulation. We conducted a comprehensive analysis of the oil's physicochemical characteristics, lipid composition and compared it with other commonly used oils in the cosmetic and supplement industry. Our findings suggest that SFO is a safe and effective ingredient for cosmetic products, with anti-oxidant properties both *in vitro* and *in situ*. In addition, we investigated the potential cosmetic properties of SFO and found it exhibited anti-hyaluronidase (anti-HAase) activity, which can be attributed to its linoleic acid and other oils content as determined by molecular docking. The SFO also demonstrated UVB protective effects in human dermal fibroblasts and anti-pigmenting effects in melanoma cell lines. As shown in a pictorial summary (Figure 8), our results suggest that SFO could constitute a promising ingredient in cosmetic products with implications for skin anti-aging, whitening, and UVB protection properties. Further studies on the *in vivo* effects of SFO and linoleic acid on anti-skin aging models should be conducted to confirm their efficacy before initiating testing on human subjects.

Data availability statement

The original contributions presented in the study are included in the article/Supplementary Material, further inquiries can be directed to the corresponding authors.

Author contributions

RP: Method, formal analysis, investigation, collected and analyzed data, visualization, composed primary draft of the manuscript and revised the manuscript. WS: Composed primary draft of the manuscript, performed the experiment, collected and analyzed data, and revised the manuscript. JJ: Investigation, method, performed the experiment, collected and analyzed the data. KK, WC, and SC: Investigation, method, performed the experiment, collected and analyzed data, composed the manuscript. YP: Conceptualization, supervision, resources, funding acquisition, writing review and editing. PD: writing, proofreading and editing the manuscript, review and critical appraisal of manuscript, project administration, and made the final decisions in preparing the manuscript. CA: Conceptualization, investigation, method, validation, writing, proofreading and editing the manuscript, review and critical appraisal of manuscript, project administration, and made the final decisions in preparing the manuscript. All authors contributed to the article and approved the submitted version.

Funding

This research project was supported by the Office of National Higher Education Science Research and Innovation Policy Council (NXPO) under Spearhead Project, Thailand.

Acknowledgments

The authors are grateful for the grant from NXPO. We would like to thank Chiang Mai University, and the Center of Excellence in Pharmaceutical Nanotechnology, Faculty of Pharmacy, Chiang Mai University, Chiang Mai 50200 Thailand, for partial support, facilitating the interdisciplinary collaboration and use of research facilities. We also thanks to Mr. Thomas McManamon for proofreading the article.

Conflict of interest

The authors declare that the research was conducted in the absence of any commercial or financial relationships that could be construed as a potential conflict of interest.

Publisher's note

References

Ahmad, A., and Ahsan, H. (2020). Lipid-based formulations in cosmeceuticals and biopharmaceuticals. *Biomed. Dermatol.* 4, 12–10. doi:10.1186/s41702-020-00062-9

Ali, J., Aziz, M. A., Rashid, M. M. O., Basher, M. A., and Islam, M. S. (2022). Propagation of age-related diseases due to the changes of lipid peroxide and antioxidant levels in elderly people: A narrative review. *Health Sci. Rep.* 5, e650. doi:10.1002/hsr2.650

Almeida, C., Rijo, P., and Rosado, C. (2020). Bioactive compounds from *Hermetia illucens* larvae as natural ingredients for cosmetic application. *Biomolecules* 10, 976. doi:10.3390/biom10070976

Almeida, C., Murta, D., Nunes, R., Baby, A. R., Fernandes, Â., Barros, L., et al. (2022). Characterization of lipid extracts from the *Hermetia illucens* larvae and their bioactivities for potential use as pharmaceutical and cosmetic ingredients. *Heliyon* 8, e09455. doi:10.1016/j.heliyon.2022.e09455

Alves, A. V., Sanjinez Argandona, E. J., Linzmeier, A. M., Cardoso, C. a. L., and Macedo, M. L. R. (2016). Chemical composition and food potential of pachymerus nucleorum larvae parasitizing Acrocomia aculeata kernels. *PloS one* 11, e0152125. doi:10.1371/journal.pone.0152125

Bandarra, N. M., Campos, R. M., Batista, I., Nunes, M. L., and Empis, J. M. (1999). Antioxidant synergy of α-tocopherol and phospholipids. *J. Am. Oil Chemists' Soc.* 76, 905–913. doi:10.1007/s11746-999-0105-4

Barroso, F. G., Sánchez-Muros, M.-J., Segura, M., Morote, E., Torres, A., Ramos, R., et al. (2017). Insects as food: Enrichment of larvae of *Hermetia illucens* with omega 3 fatty acids by means of dietary modifications. *J. Food Compos. Analysis* 62, 8–13. doi:10.1016/j.jfca.2017.04.008

Binic, I., Lazarevic, V., Ljubenovic, M., Mojsa, J., and Sokolovic, D. (2013). Skin ageing: Natural weapons and strategies. *Evidence-Based Complementary Altern. Med.* 2013, 827248. doi:10.1155/2013/827248

Botinestean, C., Hadaruga, N., Hadaruga, D., and Jianu, I. (2012). Fatty acids composition by gas chromatography-mass spectrometry (GC-MS) and most important physical-chemicals parameters of tomato seed oil. *J. Agroalimentary Process. Technol.* 18, 89–94.

Burger, P., Landreau, A., Azoulay, S., Michel, T., and Fernandez, X. (2016). Skin whitening cosmetics: Feedback and challenges in the development of natural skin lighteners. *Cosmetics* 3, 36. doi:10.3390/cosmetics3040036

Caligiani, A., Marseglia, A., Leni, G., Baldassarre, S., Maistrello, L., Dossena, A., et al. (2018). Composition of black soldier fly prepupae and systematic approaches for extraction and fractionation of proteins, lipids and chitin. *Food Res. Int.* 105, 812–820. doi:10.1016/j.foodres.2017.12.012

Caligiani, A., Marseglia, A., Sorci, A., Bonzanini, F., Lolli, V., Maistrello, L., et al. (2019). Influence of the killing method of the black soldier fly on its lipid composition. *Food Res. Int.* 116, 276–282. doi:10.1016/j.foodres.2018.08.033

Chao, K. L., Muthukumar, L., and Herzberg, O. (2007). Structure of human hyaluronidase-1, a hyaluronan hydrolyzing enzyme involved in tumor growth and angiogenesis. *Biochemistry* 46, 6911–6920. doi:10.1021/bi700382g

Da Silva Lucas, A. J., De Oliveira, L. M., Da Rocha, M., and Prentice, C. (2020). Edible insects: An alternative of nutritional, functional and bioactive compounds. *Food Chem.* 311, 126022. doi:10.1016/j.foodchem.2019.126022

Dayrit, F. M. (2015). The properties of lauric acid and their significance in coconut oil. *J. Am. Oil Chemists' Soc.* 92, 1–15. doi:10.1007/s11746-014-2562-7

De Pablo, P., Romaguera, D., Fisk, H. L., Calder, P. C., Quirke, A.-M., Cartwright, A. J., et al. (2018). High erythrocyte levels of the n-6 polyunsaturated fatty acid linoleic acid are associated with lower risk of subsequent rheumatoid arthritis in a southern European nested case–control study. *Ann. rheumatic Dis.* 77, 981–987. doi:10.1136/annrheumdis-2017-212274

Dipasquale, D., Basiricò, L., Morera, P., Primi, R., Tröscher, A., and Bernabucci, U. (2018). Anti-inflammatory effects of conjugated linoleic acid isomers and essential fatty acids in bovine mammary epithelial cells. *Animal* 12, 2108–2114. doi:10.1017/S1751731117003676

Diwakar, G., Rana, J., Saito, L., Vredeveld, D., Zemaitis, D., and Scholten, J. (2014). Inhibitory effect of a novel combination of Salvia hispanica (chia) seed and Punica granatum (pomegranate) fruit extracts on melanin production. *Fitoterapia* 97, 164–171. doi:10.1016/j.fitote.2014.05.021

Doert, M., Jaworska, K., Moersel, J.-T., and Kroh, L. W. (2012). Synergistic effect of lecithins for tocopherols: Lecithin-based regeneration of α-tocopherol. *Eur. Food Res. Technol.* 235, 915–928. doi:10.1007/s00217-012-1815-7

Dos Santos Aguilar, J. G. (2021). An overview of lipids from insects. *Biocatal. Agric. Biotechnol.* 33, 101967. doi:10.1016/j.bcab.2021.101967

Dos Santos, O. V., Dias, P. C. S., Soares, S. D., Da Conceição, L. R. V., and Teixeira-Costa, B. E. (2021). Artisanal oil obtained from insects' larvae (speciomerus ruficornis): Fatty acids composition, physicochemical, nutritional and antioxidant properties for application in food. *Eur. Food Res. Technol.* 247, 1803–1813. doi:10.1007/s00217-021-03752-8

Downer, R., and Matthews, J. (1976). Patterns of lipid distribution and utilisation in insects. *Am. Zoologist* 16, 733–745. doi:10.1093/icb/16.4.733

Driemeyer, H. (2016). *Evaluation of black soldier fly (*Hermetia illucens*) larvae as an alternative protein source in pig creep diets in relation to production, blood and manure microbiology parameters*. Stellenbosch: Stellenbosch University.

Duffy, E., Jacobs, M. R., Kirby, B., and Morrin, A. (2017). Probing skin physiology through the volatile footprint: Discriminating volatile emissions before and after acute barrier disruption. *Exp. Dermatol.* 26, 919–925. doi:10.1111/exd.13344

Ekpo, K., Onigbinde, A., and Asia, I. (2009). Pharmaceutical potentials of the oils of some popular insects consumed in southern Nigeria. *Afr. J. Pharm. Pharmacol.* 3, 51–57.

Elagbar, Z. A., Naik, R. R., Shakya, A. K., and Bardaweel, S. K. (2016). Fatty acids analysis, antioxidant and biological activity of fixed oil of Annona muricata L seeds. *J. Chem.* 2016, 1–6. doi:10.1155/2016/6948098

El-Agbar, Z. A., Naik, R. R., and Shakya, A. K. (2018). Fatty acids analysis and antioxidant activity of fixed oil of Quercus infectoria grown in Jordan. *Orient. J. Chem.* 34, 1368–1374. doi:10.13005/ojc/340324

Eruslanov, E., and Kusmartsev, S. (2010). "Identification of ROS using oxidized DCFDA and flow-cytometry," in *Advanced protocols in oxidative stress II*, 57–72.

Ewald, N., Vidakovic, A., Langeland, M., Kiessling, A., Sampels, S., and Lalander, C. (2020). Fatty acid composition of black soldier fly larvae (*Hermetia illucens*)–Possibilities and limitations for modification through diet. *Waste Manag.* 102, 40–47. doi:10.1016/j.wasman.2019.10.014

Farage, M. A., Miller, K. W., Elsner, P., and Maibach, H. I. (2008). Intrinsic and extrinsic factors in skin ageing: A review. *Int. J. Cosmet. Sci.* 30, 87–95. doi:10.1111/j.1468-2494.2007.00415.x

Feingold, K. R., and Elias, P. M. (2014). Role of lipids in the formation and maintenance of the cutaneous permeability barrier. *Biochimica Biophysica Acta (BBA)-Molecular Cell. Biol. Lipids* 1841, 280–294. doi:10.1016/j.bbalip.2013.11.007

Franco, A., Salvia, R., Scieuzo, C., Schmitt, E., Russo, A., and Falabella, P. (2021). Lipids from insects in cosmetics and for personal care products. *Insects* 13, 41. doi:10.3390/insects13010041

Girish, K. S., Kemparaju, K., Nagaraju, S., and Vishwanath, B. S. (2009). Hyaluronidase inhibitors: A biological and therapeutic perspective. *Curr. Med. Chem.* 16, 2261–2288. doi:10.2174/092986709788453078

He, Y., Hu, Y., Jiang, X., Chen, T., Ma, Y., Wu, S., et al. (2017). Cyanidin-3-O-glucoside inhibits the UVB-induced ROS/COX-2 pathway in HaCaT cells. *J. Photochem. Photobiol. B Biol.* 177, 24–31. doi:10.1016/j.jphotobiol.2017.10.006

Hehre, W. J., Ditchfield, R., Stewart, R. F., and Pople, J. A. (1970). Self-consistent molecular orbital methods. IV. Use of Gaussian expansions of slater-type orbitals. Extension to second-row molecules. *Ext. Second-Row Mol.* 52, 2769–2773. doi:10.1063/1.1673374

Henna Lu, F., Nielsen, N. S., Timm-Heinrich, M., and Jacobsen, C. (2011). Oxidative stability of marine phospholipids in the liposomal form and their applications. *Lipids* 46, 3–23. doi:10.1007/s11745-010-3496-y

Hoc, B., Francis, F., Carpentier, J., Mostade, L., Blecker, C., Purcaro, G., et al. (2021). ω3-enrichment of *Hermetia illucens* (L. 1758) prepupae from oilseed byproducts. *J. Saudi Soc. Agric. Sci.* 20, 155–163. doi:10.1016/j.jssas.2021.01.001

Horrobin, D. F. (2000). Essential fatty acid metabolism and its modification in atopic eczema. *Am. J. Clin. Nutr.* 71, 367S–372s. doi:10.1093/ajcn/71.1.367s

Huang, Z.-R., Lin, Y.-K., and Fang, J.-Y. (2009). Biological and pharmacological activities of squalene and related compounds: Potential uses in cosmetic dermatology. *Molecules* 14, 540–554. doi:10.3390/molecules14010540

Huang, T.-H., Wang, P.-W., Yang, S.-C., Chou, W.-L., and Fang, J.-Y. (2018). Cosmetic and therapeutic applications of fish oil's fatty acids on the skin. *Mar. drugs* 16, 256. doi:10.3390/md16080256

Huang, Z., Brennan, C., Zhao, H., Guan, W., Mohan, M. S., Stipkovits, L., et al. (2020). Milk phospholipid antioxidant activity and digestibility: Kinetics of fatty acids and choline release. *J. Funct. Foods* 68, 103865. doi:10.1016/j.jff.2020.103865

Hwang, H. J. (2010). Skin elasticity and sea polyphenols. *Seanol Sci. Cent. Rev.* 1, 17.

Ionescu, N., Ivopol, G.-C., Neagu, M., Popescu, M., and Meghea, A. (2015). Fatty acids and antioxidant activity in vegetable oils used in cosmetic formulations. *UPB Sci. Bull. Ser. B* 77.

Ivanova, S., Marinova, G., and Batchvarov, V. (2016). Comparison of fatty acid composition of various types of edible oils. *Bulg. J. Agric. Sci.* 22, 849–856.

Jadoon, S., Karim, S., Asad, M. H. H. B., Akram, M. R., Kalsoom Khan, A., Malik, A., et al. (2015). Anti-aging potential of phytoextract loaded-pharmaceutical creams for human skin cell longetivity. *Oxidative Med. Cell. Longev.* 2015, 709628. doi:10.1155/2015/709628

Joosten, L., Lecocq, A., Jensen, A. B., Haenen, O., Schmitt, E., and Eilenberg, J. (2020). Review of insect pathogen risks for the black soldier fly (*Hermetia illucens*) and guidelines for reliable production. *Entomologia Exp. Appl.* 168, 432–447. doi:10.1111/eea.12916

Jorge, A., Arroteia, K., Santos, I., Andres, E., Medina, S., Ferrari, C., et al. (2012). Schinus terebinthifolius R addi extract and linoleic acid from P assiflora edulis synergistically decrease melanin synthesis in B 16 cells and reconstituted epidermis. *Int. J. Cosmet. Sci.* 34, 435–440. doi:10.1111/j.1468-2494.2012.00736.x

Judde, A., Villeneuve, P., Rossignol-Castera, A., and Le Guillou, A. (2003). Antioxidant effect of soy lecithins on vegetable oil stability and their synergism with tocopherols. *J. Am. Oil Chemists' Soc.* 80, 1209–1215. doi:10.1007/s11746-003-0844-4

Kardash, E., and Tur'yan, Y. I. (2005). Acid value determination in vegetable oils by indirect titration in aqueous-alcohol media. *Croat. Chem. Acta* 78, 99–103.

Kiattisin, K., Nitthikan, N., Poomanee, W., Leelapornpisid, P., Viernstein, H., and Mueller, M. (2019). Anti-inflammatory, antioxidant activities and safety of coffea arabica leaf extract for alternative cosmetic ingredient. *Chiang Mai J. Sci.* 46, 284–294.

Kim, B., Bang, H. T., Kim, K. H., Kim, M. J., Jeong, J. Y., Chun, J. L., et al. (2020). Evaluation of black soldier fly larvae oil as a dietary fat source in broiler chicken diets. *J. Animal Sci. Technol.* 62, 187–197. doi:10.5187/jast.2020.62.2.187

Kim, C.-H., Ryu, J., Lee, J., Ko, K., Lee, J.-Y., Park, K. Y., et al. (2021). Use of black soldier fly larvae for food waste treatment and energy production in asian countries: A review. *Processes* 9, 161. doi:10.3390/pr9010161

Laothaweerungsawat, N., Sirithunyalug, J., and Chaiyana, W. (2020). Chemical compositions and anti-skin-ageing activities of Origanum vulgare L essential oil from tropical and mediterranean region. *Molecules* 25, 1101. doi:10.3390/molecules25051101

Lepage, G., and Roy, C. C. (1986). Direct transesterification of all classes of lipids in a one-step reaction. *J. lipid Res.* 27, 114–120. doi:10.1016/s0022-2275(20)38861-1

Li, X., Dong, Y., Sun, Q., Tan, X., You, C., Huang, Y., et al. (2022). Growth and fatty acid composition of black soldier fly *Hermetia illucens* (Diptera: Stratiomyidae) larvae are influenced by dietary fat sources and levels. *Animals* 12, 486. doi:10.3390/ani12040486

Lieberman, S., Enig, M. G., and Preuss, H. G. (2006). A review of monolaurin and lauric acid: Natural virucidal and bactericidal agents. *Altern. Complementary Ther.* 12, 310–314. doi:10.1089/act.2006.12.310

Limtrakul, P., Yodkeeree, S., Thippraphan, P., Punfa, W., and Srisomboon, J. (2016). Anti-aging and tyrosinase inhibition effects of Cassia fistula flower butanolic extract. *BMC Complementary Altern. Med.* 16, 497. doi:10.1186/s12906-016-1484-3

Lin, T.-K., Zhong, L., and Santiago, J. L. (2017). Anti-inflammatory and skin barrier repair effects of topical application of some plant oils. *Int. J. Mol. Sci.* 19, 70. doi:10.3390/ijms19010070

Mai, H. C., Dao, N. D., Lam, T. D., Nguyen, B. V., Nguyen, D. C., and Bach, L. G. (2019). Purification process, physicochemical properties, and fatty acid composition of black soldier fly (*Hermetia illucens Linnaeus*) larvae oil. *J. Am. Oil Chemists' Soc.* 96, 1303–1311. doi:10.1002/aocs.12263

Mapoung, S., Arjsri, P., Thippraphan, P., Semmarath, W., Yodkeeree, S., Chiewchanvit, S., et al. (2020). Photochemoprotective effects of Spirulina platensis extract against UVB irradiated human skin fibroblasts. *South Afr. J. Bot.* 130, 198–207. doi:10.1016/j.sajb.2020.01.001

Mariod, A. A. (2013). Insect oil and protein: Biochemistry, food and other uses: Review. *Agric. Sci.* 4, 76–80. doi:10.4236/as.2013.49b013

Mawazi, S. M., Ann, J., Othman, N., Khan, J., Alolayan, S. O., Al Thagfan, S. S., et al. (2022). A review of moisturizers; history, preparation, characterization and applications. *Cosmetics* 9, 61. doi:10.3390/cosmetics9030061

Morris, G. M., Huey, R., Lindstrom, W., Sanner, M. F., Belew, R. K., Goodsell, D. S., et al. (2009). AutoDock4 and AutoDockTools4: Automated docking with selective receptor flexibility. *J. Comput. Chem.* 30, 2785–2791. doi:10.1002/jcc.21256

Müller, A., Wolf, D., and Gutzeit, H. O. (2017). The black soldier fly, *Hermetia illucens*–a promising source for sustainable production of proteins, lipids and bioactive substances. *Z. für Naturforsch. C* 72, 351–363. doi:10.1515/znc-2017-0030

Orthoefer, F. T., and Eastman, J. (2005). Rice bran oil. *Bailey's industrial oil fat Prod.* 2, 465–489.

Papaemmanouil, C. D., Peña-García, J., Banegas-Luna, A. J., Kostagianni, A. D., Gerothanassis, I. P., Pérez-Sánchez, H., et al. (2022). ANTIAGE-DB: A database and server for the prediction of anti-aging compounds targeting elastase, hyaluronidase, and tyrosinase. *Hyaluronidase, Tyrosinase.* 11, 2268. doi:10.3390/antiox11112268

Pharmacopeia, T. U. S. (2017). *<401> fat and fixed oil*. Rockville, MD.

Poomanee, W., Wattananapakasem, I., Panjan, W., and Kiattisin, K. (2021). Optimizing anthocyanins extraction and the effect of cold plasma treatment on the anti-aging potential of purple glutinous rice (Oryza sativa L) extract. *Cereal Chem.* 98 (3), 571–582. doi:10.1002/cche.10399

Rabani, V., Cheatsazan, H., and Davani, S. (2019). Proteomics and lipidomics of black soldier fly (Diptera: Stratiomyidae) and blow fly (Diptera: Calliphoridae) larvae. *J. Insect Sci.* 19, 29. doi:10.1093/jisesa/iez050

Rahman, M., Islam, M., Biswas, M., and Khurshid Alam, A. (2015). *In vitro* antioxidant and free radical scavenging activity of different parts of Tabebuia pallida growing in Bangladesh. *BMC Res. notes* 8, 621–629. doi:10.1186/s13104-015-1618-6

Ravi, H. K., Vian, M. A., Tao, Y., Degrou, A., Costil, J., Trespeuch, C., et al. (2019). Alternative solvents for lipid extraction and their effect on protein quality in black soldier fly (*Hermetia illucens*) larvae. *J. Clean. Prod.* 238, 117861. doi:10.1016/j.jclepro.2019.117861

Riolo, K., Rotondo, A., La Torre, G. L., Marino, Y., Franco, G. A., Crupi, R., et al. (2023). Cytoprotective and antioxidant effects of hydrolysates from black soldier fly (*Hermetia illucens*). *Antioxidants* 12, 519. doi:10.3390/antiox12020519

Rungratanawanich, W., Abate, G., Serafini, M. M., Guarienti, M., Catanzaro, M., Marziano, M., et al. (2018). Characterization of the antioxidant effects of γ-oryzanol: Involvement of the Nrf2 pathway. *Oxid. Med. Cell. Longev.* 2018, 2987249. doi:10.1155/2018/2987249

Saffaryazdi, A., Ganjeali, A., Farhoosh, R., and Cheniany, M. (2020). Variation in phenolic compounds, α-linolenic acid and linoleic acid contents and antioxidant activity of purslane (Portulaca oleracea L.) during phenological growth stages. *Physiology Mol. Biol. Plants* 26, 1519–1529. doi:10.1007/s12298-020-00836-9

Saiki, P., Kawano, Y., Van Griensven, L. J., and Miyazaki, K. (2017). The anti-inflammatory effect of Agaricus brasiliensis is partly due to its linoleic acid content. *Food and Funct.* 8, 4150–4158. doi:10.1039/c7fo01172e

Schmitt, E., and De Vries, W. (2020). Potential benefits of using *Hermetia illucens* frass as a soil amendment on food production and for environmental impact reduction. *Curr. Opin. Green Sustain. Chem.* 25, 100335. doi:10.1016/j.cogsc.2020.03.005

Shigeta, Y., Imanaka, H., Ando, H., Ryu, A., Oku, N., Baba, N., et al. (2004). Skin whitening effect of linoleic acid is enhanced by liposomal formulations. *Biol. Pharm. Bull.* 27, 591–594. doi:10.1248/bpb.27.591

Suzuki, K., Terasaki, Y., and Uyeda, M. (2002). Inhibition of hyaluronidases and chondroitinases by fatty acids. *J. Enzyme Inhib. Med. Chem.* 17, 183–186. doi:10.1080/14756360290032930

Takenaka, A., Hosokawa, M., and Miyashita, K. (2007). Unsaturated phosphatidylethanolamine as effective synergist in combination with alpha-tocopherol. *J. Oleo Sci.* 56, 511–516. doi:10.5650/jos.56.511

Trott, O., and Olson, A. J. (2010). AutoDock Vina: Improving the speed and accuracy of docking with a new scoring function, efficient optimization, and multithreading. *J. Comput. Chem.* 31, 455–461. doi:10.1002/jcc.21334

Ushakova, N., Brodskii, E., Kovalenko, A., Bastrakov, A., Kozlova, A., and Pavlov, D. (2016). "Characteristics of lipid fractions of larvae of the black soldier fly *Hermetia illucens*," in *Doklady biochemistry and biophysics* (Springer), 209–212.

Verheyen, G. R., Ooms, T., Vogels, L., Vreysen, S., Bovy, A., Van Miert, S., et al. (2018). Insects as an alternative source for the production of fats for cosmetics. *J. Cosmet. Sci.* 69, 187–202.

Verheyen, G. R., Theunis, M., Vreysen, S., Naessens, T., Noyens, I., Ooms, T., et al. (2020). Glycine-acyl surfactants prepared from black soldier fly fat, coconut oil and palm kernel oil. *Curr. Green Chem.* 7, 239–248. doi:10.2174/2213346107999200424084626

Wang, Y.-S., and Shelomi, M. (2017). Review of black soldier fly (*Hermetia illucens*) as animal feed and human food. *Foods* 6, 91. doi:10.3390/foods6100091

Wolber, G., and Langer, T. J. (2005). LigandScout: 3-D pharmacophores derived from protein-bound ligands and their use as virtual screening filters. *J. Chem. Inf. Model.* 45, 160–169. doi:10.1021/ci049885e

Xu, Y., Zhang, J.-A., Xu, Y., Guo, S.-L., Wang, S., Wu, D., et al. (2015). Antiphotoaging effect of conditioned medium of dedifferentiated adipocytes on skin *in vivo* and *in vitro*: A mechanistic study. *Stem Cells Dev.* 24, 1096–1111. doi:10.1089/scd.2014.0321

Xu, X., Ji, H., Belghit, I., and Sun, J. (2020). Black soldier fly larvae as a better lipid source than yellow mealworm or silkworm oils for juvenile mirror carp (*Cyprinus carpio* var. specularis). *Aquaculture* 527, 735453. doi:10.1016/j.aquaculture.2020.735453

Yodkeeree, S., Thippraphan, P., Punfa, W., Srisomboon, J., and Limtrakul, P. (2018). Skin anti-aging assays of proanthocyanidin rich red rice extract, oryzanol and other phenolic compounds. *Nat. Product. Commun.* 13, 1934578X1801300. doi:10.1177/1934578x1801300812

Zhao, G., Etherton, T. D., Martin, K. R., Heuvel, J. P. V., Gillies, P. J., West, S. G., et al. (2005). Anti-inflammatory effects of polyunsaturated fatty acids in THP-1 cells. *Biochem. biophysical Res. Commun.* 336, 909–917. doi:10.1016/j.bbrc.2005.08.204

frontiers | Frontiers in Pharmacology

TYPE Original Research
PUBLISHED 04 October 2023
DOI 10.3389/fphar.2023.1213052

OPEN ACCESS

EDITED BY
Patrícia Mendonça Rijo,
Lusofona University, Portugal

REVIEWED BY
Irem I. Tatli,
Hacettepe University, Türkiye
Mohamed L. Ashour,
Ain Shams University, Egypt

*CORRESPONDENCE
Sabna Kotta,
skotta@kau.edu.sa
U. K. Ilyas,
dr.ilyasmcp@gmail.com

RECEIVED 27 April 2023
ACCEPTED 30 August 2023
PUBLISHED 04 October 2023

CITATION
Kamel FO, Karim S, Bafail DAO, Aldawsari HM, Kotta S and Ilyas UK (2023), Hepatoprotective effects of bioactive compounds from traditional herb Tulsi (*Ocimum sanctum* Linn) against galactosamine-induced hepatotoxicity in rats.
Front. Pharmacol. 14:1213052.
doi: 10.3389/fphar.2023.1213052

Hepatoprotective effects of bioactive compounds from traditional herb Tulsi (*Ocimum sanctum* Linn) against galactosamine-induced hepatotoxicity in rats

Fatemah O. Kamel[1], Shahid Karim[1], Duaa Abdullah Omer Bafail[1], Hibah Mubarak Aldawsari[2], Sabna Kotta[2]* and U. K. Ilyas[3]*

[1]Department of Clinical Pharmacology, Faculty of Medicine, King Abdulaziz University, Jeddah, Saudi Arabia, [2]Department of Pharmaceutics, Faculty of Pharmacy, King Abdulaziz University, Jeddah, Saudi Arabia, [3]Department of Pharmacognosy and Phytochemistry, Moulana College of Pharmacy, Perinthalmanna, Kerala, India

Ocimum sanctum L. (Tulsi; Family: libiaceae), also known as "The Queen of herbs" or "Holy Basil," is an omnipresent, multipurpose plant that has been used in folk medicine of many countries as a remedy against several pathological conditions, including anticancer, antidiabetic, cardio-protective, antispasmodic, diaphoretic, and adaptogenic actions. This study aims to assess *O. sanctum* L.'s hepatoprotective potential against galactosamine-induced toxicity, as well as investigate bioactive compounds in each extract and identify serum metabolites. The extraction of *O. sanctum* L as per Ayurveda was simultaneously standardized and quantified for biochemical markers: rutin, ellagic acid, kaempferol, caffeic acid, quercetin, and epicatechin by HPTLC. Hepatotoxicity was induced albino adult rats by intra-peritoneal injection of galactosamine (400 mg/kg). The quantified hydroalcoholic and alcoholic extract of *O. sanctum* L (100 and 200 mg/kg body weight/day) were compared for evaluation of hepatoprotective potential, which were assessed in terms of reduction in histological damage, change in serum enzymes such as AST, ALT, ALP and increase TBARS. Twenty chemical constituents of serum metabolites of *O. sanctum* were identified and characterized based on matching recorded mass spectra by GC-MS with those obtained from the library-Wiley/NIST. We evaluated the hepatoprotective activity of various fractions of hydroalcoholic extracts based on the polarity and investigated the activity at each phase (hexane, chloroform, and ethyl acetate) *in vitro* to determine how they affected the toxicity of CCL4 (40 mM) toward Chang liver cells. The ethyl acetate fraction of the selected plants had a higher hepatoprotective activity than the other fractions, so it was used in vacuum liquid chromatography (VLC). The ethyl acetate fraction contains high amounts of rutin (0.34% w/w), ellagic acid (2.32% w/w), kaempferol (0.017% w/w), caffeic acid (0.005% w/w), quercetin (0.038% w/w), and epicatechin (0.057% w/w) which are responsible for hepatoprotection. In comparison to standard silymarin, isolated bioactive molecules displayed the most significant hepatoprotective activity in Chang liver cells treated to CCl4 toxicity. The significant high hepatoprotection provided by standard silymarin ranged from 77.6% at 100 µg/ml to 83.95% at 200 µg/ml, purified ellagic acid ranged from 70% at

100 μg/ml to 81.33% at 200 μg/ml, purified rutin ranged from 63.4% at 100 μg/ml to 76.34% at 200 μg/ml purified quercetin ranged from 54.33% at 100 μg/ml to 60.64% at 200 μg/ml, purified epicatechin ranged from 53.22% at 100 μg/ml to 65.6% at 200 μg/ml, and purified kaempferol ranged from 52.17% at 100 μg/ml to 60.34% at 200 μg/ml. These findings suggest that the bioactive compounds in *O. sanctum* L. have significant protective effects against galactosamine-induced hepatotoxicity.

KEYWORDS

***Ocimum sanctum* Linn, galactosamine-induced rat model, hepatoprotective activity, polyphenols, serum biomarkers**

1 Introduction

Humans relied on medicinal plants for their healing properties centuries before the introduction of chemical medicines. The WHO estimates that around 80% of the people in less developed countries rely exclusively on herbal medicines for their primary healthcare. Medicinal plants serve as the backbone of traditional medicines, and nearly 3.3 billion people regularly utilize plants for therapeutic purposes in less developed countries (Davidson-Hunt, 2000). Medicinal plants are a substantial source of hepatoprotective medications. One estimate places the number of mono- and poly-herbal formulations used for treating different liver problems at over 700 in decoction, tincture, and tablets (Ilyas et al., 2016). The earliest Indian medical system, Ayurveda, has designated numerous plants for the treatment of hepatotoxicity. Given that plants have been employed as medicines for a variety of ailments and with the arrival of current synthetic medicines and their accessibility to consistent dosage forms, usage ease, and therapeutic efficiency in acute circumstances, the usage of medicinal plants has declined (Pandey et al., 2013). Traditional medications have a limited range of action and require long-term administration to be effective, working mostly on chronic illnesses, as opposed to synthetic drugs, which have a restricted spectrum of action and accompanying adverse effects (Fair and Tor, 2014). Numerous plant-based medications have been discovered to have hepatoprotective properties, including *Trigonella foenum graecum* belongs to the family Fabaceae (Zargar, 2014), *Andrographis paniculata* (Family: Acanthaceae) (Nagalekshmi et al., 2011), *Phyllanthus niruri* L. (Family: Phyllanthaceae), *Tephrosia purpurea* L. (Fabaceae), *Boerhavia diffusa* L (Nyctaginaceae) and *A. paniculata* (Family: Acanthaceae) (Dey et al., 2020), *Phyllanthus maderaspatensis* L. (Family: Phyllanthaceae) (Ilyas et al., 2015) and *Fumaria indica* L (Family: Papaveraceae) (Rathi et al., 2008). Jaundice and hepatitis are serious liver diseases with high fatality rates. An infection called hepatitis damages and inflames the liver. Swelling caused by inflammation occurs when bodily tissues are harmed or infected. Hepatitis is often classified as acute or chronic based on how long the liver has been inflamed and damaged (Schaefer and John, 2021). The five fundamental categories of viruses are categories A to E. Due to the weight of illness and mortality, these are of paramount importance. The problem may self-limit (heal on its own) or it may worsen, leading to cirrhosis and fibrosis (Eming et al., 2017). Aside from alcohol, drugs, chlorinated solvents, herbal remedies, chlorinated solvents, peroxidized fatty acids, industrial pollutants, radioactive isotope intoxication, and fungal toxins, other xenobiotics that can cause hepatic problems include parasite and viral infections, autoimmune diseases, and radio-active isotopes. In particular, types A and C induce chronic illness and are the main factors in liver cirrhosis and cancer, respectively (Ilyas et al., 2016). Only a few uncommon allopathic hepatoprotective medications are currently available for the treatment of liver disorders. Plant extracts are therefore frequently used to treat liver problems. India's semi-tropical and tropical regions are home to *Ocimum sanctum* Linn. Ayurveda and Siddha traditions have historically used various components of the plant to treat a variety of illnesses, including infections, skin problems, and hepatic abnormalities, and as an antidote for snake and scorpion stings. This plant's leaves have long been utilized for their anti-inflammatory, gastroprotective, and hepatoprotective effects (Kamyab and Eshraghian, 2013), anti-plasmodial, neuroprotective, and chemo-preventive properties (Bhattacharyya and Bishayee, 2013; Rajendran et al., 2014; Mataram et al., 2021). The plant is also effective against human pancreatic cancer, stress-induced anxiety, stress-induced oxidative and central monoaminergic changes, typhoid fever, and cerebral ischemia/reperfusion (Ahmad et al., 2012a; Ahmad et al., 2012b; Mandal et al., 2012; Shimizu et al., 2013; Singh et al., 2016). In COVID-19, Tulasi has been found to possess SARS-CoV-2 protease inhibition, lipid-lowering and antioxidant, anxiety and depression (Chatterjee et al., 2011; Suanarunsawat et al., 2011; Shree et al., 2020). This plant also contains a high concentration of polyphenolic chemicals, which have a variety of biological activities such as antiviral, antibacterial, vasodilatory, antioxidant, anti-inflammatory, and antiradical properties (Prochazkova et al., 2011), memory improvement (Spencer, 2009), gastroprotection (Mota et al., 2009), antioxidation, anti-inflammation, cardiovascular protection (Garcia-Lafuente et al., 2009), chemopreventive activity (Mohan et al., 2013) and regulate immune responses (Magrone et al., 2008). Previous research found that these plants possessed a high concentration of flavonoids, which are naturally occurring phenolic phytochemicals that have been linked to a variety of biological functions (Hollman and Katan, 1999), flavonoid glycoside is as a multi potent bioflavonoid with great potential for the prevention and treatment of disease, kaempferol glycosides is antinociceptive and anti-inflammatory (De Melo et al., 2009), anti-tyrosinase activity (Rho et al., 2010). Previously, metabolic profiling was used for a better understanding of the chemical diversity of medicinal plants. This information can be used to make comparisons with other studied taxonomically related plants and

to infer their bioactivity. Chromatography coupled with mass spectrometry is the most widely used technology for analyzing samples in extremely complex matrices, such as plant extracts (Jorge et al., 2016). Both morphologically and functionally, the galactosamine-induced experimental model system in rats is known to resemble viral hepatitis in people. Because hepatocytes have significant quantities of galactokinase and galactose-1-uridylyltransferase, galactos-amine has a greater liver selectivity than other hazardous groups, such as acetaminophen, paracetamol, and carbon tetrachloride. Hepatotoxicity, substantial portal and parenchymal infiltration, and patchy hepatocyte necrosis are all induced by galactosamine (Ilyas et al., 2015). By boosting the creation of UDP-sugar derivatives, galactosamine also causes the depletion of uridine diphosphate (UDP), which inhibits the synthesis of RNA and proteins and, in turn, deteriorates cell membranes. Chattopadhyay et al. (1992) and Jain (2015) revealed that only crude extracts are responsible for activity but did not isolate active ingredients. We identified, evaluated and isolated the most active bioactive molecules responsible for hepatoprotection in this study. The plan of the study was focused on bioactivity guided fractionation, *O. sanctum* (ethyl acetate) fractions showed significant hepatoprotective activity (cell induced with carbon tetrachloride 40 mM) as compared with other fractions, which led to the further separation of ethyl acetate fraction by vacuum Liquid chromatography and followed by the quantitative chemo profiling of the potent fraction. The chemical constituents were potent activity responsible for hepatoprotective activity will be identified and validated. A single newly developed solvent system formic acid, ethyl acetate, and toluene (1:4:5) was used for the densitometric quantification of bioactive compounds by HPTLC in aqueous alcoholic extracts with reference to respective marker compounds such as ellagic acid, rutin, kaempferol, quercetin, caffeic acid, and epicatechin in *O. sanctum*. The purpose of this study was to use GC-MS in order to investigate the metabolic profile of the hexane of the serum metabolites of *O. sanctum* and to investigate potent bioactive compounds obtained from *O. sanctum* for their hepatoprotective activity.

2 Material and methods

2.1 Reagents and chemicals

We bought reference standards from Natural Remedies Pvt. Ltd., including rutin, kaempferol, quercetin, epicatechin, caffeic acid, and catechin (Bangalore, India). We bought ALT, AST, and ALP kits from Span Diagnostics Ltd. in Surat, India. The supplier of galactosamine was SRL in Mumbai, India. Analytical-grade chemicals were employed throughout. As mobile phases for a HPTLC analysis, formic acid, ethyl acetate, toluene, and methanol (CDH Labs, Mumbai, India) were utilized. A 0.22 µm syringe-driven filter was utilized to filter all the solutions for the analysis (HIMEDIA, Mumbai, India).

2.2 Extract preparation

Fresh plant material was taken from the Maruthmallai region of Kanyakumari district, Tamilnadu, India. It was identified and authenticated by Dr. V. Chelladurai, Research Officer, Central Council for Research in Ayurveda and Siddha (Govt. of India), Tirunelveli, Tamil Nadu, India. A voucher specimen has been stored in our laboratory for future reference. Plant materials were extracted using 95% alcohol for 6 h at 37°C and an aqueous-alcoholic solvent (50%) for 5 h at 38°C. The extraction process was carried out three times. The mixed extracts were collected and dried in a rotary evaporator at 40°C under decreased pressure.

2.3 Animals experimental design

The Central Animal House facility (Registration No. 173/CPLSEA/837) provided adult Wistar rats weighing 150–200 g. The animals were fed a typical rodent diet and given access to water as needed while being kept in regular laboratory conditions (12 h light/dark cycles at 25°C with humidity levels between 45% and 65%). The animals were divided into eight groups ($n = 6$) at random. Group I acted as the vehicle control and was given regular saline for a period of 7 days. In addition to receiving normal saline (1 ml/kg, p.o.) for 7 days, Group II acted as the toxic control group. Groups III to VIII received a prophylactic treatment of a hydroalcoholic and alcoholic extract of *O. sanctum* in carbon methyl cellulose (0.1%) at various concentrations (100 and 200 mg/kg b.w.p.o) for 7 days. Silymarin (40 mg/kg, p.o.) was administered to Group VIII for 7 days. The current study evaluated the dose of *O. sanctum* extracts based on prior research studies conducted by Chattopadhyay et al. (1992). On the eighth day, 400 mg/kg ip of galactosamine was administered to Groups II to VIII to cause liver damage (Raish et al., 2016).

2.3.1 Evaluation of liver function

After giving galactosamine for 24 h, blood was drawn from the retro-orbital plexus while the groups were lightly sedated with ether (Van Herck et al., 2001). All of the groups were sacrificed immediately following blood collection. Samples of the liver were obtained for histopathological and biochemical analyses. At 37°C, serum was centrifuged to separate it, and it was then used to measure various biochemical characteristics. Using a motor-driven Teflon pestle, 10% (w/v) liver homogenates were produced in an ice-cold 0.15 M KCl solution after the liver samples were rinsed with chilled normal saline and weighed (AlSaid et al., 2015). Additional biochemical parameters, including the determination of aspartate amino transaminase (AST), alanine amino transaminase (ALT), and alkaline phosphatase (ALP), were estimated using the serum (Patlolla et al., 2011). The liver homogenate's supernatant was used to measure antioxidant enzymes, such as catalase (CAT) and superoxide dismutase (SOD), using a colorimetric technique (Weydert and Cullen, 2010). The DTNB method was used to calculate glutathione (GSDH), and a modified approach was used to calculate TBARS, an index of lipid peroxidation (Liu et al., 2020). The quickly excised liver tissues were stored in neutral buffered formalin. According to Badawi's instructions, liver slices were created for histological investigations (Badawi, 2019).

2.4 GC-MS analysis of metabolic serum

An analysis was performed on the chemical makeup of the metabolic serum. Gas chromatography (GC-MS) was used to

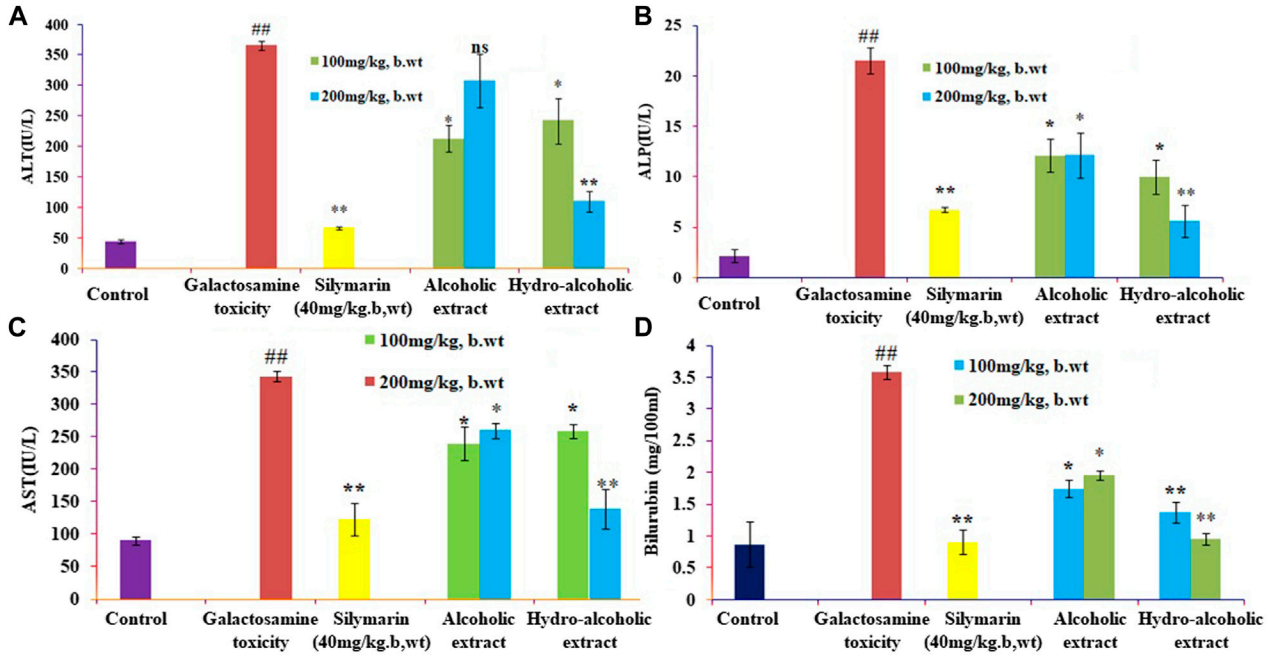

FIGURE 1
Effects of alcoholic and hydroalcoholic extracts (at two different doses of 100 and 200 mg/kg body weight, administered orally for 7 days) and standard silymarin on biochemical parameters such as ALT or alanine aminotransferase **(A)**, ALP or Alkaline phosphatase **(B)**, ASTor aspartate aminotransferase **(C)**, and bilirubin **(D)** of liver on oxidative stress induced by galactosamine. GalN was administered intraperitoneally on the eighth day as a pretreatment. Each value represents means ± standard error of the mean. ns $p > 0.05$ (non-significant), *$p < 0.05$ (significant), **$p < 0.01$ (more significant).

characterize 20 active compounds. The Agilent 7890AGC system was connected to a 5975C inert XL EI/CI MSD mass spectroscopic system, which was outfitted with a 30 m × 250 µm × 0.25 µm HP-5MS capillary column. A CTCCombiPAL injector was used, and the injection volume was 2.0 L. With a helium flow rate of 1.0 ml·min^{-1}, the inlet temperature was maintained at 270°C. Programmatically, the column's temperature was increased from 60°C to 300°C at a rate of 5°C per minute for a total run period of 40 min in SCAN mode.

2.4.1 Preparation of sample

The serum of the *O. sanctum* extract (5 ml) was extracted with acetonitrile (3 × 100). The combined acetonitrile layer was evaporated to dryness under reduced pressure at 40°C in a rotary evaporator to obtain a residue. The residue was dissolved in LC-MS-grade methanol, filtered through a 0.22 µm syringe, and injected into GC-MS.

2.5 Densitometric quantification of bioactive compounds in ethyl acetate fraction using HPTLC

2.5.1 Sample preparations

The aqueous ethanolic extract of *O. sanctum* was dissolved in 10% distilled water and was successively fractionated thrice with hexane (3 × 600 mL), chloroform (3 × 600 mL), ethyl acetate (3 × 500 mL), and water-soluble fractions. The combined fractions of *O. sanctum* were evaporated to dryness under reduced pressure at 40°C in a rotary evaporator. 100 mg of ethyl acetate fraction were accurately weighed, dissolved in 10 mL of HPLC grade methanol, sonicated for 10 min, and then made up with 10 mL of methanol. After filtering the solution, a 0.22 µm syringe was used to inject it into the HPTLC system.

2.5.2 Preparation of standard solutions

The standard solution was made by dissolving precisely weighed 10.0 mg of rutin, kaempferol, quercetin, ellagic acid, and epicatechin in 10.0 mL of methanol HPLC grade as stock solution and storing it at 4°C. These standards were further diluted to achieve the desired concentration for quantification.

2.5.3 Preparation of the plate

Prior to usage, pre-coated silica gel 60 F254 aluminium HPTLC plates (Merck, Germany) were washed in methanol and dried. The standard solution of bioactive compounds and samples were applied on an HPTLC plate in the form of bands of 4 mm width using a Linomat V applicator (Muttenz, Switzerland) with a 100 µL syringe. The application rate was kept constant at 200 nL·s^{-1}, and the space between the two bands was 9 mm.

2.5.4 Calibration curve of bioactive compounds

Standard concentrations of rutin (10–1,600 ng/band), epicatechin (100–5,000 ng/band), ellagic acid (20–200 ng/band), kaempferol (40–200 ng/band), quercetin (10–160 ng/band) were applied in triplicate on silica-gel 60 F254 plates using a CAMAG Linomat-5 Automatic Sample Spotter. The plates were developed in formic acid, ethyl acetate, and toluene (1:4:5 v/v/v) solvent in a CAMAG glass twin-trough chamber (20 cm × 100 cm) up to a distance of 8 cm. After development, the plates were dried in air and scanned at 366 nm using a CAMAG TLC Scanner 3 and Win CATS

4 software. The peak areas were recorded. Calibration curves for bioactive compounds were created by plotting peak areas versus applied ethyl acetate fractions conaining rutin, epicatechin, ellagic acid, kaempferol, quercetin respectively.

2.6 Separation and purification of bioactive compounds

The ethyl acetate fraction has been shown to have a strong hepatoprotective impact in comparison to other fractions. To separate the various components contained in the fraction, vacuum liquid chromatography (VLC) was used on this fraction. Dry slurry was made by mixing a small amount of Silica gel G (Merck) with 15 g of ethyl acetate, and this slurry was then placed onto a sintered glass funnel with Silica gel G as the stationary phase. The column was eluted with solvents of increasing polarity step-by-step under a vacuum, starting with a blend of pure toluene and ethyl acetate and finishing with pure ethyl acetate. To further clarify, the toluene levels were decreased when the ethyl acetate component was increased after initially eluting with 5% ethyl acetate in toluene. The ethyl acetate component was then increased by 5% increments up to 50% and then by 10% increments up to 100% ethyl acetate. The methanol content was increased in 5% steps after elution with ethyl acetate, elution with 5% methanol in ethyl acetate, and elution with 100% methanol. The solvents were eluted until they ran clear from the funnel. Throughout the experiment, a steady flow rate of the solvent (100 ml/min) was observed. Individual fractions were collected, and their homogeneity was checked using TLC. The same R_f values from similar fractions were merged and crystallized.

2.7 HPTLC study of column eluents of ethyl acetate fraction

The fractions obtained from the VLC were analyzed by using HPTLC, and fractions with a similar profile were combined. Aliquots of these fractions were reconstituted in methanol and subjected to an HPTLC study. Small quantities of dried eluents were dissolved in about 1 ml of HPLC-grade methanol. The sample was sprayed onto a plate at a distance of 0.8 cm from one end of the plate in the form of a narrow band using the spray-on technique with the help of a Linomate-V applicator attached to a CAMAG HPTLC system that was programmed using win-CATS software, which was included with the apparatus. Following the application of the spot, a chromatogram was generated using several solvent systems in a twin-trough chamber (20 cm × 25 cm) that had previously been saturated with a formic acid, ethyl acetate, and toluene combination (1:4:5 v/v/v). The air-dried plate was viewed under the different wavelengths of UV light and visible light. The spots were scanned using Reprostar 3; the TLC scanner 3 was designed for the densitometric evaluation of plates.

2.8 Hepatoprotective assay of fractions, bioactive compounds, and column eluents of ethyl acetate fraction

Cells were plated in 96-well plates at a density of 1×10^6 cells/well and allowed to grow there overnight. After 24 h, the medium was removed, the cells were given different quantities of treatment of each sample (100 and 200 µg/ml), and they were then incubated for 2 h in separate wells of a 96-well plate. As a benchmark, silymarin (100 and 200 µg/ml) was used. CCl4 was applied to the cell and incubated with it for 2 h. Following incubation, the cells were washed, and each well received 20 µL of MTT (5 mg/ml of MTT in PBS) for 1 h. After 2 h, a microscope was used to witness the formation of a formazan crystal. An additional hour of incubation was added if the crystal formation was not accurate. Following the removal of the medium, the leftover formazan crystals in each well were dissolved in 200 µL of DMSO. The cell culture plate was shaken for 15 min, while the absorbance was measured at 540 nm using an ELISA reader.

The following formula was used to calculate the percentage of the hepatoprotection of the polyphenols, fractions, column eluents, and silymarin:

$$\text{Percentage Hepatoprotection} = \left(\frac{\text{OD of Test sample}}{\text{OD of Control}}\right) \text{X } 100 \quad (1)$$

2.9 Statistic evaluation

The results are given as mean S.E.M. Dunnett's *post hoc* test was used after a one-way analysis of variance (ANOVA) to estimate the total variation present in a data set. $p < 0.01$ was regarded as statistically significant.

3 Results and discussion

3.1 Effect of different extracts of *O. sanctum* on biochemical parameters in rats

The present study showed that analyzed biochemical markers, which included AST, ALT, ALP, and TBARS Figures 1A–D respectively, were found to be considerably higher in galactosamine-treated rat compared to the normal control group ($p < 0.01$) There was also a substantial drop in SOD, CAT, and glutathione Figures 2A–C respectively levels in the tissue ($p > 0.05$). Hydroalcoholic extract was found to be more effective than ethanolic extracts. Figures 1, 2 shows the effect of alcoholic, hydroalcoholic and silymarin pretreatment on biochemical parameters of galactosamine-intoxicated rats. Previous study, only *O. sanctum* extract has been reported to have hepatoprotective activity against paracetamol-induced liver damage in Albino rats (Lahon and Das, 2011). The hepatoprotective and antioxidant activities of the crude fractions of the endophytic fungi of *O. sanctum* in rats were reported by Shukla et al. (2012) revealed that only crude extracts are responsible for activity but did not isolate active ingredients. Present investigation, the hepatoprotection may be attributable to numerous bioactive active moieties discovered in high concentrations in the hydroalcoholic extract of *O. sanctum*. Such moieties include bioactive compounds were simultaneously quantified using HPTLC. Bioactive active moieties act as potent free radical scavenging ability of hydroalcoholic extract provides

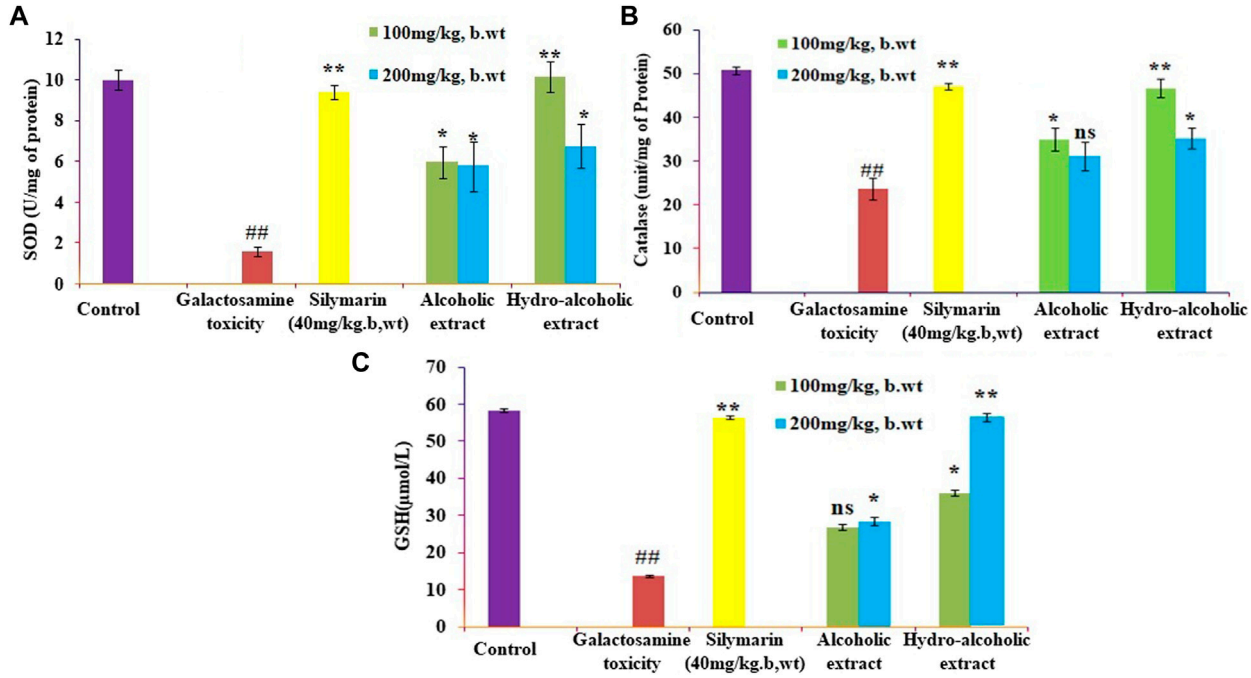

FIGURE 2
Effects of alcoholic and hydroalcoholic extracts (at two different doses of 100 and 200 mg/kg body weight, administered orally for 7 days) and standard silymarin on antioxidant parameters such as SOD or Superoxide dismutase **(A)**, GSH or Glutathione **(B)**, and CAT or catalase **(C)** of the liver on oxidative stress induced by galactosamine. GalN was administered intraperitoneally on the eighth day as a pretreatment. Each value represents means ± standard error of the mean. ns $p > 0.05$ (non-significant), *$p < 0.05$ (significant), **$p < 0.01$ (more significant).

evidence for the role of tannins and flavonoids as potential secondary metabolite responsible for hepatoprotection (Li et al., 2018). Their action may be mediated by preventing liver injury by stopping the development of lipid peroxides and inhibiting oxidative mechanisms that contribute to hepatocyte degeneration (Cichoż-Lach and Michalak, 2014).

3.2 Histopathological observation

Following histology, the normal control animals' livers had a well-defined central vein, a well-preserved cytoplasm, and a conspicuous nucleus and nucleolus. The galactosamine-treated animals' liver sections revealed severely toxic liver cells that had necrotic liver cells, focal hemorrhages in the periportal region, inflammatory cell collection, and distributed inflammation throughout the liver parenchyma. The hepatic cells with a well-preserved cytoplasm revealed that the *O. sanctum* hydroalcoholic extracts appeared to be more significant than the other extracts for the avoidance of galactosamine toxicity. Silymarin also defended against the hepatic alterations induced by galactosamine. Further, the hepatotoxic galactosamine-treated rats' liver sections underwent a histological analysis, which revealed a clear inflammatory cell infiltration around the portal triad. In the periportal region, it was found that there were necrotic liver cells and localized bleeding. However, the absence of necrosis and the development of normal hepatic cells in the liver sections of the rats given silymarin and the alcoholic and hydroalcoholic extracts of *O. sanctum* in various groups indicated signals of protection at a significant level. Figure 3 shows a histopathologic segment of liver (400X) stained with hematoxylin and eosin to reveal the cell nucleus and cytoplasm with extracellular matrix in purple blue and pink colours, respectively.

3.3 Metabolic fingerprinting of faded extract serum by GC-MS

The immunomodulatory activity of crude extract in the previous investigation by Bochu et al. (2005) was not significantly affected; however, crude extract metabolites exhibited higher immunomodulatory action than crude extract. In the current investigation, a thorough analysis was done with reference to Bochuet et al. Rat feeding trials were done with various quantities of aqueous-alcoholic (50%) extracts of chosen medicinal plants (100 and 200 mg/kg, b/w). The serum metabolites were initially analyzed using HPTLC. No distinct separation/peak was observed, which indicated that the serum was a mixture of compounds. Subsequently, the serum was analyzed using GC-MS. The serum metabolites from the extract-fed rats were identified using GC-MS, which were found to be fatty and aliphatic compounds. The process of identifying bioactive components was based on comparing the recorded mass spectra to those received from the Wiley/NIST collection. Metabolite serum, which is described in Table 1, characterized 20 different components in total. A literature review revealed that the discovered serum metabolites had no significant impact on hepatoprotective activity, thus we concentrated primarily on the ethyl acetate fraction, which

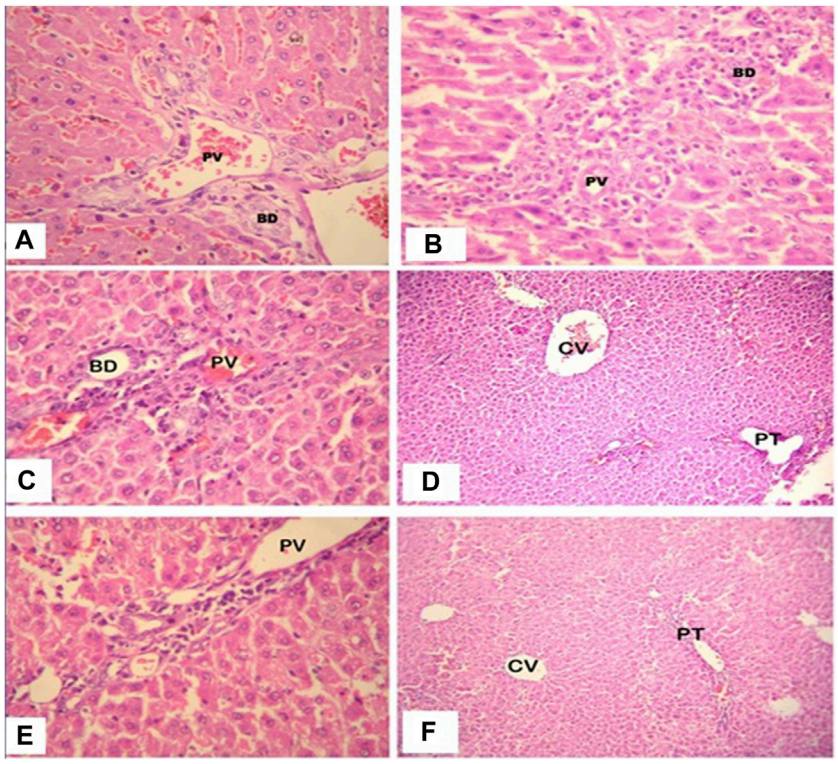

FIGURE 3
High power photomicrograph (400x) of liver section, the control group **(A)** shows normal hepatic architecture; in the galactosamine-induced necrotic liver cells and focal hemorrhages **(B)**; in the alcoholic extracts plus galactosamine **(C,D)**, there is moderate inflammatory cell infiltration; and in the hydroalcoholic extracts plus galactosamine **(E,F)**, there is only mild inflammatory cell infiltration.

contained the most significant bioactive molecule for hepatoprotection.

3.4 HPTLC quantification of bioactive compounds in ethyl acetate fraction

3.4.1 Development of the perfect mobile phase

For the simultaneous estimation of bioactive compounds, different proportions of toluene, ethyl acetate such as toluene/ethyl acetate (3:0 v/v), toluene/ethyl acetate (5:5 v/v), toluene/ethyl acetate (7:3 v/v), toluene/ethyl acetate/methanol (7:2.8:0.2 v/v/v), toluene/ethyl acetate/formic acid (7:2.5:0.5 v/v/v) and toluene/ethyl acetate/formic acid (5:4:1 v/v/v) were evaluated as the solvent systems for the development of a suitable band. All investigated solvent systems were developed under chamber saturation conditions. From the obtained results, it was observed that the solvent systems toluene/ethyl acetate (3:7 v/v), toluene/ethyl acetate (5:5 v/v), toluene/ethyl acetate (7:3 v/v), toluene/ethyl acetate/methanol (7:2.8:0.2 v/v/v), toluene/ethyl acetate/formic acid (7:2.5:0.5 v/v/v) offered the poor densitometry peaks of bioactive compounds with tailing factor. However, when the toluene/ethyl acetate/formic acid (5:4:1v/v/v) was studied, it was observed that this solvent system offered a well-separated and intact chromatographic peak of rutin at R_f = 0.08, ellagic acid at R_f = 0.55, quercetin at R_f = 0.62, kaempferol at R_f = 0.67 and epicatechin at R_f = 0.57 respectively. The typical band of the bioactive compounds and ethyl acetate fraction of *O. sanctum* was scanned at 254 nm (Figure 4). Vasilisa et al. (2020) also established the mobile phase mixture of diethyl ether, formic acid, acetic acid, water, acetophenone and heptane (30:3:9:50:30:10) (v/v/v/v/v/v) (Pedan et al., 2020). Ilyas et al. (2015) reported a solvent mixture of toluene: ethyl acetate, formic acid and methanol (3:3:0.8:0.2) (v/v/v/v) respectively, for simultaneous quantification of bioactive compounds (Ilyas et al., 2015). Bioactive compounds are naturally occurring substances with the potential to protect the liver from damage and act as antioxidants (Kamyab and Eshraghian, 2013; Saha et al., 2019). The hepatoprotective and antioxidant potential of bioactive compounds may be due to their capability to normalize impaired membrane function (De Oliveira e Silva et al., 2012).

3.5 Hepatoprotective activity of fractionated extracts of *O. sanctum*

Harsha et al. (2020) investigated cytotoxicity assay of *O. sanctum* extract on leukemic cell lines: A preliminary *in-vitro* study. We are looking into the cytotoxicity of extracts against Chang liver cells. Drugs concentrations ranging from 100 to 1000 μg/ml were used to evaluate the percentage growth inhibition of the drugs on cell lines. The drug sample exhibited a CTC50 value greater than 1000 μg/ml (concentration required to inhibit viability by 50%). We assessed the hepatoprotective activity of several *O. sanctum* fractions based on polarity and studied the activity in each phase (hexane, chloroform, and ethyl acetate) as well as against CCl4-induced hepatotoxicity. The

TABLE 1 Identification of serum metabolites of crude extract by GC-MS.

	R.T.	Area	Compound name		R.T.	Area	Compound name
1	11.733	0.65	1-tetradecene	21	25.176	1.83	Linoleic-9-Octadecyne
2	14.397	7.16	2,4-Di-tert-butylphenol	22	25.255	3.47	trans-13-Octadecenoic acid
3	14.681	0.86	Benzoic acid, 4-ethoxy-, ethyl ester	23	25.587	2.65	Octadecanoic acid
4	15.854	3.01	1-Hexadecene	24	25.926	0.72	Docosyl acetate
5	18.379	0.45	Methyl tetradecanoate	25	26.953	1.31	Methyl arachidonate
6	19.116	1.54	Tetradecanoic acid	26	27.617	0.41	2-Monoolein
7	19.545	3.08	1-Octadecene	27	29.079	0.5	N-Allylphthalimide
8	20.965	0.83	Butyl octyl phthalate	28	29.394	0.27	Cis-4-methyl-exo-tricyclo[5.2.1.0(2.6)]decane
9	21.744	0.52	Dibutyl phthalate	29	30.33	2.06	1-Monopalmitin
10	21.835	6.17	Hexadecanoic acid	30	32.904	1.1	1-Monostearin
11	21.938	0.34	2-Hexyl-3,5-dinotrobenzonitrile	31	33.2	7.66	1-Benzylidene-5,6-butano-7-azaindane
12	22.198	1.53	3,8-Di-tert-butyl-1,10-phenanthroline	32	33.6	1.15	16,17-bis(trimethylsilyloxy)androsta-1,4-diene-3-methyloxime
13	22.53	15.56	Elaol	33	34.1	0.79	Phthalic acid, isopropyl pentyl ester
14	22.729	0.3	l-(+)-Ascorbic acid 2,6-dihexadecanoate	34	34.2	0.44	Bis(7-methyloctyl) phthalate
15	22.88	2.59	Tetradecyl heptafluorobutyrate	35	34.4	0.57	Phthalic acid, butyl isopropyl ester
16	24.028	0.6	Butyl phthalate	36	34.7	0.37	Phthalic acid, neopentyl 2-propyl ester
17	24.518	1.73	Linoleic acid methyl ester	37	36.5	0.73	Propenocarbachlorin
18	24.602	2.95	Elaidic acid methyl ester	38	37.5	16.7	Cholest-5-en-3-ol (3.beta.)
19	24.693	0.76	Methyl elaidate	39	38.0	0.92	Perhydro-htx-2-one, 2-dependylacetate ester
20	24.983	3.24	Methyl stearate				

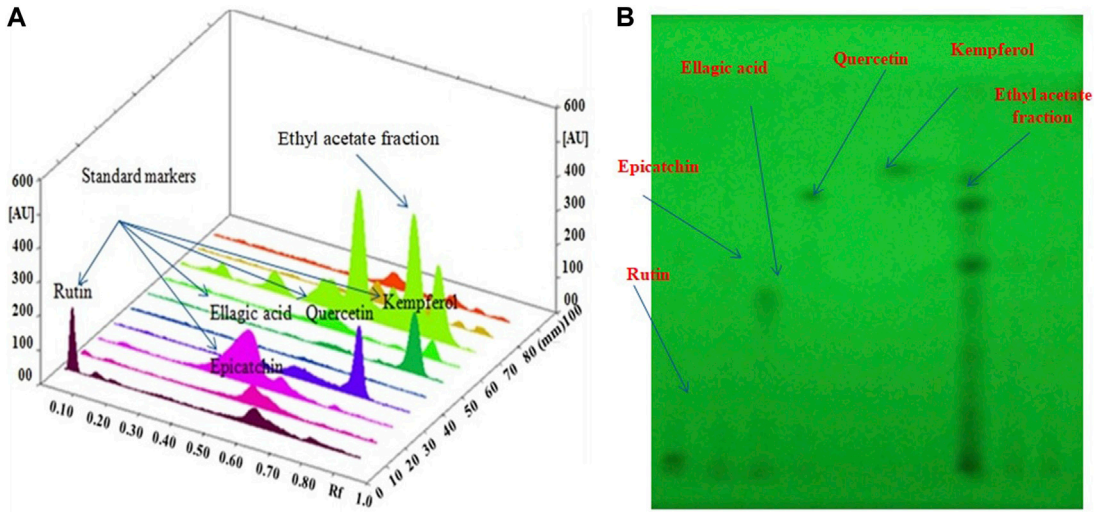

FIGURE 4
(A): 3D image of all tracks at 254 nm demonstrating that the ethyl acetate fraction had bioactive compound; **(B)**: HPTLC Chromatogram of the ethyl acetate fraction contained bioactive compound at 254 nm in the solvent system: a combination mixture of formic acid: ethyl acetate:toluene (1:4:5 v/v/v).

CCl4 treatment of Chang liver cells resulted in a considerable drop in cell viability. When compared to the other fractions, treatment with the ethyl acetate soluble fractions showed more significant dose-dependent protection against cell damage brought on by CCl4 exposure. The results are presented using the formula mean standard error mean (S.E.M.). Figure 5 shows the percentage of protection graphically.

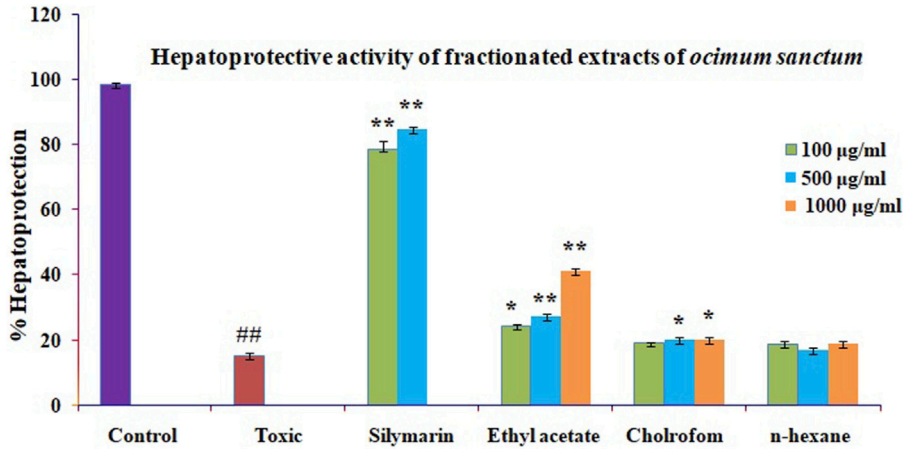

FIGURE 5
Effect of different fractions on toxicity caused by GlaN in Chang liver cells. Before being treated with GalN (40 mM) for 2 h, Chang liver cells were first incubated for 2 h in the presence or absence of extracts and their metabolites. The cells were then prepared for the MTT experiment. The findings are presented as mean S.E.M. Compared to the GalN (40 mM) control, ns $p > 0.05$, $^{**}p < 0.01$, and $^{*}p < 0.05$ are significant.

TABLE 2 Solvent combinations and R_f value of column eluents of ethyl acetate fraction of *O. sanctum*.

Tracks	Solvent combination	R_f	Tracks	Solvent combination	R_f
01	Gallic acid	**0.52**	20	Toluene + 25% ethyl acetate-1	**0.62**
02	Ellagic acid	**0.55**	21	Toluene + 25% ethyl acetate-2	0.52, 0.63, 0.74
03	Kaempferol	**0.81**	22	Toluene + 25% ethyl acetate-3	0.54
04	Quercetin	**0.73**	23	Toluene + 50% ethyl acetate-1	0.34, 0.43, 0.58, 0.77
05	Rutin	**0.08**	24	Toluene + 50% ethyl acetate-2	0.31, 0.45, 0.54,0.63
06	Epicatechin	**0.50**	25	Toluene + 50% ethyl acetate-3	0.31, 9.37, 0.45, 0.48, 0.54, 0.57, 0.62, 0.68, 0.73
07	Catechin	**0.54**	26	Toluene + 50% ethyl acetate-4	0.31, 0.38, 0.43, 0.57, 0.71
09	Caffeic acid	**0.63**	28	Toluene + 75% ethyl acetate-1	0.09, 0.32, **0.50**, **0.57**
10	Ursolic acid	Nil	29	Toluene + 75% ethyl acetate-2	0.81
11	100%Toluene-1	0.81	30	Toluene + 75% ethyl acetate-3	0.1, 0.18, **0.23**, 0.28, 0.38, 0.55
12	100% Toluene-2	0.76	31	100% ethyl acetate	0.08, **0.53**
13	10%Toluene-	**0.67**	32	5%methanol + ethyl acetate	—
14	10%Toluene-2	0.68, 0.76	33	15%methanol + ethyl acetate	—
15	Toluene + 10% ethyl acetate	0.77, 0.61	34	25% methanol + ethyl acetate-1	0.10, 0.30, 0.48, **0.52**, 0.61
16	Toluene + 10% ethyl acetate	0.61, 0.69, 0.78	35	25%methanol + ethyl acetate-2	0.06
17	Toluene + 10% ethyl acetate	0.73	36	25%methanol + ethyl acetate-3	0.32, 0.63
18	Toluene + 10% ethyl acetate	0.73	37	25%methanol + ethyl acetate-4	—
19	Toluene + 20% ethyl acetate	0.73, 0.81	38	50%methanol + ethyl acetate-	**0.63**

The following were used to identify the standards (1–10): Track No. 31 (100 percent ethyl acetate elute) was connected to ellagic acid (RF, value: 0.53); Track No. 13 (10% ethyl acetate in toluene) was connected to kaempferol (RF, value: 0.67); Track No. 20 (25% ethyl acetate in toluene elute) and quercetin (Rf value: 0.62) were identified; Track No. 28 (75% ethyl acetate in toluene elute) was paired with epicatechin (RF, value: 0.57); and rutin corresponded to Track No. 5 (Toluene + 50% ethyl acetate-2, elute), with an Rf value of 0.08.
Rf value was shown by bold values. Ethyl acetate fraction contained active substances and standard biomarkers were matched.

3.6 Vacuum liquid chromatography of potent ethyl acetate fraction

The ethyl acetate fraction of *O. sanctum* was used to perform vacuum liquid chromatography, yielding twenty-eight column eluents. HPTLC was used to evaluate these column eluents in order to identify bioactive compound from the ethyl acetate fraction of *O. sanctum* (Table 2). The different components contained in the eluents were detected by spraying with NP reagents and then comparing the Rf value to the standards

(Gallic acid, ellagic acid, Kaemferol, quercetin, rutin, epicatechin, ursolic acid and catechin). These bioactive compounds are responsible for a variety of biological functions, including anticancer (Horcajada-Molteni et al., 2000), anti-oxidant (Afanas'ev et al., 1995), chemopreventive (Araujo et al., 2011), and immunosuppressive (Yu et al., 2011). We selected the most powerful bioactive molecule for hepatoprotection in the current investigation and subsequently isolated active moieties.

3.7 Hepatoprotective activity of column eluents of ethyl acetate fractions

The hepatoprotective activity of the ten ethyl acetate column eluents previously mentioned against CCL4-induced cytotoxicity was examined by pre-incubating the cells with or without the ethyl acetate fractions or silymarin. The Chang liver cells exposed to CCl4 saw a significant reduction in cell viability. The mean standard error means (S.E.M.) formula was used to present the results. The proportion of protection is graphically shown in Figure 6. The elute from the ethyl acetate (100%) column showed that ellagic acid has significant hepatoprotective effects, followed by 75% ethyl acetate elutes (catechin and epicatechin), 50% ethyl acetate (rutin), 25% ethyl acetate (quercetin and kaempferol), and 25% methanol (caffeic acid), when compared with standard silymarin.

3.8 Hepatoprotective activity of isolated polyphenols

The mentioned bioactive compounds were examined for hepatoprotective effectiveness against CCl4-induced cytotoxicity by pre-incubating the cells with or without the silymarin or extracts. The Chang liver cells' viability significantly decreased after CCL4 therapy. The results are displayed using the mean standard error mean formula (S.E.M.). The significant high hepatoprotection provided by standard silymarin ranged from 77.6% at 100 µg/ml to 83.95% at 200 µg/ml, purified ellagic acid ranged from 70% at 100 µg/ml to 81.33% at 200 µg/ml, purified rutin ranged from 63.4% at 100 µg/ml to 76.34% at 200 µg/ml purified quercetin ranged from 54.33% at 100 µg/ml to 60.64% at 200 µg/ml, purified catechin ranged from 53.22% at 100 µg/ml to 65.6% at 200 µg/ml, and purified kaempferol ranged from 52.17% at 100 µg/ml to 60.34% at 200 µg/ml, as shown in Figure 7.

4 Conclusion

The recommended HPTLC method is unique, as it documents the first time that bioactive compounds in *O. sanctum* (Linn) were identified and quantified using a single solvent system. Feeding experiments were carried out with various concentrations (100 and 200 mg/kg, b w) of alcoholic and aqueous–alcoholic extracts (50%) of selected medicinal plants, and the identification of serum metabolites from the extract-fed rats was carried out using GC-MS. It might be concluded that the metabolites of the serum extract contain a lot of fatty and aliphatic compounds not responsible for hepatoprotective activity. The impact of pretreatment with the alcoholic and hydroalcoholic extracts of *O. sanctum* and silymarin on the biochemical parameters of the rats' given galactosamine intoxication was examined. According to the findings, the hydroalcoholic extract had a greater hepatoprotective effect than the alcoholic extracts. The hydroalcoholic extract was fractionated into petroleum ether, ethyl acetate, chloroform, and water based on polarity. *O.*

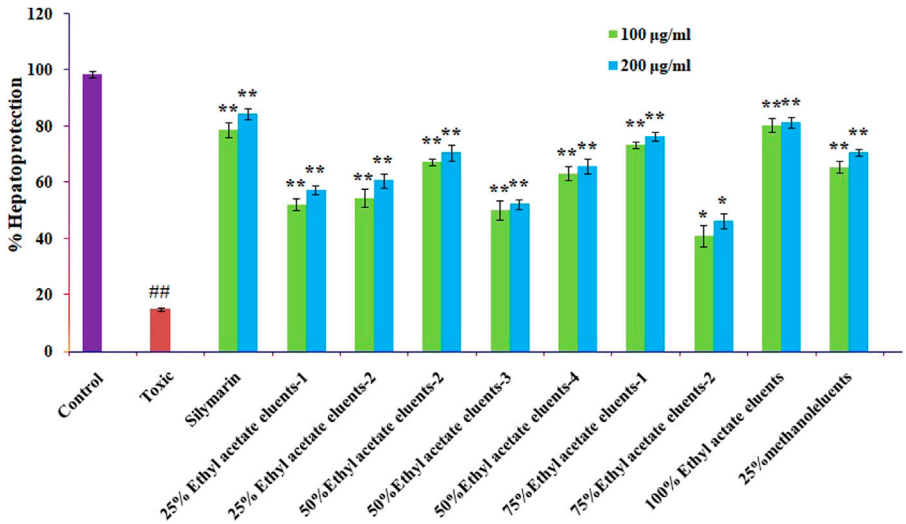

FIGURE 6
Effect of different columns eluting *O. sanctum's* ethyl acetate on CCl4-induced toxicity in Chang liver cells. Prior to being treated with CCl4 for 2 h, Chang liver cells were cultured for 2 h in the presence or absence of various columns elutes of *O. sanctum's* ethyl acetate. The cells were then prepared for the MTT experiment. The findings are presented as mean S.E.M. Compared to the CCL4 control, ns $p > 0.05$, $^{**}p < 0.01$, and $^{*}p < 0.05$ are significant.

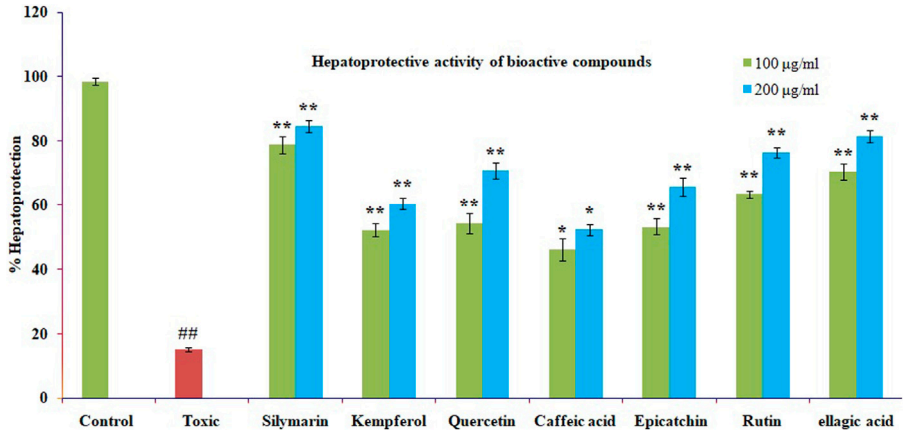

FIGURE 7
The impact of several isolated bioactive compounds on CCl4-induced toxicity in Chang liver cells. Chang liver cells were treated with CCl4 for 2 h after being cultured for 2 h with various substances in either their presence or absence. The cells were then prepared for the MTT experiment. In comparison to the CCl4 control, the data are expressed as mean S.E.M. with ns $p > 0.05$, $^{**}p < 0.01$, and $^{*}p < 0.05$ being significant.

sanctum's ethyl acetate fraction had more hepatoprotective effects than the other fractions. Hence, it was concluded that ethyl acetate is the best fraction for vacuum liquid chromatography. Our research reveals that bioactive compounds extracted from *O. sanctum* provide significant protective benefits against hepatotoxicity caused by galactosamine. This might be a result of the antioxidant and membrane-stabilizing properties of these chemicals. The results show that it is a source of structurally unique bioactive compounds, which may offer possibilities for the creation of novel semi-synthetic molecules for more current indications.

Data availability statement

The original contributions presented in the study are included in the article/Supplementary Material, further inquiries can be directed to the corresponding authors.

Ethics statement

The animal study was approved by the Jamia Hamdard, Hamdard University, New Delhi, India. The study was conducted in accordance with the local legislation and institutional requirements.

Author contributions

FK: Formal analysis, software, investigation, writing—reviewing. ShK: Software, investigation, writing—reviewing and editing; DB and HA: Investigation, reviewing and editing. SaK: Project administration, reviewing, and funding acquisition. UI: Conceptualization, methodology, supervision, writing—original draft preparation, writing—reviewing and editing. All authors contributed to the article and approved the submitted version.

Funding

This research work was funded by the institutional Fund Projects under Grant No. (IFPIP: 738-249-1443). The authors gratefully acknowledge the technical and financial support provided by the Ministry of Education and King Abdulziz University, DSR, Jeddah, Saudi Arabia.

Conflict of interest

The authors declare that the research was conducted in the absence of any commercial or financial relationships that could be construed as a potential conflict of interest.

Publisher's note

References

Afanas'ev, I. B., Ostrachovitch, E. A., Abramova, N. E., and Korkina, L. G. (1995). Different antioxidant activities of bioflavonoid rutin in normal and iron-overloading rats. *Biochem. Pharmacol.* 50, 627–635. doi:10.1016/0006-2952(95)00173-w

Ahmad, A., Rasheed, N., Chand, K., Maurya, R., Banu, N., and Palit, G. (2012a). Restraint stress-induced central monoaminergic & oxidative changes in rats & their prevention by novel *Ocimum sanctum* compounds. *Indian J. Med. Res.* 135, 548–554.

Ahmad, A., Khan, M. M., Raza, S. S., Javed, H., Ashafaq, M., Islam, F., et al. (2012b). *Ocimum sanctum* attenuates oxidative damage and neurological deficits following focal cerebral ischemia/reperfusion injury in rats. *Neurol. Sci.* 33, 1239–1247. doi:10.1007/s10072-012-0940-1

AlSaid, M., Mothana, R., Raish, M., Al-Sohaibani, M., Al-Yahya, M., Ahmad, A., et al. (2015). Evaluation of the effectiveness of Piper cubeba extract in the amelioration of CCl4-induced liver injuries and oxidative damage in the rodent model. *Biomed. Res. Int.* 2015, 359358. doi:10.1155/2015/359358

Araujo, J. R., Goncalves, P., and Martel, F. (2011). Chemopreventive effect of dietary polyphenols in colorectal cancer cell lines. *Nutr. Res.* 31, 77–87. doi:10.1016/j.nutres.2011.01.006

Badawi, M. S. (2019). Histological study of the protective role of ginger on piroxicam-induced liver toxicity in mice. *J. Chin. Med. Assoc.* 82, 11–18. doi:10.1016/j.jcma.2018.06.006

Bhattacharyya, P., and Bishayee, A. (2013). *Ocimum sanctum* Linn. (Tulsi): An ethnomedicinal plant for the prevention and treatment of cancer. *Anticancer Drugs* 7, 659–666. doi:10.1097/CAD.0b013e328361aca1

Bochu, W., Liancai, Z., and Qi, C. (2005). Primary study on the application of Serum Pharmacology in Chinese traditional medicine. Colloids Surf. B Biointerfaces. 43, 194–197. doi:10.1016/j.colsurfb.2005.04.013

Chatterjee, M., Verma, P., Maurya, R., and Palit, G. (2011). Evaluation of ethanol leaf extract of *Ocimum sanctum* in experimental models of anxiety and depression. *Pharm. Biol.* 49, 477–483. doi:10.3109/13880209.2010.523832

Chattopadhyay, R. R., Sarkar, S. K., Ganguly, S., Medda, C., and Basu, T. K. (1992). Hepatoprotective activity of *Ocimum sanctum* leaf extract against paracetamol included hepatic damage in rats. *Indian J. Pharmacol.* 24, 163–165.

Cichoż-Lach, H., and Michalak, A. (2014). Oxidative stress as a crucial factor in liver diseases. *World J. Gastroenterol.* 20 (25), 8082–8091. doi:10.3748/wjg.v20.i25.8082

Davidson-Hunt, I. (2000). Ecological ethnobotany: Stumbling toward new practices and paradigms. *MASA J.* 16, 1–13.

De Melo, G. O., Malvar Ddo, C., Vanderlinde, F. A., Rocha, F. F., Pires, P. A., Costa, E. A., et al. (2009). Antinociceptive and anti-inflammatory kaempferol glycosides from Sedum dendroideum. *J. Ethnopharmacol.* 124, 228–232. doi:10.1016/j.jep.2009.04.024

De Oliveira e Silva, A. M., Vidal-Novoa, A., Batista-González, A. E., Pinto, J. R., Portari Mancini, D. A., Reina-Urquijo, W., et al. (2012). *In vivo* and *in vitro* antioxidant activity and hepatoprotective properties of bioactive compounds from *Halimeda opuntia* (Linnaeus). *Redox Rep.* 17, 47–53. doi:10.1179/1351000212Y.0000000003

Dey, D., Chaskar, S., Bhatt, N., and Chitre, D. (2020). Hepatoprotective activity of BV-7310, a proprietary herbal formulation of *Phyllanthus niruri,Tephrosia purpurea, boerhaviadiffusa, and Andrographis paniculata,* in alcohol-induced HepG2 cells and alcohol plus a haloalkane, CCl4, induced liver damage in rats. *BMC Complement. Altern. Med.* 2020, 6428906–6428909. doi:10.1155/2020/6428906

Eming, S. A., Wynn, T. A., and Martin, P. (2017). Inflammation and metabolism in tissue repair and regeneration. *Science* 356, 1026–1030. doi:10.1126/science.aam7928

Fair, R. J., and Tor, Y. (2014). Antibiotics and bacterial resistance in the 21st century. *Perspect. Med. Chem.* 6, 25–64. doi:10.4137/PMC.S14459

Garcia-Lafuente, A., Guillamon, E., Villares, A., Rostagno, M. A., and Martinez, J. A. (2009). Flavonoids as anti-inflammatory agents: Implications in cancer and cardiovascular disease. *Inflamm. Res. official J. Eur. Histamine Res. Soc.* 58, 537–552. doi:10.1007/s00011-009-0037-3

Harsha, M., Mohan Kumar, K. P., Kagathur, S., and Amberkar, V. S. (2020). Effect of *Ocimum sanctum* extract on leukemic cell lines: A preliminary *in-vitro* study. *J. Oral Maxillofac. Pathol.* 24 (1), 93–98. doi:10.4103/jomfp.JOMFP_181_19

Hollman, P. C., and Katan, M. B. (1999). Health effects and bioavailability of dietary flavonols. *Free Radic. Res.* 31, S75–S80. doi:10.1080/10715769900301351

Horcajada-Molteni, M. N., Crespy, V., Coxam, V., Davicco, M. J., Remesy, C., and Barlet, J. P. (2000). Rutin inhibits ovariectomy-induced osteopenia in rats. *J. Bone Min. Res.* 15, 2251–2258. doi:10.1359/jbmr.2000.15.11.2251

Ilyas, U., Katare, D. P., Aeri, V., and Naseef, P. P. (2016). A review on hepatoprotective and immunomodulatory herbal plants. *Pharmacogn. Rev.* 10, 66–70. doi:10.4103/0973-7847.176544

Ilyas, U. K., Katare, D. P., and Aeri, V. (2015). Comparative evaluation of standardized alcoholic, hydroalcoholic, and aqueous extracts of *Phyllanthus maderaspatensis* Linn. against galactosamine-induced hepatopathy in albino rats. Pharmacogn. Mag. 11, 277–282. doi:10.4103/0973-1296.153079

Jain, A. N. U. R. A. G. (2015). To evaluate hepatoprotective activity of leaves of *Ocimum sanctum* using animal model. *Asian J. Pharm. Clin. Res.* 8 (4), 255–258.

Jorge, T. F., Mata, A. T., and António, C. (2016). Mass spectrometry as a quantitative tool in plant metabolomics. *Philos. Trans. A Math. Phys. Eng. Sci.* 28, 20150370. doi:10.1098/rsta.2015.0370

Kamyab, A. A., and Eshraghian, A. (2013b). Anti-inflammatory, gastrointestinal and hepatoprotective effects of *Ocimum sanctum* Linn: An ancient remedy with new application. *Inflamm. Allergy Drug Targets* 12, 378–384. doi:10.2174/1871528112666131125110017

Kamyab, A. A., and Eshraghian, A. (2013a). Anti-inflammatory, gastrointestinal and hepatoprotective effects of *Ocimum sanctum Linn*: An ancient remedy with new application. *Inflamm. &allergy drug targets* 12, 378–384. doi:10.2174/1871528112666131125110017

Lahon, K., and Das, S. (2011). Hepatoprotective activity of *Ocimum sanctum* alcoholic leaf extract against paracetamol-induced liver damage in Albino rats. *Pharmacogn. Res.* 3 (1), 13–18. doi:10.4103/0974-8490.79110

Li, S., Tan, H. Y., Wang, N., Cheung, F., Hong, M., and Feng, Y. (2018). The potential and action mechanism of polyphenols in the treatment of liver diseases. *Oxid. Med. Cell Longev.* 2018, 8394818. doi:10.1155/2018/8394818

Liu, C., Cai, Y., Wang, J., Liu, X., Ren, H., Yan, L., et al. (2020). Facile preparation of homogeneous copper nanoclusters exhibiting excellent tetraenzyme mimetic activities for colorimetric glutathione sensing and fluorimetric ascorbic acid sensing. *ACS Appl. Mat. Interfaces.* 23, 42521–42530. doi:10.1021/acsami.0c11983

Magrone, T., Candore, G., Caruso, C., Jirillo, E., and Covelli, V. (2008). Polyphenols from red wine modulate immune responsiveness: Biological and clinical significance. *Curr. Pharm. Des.* 14, 2733–2748. doi:10.2174/138161208786264098

Mandal, S., Mandal, M. D., and Pal, N. K. (2012). Enhancing chloramphenicol and trimethoprim *in vitro* activity by *Ocimum sanctum* Linn. (Lamiaceae) leaf extract against *Salmonella enterica* serovar Typhi. *Asian pac. J. Trop. Med.* 5, 220–224. doi:10.1016/S1995-7645(12)60028-5

Mataram, M. B. A., Hening, P., Harjanti, F. N., Karnati, S., Wasityastuti, W., Nugrahaningsih, D. A. A., et al. (2021). The neuroprotective effect of ethanolic extract *Ocimum sanctum* Linn. in the regulation of neuronal density in hippocampus areas as a central autobiography memory on the rat model of Alzheimer's disease. *J. Chem.Neuroanat.* 111, 101885–102111. doi:10.1016/j.jchemneu.2020.101885

Mohan, A., Narayanan, S., Sethuraman, S., and Krishnan, U. M. (2013). Combinations of plant polyphenols & anti-cancer molecules: A novel treatment strategy for cancer chemotherapy. *Anti-cancer agents Med. Chem.* 13, 281–295. doi:10.2174/1871520611313020015

Mota, K. S., Dias, G. E., Pinto, M. E., Luiz-Ferreira, A., Souza-Brito, A. R., Hiruma-Lima, C. A., et al. (2009). Flavonoids with gastroprotective activity. *Mol. (Basel, Switz.* 14, 979–1012. doi:10.3390/molecules14030979

Nagalekshmi, R., Menon, A., Chandrasekharan, D. K., and Nair, C. K. (2011). Hepatoprotective activity of Andrographis paniculata and Swertia chirayita. *Food Chem. Toxicol.* 49 (12), 3367–3373. doi:10.1016/j.fct.2011.09.026

Pandey, M. M., Rastogi., S., and Rawat, A. K. S. (2013). Indian traditional Ayurvedic system of medicine and nutritional supplementation. *Evid.based Complement. Altern. Med.* 12, 1–12. doi:10.1155/2013/376327

Patlolla, A. K., Berry, A., and Tchounwou, P. B. (2011). Study of hepatotoxicity and oxidative stress in male Swiss-Webster mice exposed to functionalized multi-walled carbon nanotubes. *Mol. Cell Biochem.* 358 (1-2), 189–199. doi:10.1007/s11010-011-0934-y

Pedan, V., Stamm, E., Do, T., Holinger, M., and Reich, E. (2020). HPTLC fingerprint profile analysis of coffee polyphenols during different roast trials. *J. Food Compos.* 94, 103610. doi:10.1016/j.jfca.2020.103610

Prochazkova, D., Bousova, I., and Wilhelmova, N. (2011). Antioxidant and prooxidant properties of flavonoids. *Fitoterapia* 82, 513–523. doi:10.1016/j.fitote.2011.01.018

Raish, M., Ahmad, A., Alkharfy, K. M., Ahamad, S. R., Mohsin, K., Al-Jenoobi, F. I., et al. (2016). Hepatoprotective activity of Lepidium sativum seeds against D-galactosamine/lipopolysaccharide induced hepatotoxicity in animal model. *BMC Complement. Altern. Med.* 16 (1), 501. doi:10.1186/s12906-016-1483-4

Rajendran, C., Begam, M., Kumar, D., Baruah, I., Gogoi, H. K., Srivastava, R. B., et al. (2014). Antiplasmodial activity of certain medicinal plants against chloroquine resistant *Plasmodium berghei* infected white albino BALB/c mice. *J.Parasit. Dis.* 38, 148–152. doi:10.1007/s12639-013-0252-2

Rathi, A., Srivastava, A. K., Shirwaikar, A., Singh Rawat, A. K., and Mehrotra, S. (2008). Hepatoprotective potential of *Fumaria indica Pugsley* whole plant extracts, fractions and an isolated alkaloid protopine. *Phytomedicine* 15 (6-7), 470–477. doi:10.1016/j.phymed.2007.11.010

Rho, H. S., Ahn, S. M., Lee, B. C., Kim, M. K., Ghimeray, A. K., Jin, C. W., et al. (2010). Changes in flavonoid content and tyrosinase inhibitory activity in kenaf leaf extract after far-infrared treatment. *Bioorg. Med. Chem. Lett.* 20, 7534–7536. doi:10.1016/j.bmcl.2010.09.082

Saha, P., Talukdar, A. D., Nath, R., Sarker, S. D., Nahar, L., Sahu, J., et al. (2019). Role of natural phenolics in hepatoprotection: A mechanistic review and analysis of regulatory network of associated genes. *Front. Pharmacol.* 10, 509. doi:10.3389/fphar.2019.00509

Schaefer, T. J., and John, S. (2021). "Acute hepatitis," in *StatPearls treasure island* (Petersburg, FL, United States: StatPearls Publishing), 400–410.

Shimizu, T., Torres, M. P., Chakraborty, S., Souchek, J. J., Rachagani, S., Kaur, S., et al. (2013). Holy Basil leaf extract decreases tumorigenicity and metastasis of aggressive human pancreatic cancer cells *in vitro* and *in vivo*: Potential role in therapy. *Cancer Lett.* 336, 270–280. doi:10.1016/j.canlet.2013.03.017

Shree, P., Mishra, P., Selvaraj, C., Singh, S. K., Chaube, R., Garg, N., et al. (2020). Targeting COVID-19 (SARS-CoV-2) main protease through active phytochemicals of ayurvedic medicinal plants -*Withaniasomnifera*(Ashwagandha),*Tinospora cordifolia*(Giloy) and *Ocimum sanctum*(Tulsi) - a molecular docking study. *J. Biomol. Struct.Dyn.* 27, 190–203. doi:10.1080/07391102.2020.1810778

Shukla, S. T., Kulkarni, V. H., Habbu, P. V., Jagadeesh, K. S., Patil, B. S., and Smita, D. M. (2012). Hepatoprotective and antioxidant activities of crude fractions of endophytic fungi of *Ocimum sanctum* Linn. in rats. *Orient Pharm. Exp. Med.* 12 (2), 81–91. doi:10.1007/s13596-012-0061-7

Singh, V., Kahol, A., Singh, I. P., Saraf, I., and Shri, R. (2016). Evaluation of anti-amnesic effect of extracts of selected *Ocimum* species using *in-vitro* and *in-vivo* models. *J. Ethnopharmacol.* 193, 490–499. doi:10.1016/j.jep.2016.10.026

Spencer, J. P. (2009). The impact of flavonoids on memory: Physiological and molecular considerations. *Chem. Soc. Rev.* 38, 1152–1161. doi:10.1039/b800422f

Suanarunsawat, T., Ayutthaya, W. D., Songsak, T., Thirawarapan, S., and Poungshompoo, S. (2011). Lipid-lowering and antioxidative activities of aqueous extracts of *Ocimum sanctum* L. leaves in rats fed with a high-cholesterol diet. *Oxid. Med. Cell.longev.* 12, 962025–962965. doi:10.1155/2011/962025

Van Herck, H., Baumans, V., Brandt, C. J., Boere, H. A., Hesp, A. P., van Lith, H. A., et al. (2001). Blood sampling from the retro-orbital plexus, the saphenous vein and the tail vein in rats: Comparative effects on selected behavioural and blood variables. *Lab. Anim.* 35 (2), 131–139. doi:10.1258/0023677011911499

Weydert, C. J., and Cullen, J. J. (2010). Measurement of superoxide dismutase, catalase and glutathione peroxidase in cultured cells and tissue. *Nat. Protoc.* 5 (1), 51–66. doi:10.1038/nprot.2009.197

Yu, C. P., Wu, P. P., Hou, Y. C., Lin, S. P., Tsai, S. Y., Chen, C. T., et al. (2011). Quercetin and rutin reduced the bioavailability of cyclosporine from Neoral, an immunosuppressant, through activating P-glycoprotein and CYP 3A4. *J. Agric. Food Chem.* 59, 4644–4648. doi:10.1021/jf104786t

Zargar, S. (2014). Protective effect of Trigonella foenum-graecum on thioacetamide induced hepatotoxicity in rats. *Saudi J. Biol. Sci.* 21 (2), 139–145. doi:10.1016/j.sjbs.2013.09.002

frontiers | Frontiers in Pharmacology

TYPE Original Research
PUBLISHED 08 November 2023
DOI 10.3389/fphar.2023.1298049

OPEN ACCESS

EDITED BY
Emel Timucin,
Acıbadem University, Türkiye

REVIEWED BY
Shahid Karim,
King Abdulaziz University, Saudi Arabia
Andrey Stoyanov Marchev,
Bulgarian Academy of Sciences, Bulgaria

*CORRESPONDENCE
Guilin Chen,
glchen@wbgcas.cn
Mingquan Guo,
guomingquan@nimte.ac.cn
Guangwan Hu,
guangwanhu@wbgcas.cn

†PRESENT ADDRESSES
Cixi Institute of Biomedical Engineering, Ningbo Institute of Materials Technology and Engineering, Chinese Academy of Sciences, Ningbo, China

RECEIVED 21 September 2023
ACCEPTED 30 October 2023
PUBLISHED 08 November 2023

CITATION
Liang C, Xu Y, Fan M, Muema FW, Chen G, Guo M and Hu G (2023), Potential antioxidative and anti-hyperuricemic components in *Rodgersia podophylla* A. Gray revealed by bio-affinity ultrafiltration with SOD and XOD. *Front. Pharmacol.* 14:1298049. doi: 10.3389/fphar.2023.1298049

Potential antioxidative and anti-hyperuricemic components in *Rodgersia podophylla* A. Gray revealed by bio-affinity ultrafiltration with SOD and XOD

Can Liang[1,2], Yongbing Xu[1,2], Minxia Fan[1,2,3], Felix Wambua Muema[1,2,3], Guilin Chen[1,2,3,4]*, Mingquan Guo[1,2]*† and Guangwan Hu[1,2,3,4]*

[1]Key Laboratory of Plant Germplasm Enhancement and Specialty Agriculture, Wuhan Botanical Garden, Chinese Academy of Sciences, Wuhan, China, [2]University of Chinese Academy of Sciences, Beijing, China, [3]Sino-Africa Joint Research Center, Chinese Academy of Sciences, Wuhan, China, [4]Hubei Jiangxia Laboratory, Wuhan, China

Rodgersia podophylla A. Gray (*R. podophylla*) is a traditional Chinese medicine with various pharmacological effects. However, its antioxidant and anti-hyperuricemia components and mechanisms of action have not been explored yet. In this study, we first assessed the antioxidant potential of *R. podophylla* with 2,2-diphenyl-1-picrylhydrazyl (DPPH), 2,2′-azino-bis(3-ethylbenzothiazoline-6-sulfonic acid) (ABTS) and ferric ion reducing antioxidant power (FRAP) assays. The results suggested that the ethyl acetate (EA) fraction of *R. podophylla* not only exhibited the strongest DPPH, ABTS radical scavenging and ferric-reducing activities, but also possessed the highest total phenolic and total flavonoid contents among the five fractions. After that, the potential superoxide dismutase (SOD) and xanthine oxidase (XOD) ligands from the EA fraction were quickly screened and identified through the bio-affinity ultrafiltration liquid chromatography-mass spectrometry (UF-LC-MS). Accordingly, norbergenin, catechin, procyanidin B2, 4-O-galloylbergenin, 11-O-galloylbergenin, and gallic acid were considered to be potential SOD ligands, while gallic acid, 11-O-galloylbergenin, catechin, bergenin, and procyanidin B2 were recognized as potential XOD ligands, respectively. Moreover, these six ligands effectively interacted with SOD in molecular docking simulation, with binding energies (BEs) ranging from −6.85 to −4.67 kcal/mol, and the inhibition constants (Ki) from 9.51 to 379.44 μM, which were better than the positive controls. Particularly, catechin exhibited a robust binding affinity towards XOD, with a BE value of −8.54 kcal/mol and Ki value of 0.55 μM, which surpassed the positive controls. In conclusion, our study revealed that *R. podophylla* possessed remarkable antioxidant and anti-hyperuricemia activities and that the UF-LC-MS method is suitable for screening potential ligands for SOD and XOD from medicinal plants.

KEYWORDS

***Rodgersia podophylla*, UF-LC-MS, antioxidative, anti-hyperuricemic, superoxide dismutase, xanthine oxidase**

1 Introduction

Rodgersia podophylla A. Gray (*R. podophylla*), a member of the Saxifragaceae family, is primarily found in the Hubei, Sichuan, Yunnan, and Tibet of China. It grows in shady and wet places such as undergrowth, shrubland, meadows, and rock crevices, at altitudes range of 1,100–3,400 m (Zhang et al., 2005). The rhizome of *R. podophylla* is used as a traditional Chinese medicine and is known by several trade names, including Suogudan and Yantuo (Zhang et al., 2015). It has been used to treat enteritis, dysentery, dysmenorrhea, menorrhagia, rheumatoid arthritis, bruises, traumatic bleeding, and scrotal eczema (Yan et al., 2017). Modern pharmacological studies also indicated that *R. podophylla* exhibited antioxidant, antibacterial, immune-enhancing, hepatoprotective, antimalarial, anticancer, and anti-inflammatory properties (Xie et al., 2022). Researchers have recently conducted extensive studies on its chemical components and revealed to contain various chemical classes, such as phenylpropanoids, flavonoids, terpenes and their derivatives, steroids, and organic acids and their derivatives (Zhang et al., 2005; Xie et al., 2022).

Reactive oxygen species (ROS) are cellular metabolites, and are normally classified into two categories: free radicals, such as superoxide anion radicals ($O_2^{\bullet-}$), and non-free radical species, such as hydrogen peroxide (Tomczyk and Malgorzata, 2021). ROS plays a crucial role in many important life processes in the human body, including cell growth (Brillo et al., 2021), proliferation, differentiation (Cheung and Vousden, 2022; Oka et al., 2022), energy supply (Yang and Lian, 2020), health, and aging (Alexey et al., 2020). However, excessive ROS in the body might expose cells to oxidative stress to inflict damage upon multiple organs, leading to a variety of health issues (Payne et al., 2013). To prevent organ damage from excess ROS, cells develop a protective system associated with redox enzymes, such as superoxide dismutase (SOD) and xanthine oxidase (XOD). Thereinto, SOD catalyzes the conversion of $O_2^{\bullet-}$ to H_2O_2 and oxygen (O_2) in the presence of transition metal ions, while H_2O_2 can be further decomposed into hydroxyl radicals (·OH) and hydroxide ions (OH^-) (Zhuang et al., 2021). XOD is a flavoproteinase that catalyzes the production of uric acid and superoxide anion ($O_2^{\bullet-}$) from xanthines and hypoxanthines (Chung et al., 1997). Excess uric acid and $O_2^{\bullet-}$ produced by XOD metabolism are closely associated with hyperuricemia (Liu et al., 2021), gout (Wang et al., 2020), hepatitis (Chung and Yu, 2000), cancer (Chung et al., 1997; Mi et al., 2020), aging, cardiovascular disease (Yu and Cheng, 2020), and chronic obstructive pulmonary disease (Rumora et al., 2020). Therefore, SOD and XOD are the potential targets for the treatment of oxidative stress injury-related diseases in humans.

At present, *R. podophylla* has been reported to exert arrestive antioxidative (Kim et al., 2020; Pyo et al., 2020) and anti-hyperuricemic activities (Wang et al., 2012), but the specific components responsible for these effects have not been revealed. Bio-affinity ultrafiltration liquid chromatography-mass spectrometry (UF-LC-MS) has been widely used to screen and identify potential ligands for biotarget enzymes from complex samples (Chen et al., 2018; Fan et al., 2022). Therefore, it is feasible to use SOD and XOD as target enzymes to screen potential bioactive compounds in *R. podophylla* that may be effective against diseases caused by oxidative damage and hyperuricemia.

In this case, due to the complex and diverse chemical compositions of *R. podophylla*, it is necessary to first screen and select its active fraction. To accomplish this, the antioxidative capacities of different solvent extracts of *R. podophylla* were evaluated using three assays: DPPH (2,2-diphenyl-1-picrylhydrazyl), ABTS (2,2′-azinobis-(3-ethylbenzthiazoline-6-sulfonic acid)), and FRAP (ferric-reducing antioxidant power). The extracts included crude extract (CE), n-hexane (n-Hex), dichloromethane (DCM), ethyl acetate (EA), and water (H_2O) fractions. At the same time, the total phenolic (TPC) and total flavonoid content (TFC) in different fractions of *R. podophylla* were detected to reveal their correlations with antioxidant activity. Then, the potential SOD and XOD ligands within the EA fraction were fast fished out with the UF-LC-MS method. Finally, molecular docking, along with the XOD inhibition assays *in vitro*, were employed to explain the interactions between the active components and the target enzymes. Consequently, this work provided a valuable reference for the development and utilization of *R. podophylla* as a natural antioxidant and anti-hyperuricemia drug or health supplement.

2 Materials and methods

2.1 Plant materials preparation and extraction

The rhizome of *R. podophylla* was collected in Xintang Township, Enshi City, Hubei Province, China, and was identified by Guangwan Hu, a senior taxonomist from the Key Laboratory of Plant Germplasm Enhancement and Specialty Agriculture (Wuhan Botanical Garden), Chinese Academy of Sciences. The voucher specimen (No. 20220705) was preserved in the herbarium of the Key Laboratory of Plant Germplasm Enhancement and Specialty Agriculture.

The dry, crushed rhizome (20 g) was soaked overnight in 200 mL of 50% ethanol at room temperature, then extracted using ultrasound for 50 min. This process was repeated three times, and the filtrate was collected. The filtrate was then concentrated using a rotary evaporator, and dried using a vacuum freeze dryer to obtain the crude extract of *R. podophylla* (CE, 4.32 g). 2 g of CE was dissolved in 100 mL of water and extracted consecutively with n-hexane (n-Hex, 100 × 3 mL), dichloromethane (DCM, 100 × 3 mL), and ethyl acetate (EA, 100 × 3 mL) to obtain n-Hex (24.3 mg), DCM (15.10 mg), EA (398.40 mg), and water (H_2O, 75.15 mg) fractions, respectively. The obtained samples were stored in a sealed container and kept in a refrigerator at 4 °C for future use.

2.2 Chemicals and reagents

The chemical standards of gallic acid, bergenin, procyanidin B2 and catechin (Purity ≥98.0%) were bought from Chengdu Alfa Biotechnology Co., Ltd (Chengdu, China). Rutin was purchased from J&K Scientific Ltd. (Beijing, China), Folin-Ciocalteu reagent, 1,3,5-tri (2-pyridyl)-2,4,6-triazine (TPTZ), 2,2′-azinobis-(3-ethylbenzthiazoline-6-sulfonic acid) (ABTS), and ascorbic acid

(vitamin C, Vc) were purchased from Sigma-Aldrich Corp (Shanghai, China). The acetonitrile (ACN) and methanol of HPLC grade were supplied by TEDIA Company Inc (Fairfield, OH, United States). All other analytical solvents and chemicals were purchased from Sinopharm Chemical Reagent Co., Ltd. (Shanghai, China). Superoxide dismutase (SOD) and xanthine oxidase (XOD) were bought from Shanghai Yuanye Bio-Technology Co., Ltd. (Shanghai, China). Ultrafiltration membranes (0.5 mL, 30 kDa) were purchased from Millipore Co. Ltd. (Bedford, MA, United States). Water (ultrapure grade) for HPLC and HPLC-UV-ESI-MS/MS analyses was prepared with EPED (Nanjing EPED Technology Development Co., Ltd. Nanjing, China).

2.3 Instruments

HPLC-UV/ESI-MS/MS was conducted with a Thermo Accela 600 series HPLC system coupled with a TSQ Quantum Access MAX mass spectrometer (Thermo Fisher Scientific, San Jose, CA, United States). As for the HPLC analysis, an Agilent 1220 LC (Santa Clara, CA, United States) with a RP-C18 column (Waters Symmetry RP-C18, 4.6 mm × 250 mm, 5 μm) was applied, and the UV absorbance was recorded by UV/VIS Spectrophotometer (UV1100, Shanghai, China). Centrifugation of samples was carried out by low-temperature high-speed centrifuge (Centrifuge 5810R, Eppendorf, Germany).

2.4 Determinations of antioxidant activity of *R. podophylla*

2.4.1 DPPH free radical scavenging activity

The DPPH radical scavenging activity of *R. podophylla* samples was determined based on a previously reported study by Muema et al. (Muema et al., 2022). Briefly, 10 μL of sample or positive control solution (Vc, 46.875–3,000 μM) was mixed with 190 μL DPPH (100 μM) in a 96-well plate. The mixture was then incubated for 30 min in the dark at room temperature. The absorbance at 517 nm was measured with a multifunctional microplate reader. Methanol was used as a blank control, and all samples and control were tested in triplicate (n = 3). The DPPH radical scavenging activity was calculated using the formula:

$$\textit{scavenging effect}\ (\%) = \frac{A_c - A_s}{A_c} \times 100\%$$

where A_c and A_s represent the absorbance values of the blank control and the tested sample or positive control, respectively. The IC_{50} value represents the concentration of the tested sample or positive control when the inhibition rate of DPPH radicals is 50%.

2.4.2 ABTS free radical scavenging activity

The ABTS free radical scavenging activity of different *R. podophylla* extracts was detected using a modified method described by Fan et al. (Fan et al., 2022). An ABTS solution (7 mM aqueous solution) was mixed with potassium persulfate (4.9 mM aqueous solution) in equal volumes (v/v) and allowed to react in the dark for 12–16 h to create a working solution ($ABTS^+$). The $ABTS^+$ solution was then diluted with methanol to ensure that its absorbance at 734 nm was approximately 0.700 ± 0.100. Next, 190 μL of the $ABTS^+$ solution was mixed with 10 μL of the sample and the absorbance was measured at 734 nm after incubating in the dark for 30 min. Methanol and Vc (31.25–1,000 μM) were used as blank and positive controls, respectively. The calculation of ABTS scavenging activity results followed the previous format in DPPH part.

2.4.3 Ferric-ion-reducing antioxidant power assay (FRAP)

The determination of ferric-iron-reducing antioxidant power (FRAP) was performed using a slightly modified method described by Xu et al. (Xu et al., 2019). The FRAP reagent (Fe^{3+}-TPTZ solution) containing 20 mM $FeCl_3.6H_2O$, 10 mM TPTZ, and 300 mM acetate buffer (3.1 g $C_2H_3NaO_2.3H_2O$ and 16 mL $C_2H_4O_2$, pH 3.6) was prepared in a ratio of 1:1:10 (v/v/v) and stored at 37°C. Next, 10 μL of appropriately diluted sample, 30 μL of ultrapure water, and 260 μL of fresh Fe^{3+}-TPTZ solution were added to a 96-well plate and incubated at 37°C for 10 min. The absorbance of the mixture at 593 nm was then measured using the multifunctional microplate reader, with three replicates per sample. $FeSO_4.7H_2O$ (62.5, 125, 250, 500, 1,000, and 2000 μM) was used as a standard to establish a calibration curve, and FRAP activity was expressed as the equivalent mM Fe^{2+} per Gram of sample (mM Fe^{2+}/g sample).

2.5 Determination of phenolic constituents

2.5.1 Determination of total phenolic content (TPC)

TPC was measured using the Folin-Ciocalteu method reported by Fan et al. (Fan et al., 2022). The reaction system was set up by sequentially adding 20 μL of the diluted sample, 20 μL of Folin-Ciocalteu reagent (diluted with pure water to 25%, v/v), 100 μL of sodium carbonate (Na_2CO_3, 1 M), and 20 μL of ultrapure water. The reaction was allowed to proceed for 1 h at room temperature in the dark. The absorbance was then recorded at 760 nm. Gallic acid solution (5–40 μg/mL) was used as a standard to establish a calibration curve. Results for TPC were expressed as milligrams of gallic acid equivalents per Gram of dry sample (mg GAE/g sample).

2.5.2 Determination of total flavonoid content (TFC)

The TFC of *R. podophylla* ethanol extract and different fractions was determined using a slightly modified method described by Chen et al. (Chen et al., 2020a). A 96-well plate was prepared by adding 20 μL of sample solution and 10 μL of sodium nitrite solution ($NaNO_2$, 5%, w/v) and incubated at room temperature for 6 min. Next, 12 μL of aluminum nitrate ($Al(NO_3)_3$, 10%, w/v) was added and incubated for an additional 6 min. Finally, 120 μL of sodium hydroxide solution (NaOH, 4%, w/v) and 58 μL of methanol solution were added, and the reaction was allowed to proceed for 15 min before measuring the absorbance at 510 nm. Rutin was used as the standard, and the results for TFC are expressed as milligrams of rutin equivalents per Gram of dry sample (mg RE/g sample).

2.6 Sample preparation and screening of the potential ligands of SOD and XOD with UF-LC-MS

Based on previous studies (Chen et al., 2020c; Fan et al., 2022), the UF-LC-MS method was applied to screen potential antioxidant components with high binding affinities to SOD and XOD in EA fractions. First, 10 mg of *R. podophylla* EA fraction was dissolved in 1 mL of Tris-HCl buffer solution (pH = 7.8) and sonicated for 30 min. Next, 180 μL of the sample solution was mixed with 20 μL of SOD (0.1 U/μL, pH 7.8) or XOD (0.2 U/μL, pH 6.8) and incubated at 37°C for 1 h. The mixed solutions were then transferred to a 30 kD ultrafiltration tube and centrifuged at 10,000 rpm for 10 min. The tube was washed three times with the appropriate PBS buffer to remove non-specifically bound components. Next, 200 μL of methanol (90%, v/v) was added and incubated for 20 min to release the enzyme-bound compounds, followed by centrifugation at 10,000 rpm for 10 min (n = 3). Finally, the ultrafiltrate was collected, dried using a termovap sample concentrator, and redissolved in 50 μL of 90% methanol for further analysis. As a negative control, an equal amount of enzyme was incubated in boiling water (100°C) for 10 min and treated in the same manner as the active enzyme group.

2.7 HPLC-UV/ESI-MS/MS analysis

The chemical compositions of the *R. podophylla* EA fraction were currently analyzed and identified with a Thermo Accela 600 HPLC system in combination with a TSQ Quantum Access MAX MS equipped with an ESI interface. Separation was performed using a Waters Sunfire RP-C18 column (4.6 mm × 250 mm, 5 μm; Waters, Wexford, Ireland). The mobile phases for HPLC elution were 0.1% (v/v) formic acid aqueous solution (A) and ACN (B). The elution conditions were as follows: 1%–5% (B) in 0–5 min, 5%–14% (B) in 5–25 min, and 14%–20% (B) in 25–60 min. The injection volume was 10 μL, the flow rate was 0.8 mL/min, and the wavelength was set at 310 nm (Wang et al., 2012). The ESI-MS/MS analysis was performed in the negative ion mode under the following conditions: the temperatures of vaporiser and capillary were 350 °C and 250 °C, respectively; the gas pressure of sheath gas (nitrogen gas, N_2) and axu gas (helium, He) was 40 psi and 10 psi, respectively; the source voltage was 3000 V and the cone voltage and collision energy were 40 V and 10 V, respectively; mass range (m/z) was from 150 to 1,500, spray voltage was 3 kV. MS data (mass range from m/z 100–1,000) was obtained in the full-scan mode. The preliminary identification of compounds in the EA fraction of *R. podophylla* was carried out by comparing the parent ions, MS fragments, and retention times with the references.

2.8 Molecular docking study

The interactions between the ligands and target enzymes were further elucidated through molecular docking. This process was based on previous studies by Fan et al. (Fan et al., 2022; Rakotondrabe et al., 2022) with minor modifications, using software such as AutoDock Tools 1.5.6, PyMOL and the Discovery Studio 4.1 software. The structures of SOD (PDB 1CBJ) and XOD (PDB 1FIQ) were obtained from the RSCB Protein Database (www.rcsb.org), while the 3D structure of the ligand was downloaded from the Traditional Chinese Medicine Systems Pharmacology Database and Analysis Platform (old.tcmsp-e.com). Next, water molecules and ligand fractions were removed using the PyMOL. Hydrogen atoms were added to proteins and ligands using AutoDock Tools, which was also used to calculate charges and perform other processing of their 3D structures. The coordinates of the active sites of SOD and XOD were (X: 6.640; Y: 23.974; Z: 58.655) and (X: 28.671; Y: 29.977; Z: 101.417) (Fan et al., 2022), respectively. A grid box was centered on the active sites of the receptors, with dimensions of 60 Å × 60 Å × 60 Å. Molecular docking analysis between ligands and receptors was then performed using AutoDock Tools, with 50 independent runs of the genetic algorithm and other default parameters. The docking conformations were ranked according to their energy scores.

2.9 Validation of potential ligands activity by XOD inhibition experiment

The XOD inhibition experiment was performed using a modified method previously reported by Wang et al. (Wang et al., 2012). In a 96-well plate, 90 μL of phosphate buffer (0.1 M, pH = 7.4), 20 μL of XOD (0.5 U/mL), and 10 μL of sample solution or positive control allopurinol solution dissolved in phosphate buffer were added and incubated at 37 °C for 30 min. Then, 80 μL of substrate (xanthine solution dissolved in phosphate buffer, 0.4 mM) was added and the plate was incubated at 37°C in the dark for 15 min. Absorbance was measured at 295 nm. Each well had a blank control without enzyme and a background control for 100% enzyme activity (only the solvent with the enzyme and the substrate). All samples and controls were tested in triplicate (n = 3). XOD inhibition was calculated as follows:

$$\textit{Inhibition}\ (\%) = \left(1 - \frac{A_{Sample} - A_{Blank}}{A_{Background} - A_{Blank}}\right) \times 100\%$$

where A_{Sample}, A_{Blank} and $A_{Background}$ are defined as the absorbance of the test sample (with the enzyme), the blank (the test sample without the enzyme) and the 100% enzyme activity (only the solvent with the enzyme and the substrate), respectively. The extent of inhibition was expressed as the concentration of sample needed to inhibit XOD activity by 50% (IC_{50}).

2.10 Statistical analysis

All data in this work were measured in triplicate and were expressed as mean ± standard deviation (SD). The IC_{50} values were calculated by plotting the percentages of scavenging activities or inhibition rates against the sample concentrations (six different concentration gradients in triplicate). Statistical analysis was performed using software of SPSS 25.0 (IBM Corp., New York, NY, United States), Origin 2021 (OriginLab Corporation, Northampton, MA, United States) and GraphPad Prism 9.0 (GraphPad Software Inc., San Diego, CA, United States).

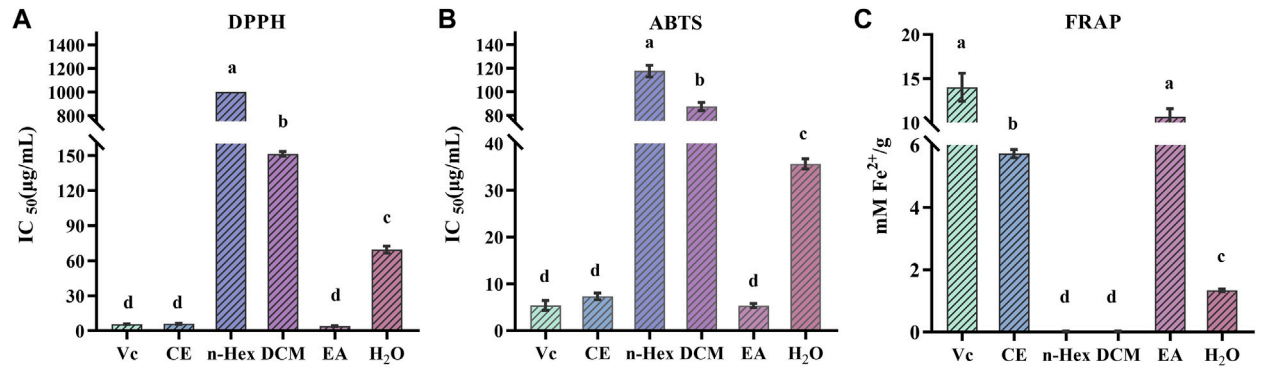

FIGURE 1
Antioxidant activity of n-hexane (n-Hex), dichloromethane (DCM), ethyl acetate (EA), H_2O and crude extracts (CE) of *R. podophylla*. **(A)** the IC_{50} value of DPPH radical scavenging assay, **(B)** the IC_{50} value of ABTS radical scavenging assay, **(C)** the FRAP assay. Mean values with different letters **(A–C)** were significantly different at a level of $p < 0.05$ (n = 3) by DMRT (Duncan's multiple range test).

3 Results and discussion

3.1 Antioxidant activities of *R. podophylla*

Due to the multiple ROS scavenging patterns and the complexity of natural phytochemicals, three representative experiments, including DPPH, ABTS, and FRAP, were selected to evaluate and compare the antioxidant activity of different *R. podophylla* extracts (Fan et al., 2020). As shown in Figure 1, the EA fraction showed the strongest scavenging effect on DPPH and ABTS free radicals compared to the other four fractions, with IC_{50} values of 3.863 ± 0.34 μg/mL and 5.537 ± 0.38 μg/mL, respectively. The IC_{50} values of the positive control Vc were 5.538 ± 0.11 μg/mL and 5.369 ± 0.86 μg/mL, respectively. The EA fraction also showed the strongest ferric iron reduction ability, with a FRAP value of 10.655 ± 0.77 mM Fe^{2+}/g, which was no significant difference with Vc (14.024 ± 1.30 mM Fe^{2+}/g). This deviated slightly from the findings presented by Zhang (Zhang et al., 2021), which might be related to the total flavonoids in *R. aesculifolia* (the *Rodgersia* genus), and exhibited a moderately higher FRAP values compared to Vc. Among the three antioxidant capacity assays, the CE fraction also showed better antioxidant activity, followed by the H_2O fraction, while the other extracts (DCM and n-Hex) showed moderate antioxidant capacities. Considering that the EA fraction showed the strongest antioxidant capacity compared to other fractions, this result aligned with Yan's findings (Yan et al., 2017) from the antioxidant activity screening of the *Rodgersia aesculifolia*, thereof the EA fraction was chosen for subsequent studies.

3.2 Total phenolic and flavonoid content

Numerous studies have demonstrated that polyphenols and flavonoids were the primary compounds with antioxidant properties, interacting with free radicals before they attack cells, thereby preventing further cellular damage (Lobo et al., 2010; Sha et al., 2021). Results from free radical scavenging experiments showed that the EA fraction had the strongest DPPH and ABTS free radical scavenging abilities, indicating that *R. podophylla* exhibited potential antioxidant activity. To further explore the potential compound types in *R. podophylla*, the TPC and TFC contents of five samples were determined using the Folin-Ciocalteu method and the aluminum nitrate colorimetric method. As shown in Table 1, the EA fraction displayed the highest TPC of 70.984 ± 3.49 mg GAE/g, followed by the CE fraction (41.970 ± 4.14 mg GAE/g). The lowest TPC was n-Hex fraction at 13.094 ± 0.06 mg GAE/g.

In addition, the TFC in the EA fraction (1,026.096 ± 8.11 mg RE/g) was also the highest among the five samples, followed by the CE fraction (595.326 ± 4.14 mg RE/g). The lowest TFC was 77.65 ± 0.13 mg RE/g at the H_2O fraction, which was about 1/13 of the EA fraction. These results further validated our previous findings and provided clues for exploring potential bioactive components in EA fraction with significant antioxidant activity.

3.3 Correlation analysis between antioxidant activities and phytochemical components

A comprehensive correlation analysis was executed to thoroughly assess the correlation between the antioxidant activity (DPPH, ABTS, FRAP) of *R. podophylla* and its TPC and TFC. The results are presented in Table 2. On the one hand, substantial correlations were observed among the three antioxidant activity determination. The Pearson correlation coefficients (R^2) between DPPH with ABTS and FRAP were notably high at 0.998 ($p < 0.01$) and −0.838 ($p < 0.05$), respectively. Furthermore, the R^2 value between ABTS and FRAP was −0.812 ($p < 0.05$). These findings suggested that these three methodologies were not only reliable but also interchangeable. On the other hand, there were also strong correlations between antioxidant activities and chemical compositions. The FRAP values showed an closely positive correlation with the TPC and TFC at 0.960 ($p < 0.01$) and 0.991 ($p < 0.01$), respectively. While the DPPH and ABTS

TABLE 1 Total phenolic and total flavonoid contents of *R. podophylla*.

Extracts	TPC(mg GAE/g dw)	TFC(mg RE/g dw)
CE	41.970 ± 4.14 [b]	595.326 ± 4.14 [b]
n-Hex	13.094 ± 0.06 [c]	99.660 ± 1.96 [c]
DCM	28.915 ± 1.15 [b]	87.472 ± 0.51 [d]
EA	70.984 ± 3.49 [a]	1,026.096 ± 8.11 [a]
H_2O	23.442 ± 0.53 [b]	77.650 ± 0.13 [d]

Note: The data were expressed as means ± SD, Means labeled by different letters (a-d) were significantly different at a level of $p < 0.05$ (n = 3) by DMRT (Duncan's multiple range test).

TABLE 2 Pearson correlation coefficients (R^2) among the antioxidant activities and phytochemical contents of *R. podophylla*.

	ABTS	FRAP	TPC	TFC
DPPH	0.998**	−0.838*	−0.795	−0.783
ABTS		−0.812*	−0.772	−0.749
FRAP			0.960**	0.991**
TPC				0.956**

Note: *and ** indicate the correlation is significant at the level of $p < 0.05$ and $p < 0.01$, respectively. DPPH, 2,2-diphenyl-1-picrylhydrazyl; ABTS, 2,2′-azino-bis(3-ethylbenzothiazoline-6-sulphonic acid); FRAP, ferric-reducing antioxidant power; TPC, total phenolic content; TFC, total flavonoid content.

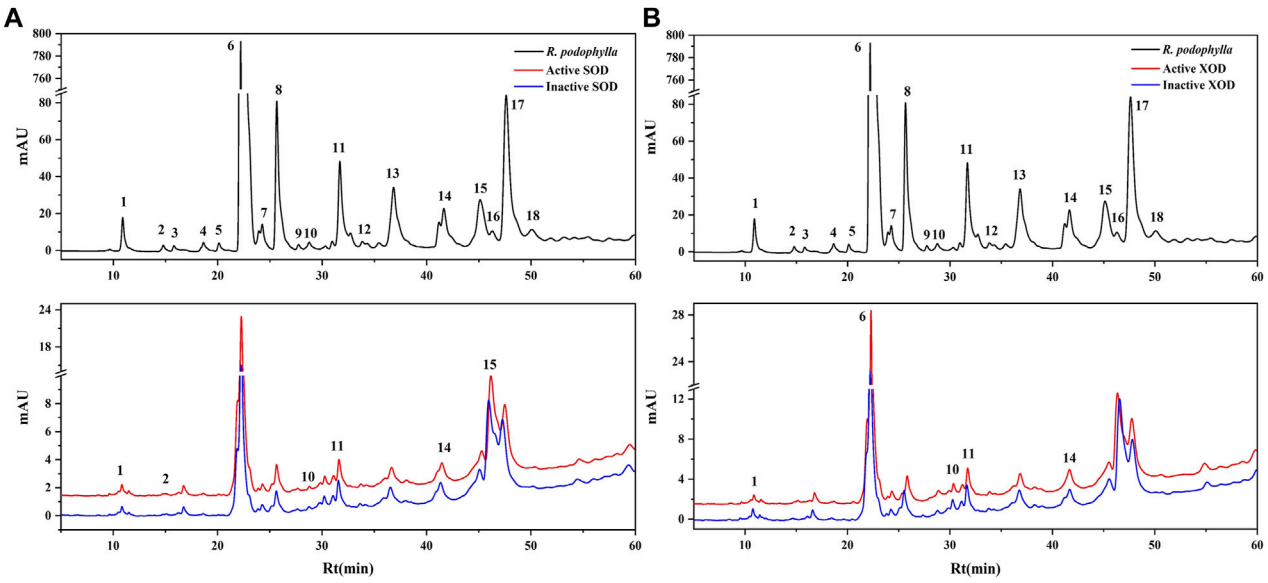

FIGURE 2
HPLC chromatograms of the chemical constituents in the EA fraction of *Rodgersia podophylla* were obtained after ultrafiltration at 310 nm. The black solid line represents HPLC profiles of the EA fraction of *R. podophylla* without ultrafiltration; the red line and blue line represent the total extract of *R. podophylla* with activated and inactivated SOD **(A)**, XOD **(B)**, respectively.

values were highly negative correlated with TPC (the R^2 value at −0.795 and −0.772) and TFC (the R^2 value at −0.783 and −0.749), respectively. The R^2 value between theTPC and TFC was found to be 0.956 ($p < 0.01$), indicating an exceptionally robust correlation. Synthesizing these findings, it was discerned that polyphenols and flavonoids could potentially be the primary contributors to the antioxidant activity exhibited by *R. podophylla*.

3.4 Screening for SOD and XOD ligands in *R. podophylla* with UF-LC-MS

Investigations have been conducted to explore the antioxidant and anti-hyperuricemic properties of *R. podophylla* through its various extracts (Wang et al., 2012). To further investigate the bioactive constituents that contribute to the antioxidant and anti-hyperuricemic effects in the EA fraction,

TABLE 3 The identification, enrichment factor (EF) and the UF-LC-MS/MS data of potential SOD and XOD ligands screened out from *R. podophylla*.

Peak NO.	Rt[a] (min)	[M-H]$^-$	Characteristic fragment (m/z)	Identification	EFs[b] (%)	
					SOD	XOD
1	10.90	169.26	169, 125, 97	Gallic acid[c]	0.54	1.00
2	14.78	313.46	313, 193, 189	Norbergenin[d]	3.35	-
6	22.20	327.20	327.30, 234, 193, 192, 207	Bergenin[c]	-	0.33
10	28.76	577.35	407, 289, 125	Procyanidin B2[c]	1.28	0.31
11	31.69	289.18	245, 203,151	Catechin[c]	2.33	0.49
14	41.65	479.38	326, 312, 207, 193, 169,125	11-O-Galloylbergenin[d]	0.96	0.55
15	45.12	479.42	327, 313, 207, 193, 169	4-O-Galloylbergenin[d]	1.17	-

[a]Rt, retention time.
[b]EFs, enrichment factors.
[c]Compared with the corresponding standards.
[d]Identified based on the published literature.

SOD and XOD were thus selected as the target enzymes for expeditious screening via bioaffinity ultrafiltration. The ligands of SOD and XOD ascertained through this methodology, might potentially constitute active compounds with antioxidant and anti-hyperuricemic properties. As depicted in Figures 2A, B, the results of the ultrafiltrate analysis via HPLC revealed 6 and 5 peaks, respectively, exhibiting varying degrees of binding capacities to SOD and XOD. In this study, the enrichment factor (EF) was employed to express the affinity between the enzyme and the ligand, calculated using the following formula:

$$EF\ (\%) = \frac{A_1 - A_2}{A_0} \times 100\%$$

Where A_1, A_2, and A_0 represent the peak areas of each chromatographic peak from the EA fraction of *R. podophylla* treated with activated, inactivated, and without SOD or XOD, respectively (Yan et al., 2017; Chen et al., 2020c; Feng et al., 2021). If the peak area of the active group exceeds that of the inactive group, it can be inferred that the group may be classified as a potential inhibitor of the target enzyme (Jiao et al., 2019). When utilized to assess the affinity between the active constituents and the enzyme, the EF value denoted the capacity of various components to bind to the target enzyme.

The EF values of potential SOD and XOD ligands in the EA fraction were summarized in Table 3. For SOD, peak 2 displayed the highest EF value (3.35%), followed by peak 11 (2.33%), peak 10 (1.28%), peak 15 (1.17%), peak 14 (0.96%), and peak 1 (0.54%). For XOD, peak 1 exhibited the highest binding force to XOD, with an EF value of 1.00%, followed by peak 14 (0.55%), peak 11 (0.49%), peak 6 (0.33%), and peak 10 (0.31%). It was observed that 6 and 5 components in the HPLC chromatograms incubated with active SOD and XOD in *R. podophylla* exhibited higher peak areas than those of the inactivated control group, respectively. The findings suggested that these constituents exhibited specific binding affinities towards SOD or XOD, and were therefore consid-ered as primary potential ligands for these enzymes.

3.5 Identification of SOD and XOD ligands in *R. podophylla* with HPLC-UV/ESI-MS/MS

The predominant peaks of the EA fraction were identified and characterized using HPLC-UV/ESI-MS/MS. The MS and MS/MS data for these peaks, including retention time (RT), deprotonated molecular ion [M-H]$^-$, and representative MS/MS spectral fragments, were presented in Table 3. Furthermore, the structures of the compounds in the EA fraction of *R. podophylla* were tentatively identified, and some representative components were depicted in Figure 3.

Peak 1 exhibited a deprotonated molecular ion at m/z 169.26 [M-H]$^-$, with characteristic fragment ions at m/z 125 and 97. Based on its exact mass, fragment ions, and retention time, as well as comparison with the standard, it was identified as gallic acid (Ren et al., 2021). Previous studies also demonstrated that this compound possessed significant antioxidant activity (Badhani et al., 2015; Yan et al., 2017), suggesting that Peak 1 might contribute partly to the antioxidant activity of *R. podophylla*.

Peak 6 displayed a deprotonated molecular ion [M-H]$^-$ at m/z 327.20, with a formula of $C_{14}H_{15}O_9$. Four major fragment ions of m/z 234 [M-H-$C_2H_6O_3$-CH_3]$^-$, m/z 207 [M-H-$C_4H_8O_4$]$^-$, m/z 193 [M-H-$C_5H_{10}O_4$]$^-$, and m/z 192 [M-H-CH_3-$C_4H_8O_4$]$^-$ were observed in the MS/MS spectrum. By comparison with previous literature and standard, Peak 6 was identified as bergenin (Li et al., 2013).

Peak 2 exhibited a deprotonated molecular ion [M-H]$^-$ at m/z 313.46. A major fragment ion at m/z 193 [M-H-$C_4H_8O_4$]$^-$ was consistent with the fragmentation mechanism of bergenin. Thus, its deprotonated molecular ion [M-H]$^-$ at m/z 313 represented bergenin with the loss of a methyl. Based on this, Peak 2 was identified as norbergenin (Ren et al., 2021).

Peak 10 produced a deprotonated molecular ion at m/z 577.35, with a formula of $C_{30}H_{25}O_{12}$. Its characteristic fragment at m/z 407 corresponded to the fragment ion at m/z 425 [$C_{22}H_{17}O_9$]$^-$, which was generated by the cleavage of procyanidins via a Retro-Diels-Alder reaction (RDA), followed by the removal of a portion of water to form the fragment at m/z 407 [$C_{22}H_{17}O_9$-H_2O]$^-$. Another characteristic fragment, at m/z 289, corresponded to the cleavage of m/z 577 [M-H]$^-$ into the catechin characteristic fragment at m/z

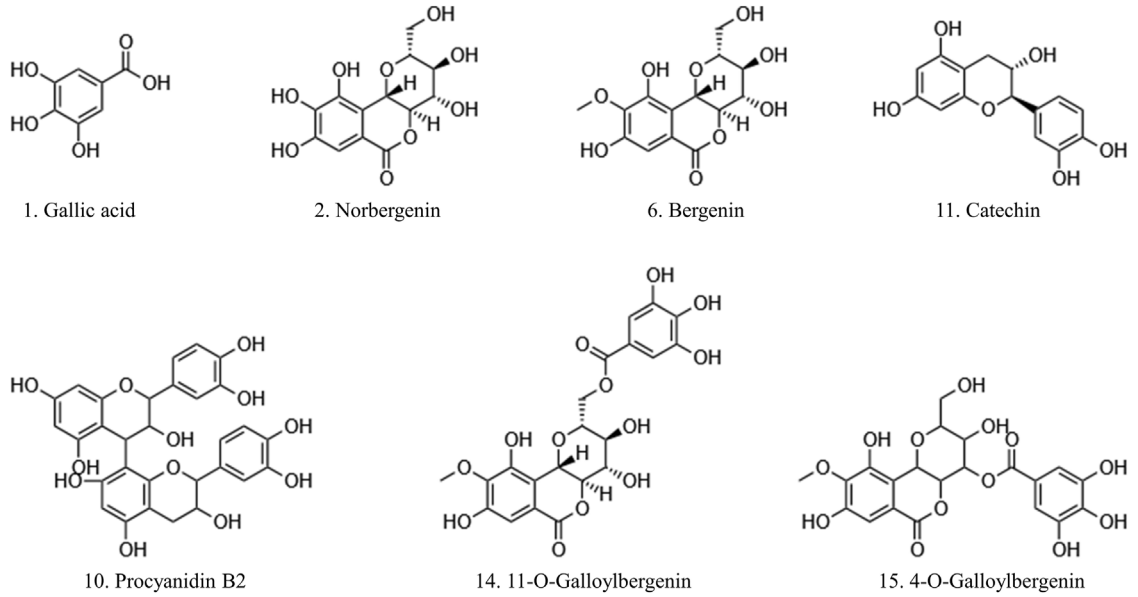

FIGURE 3
The potential ligands screened from the EA fraction of *R. podophylla* by UF-LC-MS with superoxide dismutase (SOD) and xanthine oxidase (XOD).

289 $[C_{15}H_{13}O_6]^-$. Additionally, m/z 577 also underwent C-ring cleavage to produce the characteristic fragment at m/z 125 $[C_6H_5O_3]^-$, which was also present in the fragment ion of peak 10. Through comparison with standards, peak 10 was ultimately determined as procyanidin B2 (Xiao et al., 2017).

Peak 11 presented a deprotonated molecular ion at m/z 289.18 $[M-H]^-$. A prominent fragment at m/z 245 $[M-H-CO_2]^-$ resulted from the loss of the CO_2 group (44 Da) from m/z 289, which then further lost $-C_2H_2O$ to generate m/z 203 $[M-H-CO_2-C_2H_2O]^-$. Namely, it could be inferred that peak 11 represented either catechin or epicatechin. Additionally, the fragment ion at m/z 151 $[M-H-C_6H_6O_2-CO]^-$ corresponded to the characteristic fragment ions generated by the cleavage of catechin or epicatechin via C-ring RDA in negative ion mode. Through comparison with standards, peak 11 was ultimately determined to be catechin (Liu et al., 2009; Ren et al., 2021). Previously, catechin isolated from *R. aesculifolia* exhibited its noteworthy DPPH free radical scavenging ability with an IC_{50} of 3.8231 μg/mL, showing stronger antioxidant activity than Vc (IC_{50} = 7.1391 μg/mL) (Yan et al., 2017).

Both peaks 14 and 15 exhibited the same deprotonated molecular ion at m/z 479.42 $[M-H]^-$, indicating that they were isomers with the formula $C_{21}H_{20}O_{13}$. The fragment ion at m/z 327 was characteristic of bergenins, while the fragment ions at m/z 169 $[C_7H_5O_5]^-$ and m/z 125 $[C_6H_5O_3]^-$ were characteristic of gallic acid. Thus, it can be inferred that peaks 14 and 15 represented monogalloyl bergenin. The fragment ion at m/z 327 represented $[M-H-galloyl]^-$, while the fragment ion at m/z 312 represented $[M-H-galloyl-CH_3]^-$, m/z 207 represented $[M-H-galloyl-C_4H_8O_4]^-$, and m/z 193 represented $[M-H-galloyl-C_5H_{10}O_4]^-$. In light of the available literature, it can be speculated that the phytochemical composition of genus *Rodgersia* may be galloylbergenin at the 3, 4 or 11 position. Based on the different retention times, peak 14 and peak 15 were inferred to be 11-O-galloylbergenin and 4-O-galloylbergenin, respectively (Ren et al., 2021).

3.6 Molecular docking

Molecular docking is a widely used technique for evaluating the interactions between enzymes and potential ligands, which could reveal possible interaction patterns by identifying their docking energies, sites of action, and key residues of the receptor (Chen et al., 2020b). Based on the binding degree in affinity ultrafiltration, peaks 2, 11, 10, 15, 14, and 1 were selected as SOD ligands, while peaks 1, 14, 11, 6, and 10 were selected as XOD ligands for molecular docking, respectively. Table 4 summarized the binding energy (BE), inhibition constant (Ki), and amino acids involved in hydrogen bonding. The optimal docking conformation within the binding site was illustrated in Figure 4. Dithiocarbamate (DTC) and allopurinol (ALL) were used as positive controls for SOD and XOD, respectively.

For SOD, the six compounds screened by bioaffinity ultrafiltration were lower than that of the positive control DTC (BE, −4.02 kcal/mol; Ki, 1,130.00 μM), which indicated that these compounds exhibited strong interactions with SOD. Among them, peak 11 (catechin, BE, −6.85 kcal/mol; Ki, 9.51 μM) displayed the strongest affinity with SOD, followed by peak 15 (4-O-galloylbergenin, BE, −6.67 kcal/mol; Ki, 13.01 μM), peak 14 (11-O-galloylbergenin, BE, −5.99 kcal/mol; Ki, 40.42 μM), peak 2 (norbergenin, BE, −5.71 kcal/mol; Ki, 65.32 μM), peak 1 (gallic acid, BE, −5.06 kcal/mol; Ki, 196.50 μM), and peak 10 (procyanidin B2, BE, −4.67 kcal/mol; Ki, 379.44 μM). These results were generally consistent with those obtained from bioaffinity ultrafiltration (Table 4). Through the visualization of molecular docking results, it was found that there was a pi-sigma and numerous hydrogen bonds between peak 11 (catechin) and

TABLE 4 The molecular docking results of the potential ligands in *Rodgersia podophylla* with SOD and XOD.

Peak	SOD (PDB 1CBJ)			XOD (PDB 1FIQ)		
	BE (kcal/mol)	Ki(μM)	Hydrogen bonds	BE (kcal/mol)	Ki(μM)	Hydrogen bonds
1	−5.06	196.50	Val146, Val7, Lys9	−4.9	255.89	Gln423, Lys433, Lys1128
2	−5.71	65.32	Val146, Val7, Ile149, Asn51	ND	ND	ND
6	ND	ND	ND	−5.26	139.25	Ile1229, Ser1234, Gly47
10	−4.67	379.44	Val146, Val7, Asn51, Gly148	−8.08	1.20	Arg426, Lys433, Gln423, Gly47
11	−6.85	9.51	Ala1, Ile111, Leu104, Glu107	−8.54	0.55	Glu1210, Leu1208, Asp1170
14	−5.99	40.42	Val146, Val7, Lys9, Cys144	−5.93	45.18	Gln423, Lys433, Arg426, Ala338
15	−6.67	13.01	Val146, Val7, Asn51, Lys9	ND	ND	ND
DTC[a]	−4.02	1,130.00	Val146, Gly49	ND	ND	ND
ALL[b]	ND	ND	ND	−5.03	206.23	Arg426, Glu1210

PDB, protein data bank; 1CBJ, the crystal structure accession number of SOD; 1FIQ, the crystal structure accession number of XOD; BE, binding energy; Ki, inhibition constant; a, Dithiocarbamate (DTC), positive control of SOD; b, Allopurinol (ALL), positive control of XOD; ND, not detected; Val, valine; Lys, lysine; Ile, isoleucine; Asn, asparaginate; Gly, glycine; Ala, alanine; Leu, leucine; Glu, glutamic acid; Cys, cysteine; Gln, glutamine; Ser, serine; Arg, arginine; Asp, aspartic acid.

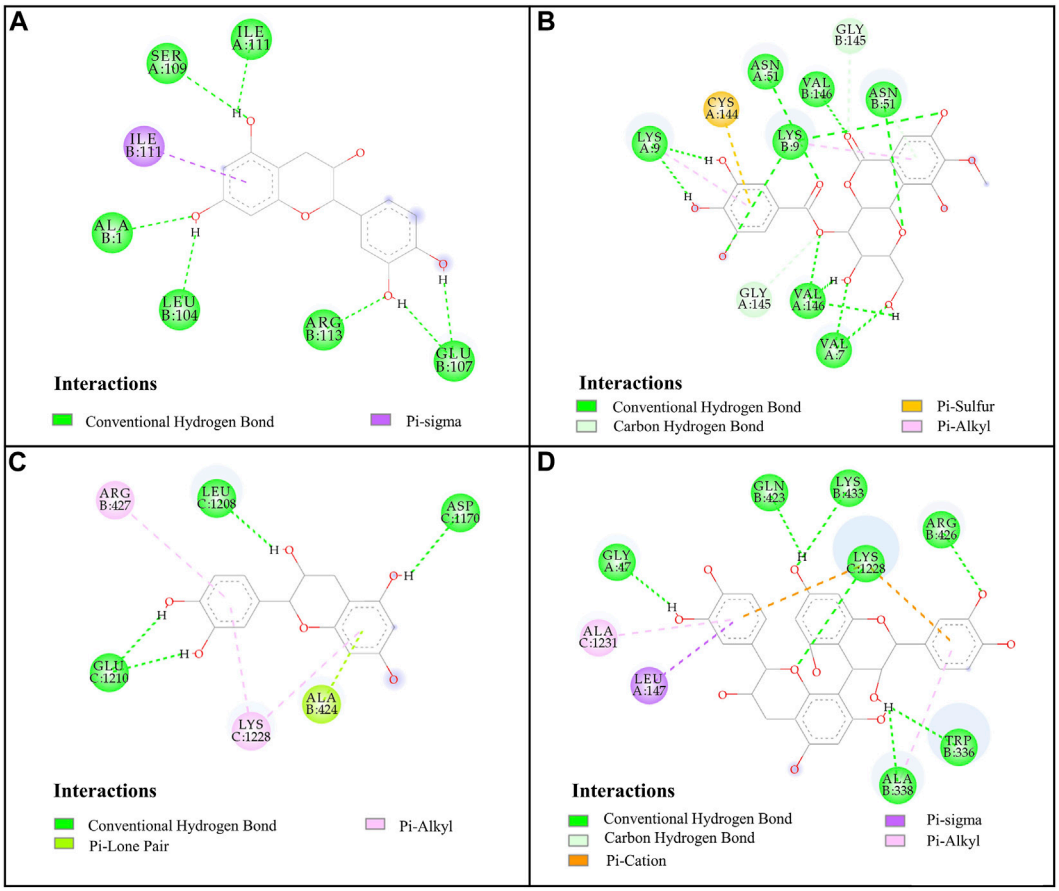

FIGURE 4
Docked complexes of SOD and XOD: **(A)**, SOD-catechin; **(B)**, SOD-4-O-galloylbergenin; **(C)**, XOD-catechin; **(D)**, XOD-procyanidin B2.

SOD. As shown in Figure 4A, Figure 7 hydrogen bonds were formed between catechin and amino acid residues such as Ala1, Ile111, Leu104 and Glu107. As depicted in Figure 4B, peak 15 (4-O-galloylbergenin) formed 12 hydrogen bonds and engaged in additional interactions, such as pi-sulfur and pi-alkyl, with amino acid residues including Val146, Val7, Asn51, and Lys9.

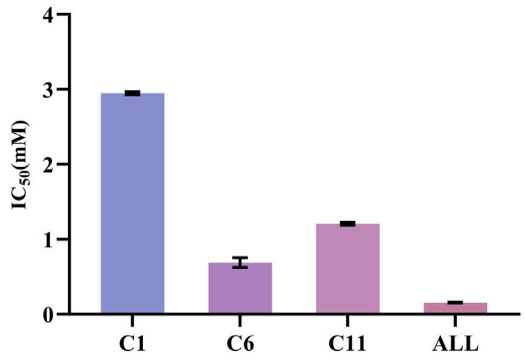

FIGURE 5
The IC_{50} of potential ligands with XOD. C1: gallic acid; C6: bergenin; C11: catechin; ALL: allopurinol.

Consequently, the stability of protein-ligand complexes was not only attributed to hydrogen bonding but also to other interaction forces.

For XOD, peak 11 (catechin) exhibited the highest interaction with XOD, with the lowest BE value of −8.54 kcal/mol and the Ki value of 0.55 μM. Figure 4C showed that catechin formed 4 hydrogen bonds with amino acid residues such as Glu1210, Leu1208 and Asp1170 of XOD and formed pi-alkyl with residues. Peak 10 (procyanidin B2, BE, −8.08 kcal/mol; Ki, 1.2 μM, Figure 4D) formed hydrogen bonds with XOD through amino acid residues such as Arg426, Lys433, Gln423, and Gly47. The presence of pi-cation, pisigma and pi-alkyl interactions increased its affinity with XOD. In addition, peak 14 (11-O-galloylbergenin, BE, −5.93 kcal/mol; Ki, 45.18 μM) and peak 6 (bergenin, BE, −5.26 kcal/mol; Ki, 139.25 μM) also exerted higher activity than the positive control ALL (BE, −5.03 kcal/mol; Ki, 206.23 μM), indicating that these compounds also had good interactions with XOD.

In summary, peaks 11, 15, 14, 2, 1, and 10 for SOD and peaks 11, 10, 14, 6 and 1 for XOD were identified as potential ligands that warranted further investigation. Their structures were shown in Figure 3, and their retention times and mass spectral fragments were presented in Table 3.

3.7 Anti-hyperuricemic capacity of potential ligands by XOD inhibition experiments

The XOD inhibition assay was conducted with a slightly modified methodology previously described by Wang et al. (Wang et al., 2012). At the concentration of 0.25 mg/mL, the *R. aesculifolia* extract achieved an XOD inhibition rate of 72.79%. This rate increased to an impressive 85.18% when the concentration was elevated to 1.25 mg/mL. Meanwhile, the XOD inhibitory activity *in vitro* of the compounds, identified through UF-LC-MS screening, was further confirmed. As shown in Figure 5, compound 6 (bergenin) displayed the strongest inhibitory effect on XOD, with an IC_{50} value of 0.680 ± 0.061 mM, which was comparable with the positive control drug, allopurinol (IC_{50} = 0.156 ± 0.005 mM) ($p > 0.05$). Compound 11 (catechin) and compound 1 (gallic acid) also showed attractive inhibitory effects, with IC_{50} values of 1.208 ± 0.015 mM and 2.949 ± 0.016 mM, respectively. To this end, the present results not only confirmed the significant XOD inhibitory activity of the compounds screened through bio-affinity ultrafiltration, but also provided a foundation for further investigation into the anti-hyperuricemia properties of *R. podophylla*.

4 Conclusion

In this study, the antioxidant capacities of *R. podophylla* extracts were firstly assessed using DPPH, ABTS, and FRAP assays. The EA fraction of *R. podophylla* exhibited the highest radical scavenging and ferric reduction abilities, with IC_{50} values of 3.863 ± 0.34 μg/mL and 5.537 ± 0.38 μg/mL for DPPH and ABTS, and the FRAP value of 10.655 ± 0.77 mM Fe^{2+}/g, respectively. Additionally, the EA fraction exhibited the highest total phenolic and flavonoid contents among all fractions, with values of 70.984 ± 3.49 mg GAE/g dw and 1,026.096 ± 8.11 mg RE/g dw, respectively. A bio-affinity ultrafiltration coupled with LC-MS/MS strategy with SOD and XOD as target enzymes was employed to screen potential antioxidant and anti-hyperuricemic compounds from the EA fraction. Based on the binding capacities, norbergenin (peak 2), catechin (peak 11), procyanidin B2 (peak 10), 4-O-galloylbergenin (peak 15), 11-O-galloylbergenin (peak 14), and gallic acid (peak 1) were identified as potential SOD ligands, while gallic acid (peak 1), 11-O-galloylbergenin (peak 14), catechin (peak 11), bergenin (peak 6), and procyanidin B2 (peak 10) were identified as potential XOD ligands, respectively. Furthermore, molecular docking revealed that these seven compounds exhibited favorable interactions with SOD and XOD through hydrogen bonding and other types of intermolecular forces. Notably, their binding affinities even surpassed those of the positive controls (DTC and ALL). Thereafter, the XOD inhibition assays *in vitro* discerned that all these molecular entities demonstrated strong XOD inhibition, especially bergenin and catechin. In summary, this study represented the first application of the UF-LC-MS method for the rapid screening of bioactive compounds in *R. podophylla* extracts, specifically targeting their antioxidant and anti-hyperuricemia properties. The research not only provided novel evidence to support the antioxidant and anti-hyperuricemic properties of *R. podophylla*, but also clarified the potential bioactive ligands for its further research and application. These bioactive compounds hold promise for future development as health supplements or natural medicines for the prevention and treatment of oxidative stress and hyperuricemia-associated diseases.

Data availability statement

The original contributions presented in the study are included in the article/Supplementary material, further inquiries can be directed to the corresponding authors.

Author contributions

CL: Data curation, Formal Analysis, Software, Writing–original draft. YX: Data curation, Software, Writing–review and editing. MF: Formal Analysis, Software, Writing–review and editing. FM: Formal

Analysis, Software, Writing–review and editing. GC: Conceptualization, Funding acquisition, Methodology, Project administration, Supervision, Validation, Writing–review and editing. MG: Writing–review and editing. GH: Methodology, Project administration, Resources, Supervision, Writing–review and editing.

Funding

The author(s) declare financial support was received for the research, authorship, and/or publication of this article. This research was funded by the Youth Innovation Promotion Association of Chinese Academy of Sciences (No. 2020337).

Conflict of interest

The authors declare that the research was conducted in the absence of any commercial or financial relationships that could be construed as a potential conflict of interest.

Publisher's note

References

Alexey, N. K., Sharma, R. P., Colangelo, A. M., Ignatenko, A., Martorana, F., Jennen, D., et al. (2020). ROS networks: designs, aging, Parkinson's disease and precision therapies. *NPJ Syst. Biol. Appl.* 6, 34. doi:10.1038/s41540-020-00150-w

Badhani, B., Sharma, N., and Kakkar, R. (2015). Gallic acid: a versatile antioxidant with promising therapeutic and industrial applications. *RSC Adv.* 5, 27540–27557. doi:10.1039/c5ra01911g

Brillo, V., Chieregato, L., Leanza, L., Muccioli, S., and Costa, R. (2021). Mitochondrial dynamics, ROS, and cell signaling: a blended overview. *Life* 11, 332. doi:10.3390/life11040332

Chen, G. L., Huang, B. X., and Guo, M. Q. (2018). Current advances in screening for bioactive components from medicinal plants by affinity ultrafiltration mass spectrometry. *Phytochem. Anal.* 29, 375–386. doi:10.1002/pca.2769

Chen, G. L., Munyao Mutie, F., Xu, Y. B., Saleri, F. D., Hu, G. W., and Guo, M. Q. (2020a). Antioxidant, anti-inflammatory activities and polyphenol profile of *Rhamnus prinoides*. *Pharm* 13, 55. doi:10.3390/ph13040055

Chen, G. L., Seukep, A. J., and Guo, M. Q. (2020b). Recent advances in molecular docking for the research and Discovery of potential marine drugs. *Mar. Drugs.* 18, 545. doi:10.3390/md18110545

Chen, G. L., Xu, Y. B., Wu, J. L., Li, N., and Guo, M. Q. (2020c). Hypoglycemic and hypolipidemic effects of *Moringa oleifera* leaves and their functional chemical constituents. *Food Chem.* 333, 127478. doi:10.1016/j.foodchem.2020.127478

Cheung, E. C., and Vousden, K. H. (2022). The role of ROS in tumour development and progression. *Nat. Rev. Cancer.* 22, 280–297. doi:10.1038/s41568-021-00435-0

Chung, H. Y., Baek, B. S., Song, S. H., Kim, M. S., Huh, J. I., Shim, K. H., et al. (1997). Xanthine dehydrogenase/xanthine oxidase and oxidative stress. *Age* 20, 127–140. doi:10.1007/s11357-997-0012-2

Chung, H. Y., and Yu, B. P. (2000). Significance of hepatic xanthine oxidase and uric acid in aged and dietary restricted rats. *Age* 23, 123–128. doi:10.1007/s11357-000-0013-x

Fan, M. X., Chen, G. L., and Guo, M. Q. (2022). Potential antioxidative components in *Azadirachta indica* revealed by bio-affinity ultrafiltration with SOD and XOD. *Antioxidants* 11, 658. doi:10.3390/antiox11040658

Fan, M. X., Chen, G. L., Zhang, Y. L., Nahar, L., Sarker, S. D., Hu, G. W., et al. (2020). Antioxidant and anti-proliferative properties of *Hagenia abyssinica* roots and their potentially active components. *Antioxidants* 9, 143. doi:10.3390/antiox9020143

Feng, H. X., Chen, G. L., Zhang, Y. L., and Guo, M. Q. (2021). Exploring multifunctional bioactive components from *Podophyllum sinense* using multi-target ultrafiltration. *Front. Pharmacol.* 12, 749189. doi:10.3389/fphar.2021.749189

Jiao, J., Yang, Y., Wu, Z., Li, B., Zheng, Q., Wei, S., et al. (2019). Screening cyclooxygenase-2 inhibitors from *Andrographis paniculata* to treat inflammation based on bio-affinity ultrafiltration coupled with UPLC-Q-TOF-MS. *Fitoterapia* 137, 104259. doi:10.1016/j.fitote.2019.104259

Kim, H. N., Kim, J. D., Park, S. B., Son, H. J., Park, G. H., Eo, H. J., et al. (2020). Anti-inflammatory activity of the extracts from *Rodgersia podophylla* leaves through activation of Nrf2/HO-1 pathway, and inhibition of nf-κb and MAPKs pathway in mouse macrophage cells. *Inflamm. Res.* 69, 233–244. doi:10.1007/s00011-019-01311-2

Li, B. H., Wu, J. D., and Li, X. L. (2013). LC-MS/MS determination and pharmacokinetic study of bergenin, the main bioactive component of *Bergenia purpurascens* after oral administration in rats. *J. Pharm. Anal.* 3, 229–234. doi:10.1016/j.jpha.2013.01.005

Liu, G. Q., Dong, J., Wang, H., Wan, L. R., Duan, Y. S., and Chen, S. Z. (2009). ESI fragmentation studies of four tea catechins. *Chem. J. Chin. Univ.* 30, 1566–1570. doi:10.3321/j.issn:0251-0790.2009.08.017

Liu, N., Xu, H., Sun, Q. Q., Yu, X. J., Chen, W. T., Wei, H. Q., et al. (2021). The role of oxidative stress in hyperuricemia and xanthine oxidoreductase (XOR) inhibitors. *Oxid. Med. Cell. Longev.* 2021, 1470380–1470415. doi:10.1155/2021/1470380

Lobo, V., Patil, A., Phatak, A., and Chandra, N. (2010). Free radicals, antioxidants and functional foods: impact on human health. *Pharmacogn. Rev.* 4, 118–126. doi:10.4103/0973-7847.70902

Mi, S. Y., Gong, L., and Sui, Z. Q. (2020). Friend or foe? An unrecognized role of uric acid in cancer development and the potential anticancer effects of uric acid-lowering drugs. *J. Cancer.* 11, 5236–5244. doi:10.7150/jca.46200

Muema, F. W., Liu, Y., Zhang, Y. L., Chen, G. L., and Guo, M. Q. (2022). Flavonoids from *Selaginella doederleinii* hieron and their antioxidant and antiproliferative activities. *Antioxidants* 11, 1189. doi:10.3390/antiox11061189

Oka, S., Tsuzuki, T., Hidaka, M., Ohno, M., Nakatsu, Y., and Sekiguchi, M. (2022). Endogenous ROS production in early differentiation state suppresses endoderm differentiation via transient FOXC1 expression. *Cell. Death Discov.* 8, 150. doi:10.1038/s41420-022-00961-2

Payne, A. C., Mazzer, A., Clarkson, G. J., and Taylor, G. (2013). Antioxidant assays - consistent findings from FRAP and ORAC reveal a negative impact of organic cultivation on antioxidant potential in spinach but not watercress or rocket leaves. *Food Sci. Nutr.* 1, 439–444. doi:10.1002/fsn3.71

Pyo, S. J., Lee, Y. J., Kang, D. G., Son, H. J., Park, G. H., Park, J. Y., et al. (2020). Antimicrobial, antioxidant, and anti-diabetic activities of *Rodgersia podophylla*. *J. Life Sci.* 30, 298–303. doi:10.5352/JLS.2020.30.3.298

Rakotondrabe, T. F., Fan, M. X., Zhang, Y. L., and Guo, M. Q. (2022). Simultaneous screening and analysis of anti-inflammatory and antiproliferative compounds from *Euphorbia maculata* combining bio-affinity ultrafiltration with multiple drug targets. *J. Anal. Test.* 6, 98–110. doi:10.1007/s41664-022-00225-z

Ren, H., Cui, X. M., Hu, J., Liu, X. M., and Chen, Z. Y. (2021). Analysis on chemical constituents in rhizomes of *Bergenia scopulosa* by UHPLC-Q exactive focus MS/MS. *Chin. J. Exp. Tradit. Med. Formulae.* 27, 118–128. doi:10.13422/j.cnki.syfjx.20210146

Rumora, L., Hlapcic, I., Popovic-Grle, S., Rako, I., Rogic, D., and Cepelak, I. (2020). Uric acid and uric acid to creatinine ratio in the assessment of chronic obstructive pulmonary disease: potential biomarkers in multicomponent models comprising IL-1beta. *PLoS One* 15, e0234363. doi:10.1371/journal.pone.0234363

Sha, Y. H., Mao, X. Y., Wu, Q. Z., Zhang, J., and Chen, W. D. (2021). Flavonoid composition and antioxidant activity of *Diaphragma juglandis* fructus. *Food Sci.* 42, 91–98. doi:10.7506/spkx1002-6630-20200423-304

Tomczyk, O., and Małgorzata, R. (2021). How to express the antioxidant properties of substances properly?. *Chem. Pap.* 75, 6157–6167. doi:10.1007/s11696-021-01799-1

Wang, W., Pang, J., Ha, E. H., Zhou, M., Li, Z., Tian, S., et al. (2020). Development of novel NLRP3-XOD dual inhibitors for the treatment of gout. *Bioorg. Med. Chem. Lett.* 30, 126944. doi:10.1016/j.bmcl.2019.126944

Wang, X. M., Xu, Q. P., Cheng, Q. N., Xu, X. H., Ma, D. D., and Quan, M. F. (2012a). *Rodgersia aesculifolia* bata extract inhibits xanthine oxidase activity and antioxidant effect. *Lishizhen Med. Mat. Med. Res.* 23, 2769–2770. doi:10.3969/j.issn.1008-0805.2012.11.047

Wang, Y., Bao, J. K., and Jin, Y. (2012b). HPLC fingerprint and chemical pattern recognition method of *Rodgersia pinnata*. *Chin. J. Exp. Tradit. Med. Formulae.* 18, 85–88. doi:10.13422/j.cnki.syfjx.2012.14.033

Xiao, Y., Hu, Z. Z., Yin, Z. T., Zhou, Y. M., Liu, T. Y., Zhou, X. L., et al. (2017). Profiling and distribution of metabolites of procyanidin B2 in mice by UPLC-DAD-ESI-IT-TOF-MS^n technique. *Front. Pharmacol.* 8, 231. doi:10.3389/fphar.2017.00231

Xie, J. L., Sun, J., Lu, Y., Zhang, X., Li, Y. J., and Liu, C. H. (2022). Research progress on *Rodgersia sambucifolia*. *Chin. J. Ethnomed.* 31, 72–81.

Xu, Y. B., Chen, G. L., and Guo, M. Q. (2019). Antioxidant and anti-inflammatory activities of the crude extracts of *Moringa oleifera* from Kenya and their correlations with flavonoids. *Antioxidants* 8, 296. doi:10.3390/antiox8080296

Yan, M. R., Ma, Y. M., Luo, G. P., Chen, C., Zhang, C. L., and Wang, X. N. (2017). Screening chemical constituents with anti-oxidative activity from *Rodgersia aesculifolia*. *Chin. Med. J. Res. Prac.* 31, 26–29. doi:10.13728/j.1673-6427.2017.05.007

Yang, S., and Lian, G. (2020). ROS and diseases: role in metabolism and energy supply. *Mol. Cell. Biochem.* 467, 1–12. doi:10.1007/s11010-019-03667-9

Yu, W., and Cheng, J. D. (2020). Uric acid and cardiovascular disease: an update from molecular mechanism to clinical perspective. *Front. Pharmacol.* 11, 582680. doi:10.3389/fphar.2020.582680

Zhang, M., Feng, B., Zhou, B. K., Liu, Y., Li, M. X., Chang, K., et al. (2015). Overview of pharmaceutical research on *Rodgersia aesculifolia* batal. *J. Anhui Agric. Sci.* 43, 33–35. doi:10.3969/j.issn.0517-6611.2015.01.010

Zhang, X. Y., Li, D. W., Wang, Y. C., and Sun, S. Q. (2005). Distribution and medical value of *Rodgeris aesculifolia* and its exploitation. *Subtrop. Plant Sci.* 34, 60–62. doi:10.3969/j.issn.1009-7791.2005.02.020

Zhang, Y., Yang, X., Liu, X., Shi, R. M., and Ma, X. T. (2021). Analysis of antioxidant activity of *Rodgersia aesculifolia*. *Batal. Sci. Technol. Chem. Ind.* 29, 28–32. doi:10.16664/j.cnki.issn1008-0511.2021.01.006

Zhuang, X. C., Chen, G. L., Liu, Y., Zhang, Y. L., and Guo, M. Q. (2021). New lignanamides with antioxidant and anti-inflammatory activities screened out and identified from *Warburgia ugandensis* combining affinity ultrafiltration LC-MS with SOD and XOD enzymes. *Antioxidants* 10, 370. doi:10.3390/antiox10030370

frontiers | Frontiers in Pharmacology

TYPE Review
PUBLISHED 17 November 2023
DOI 10.3389/fphar.2023.1304342

OPEN ACCESS

EDITED BY
Patrícia Mendonça Rijo,
Lusofona University, Portugal

REVIEWED BY
Ravindra N. Singh,
Iowa State University, United States
Kay Richards,
University of Melbourne, Australia

*CORRESPONDENCE
D. Collotta,
debora.collotta@unito.it

†These authors share first authorship

RECEIVED 29 September 2023
ACCEPTED 31 October 2023
PUBLISHED 17 November 2023

CITATION
Collotta D, Bertocchi I, Chiapello E and Collino M (2023), Antisense oligonucleotides: a novel Frontier in pharmacological strategy.
Front. Pharmacol. 14:1304342.
doi: 10.3389/fphar.2023.1304342

Antisense oligonucleotides: a novel Frontier in pharmacological strategy

D. Collotta[1*†], I. Bertocchi[1,2†], E. Chiapello[1] and M. Collino[1]

[1]Department of Neuroscience Rita Levi Montalcini, University of Turin, Turin, Italy, [2]Neuroscience Institute Cavalieri Ottolenghi (NICO), University of Turin, Turin, Italy

Antisense oligonucleotides (ASOs) are short single stranded synthetic RNA or DNA molecules, whereas double-stranded RNA nucleotide sequences are called small interfering RNA (siRNA). ASOs bind to complementary nucleic acid sequences impacting the associated functions of the targeted nucleic acids. They represent an emerging class of drugs that, through a revolutionary mechanism of action, aim to directly regulate disease-causing genes and their variants, providing an alternative tool to traditional "protein-specific" therapies. The majority of the ASOs are designed to treat orphan genetic disorders that in most of the cases are seriously disabling and still lacking an adequate therapy. In order to translate ASOs into clinical success, constant technological advances have been instrumental in overcoming several pharmacological, toxicological and formulation limitations. Accordingly, chemical structures have been recently implemented and new bio-conjugation and nanocarriers formulation strategies explored. The aim of this work is to offer an overview of the antisense technology with a comparative analysis of the oligonucleotides approved by the Food and Drug Administration (FDA) and the European Medicines Agency (EMA).

KEYWORDS

antisense oligonucleotide, siRNA, genetic disorder, gene silencing, pharmacology

1 Introduction

Last century has witnessed the drug development process primarily based on the small molecules and antibodies (Bennett, 2019). Recently, antisense oligonucleotides (ASO)-based research has gained momentum due to sequence-specific targets it employs for the therapeutic development. In particular, they represent an opportunity for strategical intervention to target RNA encoding proteins that are difficult to reach with conventional therapy, or to selectively target non-coding RNAs acting as activators/silencers of gene expression and dysregulated endogenous microRNAs that can lead to various diseases (Zamecnik and Stephenson, 1978; Levin, 2019). Although the first preclinical use of synthetic oligonucleotides to modulate RNA function dates back to 1978 (Zamecnik and Stephenson, 1978), their production as drugs has required constant improvements in chemistry, genomics, pharmacology, delivery and formulation platforms to increase their efficacy, safety and biodistribution (Levin, 2019). Recently, after many years of slow progress, ASO research is accelerating, with a variety of clinical trials that have reached their decisive stage during the years 2016–2020 (Shen and Corey, 2018). Via the interaction with different targets and through different molecular mechanisms, ASOs exert important positive effects in reducing oxidative stress, which exerts a pivotal role in several conditions, such as cancer, Alzheimer's disease, diabetes, cardiovascular and inflammatory disorders. To date, the Food and Drug Administration (FDA) has approved thirteen ASOs for clinical use,

while the European Medicines Agency (EMA) has authorised eight of them. In addition, several antisense drugs are now undergoing clinical trials for the management of cardiovascular, metabolic, endocrine, neurological, inflammatory and infectious diseases (Dhuri et al., 2020).

2 Mechanism of action of DNA and RNA antisense oligonucleotides

ASOs are polymers consisting of 15–21 nucleotides (Vegeto et al., 2019). There are different kinds of ASOs: single stranded DNA ASOs or RNA nucleotide sequences which are usually complementary to an endogenous miRNA (7), and double-stranded complexes, called short interfering RNA (siRNA) (Bajan and Hutvagner, 2020). ASOs are chemically synthesized to bind via complementary base-pairing a specific sequence of nucleic acid, as a messenger RNA (mRNA), or its nuclear precursor (pre-mRNA) (Levin, 2019).

When single stranded, ASOs have to be stable and able to be selectively addressed to their target before the degradation due to circulating nucleases. On the other hand, the duplex structure of siRNAs makes them more stable than ASOs in the blood as well as within the cells. However, systemic delivery of double-stranded siRNA is more challenging as they have larger molecular weight and negative charge. Moreover, they have hydrophilic phosphates on their outside surface, while the aromatic nucleobases are located mainly inside the duplex, thus leading to scarce interactions with plasma membranes and quite rapid renal excretion (Meister et al., 2004).

Once the ASOs has bound to the target RNA, a number of possible molecular mechanisms are triggered, which can be broadly classified as: (a) those promoting RNA cleavage through the recruitment of endogenous enzymes; (b) those that interfere with mRNA translation or maturation without promoting the degradation of the target (Ward et al., 2014). ASOs and siRNA are distinct classes of nucleic acid-based therapeutic molecules, each characterized by its own distinct mechanism of action. However, despite their individual disparities, both ASOs and siRNA possess remarkable potential as therapeutic agents, providing versatile means to modulate gene expression. This shared capacity makes them invaluable tools for addressing genetic diseases and holds the promise of reshaping disease progression through precise and targeted interventions. By collectively exploring ASOs and siRNA within the context of gene regulation strategies, we try to encompass the comprehensive landscape of nucleic acid-based therapeutics, acknowledging their distinctiveness while embracing their mutual contributions to advancing the field.

2.1 Cleavage of target RNAs by recruitment of endogenous enzymes

2.1.1 RNA degradation by activation of ribonucleases (RNase)

One of the common mechanisms for RNA target inactivation is the induction of RNase H, a family of endonucleases that selectively cleave the RNA strand of RNA/DNA hybrids (Bennett and Swayze, 2010). In the context of mRNA/ASO heteroduplexes, RNase H induces the degradation of the target mRNA.

2.1.2 RNA interference (RNAi)

siRNAs act by using the RNA interference (RNAi) pathway, a natural cellular defence mechanism evolved to recognize and degrade pathogenic RNAs (Bajan and Hutvagner, 2020). For this reason, siRNA intracellular protein association and binding to the target is generally highly selective and specific, making them suitable therapeutic tools (Schwarz et al., 2006).

siRNAs enter the physiological process of RNAi by associating with TAR RNA-binding protein (TRBP) and the argonaut 2 enzyme (AGO2), composing the RNA-Induced Silencing Complex (RISC). Once the siRNA is part of RISC, one RNA strand is cleaved and released, whereas the remaining guide strand finds the complementary mRNA, forming an RNA-RNA hybrid that induces AGO2 to degrade the target RNA (Meister et al., 2004).

The formation of RISC participates in cell-based defence, for example, against viruses. Despite that, siRNA-based drug applications are not limited to infective diseases, but they can be used for treating different types of cancers and various pathological conditions, including inflammatory disorders and neuropathies.

When the guide or sense strand binds off-target transcripts, the RNAi-related mechanism of action of siRNA may cause unwanted activity. An important safety concern related to therapeutic siRNA mechanism of action is the possible non-specific suppression of non-target mRNAs by the passenger strand. Also ASOs can induce off-target effects by association with sequences having a high degree of homology or by interactions with proteins (Chi et al., 2017).

2.2 Inactivation without mRNA degradation

Another mechanism used by ASOs for RNA inactivation is by preventing the interaction of mRNA with the ribosomes for reasons of steric hindrance. ASOs also interfere with mRNA maturation by constraining splicing or destabilizing nuclear pre-mRNA.

2.2.1 Translation or maturation blockade of messenger RNA by steric hindrance

Due to steric bulk, after pairing with the mRNA, an ASO can block the translation of the transcript with one of the following mechanisms: i) by hindering its contact with the ribosomal 40S subunit; ii) by avoiding the assemblage of the 40S/60S subunits; iii) by hampering the sliding of the ribosome along the transcript; iv) by impeding the interaction with sequences that are essential for the maturation of the transcript, such as the addition of a 7-methylguanosine cap at the 5′ end and polyadenylation at the 3′ end (Bennett and Swayze, 2010). Steric hindrance can have a crucial role also in splicing modulation, as described below.

2.2.2 Splicing modulation

The goal of ASO therapy is to block the production of an abnormal form of protein or to restore the production of a protein that is lacking or not functioning (Havens et al., 2013). ASOs can bind the primary transcript within the nucleus and interfere with the spliceosome-mediated maturation process (Figure 1). Modulation of splicing by oligonucleotides consists of

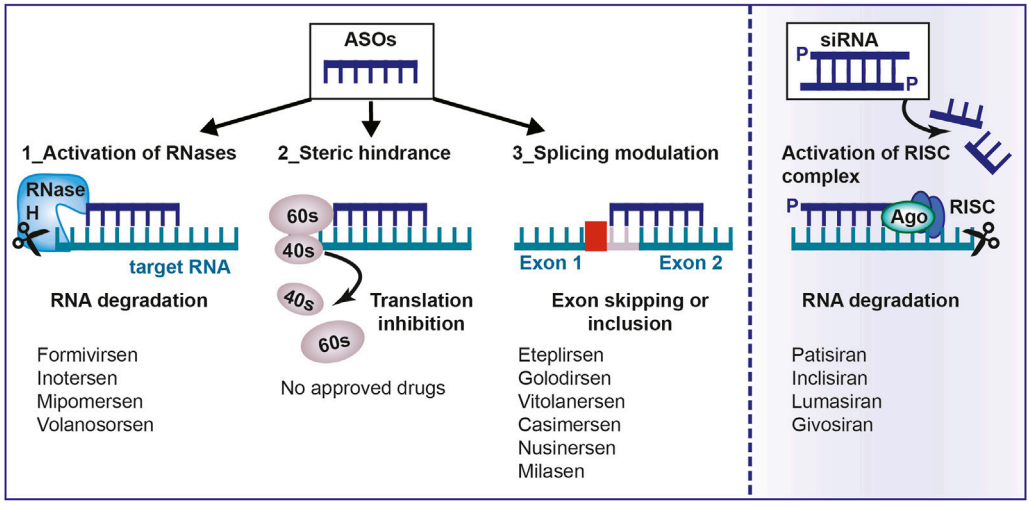

FIGURE 1
Mechanism of action of antisense oligonucleotides. Antisense oligonucleotides and siRNA can be used to target a specific, complementary (coding or non-coding) RNA. Main mechanisms of actions are: 1) RNA cleavage through the recruitment of endogenous enzymes; 2) Steric hindrance; 3) Splicing modulation; 4) Activation of RISC complex by the double-stranded siRNA. ASO, antisense oligonucleotides; aODN, siRNA: small-interfering RNA; RNase H, Ribonuclease H; RISC, RNA inducing silencing complex; mRNA, messenger RNA.

leading to exon skipping or exon inclusion. In exon skipping, ASOs bind pre-mRNAs and correct the mutation that caused the disruption of the reading frame by forming a transcript that, even if truncated, still encodes for a partially functional protein (Dhuri et al., 2020). In exon inclusion, ASOs are designed in order to target and repress regulatory elements resulting in the prevention of splicing events and the production of a full-length protein. In this regard, it is noteworthy to mention that not only linear motifs, but also RNA secondary structures that are formed because of long-distance interaction (LDI), regulate alternative splicing and can be targeted by ASOs. One of the first report about this mechanism is the study by Singh et al., 2013 who, by using cells from patients affected by spinal muscular atrophy (SMA), demonstrated the effectiveness of an ASO in correcting SMN2 exon 7 splicing, via the sequestration of the 3′ strand of an unique intra-intronic structure termed internal stem through LDI-1 (ISTL1) (Singh et al., 2013).

2.2.3 miRNA inhibition

MicroRNAs (miRNA) are small RNA molecules essential for gene regulation. They bind AGO proteins forming RISC, sharing the same proteins used by RNAi. Indeed, given that siRNA drugs compete with endogenous miRNAs to bind AGO2, it is important to optimize their dose to avoid RISC saturation and, in turn, inhibition of the RISC complex.

2.3 Aptamers

A particular class of single-stranded DNA or RNA oligonucleotides is represented by aptamers. They have a three-dimensional structure that allows a highly specific interaction with proteins (Wiraja et al., 2014), this means that aptamer binding is mainly determined by its tertiary structure and not by the primary sequence. Unlike the previous classes, aptamers are identified through the Systematic Evolution of Ligands by Exponential Enrichment (SELEX) (Ohuchi, 2012). An aptamer currently in clinical use is pegaptanib, an RNA aptamer directed against vascular endothelial growth factor (VEGF)-165, responsible for pathological ocular neovascularization associated with age-related macular degeneration (Ng et al., 2006). Another aptamer that has been recently approved for the treatment of geographic atrophy, also secondary to age-related macular degeneration, is avacincaptad pegol, an inhibitor of the complement component 5 (Kang, 2023).

3 Pharmacokinetics

Having explored the diverse mechanisms by which ASOs exert their effects on target RNA, it is crucial to delve into their pharmacokinetics to better understand how these therapeutic molecules behave within the body. Understanding of pharmacokinetics is important in the drug development and safety field. This is particularly true for ASOs, where pharmacokinetics is intricately intertwined with the chemical properties of these therapeutic molecules. ASOs undergo various chemical modifications that impact their internucleotide links (first generation ASOs), the connecting rings between the ASO backbone and nucleobases (second generation ASOs), and the nucleobases themselves, which play a vital role in complementary base pairing with target RNA. These chemical alterations not only define the structural characteristics of ASOs but also govern their pharmacokinetic behavior, ultimately influencing their therapeutic effectiveness and safety profiles (Shadid et al., 2021).

The main route of administration for ASOs is the parenteral one (either intravenous or subcutaneous) (Geary et al., 2015). After subcutaneous (SC) infusion, ASOs move into the circulation, with peak concentrations reached within 3–4 h for the second generation of ASOs (Levin et al., 2007). Plasma concentration decrease in a

multi-exponential mode characterised by a dominant rapid first phase of distribution in which the drug is transported to tissues (minutes/hours) (Geary et al., 2015), followed by a slower second phase of elimination (the half-life can reach up to several weeks for ASOs with both backbone and sugar modifications). The first phase of distribution is largely driven by backbone chemistry (Levin et al., 2007). The phosphorothioate (PS) backbone gives an important pharmacokinetic benefit, given that the increased binding to proteins allows a significant release to many tissues. Indeed, tissue distribution of PS-modified ASOs is relatively broad, with the organs reaching the highest concentration being the liver and kidney, followed by bone marrow, adipocytes and lymph nodes (Vegeto et al., 2019). At the tissue level, intracellular uptake of ASOs occurs by endocytosis mediated by surface receptors (integrins, scavenger receptors and Toll-like receptors) (Vegeto et al., 2019). Passive diffusion of ASOs into cells is limited by the fact that they are large molecules (single-stranded ASOs are 4–10 kDa, double-stranded siRNA are 14 kDa) and have a negatively charged surface because of phosphate groups, resulting in electrostatic repulsion with the cell membrane (Roberts et al., 2020). Systemically delivered drugs directed at the central nervous system (CNS) encounter a further impediment to their action, namely, the blood-brain barrier (Bennett et al., 2017).

Subsequent to their release from the endolysosome, ASOs navigate to their designated site of action, endeavoring to evade degradation or re-exportation via exocytosis (Sahay et al., 2013). Following their liberation from the endolysosome, these ASOs exhibit extended half-lives (ranging from 2 to 4 weeks) and exert prolonged inhibitory effects on the expression of their target RNA (Geary et al., 2015). The subsequent elimination phase operates through a diverse array of intricate mechanisms, collectively ensuring the methodical clearance of ASOs from the biological system. Among these mechanisms, direct excretion via the renal glomerular filtration system emerges as a crucial avenue, facilitated by the kidneys' finely tuned filtration capabilities. Concurrently, ubiquitous tissue and serum endo- and exonucleases engage in a metabolic interplay, progressively degrading ASOs and priming them for subsequent elimination. The orchestrated choreography extends to circulating macrophages, vigilant custodians of the endothelial reticulum system, engaging in the meticulous task of phagocytic uptake. These sentinel cells envelop the ASOs, facilitating their eventual removal from circulation. Additionally, specific plasma proteins contribute to the orchestration of this elimination phase, potentially inactivating or sequestering ASOs and guiding their transition from active therapeutic agents to inert remnants (Kilanowska and Studzińska, 2020). Currently, all approved ASOs are either administered locally, such as directly into the eye and the cerebrospinal fluid, or act in the liver after parenteral administration (Roberts et al., 2020). Intravitreal administration limits systemic absorption to 1% of the administered dose, minimising the toxicological risk (Bennett et al., 2017). This route has been used for the delivery of fomivirsen, to treat cytomegalovirus retinitis. Intrathecal administration is required to treat diseases of the CNS. It ensures a high distribution in the cortical tissue and spinal cord and a lower concentration in deeper brain structures (Geary et al., 2015). Lastly, drug delivery to the liver by parenteral administration is facilitated by several factors: the high perfusion of the liver, the presence of a fenestrated sinusoidal endothelium that allows the passage of ASOs and the high concentration on the hepatocyte membrane of receptors that can facilitate the endocytotic process (e.g., the asialoglycoprotein receptor, ASGR) (Tanowitz et al., 2017). In contrast, the development of technologies for extra hepatic delivery is still the main goal in the field of ASOs.

4 Strategy to enhance delivery

4.1 Chemical modification

The use of chemical modifications has been crucial to increase ASO enzymatic stability, target recognition, binding efficiency, tissue distribution and, at the same time, to reduce their toxicity, leading to significant improved antisense drugs (Edvard Smith and Zain, 2019). The most common and relevant modifications of currently marketed oligonucleotides are applied at the level of the backbone (first generation ASOs), the heterocycle and the sugar, as discussed below. The key role played by the introduced chemical components is demonstrated by the fact that most of the ASOs approved to date are "naked", i.e., without an additional delivery vehicle (Roberts et al., 2020).

4.1.1 Backbone modifications/phospodiester linkage modifications

The primary reason for modification of the oligonucleotide backbone is the inherent instability of the phosphodiester bond to nucleases. This can be prevented by the non-bridging replacement of the phosphodiester bond with a sulphur atom (Eckstein, 2000). The phosphorothioate (PS) backbone confers a delay in renal clearance by increasing both resistance to nucleases action and binding to plasma (e.g., albumin) and intracellular (e.g., nucleolin) proteins (Gaus et al., 2019). PS ASOs, (first generation), are stable in plasma and tissues (half-life: 2–3 days). PS binding allows the activation of RNase H. Although it creates a minor reduction in binding affinity to the target, it is possible balance it by some modifications, such as, e.g., additional modifications to the sugar backbone portions (Roberts et al., 2020; Oberemok et al., 2018). Moreover, PS ASOs enter cells more easily: PS is recognised by scavenger receptors (such as STAB1 and STAB2 stabilins) that facilitate internalisation in tissues such as the liver (Miller et al., 2018). Despite this, *in vivo* studies have demonstrated the necessity of high and repeated doses to achieve the therapeutic effect (Vegeto et al., 2019). A toxicological limitation of PS ASOs is the triggering of immune reactions by activation of Toll-like receptors (TLRs) (Vegeto et al., 2019). Moreover, an extra sulfur atom can be added into the PS linkage, resulting in a chiral centre at each modified phosphorous atom, producing two possible stereoisomeric forms having different physiochemical properties and pharmacological activity (Roberts et al., 2020).

Besides the modifications of the phosphorodextrin backbone linkage, isosteric substitutions of the phosphoriboside group have been implemented giving rise to two classes of ASO analogues: phosphorodiamidate morpholino oligomers (PMOs) and nucleic peptide acids (PNAs). PMOs are characterized by the substitution of ribose with morpholino and of the phosphorodextere bond with a

phosphorodiamine bond. PNAs, on the other hand, are synthetic nucleic acid imitations containing neutral N-2-aminoethyl glycine units, with nucleobases linked by a flexible methyl carbonyl linker (Dhuri et al., 2020). Both classes are neutral and therefore form very stable hybrids with the target RNA and have high resistance to nuclease action (Bennett et al., 2017). However, they do not support the activity of endogenous enzymes such as RNAse H or AGO2 and exert their action through mechanisms of steric hindrance and splicing modulation (Bennett et al., 2017). The lack of binding to serum proteins results in a rapid renal clearance.

4.1.2 Heterocycle/nucleobase modifications

The main positive effect of modifications applied to the heterocycle is the increase of the binding affinity to the target (Herdewijn, 2000). One of the most implemented adjustment is the replacement of the C5 hydrogen of deoxycytidine with a methyl group (Vasquez et al., 2021). The introduction of the methyl group between the nitrogenous bases in the major groove confers increased thermal stability to the duplex (Sahay et al., 2013). This modification supports RNase H activity and is used to reduce the immunostimulatory potential of PS ASOs (Bennett et al., 2017).

4.1.3 Ribose sugar modifications

Currently, modifications of the hydroxyl in the 2′ position of the sugar portion of deoxyribose in DNA and ribose in RNA, respectively, have made the greatest contribution in increasing the pharmacological properties of oligonucleotides by creating second-generation ASOs (Bennett et al., 2017). The most commonly used substitutions are the fluorine group (2′-F), the methyl group (2′-O-Me) and the methoxymethyl group (2′-O-MOE) (Tanowitz et al., 2017). This variation is notable, on one hand, for its increased nuclease resistance, as it blocks the nucleophilic portion of the hydroxyl at the 2′ position of the sugar, and, on the other hand, for its increased thermal stability at complementary hybridisation, which allows tighter binding and the use of shorter oligonucleotides (Shen and Corey, 2018). Unfortunately, modifications at the 2′ position are not compatible with RNAse H-mediated cleavage activity (Shen and Corey, 2018). This limitation was minimised through the use of the gapmers strategy. This method makes use of a central region of unmodified DNA or RNA ASOs supporting RNase H activity flanked by ends of 20 nucleotides modified in 2' (Tanowitz et al., 2017). For siRNA, the situation is more complex as they must retain the ability to be recognised by the AGO2 cleavage enzyme. However, the RNAi machinery is remarkably tolerant to chemical modifications carried out at the 2′ position of the sugar (e.g., givosiran) (Roberts et al., 2020; Allerson et al., 2005).

Instead Bridged nucleic acids (BNAs) contain a constrained bridge between 2′ oxygen and 4' carbon of the ribose ring (Dhuri et al., 2020). These bicyclic systems have been fused into the flanking regions of gapmers as they have an ideal conformation to interact with complementary DNA or RNA sequences showing a strong increase in binding affinity (Roberts et al., 2020).

4.1.4 Terminal modification

Phosphorylation at the 5′ end of the siRNA guide strand is crucial for activity, because it mediates the binding to AGO2 (Schirle and MacRae, 2012; Frank et al., 2010). To limit the subtraction of this group by cellular phosphatases, the introduction of 5′-vinyl phosphonate as an imitation phosphate that is not a substrate of phosphatases has been functionally introduced (Haraszti et al., 2017). Terminal modifications can drastically improve the therapeutic efficacy of small ASOs. For instance, the incorporation of PEG-282 and propyl modifications at the 5′ and 3′ ends, respectively, of a small ASO (8-mer), ameliorated its effectiveness *in vivo*, leading to improved symptoms in both severe and mild mouse models of spinal muscular atrophy (SMA) (Keil et al., 2014).

4.2 Nanoformulation-based delivery

Advances in nanotechnology make it possible to overcome certain pharmacokinetic limitations of ASOs, including plasma and endosomal degradation, direct renal clearance and intracellular transmembrane delivery (Roberts et al., 2020). The nanoparticles, absorbed by endocytosis, are, however, heterogeneously sized (around 100 nm) with limited biodistribution due to difficulty of diffusion through the extracellular matrix of tissues (Tanowitz et al., 2017). Their action is mainly concentrated in the liver and in the reticuloendothelial system, since the sinusoidal capillary endothelium has sufficient openings to allow nanocarriers in (Wisse et al., 2008). Nanocarriers are also a potential approach in the field of oncology, as they show an accumulation in the tumour environment due to the EPR (enhanced permeability and retention) effect (Dhuri et al., 2020).

4.2.1 Lipoplexes and liposomes

Lipid-based delivery systems, such as lipoplexes and liposomes, derive from mixing polyanionic oligonucleotides with lipids. These formulations are able to mask the negative charge of the ASOs in order to reduce electrostatic repulsion with the cell surface (Vegeto et al., 2019). Specifically, polyplexes result from the direct interaction between polyanionic ASOs and polycationic lipids (Rehman et al., 2013). In contrast, liposomes are closed and stable vesicular systems characterised by a lipid bilayer in which the ASO is confined within the aqueous space (Ickenstein and Garidel, 2019). Some lipid nanoparticles (LNPs, stable nucleic acid lipid particles) consist in polycationic lipids (Roberts et al., 2020). In order to minimise the interaction with plasma opsonins, which lead to rapid degradation by phagocytes of the reticuloendothelial system, a shielding strategy has been adopted. The most commonly used polymer to create a superficial steric barrier to shield the residual charge is polyethylene glycol (PEG) (Ambegia et al., 2005). An example of LNP-based siRNA formulation is Patisiran used to treat transthyretin-mediated amyloidosis.

4.2.2 Polymeric nanoparticles

Polymeric nanoparticles result from the non-covalent complexation between negatively charged ASOs and cationic polymers, including PEI (polyethylenimine), PBAE (poly-(beta-amino ester)) or poly-L-lysine (Geary et al., 2002). After endocytosis, in order to transport the ASO from the endolysosome to the cytoplasmic compartment, PEI and PBAE have an effect known as the "proton-sponge effect" (Benjaminsen

et al., 2013), whereas poly-L-lysine-based nanoparticles incorporate fusogenic peptides or lytic domains capable of destabilising the endosomal membrane (Geary et al., 2002). However, the clinical advancement of polymeric nanoparticles has been limited by bioincompatibility and the inevitable toxicity in chronic use resulting from the undesired interaction between the chaperone charge and serum and tissue proteins (Dhuri et al., 2020).

4.2.3 Exosomes

Exosomes are biological nanoparticles whose use as delivery systems is current under study at a preclinical level. In particular, exosomes are extracellular bilayer vesicles, ranging in size from 30 to 100 nm, whose function is to facilitate intercellular communication through the transfer of nucleic acids, lipids and proteins (Tanowitz et al., 2017). Exosomes show many benefits related to oligonucleotide drug delivery as they are able to cross biological membranes, are protected from phagocytosis and are not toxic (Roberts et al., 2020).

4.2.4 Spherical nucleic acid (SNA)

SNA particles consist of a densely packed shell of nucleic acids, which are oriented around a hollow or solid core nanoparticle. SNA particles are currently undergoing clinical trials for the administration of ASOs to tumors (such as glioblastoma) or for their topical administration in the treatment of psoriasis (Kapadia et al., 2018).

4.3 Conjugation strategies

The potential delivery of ASOs to DNA and RNA can be enhanced by conjugation with ligands able to promote cellular uptake and active targeting by interaction with superficial receptors and, on the other hand, to reduce the direct renal clearance of ASOs by increasing their size (Roberts et al., 2020). The most commonly used ligands are lipids, sugars, peptides, aptamers or antibodies. Unlike nanoparticles, they are well-defined molecular entities characterised by standard techniques, with a favourable biodistribution profile (Tanowitz et al., 2017).

4.3.1 Lipid conjugates

The main result of this technological approach concern exposure to the liver, that have been achieved through conjugation with cholesterol and lipid groups such as long-chain fatty acids and α-tocopherol (Bennett et al., 2017). It has been shown that the *in vivo* activity of lipid-conjugated ASOs depends on their ability to bind plasma lipoproteins and thus exploit the endogenous system for lipid transport and uptake (Roberts et al., 2020).

4.3.2 GalNac conjugates

An optimal delivery strategy to hepatocytes is trivalent conjugation of N-acetyl-galactosamine (GalNac) to the siRNA passenger strand or single-stranded DNA ASOs (Prakash et al., 2014). This ligand is a carbohydrate portion with high affinity and selectivity for asialoglycoprotein receptor 1 (ASGR1), which is densely expressed at the plasma membrane of hepatocytes (approximately 5*105 copies per hepatocyte) (Tanowitz et al., 2017). Upon ligand binding, the receptor-ligand pair is internalised in the endosomes. The acidic endomembrane environment promotes dissociation of the ligand from the receptor, allowing the receptor to coming back to the plasma membrane and the ligand-conjugate to be available for pharmacological action (Springer and Dowdy, 2018). Subsequently, the GalNac portion undergoes enzymatic degradation. Conjugation with GalNac increases the power of the ASO by approximately 30-fold and increases entry into hepatocytes (otherwise unconjugated ASOs have been detected mainly in non-parenchymal liver cells) (Roberts et al., 2020). This evidence results in an increase in the therapeutic index and, consequently, in a lower dose and/or a lower frequency of administration. In clinic, there are two examples of GalNac-conjugated siRNA: Givosiran, monthly administered to treat acute hepatic porphyria; and Inclisiran, administered twice a year in patients with familial hypercholesterolaemia. However, these important results are partly due to the liver being one of the main tissues of oligonucleotide accumulation and partly to ASGR1 receptor having many desirable features such as high expression levels, rapid internalisation and recycling (turnover of about 20 min) (Tanowitz et al., 2017).

4.3.3 Peptide conjugates

Cell-penetrating peptides (CPPs) are short peptide sequences with positive charge that have been identified as carrying neutrally charged ASOs, with which they are linked, such as PMO and PNA, across cell membranes. CPPs can penetrate into the cell through endocytosis or by perturbing the plasma membrane lipid bilayer (Tréhin et al., 2004). The use of ASO conjugated with peptides is also found in the CRISPR-Cas9 system. CRISPR-Cas9 is composed of a nonspecific nuclease (Cas9) and a series of programmable sequence-specific CRISPR RNA (crRNA), which lead to DNA cleavage by Cas9 and produce double-strand breaks once the target sites are identified (Karimian et al., 2019).

4.3.4 Antibodies and aptamer conjugates

Even though a number of technologies for hepatic delivery are available, extrahepatic targeting is still a challenge (Bennett et al., 2017). Currently, antibody- and aptamer-conjugated ASOs are in the early stages of testing in order to exploit their interaction with specific superficial receptors (e.g., transferrin receptor highly expressed in skeletal and cardiac muscle) (Roberts et al., 2020). Aptamers have a number of advantages over antibodies, including facilitating the production by chemical synthesis, low immunogenicity and lower cost (Vegeto et al., 2019).

5 Toxicology

The most toxicologically characterised classes of ASOs are the first-generation ones (ASO-PS) and the second-generation ASOs with 2′-O-MOE sugar adjustments due to the larger number of drugs in clinical use. The toxicity of ASOs is dose-proportional and can be affected by both the oligonucleotide and the formulation (Bennett et al., 2017).

5.1 Toxicity linked to the oligonucleotide

The toxicity of ASOs is commonly categorised into: hybridization-dependent or hybridization-independent way (Frazier, 2015).

5.1.1 Hybridization-dependent

Hybridization-dependent toxicity includes both excessive pharmacological effects that occur between the ASO and the target; and non-specific effects due to complementary or partial recognition of unwanted transcripts (Batista-Duharte et al., 2020).

Off-target toxicity can be avoided or minimised by implementing bioinformatics analyses for target RNA selection and sequence homology detection, performing accurate characterisation of pharmacology and toxicology in preclinical models and implementing chemical modifications (Bennett et al., 2017). A recent study conducted by Scharner et al. shows the *in vitro* effects of splice-modulating ASOs on 108 potential off-targets predicted on the basis of sequence complementarity, and identified 17 mis-splicing events for one of the ASOs tested (Scharner et al., 2020). Based on analysis of data from two overlapping ASO sequences, they conclude that off-target effects are difficult to predict, and the choice of ASO chemistry influences the extent of off-target activity. The off-target events caused by the uniformly modified ASOs tested in their study were significantly reduced with mixed-chemistry ASOs of the same sequence. Furthermore, using shorter ASOs, combining two ASOs and delivering ASOs by free uptake also reduced off-target activity. Finally, ASOs with strategically placed mismatches can be used to reduce unwanted off-target splicing events.

A more practical example that highlights the importance of implementing better ASO design is the results obtained by Ottesen et al. (2021). In this study, the transcriptome of SMA patient cells treated with 100 nM of Anti-N1 for 30 h was analyzed. While 100 nM of Anti-N1 substantially stimulated SMN2 exon 7 inclusion, it also caused massive perturbations in the transcriptome and triggered widespread aberrant splicing, affecting expression of essential genes associated with multiple cellular processes. The authors also showed a substantial reduction in off-target effects with shorter ISS-N1-targeting ASOs.

At the clinical level, toxicity may be negligible as not all RNA sites are accessible, not all tissues have pharmacological ASO concentrations and gene silencing does not necessarily lead to toxicity.

5.1.2 Hybridization-independent

There are four subcategories of non-pharmacological toxicity:

i. Tissue accumulation in the kidney and liver - The consequences related to the concentration of ASOs in the kidney and liver tissues are the most frequently encountered in preclinical toxicity studies through *in vivo* and *in vitro* studies (Frazier, 2015). They are related to the distribution and metabolism of ASOs. In the liver, ASO accumulation is mainly mediated by sinusoidal endothelial cells, followed by hepatocytes and Kupffer cells (Vegeto et al., 2019). In the kidney, accumulation of ASOs occurs at high doses by reabsorption in the cells of the proximal convoluted tubule following glomerular filtration. The main symptom of liver toxicity occurs with increased levels of circulating liver enzymes; in contrast, increased tubular proteinuria (rarely glomerular nephritis) due to disruption of tubular reabsorption capacities is the main indication of renal damage (Vegeto et al., 2019). Histological analysis of both liver and kidney tissues shows the presence of ASOs in basophilic granules at the level of the cytoplasm of epithelial cells related to an increased incidence of degenerative alterations especially in chronic use. A second common histological change is the increase in granular or vacuolated macrophages linked to cellular activation and the secretion of pro-inflammatory cytokines (Frazier, 2015).

ii. Aptamer binding - The interaction of the ASO in plasma, intracellular or cell surface proteins is known as the "aptamer effect." A common consequence is the activation of complement, coagulation and immunity (Bennett and Swayze, 2010). Generally, this toxicity is influenced by the oligonucleotide chemical class and does not depend on the sequence (Geary et al., 2015). An exception is the activation of the Toll-like receptor of innate immunity, which has shown to be dependent on sequences rich in guanine and uracil at the 3′ end (Krieg, 2006). This immunomodulatory effect, however, can be easily minimised by avoiding these sequence motifs.

iii. Pro-inflammatory mechanisms - Reactions at the injection site, fever, chills and nuchal rigidity were commonly observed during clinical trials of phosphorothioate ASOs (e.g., mipomersen) (Levin, 2019).

iv. Thrombocytopenia - At the clinical level, thrombocytopenia is a side effect that may hamper the development of ASOs after the use of gapmer PS-2′-O-MOE (Sahay et al., 2013). For example, severe thrombocytopenia has been reported in patients with transthyretin-mediated hereditary amyloidosis treated with inotersen. In these patients, monitoring of platelet counts and, if necessary, adjustment of the medicine dose is required.

5.2 Adverse effects caused by formulation

Proinflammatory and immunostimulatory effects are linked to the residual positive surface charge of some lipid nanoparticles used to promote siRNA biodistribution. Therefore, lipid nanoparticle formulations, as in the case of patisiran, require premedication with antihistamines, glucocorticoids and non-steroidal anti-inflammatory medicines to avoid unwanted effects (Coelho et al., 2013).

5.3 ASOs as interesting tools against oxidative stress

Encouraging results obtained mainly in preclinical studies suggest ASOs as interesting tools against oxidative stress. In C57BL/6J mice, an ASO was demonstrated to modulate the activity of a phosphatidylethanolamine N-methyltransferase (PEMT), that positively regulates mitochondrial ubiquinone (CoQ) content. Acute PEMT disruption mediated by ASOs was sufficient to increase mitochondrial CoQ and decrease superoxide, resulting in the preservation of insulin sensitivity and an improvement of glucose and insulin responses in high fat diet (HFD)-fed mice (Ayer et al., 2021).

Moreover, in HFD-fed mice, the treatment with generation 2.5 ASOs, which are highly potent and contain 2′–4′ constrained ethyl (cEt)-modifications that allow the binding to RNase H1.20, were used against the mammalian STE20-like protein kinase 3

(MST3) and resulted in protection against diet-induced oxidative stress at hepatic level, improving the full spectrum of HFD-induced nonalcoholic fatty liver disease, including suppressed liver steatosis, inflammation, fibrosis, and cellular damage (Caputo et al., 2021). In particular, Mst3 ASOs was able to blunt lipogenic gene expression, and accumulation of acetyl-CoA carboxylase (ACC) protein leading to a reduction of the oxidative and ER stress induced by hepatic lipotoxicity in obese mice.

The same authors had previously reported that the knockdown of MST3 in cultured human hepatocytes stimulates β-oxidation and triacylglycerol (TAG) and inhibits fatty acid influx and lipid synthesis, instead MST3 overexpression increases lipid accumulation in mouse and human liver cells. This resulted in an increase in density and size of intracellular lipid droplets, which is known to cause cellular dysfunction and contribute to the development of lipid-related metabolic disorders. The authors in fact reported that reducing or increasing MST3 abundance in human cultured hepatocytes leads to a suppression or an aggravation of oxidative stress, respectively (Cansby et al., 2019).

In a murine model of Alzheimer disease (AD), a phosphorothionated antisense against glycogen synthase kinase (GSK)-3β, GAO, lead to an improvement of learning and memory abilities coupled with a reduction of protein oxidation and lipid peroxidation markers (Farr et al., 2014). This decrease in oxidative stress was associated to a concomitant increased levels of the antioxidant transcription factor nuclear factor-E2-related factor 2 (Nrf2), which is negatively regulated by GSK-3β.

Similarly, siRNA directed against another negative modulator of Nrf2 protected against oxidative stress *in vitro* and showed protective effects against MPTP-induced dopaminergic terminal damage *in vivo* when injected into the striatum (Williamson et al., 2012).

Other reports revealed suppressive effects of an ASO with an analogous structure as nusinersen on CNS oxidative stress and microglial activation, suggesting also a new role of SMN protein in microglia (Ando et al., 2020). In addition, in Spinal muscular atrophy (SMA) type 1 patients, preliminary results suggest that the therapy with nusinersen is indeed effective in reducing inflammation and oxidative stress (Bianchi et al., 2021). In fact, 6 months after starting treatment it was observed a reversion of the cerebrospinal fluid protein pattern from patient cohort to that of control donors. Remarkably, an upregulation of apolipoprotein A1 and E were detected. Since these multifunctional proteins are critically active in biomolecular processes aberrant in SMA, i.e., neuronal survival and plasticity, inflammation, and oxidative stress control, their nusinersen induced modulation may support SMN improved-expression effects.

Lastly, regarding miRNA inhibitors, an anti-miR-21 was demonstrated to be highly effective in murine models of Alport nephropathy: in particular, anti-miR-21 was able to reduce TGF-β-mediated stress response in glomeruli, to mitigate the expression of PPAR-α and its downstream fatty acid oxidation, to inhibit pro-inflammatory and profibrotic signals and to control the production of reactive oxygen species (Ben-Nun et al., 2020). Based on these evidences, clinical trials have been started with two miR-21 inhibitors, RG-012 and Lademirsen (SAR339375), in patients with kidney fibrosis as a result of Alport syndrome (Available from: https://clinicaltrials.gov/ct2/show/NCT03373786 and https://clinicaltrials.gov/ct2/show/NCT02855268).

6 FDA and EMA-approved formulations

As shown in Table 1 and Figure 2 there are already different ASOs approved from FDA and EMA for the treatment of several disorders, including metabolic/endocrine, neurological/neuromuscular, cardiovascular and infectious diseases.

6.1 Infectious diseases

6.1.1 Fomivirsen

The first oligonucleotide available for therapy was fomivirsen, a phosphorothioate ASO approved by the FDA and EMA respectively in 1998 and 1999 for the second-line treatment of cytomegalovirus (CMV) retinitis in patients with acquired immunodeficiency syndrome (AIDS) (Geary et al., 2002). Fomivirsen, administered locally by intravitreal injection, had a complementary structure to the viral messenger RNA encoding CMV immediate-early (IE)-2 protein, required for viral replication (Geary et al., 2002). Clinical efficiency was demonstrated in a randomised clinical trial, in which fomivirsen slowed the progression of the disease over 71 days compared to 13 days in the control group (Hutcherson and Lanz, 2002). The progression of the disease happened in 44% of treated patients compared to 70% in untreated patients (Hutcherson and Lanz, 2002). Although a milestone in the field of ASOs, this treatment was used for a limited period, as the incidence of cytomegalovirus retinitis was dramatically reduced by the development of highly active antiretroviral therapy (HAART) (Yin and Rogge, 2019). Developed by Ionis Pharmaceuticals and subsequently licensed to Novartis, it was revoked in 2002 in the European Union and in 2006 in the United States (Stein and Castanotto, 2017).

6.2 Cardiovascular diseases

6.2.1 Mipomersen

The first systemically approved ASO therapy was mipomersen, an antisense 20-mer phosphorothioate 2′-methoxy-ethoxy (MOE) gapmer, developed by Genzyme for adult patients with homozygous familial hypercholesterolaemia (HoFH) (Thomas et al., 2013). HoFH is an autosomal dominant genetic disorder characterised by high levels of low-density lipoprotein cholesterol (LDL-C) with a risk of developing coronary heart disease by the age of 30 (Cuchel et al., 2014). The disease is characterized by loss of function mutations in both LDL-receptor genes, causing the reduced liver uptake of plasma LDL cholesterol. Mipomersen forms a heteroduplex with a complementary mRNA sequence encoding for apolipoprotein B, the main component of LDL-C produced by the liver, resulting in the activation of RNase H (Akdim et al., 2010). The decreased production of apolipoprotein B consequently reduces the export of LDL-C from the liver, preventing the atherosclerotic process (Akdim et al., 2010). It is administered by subcutaneous injection at a dose of 200 mg once a week in addition

TABLE 1 FDA and EMA approved antisense drugs.

Name (market name)Company	Chemistry	Mechanism of action	Target/organ	Indication	Route/Dosing	Year of approval	Designation
Fomivirsen (Vitravene™), Ionis Pharma, Novartis	21 mer PS DNA	RNase H1	CMV IE-2 mRNA/eye	CMV retinitis	IVT/300 μg every 4 weeks	FDA (1998) EMA (1999)	-
Mipomersen (Kynamro™), Ionis Pharma, Genzyme, Kastle Tx	20 mer, 2′-O-MOE, PS, 5-methyl cytosine	RNase H1	Apo-B-100 mRNA/ liver	HoFH	SC/200 mg once weekly	FDA (2013)	Orphan
Eteplirsen (Exondys 51®), Sarepta Tx	30 mer PMO	Exon skipping	DMD pre-mRNA exon 51/Skeletal muscle	DMD	I.V. infusion/ 30 mg/kg once weekly	FDA (2016)	Orphan
Nusinersen (Spinraza®), Ionis Pharma, Biogen	18 mer PS, 2′-O-MOE, 5-methyl cytosine	Exon inclusion	SMN2 pre-mRNA exon 7/CNS	SMA	ITH/12 mg once every 4 months	FDA (2016) EMA (2017)	Orphan
Patisiran (Onpattro®), Alnylam	2′-O-Me, 2′F, PS siRNA	AGO2	TTR mRNA/liver	hATTR	I.V. infusion 0.3 mg/kg once every 3 weeks	FDA (2018) EMA (2018)	Orphan
Inotersen (Tegsedi®), Ionis Pharma, Akcea Pharma	20 mer 2′-O-MOE, PS	RNase H1	TTR mRNA/liver	hATTR	SC/300 mg once weekly	FDA (2018) EMA (2018)	Orphan
Vutrisiran/ALN-TTRSC02	2′-O-Me, 2′-F,PS	RNase H1	TTR mRNA/liver	hATTR	SC/25 mg every 3 months	FDA (2022)	Orphan
Milasen Boston Children's Hospital	22 mer 2′-O-MOE, PS, 5-methyl cytosine	Splicing modulation	Intron 6 spice acceptor cryptic site/CNS	CLN7	ITH/42 mg once every 3 months	FDA (2018)	Orphan
Volanesorsen (Waylivra®), Ionis Pharma, Akcea Pharma	20 mer, PS,2′-O-MOE	RNAse H	mRNA APOCIII/ liver	FCS	SC/285 mg once weekly	EMA (2019)	Orphan
Givosiran (Givlaari®), Alnylam	PS - SiRNA GalNAc	AGO2	ALAS1 mRNA/liver	AHP	SC/2,5 mg/kg once every months	FDA (2019), EMA (2020)	Orphan
Golodirsen (Vyondys 53™), Sarepta Tx	25 mer PMO	Exon-Skipping	DMD pre-mRNA/ muscle	DMD	I.V/30 mg/kg once weekly	FDA (2019)	Orphan
Viltolanersen (Viltepso™), NS Pharma	PMO	Exon-skipping	DMD pre-mRNA/ muscle	DMD	IV/80 mg/kg once weekly	FDA (2020)	Orphan
Lumasiran (Oxlumo™), Alnylam	siRNA	AGO2	HA01 mRNA/liver	PH1	SC/dose and frequency depend on the patient's weight	FDA (2020) EMA (2020)	Orphan
Inclisiran (Leqvio®), The Medicines Company, Novartis	2′F, 2′-O-Me, PS siRNA- GalNAc	AGO2	mRNA PCSK9/liver	FH	SC/300 mg once every 6 months	EMA (2020) FDA (2021)	-
Casimersen (Amondys 45 ™), Sarepta	22 mer PMO	Exon-Skipping	DMD pre-mRNA/ muscle	DMD	30 mg/kg once weekly	FDA (2021)	Orphan
Tofersen	2′-O-MOE-PS	RNase H1	SOD1 mRNA/brain	ALS	100mg/15 mL (6.7 mg/mL) single-dose vial	FDA (2023)	

Antisense medicines approved by the Food and Drug Administration (FDA) or European Medicines Agency (EMA). 2′- F— 2′-Fluoro, 2′-O- MOE—2′-O-methoxyethyl, AHP—acute hepatic porphyria, ALAS—Aminolevulinate synthase, Apo—Apolipoprotein, CLN7— Neuronal Ceroid Lipofuscinosis, CMV—cytomegalovirus, CNS—central nervous system, DMD—Duchenne muscular dystrophy, FCS—Familial chylomicronemia syndrome, FH—Familial hypercholesterolemia, GAlNAc—N-acetylgalactosamine, HAO1— Hydroxyacid oxidase 1, hATTR—hereditary transthyretin amyloidosis, HoFH—omozygous familial hypercolesterolaemia, ITH—Intrathecal, IV—Intravenous, IVT—intravitreal, PCSK9—Proprotein convertase subtilisin/kexin type 9, PH1 — Hyperoxaluria type 1, PMO, Phosphorodiamidate morpholino; PS, Phosphorothioate, SC—Subcutaneous, siRNA—Small interfering RNA, SMA—spinal muscular atrophy, SMN—survival of motor neurons, TTR—Transthyretin.

to the maximum dose of hypolipidemic therapy and diet. Mipomersen was approved by the FDA in January 2013 on the basis of results obtained in four phase III clinical studies (Stein and Castanotto, 2017) in which mipomersen reduced plasma C-LDL concentration by 25%–37% compared to baseline (primary endpoint) in patients with HoFH already treated with a

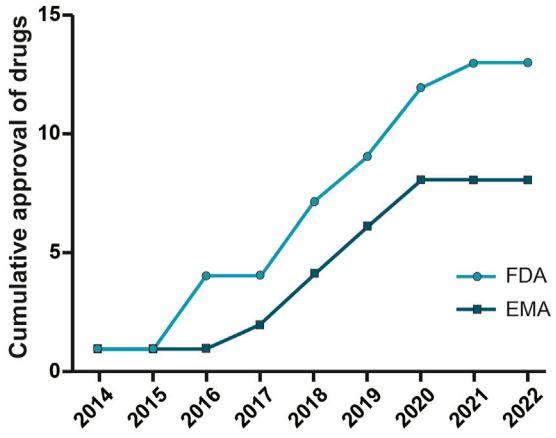

FIGURE 2
Oligonucleotide drugs approved by FDA and EMA. ASO drugs for different therapeutic areas (neurological and neuromuscular, metabolic and endocrine, and infection diseases) approved by the Food and Drug Administration and European Medicines Agency from 2013 to 2022.

hypolipidemic drug (Hair et al., 2013). There were also reductions in total cholesterol, apolipoprotein B and lipoprotein (a) (Hair et al., 2013). In contrast, the EMA denied the marketing authorisation on 13 December 2012 due to concerns about side effects of a drug intended for long-term use, including liver toxicity and cardiovascular risk (Il GEB, 2013). Mipomersen did not accomplish a successful marketing as it was outperformed for minor hepatotoxic effects by a small molecule (lopitamide) (Stein and Castanotto, 2017). Its uncertain future is also linked to the competition of PCSK9 (Proprotein convertase subtilisin/kexin type 9) inhibitors, monoclonal antibodies (e.g., evolocumab and alirocumab) and oligonucleotide molecules recently approved (inclisiran) (Stein and Castanotto, 2017).

6.2.2 Volanesorsen

Volesorsen is a PS, 2′-O-MOE gapmer, approved by the EMA in May 2019, suitable for use in adults affected by familial chylomicronemia syndrome (FCS), a rare genetic disorder with high risk of pancreatitis, in case the response to diet and the therapeutic lowering of triglycerides is insufficient (Paik and Duggan, 2019). Volanesorsen, inhibits hepatic apolipoprotein CIII (APOCIII) mRNA, resulting in reduced plasma apolipoprotein C-III levels (Paik and Duggan, 2019). Also the inhibition of APOC3, which encodes a protein involved in triglyceride (TG)-rich lipoproteins (TGRLs) removal, has been reported to be an original target to treat severe hypertriglyceridemia (sHTG). It is administered by subcutaneous injection at a dose of 285 mg once a week for the first 3 months of treatment and then once every 2 weeks. The frequency of administration is adjusted again after six and 9 months according to the patient's clinical condition. Thrombocytopenia, observed in clinical trials, should be monitored in patients receiving the medicine (Witztum et al., 2019). The approval followed the results of the multinational phase III APPROACH study in which patients treated with volanesorsen showed a 77% reduction in average triglyceride levels and a significant reduction in pancreatitis attacks (Witztum et al., 2019). Additional clinical trials are ongoing to evaluate its efficacy in hypertriglyceridemia, familial chylomicronemia syndrome (FCS) and partial lipodystrophy (Paik and Duggan, 2019).

6.2.3 Defibrotide

Defibrotide is approved by EMA and by FDA, respectively in 2013 and in 2016, for the treatment of patients with hepatic veno-occlusive disease (VOD) that occurs after high dose chemotherapy and autologous bone marrow transplantation (HSCT) (Stein and Castanotto, 2017). Liver veno-occlusive disease results from damage and occlusion of small hepatic venules due to endothelial cells activity triggered by local release of cytokines as part of pro-inflammatory and pro-thrombotic states and activation of the fibrinolytic pathway (Dalle and Giralt, 2016). Hepatic sinusoids become fibrous with necrosis of perivascular hepatocytes. Patients may develop jaundice, painful hepatomegaly, fluid retention, ascites and weight gain with progressive organ failure (up to 80% mortality) (Dalle and Giralt, 2016). Defibrotide is a mixture containing femtomolar concentration of single- (90%) and double-stranded (10%) ASOs derived from porcine intestinal mucosal DNA (Kornblum et al., 2006). The concentration of any specific sequence in the mixture is approximately in the femtomolar range. Therefore, defibrotide cannot act through an antisense mechanism but, most likely, through charge-charge interactions of its phosphodiester constituents with proteins (Stein and Castanotto, 2017). Although the mechanism of action is uncertain, defibrotide has antithrombotic and anti-inflammatory properties. Defibrotide is in fact able to increase the expression of systemic tissue factor pathway inhibitor (TFPI), tissue plasminogen activator (t-PA) and thrombomodulin (TM); reducing expression of von Willebrand factor (vWF) and plasminogen activator inhibitor-1 (PAI-1); and enhancing plasmin enzyme activity to promote hydrolysis of fibrin clots (Richardson et al., 2017). The recommended dose is 6.25 mg/kg body weight every 6 h (25 mg/kg/day) administered by intravenous infusion for at least 21 days and is to be continued until symptoms and signs of severe VOD have resolved (Stein and Castanotto, 2017). The study had two endpoints: the primary one was the patient survival rate at day +100 post-HSCT. The percentage of patients alive in the DF group was 38.2% (39/102) versus 25% (8/32) in the control group. The secondary one was the complete response rate (defined as total bilirubin levels below 2 mg/dL), with a rate of 23.5% (24/102) observed in the DF-treated group and a rate of 9.4% (3/32) in the control group (Richardson et al., 2016).

6.2.4 Inclisiran

Inclisiran is a 2′F, 2′-O-Me, PS siRNA-GalNAc, approved by both the EMA and FDA on the basis of surrogate endpoints for the use in adults with primary hypercholesterolaemia or mixed dysplidaemia as a supplement to standard diet and therapy (Food and Drug Admi nistration, 2020). These diseases result in elevated blood cholesterol levels with a predisposition to atherosclerotic disease.

Inclisiran should be used in combination in patients who, with the maximum tolerated dose of statins, are unable to reach low-density lipoprotein cholesterol goals. Inclisiran, by activating AGO2, induces cleavage of the mRNA encoding for proprotein convertase

subtilisin-kexin type 9 (PCSK9), an enzyme that negatively regulates the turnover and therefore LDL receptor (LDLR) levels on the hepatocyte membrane (Dyrbuś et al., 2020). This results in increased uptake of LDL from the bloodstream due to increased expression of LDLR levels (Dyrbuś et al., 2020). Chemical modifications and conjugation with three N-acetyl-galactosamine molecules significantly improve the biodistribution of the drug, allowing the cholesterol-lowering effect to be maintained for up to 6 months with a single subcutaneous injection of the medicine (Fitzgerald et al., 2017). Evidence supporting the efficacy of inclisiran comes from randomised, placebo-controlled phase III clinical trials. Among these studies, ORION-10 and ORION-11 were the studies with the highest number of patients (Dyrbuś et al., 2020). ORION-10 tested the medicine in 1,561 patients with atherosclerotic cardiovascular disease (ASCVD) and ORION-11 included 1,617 subjects with ASCVD or equivalent cardiovascular risk. At the end of the follow-up period (day 510), inclisiran reduced LDL-C levels by 52.3% in ORION-10% and 49.9% in ORION-11 (Dyrbuś et al., 2020). Currently, the ORION-4 study is underway to examine the impact of inclisiran (in addition to standard therapy and diet) in reducing the risk of major adverse cardiovascular events in approximately 15,000 ASCVD patients.

6.3 Metabolic and endocrine diseases

6.3.1 Givosiran

Givosiran is a GalNAc-conjugated PS-siRNA used to treat acute hepatic porphyria (AHP) in adults and adolescents over 12 years of age (Scott, 2020). Givosiran binds a ligand that enable the specific delivery of the siRNA to the liver, where it acts against the aminolevulinate synthase 1 (ALAS1) mRNA, resulting in decreased levels of neurotoxic δ-aminolevulinic acid and porphobilinogen, that are associated with acute porphyria attacks (Balwani et al., 2020). Administered by subcutaneous injection at a dose of 2.5 mg/kg once a month, givosiran enters the hepatocytes and degrades the mRNA encoding for ALAS1 by activation of AGO 2 (Scott, 2020). Approved by the FDA in 2019 and by the EMA in 2020, the efficacy of givosiran was evaluated in a randomised, double-blind, placebo-controlled clinical trial in a 1:1 ratio (ENVISION NCT03338816) (Balwani et al., 2020). Out of a total of 94 patients with AHP, 74% of patients treated with givosiran showed a reduction in porphyria attacks. Givosiran was well tolerated with common side effects such as nausea and injection site reactions (Balwani et al., 2020). Liver function and allergic reactions should be monitored during and after treatment (Dhuri et al., 2020).

6.3.2 Lumasiran

Developed by Alnylam Pharmaceuticals and approved in November 2020 by both the FDA and the EMA, lumasiran is a subcutaneously administered siRNA specifically to reduce hepatic overproduction of oxalate in patient with primary hyperoxaluria type 1 (PH1) (Scott and Keam, 2021). A high level of oxalate in the urine can cause kidney stones or kidney failure (Frishberg et al., 2019). By targeting the hydroxyacid oxidase 1 (HAO1) mRNA in the liver, lumasiran decrease the production of glycolate oxidase. The reduced production of this enzyme results in an increase in the concentration of the precursor glycolate, which being soluble, is readily eliminated by the kidney (Scott and Keam, 2021). The drug dose is based on body weight. The clinical efficacy of lumasiran was evaluated in a randomized, double-blind trial comparison study between lumasiran and placebo in 39 patients aged 6 and 60 years with primary hyperoxaluria type 1. After 6 months of treatment, the level of oxalate in urine was reduced by 65% on average in patients on lumasiran compared with 12% in patients who received placebo (Garrelfs et al., 2021).

6.4 Neurological and neuromuscular diseases

6.4.1 Nusinersen

Nusinersen is an antisense 18-mer phosphorothioate 2′-methoxy-ethoxy (MOE) gapmer engineered to treat patients with Spinal muscular atrophy 5q (SMA), an autosomal recessive degenerative motor neuron disease (Chiriboga, 2017). This disease is caused by a deletion or mutation with total loss of function of the survival motor neuron 1 (SMN1) on chromosome 5q. SMN protein deficiency causes weakness and atrophy of the limbs and respiratory and bulbar muscles (Chiriboga, 2017). Typically, humans have SMN2, a paralogous copy of the SMN1 gene. SMN2 differs from SMN1 by a basic cytosine to thymine transition in exon 7 that results in a weakened splice site. Consequently, 90% of the transcripts derived from SMN2 induce the splicing of this exon resulting in a truncated protein that is rapidly degraded.

ASO-based approaches aimed at exon 7 splicing correction (Hua et al., 2008) have employed several targets including the 3′ splice site (3′ ss) of exon 8, element 1, GC-rich sequence (GCRS), ISTL1 and ISS-N2 and the 100th position of intron 7. Among these, the largest number of studies has been done on Intronic Splice Silencing site (ISS-N1)-targeting ASOs (Singh et al., 2015).

Nusinersen increases the inclusion rate of exon 7 in SMN2 gene transcripts by binding to ISS-N1 and displacing splicing factors by steric hindrance (Singh et al., 2006; Singh et al., 2017; Goodkey et al., 2018). It is administered intrathecally at a dose of 12 mg. Treatment with nusinersen involves four loading doses (12 mg) on days 0, 14, 28 and 63 and a maintenance dose administered every 4 months (Wurster et al., 2019).

Nusinersen was approved in December 2016 by FDA and in May 2017 by EMA on the basis of increased survival and improved motor function demonstrated in two randomised, double-blind, simulation-controlled phase III clinical trials (Finkel et al., 2017; Mercuri et al., 2018). The clinical benefit shown, allowed to stopped early the placebo-controlled studies in order to generate an open-label study to receive the treatment (Yin and Rogge, 2019). Osredkar et al. recently have conducted a two-center study (in Slovenia and Czech Republic) which confirm the efficacy and safety of nusinersen after 14 months of treatment. The patient population under consideration included 61 subjects aged between 2 months and 19 years with a genetically confirmed diagnosis of SMA (Osredkar et al., 2021). Specifically, the results showed that all patients benefited from the drug. However, better outcomes were recorded with an earlier age of treatment initiation and a higher number of SMN2 copies. Neonatal screening may therefore be

necessary to maximize drug efficacy. In terms of safety, no side effects made it necessary to stop treatment (Osredkar et al., 2021).

6.4.2 Milasen

Milasen is an outstanding example of ASO-based personalised medicine as it is an ASO specifically designed for a girl suffering from neuronal ceroid lipofuscinosis 7 (CLN7), a disease that primarily affects the nervous system causing vision loss, dysarthria, ataxia and dysphagia (Kim et al., 2019). It is caused by an alteration in the transcript splicing due to the insertion of an SVA retrotransposon (SINE-VNTR-Alu) into the MFSD8 gene (also called CLN7). Milasen restores correct splicing by binding cryptic splice sites in the pre-mRNA (Kim et al., 2019). It is administered as an intrathecal bolus starting with 3.5 mg and increasing the dose every 2 weeks to 42 mg. After the dose increase, two additional loading doses are administered, followed by a maintenance dose approximately every 3 months (Kim et al., 2019). The safety of milasen has been assessed in preclinical toxicity studies (Dhuri et al., 2020).

6.4.3 Patisiran

Transthyretin-mediated hereditary amyloidosis (hATTR) is caused by a mutation in the gene coding for transthyretin (TTR), a protein produced by the liver that transports thyroxine and retinol in the plasma and cerebrospinal fluid (Hanna, 2014). The result of the mutation is the formation of an oversized protein that accumulates as insoluble amyloid fibrils in the nerves, heart and gastrointestinal tract. In addition to polyneuropathy, this disease leads to a decline in cardiac function with a life expectancy of 3–15 years after the appearance of symptoms (Hanna, 2014). Patisiran, a 2′-O-Me, 2′F, PS siRNA formulated in a lipid nanoparticle, is directed at gene silencing of a transthyretin-coding mRNA sequence by activation of AGO2 (Hoy, 2018). The recommended medicine dose is 300 mg/kg body weight administered by intravenous infusion once every 3 weeks. Premedication with dexamethasone, acetaminophen/paracetamol and H1 and H2 antagonists is required to reduce the pro-inflammatory effect of the formulation (Adams et al., 2017). In 2018, it was approved by both FDA and EMA on the basis of robust evidence of clinical efficacy with an acceptable safety profile in patients with hereditary transthyretin-mediated amyloidosis with polyneuropath, demonstrated in a double-blind, randomised, placebo-controlled phase III study (APOLLO II; NCT01960348) (Hoy, 2018; Adams et al., 2017). Both the primary endpoint of the study (mNIS + 7, modified Neuropathy Impairment Score +7) and the secondary endpoints (quality of life, muscle strength, gait speed, nutritional status and autonomic function) were widely demonstrated (Adams et al., 2017). Compared to inotersen, there were no serious side effects. Three post-approval clinical studies are currently underway. The aim of the first study is to evaluate the long-term efficacy and safety of patisiran (expected end date August 2022); the second study evaluates the safety and efficacy of patisiran in patients with hATTR after liver transplantation; the third study compares the efficacy of vitrusiran with patisiran for the treatment of hATTR (Dhuri et al., 2020).

6.4.4 Inotersen

Inotersen is a 2′-O-MOE PS gapmer ASO that has been approved by both the EMA and FDA in 2018 for the treatment of hATTR (Goodkey et al., 2018). Inotersen mediates the cleavage of mRNA encoding for transthyretin through the activation of RNAse H (Goodkey et al., 2018). It is administered by subcutaneous injection at a dosage of 284 mg once a week. The clinical efficacy of inotersen was demonstrated in a randomised, double-blind, placebo-controlled clinical trial (NEURO-TTR, NCT01737398) (Benson et al., 2018). However, there were two significant adverse reactions in the treatment group: thrombocytopenia and glomerulonephritis, which required the introduction of metabolic and haematological monitoring (Dhuri et al., 2020). Interesting are the results obtained in a study conducted to evaluate the long term safety and efficacy of inotersen in transthyretin cardiomyopathy (Dasgupta et al., 2020). As cardiomyopathy is a major cause of death in patients with systemic transthyretin amyloidosis, this results showed that inotersen is safe and effective in this context (Dasgupta et al., 2020).

6.4.5 Eteplirsen

Duchenne muscular dystrophy (DMD) is an autosomal recessive myophathy caused by mutations in the dystrophin gene. Patients usually experience premature death around 30/40 years of age due to respiratory or cardiac failure (Aartsma-Rus and Krieg, 2017). Dystrophin deficiency occurs at the age of 2–5 years with delayed walking, hypotonic limbs, weakness and loss of muscle function. Gold-standards in the management of complications are corticosteroids and artificial respirators. Additionally, drug therapies including eteplirsen have been approved by the FDA to treat specific types of DMD. Eteplirsen is a 30-nucleotide PMO indicated for the treatment of DMD in patients with a specific genetic mutation that causes the deletion of exons 49–50, leading to the formation of a stop signal on codon 51. It is designed to bind to exon 51 of dystrophin pre-mRNA and promote the skipping of exon 51, excluding this exon from the primary dystrophin transcript (Vegeto et al., 2019). The final transcript results in a truncated but partially functional protein, as occurs in Becker muscular dystrophy (milder form of the dystrophic phenotype) (Beckers et al., 2021). It is administered by weekly venous infusion at a dose of 30 mg/kg. The clinical efficacy of eteplirsen was evaluated in a small group of patients in a phase II study in which the primary endpoints were the distance covered in 6 minutes and the percentage of dystrophin-positive fibres (Mendell et al., 2013). There were no significant differences in the gait test between groups and a moderate increase in dystrophin expression in muscle tissue was detected by immunohistochemical analysis (from 0.16% at baseline to 0.48% at week 48) (Mendell et al., 2013). The reasons for a weak physiological response to eteplirsen are due to a reduced absorption in muscle and a rapid renal filtration due to low plasma protein binding (Levin, 2019). In 2016 the FDA granted controversial accelerated approval based on surrogate endpoints (Mendell et al., 2013) to eteplirsen given the unsatisfied medical need, the severity and progressive nature of the disease. This authorization is subject to the completion of further studies confirming the function benefit from eteplirsen treatment. Otherwise, in 2018, the EMA refused the marketing of the medicine due to lack of data about the clinical benefit (Aartsma-Rus and Goemans, 2019).

6.4.6 Golodirsen

Golodirsen is a ASO with 25 monomers suitable for the treatment of DMD (Heo, 2020). Similar to eteplirsen, it has a neutral synthetic backbone (PMO chemistry), however, it is

TABLE 2 Investigational antisense drugs.

Drug candidate NCT ID	Chemistry	Mechanism of action	Target/organ	Indication	Route	Company
Tominersen (RG6042)	2′-O-MOE-PS	RNase H1	HTT mRNA/brain	Huntington's disease	ITH	Ionis
Casimersen	PMO	Exon skipping	DMD exon 45/muscle	DMD	IV	Sarepta
AKCEA-TTR-LRx 04136171	siRNA GalNAc	RNAi	TTR mRNA/liver	ATTR with cardiomyopathy	SC	Ionis
QPI-1002	siRNA	RNAi	p53 mRNA/kidney	Cardiac surgery/kidney delayed graft function/acute kidney injury	IV	Quark
Fitusiran/ALN-AT3	siRNA GalNAc	RNAi	Anti-thrombin mRNA/liver	Haemophilia A and B	SC	Genzyme
Volanesorsen	2′-O-MOE-PS	RNase H1	ApoC-III mRN/liver	FCS/Lipoprotein Lipase Deficiency/Hyperlipo proteinemia type 1	SC	Ionis
Alicaforsen	PS	RNase H1	ICAM1 mRNA/colon	Pouchitis	E	Atlantic
Tivanisiran	siRNA	RNAi	TRPV1/eye	Dry eye syndrome	IVT	Sylentis
IONIS-TTR Rx	2′-O-MOE-PS	RNAse H1	TTR mRNA/liver	FAP/CS	SC	Ionis

Antisense drugs that showed promise in phase III, clinical trials 2′-O- MOE—2′-O-methoxyethyl, ALS—amyotrophic lateral sclerosis, ATTR—Transthyretin amyloidosis, DMD—Duchenne muscular dystrophy, E—Enema, Apo—Apolipoprotein, FAP—familial amyloid poly neuropathy, FCS—Familial chylomicronemia syndrome, GAlNAc—N-acetylgalactosamine, HTT—Huntingtin, ICAM—Intercellular adhesion molecule, ITH—Intrathecal, IV—Intravenous, IVT—intravitreal, PMO, Phosphorodiamidate morpholino; PS, Phosphorothioate, SC—Subcutaneous, siRNA—Small interfering RNA, SOD1 —Superoxide dismutase, TTR—Transthyretin, p53—Tumor protein, TRPV1—Transient Receptor Potential Vanilloid 1.

targeted at patients with a different genetic mutation. Specifically, it is recommended for the treatment of DMD in subjects with a confirmed mutation in the dystrophin gene susceptible to skipping exon 53 (approximately 8% of DMD patients). Golodirsen is engineered to make exon 53 skip in the dystrophin gene, enabling the production of a truncated but still functional form of dystrophin, which is a deficient protein in the disease (Heo, 2020). The recommended dose of golodirsen is 30 mg/kg, administered by intravenous infusion (Heo, 2020). Renal function should be monitored in patients taking the medicine, as renal toxicity has been observed during preclinical *in vivo* studies (Frank et al., 2020). Golodirsen was approved in December 2019 by the FDA following positive results from a phase I/II clinical trial, which demonstrated increased dystrophin expression at the muscle level (Frank et al., 2020). The approval is subject to the implementation of further clinical studies confirming drug efficacy, i.e., improvement in mobility function, measured as the change in the 6-min walk test (6MWT) from baseline to week 26. The multicentre, randomised, double-blind, placebo-controlled phase III ESSENCE study is currently taking place and is expected to be completed by 2024. This study aims at assessing not only the safety and efficacy of golodisen but also of casimersen, an oligonucleotide that was approved by FDA for DMD patients with a mutation in dystrophin exon 45.

6.4.7 Viltolanersen

Viltolarsen, an antisense phosphorodiamidate morpholino oligonucleotide, is specific for exon 53 of the dystrophin mRNA precursor. It has the capability to induce exon 53 skipping, generating a functional truncated dystrophin protein in DMD patients with a specific mutation (Dhillon). It is administered intravenously once a week for 1 h at a dose of 80 mg/kg. Renal function monitoring is required for patients receiving viltolanersen. Viltolanersen received accelerated marketing approval from the FDA in August 2020 on the basis of a multicentre phase II clinical trial, which showed increases in *de novo* dystrophin production in muscle (surrogate endpoint) and clinical improvements in time-based functional tests (Clemens et al., 2020).

6.4.8 Casimersen

Casimersen is an antisense phosphorodiamidate oligonucleotide designed for exon skipping in patients diagnosed with DMD confirmed by the susceptible exon 45 skip genotype (Shirley, 2021). This drug allows the increase of dystrophin production at the skeletal muscle level through the synthesis of an internally truncated but partially functional protein in patients with DMD.

Casimersen is administered by intravenous infusion at the dose of 30 mg/kg once weekly (Shirley, 2021).

In February 2021, Casimersen received accelerated approval from the FDA based on the results of the ongoing, double-blind, placebo-controlled phase 3 study. Intermediate results showed a greater change in dystrophin expression from baseline in the casimersen treated group compared to placebo controls.

7 Future perspectives

The number of ASO molecules under investigation for the treatment of several diseases is considerable. The main candidates in phase III clinical trials are briefly described below in Table 2. It should be noted that, to date, these molecules are still mainly intended for local delivery (to the eye by intravitreal injection, to the central nervous system by intrathecal administration, to the colon by enema); and for delivery to the liver and kidney, the major organs where ASOs accumulate. As documented by the most recently approved drugs, oligonucleotides can be used both in personalised medicine (e.g., milasen) and for the treatment of a significant population of individuals (e.g., inclisiran). In the context

of optimizing the development of ASOs, it is important to discuss the critical aspects of their design. The size of ASOs appears to play a pivotal role in reducing off-target effects, and careful consideration should be given to this parameter. Moreover, more extensive RNA-Seq and proteomic studies are needed to gain a deeper understanding of off-target effects that cannot be reliably predicted by currently available bioinformatic algorithms. These studies provide detailed information about how proteins are produced and how genes are expressed at the RNA level. This information can be crucial for assessing their off-target effects and also ensuring the safety and efficacy of ASOs in clinical applications. Additionally, a key challenge in the advancement of ASO-based therapeutics is the identification of chemical structures able to ensure better pharmacokinetics and pharmacodynamic properties. While GAlNAc conjugates and encapsulation in lipid nanoparticles (LNPs) have demonstrated excellent delivery to the liver, particularly for metabolic liver-related diseases, further research and advancements are required to achieve meaningful and widespread delivery to other tissues. Tissue-specific targeting represents a promising avenue for achieving pharmacological effect at lower doses and, at the same time, decrease the main causes of unresolved toxicity, including off-target accumulation in renal and hepatic tissues and proinflammatory effects.

8 Conclusion

Major chemical and technological improvements have been made to diminish the toxicity and increase the efficacy of ASOs. This process has recently led to a great number of ASO-based medicines being used in clinical practice and to a renewed interest from big pharma, resulting in a multibillion-dollar market, comparable to that of small molecules. ASOs may be used in monotherapy or in combination with traditional therapy. They constitute a valid therapeutic alternative for diseases with no cure or effective therapies (orphan genetic diseases).

Thanks to their properties, ASOs are able to regulate oxidative stress and inflammatory response that are common mechanisms altered in many disorders. Currently, ASOs are primarily intended for the treatment of neurological, neuromuscular and metabolic disorders. However, thanks to further technological innovations, ASOs are expected to be used as advanced therapeutics for many other disorders in the next future.

Author contributions

DC: Writing–review and editing. IB: Writing–review and editing. EC: Writing–original draft. MC: Supervision, Writing–review and editing.

Funding

The author(s) declare that no financial support was received for the research, authorship, and/or publication of this article.

Conflict of interest

The authors declare that the research was conducted in the absence of any commercial or financial relationships that could be construed as a potential conflict of interest.

The author(s) declared that they were an editorial board member of Frontiers, at the time of submission. This had no impact on the peer review process and the final decision.

Publisher's note

References

Aartsma-Rus, A., and Goemans, N. (2019). A sequel to the eteplirsen saga: eteplirsen is approved in the United States but was not approved in europe. *Nucleic Acid. Ther.* 29 (1), 13–15. doi:10.1089/nat.2018.0756

Aartsma-Rus, A., and Krieg, A. M. (2017). FDA approves eteplirsen for duchenne muscular dystrophy: the next chapter in the eteplirsen saga. *Nucleic Acid. Ther.* 27, 1–3. doi:10.1089/nat.2016.0657

Adams, D., Suhr, O. B., Dyck, P. J., Litchy, W. J., Leahy, R. G., Chen, J., et al. (2017). Trial design and rationale for APOLLO, a Phase 3, placebo-controlled study of patisiran in patients with hereditary ATTR amyloidosis with polyneuropathy. *BMC Neurol.* 17 (1), 181–212. doi:10.1186/s12883-017-0948-5

Akdim, F., Stroes, E. S. G., Sijbrands, E. J. G., Tribble, D. L., Trip, M. D., Jukema, J. W., et al. (2010). Efficacy and safety of mipomersen, an antisense inhibitor of apolipoprotein B, in hypercholesterolemic subjects receiving stable statin therapy. *J. Am. Coll. Cardiol.* 55 (15), 1611–1618. doi:10.1016/j.jacc.2009.11.069

Allerson, C. R., Sioufi, N., Jarres, R., Prakash, T. P., Naik, N., Berdeja, A., et al. (2005). Fully 2′-modified oligonucleotide duplexes with improved *in vitro* potency and stability compared to unmodified small interfering RNA. *J. Med. Chem.* 48, 901–904. doi:10.1021/jm049167j

Ambegia, E., Ansell, S., Cullis, P., Heyes, J., Palmer, L., and MacLachlan, I. (2005). Stabilized plasmid-lipid particles containing PEG-diacylglycerols exhibit extended circulation lifetimes and tumor selective gene expression. *Biochim. Biophys. Acta - Biomembr.* 1669, 155–163. doi:10.1016/j.bbamem.2005.02.001

Ando, S., Osanai, D., Takahashi, K., Nakamura, S., Shimazawa, M., and Hara, H. (2020). Survival motor neuron protein regulates oxidative stress and inflammatory response in microglia of the spinal cord in spinal muscular atrophy. *J. Pharmacol. Sci.* 144 (4), 204–211. doi:10.1016/j.jphs.2020.09.001

Ayer, A., Fazakerley, D. J., Suarna, C., Maghzal, G. J., Sheipouri, D., Lee, K. J., et al. (2021). Genetic screening reveals phospholipid metabolism as a key regulator of the biosynthesis of the redox-active lipid coenzyme Q. *Redox Biol.* 46, 102127. doi:10.1016/j.redox.2021.102127

Bajan, S., and Hutvagner, G. (2020). RNA-based therapeutics: from antisense oligonucleotides to miRNAs. *Cells* 9 (1), 137–227. doi:10.3390/cells9010137

Balwani, M., Sardh, E., Ventura, P., Peiró, P. A., Rees, D. C., Stölzel, U., et al. (2020). Phase 3 trial of RNAi therapeutic givosiran for acute intermittent porphyria. *N. Engl. J. Med.* 382 (24), 2289–2301. doi:10.1056/NEJMoa1913147

Batista-Duharte, A., Sendra, L., Herrero, M. J., Téllez-Martínez, D., Carlos, I. Z., and Aliño, S. F. (2020). Progress in the use of antisense oligonucleotides for vaccine improvement. *Biomolecules* 10 (2), 316. doi:10.3390/biom10020316

Beckers, P., Caberg, J. H., Dideberg, V., Dangouloff, T., den Dunnen, J. T., Bours, V., et al. (2021). Newborn screening of duchenne muscular dystrophy specifically targeting deletions amenable to exon-skipping therapy. *Sci. Rep.* 11 (1), 3011. doi:10.1038/s41598-021-82725-z

Benjaminsen, R. V., Mattebjerg, M. A., Henriksen, J. R., Moghimi, S. M., and Andresen, T. L. (2013). The possible "proton sponge " effect of polyethylenimine

(PEI) does not include change in lysosomal pH. *Mol. Ther.* 21 (1), 149–157. doi:10.1038/mt.2012.185

Bennett, C. F. (2019). Therapeutic antisense oligonucleotides are coming of age. *Annu. Rev. Med.* 70 (1), 307–321. doi:10.1146/annurev-med-041217-010829

Bennett, C. F., Baker, B. F., Pham, N., Swayze, E., and Geary, R. S. (2017). Pharmacology of antisense drugs. *Annu. Rev. Pharmacol. Toxicol.* 57 (1), 81–105. doi:10.1146/annurev-pharmtox-010716-104846

Bennett, C. F., and Swayze, E. E. (2010). RNA targeting therapeutics: molecular mechanisms of antisense oligonucleotides as a therapeutic platform. *Annu. Rev. Pharmacol. Toxicol.* 50 (1), 259–293. doi:10.1146/annurev.pharmtox.010909.105654

Ben-Nun, D., Buja, L. M., and Fuentes, F. (2020). Prevention of heart failure with preserved ejection fraction (HFpEF): reexamining microRNA-21 inhibition in the era of oligonucleotide-based therapeutics. *Cardiovasc Pathol.* 49, 107243. doi:10.1016/j.carpath.2020.107243

Benson, M. D., Waddington-Cruz, M., Berk, J. L., Polydefkis, M., Dyck, P. J., Wang, A. K., et al. (2018). Inotersen treatment for patients with hereditary transthyretin amyloidosis. *N. Engl. J. Med.* 379, 22–31. doi:10.1056/NEJMoa1716793

Bianchi, L., Sframeli, M., Vantaggiato, L., Vita, G. L., Ciranni, A., Polito, F., et al. (2021). Nusinersen modulates proteomics profiles of cerebrospinal fluid in spinal muscular atrophy type 1 patients. *Int. J. Mol. Sci.* 22 (9), 4329–29. doi:10.3390/ijms22094329

Cansby, E., Kulkarni, N. M., Magnusson, E., Kurhe, Y., Amrutkar, M., Nerstedt, A., et al. (2019). Protein kinase MST3 modulates lipid homeostasis in hepatocytes and correlates with nonalcoholic steatohepatitis in humans. *FASEB J.* 33 (9), 9974–9989. doi:10.1096/fj.201900356RR

Caputo, M., Kurhe, Y., Kumari, S., Cansby, E., Amrutkar, M., Scandalis, E., et al. (2021). Silencing of STE20-type kinase MST3 in mice with antisense oligonucleotide treatment ameliorates diet-induced nonalcoholic fatty liver disease. *FASEB J.* 35 (5), 215677–e21617. doi:10.1096/fj.202002671RR

Chi, X., Gatti, P., and Papoian, T. (2017). Safety of antisense oligonucleotide and siRNA-based therapeutics. *Drug Discov. Today* 22 (5), 823–833. doi:10.1016/j.drudis.2017.01.013

Chiriboga, C. A. (2017). Nusinersen for the treatment of spinal muscular atrophy. *Expert Rev. Neurother.* 17 (10), 955–962. doi:10.1080/14737175.2017.1364159

Clemens, P. R., Rao, V. K., Connolly, A. M., Harper, A. D., Mah, J. K., Smith, E. C., et al. (2020). Safety, tolerability, and efficacy of viltolarsen in boys with duchenne muscular dystrophy amenable to exon 53 skipping: a phase 2 randomized clinical trial. *JAMA Neurol.* 77 (8), 982–991. doi:10.1001/jamaneurol.2020.1264

Coelho, T., Adams, D., Silva, A., Lozeron, P., Hawkins, P. N., Mant, T., et al. (2013). Safety and efficacy of RNAi therapy for transthyretin amyloidosis. *N. Engl. J. Med.* 369, 819–829. doi:10.1056/NEJMoa1208760

Cuchel, M., Bruckert, E., Ginsberg, H. N., Raal, F. J., Santos, R. D., Hegele, R. A., et al. (2014). Homozygous familial hypercholesterolaemia: new insights and guidance for clinicians to improve detection and clinical management. A position paper fromthe Consensus Panel on Familial Hypercholesterolaemia of the European Atherosclerosis Society. *Eur. Heart J.* 35 (32), 2146–2157. doi:10.1093/eurheartj/ehu274

Dalle, J. H., and Giralt, S. A. (2016). Hepatic veno-occlusive disease after hematopoietic stem cell transplantation: risk factors and stratification, prophylaxis, and treatment. *Biol. Blood Marrow Transplant.* 22, 400–409. doi:10.1016/j.bbmt.2015.09.024

Dasgupta, N. R., Rissing, S. M., Smith, J., Jung, J., and Benson, M. D. (2020). Inotersen therapy of transthyretin amyloid cardiomyopathy. *Amyloid* 27 (1), 52–58. doi:10.1080/13506129.2019.1685487

Dhillon, S. (2020). Viltolarsen: first approval. Drugs 80(10):1027–1031. doi:10.1007/s40265-020-01339-3

Dhuri, K., Bechtold, C., Quijano, E., Pham, H., Gupta, A., Vikram, A., et al. (2020). Antisense oligonucleotides: an emerging area in drug discovery and development. *J. Clin. Med.* 9 (6), 2004. doi:10.3390/jcm9062004

Dyrbuś, K., Gąsior, M., Penson, P., Ray, K. K., and Banach, M. (2020). Inclisiran—new hope in the management of lipid disorders? *J. Clin. Lipidol.* 14, 16–27. doi:10.1016/j.jacl.2019.11.001

Eckstein, F. (2000). Phosphorothioate oligodeoxynucleotides: what is their origin and what is unique about them? *Antisense Nucleic Acid Drug Dev.* 10, 117–121. doi:10.1089/oli.1.2000.10.117

Edvard Smith, C. I., and Zain, R. (2019). Therapeutic oligonucleotides: state of the art. *Annu. Rev. Pharmacol. Toxicol.* 59, 605–630. doi:10.1146/annurev-pharmtox-010818-021050

Farr, S. A., Ripley, J. L., Sultana, R., Zhang, Z., Niehoff, M. L., Platt, T. L., et al. (2014). Antisense oligonucleotide against GSK-3β in brain of SAMP8 mice improves learning and memory and decreases oxidative stress: involvement of transcription factor Nrf2 and implications for Alzheimer disease. *Free Radic. Biol. Med.* 67, 387–395. doi:10.1016/j.freeradbiomed.2013.11.014

Finkel, R. S., Mercuri, E., Darras, B. T., Connolly, A. M., Kuntz, N. L., Kirschner, J., et al. (2017). Nusinersen versus sham control in infantile-onset spinal muscular atrophy. *N. Engl. J. Med.* 377 (18), 1723–1732. doi:10.1056/NEJMoa1702752

Fitzgerald, K., White, S., Borodovsky, A., Bettencourt, B. R., Strahs, A., Clausen, V., et al. (2017). A highly durable RNAi therapeutic inhibitor of PCSK9. *N. Engl. J. Med.* 376 (1), 41–51. doi:10.1056/NEJMoa1609243

Food and Drug Administration (2020). *Leqvio inclisiran*.

Frank, D. E., Schnell, F. J., Akana, C., El-Husayni, S. H., Desjardins, C. A., Morgan, J., et al. (2020). Increased dystrophin production with golodirsen in patients with Duchenne muscular dystrophy. *Neurology* 94 (21), e2270–e2282. doi:10.1212/WNL.0000000000009233

Frank, F., Sonenberg, N., and Nagar, B. (2010). Structural basis for 5′-nucleotide base-specific recognition of guide RNA by human AGO2. *Nature* 465, 818–822. doi:10.1038/nature09039

Frazier, K. S. (2015). Antisense oligonucleotide therapies:the promise and the challenges from a toxicologic pathologist's perspective. *Toxicol. Pathol.* 43 (1), 78–89. doi:10.1177/0192623314551840

Frishberg, Y., Deschenes, G., Cochat, P., Magen, D., Groothoff, J., Hulton, S. A., et al. (2019). A safety and efficacy study of lumasiran, an investigational RNA interference (RNAi) therapeutic, in adult and pediatric patients with primary hyperoxaluria type 1. *Eur. Urol. Suppl.* 18, e388–e389. doi:10.1016/s1569-9056(19)30291-x

Garrelfs, S. F., Frishberg, Y., Hulton, S. A., Koren, M. J., O'Riordan, W. D., Cochat, P., et al. (2021). Lumasiran, an RNAi therapeutic for primary hyperoxaluria type 1. *N. Engl. J. Med.* 384 (13), 1216–1226. doi:10.1056/NEJMoa2021712

Gaus, H. J., Gupta, R., Chappell, A. E., Østergaard, M. E., Swayze, E. E., and Seth, P. P. (2019). Characterization of the interactions of chemically-modified therapeutic nucleic acids with plasma proteins using a fluorescence polarization assay. *Nucleic Acids Res.* 47, 1110–1122. doi:10.1093/nar/gky1260

Geary, R. S., Henry, S. P., and Grillone, L. R. (2002). Fomivirsen: clinical pharmacology and potential drug interactions. *Clin. Pharmacokinet.* 41, 255–260. doi:10.2165/00003088-200241040-00002

Geary, R. S., Norris, D., Yu, R., and Bennett, C. F. (2015). Pharmacokinetics, biodistribution and cell uptake of antisense oligonucleotides. *Adv. Drug Deliv. Rev.* 87, 46–51. doi:10.1016/j.addr.2015.01.008

Goodkey, K., Aslesh, T., Maruyama, R., and Yokota, T. (2018). Nusinersen in the treatment of spinal muscular atrophy. *Methods Mol. Biol.* 1828, 69–76. doi:10.1007/978-1-4939-8651-4_4

Hair, P., Cameron, F., and McKeage, K. (2013). Mipomersen sodium: first global approval. *Drugs* 73, 487–493. doi:10.1007/s40265-013-0042-2

Hanna, M. (2014). Novel drugs targeting transthyretin amyloidosis. *Curr. Heart Fail Rep.* 11, 50–57. doi:10.1007/s11897-013-0182-4

Haraszti, R. A., Roux, L., Coles, A. H., Turanov, A. A., Alterman, J. F., Echeverria, D., et al. (2017). 5'-Vinylphosphonate improves tissue accumulation and efficacy of conjugated siRNAs *in vivo*. *Nucleic Acids Res.* 45, 7581–7592. doi:10.1093/nar/gkx507

Havens, M. A., Duelli, D. M., and Hastings, M. L. (2013). Targeting RNA splicing for disease therapy. *Wiley Interdiscip. Rev. RNA* 4 (3), 247–266. doi:10.1002/wrna.1158

Heo, Y. A. (2020). Golodirsen: first approval. Drugs. doi:10.1007/s40265-020-01267-2

Herdewijn, P. (2000). Heterocyclic modifications of oligonucleotides and antisense technology. *Antisense Nucleic Acid Drug Dev.* 10, 297–310. doi:10.1089/108729000421475

Hoy, S. M. (2018). Patisiran: first global approval. *Drugs* 78, 1625–1631. doi:10.1007/s40265-018-0983-6

Hua, Y., Vickers, T. A., Okunola, H. L., Bennett, C. F., and Krainer, A. R. (2008). Antisense masking of an hnRNP A1/A2 intronic splicing silencer corrects SMN2 splicing in transgenic mice. *Am. J. Hum. Genet.* 82 (4), 834–848. doi:10.1016/j.ajhg.2008.01.014

Hutcherson, S. L., and Lanz, R. (2002). A randomized controlled clinical trial of intravitreous fomivirsen for treatment of newly diagnosed peripheral cytomegalovirus retinitis in patients with aids. *Am. J. Ophthalmol.* doi:10.1016/S0002-9394(02)01327-2

Ickenstein, L. M., and Garidel, P. (2019). Lipid-based nanoparticle formulations for small molecules and RNA drugs. *Expert Opin. Drug Deliv.* 16 (11), 1205–1226. doi:10.1080/17425247.2019.1669558

Il Geb, V. *Rifiuto dell ' autorizzazione all ' immissione in commercio per Kynamro (mipomersen)*. 2013.

Kang, C. (2023). Avacincaptad pegol: first approval. *Drugs* 83, pages1447–1453. doi:10.1007/s40265-023-01948-8

Kapadia, C. H., Melamed, J. R., and Day, E. S. (2018). Spherical nucleic acid nanoparticles: therapeutic potential. *BioDrugs* 32, 297–309. doi:10.1007/s40259-018-0290-5

Karimian, A., Azizian, K., Parsian, H., Rafieian, S., Shafiei-Irannejad, V., Kheyrollah, M., et al. (2019). CRISPR/Cas9 technology as a potent molecular tool for gene therapy. *J. Cell Physiol.* 234 (8), 12267–12277. doi:10.1002/jcp.27972

Keil, J. M., Seo, J., Howell, M. D., Hsu, W. H., Singh, R. N., and DiDonato, C. J. (2014). A short antisense oligonucleotide ameliorates symptoms of severe mouse models of spinal muscular atrophy. *Mol. Ther. Nucleic Acids* 3 (7), e174. doi:10.1038/mtna.2014.23

Kilanowska, A., and Studzińska, S. (2020). *In vivo* and in vitrostudies of antisense oligonucleotides - a review. *RSC Adv.* 10 (57), 34501–34516. doi:10.1039/D0RA04978F

Kim, J., Hu, C., Moufawad El Achkar, C., Black, L. E., Douville, J., Larson, A., et al. (2019). Patient-customized oligonucleotide therapy for a rare genetic disease. *N. Engl. J. Med.* 381, 1644–1652. doi:10.1056/NEJMoa1813279

Kornblum, N., Ayyanar, K., Benimetskaya, L., Richardson, P., Iacobelli, M., and Stein, C. A. (2006). Defibrotide, a polydisperse mixture of single-stranded phosphodiester oligonucleotides with lifesaving activity in severe hepatic veno-occlusive disease: clinical outcomes and potential mechanisms of action. *Oligonucleotides* 16, 105–114. doi:10.1089/oli.2006.16.105

Krieg, A. M. (2006). Therapeutic potential of toll-like receptor 9 activation. *Nat. Rev. Drug Discov.* 5, 471–484. doi:10.1038/nrd2059

Levin, A. A. (2019). Treating disease at the RNA level with oligonucleotides. *N. Engl. J. Med.* 380 (1), 57–70. doi:10.1056/NEJMra1705346

Levin, A. A., Yu, R. Z., and Geary, R. S. (2007). "Basic principles of the pharmacokinetics of antisense oligonucleotide drugs," in *Antisense drug technology: principles, strategies, and applications* (Boca Raton, Florida, USA: CRC Press).

Meister, G., Landthaler, M., Patkaniowska, A., Dorsett, Y., Teng, G., and Tuschl, T. (2004). Human Argonaute2 mediates RNA cleavage targeted by miRNAs and siRNAs. *Mol. Cell* 15 (2), 185–197. doi:10.1016/j.molcel.2004.07.007

Mendell, J. R., Rodino-Klapac, L. R., Sahenk, Z., Roush, K., Bird, L., Lowes, L. P., et al. (2013). Eteplirsen for the treatment of Duchenne muscular dystrophy. *Ann. Neurol.* 74 (5), 637–647. doi:10.1002/ana.23982

Mercuri, E., Darras, B. T., Chiriboga, C. A., Day, J. W., Campbell, C., Connolly, A. M., et al. (2018). Nusinersen versus sham control in later-onset spinal muscular atrophy. *N. Engl. J. Med.* 378, 625–635. doi:10.1056/NEJMoa1710504

Miller, C. M., Tanowitz, M., Donner, A. J., Prakash, T. P., Swayze, E. E., Harris, E. N., et al. (2018). Receptor-mediated uptake of phosphorothioate antisense oligonucleotides in different cell types of the liver. *Nucleic Acid. Ther.* 28 (3), 119–127. doi:10.1089/nat.2017.0709

Ng, E. W. M., Shima, D. T., Calias, P., Cunningham, E. T., Guyer, D. R., and Adamis, A. P. (2006). Pegaptanib, a targeted anti-VEGF aptamer for ocular vascular disease. *Nat. Rev. Drug Discov.* 5, 123–132. doi:10.1038/nrd1955

Oberemok, V. V., Laikova, K. V., Repetskaya, A. I., Kenyo, I. M., Gorlov, M. V., Kasich, I. N., et al. (2018). A half-century history of applications of antisense oligonucleotides in medicine, agriculture and forestry: we should continue the journey. *Molecules* 23 (6), 1302. doi:10.3390/molecules23061302

Ohuchi, S. (2012). Cell-Selex technology. *Biores Open Access* 1 (6), 265–272. doi:10.1089/biores.2012.0253

Osredkar, D., Jílková, M., Butenko, T., Loboda, T., Golli, T., Fuchsová, P., et al. (2021). Children and young adults with spinal muscular atrophy treated with nusinersen. *Eur. J. Paediatr. Neurol.* 30, 1–8. doi:10.1016/j.ejpn.2020.11.004

Ottesen, E. W., Luo, D., Singh, N. N., and Singh, R. N. (2021). High concentration of an ISS-N1-targeting antisense oligonucleotide causes massive perturbation of the transcriptome. *Int. J. Mol. Sci.* 22 (16), 8378. doi:10.3390/ijms22168378

Paik, J., and Duggan, S. (2019). Volanesorsen: first global approval. *Drugs* 79, 1349–1354. doi:10.1007/s40265-019-01168-z

Prakash, T. P., Graham, M. J., Yu, J., Carty, R., Low, A., Chappell, A., et al. (2014). Targeted delivery of antisense oligonucleotides to hepatocytes using triantennary N-acetyl galactosamine improves potency 10-fold in mice. *Nucleic Acids Res.* 42, 8796–8807. doi:10.1093/nar/gku531

Rehman, Z. U., Hoekstra, D., and Zuhorn, I. S. (2013). Mechanism of polyplex- and lipoplex-mediated delivery of nucleic acids: real-time visualization of transient membrane destabilization without endosomal lysis. *ACS Nano* 7, 3767–3777. doi:10.1021/nn3049494

Richardson, P. G., Grupp, S. A., Pagliuca, A., Krishnan, A., Ho, V. T., and Corbacioglu, S. (2017). Defibrotide for the treatment of hepatic veno-occlusive disease/sinusoidal obstruction syndrome with multiorgan failure. *Int. J. Hematol. Oncol.* 6, 75–93. doi:10.2217/ijh-2017-0015

Richardson, P. G., Riches, M. L., Kernan, N. A., Brochstein, J. A., Mineishi, S., Termuhlen, A. M., et al. (2016). Phase 3 trial of defibrotide for the treatment of severe veno-occlusive disease and multi-organ failure. *Blood* 127, 1656–1665. doi:10.1182/blood-2015-10-676924

Roberts, T. C., Langer, R., and Wood, M. J. A. (2020). Advances in oligonucleotide drug delivery. *Nat. Rev. Drug Discov.* 19 (10), 673–694. doi:10.1038/s41573-020-0075-7

Sahay, G., Querbes, W., Alabi, C., Eltoukhy, A., Sarkar, S., Zurenko, C., et al. (2013). Efficiency of siRNA delivery by lipid nanoparticles is limited by endocytic recycling. *Nat. Biotechnol.* 31, 653–658. doi:10.1038/nbt.2614

Scharner, J., Ma, W. K., Zhang, Q., Lin, K. T., Rigo, F., Bennett, C. F., et al. (2020). Hybridization-mediated off-target effects of splice-switching antisense oligonucleotides. *Nucleic Acids Res.* 48 (2), 802–816. doi:10.1093/nar/gkz1132

Schirle, N. T., and MacRae, I. J. (2012). The crystal structure of human argonaute2. *Science* 336, 1037–1040. doi:10.1126/science.1221551

Schwarz, D. S., Ding, H., Kennington, L., Moore, J. T., Schelter, J., Burchard, J., et al. (2006). Designing siRNA that distinguish between genes that differ by a single nucleotide. *PLoS Genet.* 2 (9), 1400–e218. doi:10.1371/journal.pgen.0020140

Scott, L. J. (2020). Givosiran: first approval. *Drugs* 80, 335–339. doi:10.1007/s40265-020-01269-0

Scott, L. J., and Keam, S. J. (2021). Lumasiran: first approval. *Drugs* 81, 277–282. doi:10.1007/s40265-020-01463-0

Shadid, M., Badawi, M., and Abulrob, A. (2021). Antisense oligonucleotides: absorption, distribution, metabolism, and excretion. *Expert Opin. Drug Metab. Toxicol.* 17 (11), 1281–1292. doi:10.1080/17425255.2021.1992382

Shen, X., and Corey, D. R. (2018). Chemistry, mechanism and clinical status of antisense oligonucleotides and duplex RNAs. *Nucleic Acids Res.* 46 (4), 1584–1600. doi:10.1093/nar/gkx1239

Shirley, M. (2021). Casimersen: first approval. *Drugs*. doi:10.1007/s40265-021-01512-2

Singh, N. K., Singh, N. N., Androphy, E. J., and Singh, R. N. (2006). Splicing of a critical exon of human Survival Motor Neuron is regulated by a unique silencer element located in the last intron. *Mol. Cell Biol.* 26 (4), 1333–1346. doi:10.1128/MCB.26.4.1333-1346.2006

Singh, N. N., Howell, M. D., Androphy, E. J., and Singh, R. N. (2017). How the discovery of ISS-N1 led to the first medical therapy for spinal muscular atrophy. *Gene Ther.* 24 (9), 520–526. doi:10.1038/gt.2017.34

Singh, N. N., Lawler, M. N., Ottesen, E. W., Upreti, D., Kaczynski, J. R., and Singh, R. N. (2013). An intronic structure enabled by a long-distance interaction serves as a novel target for splicing correction in spinal muscular atrophy. *Nucleic Acids Res.* 41 (17), 8144–8165. doi:10.1093/nar/gkt609

Singh, N. N., Lee, B. M., DiDonato, C. J., and Singh, R. N. (2015). Mechanistic principles of antisense targets for the treatment of spinal muscular atrophy. *Future Med. Chem.* 7 (13), 1793–1808. doi:10.4155/fmc.15.101

Springer, A. D., and Dowdy, S. F. (2018). GalNAc-siRNA conjugates: leading the way for delivery of RNAi therapeutics. *Nucleic Acid. Ther.* 28, 109–118. doi:10.1089/nat.2018.0736

Stein, C. A., and Castanotto, D. (2017). FDA-approved oligonucleotide therapies in 2017. *Mol. Ther.* 25 (5), 1069–1075. doi:10.1016/j.ymthe.2017.03.023

Tanowitz, M., Hettrick, L., Revenko, A., Kinberger, G. A., Prakash, T. P., and Seth, P. P. (2017). Asialoglycoprotein receptor 1 mediates productive uptake of N-acetylgalactosamine-conjugated and unconjugated phosphorothioate antisense oligonucleotides into liver hepatocytes. *Nucleic Acids Res.* 45 (21), 12388–12400. doi:10.1093/nar/gkx960

Thomas, G. S., Cromwell, W. C., Ali, S., Chin, W., Flaim, J. D., and Davidson, M. (2013). Mipomersen, an apolipoprotein b synthesis inhibitor, reduces atherogenic lipoproteins in patients with severe hypercholesterolemia at high cardiovascular risk: a randomized, double-blind, placebo-controlled trial. *J. Am. Coll. Cardiol.* 62, 2178–2184. doi:10.1016/j.jacc.2013.07.081

Tréhin, R., Nielsen, H. M., Jahnke, H. G., Krauss, U., Beck-Sickinger, A. G., and Merkle, H. P. (2004). Metabolic cleavage of cell-penetrating peptides in contact with epithelial models: human calcitonin (hCT)-derived peptides, Tat(47-57) and penetratin(43-58). *Biochem. J.* 382 (3), 945–956. doi:10.1042/BJ20040238

Vasquez, G., Freestone, G. C., Wan, W. B., Low, A., De Hoyos, C. L., Yu, J., et al. (2021). Site-specific incorporation of 5'-methyl DNA enhances the therapeutic profile of gapmer ASOs. *Nucleic Acids Res.* 49 (4), 1828–1839. doi:10.1093/nar/gkab047

Vegeto, E., Maggi, A., and Minghetti, P. (2019). *Farmaci biotecnologici aspetti farmacologici e clinici*. Rozzanop: Universita Degli Studi Di Milani, 173–191. http://hdl.handle.net/2434/708678.

Ward, A. J., Norrbom, M., Chun, S., Bennett, C. F., and Rigo, F. (2014). Nonsense-mediated decay as a terminating mechanism for antisense oligonucleotides. *Nucleic Acids Res.* 42 (9), 5871–5879. doi:10.1093/nar/gku184

Williamson, T. P., Johnson, D. A., and Johnson, J. A. (2012). Activation of the Nrf2-ARE pathway by siRNA knockdown of Keap1 reduces oxidative stress and provides partial protection from MPTP-mediated neurotoxicity. *Neurotoxicology* 33 (3), 272–279. doi:10.1016/j.neuro.2012.01.015

Wiraja, C., Yeo, D., Lio, D., Labanieh, L., Lu, M., Zhao, W., et al. (2014). Aptamer technology for tracking cells' status and function. *Mol. Cell Ther.* 2 (1), 33. doi:10.1186/2052-8426-2-33

Wisse, E., Jacobs, F., Topal, B., Frederik, P., and De Geest, B. (2008). The size of endothelial fenestrae in human liver sinusoids: implications for hepatocyte-directed gene transfer. *Gene Ther.* 15, 1193–1199. doi:10.1038/gt.2008.60

Witztum, J. L., Gaudet, D., Freedman, S. D., Alexander, V. J., Digenio, A., Williams, K. R., et al. (2019). Volanesorsen and triglyceride levels in familial chylomicronemia syndrome. *N. Engl. J. Med.* 381 (6), 531–542. doi:10.1056/NEJMoa1715944

Wurster, C. D., Winter, B., Wollinsky, K., Ludolph, A. C., Uzelac, Z., Witzel, S., et al. (2019). Intrathecal administration of nusinersen in adolescent and adult SMA type 2 and 3 patients. *J. Neurol.* 266, 183–194. doi:10.1007/s00415-018-9124-0

Yin, W., and Rogge, M. (2019). Targeting RNA: a transformative therapeutic strategy. *Clin. Transl. Sci.* 12 (2), 98–112. doi:10.1111/cts.12624

Zamecnik, P. C., and Stephenson, M. L. (1978). Inhibition of Rous sarcoma virus replication and cell transformation by a specific oligodeoxynucleotide. *Proc. Natl. Acad. Sci. U. S. A.* 75, 280–284. doi:10.1073/pnas.75.1.280

Glossary

2′- F	2′-Fluoro
2′-O-Me	2′-O-methyl
2′-O-MOE	2′-O-methoxyethyl
6 MWT	6 min walk test
AGO-2	Argonaut 2
AHP	Acute hepatic porphyria
AIDS	Acquired immunodeficiency syndrome
ALAS	Aminolevulinate synthase
ALS	amyotrophic lateral sclerosis
aODN	antisense OligoDesoxiNucleotides
APO	Apolipoprotein
ATTR	Transthyretin amyloidosis
ASCVD	Atherosclerotic cardiovascular disease
ASGR	Asialoglycoprotein receptor
ASO	Antisense Oligonucleotides
BNA	Bridged nucleic acid
CLN7	Neuronal Ceroid Lipofuscinosis
CMV	Cytomegalovirus
CNS	Central nervous system
CPP	Cell-penetrating peptides
CRISP	Clustered Regularly Interspaced Short Palindromic Repeats
crRNA	CRISP RNA, DNADeoxyriboNucleic Acid
DF	Defibrotide
DMD	Duchenne muscular dystrophy
EMA	European Medicines Agency
E	Enema
EPR	Enhanced permeability and retention
FAP	Familial amyloid poly Neuropathy
FCS	Familial chylomicronemia syndrome
FDA	Food and Drug Administration
FH	Familial hypercholesterolemia
GAlNAc	N-acetylgalactosamine
HAART	Highly active antiretroviral therapy
HAO1	Hydroxyacid oxidase 1
hATTR	Hereditary Transthyretin amyloidosis
HoF	HOmozygous familial hypercolesterolaemia
HSCT	Hematopoietic stem cell transplantation, HTTHuntingtin
ICAM	Intercellular adhesion molecule
IE2	Immediate early 2
ITH	Intrathecal
IV	Intravenous
IVT	intravitreal
LDL-C	Low-density lipoprotein cholesterol
LDL-R	Low-density lipoprotein receptor
LNP	lipid nanoparticles
mRNA	RNA messenger
MFSD8	Major Facilitator superfamily domain containing 8
miRNA	microRNA
mNIS+7	modified neuropathy impairment score +7
p53	Tumor protein, PAI—plasminogen activator inhibitor
PBAE	poly-(beta-amino-ester)
PCSK9	Proprotein convertase subtilisin/kexin type 9
PEG	Polyethylene glycol
PEI	Polyethylenimine
PH1	Hyperoxaluria type 1
PMO	Phosphorodiamidate morpholino
PNA	Nucleic peptide acid
pre-mRNA	precursor RNA messenger
PS	Phosphorothioate
QOL-DN	Norfolk Quality of Life-Diabetic Neuropathy
RISC	RNA Induced Silencing RNA
RNA	RiboNucleic Acid
RNAi	RNA interference
RNAse H	ribonuclease H
SC	Subcutaneous
SELEX	Systematic Evolution of Ligands by Exponential Enrichment
sHTG	severe hypertriglyceridemia
siRNA	Small interfering RNA
SMA	Spinal muscular atrophy
SMN	Survival of motor neuron
SNA	Spherical nucleic Acid
SOD1	Superoxide dismutase
SOS	Sinusoidal obstruction syndrome
STAB	stabilin
SVA	SINE-VNTR-Alu
TG	Triglyceride
TGRL	Triglyceride rich lipoprotein
TFPI	Tissue factor pathway inhibitor
TLR	Toll-like receptor
TM	thrombomodulin
tPA	tissue plasminogen activator
TRBP	TAR RNA binding protein

TRPV1	Transient Receptor Potential Vanilloid 1
TTR	Transthyretin
VEGF	vascular endothelial growth factor
VOD	Veno-occlusive disease
vWF	von Willebrand factor

frontiers | Frontiers in Pharmacology

TYPE Original Research
PUBLISHED 05 December 2023
DOI 10.3389/fphar.2023.1307799

OPEN ACCESS

EDITED BY
Patrícia Mendonça Rijo,
Lusofona University, Portugal

REVIEWED BY
Shahid Karim,
King Abdulaziz University, Saudi Arabia
Debora Collotta,
University of Turin, Turin, Italy

*CORRESPONDENCE
Anjana Goel,
anjana.goel@gla.ac.in
Zhijian Lin,
linzhijian@bucm.edu.cn

RECEIVED 05 October 2023
ACCEPTED 20 November 2023
PUBLISHED 05 December 2023

CITATION
Sharma A, Goel A and Lin Z (2023), Analysis of anti-rheumatic activity of *Nyctanthes arbor-tristis* via *in vivo* and pharmacovigilance approaches. *Front. Pharmacol.* 14:1307799. doi: 10.3389/fphar.2023.1307799

Analysis of anti-rheumatic activity of *Nyctanthes arbor-tristis* via *in vivo* and pharmacovigilance approaches

Ayushi Sharma[1], Anjana Goel[1]* and Zhijian Lin[2]*

[1]Department of Biotechnology, Institute of Applied Sciences and Humanities, GLA University, Mathura, Uttar Pradesh, India, [2]Department of Clinical Chinese Pharmacy, School of Chinese Materia Medica, Beijing University of Chinese Medicine, Beijing, China

Introduction: Rheumatoid arthritis (RA) is an immune-mediated disease associated with chronic inflammation of numerous joints. *Nyctanthes arbor-tristis* (NAT) is a traditional remedy for RA, a chronic inflammatory disorder.

Aim: The current project aims to demonstrate the role of the NAT extracts in subacute toxicity, pharmacovigilance, and anti-rheumatic biomarkers.

Method: Hydroethanolic extract (1:1) of plant leaves was prepared by using the reflux method. The safety of the dose was evaluated in Sprague–Dawley rats, and the anti-inflammatory effects of NAT on RA symptoms, including paw volumes, body weight, arthritic index, withdrawal latency, hematology and serological test, radiology, and histopathology, were evaluated in Freund's complete adjuvant (FCA)-induced arthritis Sprague–Dawley rat models. The inflammatory (TNF-α and COX-2) and anti-inflammatory markers (IL-10) were analyzed in control and experimental groups.

Result: The study showed that 500 mg/kg BW NAT leaf extract was found to be least toxic without showing any subacute toxicity symptoms. The pharmacovigilance study highlighted the potential side effects of NAT, such as drowsiness, sedation, and lethargy, at high dosages. Treatment with the plant extract mitigated paw edema, restored the immune organ and body weights, and ameliorated the level of blood parameters such as hemoglobin, red blood cells, platelets, white blood cells, aspartate aminotransferase (AST), alanine transaminase (ALT), C-reactive proteins, and rheumatoid factor. Treatment with the plant extracts also reduced the level of cyclooxygenase 2 and TNF-α and increased the level of IL-10 in the serum of arthritic rats dose-dependently. Radiographic analysis of the ankle joint showed an improvement in the hind legs. Histological examination of the ankle joints revealed that the plant extract treatment decreased pannus formation, inflammation, and synovial hyperplasia in arthritic animals.

Conclusion: NAT 500 mg/kg could serve as a promising therapeutic option for the treatment of inflammatory arthritis.

KEYWORDS

Harsingar, anti-inflammatory, rheumatoid arthritis, cytokines, Freund's complete adjuvant, indomethacin

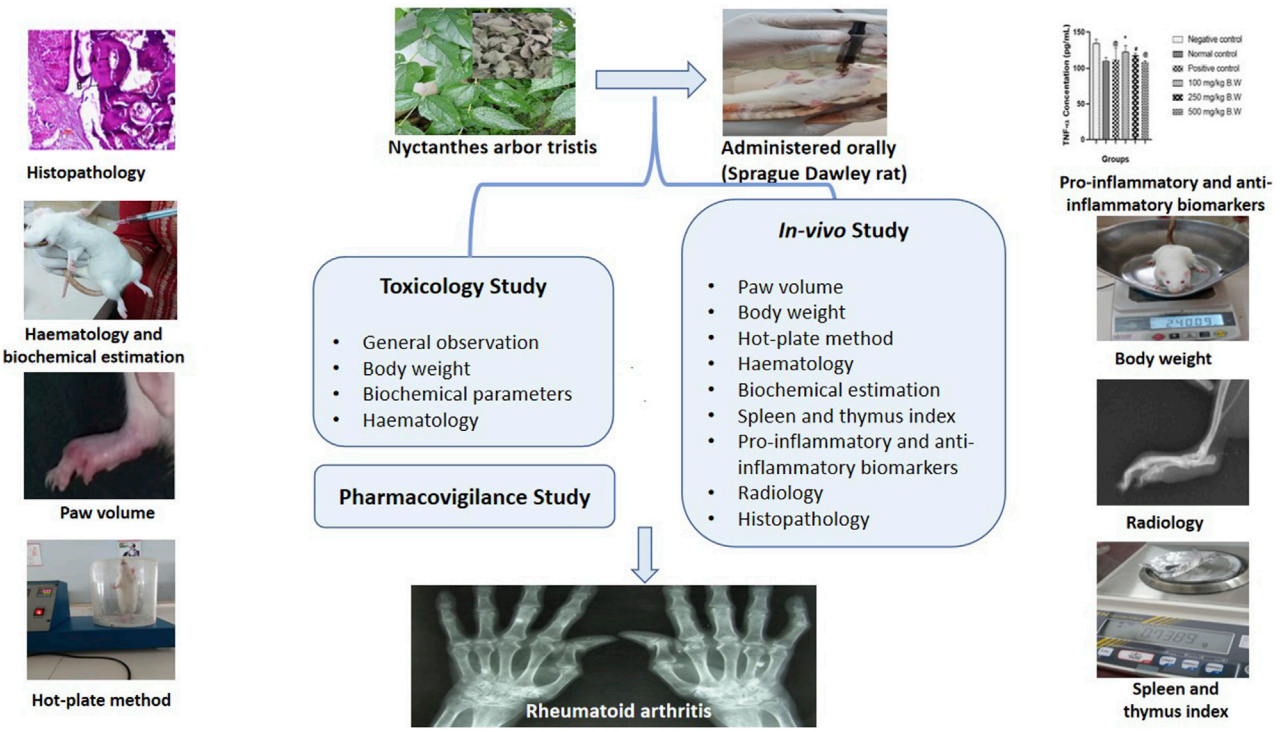

GRAPHICAL ABSTRACT

1 Introduction

Rheumatoid arthritis (RA) is an immune-mediated disease associated with chronic inflammation of numerous joints. RA symptoms include persistent joint synovial inflammation, pannus development, and subsequent destruction of adjacent bone/cartilage tissue (Marsh et al., 2021). It can rapidly progress to inflammation, affecting various systems with irreversible joint dysfunction, resulting in early mortality, debility, reduced quality of life, and even mortality (Radu and Bungau, 2021). Articular cartilage hyperplasia is a key step in the pathogenesis of RA, which is facilitated by macrophages, T and B lymphocytes, fibroblasts, and pro-inflammatory cytokines, most prominently interleukins (IL-6, IL-1, and TNF-α) (Nygaard and Firestein, 2020). Increased oxidative stress, along with an increase in pro-inflammatory cytokines, is thought to be a significant risk factor for joint deterioration in RA. When inflammatory cells like macrophages and neutrophils stimulate cytokine production, they release reactive oxygen species (ROS) and may damage tissues (Warmink et al., 2023).

Traditional non-steroidal anti-inflammatory medicines (NSAIDs) and disease-modifying anti-rheumatic drugs (DMARDs) have been replaced by innovative biological agents such as TNF monoclonal antibodies, which have improved the treatment strategies for RA patients in recent years (Ben Mrid et al., 2022). Existing medications for rheumatoid arthritis have demonstrated restricted effectiveness in achieving remission in specific patients and are associated with a range of side effects, encompassing systemic organ toxicity affecting the gastrointestinal tract, skin, and kidneys, as well as immunotoxicity, which heightens the risk of infections (Martu et al., 2021). Herbal therapies have been used conveniently for some time with no obvious toxicity or adverse effects, prompting a fresh wave of research into conventional methods currently. Sharma and Goel (2023) suggest that now is the time to look for new and improved natural medicines that can be used for the long-term treatment of RA.

Night jasmine, scientifically known as *Nyctanthes arbor-tristis* Linn and commonly referred to as night jasmine, belongs to the Oleaceae family (Solanki et al., 2021). This plant species is indigenous to South Asia, with its presence documented in regions spanning India (Assam, Arunachal Pradesh, and the area extending southward to the central region of Godavari), Nepal, Bhutan, Java, Sri Lanka, and Sumatra (Pundir et al., 2022). In Ayurveda, *Nyctanthes arbor-tristis* holds significant medicinal potential. It has been identified as a valuable source of bioactive compounds that can serve both as medicines and as intermediates for the development of novel therapeutic agents in modern medicine (Wang et al., 2023). Historically, *Nyctanthes arbor-tristis* has demonstrated a wide range of therapeutic properties, including antimicrobial, antioxidant, antiviral, antidiabetic, antimalarial, antifungal, anti-inflammatory, anticancer, central nervous system depressant, hepatoprotective, and immunostimulant activities. Comprehensive studies, both *in vitro* and *in vivo*, have scientifically validated the presence of these pharmacologically active constituents throughout various parts of the plant (Rawat et al., 2021). Traditionally, the leaves of this plant have been used to prepare decoctions and juices for treating inflammatory disorders such as arthritis and rheumatism. Additionally, the flowers of *Nyctanthes arbor-tristis* have been recognized for their beneficial properties in addressing conditions such as indigestion, flatulence, and stomachic issues; promoting bowel regularity; addressing piles;

and managing various skin ailments (Chakraborty and Datta, 2022). In the realm of rheumatic joint pain relief, the powdered stem bark has historically been employed, albeit with limited scientific documentation. The objective of this study was to assess the potential toxicity resulting from the daily administration of hydroethanolic extracts derived from the *Nyctanthes arbor-tristis* leaves for over a 28-day period. Additionally, we aimed to investigate their *in vivo* anti-edematous and anti-arthritic activities as well as their impact on cytokine profiles in a model of Freund's complete adjuvant (FCA)-induced experimental arthritis.

2 Materials and methods

2.1 Authentication and procurement of the plant

From January to March, leaves were collected from the GLA University campus in India. At the Agharkar Research Institute in Pune, India, the plant specimens were identified and authenticated using the voucher specimen (AUTH 22-48). Fresh leaves were thoroughly washed in distilled water and tap water before being air-dried. When not in use, the dried leaves were coarsely crushed with an electric mixer and stored in sealed plastic bags.

2.2 Preparation of hydroethanolic extract

The phytoconstituents were extracted using a hydroethanolic solvent in a 1:1 ratio, employing a reflux apparatus. The resulting extract was then concentrated at 45°C by using a rotary vacuum evaporator from Yamato Scientific Co., Japan. In preparation for the *in vivo* study, the concentrated extract was subsequently stored at −20°C.

2.3 Experimental animal

The study protocol was approved by the Institutional Animal Ethical Committee (IAEC) of the Dept. of Biotechnology and Institute of Pharmaceutical Research, GLA University, Mathura, India, in accordance with the regulations of CPCSEA (1260/PO/AC/09/CPCSE). Female Sprague–Dawley (SD) rats were obtained from the "National Institute of Biologicals," Noida, India. The animals were housed in a typical animal housing facility with a temperature of 24 ± 1°C, relative humidity of (45%–50%), and a light/dark cycle of 12 h. The animals were fed a conventional pellet chow diet and were given unlimited access to water. The animals were allowed to acclimate for at least 10 days before the experiments.

2.4 Selection of doses and sub-acute toxicity studies

The dose was chosen based on prior toxicity tests, which showed that a dose of 2 g/kg BW did not cause mortality in rats (Hazarika et al., 2022). As a result, the maximal dose in this investigation was set at 2 g/kg BW. The oral toxicity investigation was conducted based on OECD Guideline 407 (Balkrishna et al., 2023). The animals were divided into six groups of six each (females). Group 1 was treated as the vehicle control. Extract doses of 100, 250, 500, 1,000, and 2,000 mg/kg/BW were administered to groups 2, 3, 4, 5, and 6 and the vehicles, respectively, for 28 days. All the extracts were given via oral gavage.

2.4.1 General observation and mortality

Death, any sign of illness, and response to therapy were recorded twice daily, along with other general observations like changes in the skin, drowsiness, sedation, eye color, general physique, coma, and death. The procedures were conducted following the guidelines for the recognition, evaluation, and use of clinical signs as the human endpoint for the safety evaluation of experiments involving animals.

2.4.2 Body weight

During the experiment, the body weight was recorded at 0 days and after 7-day intervals up to 28 days by using a digital weighing balance.

2.4.3 Hematological and biochemical analysis

All the animals were made to fast overnight before drawing the blood for analysis of the hematology and biochemical parameters. The animals were provided free access to water. The rats were anesthetized before drawing blood samples directly from the heart, and the samples were stored in EDTA-coated and plain vials. Hemoglobin, white blood cell count, red blood cell count, platelets, protein, albumin, gamma globulin, urea, uric acid, creatinine, AST, ALT, bilirubin, and cholesterol of the control and plant-treated groups were estimated using an automatic hematology analyzer (hematology auto analyzer MEK-6420P) and clinical chemistry analyzer (semi-automated biochemistry analyzer Erba Chem 5X).

2.5 Pharmacovigilance study

In this research, we conducted a pharmacovigilance study, including the detection, assessment, understanding, and prevention of the potential risk of NAT, through literature reviewing, *in vivo* experiments, and surveillance database mining.

2.5.1 Detection

This involves identifying potential adverse drug reactions (ADRs) associated with the use of *Nyctanthes arbor-tristis*. This can be done through spontaneous reporting, clinical trials, systematic reviews, and observational studies. There is limited scientific evidence available on the potential ADRs associated with *Nyctanthes arbor-tristis*, as it is a traditional herbal medicine and has not been extensively studied in clinical trials. From the Chinese Field Herbarium official website (http://www.cfh.ac.cn/), the term *Nyctanthes arbor-tristis* was entered, and the relevant species information card (http://www.cfh.ac.cn/34781.sp) was used to find the nickname of *Nyctanthes arbor-tristis*. With regard to the detection of potential safety issues, this study systematically searched the China National Medical Product

Administration website, the FDA Adverse Event Reporting System, the Canadian Institutes of Health Research, and the Medicinal plant database, Botanical Survey of India, India (https://bsi.gov.in/page/en/medicinal-plant-database) and comprehensively identified adverse reactions associated with *Nyctanthes arbor-tristis*. In addition, we also searched published articles from PubMed, China National Knowledge Infrastructure Database, and Google Scholar to detect the potential risk of *Nyctanthes arbor-tristis*.

2.5.2 Assessment

After identifying the ADRs of *Nyctanthes arbor-tristis*, further research should be conducted to assess the severity and frequency of these reactions. Since *Nyctanthes arbor-tristis* is a traditional herb commonly used mostly in India and China, and there is no patent drug made from just *Nyctanthes arbor-tristis*, we searched the database of clinical trials in China (http://www.chictr.org.cn), NIH U.S. National Library of Medicine (https://clinicaltrials.gov), and India to conduct the risk assessment.

2.5.3 Understanding

Based on the literature search, there are some potential ADRs related to the risks of *Nyctanthes arbor-tristis*, and this research conducted a safety experiment to find out the mechanism of the risk of *Nyctanthes arbor-tristis*. This study promoted the understanding of the potential risk of *Nyctanthes arbor-tristis*. Further research can be conducted to understand the mechanisms behind these reactions and the risk factors for developing them.

2.5.4 Prevention

Based on the results of the risk assessment, appropriate risk minimization strategies are developed and implemented. Based on the pharmacovigilance study, we should pay attention to the dosage and duration of *Nyctanthes arbor-tristis* in medical use. If there is any adverse reaction monitored, it will be necessary to discontinue the use of *Nyctanthes arbor-tristis* and treat the ADR symptoms.

2.6 Anti-rheumatic activity

2.6.1 Induction of RA by FCA

Subcutaneous injection of approximately 0.1 mL of FCA was administered to the subplantar region of the left hind paw on both the first and seventh days to all the animals in every group, except for those in the vehicle control group (Singh et al., 2021).

For the study of FCA-induced arthritis, the rats were split into six groups with six rats in each group.

Group I: vehicle control: normal saline was given as an oral 1% w/v suspension.
Group II: arthritic control: normal saline was given as an oral 1% w/v suspension.
Group III: arthritic animals were given 10 mg/kg of body weight of indomethacin, a commonly used anti-inflammatory medication.
Group IV: rheumatic arthritic animals were treated orally with a hydroethanolic fraction of NAT at a dose of 100 mg/kg body weight.
Group V: rheumatic arthritic animals were treated orally with a hydroethanolic fraction of NAT at a dose of 250 mg/kg body weight.
Group VI: rheumatic arthritic animals were treated orally with a hydroethanolic fraction of NAT at a dose of 500 mg/Kg body weight.

At the conclusion of the experiment, the rats were anesthetized using 7% chloral hydrate (400 mg/kg, administered intraperitoneally; supplied by Sinopharm Chemical Reagent Co., Ltd.). It was verified that the rats exhibited no indications of peritonitis, pain, or discomfort as a result of anesthesia. Following anesthesia, blood was drawn from the live anesthetized rats from the abdominal aorta. After obtaining 5 mL of blood, the rats were subsequently euthanized through cervical dislocation. Furthermore, the ankle joints, synovial tissue, and spleen were collected from each animal.

2.6.2 Evaluation of paw volume

A "plethysmometer (Ugo, Basile, Italy)" was used to measure the left paw volume up to the lateral malleolus before FCA injection on the first day and at 7-day intervals thereafter until the 28th day (Shakeel et al., 2021).

2.6.3 Determination of body weight

During the experiment, the body weight was measured by using a digital scale (Sartorius 1413, MP 8/8-1, Bohemia, NY, United States) before the first FCA injection on the first day and then at different times until the 28th day (Singh et al., 2021).

2.6.4 Analgesic assessment using the hot plate test

Analgesic activity was evaluated using a modified version of Eddy's hot plate method (Gurung et al., 2020). The temperature of the plate used to house the rats was maintained at 55 ± 1°C. There was a log detailing how long the rats took for paw licking and how long they took for jumping. Each rat's reaction time, measured in seconds, was recorded as it took flight from the plate. The nociceptive response was assessed at 15-min intervals for 90 min before and after the administration of the vehicle; NAT hydroethanolic extracts at 100, 250, and 500 mg/kg and indomethacin at 10 mg/kg.

2.6.5 Radiological analysis of ankle joints

On day 28, after injecting FCA into the animal's hind paws, they were anesthetized using ketamine anesthesia for X-rays analyzed by (GE DX-300). At 40 kV peak and 12 Ms, radiographs of the hind paw were taken. The radiographic alterations were deduced from the X-ray image (Alamgeer et al., 2017).

2.6.6 Determination of spleen and thymus weight

Rats were slaughtered using ketamine anesthesia after the experiments. The weights of all the thymus and spleens were measured.

2.6.7 Parameter of biochemical estimation

The blood was taken on the 28th day of the experiment. Aspartate aminotransferase (AST), alanine transaminase (ALT), C-reactive protein (CRP) level, and rheumatoid factor (RF) were estimated in the serum (Vijeesh et al., 2022).

TABLE 1 General appearance and behavioral observations of the sub-acute toxicity study for the control and treated groups.

Groups	Change in skin	Drowsiness	Sedation	Eye color	General physique	Coma	Death
Vehicle control	No effect	Not present	Not observed	No effect	Normal	Not present	Alive
NAT (100 mg/kg)	No effect	Not present	Not observed	No effect	Normal	Not present	Alive
NAT (250 mg/kg)	No effect	Not present	Not observed	No effect	Normal	Not present	Alive
NAT (500 mg/kg)	No effect	Not present	Not observed	No effect	Normal	Not present	Alive
NAT (1,000 mg/kg)	No effect	Present	Observed	No effect	Lethargy	Not present	Alive
NAT (2,000 mg/kg)	No effect	Present	Observed	No effect	Lethargy	Not present	Alive

2.6.8 Estimation of inflammatory biomarkers (TNF-α, COX-2, and IL-10)

Pro-inflammatory and anti-inflammatory biomarkers, including TNF-α (DY510-05), COX-2 (ELK7718), and IL-10 (DY522-05), were analyzed using the R&D Systems DuoSet Development Kit with pre-made ELISA reagent kits as per the instruction of the manual by ELISA (i-mark microplate absorbance reader Bio-Rad (Felipe et al., 2020).

2.6.9 Histopathological assessment of joints

For histological analysis, the paws were removed from treated and control rats and their ankle joints were transacted between the medial and lateral malleoli. The rats' feet were then placed in 10% formalin (Uttra et al., 2019).

2.7 Data and statistical analysis

The data are presented in the form of mean ± SEM for a sample size of six animals. We conducted statistical analysis on the experimental results using one-way ANOVA followed by the Dunnett test, employing GraphPad InStat software. A significance level of $p < 0.05$ was employed to determine statistical significance.

3 Result

3.1 Sub-acute toxicity study

The sub-acute toxic study of the tested plant extract was determined as per OECD guideline 407.

3.1.1 General observation and mortality

In the experiment groups and the control group, no treatment-related deaths were reported. Throughout the 28-day study period, neither physical nor behavioral changes were seen in the groups, but drowsiness, sedation, and lethargy were observed in 1,000 and 2,000 mg/kg BW animals, as shown in Table 1.

3.1.2 Change in body weight

There was no statistically significant difference found in average body weight between the vehicle control and the NAT group at doses of 100, 250, 500, 1,000, and 2,000 mg/kg, but in the 1,000 and 2,000 mg/kg BW group animals, decrease in body weight was observed compared to other groups. The effect of NAT extract on body weight is shown in Table 2 ($p > 0.05$).

3.1.3 Effect of the plant extract on hematological and biochemical parameters

The results of the various hematological and biochemical parameters tests on the experimental and vehicle groups are summarized in (Tables 3, 4, and 5). Oral administration of NAT at doses of 100, 250, 500, 1,000, and 2,000 mg/kg did not cause statistically significant changes in hematological and biochemical parameters, such as protein, albumin, gamma-globulin, urea, sodium, creatinine, uric acid, SGOT (AST), SGPT (ALT), bilirubin, and total cholesterol levels, when compared to the control group, but increased levels of SGOT, SGPT, bilirubin, and total cholesterol showed toxicity were observed when compared to the vehicle control.

3.2 Pharmacovigilance finding and measures

Nyctanthes arbor-tristis is a traditional herbal medicine commonly used in China, India, and other Asian countries. It is very important to conduct pharmacovigilance research for *Nyctanthes arbor-tristis*. Based upon the theory, science, and activities of pharmacovigilance, conducting pharmacovigilance research for *Nyctanthes arbor-tristis* involves several steps given as follows

3.2.1 Detection

On the PubMed website (https://pubmed.ncbi.nlm.nih.gov/), the terms *Nyctanthes arbor-tristis* Linn, Bruschia macrocarpa Bertol, *Nyctanthes* dentata Blume, *Nyctanthes tristis* Salisb, *Parilium arbor-tristis* (L.) Gaertn, *Scabrita scabra* L, and *Scabrita triflora* L were entered and relevant literature on adverse reactions was searched for one by one. Some possible ADRs that have been reported in traditional medicine practices include gastrointestinal complaints such as stomach pain, gastric ulcer, nausea, vomiting, and diarrhea, which have been reported in some cases (Saxena et al., 1987; Godse et al., 2016); allergic reactions such as skin rash, itching, and hives have been reported in some individuals; central nervous system effects such as drowsiness, headache, and dizziness have been reported in some cases; some cases also report liver and kidney damage (Das et al., 2008). It is important to note that these ADRs are based on traditional medical practices and may not have been rigorously studied in clinical trials. In addition, there are no

TABLE 2 Effect of different concentrations of NAT extracts on body weight.

Groups	Body weight on different days (g)					
	Day 0	Day 7	Day 14	Day 21	Day 28	Change in % (Days 0–28)
Vehicle control	212.3 ± 23.6	210.5 ± 21.3	216.5 ± 22.7	218.6 ± 23.2	216.1 ± 21.9	1.78
NAT (100 mg/kg)	234.66 ± 22.6	239 ± 24.3	245.3 ± 25.5	246.83 ± 22.9	247.3 ± 24.9	5.38
NAT (250 mg/kg)	217.33 ± 7.2	218.4 ± 7.3	234.5 ± 12.7	235.7 ± 11.3	234.4 ± 10.9	7.85
NAT (500 mg/kg)	212.5 ± 14.9	226.8 ± 16.3	243.813.8	247.4 ± 14.7	248 ± 11	16.70
NAT (1,000 mg/kg)	215 ± 40.8	223.8 ± 39.9	213 ± 43.6	198.5 ± 39.9	195.6 ± 37.6	−9.02
NAT (2,000 mg/kg)	240.33 ± 22.23	236 ± 17.2	220.33 ± 39.2	212.5 ± 39.9	208.4 ± 37.5	−13.28

TABLE 3 Renal profile of the control group and rats treated with NAT leaf extract measured during the sub-acute toxicity study.

Parameters	Vehicle control	NAT (100 mg/kg)	NAT (250 mg/kg)	NAT (500 mg/kg)	NAT (1,000 mg/kg)	NAT (2,000 mg/kg)
Urea (mg/dL)	30.33 ± 4.72	32.2 ± 5.40	30.7 ± 5.70	34.74 ± 7.31	35.44 ± 6.10	35.17 ± 2.50
Uric acid (mg/dL)	3.73 ± 0.75	3.55 ± 0.71	3.95 ± 0.62	3.87 ± 0.44	3.89 ± 0.25	4.04 ± 0.36
Creatinine (mg/dL)	0.71 ± 0.14	0.68 ± 0.12	0.72 ± 0.10	0.62 ± 0.14	0.73 ± 0.13	0.85 ± 0.06

TABLE 4 Liver profile of the control group and rats treated with NAT leaf extract measured during the sub-acute toxicity study.

Parameters	Vehicle control	NAT (100 mg/kg)	NAT (250 mg/kg)	NAT (500 mg/kg)	NAT (1,000 mg/kg)	NAT (2,000 mg/kg)
SGOT (AST) (IU/L)	162 ± 37.24	168.5 ± 41.41	163 ± 20.92	167.5 ± 39.68	178.7 ± 66.70	214.5 ± 42.65
SGPT (ALT) (IU/L)	134.66 ± 40.5	142.04 ± 38.83	143.6 ± 16.5	143.75 ± 42.30	165.4 ± 47.17	181 ± 22.32
Bilirubin (g/dL)	0.40 ± 0.09	0.45 ± 0.16	0.58 ± 0.15	0.58 ± 0.1	0.62 ± 0.05	0.64 ± 0.10
Total cholesterol (mg/dL)	96.43 ± 9.22	93.75 ± 16.98	98.74 ± 8.38	98.9 ± 12.72	108.24 ± 52.6	116.52 ± 48.5

TABLE 5 Hematological parameters of the control group and rats treated with NAT leaf extract measured during the sub-acute toxicity study.

Parameters	Vehicle control	NAT (100 mg/kg)	NAT (250 mg/kg)	NAT (500 mg/kg)	NAT (1,000 mg/kg)	NAT (2,000 mg/kg)
`Q Protein (g/dL)	6.67 ± 0.64	6.28 ± 0.42	6.42 ± 0.36	6.39 ± 0.38	6.59 ± 0.88	6.77 ± 0.53
Albumin (g/dL)	3.9 ± 0.57	3.52 ± 0.48	3.66 ± 0.38	3.80 ± 0.09	3.84 ± 0.76	3.33 ± 0.32
γ-Globulin (g/dL)	3.34 ± 0.37	2.62 ± 0.72	2.62 ± 0.46	2.49 ± 0.52	3.07 ± 0.24	2.93 ± 0.58
Hemoglobin (g/L)	11.96 ± 0.28	12.93 ± 0.4	13 ± 0.5	14.4 ± 0.2	12.35 ± 0.38	11.5 ± 0.7
WBC (10^9/L)	9733.33 + 1150	9830 + 2600	9600 + 731.81	9533.33 + 500	9800 + 1699	9950 + 1681.93
Total RBC (10^{12}/L)	8.62 ± 0.51	8.74 ± 1.52	9.05 ± 0.71	10.17 ± 0.93	10.21 ± 1.47	9.14 ± 1.03
Platelets (10^3/?L)	708.40 ± 117.74	881.70 ± 56.09	764.50 ± 272.37	835.00 ± 290.60	718.67 ± 111.74	697.88 ± 69.91

adverse drug reactions in the ADR monitoring system in China, the United States, Canada, and India. Therefore, it is essential to use caution when using *Nyctanthes arbor-tristis* and to consult with a healthcare professional before taking this herbal medicine.

3.2.2 Assessment

No clinical trial registration was found. *Nyctanthes arbor-tristis* is not a patent medication authorized by the China National Medical Products Administration or by the Indian government. There were

TABLE 6 Effect of the plant extract on Freund's complete adjuvant (FCA)-induced paw volume of rats.

Groups	Paw volume on different days (mL)					
	Day 0	Day 7	Day 14	Day 21	Day 28	Change in % (Day 0–28)
Arthritic control	0.46 ± 0.08	1.36 ± 0.19	1.31 ± 0.07	1.19 ± 0.11	1.0 ± 0.16	117.39
Vehicle control	0.46 ± 0.08	0.47 ± 0.07	0.49 ± 0.09	0.50 ± 0.10	0.52 ± 0.12#	13.04
NAT (100 mg/kg)	0.48 ± 0.09	1.39 ± 0.15	1.30 ± 0.17	0.95 ± 0.18	0.94 ± 0.29	95.83
NAT (250 mg/kg)	0.43 ± 0.08	1.27 ± 0.20	1.13 ± 0.19	0.87 ± 0.14*	0.65 ± 0.10*	51.16
NAT (500 mg/kg)	0.45 ± 0.05	1.32 ± 0.24	0.95 ± 0.15*	0.71 ± 0.12#	0.48 ± 0.08#	6.66
Positive control	0.43 ± 0.05	1.30 ± 0.15	1.05 ± 0.14*	0.77 ± 0.17*	0.56 ± 0.14#	30.23

Values are expressed as mean ± SEM for six animals. Symbols represent statistical significance: ∗ = < 0.05, # = < 0.01, @ = < 0.001 when compared to arthritic control. Bonferroni post-test after a two-way analysis of variance.

no post-marketing ADR monitoring data. In this case, it is difficult to conduct the benefit–risk assessment. More data and clinical evidence should be collected for future assessment to balance the benefits and risks of *Nyctanthes arbor-tristis*.

3.2.3 Understanding

In this study, we carried out *in vivo* studies, as well as pharmacokinetic and pharmacodynamic analyses, and we identified the mechanism. In this study, we observed that NAT can cause drowsiness, sedation, and lethargy at the high dosages of 1,000 mg/kg and 2,000 mg/kg. Some other studies indicated that the inhibition of AchE activity is reduced in malathion-treated serum and brain tissue samples of mice treated with NAT extract. The hot infusion of NAT flowers has shown sedative potential in mice. The ethanolic extract of NAT flowers, seeds, and leaves has shown central nervous system depression activity. The potential bioactive compounds might include arbortristoside-A, arbortristoside-B, astragalin, nicotiflorin, and quercetin (Sharma et al., 2021).

3.2.4 Prevention

We have identified certain risks of *Nyctanthes arbor-tristis* with potential ADRs. Hence, we should develop some strategies and measures to prevent or minimize the risks associated with *Nyctanthes arbor-tristis*. We should pay attention to the dosage and duration of the medical use of *Nyctanthes arbor-tristis*. It will be necessary to discontinue the use of *Nyctanthes arbor-tristis* and treat the ADR symptoms when ADRs are monitored. Further research should be conducted for implementing risk mitigation strategies, such as toxic study changes, mechanism and potential risk component identification, patient education or training of healthcare professionals about the safe and rational use of this herbal medication, and even post-marketing surveillance after marketing authorization.

3.3 Anti-arthritic activity

3.3.1 FCA-induced arthritis

The subplantar injection of FCA in the left hind paw of the rats resulted in a progressive increase in the volume of the ipsilateral (injected) paw as well as the contralateral (non-injected) paw.

3.3.2 Effect of the extract on paw volume

FCA was administered on the first and third day, which resulted in a progressive increase in paw volume. The treatment with standards (indomethacin) and plant concentration (NAT) started from day 0 and continued to day 28. As presented in Table 6, it can be seen that treatment with standards as well as the plant extract caused significant abatement of paw volume, which was noticed from day 14 to day 28. NAT (500 mg/kg) demonstrated a high level of anti-arthritic effects (63.63%) compared to that of indomethacin (56.92%). However, the anti-arthritic effects of NAT (250 mg/kg) (48.81%) were found to be significantly lower than those of indomethacin and NAT (500 mg/kg). Hence, NAT (500 mg/kg) could be used as an alternative to indomethacin in the treatment of RA.

3.3.3 Body weight

All animals injected with FCA showed a reduction in body weight, which might be due to the decreased absorption of nutrients through the intestine (Taylor et al., 2009). However, the treatment with standards (indomethacin) and the plant extract showed an increase in the body weight from the 14th day onward. The NAT (500 mg/kg) and NAT (250 mg/kg) were found to restore the body weight and also increase it (5.25% and 2.02%) in a progressive manner, such as in the case of indomethacin (2.93%), as shown in Table 7. Overall, both NAT (500 mg/kg) and NAT (250 mg/kg) were found to have a good impact on the body weight of the rats.

3.3.4 Hot plate method

The analgesic effect can be assessed in the hot plate test. The effect of NAT at 100–500 mg/kg BW on hot-plate response latency is shown in Table 8. The hot-plate response latency in animals treated with 100, 250, and 500 mg/kg BW NAT was significantly different from that of the negative control. NAT (100 mg/kg) shows significant result from 60 to 90 min ($0 < 0.05$), and NAT (250 mg/kg) and NAT (500 mg/kg) show significant results from 30 to 180 min ($p < 0.001$). A typical analgesic effect was seen in the NAT group rats.

3.3.5 Radiological analysis of ankle joints

Figure 1 shows the radiographs of the joints in the rats with and without treatment for FCA-induced arthritis. In addition to normal joint spaces and connective tissue, the joints of vehicle control rats

TABLE 7 Effect of the plant extract on body weight.

Groups	Body weight on different days (g)					
	Day 0	Day 7	Day 14	Day 21	Day 28	Change in % (Day 0–28)
Arthritic control	252.8 ± 9.2	241.5 ± 5.6	232.7 ± 6.1	229.5 ± 7.6	226.5 ± 9.3	−10.40
Vehicle control	255 ± 6.1	258.2 ± 5.9	262.4 ± 6.1	264.8 ± 5.6	266.8 ± 5.8	4.62
NAT (100 mg/kg)	253.1 ± 22.4	247.2 ± 23.1	246 ± 23.2	244.7 ± 23	245.2 ± 23.4	−3.12
NAT (250 mg/kg)	252.4 ± 5.9	248.7 ± 5.7	249.4 ± 4.9$^{\#}$	251.8 ± 5.4$^{\#}$	257.5 ± 7$^{\#}$	2.02
NAT (500 mg/kg)	251.4 ± 16.1	256.2 ± 15.7	259 ± 15.5$^{\#}$	261.8 ± 15.5$^{\#}$	264.6 ± 15.6$^{\#}$	5.25
Positive control	255.2 ± 10.8	251.6 ± 10.4	252.5 ± 11.1$^{\#}$	256.8 ± 11.1$^{\#}$	262.7 ± 8.8$^{\#}$	2.93

Values are expressed as mean ± SEM for six animals. Symbols represent statistical significance: ∗ = < 0.05, # = < 0.01, @ = < 0.001 when compared to arthritic control. Bonferroni post-test after a two-way analysis of variance.

TABLE 8 Effects of *Nyctanthes arbor-tristis* and indomethacin on pain induced by analgesic assessment using the hot plate test.

Groups	Time of reaction (Sec)						
	0 min	30 min	60 min	90 min	120 min	150 min	180 min
Arthritic control	3.83 ± 0.35	4.02 ± 0.30	3.80 ± 0.20	4.07 ± 0.20	3.75 ± 0.30	3.73 ± 0.25	3.53 ± 0.24
Vehicle control	4.00 ± 0.23	4.22 ± 0.60	4.08 ± 0.29	4.15 ± 0.21	4.25 ± 0.41	4.17 ± 0.30	4.17 ± 0.57
NAT (100 mg/kg)	3.88 ± 0.42	4.22 ± 0.53	4.45 ± 0.50*	4.65 ± 0.49*	4.33 ± 0.49*	4.20 ± 0.50	3.98 ± 0.40
NAT (250 mg/kg)	4.10 ± 0.28	5.24 ± 0.70$^{@}$	6.03 ± 0.42$^{@}$	7.35 ± 0.29$^{@}$	6.32 ± 0.33$^{@}$	6.00 ± 0.35$^{@}$	5.28 ± 0.32$^{@}$
NAT (500 mg/kg)	4.28 ± 0.22	5.02 ± 0.29$^{@}$	6.47 ± 0.23$^{@}$	7.68 ± 0.32$^{@}$	6.80 ± 0.22$^{@}$	6.43 ± 0.23$^{@}$	5.78 ± 0.40$^{@}$
Positive control	4.60 ± 0.43$^{\#}$	5.05 ± 0.30$^{@}$	5.78 ± 0.56$^{@}$	6.25 ± 0.37$^{@}$	6.85 ± 0.45$^{@}$	6.43 ± 0.50$^{@}$	5.78 ± 0.37$^{@}$

Values are expressed as mean ± SEM for six animals. Symbols represent statistical significance: ∗ = < 0.05, # = < 0.01, @ = < 0.001 when compared to arthritic control. Bonferroni post-test after a two-way analysis of variance.

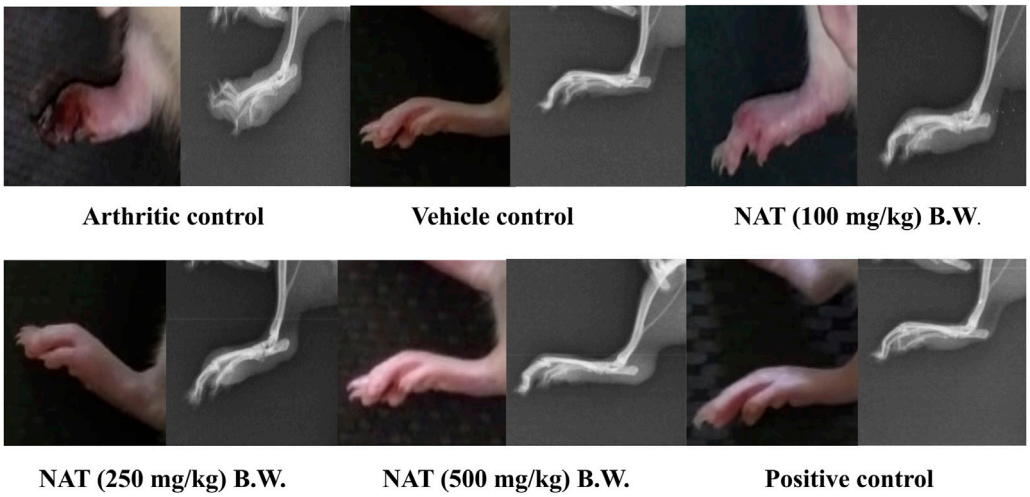

FIGURE 1
Radiographic analysis of left hind limbs of FCA-induced arthritic rats treated with *Nyctanthes arbor-tristis* extract.

did not exhibit focal cartilage bone erosion or joint tissue swelling. All of the treatments had a positive impact on the radiographic changes in the joints of the adjuvant-injected control rats, including extensive phalangeal bone erosion; periarticular bone resorption; no discernible joint spaces; extensive joint deformity; diffuse soft tissue swelling; and thickened, significantly enlarged, and dense connective

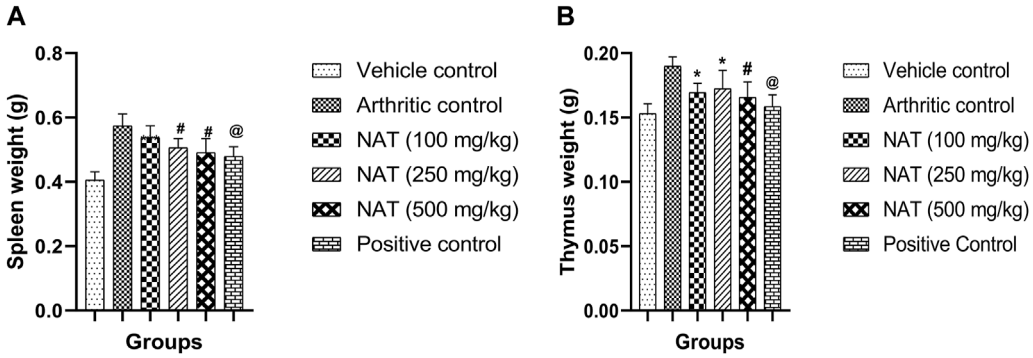

FIGURE 2
Effect of *Nyctanthes arbor-tristis* extract on spleen **(A)** and thymus **(B)** weights in FCA-induced arthritic rats. Values are expressed as mean ± SEM for six animals. ∗ = < 0.05, # = < 0.01, @ = < 0.001 when compared to arthritic control rats. We performed a one-way analysis of variance followed by the Dunnett test.

tissue. The prophylactic administration of NAT at doses of 250 mg/kg and 500 mg/kg significantly reduced the radiographic changes in the arthritic control group. Additionally, NAT (250 mg/kg) treatment moderately reduced bone erosion and resorption as well as noticeable joint deformity. NAT administration (100 mg/kg) had only marginally protective effects. Additionally, indomethacin-treated rats' radiographs showed a mild-to-moderate level of protection against the radiographic changes seen in the adjuvant control group.

3.3.6 Measurement of spleen and thymus weights

Immunological functions are related to the thymus and spleen indexes. On the 28th day, the rats were sacrificed and the thymus index and spleen index were determined. As presented in Figure 2, the weights of the spleen and thymus for the NAT (500 mg/kg) group animals were found to be significantly lower than those of the arthritic control group ($p < 0.01$). NAT (250 mg/kg) and NAT (100 mg/kg) groups also showed increase in thymus weight (0.17 ± 0.014 g and 0.16 ± 0.007 g) but slight decrease in spleen weight (0.50 ± 0.028 g and 0.53 ± 0.036 g). Based on these observations, NAT (500 mg/kg) was found to be much better than NAT (250 mg/kg) in reducing the thymus and spleen weights.

3.3.7 Serum lysosomal enzymes in FCA-induced arthritis

During the inflammatory response, enzymes like alanine aminotransferase (AST) and alanine transaminase (ALT) play crucial roles in the production of chemical mediators like bradykinins (Cheng et al., 2015). In addition, serum alanine aminotransferase (AST) and alanine aminotransferase (ALT) are specific biomarkers helpful in assessing liver damage (Agrawal and Pal, 2013). Therefore, AST and ALT concentrations were assessed. The FCA treatment increased enzyme levels in all animal groups, and serum CRP and RF are the markers of inflammation and the creation of antibodies against the injected FCA. In the FCA control group animals, high levels of CRP (7.0 mg/L) and RF (57.68 IU/L) were found. However, as shown in Figure 3, NAT (500 mg/kg), NAT (250 mg/kg), NAT (100 mg/kg), and indomethacin (10 mg/kg) markedly decreased the levels of AST, ALT, CRP, and RF. NAT (500 mg/kg) treatment was more effective than that of NAT (250 mg/kg) in lowering the serum levels of AST, ALT, CRP, and RF.

3.3.8 Hematological parameters in FCA-induced arthritis

When comparing arthritic control rats to other groups, NAT (500 mg/kg) showed a significant decrease ($p < 0.001$) in red blood cell (RBC) and platelet (Plt) levels, while the latter (NAT (250 mg/kg)) showed a significant change ($p < 0.01$) in WBC and hemoglobin levels. When compared to arthritic control rats, those given NAT (250 mg/kg) showed statistically significant changes ($p < 0.05$) in RBC and Hb levels and significant decreases ($p < 0.05$) in WBC and platelets. However, the hematological changes induced by FCA were lessened more by indomethacin (10 mg/kg) than by NAT (250 mg/kg and 500 mg/kg) treatment, as shown in Figure 4.

3.3.9 Effect of NAT on TNF-α, IL-10, and COX-2

TNF- α and COX-2, two pro-inflammatory cytokines, and IL-10, an anti-inflammatory cytokine, are crucial in the pathogenesis of RA. To determine the levels of TNF- α, IL-10, and COX-2 cytokines in the serum of arthritic rats, an analysis was conducted. The results are depicted in Figure 5. Rats with FCA-induced arthritis had significantly higher levels of TNF- α, IL-10, and COX-2 ($p < 0.01$). However, the elevated serum levels of TNF- α, IL-10, and COX-2 were decreased in the arthritic rats treated with NAT. This impact was nearly identical to that of regular indomethacin. While serum TNF- α, IL-10, and COX-2 levels were reduced in arthritic rats treated with NAT compared to the controls, their level was still higher than that of both NAT and the standards ($p < 0.05$).

3.3.10 Histopathological study of NAT-treated rats

Rats with normal ankle joints showed intact articular cartilage, normal synovial tissue, and joint space free of inflammation upon histopathological examination. Additionally, NAT (250 mg/kg) and NAT (500 mg/kg) administration significantly reduced the arthritic control animals' ankle joint modifications, such as prominent synovial lining hyperplasia, noticeable synoviocyte proliferation, inflammatory cell infiltration into joint capacity, pannus invasion

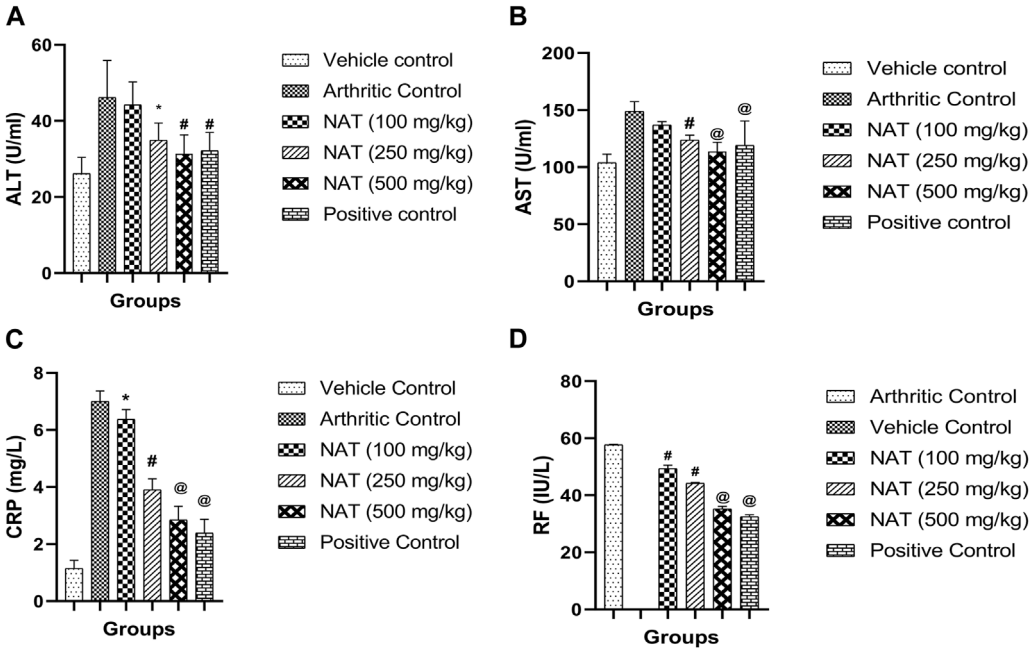

FIGURE 3
Effect of *Nyctanthes arbor-tristis* extract on serum lysosomal enzymes: ALT **(A)**, AST **(B)**, CRP **(C)** and RF **(D)** in FCA-induced arthritic rats. Values are expressed as mean ± SEM for six animals. ∗ = < 0.05, # = < 0.01, @ = < 0.001 when compared to arthritic control rats. We performed a one-way analysis of variance followed by the Dunnett test.

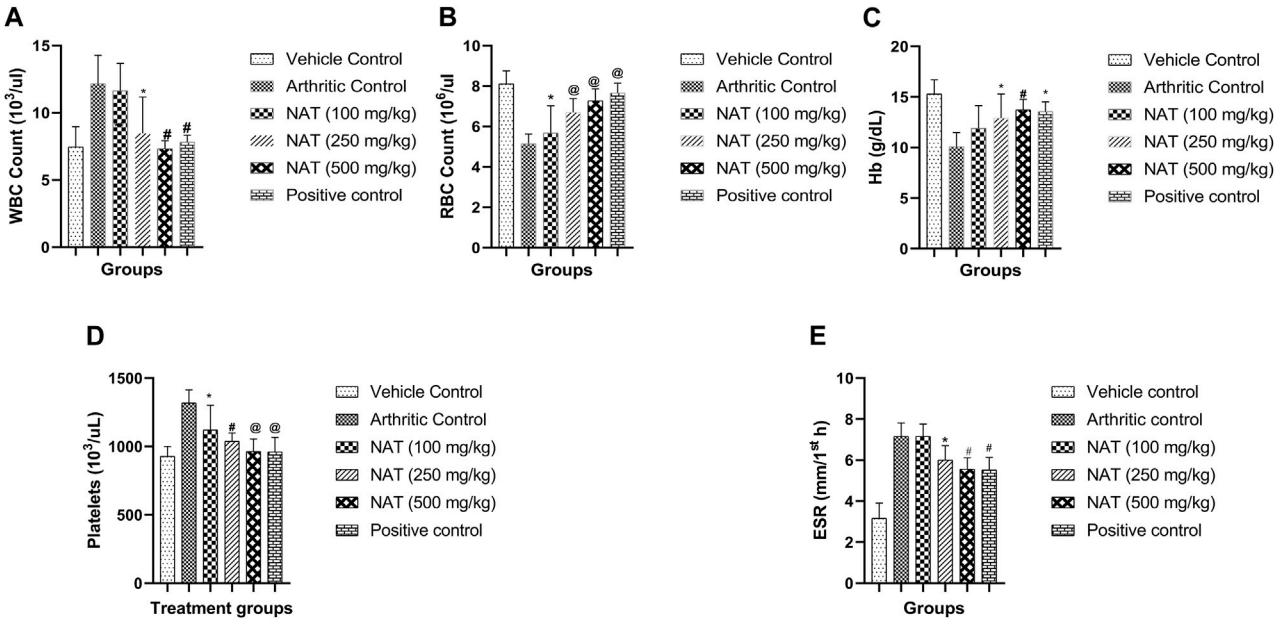

FIGURE 4
Effect of *Nyctanthes arbor-tristis* extract on Hematological parameters: WBC **(A)**, RBC **(B)**, Hb **(C)**, Platelets **(D)** and ESR **(E)** in FCA-induced arthritic rats. Values are expressed as mean ± SEM for six animals. ∗ = < 0.05, # = < 0.01, @ = < 0.001 when compared to arthritic control rats. We performed a one-way analysis of variance followed by the Dunnett test.

of subchondral bone with subsequent articular cartilage, and bone erosion. Additionally, NAT (100 mg/kg) treatment slightly decreased the histopathological signs of arthritis. Furthermore, rats treated with NAT (500 mg/kg) showed significant histopathological changes. The information also demonstrates that oral administration of indomethacin to control rats with

10.3389/fphar.2023.1307799

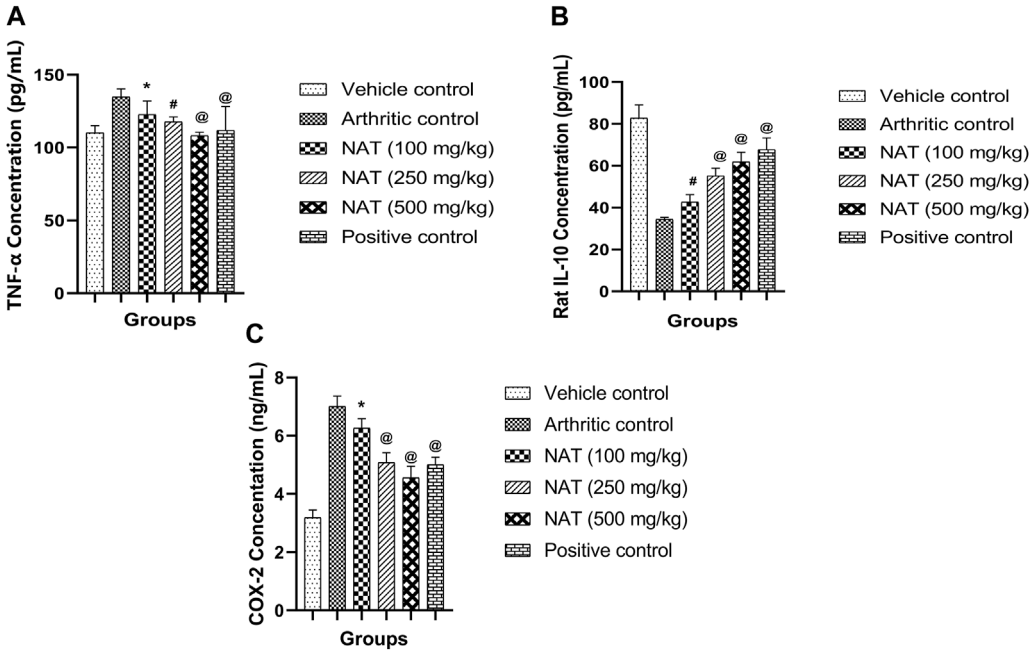

FIGURE 5
Effect of *Nyctanthes arbor-tristis* extract on cytokines: TNF-α **(A)**, IL-10 **(B)**, COX-2 **(C)** production in serum. Values are expressed as mean ± SEM for six animals. ∗ = < 0.05, # = < 0.01, @ = < 0.001 when compared to arthritic control. We performed a one-way analysis of variance followed by the Dunnett test.

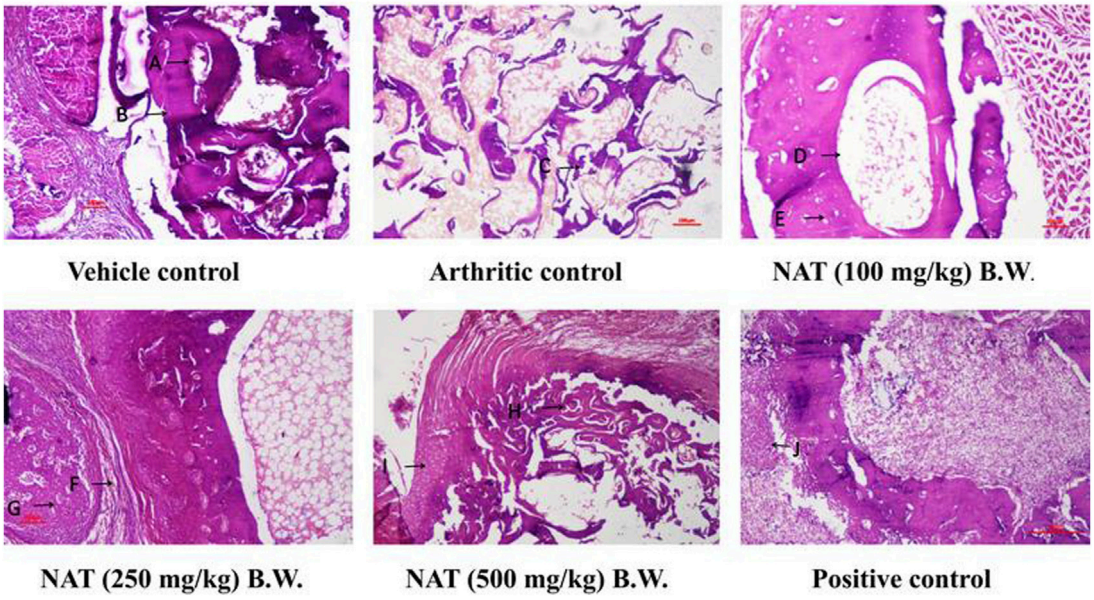

FIGURE 6
Evaluation of the extract of *Nyctanthes arbor-tristis* on the ankle joint of arthritic rats injected with FCA. Vehicle control: adequate no. of osteocytes in bone matrix **(A)** osteoblasts surrounding the border of the matrix **(B)**. H&E x 100x, arthritic control: disintegrated bone matrix with vacant lacuna containing no osteocyte **(C)**.H&E x 100x, NAT (100 mg/kg) BW: very few osteocyte lacunae in bone marrow matrix **(D)** surrounding the yellow bone marrow **(E)**. H&E x 100, NAT (250 mg/kg) BW: decreased bone marrow surrounded with fibrous tissue **(F)**. Osteocytes present in deep trabeculae. The proliferation of osteoblastic cells lining the border of the bone matrix **(G)**. H&E x 100 NAT (500 mg/kg) BW: decreased size and no. of trabeculae bone matrix **(H)**. Hyperplastic chondrocyte with increased activity **(I)**. H&E x 100, positive control: hyperplastic chondrocyte with increased activity **(J)** H&E x 100.

arthritis significantly protected them from histopathological changes (Figure 6).

4 Discussion

Nyctnathes arbor-tristis has been suggested as a potential medicinal agent for the treatment and prevention of painful joints and rheumatism. In our earlier studies, we found a significant activity of NAT hydroethanolic extract in *in vitro and* in silico studies (Sharma et al., 2023). The current study demonstrates that hydroethanolic extract of the aerial part of *Nyctnathes arbor-tristis* protects against adjuvant-induced arthritis in rats, an extensively used inflammatory arthritic animal model that replicates the pathological and clinical features of human RA. Following an injection of FCA, the inflammatory reaction typically starts between 1 and 3 days in the form of initial lesions, and then secondary lesions appear between 11 and 14 days later. Edema has been linked to increased vascular permeability, extravasation of fluid and proteins, and cellular invasion at the inflammatory sites (Bose et al., 2014). According to our analysis, the disease control group showed signs of persistent inflammation up to day 28 due to persistent edema and cellular invasion. In contrast to arthritic control rats, however, the treated animals showed remarkable protection against the morphological abnormalities of RA, with peak inflammation occurring up to the third day, followed by a rapid decline in paw edema. This decrease in edema may be related to a reduction in the production of prostaglandins as well as an increase in the invasion of neutrophils. Another study (Qasim et al., 2020) reported that the reduction in prostaglandin production corresponds to an elevation in neutrophil infiltration. The animal groups subjected to NAT treatments exhibited a notable increase in rat body weight when compared to the arthritic control group. The decrease in nutrient absorption from the intestine in FCA-challenged rats resulted in a significant reduction in rat body weight (Allawadhi et al., 2022). Similar to the effects observed with standard medications such as indomethacin, NAT substantially restored the rats' body weight, possibly due to an improvement in their arthritic condition, which could subsequently normalize nutrient absorption from the intestine. These results align well with previous findings on the treatment of Freund's complete adjuvant-induced arthritis using a cerium oxide nanoparticle (Akhtar et al., 2022).

In cases of adjuvant arthritis, the spleen plays a crucial role in generating cells and antibodies responsible for immunological responses. The spleens of arthritic rats exhibit an increase in cellularity (Khanfar et al., 2022). There is an observed rise in spleen cell weight in arthritic rats in the present study. We observed a clear increase in the organ weights of the spleen and thymus in FCA-induced rats. The administration of NAT led to a decrease in spleen and thymus weights, likely due to the suppression of splenic lymphocytes and the inhibition of lymphocyte infiltration into the synovium. These findings are consistent with those of earlier research involving the treatment of FCA-induced arthritic rats using β-sitosterol-loaded solid lipid nanoparticles (Zhang et al., 2020).

Further confirmation of the anti-arthritic capabilities of NAT and indomethacin was achieved through the evaluation of several biochemical markers in rat serum. These markers, including AST, ALT, CRP, and RF, serve as crucial indicators for assessing the anti-arthritic potential of the drug. Reduced RF and CRP levels, with RF serving as a potential marker for RA, were characterized by a notable increase in distal interphalangeal arthritis incidence (Sharma et al., 2023). Additionally, a persistently high serum CRP level is recognized as a strong indicator of RA (Petchi et al., 2015). Elevated serum levels of AST, ALT, and ALP were observed, while the total protein level decreased. Evaluating serum AST, ALT, and ALP levels offers a straightforward and effective method for assessing the drug's anti-arthritic activity. Aminotransferase and ALP activities notably increased in arthritic rats, serving as reliable indicators of liver and kidney impairment, which is a known feature of adjuvant arthritis. It is worth noting that serum AST and ALT have been reported to play a significant role in the generation of biologically active chemical mediators, such as bradykinins, in the inflammatory process (Kadam and Bodhankar, 2013). In this investigation, the treatment of arthritic rats with NAT and indomethacin resulted in a significant reduction in the elevated levels of AST, ALT, CRP, and RF as compared to arthritic control rats. These findings suggest the therapeutic potential of the studied NAT in RA treatment. Additionally, the significant decrease in the elevated serum levels of AST and ALT indicates that the studied fractions did not induce liver injury in the rats. In summary, the results of lysosomal enzyme measurements are consistent with prior reports in the literature regarding *Calotropis procera* leaves (Singh et al., 2021).

Anemia is a prevalent condition in rheumatoid arthritis, characterized by reduced levels of red blood cells (RBCs) and hemoglobin (Hb) content (Mahnashi et al., 2021). This anemic state arises from abnormalities in iron storage within the synovial tissue and the reticuloendothelial system (Das et al., 2021). Furthermore, the reduced capacity of the bone marrow to produce sufficient blood cells is another contributing factor to the decline in RBC and Hb levels (Hess and D'Alessandro, 2022). In RA, immune system activation in response to antigenic assaults results in elevated white blood cell (WBC) and platelet levels (Manan et al., 2020). An increase in WBC count is linked to heightened immune system activity against destructive pathogens, ultimately triggering the activation of inflammatory signaling molecules (Ge et al., 2021). Platelets play a significant role in inflammation and immunomodulation, as microparticles released from platelets interact with WBCs and contribute to systemic and joint inflammation in RA (Harifi and Sibilia, 2016). Treatment with NAT led to an increase in RBC and Hb levels and reduced WBC and platelet levels when compared to the arthritic control group, thereby confirming the anti-arthritic potential of NAT. The outcomes of the hematological assessments closely mirrored the findings previously documented in the literature for the extract derived from methanolic, n-hexane, and ethyl acetate fractions of the bark of *Acacia modesta* (Mashaal et al., 2023).

It was hypothesized that administering FCA stimulates T cells, which in turn excite macrophages and monocytes, leading to an upregulation of lysosomal enzymes and the release of pro-inflammatory cytokines. Arthritic joints are characterized by the uncontrolled spread of synovial tissue, joint dysfunction, tissue destruction, bone erosion, and programmed cell death, all of which may be traced back to the overexpression of pro-inflammatory cytokines (Komatsu and Takayanagi, 2012). In this

study, we used ELISA to examine the impact of NAT hydroethanolic extract on blood COX-2 and TNF-α levels. In this research, rats treated with indomethacin and NAT showed a significant decrease in elevated TNF-α levels seen in disease control rats, indicating the potential of the plant to reduce arthritis and inflammation. The transcription factor NF-κB was shown to regulate TNF-α expression, whereas TNF-α itself was shown to act as a potent stimulator of NF-κB (Makrov, 2001). Because NF-κB is required to produce pro-inflammatory cytokines, reducing TNF-α has a net beneficial impact of reducing their levels (Wong et al., 2008). Current research has shown that the plant extract significantly suppressed TNF-α expression, which may have resulted from a decrease in NF-κB expression levels, as was previously observed. Additionally, in rheumatoid synovium, the COX-2 (cyclooxygenase) pathway's generation of PGE2 through arachidonic acid metabolism is particularly important (Cheng et al., 2015). Cartilage and bone erosions, fluid extravasation, discomfort, vasodilation, and similar conditions may all be accelerated by elevated PGE2 concentrations (Fattahi and Mirshafiey, 2012). While the current investigation found elevated COX-2 levels in arthritic control animals, a substantial decrease was seen in NAT-administered rats, suggesting that NAT may have protected inflamed joints from further damage by reducing prostaglandin production as a result of subdual COX-2 generation. So NAT's anti-arthritic impact may also be due to its potential to block the metabolism of arachidonic acid. As an immunomodulatory cytokine, IL-10 alters the progression of RA synovitis (Sharma et al., 2023). In RA pathogenesis, IL-10 does more than only inhibit the production of Th1 cell-generated cytokines (GM-CSF, IL-1, IFN-γ, and TNF-α); it preserves joint tissue, prevents the activity of antigen-presenting cells, and suppresses the production of IL-18 mRNA (Lin et al., 2013). Arthritic control rats showed a large decrease in IL-10 levels, whereas all treatment groups, including those given indomethacin, showed a significant increase, suggesting an anti-inflammatory/immunomodulatory effect of NAT in this condition. These findings align with the outcomes documented for the *Ephedra gerardiana* aqueous ethanolic extract and fractions, as reported in a previous study (Uttra et al., 2019).

Radiographic images are employed for the assessment of tissue swelling, erosions, and joint deformities in arthritis patients. These images provide insight into soft tissue lesions, often serving as early indicators of arthritis. Additionally, bone erosion and the deterioration of trabecular bone are characteristic pathological changes observed in human arthritis (Almarestani et al., 2011). In the case of FCA-induced arthritic rats, there was a noticeable presence of soft tissue swelling and a narrowing of joint spaces, indicating bone damage associated with arthritic conditions. The radiographic observations of the treatment groups receiving NAT demonstrated mitigation of arthritis-related joint alterations are given in Figure 1.

The histopathological findings also indicated that NAT possesses the ability not just to reduce inflammation but also to shield cartilage and bones from erosion. These observations complement the data acquired from other biochemical measurements. Arthritis is characterized by the infiltration of inflammatory cells, subcutaneous inflammation, and synovial inflammation (Vishnu and Krishnan, 2018). These findings were consistent with the outcomes reported in studies involving the treatment of rats with complete Freund's adjuvant-induced arthritis using chrysin (Faheem et al., 2023).

5 Conclusion

According to the findings, oral administration of *Nyctanthes arbor-tristis* to arthritic rats significantly reduced paw edema and restored body weight; re-established an altered biochemical and hematological profile and inflammatory mediators' serum expression levels; and decreased bone and cartilage destruction. Hence, the capacity of the tested plant to reduce TNF-α, increase IL-10 levels, and reduce the concentrations of the inflammatory enzyme COX-2 seems to be linked to its anti-rheumatic and immunomodulatory capabilities. As a result, *Nyctanthes arbor-tristis* may be the best strategy to treat RA. However, further research is essential to pinpoint and separate the potential phytoconstituents responsible for the anti-arthritic potential, thus enabling the use of *Nyctanthes arbor-tristis* in the treatment of arthritic conditions.

Data availability statement

The original contributions presented in the study are included in the article/Supplementary material; further inquiries can be directed to the corresponding authors.

Ethics statement

The animal study was approved by the Institutional Animal Ethics committee, GLA University, Mathura. The study was conducted in accordance with the local legislation and institutional requirements.

Author contributions

AS: data curation, formal analysis, methodology, and writing–original draft. AG: conceptualization, supervision, and writing–review and editing. ZL: funding acquisition, software, and writing–review and editing.

Funding

The author(s) declare financial support was received for the research, authorship, and/or publication of this article. This work was supported by the Beijing Municipal Natural Science Foundation (7212178), China, the Department of Biotechnology, GLA University, Mathura, India, and the Innovation Team and Talents Cultivation Program of National Administration of Traditional Chinese Medicine (ZYYCXTD-C-2020005-11).

Conflict of interest

The authors declare that the research was conducted in the absence of any commercial or financial relationships that could be construed as a potential conflict of interest.

Publisher's note

References

Agrawal, J., and Pal, A. (2013). Nyctanthes arbor-tristis Linn—a critical ethnopharmacological review. *J. Ethnopharmacol.* 146, 645–658. doi:10.1016/j.jep.2013.01.024

Akhtar, M. F., Raza, S. A., Saleem, A., Hamid, I., Ashraf Baig, M. M. F., Sharif, A., et al. (2022). Appraisal of anti-arthritic and anti-inflammatory potential of folkloric medicinal plant peganum harmala. *Endocr. Metab. Immune Disord. Drug Targets* 22, 49–63. doi:10.2174/1871530321666210208211310

Alamgeer, H., Uttra, A., and Hasan, U. (2017). Anti-arthritic activity of aqueous-methanolic extract and various fractions of Berberis orthobotrys Bien ex Aitch. *BMC Complement. Altern. Med.* 17, 371. doi:10.1186/s12906-017-1879-9

Allawadhi, P., Khurana, A., Sayed, N., Godugu, C., and Vohora, D. (2022). Ameliorative effect of cerium oxide nanoparticles against Freund's complete adjuvant-induced arthritis. *Nanomedicine* 17, 383–404. doi:10.2217/NNM-2021-0172

Almarestani, L., Fitzcharles, M. A., Bennett, G. J., and Ribeiro-Da-Silva, A. (2011). Imaging studies in Freund's complete adjuvant model of regional polyarthritis, a model suitable for the study of pain mechanisms, in the rat. *Arthritis Rheum.* 63, 1573–1581. doi:10.1002/art.30303

Balkrishna, A., Singh, S., Srivastava, D., Mishra, S., Sharma, S., Mishra, R., et al. (2023). A systematic review on traditional, ayurvedic, and herbal approaches to treat solar erythema. *Int. J. Dermatol* 62, 322–336. doi:10.1111/IJD.16231

Ben Mrid, R., Bouchmaa, N., Ainani, H., El Fatimy, R., Malka, G., and Mazini, L. (2022). Anti-rheumatoid drugs advancements: new insights into the molecular treatment of rheumatoid arthritis. *Biomed. Pharmacother.* 151, 113126. doi:10.1016/j.biopha.2022.113126

Bose, M., Chakraborty, M., Bhattacharya, S., Bhattacharjee, P., Mandal, S., Kar, M., et al. (2014). Suppression of NF-κB p65 nuclear translocation and tumor necrosis factor-α by Pongamia pinnata seed extract in adjuvant-induced arthritis. *J. Immunotoxicol.* 11, 222–230. doi:10.3109/1547691X.2013.824931

Bozkurt, F., Yetkin, Z., Berker, E., Tepe, E., and Akkus , , S. (2006). Anti-inflammatory cytokines in gingival crevicular fluid in patients with periodontitis and rheumatoid arthritis: a preliminary report. *Cytokine* 35, 180–185. doi:10.1016/j.cyto.2006.07.020

Chakraborty, R., and Datta, S. (2022). A brief overview on the Health benefits of Nyctanthes arbor-tristisLinn.-A wonder of mother nature. *Indo Glob. J. Pharm. Sci.* 12, 197–204. doi:10.35652/igjps.2022.12024

Cheng, X. L., Liu, X. G., Wang, Q., Zhou, L., Qi, L. W., Li, P., et al. (2015). Antiinflammatory and anti-arthritic effects of guge fengtong formula: *in vitro* and *in vivo* studies. *Chin. J. Nat. Med.* 13, 842–853. doi:10.1016/S1875-5364(15)30088-1

Das, C., Ghosh, G., Bose, A., and Das, D. (2021). Prophylactic efficacy of bioactive compounds identified from GC-MS analysis of Balarista formulation on adjuvant induced arthritic rats by inhibiting COX-2 inhibitor. *South Afr. J. Bot.* 141, 200–218. doi:10.1016/j.sajb.2021.04.033

Das, S., Samsal, S., and Basu, S. (2008). Evaluation of CNS depressant activity of different plant parts of Nyctanthes arbortristis linn. *Indian J. Pharm. Sci.* 70, 803–806. doi:10.4103/0250-474X.49129

Faheem, M. A., Akhtar, T., Naseem, N., Aftab, U., Zafar, M. S., Hussain, S., et al. (2023). Chrysin is immunomodulatory and anti-inflammatory against complete Freund's adjuvant-induced arthritis in a pre-clinical rodent model. *Pharmaceutics* 15, 1225. doi:10.3390/PHARMACEUTICS15041225

Fattahi, M. J., and Mirshafiey, A. (2012). Prostaglandins and rheumatoid arthritis. *Arthritis* 2012, 239310. doi:10.1155/2012/239310

Felipe, N., Fernando, S., Gabriela, C., Fernanda, R., Pablo, S. P., Lleretny, R. A., et al. (2020). Assessment of the anti-inflammatory and engraftment potential of horse endometrial and adipose mesenchymal stem cells in an *in vivo* model of post breeding induced endometritis. *Theriogenology* 155, 33–42. doi:10.1016/J.THERIOGENOLOGY.2020.06.010

Ge, Y., Huang, M., and Yao, Y. M. (2021). The effect and regulatory mechanism of high mobility group box-1 protein on immune cells in inflammatory diseases. *Cells* 10, 1044. doi:10.3390/CELLS10051044

Godse, C., Tadhed, P., Talwalkar, S., Vaidya, R., Amonkar, A., Vaidya, A., et al. (2016). Antiparasitic and disease-modifying activity of Nyctanthes arbor-tristis Linn. in malaria: an exploratory clinical study. *J. Ayurveda Integr. Med.* 7, 238–248. doi:10.1016/j.jaim.2016.08.003

Gurung, R., Adhikari, S., Koirala, N., and Parajuli, K. (2020). Extraction and evaluation of anti-inflammatory and analgesic activity of mimosa rubicaulis in Swiss albino rats. *Antiinfect Agents* 19, 6–13. doi:10.2174/2211352518999201009125006

Harifi, G., and Sibilia, J. (2016). Pathogenic role of platelets in rheumatoid arthritis and systemic autoimmune diseases: perspectives and therapeutic aspects. *Saudi Med. J.* 37, 354–360. doi:10.15537/smj.2016.4.14768

Hazarika, A., Deka, D. K., Phukan, S. C., and Hussain, J. (2022). *In vitro* anthelmtic activity of Nyctanthes arbortristis leaves against ascaridia galli. *Int. J. Bio-resource Stress Manag.* 13, 1221–1225. doi:10.23910/1.2022.2759

Hess, J. R., and D'Alessandro, A. (2022). Red blood cell metabolism and preservation. *Rossi's Princ. Transfus. Med.*, 143–157. doi:10.1002/9781119719809.CH14

Kadam, P., and Bodhankar, S. L. (2013). Antiarthritic activity of ethanolic seed extracts of Diplocyclos palmatus (L) C. *Jeffrey Exp. animals. Der. Pharm. Lett* 5, 233–242.

Khanfar, E., Olasz, K., Gajdócsi, E., Jia, X., Berki, T., Balogh, P., et al. (2022). Splenectomy modulates the immune response but does not prevent joint inflammation in a mouse model of RA. *Clin. Exp. Immunol.* 209, 201–214. doi:10.1093/CEI/UXAC052

Komatsu, N., and Takayanagi, H. (2012). Inflammation and bone destruction in arthritis: synergistic activity of immune and mesenchymal cells in joints. *Front. Immunol.* 3, 77. doi:10.3389/fimmu.2012.00077

Lin, B., Zhang, H., Zhao, X. X., Rahman, K., Wang, Y., Maa, X. Q., et al. (2013). Inhibitory effects of the root extract of Litsea cubeba (lour.) pers. on adjuvant arthritis in rats. *J. Ethnopharmacol.* 147, 327–334. doi:10.1016/j.jep.2013.03.011

Mahnashi, M. H., Jabbar, Z., Alamgeer, Irfan, H. M., Asim, M. H., Akram, M., et al. (2021). Venlafaxine demonstrated anti-arthritic activity possibly through down regulation of TNF-α, IL-6, IL-1β, and COX-2. *Inflammopharmacology* 29, 1413–1425. doi:10.1007/s10787-021-00849-0

Makrov, S. S. (2001). NF-kappa B in rheumatoid arthritis: a pivotal regulator of inflammation, hyperplasia, and tissue destruction. *Arthritis Res.* 3, 200–206. doi:10.1186/ar300

Manan, M., Saleem, U., Hamid Akash, M. S., Qasim, M., Hayat, M., Raza, Z., et al. (2020). Antiarthritic potential of comprehensively standardized extract of alternanthera bettzickiana: *in vitro* and *in vivo* studies. *ACS Omega* 5, 19478–19496. doi:10.1021/acsomega.0c01670

Marsh, L. J., Kemble, S., Reis Nisa, P., Singh, R., and Croft, A. P. (2021). Fibroblast pathology in inflammatory joint disease. *Immunol. Rev.* 302, 163–183. doi:10.1111/imr.12986

Martu, M. A., Maftei, G. A., Luchian, I., Stefanescu, O. M., Scutariu, M. M., and Solomon, S. M. (2021). The effect of acknowledged and novel anti-rheumatic therapies on periodontal tissues—a narrative review. *Pharmaceuticals* 14, 1209. doi:10.3390/ph14121209

Mashaal, K., Shabbir, A., Khan, M. A., Hameed, H., Shahzad, M., Irfan, A., et al. (2023). Anti-arthritic and immunomodulatory potential of methanolic, n-hexane, and ethyl acetate fractions of bark of Acacia modesta on complete Freund's adjuvant-induced arthritis in rats. *Pharmaceutics* 15, 2228. doi:10.3390/pharmaceutics15092228

Nygaard, G., and Firestein, G. S. (2020). Restoring synovial homeostasis in rheumatoid arthritis by targeting fibroblast-like synoviocytes. *Nat. Rev. Rheumatol.* 16, 316–333. doi:10.1038/s41584-020-0413-5

OECD (2000). "Guidance document on the recognition, assessment and use of clinical signs as human endpoints for experimental animals used in safety evaluation," in *Environmental Health and safety monograph series on testing and assessment (OECD #19)* (USA: OECD).

Petchi, Rr., Parasuraman, S., Vijaya, C., Gopala Krishna, S., and Kumar, Mk. (2015). Antiarthritic activity of a polyherbal formulation against Freund′s complete adjuvant induced arthritis in Female Wistar rats. *J. Basic Clin. Pharm.* 6, 77–83. doi:10.4103/0976-0105.160738

Pundir, S., Gautam, G. K., and Zaidi, S. (2022). A review on pharmacological activity of Nyctanthes arbor-tristis. *Res. J. Pharmacogn. Phytochemistry* 14, 69–72. doi:10.52711/0975-4385.2022.00014

Qasim, S., Alamgeer Kalsoom, S., Shahzad, M., Irfan, H. M., Zafar, M. S., et al. (2020). Appraisal of disease-modifying potential of amlodipine as an anti-arthritic agent: new indication for an old drug. *Inflammopharmacology* 28, 1121–1136. doi:10.1007/s10787-020-00692-9

Radu, A. F., and Bungau, S. G. (2021). Management of rheumatoid arthritis: an overview. *Cells* 10, 2857. doi:10.3390/cells10112857

Rawat, H., Verma, Y., Saini, N., Negi, N., Chandra Pant, H., Mishra, A., et al. (2021). Nyctanthes arbor-tristis: a traditional herbal plant with miraculous potential in medicine. *Int. J. Bot. Stud.* 6, 427–440.

Saxena, R., Gupta, B., Saxena, K., Srivastva, V., and Prasad, D. (1987). Analgesic, antipyretic and ulcerogenic activity of Nyctanthes arbor tristis leaf extract. *J. Ethnopharmacol.* 19, 193–200. doi:10.1016/0378-8741(87)90041-9

Shakeel, F., Alam, P., Ali, A., Alqarni, M. H., Alshetaili, A., Ghoneim, M. M., et al. (2021). Investigating antiarthritic potential of nanostructured clove oil (Syzygium aromaticum) in fca-induced arthritic rats: Pharmaceutical action and delivery strategies. *Molecules* 26, 7327. doi:10.3390/molecules26237327

Sharma, A., and Goel, A. (2023). Pathogenesis of rheumatoid arthritis and its treatment with anti-inflammatory natural products. *Mol. Biol. Rep.* 50, 4687–4706. doi:10.1007/s11033-023-08406-4

Sharma, A., Goel, A., Gupta, N., and Sharma, B. (2023). Phytochemicals from Nyctanthes arbor-tristis and their biomedical implications. *J. Med. Pharm. Allied Sci.* 12, 6012–6020. doi:10.55522/jmpas.v12i4.5284

Sharma, L., Dhiman, M., Singh, A., and Sharma, M. (2021). Nyctanthes arbor-tristis L.: "an unexplored plant of enormous possibilities for economic revenue". *Proc. Natl. Acad. Sci.i* 91, 241–255. doi:10.1007/s40011-020-01213-y

Shirsat, M. K., Gupta, S. K., Vaya, R., and Dwivedi, J. (2011). Histological study of different part of Calotropis gigantea Linn. *J. Glob. Pharma Technol.* 3, 18–20. doi:10.1234/jgpt.v3i2.348

Singh, V. S., Dhawale, S. C., Shakeel, F., Faiyazuddin, M., and Alshehri, S. (2021). Antiarthritic potential of calotropis procera leaf fractions in fca-induced arthritic rats: involvement of cellular inflammatory mediators and other biomarkers. *Agric. Switz.* 11, 68–16. doi:10.3390/agriculture11010068

Solanki, M., Rajhans, S., Pandya, H. A., and Mankad, A. U. (2021). Nyctanthes arbor-tristis Lin: a short review linn: a short review. *World J. Pharm. Pharm. Sci.* 10, 1047–1054. doi:10.20959/wjpps20213-18575

Taylor, S. L., Krempel, R. L., and Schmaljohn, C. S. (2009). Inhibition of TNF-alpha-induced activation of NF-kappaB by Hantavirus nucleocapsid proteins. *Ann. N. Y. Acad. Sci.* 1171, 86–93. doi:10.1111/j.1749-6632.2009.05049.x

Uttra, A. M., Alamgeer Shahzad, M., Shabbir, A., Jahan, S., Bukhari, I. A., et al. (2019). Ribes orientale: a novel therapeutic approach targeting rheumatoid arthritis with reference to pro-inflammatory cytokines, inflammatory enzymes and anti-inflammatory cytokines. *J. Ethnopharmacol.* 237, 92–107. doi:10.1016/j.jep.2019.03.019

Vijeesh, V., Vysakh, A., Jisha, N., and Latha, M. S. (2022). *In vitro* enzyme inhibition and *in vivo* anti-hyperuricemic potential of malic acid: an experimental approach. *J. Biol. Act. Prod. Nat.* 12, 344–352. doi:10.1080/22311866.2022.2124192

Vishnu, R., and Krishnan, R. (2018). Preclinical evaluation of anti-rheumatoid effect of chrysin in Freund's complete adjuvant induced arthritis in Wistar Albino rats. *Asian J. Pharm. Pharmacol.* 4, 74–78. doi:10.31024/ajpp.2018.4.1.13

Wang, H., Wang, Z., Zhang, Z., Liu, J., and Hong, L. (2023). β-Sitosterol as a promising anticancer agent for chemoprevention and chemotherapy: mechanisms of action and future prospects. *Adv. Nutr.* 14, 1085–1110. doi:10.1016/j.advnut.2023.05.013

Warmink, K., Vinod, P., Korthagen, N. M., Weinans, H., and Rios, J. L. (2023). Macrophage-driven inflammation in metabolic osteoarthritis: implications for biomarker and therapy development. *Int. J. Mol. Sci.* 24, 6112. doi:10.3390/ijms24076112

Wong, M., Ziring, D., Korin, Y., Desai, S., Kim, S., Lin, J., et al. (2008). TNFalpha blockade in human diseases: mechanisms and future directions. *Clin. Immunol.* 126, 121–136. doi:10.1016/J.CLIM.2007.08.013

Zhang, F., Liu, Z., He, X., Li, Z., Shi, B., and Cai, F. (2020). β-Sitosterol-loaded solid lipid nanoparticles ameliorate complete Freund's adjuvant-induced arthritis in rats: involvement of NF-κB and HO-1/Nrf-2 pathway. *Drug Deliv.* 27, 1329–1341. doi:10.1080/10717544.2020.1818883

frontiers | Frontiers in Pharmacology

TYPE Original Research
PUBLISHED 07 February 2024
DOI 10.3389/fphar.2024.1306273

OPEN ACCESS

EDITED BY
Valeria Bruno,
Sapienza University of Rome, Italy

REVIEWED BY
Debora Collotta,
University of Turin, Italy
Jose Alberto Choreño-Parra,
National Institute of Respiratory Diseases-Mexico (INER), Mexico

*CORRESPONDENCE
Zeynep Tokcaer Keskin,
zeynep.keskin@acibadem.edu.tr

†These authors have contributed equally to this work and share first authorship

RECEIVED 03 October 2023
ACCEPTED 22 January 2024
PUBLISHED 07 February 2024

CITATION
Koni E, Congur I and Tokcaer Keskin Z (2024), Overexpression of CXCL17 increases migration and invasion of A549 lung adenocarcinoma cells.
Front. Pharmacol. 15:1306273.
doi: 10.3389/fphar.2024.1306273

Overexpression of CXCL17 increases migration and invasion of A549 lung adenocarcinoma cells

Ekin Koni[1†], Irem Congur[1†] and Zeynep Tokcaer Keskin[1,2*]

[1]Graduate School of Natural and Applied Sciences, Department of Molecular and Translational Biomedicine, Acibadem Mehmet Ali Aydinlar University, Istanbul, Türkiye, [2]Faculty of Engineering and Natural Sciences, Department of Molecular Biology and Genetics, Acibadem Mehmet Ali Aydinlar University, Istanbul, Türkiye

Lung cancer is one of the most frequently diagnosed malignancies and is a widespread disease that affects millions of individuals globally. CXCL17 is a member of the CXC chemokine family that attracts myeloid cells and is associated with the mucosa. CXCL17 can both support and suppress tumor growth in certain types of cancer. A549 LUAD cells were transfected with N-Terminal p3XFLAG-CMV or N-Terminal p3XFLAG-CMV-CXCL17 to establish stably transfected CXCL17-overexpressing cells. Reverse-transcription polymerase chain reaction (RT-PCR) and Enzyme Linked Immunosorbent Assay (ELISA) were performed to verify the levels of CXCL17 mRNA and of CXCL17 protein concentration of stably transfected A549 cells respectively. Wound healing, CCK8, and matrigel invasion assays were performed to assess the effect of CXCL17 overexpression on migration, proliferation, and invasion of A549 cells. When compared to control groups, proliferative capacity of A549 cells were unaffected by CXCL17 overexpression; however, the wound area in the CXCL17 overexpression group had dramatically decreased after 48 h. Similarly, the number of invasion cells was significantly higher in the CXCL17-overexpressing group than in the control ones after 48 h. CXCL17 overexpression significantly increased the ability of A549 cells to migrate and invade, without affecting their proliferative abilities.

KEYWORDS

CXCL17, A549, migration, invasion, proliferation

1 Introduction

Lung cancer is one of the most frequently diagnosed malignancies and is a widespread disease that affects millions of individuals globally, which is still the largest cause of cancer-related death worldwide. This disease occurs when abnormal cells in the lungs grow out of control, frequently creating a tumor that can spread to other body organs (Gridelli et al., 2015). According to a pathological perspective, the two main classifications of lung cancer are small cell lung cancer (SCLC) and non-small cell lung cancer (NSCLC) (Fois et al., 2021). The characteristics of SCLC include an elevated rate of metastasis and proliferation, as well as a favorable early response to radiotherapy and chemotherapy (Wang et al., 2020). NSCLC refers to any form of epithelial lung cancer other than SCLC (PDQ Adult Treatment Editorial Board, 2023). 40% of NSCLC instances are lung adenocarcinomas (LUAD), followed by 25% of squamous cell carcinomas and 12% of large cell carcinomas (Schabath

and Cote, 2019). Currently, 85% of lung cancer cases seen globally are caused by NSCLC. Oncologists can now tailor the therapy options due to recent advancements in the understanding of pathways, techniques for identifying genetic lesions that can be treated, and newly developed medications to block the actions of the pathways. The prognosis and available treatments for NSCLC are significantly influenced by the disease stage at the time of diagnosis (Herbst et al., 2018). Moreover, more than 90% of cancer deaths are attributed to metastasis. Metastasis is a systemic condition as opposed to primary tumors, which can frequently be treated with local surgery or radiation. Surgery is the first line of defense against lung adenocarcinoma, followed by chemotherapy and radiation therapy. However, cancer frequently returns despite treatment. In fact, within 5 years of diagnosis, 25% of patients with lung adenocarcinoma will experience the onset of metastatic disease (Wu et al., 2022). CXCL17 is a member of the CXC chemokine family that attracts myeloid cells (Gowhari Shabgah et al., 2022). The mucosal tissues of the lungs, trachea, bronchi, stomach, and intestinal lumens—organs of the respiratory and gastrointestinal tract—structurally express *CXCL17*. As a result, CXCL17 is regarded as a chemokine associated with the mucosa (Choreño-Parra et al., 2020). The angiogenic activity of CXCL17, also known as VCC-1 (VEGF-Coregulated Chemokine 1), encourages tumorigenesis (Li et al., 2021). Immune cells are activated and move toward the site of inflammation when CXCL17 binds to its receptor, starting a signaling cascade (Choreño-Parra et al., 2020). Chemokines have been demonstrated to have a significant impact on how cells enter the tumor microenvironment and control how the body's immune system responds to all cancer cells (Marcuzzi et al., 2018). Even though numerous studies have demonstrated that CXCL17 is highly expressed in primary tumor samples and cancer cell lines, other studies have demonstrated that this cytokine is underexpressed in cancers. CXCL17 has the ability to both support and suppress tumor growth in certain types of cancer (Gowhari Shabgah et al., 2022). CXCL17 promotes angiogenesis and cell proliferation, which, according to numerous studies, aids in the development of tumors in breast and colon malignancies (Mu et al., 2009). Colorectal, breast, hepatocellular, and type I endometrial cancer all showed significantly lower levels of CXCL17 mRNA or protein compared to type I endometrial cancer and pancreatic intraductal papillary mucinous carcinoma (Weinstein et al., 2006). Additionally, the MDA-MB231 cell line's tendency for cell migration and proliferation is decreased by the downregulation of the gene (Xiao et al., 2021). When pathogen materials are induced, the expression of CXCL17 at steady levels may increase, which might decrease immune responses to support homeostasis and prevent unfavorable immunological reactions (Liu et al., 2020). Additionally, the MDA-MB231 cell line's tendency for cell migration and proliferation is decreased by the downregulation of the gene (Xiao et al., 2021). According to studies on CXCL17 gene expression in breast cancer (Hashemi and Khorramdelazad, 2023), a high level of CXCL17 gene expression in patients is associated with a worse overall survival. When pathogen materials are induced, the expression of CXCL17 at steady levels may increase, which might decrease immune responses to support homeostasis and prevent unfavorable immunological reactions (Liu et al., 2020). According to a recent study, CXCL17 may be involved in how lung adenocarcinoma (LUAD) spreads to the spine. The data show that CXCL17 activates Src/FAK signaling and promotes mononuclear macrophage chemotaxis.

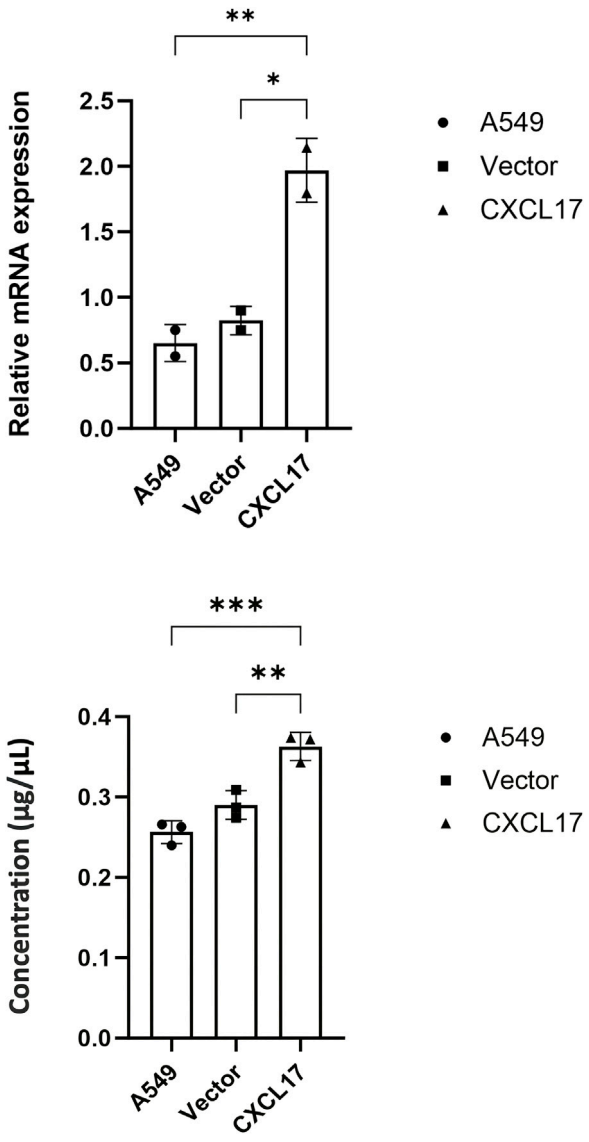

FIGURE 1
CXCL17 overexpression in CXCL17-gene transfected A549 cells. **(A)** RT-PCR analysis demonstrated the CXCL17 mRNA levels were significantly higher in the CXCL17 group compared to A549 and vector groups. Results are displayed as mean ± SD of two independent experiments. *p*-value<0.05; *0.0145, **0.0098. **(B)** ELISA results showed the protein levels of CXCL17 were significantly higher in CXCL17 group compared to A549 and vector groups. Results are displayed as mean ± SD of two independent experiments. *p*-value<0.05; **0.0039, ***0.0005.

The treatment of NSCLC has multiple treatment options according to NCCN guidelines version 1.2024. However, there is still a need for new targeted therapies to prevent the spread and provide a full treatment for lung cancer patients. CXCL17 with all the information provided in the literature has a potential to be a great target for drug candidates.

Online databases UALCAN and GEPIA offer resources for the analysis of gene expression data to researchers studying cancer.

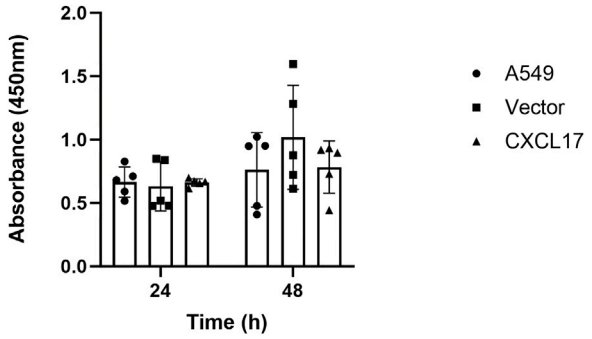

FIGURE 2
CXCL17 overexpression has no impact on the proliferation of A549 cells. A bar graph displaying each group's (A549, vector, CXCL17) absorbance at 450 nm after 24 and 48 h. There was no significant difference in the proliferative abilities of these groups at both time points. Results are displayed as mean ± SD of five independent experiments.

According to the UALCAN database, LUAD patients had lower levels of CXCL17 gene expression compared to healthy individuals, whereas the GEPIA database demonstrated that LUAD patients had higher levels of gene expression for CXCL17 relative to normal (Chandrashekar et al., 2017; Tang et al., 2017). The lack of information in the literature and the small sample size can be attributed for the misinterpretation of such information. This can lead to inaccurate or incomplete understanding of the topic. In order to solve this unknown concept, we aimed to investigate how CXCL17 overexpression affects the migration, proliferation and invasion capabilities of A549 LUAD cells *in vitro*. Our results demonstrated that increased levels of CXCL17 significantly enhanced migration and invasion capacities of A549 cells but not proliferation.

2. Results

2.1 Establishment of CXCL17-overexpressing A549 LUAD cells

To investigate whether CXCL17 overexpression affects LUAD cell migration, proliferation, and invade, we first transfected A549 cells with N-Terminal p3XFLAG-CMV-CXCL17 or vector only. The mRNA and protein levels of CXCL17 in A549 cells were verified using RT-PCR and ELISA after the development of stable clones with CXCL17 overexpression. The relative mRNA levels in *CXCL17* transfected cells (CXCL17) were significantly higher than untransfected (A549) and vector only transfected (vector) cells having *p*-values of 0.0098 and 0.0145, respectively (Figure 1A). CXCL17 protein concentrations detected by ELISA were significantly higher in the CXCL17 group compared to A549 and vector groups having *p*-values of 0.0005 and 0.0039, respectively (Figure 1B).

2.2. CXCL17 overexpression has no effect on the proliferation of A549 cells

We performed CCK8 assay to assess the proliferative capacity in each group in order to examine the effect of CXCL17 overexpression on the proliferation of A549 cells. As shown in Figure 2, A549, vector, and CXCL17 groups all had very similar proliferative capacities at both 24 and 48 h. These findings indicated that overexpression of CXCL17 had no significant effect on the proliferation of A549 cells.

2.3 CXCL17 overexpression has an impact on migration abilities of A549 cells

In order to determine how CXCL17 overexpression affects the migration of A549 cells, we performed the wound healing assay. As shown in Figure 3A, the CXCL17 group had more than 60% of the scratch's surface closed after 24 h, compared to 35%–40% for the A549 and vector groups. At the end of 48 h, the wound area of the CXCL17 group significantly decreased as compared to the A549 and vector groups, with *p*-values of 0.0001 and 0.0153, respectively (Figure 3B). These findings suggested that A549 cells had an enhanced capacity for migration when CXCL17 is overexpressed.

2.4 CXCL17 overexpression has an impact on invasion capabilities of A549 cells

To further explore the role of CXCL17, we conducted a Matrigel invasion assay to evaluate the impact of CXCL17 overexpression on the ability of A549 cells to invade. After 24 h, we observed that there was not a significant difference between the number of invaded cells within each group. Nevertheless after 48 h, the CXCL17 group had significantly more invaded cells than the A549 and vector groups, with *p*-values of 0.0028 and 0.0034, respectively (Figure 4). These results demonstrated that overexpressed CXCL17 plays an essential role for cell invasion.

3 Discussion

CXCL17 plays a crucial part in angiogenesis, which is essential for supplying nutrients to cancer cells, encouraging cancer growth, and enabling invasion. One of the main methods for managing NSCLC is the current treatment with antiangiogenic drugs such as bevacizumab, which blocks VEGF. Some patients, however, may develop resistance to bevacizumab due to the activation of alternative angiogenic pathways that are unaffected by VEGF inhibition (Russo et al., 2017). The proangiogenic factor FGF signaling, which is controlled by CXCL17, is one of these compensatory mechanisms. Therefore, concentrating on CXCL17 may be a promising strategy to increase the effectiveness of anti-VEGF medications in the treatment of NSCLC (Choreño-Parra et al., 2020). With the UALCAN database analysis (Chandrashekar et al., 2017), we discovered that LUAD patients had significantly lower expression of the CXCL17 gene compared to healthy controls. These findings led us to hypothesize that CXCL17 could promote tumor growth and induce metastasis. As the precise function of CXCL17 in NSCLC is still unclear, in this study, we evaluated the proliferative, migratory, and invasion potential of A549 cells that overexpress CXCL17 to learn more about the effects of CXCL17 in NSCLC cells. Understanding this molecular pathway will facilitate the search

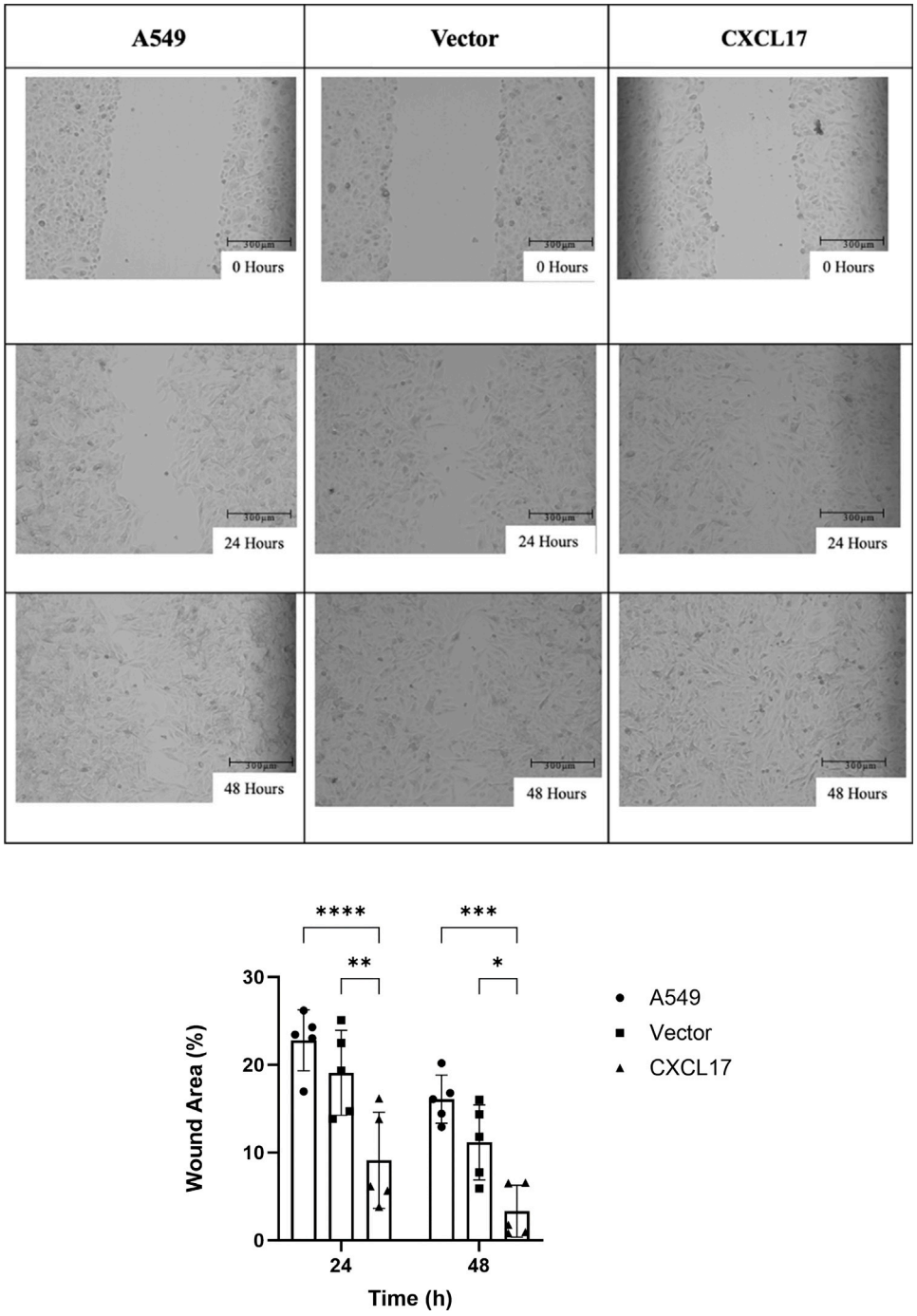

FIGURE 3
CXCL17 overexpression affects migration of A549 cells. **(A)** The best representation of the wound areas is shown in 10X microscope images taken at three different time intervals (0, 24, and 48 h). Scale bar 300 μm. The ability of cells to migrate had been significantly enhanced in the CXCL17 group. **(B)** A bar graph displaying each group's (A549, vector, CXCL17) wound area% at 24 and 48 h. Wound area of the CXCL17 group was significantly decreased compared to others. Results are displayed as mean ± SD of five independent experiments. *p*-value<0.05; *0.0153, **0.0021, ***0.0001 ****<0.0001.

for new active compounds that could interact with CXCL17 of some of the proteins that directly or indirectly affects the metastatic properties of lung adenocarcinomas.

Numerous studies show that in addition to promoting the movement of white blood cells, chemokines, like CXCL17, also play a part in a number of physiological processes. In contrast to a new group of macrophage-like cells that were more prevalent, alveolar macrophages were found to be less common in mice lacking the CXCL17 protein. These findings imply that CXCL17 also functions as a novel macrophage chemoattractant in mucosal tissues (Xiao et al., 2021). Breast and colon cancers express CXCL17 at significantly higher levels, where it promotes

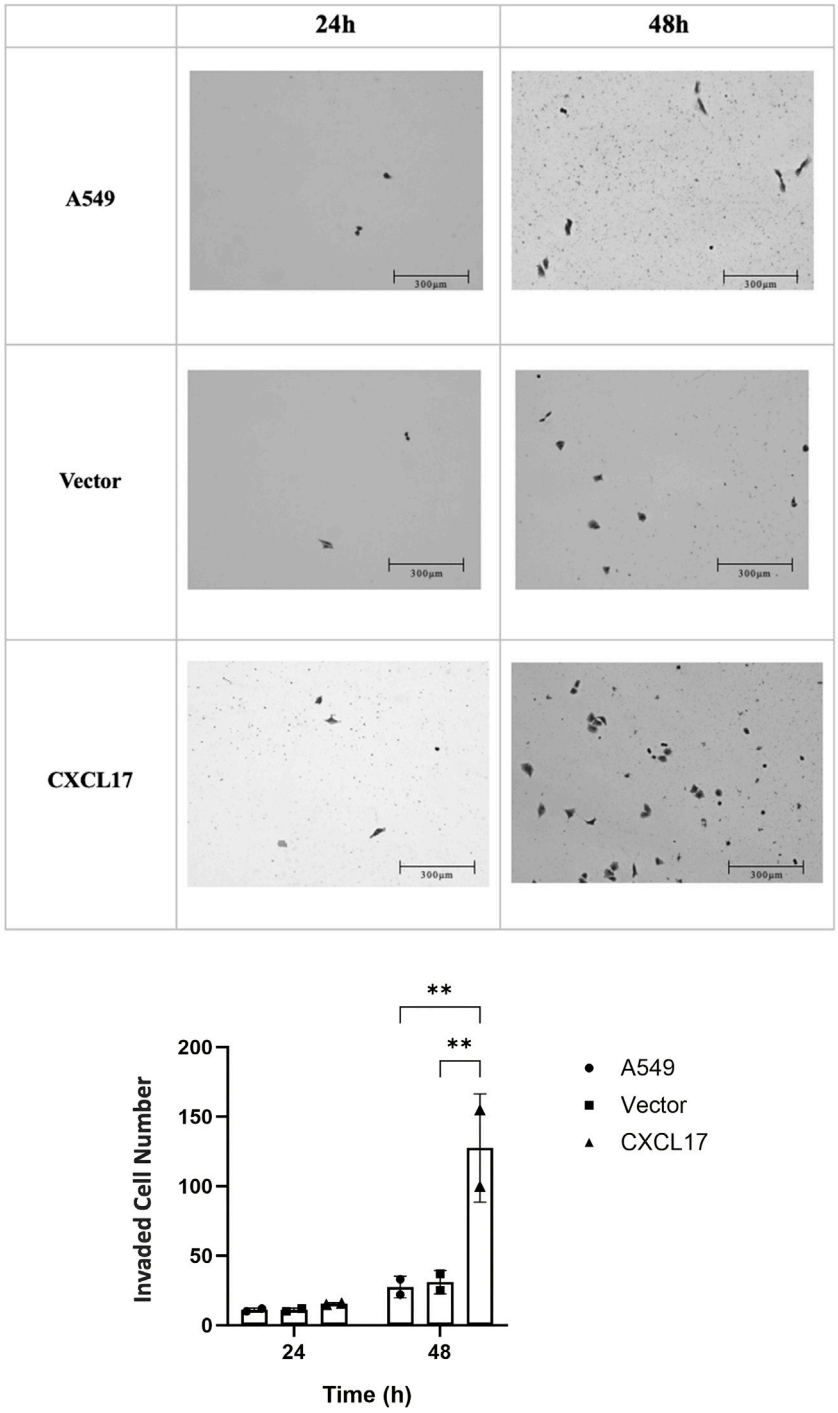

FIGURE 4
CXCL17 overexpression affects invasion of A549 cells. **(A)** The best representation of the invaded cells is shown in 10X microscope images taken at two different time intervals (24, and 48 h). Scale bar 300 μm. The CXCL17 group demonstrated a markedly increased capacity for cell invasion. **(B)** A bar graph displaying the number of invaded cells in each group (A549, vector, CXCL17). The CXCL17 group had a significantly higher number of invaded cells than the other groups. Results are displayed as mean ± SD of two independent experiments. *p*-value<0.05; **0.0028 and **0.0034, A549 vs. CXCL17 and vector vs. CXCL17, respectively.

angiogenesis, the spread of cancerous cells, and the development of the disease (Burkhardt et al., 2014). CXCL17 can promote the growth of SMMC7721 hepatoma carcinoma cells both *in vivo* and in (9). In a recent study, the MTT assay revealed that high levels of *CXCL17* helped the hepatocellular carcinoma cell lines HepG2 and Hepa1-6 survive. This suggests that CXCL17 encourages HCC cell proliferation (Wang et al., 2019). An essential component of tissue formation and regeneration is the control of cell

proliferation (Duronio and Xiong, 2013). Therefore, we performed CCK8 assay to evaluate the proliferative capacity of A549 cells. However, in our study it was demonstrated that the proliferative states of the cells were not affected significantly with the overexpression of CXCL17 in A549 cells. In one study, researchers tested the tumorigenic potential of NIH3T3-mouse embryonic fibroblast cells that had CXCL17 overexpressed. They noticed that the level of CXCL17-3T3 cell proliferation was unaffected in comparison to the control under typical adherent culture conditions. However, compared to mock transfected cells, CXCL17-3T3 cells developed tumors more quickly when subcutaneously injected into nude mice (Matsui et al., 2012). This circumstance may also help us explain our findings. We performed wound healing and Matrigel invasion assays to examine the ability of A549 cells to migrate and invade, respectively. Our findings showed that overexpressing CXCL17 significantly increased A549 cells' migration and invasion. In addition to contributing to the immune response, CXCL17 affects cellular migration which is the onset of diseases such as inflammation and tumor metastasis. Cell migration is, in fact, a crucial component of many physiological phenomena. Invasion, migration, and cell viability play important roles in the pathogenesis of cancer and other biological processes. Cancer metastases are formed when cancer cells disseminate to distant organs as a result of numerous stochastic and complex events. These cells may disperse to distant organs on their own or in response to pressure from the outside world. The ability of the cells to move is a crucial component of cancer metastases (Fares et al., 2020). Moreover, as our results regarding proliferation clearly indicated that CXCL17 overexpression did not change proliferation, wound healing and transwell assay results could be purely attributed to the intrinsic mechanisms that change the mobility of the cells. Wang et al., 2019, demonstrated in hepatocellular carcinoma that CXCL17 promoted this activity via autophagy.Many tumors have been shown to overexpress CXCL17 as a result of proangiogenic agents such as VEGF, CXCL1, and CXCL8. TAMs are immune cells that are activated by high CXCL17 levels in lung adenocarcinomas through the Src/FAK pathway. Then, these TAMs promote the growth and metastasis of malignancies by cultivating an environment that suppresses immunity. Thus, focusing on CXCL17 or its downstream Src/FAK pathway components could be one strategy for treating lung cancer (Hashemi and Khorramdelazad, 2023).

Our research shows that CXCL17 stimulates lung cancer tumor growth and spread. These results imply that CXCL17 might be a viable target for novel cancer treatments. Our findings are in line with earlier studies that demonstrate CXCL17 has a function in tumor development and progression and is overexpressed in a number of cancer types. However, our research is the first to demonstrate that the overexpression of CXCL17 encourages the A549 lung cancer cells to migrate and invade.

A recent study performed in colorectal cancer (CRC) cells used highly expressed GPR35 and CXCL17 in drug-resistant tumor cells. GPR35 expression was shown to be significantly reduced upon CXCL17 knockdown (Bu et al., 2023). In oral squamus cell carcinoma one recent study showed the inhibition of CXCL17 and MUC1 by *Porphyromonas gingivalis* (Lan et al., 2023). Another study performed with HPV-associated cervical cancer pinpointed CXCL17 in relation with Akt pathway and tumor progression (Olwal et al., 2023). The high expression of CXCL17 was also linked with glioblastoma prognosis (Wang et al., 2023). With all the research related with different cancer types show the involvement and the importance of CXCL17 in tumor progression which makes CXCL17 a possible target of candidate drugs and the overexpression model we generated could be a good *in vitro* system to analyze the active compounds and drug candidates while investigating the properties of the drugs and their action mechanisms.

Our studies were conducted *in vitro*, that's why it is possible that the findings may not fully recapitulate the molecular interactions *in vivo* settings. Moreover, in this study the subcellular localization of CXCL17 and its direct effect in wound healing and invasion was not shown due to study design. Despite these limitations, the results of this study provide valuable insights into the role of CXCL17 gene in NSCLC. Further research, including *in vivo* experiments and studies to reveal the molecular mechanisms, are required to fully understand the molecular interactions and the role of this gene in NSCLC.

To conclude overexpressing CXCL17 in A549 cells did not increase their capacity for proliferating *in vitro*, however, it did increase their capacity to migrate and invade.

4 Materials and methods

4.1 Cell culture

The human non-small cell lung cancer cell line A549 was cultured in high glucose DMEM (Gibco™, catalog no. 11965092) supplemented with 10% fetal bovine serum (FBS) (Gibco™, catalog no. 10270106) and 1% pen-strep (Gibco™, catalog no. 15140122) and incubated at 37°C, 5% CO_2.

4.2 Reverse transcription polymerase chain reaction

From the ENSEMBL database (https://www.ensembl.org/index.html) (Cunningham et al., 2021), *CXCL17* cDNA sequences were acquired. To be able to select a restriction enzyme to avoid digestion of cDNA sequence, restriction enzymes having "0 cutter" were examined in the NEBcutter software (http://nc2.neb.com/NEBcutter2/) (Vincze et al., 2003). The N-Terminal p3XFLAG-CMV plasmid-compatible restriction enzymes *Eco*RI and *Kpn*I have been chosen as appropriate enzymes for the CXCL17 gene.

Total RNA from A549 cell line was isolated using the iNtRON Biotechnology RNA-spinTM Total RNA Extraction Kit (for Cell/Tissue) (Catalog no. 17211). The cDNA of A549 RNA was generated from 1 μg total RNA per sample using Vazyme HiScript III RT SuperMix for qPCR (+gDNA wiper) kit (Catalog no. R323). New England BioLabs Taq DNA Polymerase with Standard Taq (Mg-free) Buffer kit (Catalog no. M0320S) was used to amplify the CXCL17 gene from 1 μg cDNA using QIAmplifier 96 PCR equipment. *Cyclophilin A* was used as a positive control.

The sequence of primers (Thorvacs Biotechnology LLC) used:

CXCL17 Forward: 5′GCGAATTCAAAAGTTCTAATCTCT TCCCTCCTCCT 3′

CXCL17 Reverse: 5′GCGGTACCCTACAAAGGCAGAGCA AAGCTTC 3′

CYCLOPHILIN A Forward: 5′AATGGCACTGGTGGCAAG TC 3′

CYCLOPHILIN A Reverse: 5′ GCTCCATGGCCTCCACAA TA 3′

FLAG TAG Forward: 5′ GACTACAAAGACCATGACGGT 3′

4.3 Establishment of CXCL17-overexpressing cells

N-Terminal p3xFLAG-CMV vector was used to establish stably transfected *CXCL17*-overexpressing cells. To construct the N-Terminal p3XFLAG-CMV plasmid, the consensus coding sequence (CCDS) of human CXCL17 gene was amplified with RT-PCR from RNA obtained from A549 cells with primers omitting ATG start codon to enable FLAG fusion. The product of this amplification was digested with *Eco*RI and *Kpn*I and inserted into an *Eco*RI- and *Kpn*I -cleaved N-Terminal p3XFLAG-CMV vector and ligated with T4 DNA Ligase according to the manufacturer's protocol. Restriction enzymes and T4 DNA ligase were purchased from New England Biolabs. The engineered plasmids were sent to Sanger sequencing to verify the correct clone.

jetOPTIMUS® transfection reagent (Catalog no. 101000051) was used for the transfection of cells. A549 cells were transfected with N-Terminal p3XFLAG-CMV or N-Terminal p3XFLAG-CMV-CXCL17 using 10 μg DNA and 10 μL JetOPTIMUS reagent, according to the manufacturer's protocol (Catalog no. 101000051). 3 days post transfection, cells were treated with 700 μg/mL G418 to select stable transfected cells. Medium was changed every 3 days until all the cells that were not transfected died.

After selection, all experiments were performed on 3 groups: The CXCL17 overexpressing cells (will be referred as CXCL17) The cells transfected with unmodified vector only (will be referred as vector) and untransfected naive A549 cells (will be referred as A549).

4.4 Enzyme linked immunosorbent assay

In order to extract protein from A549 cells, 200 μL of RIPA buffer (ABT, catalog no. B08-01-01) containing 1X protease inhibitor cocktail (BOSTER, catalog no. AR1182) was used. The BCA assay (Thermo Fisher Scientific, catalog no. 23225) was used to calculate the total protein concentration. For the purpose of confirming overexpression from cell lysates, the ELK Biotechnologies ELISA Kit (Catalog no. ELK3130) was used. The experiment was conducted in accordance with the manual for the kit's instructions. Protein levels were normalized to total protein concentration. The assay was run as 3 replicates in total.

4.5 Cell counting kit—8 (CCK8) assay

Cell proliferation was analyzed using CCK8 assay (Sigma-Aldrich, catalog no. 96992) to quantitate the number of viable cells. In the first experiment, 500 cells from each group (A549, vector, CXCL17) were seeded into 96-well plates The assay was repeated at two independent experiments with a total of 5 replicates. 10 μL of CCK8 solution was added into each well 24 and 48 h after seeding and incubated for 4 h at 37°C. The absorbance value was read at 450 nm using a microplate reader (Thermo Scientific Varioskan Flash).

4.6 Wound healing assay

In 6-well plates, 350.000 cells from each group (A549, vector, CXCL17) were plated in high glucose DMEM containing 2% FBS as a total of as a total of 3 replicates in first trial, while in the second trial, 2 replicates were performed. The experiment was completed with a total of 5 replicates in two separate times. A 200 μL pipette tip was used to scratch the cell monolayer's surface in the center of the wells after 24 h had passed and it had reached 80% confluence. 24 and 48 h after creating the scratch, 10 photographs were taken with an EVOS M500 microscope on 10 × and the wound area was calculated using ImageJ wound healing size tool at every time point.

4.7 Matrigel invasion assay

24-well Transwell plates with 0.8um membrane inserts (Corning® Costar® Transwell® cell culture inserts, catalog no. CLS3464) were coated with 50 μL of 1:50 diluted Matrigel (Corning® Matrigel® Basement Membrane Matrix, LDEV-free, 10 mL, catalog no. 354234) with high glucose DMEM and then incubated at 37°C for 1 h to gel. The surface was aspirated to remove the non-gelling solution. 10.000 cells from each group (A549, vector, CXCL17) were seeded into the upper chamber in high glucose DMEM containing 1% FBS in 2 replicates at 2 independent experiments with 4 total replicates. High glucose DMEM containing 10% FBS medium was added to the lower chamber to attract cells. One of these plates was set up to be incubated for 24 h, and the other for 48. After 24 and 48 h, cells invade to the bottom chamber were fixed using ice cold 100% methanol for 10 min and stained with Giemsa stain (Merck, catalog no. 1.09204.0500) for 5 min. Photographs of invaded cells were taken with an EVOS M500 microscope on 10X and analyzed with ImageJ.

4.8 Statistical analysis

All experiments were conducted at least twice, and the Graphpad Prism 9 program was used to perform all statistical analyses. The results were displayed as the mean ± standard deviation. One-way analysis of variance (ANOVA) was performed to assess the differences of mRNA and protein levels of each group using Tukey's multiple comparisons test. Two-way ANOVA was performed to assess the differences of proliferated and invaded cells using Šídák's multiple comparisons test. Two-way ANOVA was performed to assess the differences of migrated cells using Tukey's multiple comparisons test. The threshold for significance was set at $p < 0.05$.

Data availability statement

The original contributions presented in the study are included in the article/Supplementary material, further inquiries can be directed to the corresponding author.

Ethics statement

Ethical approval was not required for the studies on humans in accordance with the local legislation and institutional requirements because only commercially available established cell lines were used. Ethical approval was not required for the studies on animals in accordance with the local legislation and institutional requirements because only commercially available established cell lines were used.

Author contributions

EK: Writing–review and editing, Data curation, Formal Analysis, Investigation, Validation, Visualization, Writing–original draft. IC: Data curation, Formal Analysis, Investigation, Validation, Visualization, Writing–original draft, Writing–review and editing. ZT: Validation, Writing–review and editing, Conceptualization, Funding acquisition, Methodology, Project administration, Resources, Supervision.

Funding

The author(s) declare financial support was received for the research, authorship, and/or publication of this article. This research was funded by the Health Institutes of Türkiye (TUSEB), project No. 11899.

Acknowledgments

We would like to thank Acıbadem University for providing materials support. We also thank Prof. Dr. Uygar H. Tazebay for providing the study vector and Dr. Nazlı Keskin Toklu for providing chemically competent cells, *E. coli* DH5α.

Conflict of interest

The authors declare that the research was conducted in the absence of any commercial or financial relationships that could be construed as a potential conflict of interest.

Publisher's note

All claims expressed in this article are solely those of the authors and do not necessarily represent those of their affiliated organizations, or those of the publisher, the editors and the reviewers. Any product that may be evaluated in this article, or claim that may be made by its manufacturer, is not guaranteed or endorsed by the publisher.

References

Bu, J., Yan, W., Huang, Y., and Lin, K. (2023). Activation of the IL-17 signalling pathway by the CXCL17-GPR35 axis affects drug resistance and colorectal cancer tumorigenesis. *Am. J. Cancer Res.* 13 (5), 2172–2187. PMID: 37293165; PMCID: PMC10244108.

Burkhardt, A. M., Maravillas-Montero, J. L., Carnevale, C. D., Vilches-Cisneros, N., Flores, J. P., Hevezi, P. A., et al. (2014). CXCL17 is a major chemotactic factor for lung macrophages. *J. Immunol.* 193 (3), 1468–1474. Epub 2014 Jun 27. PMID: 24973458; PMCID: PMC4142799. doi:10.4049/jimmunol.1400551

Chandrashekar, D. S., Bashel, B., Balasubramanya, S. A. H., Creighton, C. J., Ponce-Rodriguez, I., Chakravarthi, BVSK, et al. (2017). UALCAN: a portal for facilitating tumor subgroup gene expression and survival analyses. *Neoplasia* 19 (8), 649–658. Epub 2017 Jul 18. PMID: 28732212; PMCID: PMC5516091. doi:10.1016/j.neo.2017.05.002

Choreño-Parra, J. A., Thirunavukkarasu, S., Zúñiga, J., and Khader, S. A. (2020). The protective and pathogenic roles of CXCL17 in human health and disease: potential in respiratory medicine. *Cytokine Growth Factor Rev.* 53, 53–62. Epub 2020 Apr 23. PMID: 32345516; PMCID: PMC7177079. doi:10.1016/j.cytogfr.2020.04.004

Cunningham, F., Allen, J. E., Allen, J., Alvarez-Jarreta, J., Amode, M., Armean, I., et al. (2021). Ensembl 2022. *Nucleic Acids Res.* 50, D988–D995. doi:10.1093/nar/gkab1049

Duronio, R. J., and Xiong, Y. (2013). Signaling pathways that control cell proliferation. *Cold Spring Harb. Perspect. Biol.* 5 (3), a008904. PMID: 23457258; PMCID: PMC3578363. doi:10.1101/cshperspect.a008904

Fares, J., Fares, M. Y., Khachfe, H. H., Salhab, H. A., and Fares, Y. (2020). Molecular principles of metastasis: a hallmark of cancer revisited. *Signal Transduct. Target Ther.* 5 (1), 28. PMID: 32296047; PMCID: PMC7067809. doi:10.1038/s41392-020-0134-x

Fois, S. S., Paliogiannis, P., Zinellu, A., Fois, A. G., Cossu, A., and Palmieri, G. (2021). Molecular epidemiology of the main druggable genetic alterations in non-small cell lung cancer. *Int. J. Mol. Sci.* 22 (2), 612. doi:10.3390/ijms22020612

Gowhari Shabgah, A., Jadidi-Niaragh, F., Ebrahimzadeh, F., Mohammadi, H., Askari, E., Pahlavani, N., et al. (2022). A comprehensive review of chemokine CXC17 (VCC1) in cancer, infection, and inflammation. *Cell Biol. Int.* 46 (10), 1557–1570. Epub 2022 Jul 10. PMID: 35811438. doi:10.1002/cbin.11846

Gridelli, C., Rossi, A., Carbone, D. P., Guarize, J., Karachaliou, N., Mok, T., et al. (2015). Non-small-cell lung cancer. *Nat. Rev. Dis. Prim.* 1, 15009. PMID: 27188576. doi:10.1038/nrdp.2015.9

Hashemi, S. F., and Khorramdelazad, H. (2023). The cryptic role of CXCL17/CXCR8 axis in the pathogenesis of cancers: a review of the latest evidence. *J. Cell Commun. Signal* 17 (3), 409–422. Epub 2022 Nov 9. PMID: 36352331; PMCID: PMC10409701. doi:10.1007/s12079-022-00699-7

Herbst, R. S., Morgensztern, D., and Boshoff, C. (2018). The biology and management of non-small cell lung cancer. *Nature* 553, 446–454. doi:10.1038/nature25183

Lan, Z., Zou, K. L., Cui, H., Zhao, Y. Y., and Yu, G. T. (2023). Porphyromonas gingivalis suppresses oral squamous cell carcinoma progression by inhibiting MUC1 expression and remodeling the tumor microenvironment. *Mol. Oncol.* 2023, 13517. Epub ahead of print. PMID: 37666495. doi:10.1002/1878-0261.13517

Li, Y., Wu, T., Gong, S., Zhou, H., Yu, L., Liang, M., et al. (2021). Analysis of the prognosis and therapeutic value of the CXC chemokine family in head and neck squamous cell carcinoma. *Front. Oncol.* 10, 570736. PMID: 33489879; PMCID: PMC7820708. doi:10.3389/fonc.2020.570736

Liu, W., Xie, X., and Wu, J. (2020). Mechanism of lung adenocarcinoma spine metastasis induced by CXCL17. *Cell Oncol. (Dordr)* 43 (2), 311–320. Epub 2019 Dec 12. PMID: 31832986. doi:10.1007/s13402-019-00491-7

Marcuzzi, E., Angioni, R., Molon, B., and Calì, B. (2018). Chemokines and chemokine receptors: orchestrating tumor metastasization. *Int. J. Mol. Sci.* 20 (1), 96. doi:10.3390/ijms20010096

Matsui, A., Yokoo, H., Negishi, Y., Endo-Takahashi, Y., Chun, N. A., Kadouchi, I., et al. (2012). CXCL17 expression by tumor cells recruits CD11b+Gr1 high F4/80- cells and promotes tumor progression. *PLoS One* 7 (8), e44080. PMC3430639 PMID: 22952881. doi:10.1371/journal.pone.0044080

Mu, X., Chen, Y., Wang, S., Huang, X., Pan, H., and Li, M. (2009). Overexpression of VCC-1 gene in human hepatocellular carcinoma cells promotes cell proliferation and invasion. *Acta Biochim. Biophys. Sin. (Shanghai).* 41 (8), 631–637. PMID: 19657564. doi:10.1093/abbs/gmp051

Olwal, C. O., Fabius, J. M., Zuliani-Alvarez, L., Eckhardt, M., Kyei, G. B., Quashie, P. K., et al. (2023). Network modeling suggests HIV infection phenocopies PI3K-AKT pathway mutations to enhance HPV-associated cervical cancer. *Mol. Omics* 19 (7), 538–551. PMID: 37204043; PMCID: PMC10524288. doi:10.1039/d3mo00025g

PDQ Adult Treatment Editorial Board (2023). *Non-small cell lung cancer treatment (PDQ®)–Health professional version*. Bethesda (MD): National Cancer Institute.

Russo, A. E., Priolo, D., Antonelli, G., Libra, M., McCubrey, J. A., and Ferra√π, F. (2017). Bevacizumab in the treatment of NSCLC: patient se-lection and perspectives.

Lung Cancer (Auckl) 8, 259–269. PMID: 29276417; PMCID: PMC5733913. doi:10.2147/LCTT.S110306

Schabath, M. B., and Cote, M. L. (2019). Cancer progress and priorities: lung cancer. *Cancer Epidemiol. Biomarkers Prev.* 28, 1563–1579. doi:10.1158/1055-9965.EPI-19-0221

Tang, Z., Li, C., Kang, B., Gao, G., Li, C., and Zhang, Z. (2017). GEPIA: a web server for cancer and normal gene expression profiling and interactive analyses. *Nucleic Acids Res.* 45 (W1), W98–W102. PMID: 28407145; PMCID: PMC5570223. doi:10.1093/nar/gkx247

Vincze, T., Posfai, J., and Roberts, R. J. (2003). NEBcutter: a program to cleave DNA with restriction enzymes. *Nucleic Acids Res.* 31, 3688–3691. doi:10.1093/nar/gkg526

Wang, L., Li, H., Zhen, Z., Ma, X., Yu, W., Zeng, H., et al. (2019). CXCL17 promotes cell metastasis and inhibits autophagy via the LKB1-AMPK pathway in hepatocellular carcinoma. *Gene* 690, 129–136. Epub 2018 Dec 28. PMID: 30597237. doi:10.1016/j.gene.2018.12.043

Wang, R., Li, Q., Chu, X., Li, N., Liang, H., and He, F. (2023). Sequencing and Bioinformatics analysis of lncRNA/circRNA-miRNA-mRNA in Glioblastoma multiforme. *Metab. Brain Dis.* 38 (7), 2289–2300. Epub 2023 Jun 30. PMID: 37389689. doi:10.1007/s11011-023-01256-w

Wang, Y., Zou, S., Zhao, Z., Liu, P., Ke, C., and Xu, S. (2020). New insights into small-cell lung cancer development and therapy. *Cell Biol. Int.* 44, 1564–1576. doi:10.1002/cbin.11359

Weinstein, E. J., Head, R., Griggs, D. W., Sun, D., Evans, R. J., Swearingen, M. L., et al. (2006). VCC-1, a novel chemokine, promotes tumor growth. *Biochem. Biophys. Res. Comm.* 10 (350), 74–81. doi:10.1016/j.bbrc.2006.08.194

Wu, B., Chen, J., Zhang, X., Feng, N., Xiang, Z., Wei, Y., et al. (2022). Prognostic factors and survival prediction for patients with metastatic lung adenocarcinoma: a population-based study. *Med. Baltim.* 101 (49), e32217. PMID: 36626448; PMCID: PMC9750683. doi:10.1097/MD.0000000000032217

Xiao, S., Xie, W., and Zhou, L. (2021). Mucosal chemokine CXCL17: what is known and not known. *Scand. J. Immunol.* 93 (2), e12965. doi:10.1111/sji.12965

frontiers | Frontiers in Pharmacology

TYPE Original Research
PUBLISHED 02 April 2024
DOI 10.3389/fphar.2024.1367469

OPEN ACCESS

EDITED BY
Patricia Rijo,
Lusofona University, Portugal

REVIEWED BY
Joanna Gdula-Argasinska,
Jagiellonian University Medical College, Poland
Gul Ilbay,
Kocaeli University, Türkiye
Elysia A. Masters,
U.S. Food and Drug Administration,
United States

*CORRESPONDENCE
Güldal Süyen,
guldal.suyen@acibadem.edu.tr

RECEIVED 08 January 2024
ACCEPTED 15 March 2024
PUBLISHED 02 April 2024

CITATION
Yavuz M, Dayanc ED, Merve Antmen F, Keskinöz E, Altuntaş E, Dolu G, Koç B, Tunçcan E, Şakar D, Canözer U, Büyüker C, Polat E, Erkaya M, Azevedo R, Öz Arslan D, Almeida A and Süyen G (2024), Relationships between trace elements and cognitive and depressive behaviors in sprague dawley and wistar albino rats.
Front. Pharmacol. 15:1367469.
doi: 10.3389/fphar.2024.1367469

Relationships between trace elements and cognitive and depressive behaviors in sprague dawley and wistar albino rats

Melis Yavuz[1], Ekin Dongel Dayanc[2,3], Fatma Merve Antmen[2,4], Elif Keskinöz[5], Esra Altuntaş[6], Gökçen Dolu[6], Berkcan Koç[7], Emre Tunçcan[8], Damla Şakar[8], Ufuk Canözer[8], Ceyda Büyüker[8], Ece Polat[6], Metincan Erkaya[8], Rui Azevedo[9], Devrim Öz Arslan[10], Agostinho Almeida[9] and Güldal Süyen[11]*

[1]Department of Pharmacology, Faculty of Pharmacy, Acibadem Mehmet Ali Aydinlar University, Istanbul, Türkiye, [2]Department of Physiology, Institute of Health Sciences, Acibadem Mehmet Ali Aydinlar University, Istanbul, Türkiye, [3]Department of Medical Laboratory Techniques, Vocational School of Health Services, Acibadem Mehmet Ali Aydinlar University, Istanbul, Türkiye, [4]Biobank Unit, Acibadem Mehmet Ali Aydinlar University, Istanbul, Türkiye, [5]Department of Anatomy, School of Medicine, Acibadem Mehmet Ali Aydinlar University, Istanbul, Türkiye, [6]Faculty of Pharmacy, Acibadem Mehmet Ali Aydinlar University, Istanbul, Türkiye, [7]Department of Biophysics, Institute of Health Sciences, Acibadem Mehmet Ali Aydinlar University, Istanbul, Türkiye, [8]School of Medicine, Acibadem Mehmet Ali Aydinlar University, Istanbul, Türkiye, [9]LAQV/REQUIMTE, Department of Chemical Sciences, Faculty of Pharmacy, University of Porto, Porto, Portugal, [10]Department of Biophysics, School of Medicine, Acibadem Mehmet Ali Aydinlar University, Istanbul, Türkiye, [11]Department of Physiology, School of Medicine, Acibadem Mehmet Ali Aydinlar University, Istanbul, Türkiye

Introduction: This study investigates the effects of social isolation on mental health and cognitive functions in Sprague Dawley (SD) and Wistar Albino (WIS) rat strains, prompted by the heightened awareness of such impacts amid the COVID-19 pandemic. This study aims to explore the impact of social isolation on memory, learning, and behavioral changes in middle-aged SD and WIS rat strains and to investigate cortical trace element levels, seeking potential correlations between these levels and the observed behavioral responses to social isolation.

Methods: Four groups of 14-month-old male rats were established: control and isolated SDs and WIS rats (CONT-SD, ISO-SD, CONT-WIS, ISO-WIS). Morris Water Maze and Porsolt Forced Swimming tests were conducted for behavioral assessment. Following behavioral tests, rats were sacrificed under general anesthesia, and cortices were isolated for analysis of macro and trace element levels (ICP/MS).

Results: In behavioral tests, CONT-SD rats exhibited superior performance in the Morris Water Maze test compared to CONT-WIS rats, but displayed increased depressive behaviors following social isolation, as evident in the Porsolt Forced Swimming test ($p < 0.05$). ISO-SD rats showed elevated levels of Co and Cu, along with reduced levels of Cs and As, compared to ISO-WIS rats. Moreover, isolation resulted in decreased Cu and Mo levels but increased Rb levels in WIS rats. Comparison of trace element levels in naïve groups from different strains revealed lower Zn levels in the WIS group compared to SD rats.

Discussion: The findings suggest that the SD strain learns faster, but is more susceptible to depression after isolation compared to the WIS strain. Increased Co

and Cu levels in ISO-SD align with previous findings, indicating potential trace element involvement in stress responses. Understanding these mechanisms could pave the way for preventive treatment strategies or therapeutic targets against the consequences of stressors, contributing to research and measures promoting a balanced diet to mitigate neurobehavioral abnormalities associated with social isolation in the future.

KEYWORDS

social isolation, memory, Strain, sprague Dawley, Wistar, middle-aged, trace elements, depression

1 Introduction

The COVID-19 pandemic has highlighted the importance of social isolation. Therefore, understanding the effects of social isolation on behavioral and cognitive functions has been clearly felt. Social isolation is considered a potent stressor for both animals and humans (Liu et al., 2010) with significant adverse effects on the mental and cognitive health of people of all ages (Cacioppo and Hawkley, 2009). Numerous animal studies have shown that stress resulting from social isolation can cause anxiety-like behaviors and a tendency toward depression (Lukkes et al., 2009; Amiri et al., 2015). Specifically, depression and anxiety-like behavior have been shown to develop after 3 weeks of social isolation (Filipović et al., 2011; Martinovic et al., 2014). Porsolt et al. initially designed the forced swim test to assess the effectiveness of antidepressant drugs in rodents, mainly rats and mice, in their studies from 1977 to 1978 (Porsolt et al., 1977). In addition to this, this test has also been used to assess how exposure to stressful situations, which can induce depression-like behaviors, affects individuals (Armario, 2021).

Several studies have indicated long-term social isolation impairs synaptic plasticity and spatial memory (Wang et al., 2019). The Morris water maze test is a major behavioral test used to measure learning and memory function in animals. A study, assessing learning and memory functions in male albino Wistar (WIS) rats revealed that memory performance was impaired in isolated rats compared to those living in a social and enriched environment (Keloglan et al., 2022). Furthermore, social isolation increases the risk of future cognitive impairment and enhances the rate of memory decline in older people (Bassuk et al., 1999; Ertel et al., 2008). The risk of Alzheimer's disease, which causes cognitive decline and loss of memory function, doubles in solitary individuals (Wilson et al., 2007).

Most studies on social isolation have been conducted on animals, particularly during the post-weaning, developmental or post-natal period, often as a model for autism spectrum disorders or other neurodevelopmental disorders. However, studies on middle-aged rats are rare (Flurkey et al., 2007; Flurkey and Currer, 2009; Stowie and Glass, 2015). Given that the middle-aged or elderly were mainly impacted by social isolation, which affects memory, during the pandemic, understanding the mechanisms underlying the effects of social isolation in middle-aged individuals is important, just as in adulthood.

Trace elements play crucial roles in mental illnesses (Młyniec et al., 2015; Alghadir et al., 2016). Numerous studies have shown an imbalance in the serum or plasma levels of trace and macro elements such as Zn, Cu, Fe and Mg, in individuals with depression compared to those without (Chang et al., 2014; Stanisławska et al., 2014). A study revealed that rats resistant to depression exhibited higher levels of Fe, Na, S, Mn and Co in their brain samples compared to the sensitive group. Conversely, the sensitive group displayed lower plasma levels of Ca, K, S, Se and Co compared to the resistant group (Xu et al., 2020).

In this study, we hypothesized that the prolonged social isolation experienced during the COVID-19 pandemic would exert significant effects on behavior and cognitive functions in middle-aged rats, manifesting as anxiety-like behaviors, depression, and cognitive decline in both WIS and Sprague Dawley (SD) strains. Additionally, our hypothesis posits that the protracted social isolation may lead to compromised synaptic plasticity and spatial memory, with a potential correlation to the imbalance of trace elements, particularly Zn, Cu, Fe, Mg, within the cortex. Through this study, we aim to provide insights into the underlying mechanisms of memory impairment, explore the association between trace elements and cognitive outcomes, and discern the suitability of WIS and SD rat strains for experimental investigations into the impacts of social isolation.

2 Materials and methods

2.1 Animals and housing

The rats were bred and housed in cages (n = 3 rats/cage) in the laboratory of Acıbadem Mehmet Ali Aydınlar University, Experimental Animals Application and Research Center (ACUDEHAM) (Protocol no: 2021/471). All animal experiments conformed with the EU Directive 2010/63/EU and ARRIVE guidelines. Before the experiment, the animals were subjected to a 12:12 h light-dark cycle, at a constant temperature environment (21°C ± 3°C) with 51% humidity with food and water *ad libitum*. The food provided to all animals was a standard maintenance diet for rats and mice involving constant levels of minerals and trace elements (Rats and Mice Maintenance, Carfil Quality). The rats in the social isolation group were housed individually in cages. Cotton and disposable non-transparent cardboard cylinders were placed in all cages (22 cm wide, 37 cm 18 cm high) for "enrichment". Using 14-month-old male SD and WIS rats the experiments were performed between 10:00 a.m. and 7:00 p.m. after 4 weeks of housing.

2.2 Experimental design

The rats were divided into two groups. The control groups were kept in standard housing conditions, as shown above. After 4 weeks

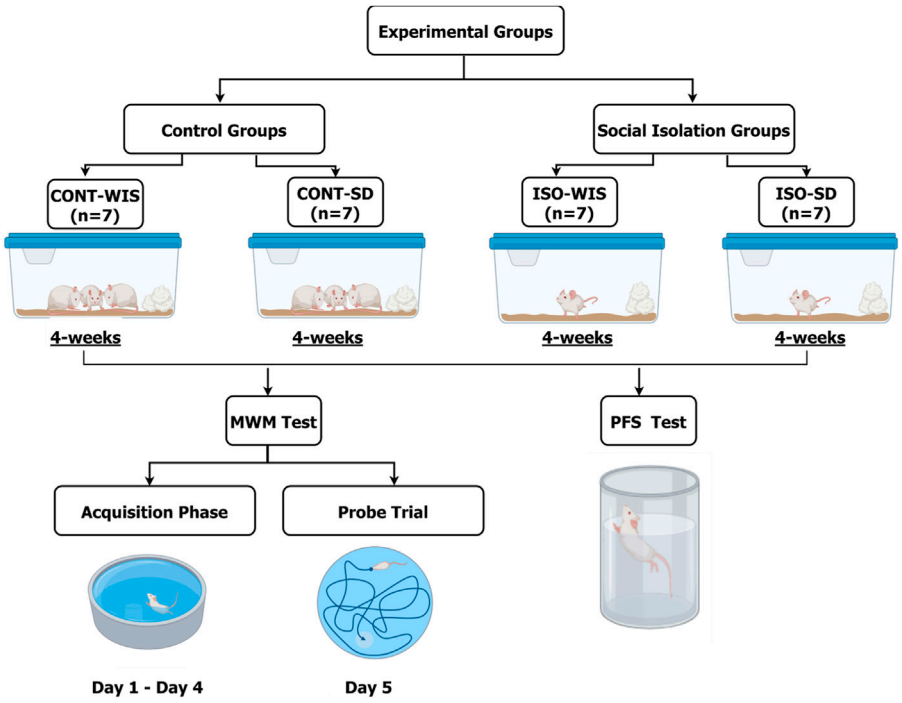

FIGURE 1
Experimental design of the study. CONT-WIS: Wistar control group, CONT-SD: Sprague Dawley control group, ISO-WIS: Wistar rats exposed to the social isolation, ISO-SD: Sprague Dawley rats exposed to the social isolation, MWM: Morris Water Maze. The rats were grouped as shown. CONT-WIS and CONT-SD are the control group of WIS and SD strains, respectively; ISO-WIS and ISO-SD are the corresponding social isolation groups. After 4 weeks, the MWM test was carried out on days 1–4 (acquisition phase) and on day 5 (probe trial). Created partially with BioRender.com.

of social isolation, Morris Water Maze tests were performed for four consecutive days, first on the isolated rats, and then on the control group. The rats were placed in the laboratory 1 hour before the experiments started to allow them to acclimatize. The tests were initiated at 10 a.m. The control groups of each strain (WIS and SD) were named CONT-WIS (n = 10) and CONT-SD (n = 7), while social isolation groups were called ISO-WIS (n = 9) and ISO-SD (n = 8) (Figure 1).

2.3 Social isolation protocol

The rats in the ISO-WIS and ISO-SD groups were housed individually in enriched cages for 4 weeks. The rats in the control groups (CONT-WIS and CONT-SD) were housed in groups (n = 3–4/group). There was no physical contact between the isolated rats and their conspecifics. Due to the potential effects of handling on the results (Song et al., 2021), the researchers did not handle the rats before the experiments. The same person cleaned and changed the cages twice a week to reduce handling and interaction.

2.4 Behavioral tests

After the rats were acclimatized to the laboratory and researchers, the Morris Water Maze test was performed. Environmental cues were placed on the testing room's walls. All tests were recorded with a video camera placed on the ceiling of the testing room. The images were transferred to a computer and analyzed with EthoVision XT 9 video tracking software.

2.4.1 Morris water maze test

The study was conducted in a black circular pool (180 cm diameter, 60 cm depth) with water at a constant temperature (24°C–26°C). Visual cues, such as plus, circle, and rectangle signs were placed on the room's walls, where the pool was located. The pool was divided into four hypothetical equal quadrants to decide where the animal should be released into the pool. A constant black platform (40 cm high, 2 cm below water) was placed in the middle of one quadrant.

The rats were tested twice daily over 4 days, and each session involved four releases from different quadrants. They swam for 90 s to locate the platform. Upon finding it, the rat waited on the platform for 30 s before being placed back into the pool from a different starting point. If the platform could not be found, the rats were put on the platform by the researcher for 30 s. Escape latency, the time taken to find the platform was recorded for each session, and daily averages were calculated.

During the probe trial to assess the memory on the fifth day, the platform was removed to examine the rats' memory functions. During a single 90-s swimming session, the duration spent in the quadrant where the platform was initially positioned, the number of platform crossings, the distance covered, and swimming velocity were recorded.

2.4.2 Porsolt forced swimming test

A transparent cylindrical Plexiglas tank (60 cm high, 20 cm in diameter) was employed to evaluate depression and learned helplessness. The tank was filled with water at 25°C, reaching a depth of 30 cm from surface level to prevent possible escape. A camera was placed above the cylinder to capture the test. The procedure involved placing a rat inside the tank and starting both a stopwatch and the video camera as soon as the rat entered the water. The durations for climbing, swimming and immobility exhibited by the rats were recorded over 2 days. The pre-test was conducted 2 days after Morris Water Maze. The initial day served as a pre-test, during which the animal remained in the water tank for 15 min, with its behavior being thoroughly documented using the Ethovision XT nine software. After each trial, the rats were carefully dried with a towel and a hairdryer before being returned to their respective cages. The next day the testing phase took place, with the animal placed in the tank again, this time for 5 min. The same parameters and measurement criteria were applied, and the rat was removed from the tank after the test and dried as described before.

2.5 Cortical tissue isolations

The day after the Porsolt test, the rats were decapitated under isoflurane anesthesia and their cortices were dissected in ice-cold saline (+4°C, 50 mL). The isolated cortex was used for trace element analysis by ICP-MS.

2.6 ICP-MS analysis of trace elements in rat cortices

2.6.1 Sample pretreatment

The isolated cortex samples were weighed in acid-washed Eppendorf tubes and dried at 80 °C (drying oven) until constant weight. Then, the samples (approximately 1 mg) were transferred to 15 mL polypropylene tubes. Then 250 µL of high-purity HNO_3 (≥69%, TraceSELECT, Fluka) and 50 µL of high-purity H_2O_2 (30%, Suprapur, Supelco) were added to digest the sample for 72 h at room temperature and 1 h at 60°C. After sample digestion, the volume was adjusted with ultrapure water and internal standards (IS) solution to a final volume of 10 mL. Sample blanks were obtained using the same procedure. The analytical quality was assessed using two certified reference materials (CRM) were used: Mussel tissue (ERM-CE278K) and Skimmed Milk Powder (ERM-BD151), both from the European Commission's Joint Research Centre (JRC). These CRMs were pre-treated and analyzed using the same procedure as the samples. The obtained solutions were stored at 4°C until analysis.

2.6.2 Trace element analysis

The samples were analyzed using inductively coupled plasma mass spectrometry (ICP-MS)with an iCAP Q instrument (Thermo Fisher Scientific), equipped with a Meinhard TQ + concentric quartz nebulizer, a Peltier-cooled high-purity quartz baffled cyclonic spray chamber, and a demountable quartz torch with a 2.5 mm i. d. quartz injector. The interface consisted of two Ni cones (sampler and skimmer). High-purity argon (99.9997%) was used as nebulizer and plasma gas. The sample solutions and calibration standards were introduced into the ICP-MS instrument using a CETAC ASX-520 autosampler (Teledyne CETAC Technologies). Before each run, the instrument was tuned for maximum sensitivity and signal stability to minimize the formation of oxides and double-charge ions. The main operational parameters of the ICP-MS were: nebulizer gas flow, 1.14 L/min; auxiliary gas flow, 0.79 L/min; plasma gas flow, 13.9 L/min; radiofrequency generator power, 1550 W; and dwell time, 1–10 m. The isotopes 7Li, 25Mg, 27Al, 31P, 43Ca, 52Cr, 55Mn, 57Fe, 59Co, 60Ni, 65Cu, 66Zn, 75As, 82Se, 85Rb, 88Sr, 111Cd, 121Sb, 133Cs, 137Ba, 205 TL and 208 Pb were measured for analytical determination and the isotopes 6Li, 45Sc, 71Ga, 89Y, 103Rh, 193Ir and 209Bi were monitored as IS (Azevedo et al., 2023).

2.7 Statistical analysis

Data analysis was conducted using the statistical software package SPSS version 22. Graphs were generated in the Graphpad Prism 10.2.1. A one-way analysis of variance (ANOVA) was employed to examine the effects of the time spent in the platform area (duration), the number of platform crossings (frequency), the average speed in the pool (velocity) and the total distance (distance) in the probe trial (CONT-WIS, ISO-WIS, CONT-SD and ISO-SD). Prior to conducting the ANOVA, assumptions of normality, homogeneity of variances were assessed through visual inspection of histograms, and Levene's test, respectively. Subsequently, to test specific hypotheses regarding the linear trend across group means, a linear contrast analysis was performed. Three contrasts were created to assess linear trends across the groups. Trace element analysis was performed with One-Way ANOVA and the data is represented as "F (DFn, DFd) = Fvalue, p-value" with $p < 0.05$ significant difference. The analysis of immobility time was performed with repeated-measures analysis of variance (ANOVA) followed by *post hoc* Dunnett test, designed with two factors, "time" and "treatment," followed by the Dunnett test, was used.

3 Results

3.1 Morris water maze

3.1.1 Time spent to find the platform (escape latency) over the course of four days

Briefly, all rats learned to find the platform, as shown by the significant decrease in escape latency compared to the first day within each group. There was no statistically significant difference in the time spent to find the platform between all groups on day 1. However, significant differences were observed between the time points, but no significant results were observed with the effect of strain or social [F (2,252, 67,55) = 71,82, $p < 0.05$] significant differences of first day of the second, third and fourth days (Figure 2).

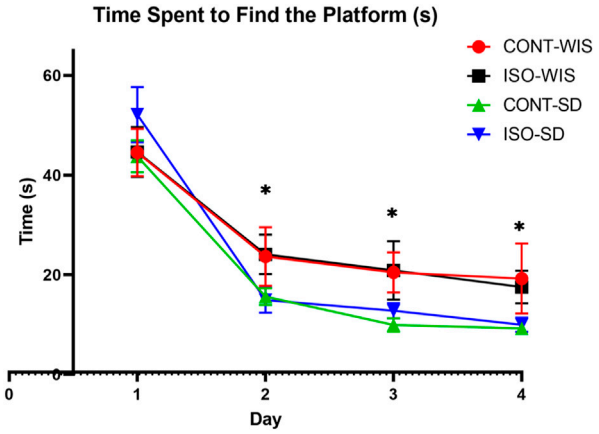

FIGURE 2
Time spent by the rats to find the platform (seconds). All data are expressed as mean ± SEM. *$p < 0.05$ indicates a significant difference between the time points of first and second day. No significant differences were found between the groups.

3.1.2 Probe trial

In the probe trial, memory performance was assessed by time spent in the target quadrant, number of platform crossings, average velocity, and total distance swam. Statistical differences were found in the distance travelled (t = 0.205, $p < 0.05$) and velocity (t = 0.205, $p < 0.05$) between ISO-WIS and ISO-SD (Figures 3D–H Supplementary Figure S4) and between the CONT-SD and ISO-SD (Figures 3B, F).

No significant linear contrasts were observed for groups that the time spent in target quadrant and the number of platform crossings were compared ($p > 0.05$; Figure 4).

3.2 Porsolt forced swimming test

The Porsolt Forced Swimming test results were compared between all groups. Two-Way Anova results showed a significant difference between groups in immobility time ($p < 0.05$) at 1, 2, 3, 4 and 5 min. There was also a significant difference in isolated animals ($p < 0.005$). The difference in the immobility time between the ISO-WIS and CONT-WIS, CONT-SD and CONT-WIS as well as CONT-SD and ISO-SD groups were statistically significant [strain or social isolation effect; F (Van der Borght et al., 2005; Lukkes et al., 2009) = 6,583, $p < 0.05$](Figure 5).

3.3 Trace element levels in the cortex

The trace element levels (As, Ba, Ca, Co, Cr, Cs, Fe, Hg, Li, Mg, Mn, Mo, P, Rb, Se, Sr, Tl, Zn) were measured in the rat cortices from all groups (See Supplementary Material for other trace element levels for all elements: ^{7}Li, ^{25}Mg, ^{27}Al, ^{31}P, ^{43}Ca, ^{52}Cr, ^{55}Mn, ^{57}Fe, ^{59}Co, ^{60}Ni, ^{65}Cu, ^{66}Zn, ^{75}As, ^{82}Se, ^{85}Rb, ^{88}Sr, ^{111}Cd, ^{121}Sb, ^{133}Cs, ^{137}Ba, ^{205}TL and ^{208}Pb). The levels of Co, Cu, Zn, As, Rb, Mo and Cs were significantly different between some groups. Co and Cu levels were significantly higher in the ISO-SD group than the ISO-WIS group (F (Rex et al., 2004; Lukkes et al., 2009) = 1.284; $p = 0.3014$; F (Rex et al., 2004; Lukkes et al., 2009) = 6.776; $p = 0.0017$; respectively, Figure 6). Whereas Cs and As levels were significantly lower in the ISO-SD group compared to the ISO-WIS group (F (Rex et al., 2004; Lukkes et al., 2009) = 5.421; $p = 0.0052$; F (Rex et al., 2004; Lukkes et al., 2009) = 6.616; $p = 0.0019$; respectively, Figure 6). After social isolation, Cu and Mo levels were lower (F (Rex et al., 2004; Lukkes et al., 2009) = 3.191; $p = 0.0409$) in the CONT-WIS group than the ISO-WIS group (F (Rex et al., 2004; Lukkes et al.,

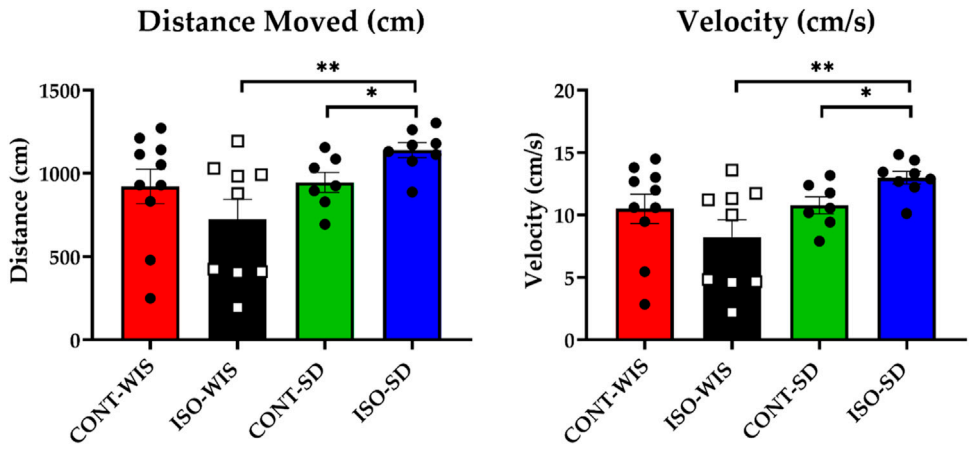

FIGURE 3
Results of the probe trial: Distance Travelled (cm) and Velocity (cm/s) for each group. All data are expressed as mean ± SEM. *$p < 0.05$, **$p < 0.01$ denote significant differences. The distance travelled was compared based on the effect of social isolation or strain differences between the groups of CONT-WIS vs. ISO-WIS, CONT-SD vs. ISO-SD, CONT-WIS vs. CONT-SD, and ISO-WIS vs. ISO-SD. Velocity was compared based on the effect of social isolation on compared based on the effect of social isolation or strain differences between the groups of CONT-WIS vs. ISO-WIS, CONT-SD vs. ISO-SD, CONT-WIS vs. CONT-SD, and ISO-WIS vs. ISO-SD.

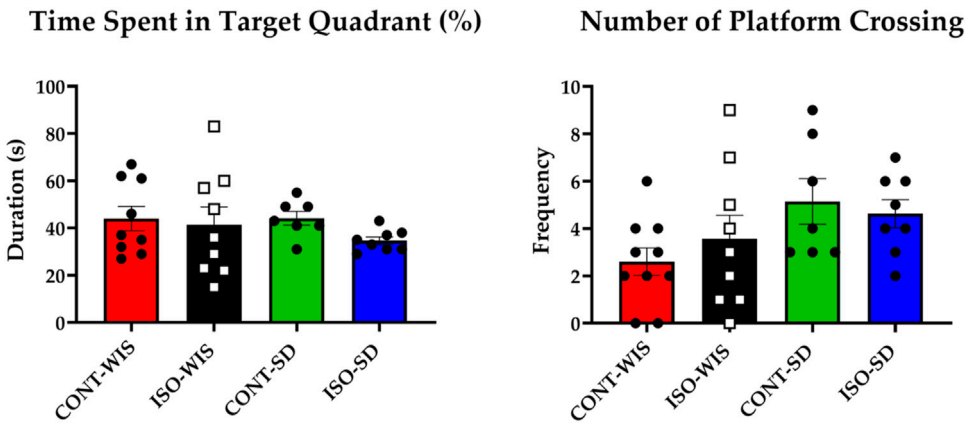

FIGURE 4
Probe trial parameter results: Time Spent in the Target Quadrant (Duration; s) and the Number of Platform Crossings (Frequency) for each group. All data are expressed as mean ± SEM. Time spent in the target quadrant and the number of platform crossings based on the effect of social isolation or strain differences between the groups of CONT-WIS vs. ISO-WIS, CONT-SD vs. ISO-SD, CONT-WIS vs. CONT-SD, and ISO-WIS vs. ISO-SD. Velocity was compared based on the effect of social isolation on compared based on the effect of social isolation or strain differences between the groups of CONT-WIS vs. ISO-WIS, CONT-SD vs. ISO-SD, CONT-WIS vs. CONT-SD, and ISO-WIS vs. ISO-SD.

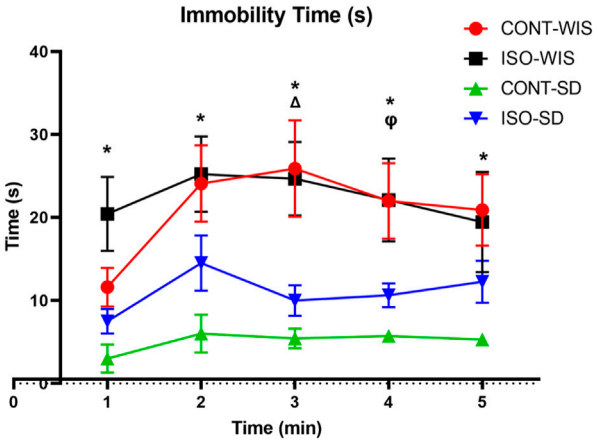

FIGURE 5
Time of Immobility (seconds). All data are expressed as mean ± SEM. *$p < 0.05$, indicate significant difference. The significant differences between groups are denoted as follows: *$p < 0.05$, CONT-WIS and CONT-SD; $^{\Delta}$ $p < 0.05$, ISO-WIS and ISO-SD; $^{\square}$ $p < 0.05$, CONT-SD and ISO-SD.

2009) = 4.750; $p = 0.0093$), while Rb levels were higher. In the naïve strains were compared, it was observed that Zn levels were lower in the WIS group that in the SD rats (F (Weiss et al., 2000; Lukkes et al., 2009) = 4.114; $p = 0.0173$; Figure 6).

4 Discussion

Until now, a direct and comprehensive assessment of trace elements in the brain, such as a comparative analysis between two different rat strains following social isolation has not been done yet. Therefore, our objective was to discern potential associations between trace element levels, strain responses to social isolation, and subsequent impacts on depressive behavior and memory functions. Our findings revealed differences in trace element levels between two rat strains subjected to social isolation. Specifically, Co and Cu levels were elevated, while As and Cs levels were reduced in the socially isolated SD group compared to the WIS group.

Our findings showed that, compared to the first day, the time spent finding the platform gradually decreased for all groups. In summary: (Liu et al., 2010): although the distance to find the platform in the probe trial was not affected by isolation in the WIS groups, it had a drastic effect on the SD groups; (Cacioppo and Hawkley, 2009); the velocity of the isolated SD was higher than the SD control and isolated WIS groups. No differences were found between CONT-SD and CONT-WIS groups; (Lukkes et al., 2009); isolated SD rats found the platform faster than control SD rats, but no other differences were found regarding velocity; (Amiri et al., 2015); there were significant differences in the cortical trace element levels between groups. Specifically, within the ISO-SD group, unlike the ISO-WIS group, the Co and Cu levels were higher, while the Cs and As levels were lower; (Filipović et al., 2011); isolation led to decreased levels of Cu and Mo, but increased the Rb levels in WIS rats. Comparing trace element levels in naïve groups of different strains, Zn levels were lower in the WIS group than in the SD rats; (Martinovic et al., 2014); the CONT-SD and ISO-SD groups outperformed the CONT-WIS group in locating the platform over 4 days although statistically not significant.

Our results suggest that social isolation may impact ISO-SD rats more. Existing literature on the behavioral consequences of social isolation in various rat strains varies widely. Specifically, one study documented a substantial decline in pre-pulse inhibition among SD rats compared to WIS rats after 12 weeks of isolation (Weiss et al., 2000). In our research, ISO-SD rats had increased velocity and distance moved that might show it takes more effort to find the platform, which might indicate a potential memory deficit. Our results also revealed that isolation elicited a comparatively more discernible impact on SD than WIS rats. Previous reports have

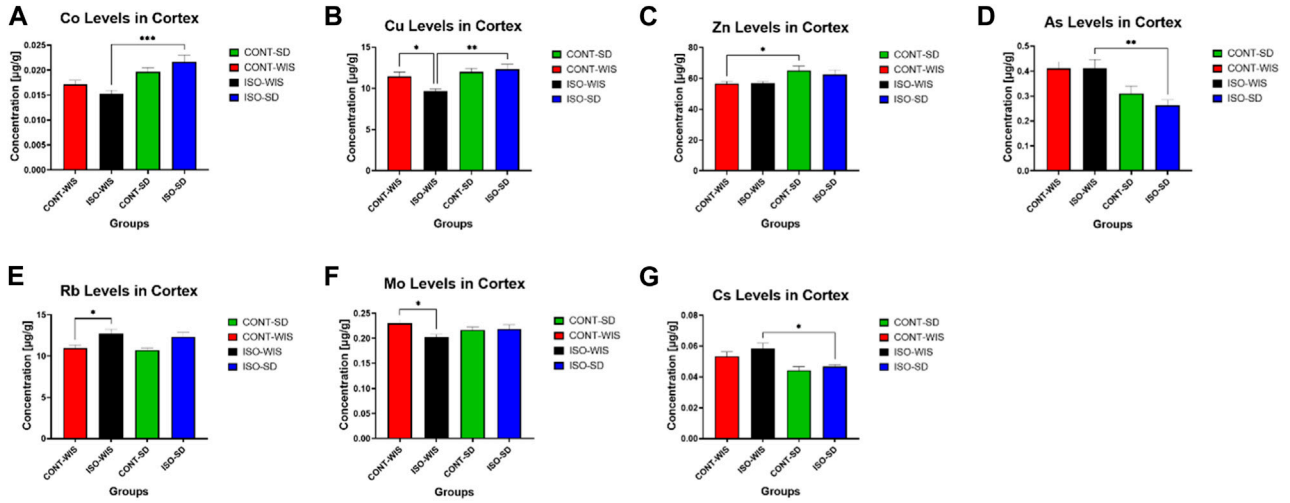

FIGURE 6
Cortical trace element levels. **(A)** Co levels in the cortex in all groups, **(B)** Cu levels in the cortex in all groups, **(C)** Zn levels in the cortex in all groups, **(D)** As levels in the cortex in all groups, **(E)** Rb levels in the cortex in all groups, **(F)** Mo levels in the cortex in all groups, **(G)** Cs levels in the cortex in all groups. All data are expressed as mean ± SEM. The significant differences between groups are denoted as follows: *$p < 0.05$, Cu levels between the CONT-WIS and ISO-WIS, Zn levels between CONT-WIS and CONT-SD, Rb levels between CONT-WIS and ISO-WIS, Mo levels between CONT-WIS and ISO-WIS, Cs levels between ISO-WIS and ISO-SD groups. **$p < 0.01$, Cu levels between the ISO-WIS and ISO-SD, As levels between ISO-WIS and ISO-SD. ***$p < 0.001$, Co levels between the ISO-WIS and ISO-SD.

suggested that environmental conditions do not significantly impact the social behavior of SD rats, while they affect WIS rats indicating that WIS rats generally tend to be more anxious (Rex et al., 2004).

The Morris Water Maze test is used for evaluating memory functions and spatial learning mainly the time spent in the target quadrant and the number of platform crossings. Total distance travelled and the average swimming speed of the rats was also included as it was shown in prior studies that anxiety and age affected these parameters as well, as well as to understand the thigmotactic behaviors (Belviranli et al., 2012). Repeated testing was conducted for 4 days to assess spatial learning, and a probe trial day to assess the reference memory performance (Morris, 1984). In both control and isolated groups, SD rats performed better than WIS rats in locating the platform over 4 days as seen in the graphs although there was no statistical significance. This might suggest that SD rats might possess better spatial learning and memory ability than the WIS rats, but more studies are needed to confirm this. Adult SD rats have been previously shown to perform better than WIS rats in autoshaping, lever press response, maze testing (Andrews et al., 1995), and the latency to find the maze (Inostroza et al., 2011). However, another study comparing WIS and SD rats reported contradictory results. Although both strains performed equally during training, WIS rats exhibited better cueing results in the Morris Water Maze test (Van der Borght et al., 2005). Which might be in line with the increased velocity and distance taken by SD rats in the probe trial. Another study comparing three rat strains revealed that SD rats are superior to spontaneous hypertensive rats. A genetic model of attention deficit hyperactivity disorder also localized the platform in the maze more rapidly (Cao et al., 2013). Furthermore, compared with WIS Kyoto rats and spontaneous hypertensive rats, SD rats exhibited elevated docosahexaenoic acid levels in their hippocampus, prefrontal cortex, and corpus striatum, and reduced docosahexaenoic acid levels in the corpus callosum, parietal lobe, and temporal lobe. Our findings are consistent with the studies on aged rats.

Using the Porsolt forced swimming test we evaluated depressive-like behavior in rats using immobility time. We observed significant differences between CONT-WIS and CONT-SD groups throughout the experiments. The immobility time for CONT-WIS rats was longer than that of CONT-SD rats for each time period, suggesting that WIS rats exhibited more anxiety than naturally middle-aged SD rats. Although also a statistically significant difference was observed between isolated WIS/SD rats, it is difficult to interpret this due to the baseline difference in anxiety. The duration of immobility of WIS rats was shown to be longer than that of SD rats, which might be because WIS rats have more dopamine receptors (Zamudio et al., 2005). Furthermore, the ISO-WIS group showed longer immobility time than the CONT-WIS group in the first minute, but without statistical significance. A study on 15-week-old rats showed no significant difference between isolated and control WIS rats regarding immobility time (Hall et al., 1998). As a limitation of our study, we initially conducted behavioral tests with the isolated group while many animals were in the groups. This ensured that the time spent in the cages during social isolation was evenly distributed, involving 17 animals first, considering constraints related to daylight hours and the duration of behavioral tests.

While direct associations are challenging to establish, there is evidence of altered levels of trace elements that may indicate a potential association with social isolation and its outcomes. For instance, Zn levels were higher in the SD control group, aligning with previous research associating Zn with stress-related responses. Zn deficiency or social isolation alone induces anxious or depressive symptoms (Mitsuya et al., 2015). In previous findings, socially-isolated rats showed reduced serum Zn levels but increased Cu levels in the prefrontal cortex of SD rats (Famitafreshi and Karimian,

2016). In our study, Zn was also initially higher in the control group of SD. Similarly, the activity of total superoxide dismutase, including Cu/Zn superoxide dismutase (CuZnSOD) and catalase was increased in the cerebral cortex of WIS rats exposed to social isolation (Pejic et al., 2016). Another study reports increased activity of CuZnSOD in socially isolated rats (Pajović et al., 2006; Stanisavljevic et al., 2017). These increases in the Cu and Zn may be related to the increases in the need for the catalase activities. Zn was also associated with depressive-like and anxiety-related behavior (Takeda et al., 2007; Watanabe et al., 2010). The effects of Zn were studied in the forced swimming (Porsolt's) test in mice. Zn (ZnSO4) at a dose of 30 mg/kg (but not at a dose of 10 mg/kg), similar to imipramine (30 mg/kg), reduced the immobility time in that test. Moreover, Zn at both doses reduced the locomotor activity. The obtained results indicate that Zn induces an antidepressant-like effect in the forced swimming test. Since Zn reduces locomotor activity, this antidepressant-like effect is not related to the alteration of general activity (Kroczka et al., 2000). In our study, not many differences were found due to social isolation. Still, SD rats had higher intrinsic levels of Zn, which may be associated with an intrinsic protection mechanism against possible stressors. In contrast, SD rats appear more prone to stress-related immobility behaviors.

The antidepressant, psychostimulant, and nootropic effects of several major and trace elements including KCl, RbNO3, and magnesium sulphate were studied on models of behavioral despair using Porsolt and conditioned passive avoidance tests. This preparation was found to shorten the immobilization time in the Porsolt test and promote retention of the conditioned passive avoidance. The most pronounced psychostimulant effect of the substance was observed in a dose-dependent manner (Afanasieva et al., 2013). Other trace elements have been associated with neurological symptoms or irritability such as Mo, Rb, exposure to As and elevated Co levels (Rex et al., 2004; Tower, 2010; Kyi-Tha-Thu et al., 2023). We have found elevated Rb levels only in socially isolated WIS rats, thus supporting the anticipated association between their breed disposition and elevated Rb levels under isolation conditions (Rex et al., 2004). We have found decreased Mo levels in the ISO-WIS group. Animal studies have shown reduced exploratory behavior and a potential decline in passive avoidance learning in subjects exposed to higher doses of Co (Czarnota et al., 1998). It has also been demonstrated that top-down control of passive coping behavior by the medial prefrontal cortex can collaborate with the bottom-up action of glucocorticoids to improve memory consolidation of the immobility response. In this regard, the immobility response can be attributed to the accumulation of passive avoidance behavior (Lingg et al., 2020). In line with these findings, isolated SD rats in our study showed greater immobility compared to isolated WIS rats in the Porsolt forced swimming test, as well as increased Co levels, which may be a possible association of correlated neurobehavioral changes. In male rats, chronic exposure to As resulted in anxiety- and depression-like behaviors along with memory impairment. These effects were observed through reduced time spent in open areas (elevated plus maze), increased immobility time (forced swimming test), and decreased performance in spatial memory tasks (Morris water maze test) (Samad et al., 2021). In the course of our research, elevated As levels were noted in ISO-WIS rats in comparison to ISO-SD rats. This observation aligns with the inherently anxious disposition of WIS rats and previous research indicating the anxiogenic effects of As. Furthermore, a disparity emerged in the Porsolt forced swimming test between ISO-WIS and ISO-SD rats only in the third minute, with ISO-WIS rats displaying significantly greater immobility compared to ISO-SD. While consistent with earlier findings on the impact of As, it is noteworthy that social isolation exerts a more pronounced influence on the SD strain. One study associated Cs with impaired learning and spatial memory and increased anxiety (Bellés et al., 2016). Further, regarding anxiety, which is expected to be higher in WIS rats, our results show that CONT-WIS had higher levels of Cs compared to CONT-SD, consistent with previous findings.

In summary, distinct patterns were evident in both trace element analysis and behavioral tests. The comprehensive findings indicate elevated Co and Cu levels, coupled with decreased Cs and As levels in socially isolated SD rats compared to WIS rats. Furthermore, isolation may have exerted varying influences on Zn, Mo, and Rb levels within each strain. This divergence in trace element profiles is perceived as offering valuable insights into factors contributing to resilience. Moreover, the present results hold promise for identifying novel targets for the treatment and dietary prevention of depressive and mental disorders during stressful periods in the future. The study emphasizes the strain-specific responses to isolation, providing an in-depth view of the neurobehavioral effects of trace elements and contributing valuable information to the comprehension of behavioral consequences in socially isolated rats. Other factors also must be considered to draw direct associations between these associations.

5 Conclusion

Studies suggest that strain differences might be the underlying reason behind the conflicting results in any behavioral paradigm. A strain's performance in one task does not reliably predict its performance on another. Our findings indicate that SD rats are more sensitive to social isolation as shown in previous studies. Therefore, using SD rats to study the effects of stress and isolation is more plausible. Furthermore, we emphasized strain-specific responses to isolation and the association of specific neurobehavioral effects with trace elements. Our results might contribute to the future on designing a balanced diet to prevent neurobehavioral abnormalities due to social isolation.

Data availability statement

The original contributions presented in the study are included in the article/Supplementary Material, further inquiries can be directed to the corresponding author.

Ethics statement

The animal study was approved by the Acibadem University Experimental Animals Ethical Committee. The study was conducted

in accordance with the local legislation and institutional requirements.

Author contributions

MY: Conceptualization, Data curation, Formal Analysis, Funding acquisition, Investigation, Methodology, Project administration, Resources, Validation, Visualization, Writing–original draft, Writing–review and editing. EDD: Conceptualization, Data curation, Investigation, Methodology, Validation, Writing–original draft. FMA: Data curation, Investigation, Methodology, Project administration, Supervision, Writing–original draft. EK: Data curation, Methodology, Writing–original draft. EA: Data curation, Formal Analysis, Investigation, Methodology, Writing–original draft. GD: Data curation, Formal Analysis, Investigation, Methodology, Validation, Writing–original draft. BK: Data curation, Methodology, Writing–original draft. ET: Data curation, Formal Analysis, Methodology, Software, Writing–original draft. DS: Data curation, Writing–original draft. UC: Data curation, Writing–original draft. CB: Data curation, Writing–original draft. EP: Data curation, Writing–original draft. ME: Data curation, Writing–original draft. RA: Data curation, Formal Analysis, Investigation, Methodology, Writing–original draft. DÖA: Methodology, Resources, Writing–review and editing. AA: Formal Analysis, Methodology, Resources, Supervision, Writing–review and editing. GS: Conceptualization, Formal Analysis, Investigation, Methodology, Project administration, Resources, Software, Supervision, Writing–review and editing.

Funding

The author(s) declare financial support was received for the research, authorship, and/or publication of this article. FMA is funded by TUBITAK-BIDEB 2244 Industrial Ph.D. Program [Grant Number 118C082]. Gokcen GD has received a travel grant from the Kerem Aydinlar Foundation.

Conflict of interest

The authors declare that the research was conducted in the absence of any commercial or financial relationships that could be construed as a potential conflict of interest.

Publisher's note

All claims expressed in this article are solely those of the authors and do not necessarily represent those of their affiliated organizations, or those of the publisher, the editors and the reviewers. Any product that may be evaluated in this article, or claim that may be made by its manufacturer, is not guaranteed or endorsed by the publisher.

Supplementary material

The Supplementary Material for this article can be found online at: https://www.frontiersin.org/articles/10.3389/fphar.2024.1367469/full#supplementary-material

SUPPLEMENTARY FIGURE 1
Cortical trace element levels. Co, Mg, P, Ca, Cr, Mn, Fe, Co, Cu levels in the cortex in all groups. All data are expressed as mean ± SEM. The significant differences between groups are denoted as follows: *$p < 0.05$, Cu levels between the CONT-WIS and ISO-WIS, **$p < 0.01$, Cu levels between the ISO-WIS and ISO-SD, ***$p < 0.001$, Co levels between the ISO-WIS and ISO-SD.

SUPPLEMENTARY FIGURE 2
Cortical trace element levels. Zn, As, Se, Rb, Sr, Mo, Cs, Ba, Hg levels in the cortex in all groups. All data are expressed as mean ± SEM. The significant differences between groups are denoted as follows: *$p < 0.05$, Zn levels between the CONT-WIS and CONT-SD, Rb levels between the CONT-WIS and ISO-WIS, Mo levels between CONT-WIS and ISO-WIS, Cs levels ISO-WIS and ISO-SD, **$p < 0.01$, As levels between the ISO-WIS and ISO-SD.

References

Afanasieva, O. G., Suslov, N. I., and Shilova, I. V. (2013). Antidepressant, psychostimulant, and nootropic effects of major and trace element composition. *Bull. Exp. Biol. Med.* 155 (2), 204–206. doi:10.1007/s10517-013-2113-5

Alghadir, A. H., Gabr, S. A., and Al-Eisa, E. (2016). Effects of physical activity on trace elements and depression related biomarkers in children and adolescents. *Biol. trace Elem. Res.* 172, 299–306. doi:10.1007/s12011-015-0601-3

Amiri, S., Haj-Mirzaian, A., Rahimi-Balaei, M., Razmi, A., Kordjazy, N., Shirzadian, A., et al. (2015). Co-occurrence of anxiety and depressive-like behaviors following adolescent social isolation in male mice; possible role of nitrergic system. *Physiology Behav.* 145, 38–44. doi:10.1016/j.physbeh.2015.03.032

Andrews, J. S., Jansen, J. H. M., Linders, S., Princen, A., and Broekkamp, C. L. E. (1995). Performance of four different rat strains in the autoshaping, two-object discrimination, and swim maze tests of learning and memory. *Physiology Behav.* 57 (4), 785–790. doi:10.1016/0031-9384(94)00336-x

Armario, A. (2021). The forced swim test: historical, conceptual and methodological considerations and its relationship with individual behavioral traits. *Neurosci. Biobehav Rev.* 128, 74–86. doi:10.1016/j.neubiorev.2021.06.014

Azevedo, R., Oliveira, A. R., Almeida, A., and Gomes, L. R. (2023). Determination by ICP-ms of essential and toxic trace elements in gums and carrageenans used as food additives commercially available in the Portuguese market. *Foods Basel, Switz.* 12 (7), 1408. doi:10.3390/foods12071408

Bassuk, S. S., Glass, T. A., and Berkman, L. F. (1999). Social disengagement and incident cognitive decline in community-dwelling elderly persons. *Ann. Intern. Med.* 131 (3), 165–173. doi:10.7326/0003-4819-131-3-199908030-00002

Bellés, M., Heredia, L., Serra, N., Domingo, J. L., and Linares, V. (2016). Exposure to low doses of 137cesium and nicotine during postnatal development modifies anxiety levels, learning, and spatial memory performance in mice. *Food Chem. Toxicol.* 97, 82–88. doi:10.1016/j.fct.2016.08.032

Belviranli, M., Atalik, K. E. N., Okudan, N., and Gökbel, H. (2012). Age and sex affect spatial and emotional behaviors in rats: the role of repeated elevated plus maze test. *Neuroscience* 227, 1–9. doi:10.1016/j.neuroscience.2012.09.036

Cacioppo, J. T., and Hawkley, L. C. (2009). Perceived social isolation and cognition. *Trends cognitive Sci.* 13 (10), 447–454. doi:10.1016/j.tics.2009.06.005

Cao, A., Yu, L., Wang, Y., Wang, G., and Lei, G. (2013). Composition of long chain polyunsaturated fatty acids (LC-PUFAs) in different encephalic regions and its association with behavior in spontaneous hypertensive rat (SHR). *Brain Res.* 1528, 49–57. doi:10.1016/j.brainres.2013.05.029

Chang, M.-Y., Tseng, C.-H., and Chiou, Y.-L. (2014). The plasma concentration of copper and prevalence of depression were positively correlated in shift nurses. *Biol. Res. Nurs.* 16 (2), 175–181. doi:10.1177/1099800413479156

Czarnota, M., Whitman, D., and Berman, R. (1998). Activity and passive-avoidance learning in cobalt-injected rats. *Int. J. Neurosci.* 93 (1-2), 29–33. doi:10.3109/00207459808986409

Ertel, K. A., Glymour, M. M., and Berkman, L. F. (2008). Effects of social integration on preserving memory function in a nationally representative US elderly population. *Am. J. public health* 98 (7), 1215–1220. doi:10.2105/AJPH.2007.113654

Famitafreshi, H., and Karimian, M. (2016). Paradoxical regulation of copper and zinc and changes in neurogenesis, alcohol preference and salt appetite in isolated male rats. *Ssu-ijml.* 3 (4), 249–261.

Filipović, D., Zlatković, J., Inta, D., Bjelobaba, I., Stojiljkovic, M., and Gass, P. (2011). Chronic isolation stress predisposes the frontal cortex but not the hippocampus to the potentially detrimental release of cytochrome c from mitochondria and the activation of caspase-3. *J. Neurosci. Res.* 89 (9), 1461–1470. doi:10.1002/jnr.22687

Flurkey, K., and Currer, J. M. (2009). *The Jackson Laboratory handbook on genetically standardized mice: jackson Laboratory*.

Flurkey, K., Currer, J. M., and Harrison, D. (2007). Mouse models in aging research. *The mouse in biomedical research*. Elsevier, 637–672.

Hall, F. S., Huang, S., Fong, G. F., and Pert, A. (1998). The effects of social isolation on the forced swim test in Fawn hooded and Wistar rats. *J. Neurosci. Methods* 79 (1), 47–51. doi:10.1016/s0165-0270(97)00155-6

Inostroza, M., Cid, E., Brotons-Mas, J., Gal, B., Aivar, P., Uzcategui, Y. G., et al. (2011). Hippocampal-dependent spatial memory in the water maze is preserved in an experimental model of temporal lobe epilepsy in rats. *PLOS ONE* 6 (7), e22372. doi:10.1371/journal.pone.0022372

Keloglan, M. S., Ozturk, D. M., Sahin, L., Cevik, O. S., and Cevik, K. (2022). Environmental enrichment as a strategy: attenuates the anxiety and memory impairment in social isolation stress. *Int. J. Dev. Neurosci.* 82 (6), 499–512. doi:10.1002/jdn.10205

Kroczka, B., Zieba, A., Dudek, D., Pilc, A., and Nowak, G. (2000). Zinc exhibits an antidepressant-like effect in the forced swimming test in mice. *Pol. J. Pharmacol.* 52 (5), 403–406.

Kyi-Tha-Thu, C., Htway, S.-M., Suzuki, T., Nohara, K., and Win-Shwe, T.-T. (2023). Gestational arsenic exposure induces anxiety-like behaviors in F1 female mice by dysregulation of neurological and immunological markers. *Environ. Health Prev. Med.* 28, 43. doi:10.1265/ehpm.23-00046

Lingg, R. T., Johnson, S. B., Emmons, E. B., Anderson, R. M., Romig-Martin, S. A., Narayanan, N. S., et al. (2020). Bed nuclei of the stria terminalis modulate memory consolidation via glucocorticoid-dependent and -independent circuits. *Proc. Natl. Acad. Sci. U. S. A.* 117 (14), 8104–8114. doi:10.1073/pnas.1915501117

Liu, L.-J., Sun, X., Zhang, C.-L., Wang, Y., and Guo, Q. (2010). A survey in rural China of parent-absence through migrant working: the impact on their children's self-concept and loneliness. *BMC public health* 10 (1), 32–38. doi:10.1186/1471-2458-10-32

Lukkes, J. L., Mokin, M. V., Scholl, J. L., and Forster, G. L. (2009). Adult rats exposed to early-life social isolation exhibit increased anxiety and conditioned fear behavior, and altered hormonal stress responses. *Hormones Behav.* 55 (1), 248–256. doi:10.1016/j.yhbeh.2008.10.014

Martinovic, J., Todorović, N., Bošković, M., Pajović, S., Demajo, M., and Filipovic, D. (2014). Different susceptibility of prefrontal cortex and hippocampus to oxidative stress following chronic social isolation stress. *Mol. Cell. Biochem.* 393, 43–57. doi:10.1007/s11010-014-2045-z

Mitsuya, H., Omata, N., Kiyono, Y., Mizuno, T., Murata, T., Mita, K., et al. (2015). The co-occurrence of zinc deficiency and social isolation has the opposite effects on mood compared with either condition alone due to changes in the central norepinephrine system. *Behav. Brain Res.* 284, 125–130. doi:10.1016/j.bbr.2015.02.005

Młyniec, K., Gaweł, M., Doboszewska, U., Starowicz, G., Pytka, K., Davies, C. L., et al. (2015). Essential elements in depression and anxiety. Part II. *Pharmacol. Rep.* 67 (2), 187–194. doi:10.1016/j.pharep.2014.09.009

Morris, R. (1984). Developments of a water-maze procedure for studying spatial learning in the rat. *J. Neurosci. methods* 11 (1), 47–60. doi:10.1016/0165-0270(84)90007-4

Pajović, S. B., Pejić, S., Stojiljković, V., Gavrilović, L., Dronjak, S., and Kanazir, D. T. (2006). Alterations in hippocampal antioxidant enzyme activities and sympatho-adrenomedullary system of rats in response to different stress models. *Physiol. Res.* 55 (4), 453–460. doi:10.33549/physiolres.930807

Pejic, S., Stojikjkovic, V., Todorovic, A., Gavrilovic, L., Pavlovic, I., Popovic, N., et al. (2016). Antioxidant enzymes in brain cortex of rats exposed to acute, chronic and combined stress. *Folia Biol. (Krakow).* 64 (3), 189–195. doi:10.3409/fb64_3.189

Porsolt, R. D., Bertin, A., and Jalfre, M. (1977). Behavioral despair in mice: a primary screening test for antidepressants. *Arch. Int. Pharmacodyn. Ther.* 229 (2), 327–336.

Rex, A., Voigt, J.-P., Gustedt, C., Beckett, S., and Fink, H. (2004). Anxiolytic-like profile in Wistar, but not Sprague–Dawley rats in the social interaction test. *Psychopharmacology* 177 (1), 23–34. doi:10.1007/s00213-004-1914-7

Samad, N., Rao, T., Rehman, M. H. U., Bhatti, S. A., and Imran, I. (2021). Inhibitory effects of selenium on arsenic-induced anxiety-/depression-like behavior and memory impairment. *Biol. Trace Elem. Res.* 200, 689–698. doi:10.1007/s12011-021-02679-1

Song, M. K., Lee, J. H., and Kim, Y.-J. (2021). Effect of chronic handling and social isolation on emotion and cognition in adolescent rats. *Physiology Behav.* 237, 113440. doi:10.1016/j.physbeh.2021.113440

Stanisavljevic, A., Peric, I., Pantelic, M., and Filipovic, D. M. (2017). Olanzapine alleviates oxidative stress in the liver of socially isolated rats. *Can. J. physiology Pharmacol.* 95 (6), 634–640. doi:10.1139/cjpp-2016-0598

Stanisławska, M., Szkup-Jabłońska, M., Jurczak, A., Wieder-Huszla, S., Samochowiec, A., Jasiewicz, A., et al. (2014). The severity of depressive symptoms vs serum Mg and Zn levels in postmenopausal women. *Biol. trace Elem. Res.* 157, 30–35. doi:10.1007/s12011-013-9866-6

Stowie, A. C., and Glass, J. D. (2015). Longitudinal study of changes in daily activity rhythms over the lifespan in individual male and female C57BL/6J mice. *J. Biol. Rhythms* 30 (6), 563–568. doi:10.1177/0748730415598023

Takeda, A., Tamano, H., Kan, F., Itoh, H., and Oku, N. (2007). Anxiety-like behavior of young rats after 2-week zinc deprivation. *Behav. Brain Res.* 177 (1), 1–6. doi:10.1016/j.bbr.2006.11.023

Tower, S. S. (2010). Arthroprosthetic cobaltism: neurological and cardiac manifestations in two patients with metal-on-metal arthroplasty: a case report. *Jbjs* 92 (17), 2847–2851. doi:10.2106/JBJS.J.00125

Van der Borght, K., Wallinga, A. E., Luiten, P. G. M., Eggen, B. J. L., and Van der Zee, E. A. (2005). Morris water maze learning in two rat strains increases the expression of the polysialylated form of the neural cell adhesion molecule in the dentate gyrus but has No effect on hippocampal neurogenesis. *Behav. Neurosci.* 119, 926–932. doi:10.1037/0735-7044.119.4.926

Wang, B., Wu, Q., Lei, L., Sun, H., Michael, N., Zhang, X., et al. (2019). Long-term social isolation inhibits autophagy activation, induces postsynaptic dysfunctions and impairs spatial memory. *Exp. Neurol.* 311, 213–224. doi:10.1016/j.expneurol.2018.09.009

Watanabe, M., Tamano, H., Kikuchi, T., and Takeda, A. (2010). Susceptibility to stress in young rats after 2-week zinc deprivation. *Neurochem. Int.* 56 (3), 410–416. doi:10.1016/j.neuint.2009.11.014

Weiss, I. C., Di Iorio, L., Feldon, J., and Domeney, A. M. (2000). Strain differences in the isolation-induced effects on prepulse inhibition of the acoustic startle response and on locomotor activity. *Behav. Neurosci.* 114, 364–373. doi:10.1037/0735-7044.114.2.364

Wilson, R. S., Krueger, K. R., Arnold, S. E., Schneider, J. A., Kelly, J. F., Barnes, L. L., et al. (2007). Loneliness and risk of Alzheimer disease. *Archives general psychiatry* 64 (2), 234–240. doi:10.1001/archpsyc.64.2.234

Xu, L., Zhang, S., Chen, W., Yan, L., Chen, Y., Wen, H., et al. (2020). Trace elements differences in the depression sensitive and resilient rat models. *Biochem. Biophysical Res. Commun.* 529 (2), 204–209. doi:10.1016/j.bbrc.2020.05.228

Zamudio, S., Fregoso, T., Miranda, A., De La Cruz, F., and Flores, G. (2005). Strain differences of dopamine receptor levels and dopamine related behaviors in rats. *Brain Res. Bull.* 65 (4), 339–347. doi:10.1016/j.brainresbull.2005.01.009

frontiers | Frontiers in Pharmacology

TYPE Brief Research Report
PUBLISHED 16 April 2024
DOI 10.3389/fphar.2024.1365151

OPEN ACCESS

EDITED BY
Patricia Rijo,
Lusofona University, Portugal

REVIEWED BY
Srinivasa Rao Sirasanagandla,
Sultan Qaboos University, Oman
Roberta Okamoto,
São Paulo State University, Brazil

*CORRESPONDENCE
Amy L. Inselman,
amy.inselman@fda.hhs.gov

†PRESENT ADDRESS
Sybil Swift, Scientific and Regulatory Affairs, CBD Industries, LLC, Charlotte, NC, United States

‡Gemma Kuijpers, Retired, Laurel, MD, United States

RECEIVED 03 January 2024
ACCEPTED 01 April 2024
PUBLISHED 16 April 2024

CITATION
Inselman AL, Masters EA, Moore JN, Agarwal R, Gassman A, Kuijpers G, Beger RD, Delclos KB, Swift S, Camacho LD, Vanlandingham MM, Sloper D, Nakamura N, Gamboa da Costa G, Woodling K, Bryant M, Trbojevich R, Wu Q, McLellen F and Christner D (2024), The effect of black cohosh extract and risedronate coadministration on bone health in an ovariectomized rat model. *Front. Pharmacol.* 15:1365151. doi: 10.3389/fphar.2024.1365151

The effect of black cohosh extract and risedronate coadministration on bone health in an ovariectomized rat model

Amy L. Inselman[1]*, Elysia A. Masters[1], Jalina N. Moore[1], Rajiv Agarwal[2], Audrey Gassman[3], Gemma Kuijpers[3‡], Richard D. Beger[1], Kenneth B. Delclos[4], Sybil Swift[5†], Luísa Camacho[4], Michelle M. Vanlandingham[4], Daniel Sloper[1], Noriko Nakamura[1], Gonçalo Gamboa da Costa[6], Kellie Woodling[4], Matthew Bryant[7], Raul Trbojevich[7], Qiangen Wu[4], Florence McLellen[7] and Donna Christner[2]

[1]Division of Systems Biology, National Center for Toxicological Research, U.S. Food and Drug Administration, Jefferson, AR, United States, [2]Office of New Drug Products, Office of Pharmaceutical Quality, Center for Drug Evaluation and Research, U.S. Food and Drug Administration, Silver Spring, MD, United States, [3]Division of Urology, Obstetrics and Gynecology, Center for Drug Evaluation and Research, U.S. Food and Drug Administration, Silver Spring, MD, United States, [4]Division of Biochemical Toxicology, National Center for Toxicological Research, U.S. Food and Drug Administration, Jefferson, AR, United States, [5]Office of Dietary Supplement Program, Center for Food Safety and Nutrition, U.S. Food and Drug Administration, College Park, MD, United States, [6]Office of the Center Director, National Center for Toxicological Research, U.S. Food and Drug Administration, Jefferson, AR, United States, [7]Office of Scientific Coordination, National Center for Toxicological Research, U.S. Food and Drug Administration, Jefferson, AR, United States

Preparations of black cohosh extract are sold as dietary supplements marketed to relieve the vasomotor symptoms of menopause, and some studies suggest it may protect against postmenopausal bone loss. Postmenopausal women are also frequently prescribed bisphosphonates, such as risedronate, to prevent osteoporotic bone loss. However, the pharmacodynamic interactions between these compounds when taken together is not known. To investigate possible interactions, 6-month-old, female Sprague-Dawley rats underwent bilateral ovariectomy or sham surgery and were treated for 24 weeks with either vehicle, ethinyl estradiol, risedronate, black cohosh extract or coadministration of risedronate and black cohosh extract, at low or high doses. Bone mineral density (BMD) of the femur, tibia, and lumbar vertebrae was then measured by dual-energy X-ray absorptiometry (DEXA) at weeks 0, 8, 16, and 24. A high dose of risedronate significantly increased BMD of the femur and vertebrae, while black cohosh extract had no significant effect on BMD individually and minimal effects upon coadministration with risedronate. Under these experimental conditions, black cohosh extract alone had no effect on BMD, nor did it negatively impact the BMD-enhancing properties of risedronate.

KEYWORDS

black cohosh, risedronate, bone mineral density, dietary supplements, bisphosphonates, postmenopausal osteoporosis

1 Introduction

Dietary supplements are often viewed as a safe alternative for the prevention and treatment of disease, frequently leading to their usage being under-reported to physicians. Combining dietary supplements with prescription medications, however, may alter the efficacy, and even safety, of a medication. The present study was designed to evaluate the potential pharmacodynamic interactions of black cohosh extract, a dietary supplement marketed to relieve the vasomotor symptoms of menopause, and the FDA-approved osteoporosis drug risedronate, prescribed to post-menopausal women to improve bone health.

Black cohosh extract is made from the roots and rhizomes of *Actaea racemosa* L. (synonym *Cimicifuga racemosa* (L.) Nutt), a perennial plant native to North America (Betz et al., 2009). Dietary supplements containing black cohosh extract are available in a variety of forms (dried extracts, liquid extracts, dried whole herb) and vary widely in their chemical composition, with some standardized on the ratio of herbal drug to native extract and others to total triterpene glycoside content (National Institutes of Health, 2023). While there are no data available on the specific number of individuals who take black cohosh extracts, it was the 20th ranked top-selling herbal supplement in 2021 (Smith et al., 2022). Black cohosh has a long history of use for women's reproductive health (Foster, 1999), with numerous clinical studies investigating whether it can alleviate the vasomotor symptoms of menopause (Nappi et al., 2005; Osmers et al., 2005; Newton et al., 2006; Wuttke et al., 2006; Bai et al., 2007; Geller et al., 2009; Leach and Moore, 2012; Franco et al., 2016). While some studies indicated a positive effect (lessening of symptoms), others indicated worsening of symptoms or shown no benefit over placebo. The inconsistent reports on the efficacy of black cohosh products may be due to the variability of the test article used, as few include characterization or standardization (Swanson, 2002). Adulteration of black cohosh products with related species of *Actaea* has also been documented (Foster, 2013).

In addition to providing relief from the vasomotor symptoms of menopause, extracts of black cohosh have also been reported to protect against postmenopausal bone loss. Qui and others demonstrated that 25-acetylcimigenol xylopyranoside (ACCX), a component isolated from black cohosh, inhibited receptor activator of nuclear factor kappa B ligand (RANKL)-induced osteoclast differentiation of mouse bone marrow macrophages (Qiu et al., 2007). Black cohosh extract has also been associated with decreased bone loss in the ovariectomized (OVX) rat model, as well as increased bone mineral density (BMD) and enhanced callus formation in a OVX rat tibia fracture healing model (Nisslein and Freudenstein, 2003; Kolios et al., 2010; Seidlová-Wuttke et al., 2012).

Risedronate sodium is one of several bisphosphonates approved by the U.S. FDA for the treatment and prevention of osteoporosis in postmenopausal women and in 2012 was the leading branded oral bisphosphonate on the market in the U.S. (U.S. Securities and Exchange Commission, 2012). Bisphosphonates prevent bone loss by binding hydroxyapatite and inhibiting the bone resorbing action of osteoclasts through inhibition of RANKL (Yasuda et al., 1998). Nitrogen-containing bisphosphonates, such as risedronate, also block osteoclast activity by inhibiting the enzyme farnesyl pyrophosphate synthase (FPPS) (Kavanagh et al., 2006; Russell, 2011). It is possible that black cohosh extract and risedronate both protect against bone loss; risedronate via binding hydroxyapatite and inhibition of FPPS, and risedronate and black cohosh extract via inhibition of RANKL-mediated osteoclast differentiation. However, it is not known whether there are pharmacodynamic interactions when taken together that could impact the efficacy of FDA-approved bisphosphonates.

Here we investigated the individual and combined effects of black cohosh extract and risedronate at high and low doses, as well as ethinyl estradiol as a positive control, on BMD in the OVX rat, an established model of postmenopausal osteoporosis (Kalu, 1991). Risedronate treatment increased BMD compared to the OVX-vehicle controls, while black cohosh extract had no effect on BMD when administered individually. When co-administered with risedronate, black cohosh extract had some positive effects; however, BMD increases were not significantly different from animals administered risedronate alone. Taken together, the results suggest that black cohosh extract did not inhibit the effectiveness of risedronate.

2 Materials and methods

2.1 Test compounds

Risedronate sodium (Cat. No. SML0650), ethinyl estradiol (Cat No. E4876) and carboxymethylcellulose (CMC; Cat. No. C4888) were purchased from Sigma-Aldrich (St. Louis, MO). A standardized black cohosh dry extract (Cat. No. 398014; USA sourced, water/ethanol extraction; total triterpene glycoside content, 2.7%) was obtained from Euromed USA, Inc. (Presto, PA) and was considered a representative market sample. Detailed methods for test compound characterization/verification and dose certification are provided in the Supplementary Data S1.

2.2 Animals and experimental design

Animal procedures were approved by the NCTR Institutional Animal Care and Use Committee and followed the guidelines set forth in the Care and Use of Laboratory Animals (National Research Council, 2011). Animal rooms were maintained at 23°C ± 3°C with a relative humidity of 50% ± 20% and a 12-h light/dark cycle. Animals were housed in solid-bottom polysulfone cages with microisolator tops. Millipore-filtered tap water was provided in glass bottles with silicone stoppers. Animals were maintained on 5K96 verified casein diet 10 IF (LabDiet, St. Louis, MO), to minimize background exposure to phytoestrogens; detailed analysis of isoflavone measurements are provided in the Supplementary Data S1. Food and water were provided *ad libitum*.

A total of 230 virgin female Sprague-Dawley rats were purchased from Harlan Industries (Indianapolis, IN) and delivered at approximately 3 months of age. At 6 months of age, animals were assigned to treatment groups such that the mean initial weights were comparable and underwent bilateral ovariectomy or a sham surgery. In brief, surgery was conducted under isoflurane anesthesia. Bilateral dorsal incisions were made to allow visualization of the viscera. The ovaries were located, removed by cauterization, and incisions closed

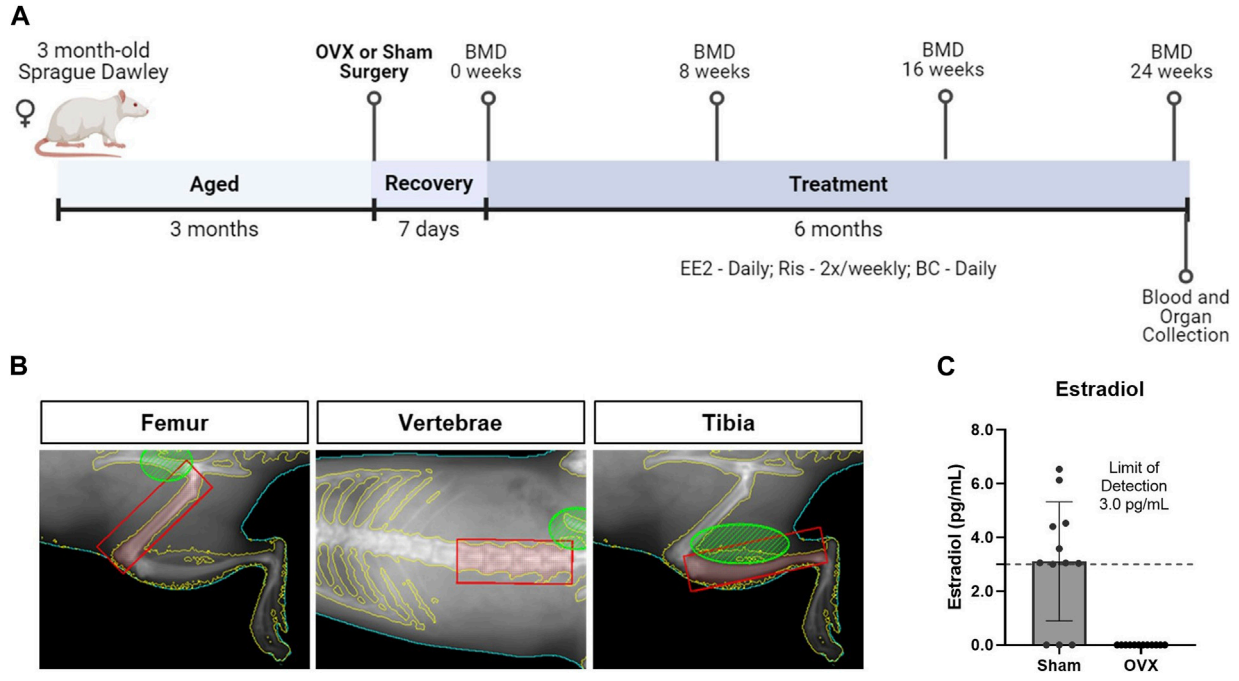

FIGURE 1
Study design to evaluate changes in bone quality in the ovariectomized rat, an established model of postmenopausal osteoporosis. **(A)** At 6 months of age, female Sprague Dawley rats underwent sham or bilateral ovariectomy (OVX). Following a 7-day recovery period, animals were treated with vehicle or test articles for 24 weeks. **(B)** Representative DEXA images show regions of interest in shaded red boxes used to quantify bone mineral density (BMD) for the femur, lumbar vertebrae (L1-L4), and tibia. All images depicted are from the same rat. **(C)** Estradiol levels, measured by ELISA, were significantly greater in sham animals compared to OVX-vehicle animals ($p < 0.0001$, n = 12). The lower limit of detection in the assay was 3 pg/mL (dashed line).

with wound clips. In the sham control group, surgery was conducted as described, but ovaries were left intact. Animals recovered for 7 days before initial BMD assessment; dosing began the following day and continued for 24 weeks (Figure 1A).

Animals were euthanized at 1 year of age by over-exposure to carbon dioxide followed by exsanguination. Liver, kidney (paired), and uterine weights were obtained. OVX animals were examined to verify removal of ovarian tissue; three animals (n = 2 OVX-vehicle; n = 1 low dose black cohosh extract/high dose risedronate) were excluded from analysis, due to incomplete ovariectomy.

Four animals died during the study or were euthanized before the scheduled euthanasia date due to health concerns. One of the animals had a nephroblastoma, one had focal caseous pleuropneumonia due to a gavage accident, and the cause of morbidity in the other two animals could not be determined.

2.3 Dose selection and treatment groups

There was a total of 12 treatment groups with 18 animals assigned to each group (Table 1).

Risedronate was solubilized in Millipore®-filtered water and the animals were dosed twice weekly (Monday and Thursday) by subcutaneous injection at 1.5 or 5 μg/kg bw, modeling previous bone pharmacology studies (Li et al., 1999; Yao et al., 2007; Cheng et al., 2009; Uyar et al., 2009; Shahnazari et al., 2010).

Dry black cohosh extract was mixed with 0.5% aqueous CMC. Animals were dosed daily by gavage at 10 or 100 mg/kg bw using an automated Hamilton Microlab® pump (Hamilton Co., Reno, NV). Black cohosh dose selection was based on literature reports demonstrating a positive effect on bone with no reported toxicity (Seidlová-Wuttke et al., 2003a; Kolios et al., 2010). Additionally, the 10 mg/kg bw dose is similar to the upper end of the suggested human dose for treatment of menopausal symptoms (20–40 mg twice per day) (Reagan-Shaw et al., 2008).

Ethinyl estradiol, was solubilized in 0.3% aqueous CMC and administered daily by gavage at 2.5 or 15 μg/kg bw. Initially, doses of 10 and 100 μg/kg bw were selected, based on literature reports demonstrating that oral concentrations of 30 μg/kg bw reversed OVX-induced bone loss, with a dose as high as 100 μg/kg bw showing no evidence of toxicity (Ke et al., 1997; Picherit et al., 2000; Coelingh Bennink et al., 2008). However, after problems with solubility and toxicity (i.e., weight loss) concentrations were adjusted downward after three or four weeks of treatment.

2.4 Dual-energy X-ray absorptiometry

BMD of the femur, tibia, and L1-L4 lumbar vertebrae were measured by DEXA at weeks 0 (one day prior to start of dosing), 8, 16, and 24 (one day prior to euthanasia). The DEXA instrument (PIXImus, Lunar GE Medical Systems, Madison, WI) was calibrated using the manufacturer's phantom mouse. All animals were anesthetized with isoflurane and placed on the DEXA tray in the ventral position with the limbs held splayed. Each animal was positioned to scan the right leg, then positioned to scan the spine

TABLE 1 Treatment groups and dosing.

	Treatment group	Compound(s) administered	Concentration	Route and Frequency of administration
1	Sham	CMC	0.5%	Oral Gavage; daily
2	Vehicle (OVX)	CMC	0.5%	Oral Gavage; daily
3	Lo EE2	Ethinyl Estradiol	2.5 μg/kg bw	Oral Gavage; daily
4	Hi EE2	Ethinyl Estradiol	15.0 μg/kg bw	Oral Gavage; daily
5	Lo Ris	Risedronate	1.5 μg/kg bw	Subcutaneous; biw
6	Hi Ris	Risedronate	5.0 μg/kg bw	Subcutaneous; biw
7	Lo BC	Black Cohosh Extract	10 mg/kg bw	Oral Gavage; daily
8	Hi BC	Black Cohosh Extract	100 mg/kg bw	Oral Gavage; daily
9	Lo BC + Lo Ris	Black Cohosh Extract	10 mg/kg bw	Oral Gavage; daily
		Risedronate	1.5 μg/kg bw	Subcutaneous; biw
10	Lo BC + Hi Ris	Black Cohosh Extract	10 mg/kg bw	Oral Gavage; daily
		Risedronate	5.0 μg/kg bw	Subcutaneous; biw
11	Hi BC + Lo Ris	Black Cohosh Extract	100 mg/kg bw	Oral Gavage; daily
		Risedronate	1.5 μg/kg bw	Subcutaneous; biw
12	Hi BC + Hi Ris	Black Cohosh Extract	100 mg/kg bw	Oral Gavage; daily
		Risedronate	5.0 μg/kg bw	Subcutaneous; biw

CMC, carboxymethylcellulose.
biw = twice a week.

area. Each region was scanned twice with repositioning of the animal between scans. The software's inclusion and exclusion areas were used to outline the femur, tibia, and lumbar vertebrae regions of interest (ROI) (Figure 1B). BMD data for each ROI were analyzed by averaging the technical replicates. To limit repeated isoflurane exposure, only a subset of animals were subjected to DEXA scanning at weeks 8 and 16 (n = 10/group); all animals were scanned at weeks 0 and 24.

2.5 ELISA assays

For measurement of estradiol levels and serum bone markers, blood was collected at euthanasia by cardiac puncture into Vacutainer® tubes (BD, Franklin Lakes, NJ). Samples were centrifuged at 3,000 *x g* for 10 min at room temperature; the serum was aliquoted and stored at −80°C until use.

Serum estradiol was measured using a mouse/rat estradiol ELISA kit (Cat. No. ES180S-100) from Calbiotech (Spring Valley, CA) per the manufacturer's instructions. Samples were read on a Molecular Devices Spectramax M2 spectrophotometer (Sunnyvale, CA) and analyzed with Softmax Pro 5 software. The lower limit of detection (LOD) for estradiol was 3 pg/mL; samples below the LOD were set to zero for analysis.

2.6 Statistical analysis

Differences between groups were analyzed using GraphPad Prism Version 6.0 (GraphPad Software, Inc., LaJolla, CA). Differences between multiple treatment groups at single timepoints (body weight, organ weights, and BMD) were evaluated using one-way ANOVA followed by Sidak's post-hoc test for multiple comparisons; comparisons included vehicle vs. all other groups, low risedronate treatment vs. low/high black cohosh extract + low risedronate treatment and high risedronate treatment vs. low/high black cohosh extract + high risedronate treatment. Difference in estradiol levels were evaluated using unpaired t-tests. p values less than 0.05 were considered significant. Data are presented as means ± standard deviation (SD), unless noted.

3 Results

3.1 Estradiol levels

Serum estradiol levels were quantified in a subset of animals from the sham and OVX-vehicle groups. Three of the twelve sham animals had estradiol levels below the LOD, while all twelve OVX-vehicle animals had undetectable levels (Figure 1C). The average estradiol concentration of the sham animals was significantly greater than the OVX-vehicle-treated group, which were 3.11 and 0 pg/mL, respectively.

3.2 Body and organ weights

Body weights of animals treated with risedronate or black cohosh extract, alone or with coadministration, did not

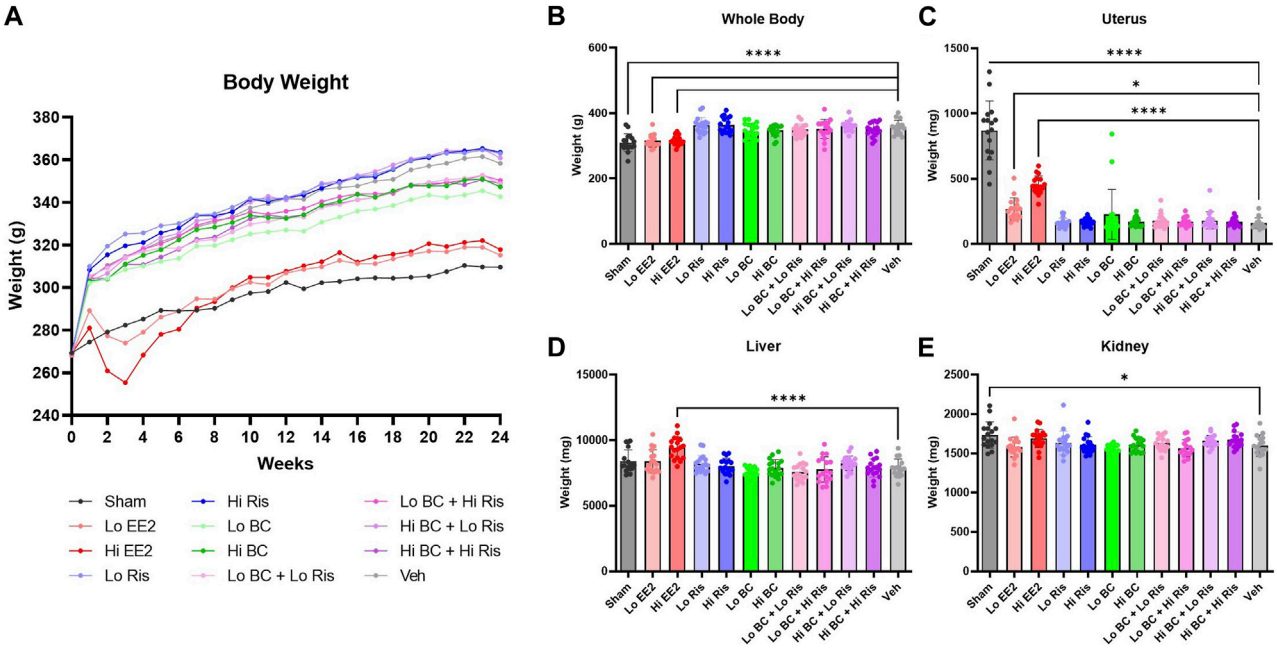

FIGURE 2
Longitudinal body, terminal body, and absolute organ weight measurements. **(A)** Mean weekly body weight measurements are plotted for each treatment group. Due to significant reductions in body weight, doses of EE2 were adjusted downward to 2.5 and 15 μg/kg body weight per day after three or four weeks of treatment for load one and load two animals. Animals in loads three and four only received the lowered doses. **(B)** Sham surgery and EE2 treatment groups had significantly lower body weight measurements at week 24, while all risedronate and black cohosh extract treatment groups showed no significant differences compared to OVX-vehicle control. **(C–E)** Uterine, liver and kidney weights at week 24 showed no significant differences associated with risedronate or black cohosh extract treatments compared to OVX-vehicle. Data plotted as mean ± SD. Significance was evaluated by one-way ANOVA with Sidak's post-hoc for multiple comparisons. * Indicates difference vs. OVX-vehicle control; *$p < 0.05$, **$p < 0.01$, ***$p < 0.001$, ****$p < 0.0001$; n = 16–18. EE2 = ethinyl estradiol; BC = black cohosh extract; Ris = risedronate sodium; Veh = OVX-vehicle control.

significantly differ from OVX-vehicle controls. Estradiol and sham surgery groups had lower mean body weights than OVX-vehicle controls from week 0 through 24 (Figure 2A), with the difference reaching statistical significance at week 24 (Figure 2B).

Ovariectomy decreased uterine weights in all groups relative to the sham controls (Figure 2C). However, a dose-related increase in uterine weight was observed in the low and high ethinyl estradiol treatment groups (1.7 and 2.8-fold increase vs. OVX-vehicle, respectively). High ethinyl estradiol treatment and sham surgery groups also showed increased liver and kidney weights, respectively, at the time of sacrifice compared to OVX-vehicle controls (Figures 2D, E).

3.3 BMD

Femur, vertebrae, and tibia BMD were measured at 0, 8, 16 and 24 weeks. Mean BMD for ethinyl estradiol, risedronate, black cohosh extract and coadministration treatment groups were plotted separately to visualize trends over time (Figure 3A). Longitudinal BMD measurements revealed similar trends for femur and vertebrae BMD measurements across treatment groups, while tibia BMD trends were less apparent. In the femur and vertebrae, BMD of ethinyl estradiol (red) and risedronate (blue) groups trend higher than OVX-vehicle control but remain lower than sham surgery from 0 to 24 weeks. In contrast, treatment with black cohosh extract (green) showed minimal changes in BMD compared to OVX-vehicle control in the femur and vertebrae. Coadministration of risedronate and black cohosh extract (purple) produced modest changes in BMD of all ROIs compared to risedronate treatment alone. Net changes in tibial BMD were minimal across all control and treatment groups.

BMD at week 24 was normalized to baseline (week 0) for each animal and plotted for each ROI (Figures 3B–D). Mean BMD measurements of the femur, vertebrae, and tibia at weeks 0 and 24 are shown in Supplementary Tables S2-S4. Statistical analysis confirmed that sham surgery femurs had significantly higher BMD compared to OVX-vehicle (Figure 3B). In all high-dose risedronate treatment groups, individually and when co-administered with black cohosh extract, the BMD of the femur at week 24 was significantly greater compared to OVX-vehicle control. Black cohosh extract alone had no statistically significant effect on femur BMD, as compared to OVX-vehicle control. Interestingly, low risedronate when co-administered with high-dose black cohosh extract showed a significant increase in femur BMD as compared to OVX-vehicle control, while low risedronate treatment alone had no significant effect. However, femur BMD in this high black cohosh extract/low risedronate group was not significantly different than low-dose risedronate treatment alone ($p = 0.6281$).

Vertebral BMD followed similar trends as the femur (Figure 3C); however, the magnitude of changes in BMD were the largest among the three ROIs. The sham surgery group showed the highest mean vertebral BMD at week 24 and was 1.3-fold greater than OVX-vehicle control. Both ethinyl estradiol dose groups also had significantly higher vertebral

10.3389/fphar.2024.1365151

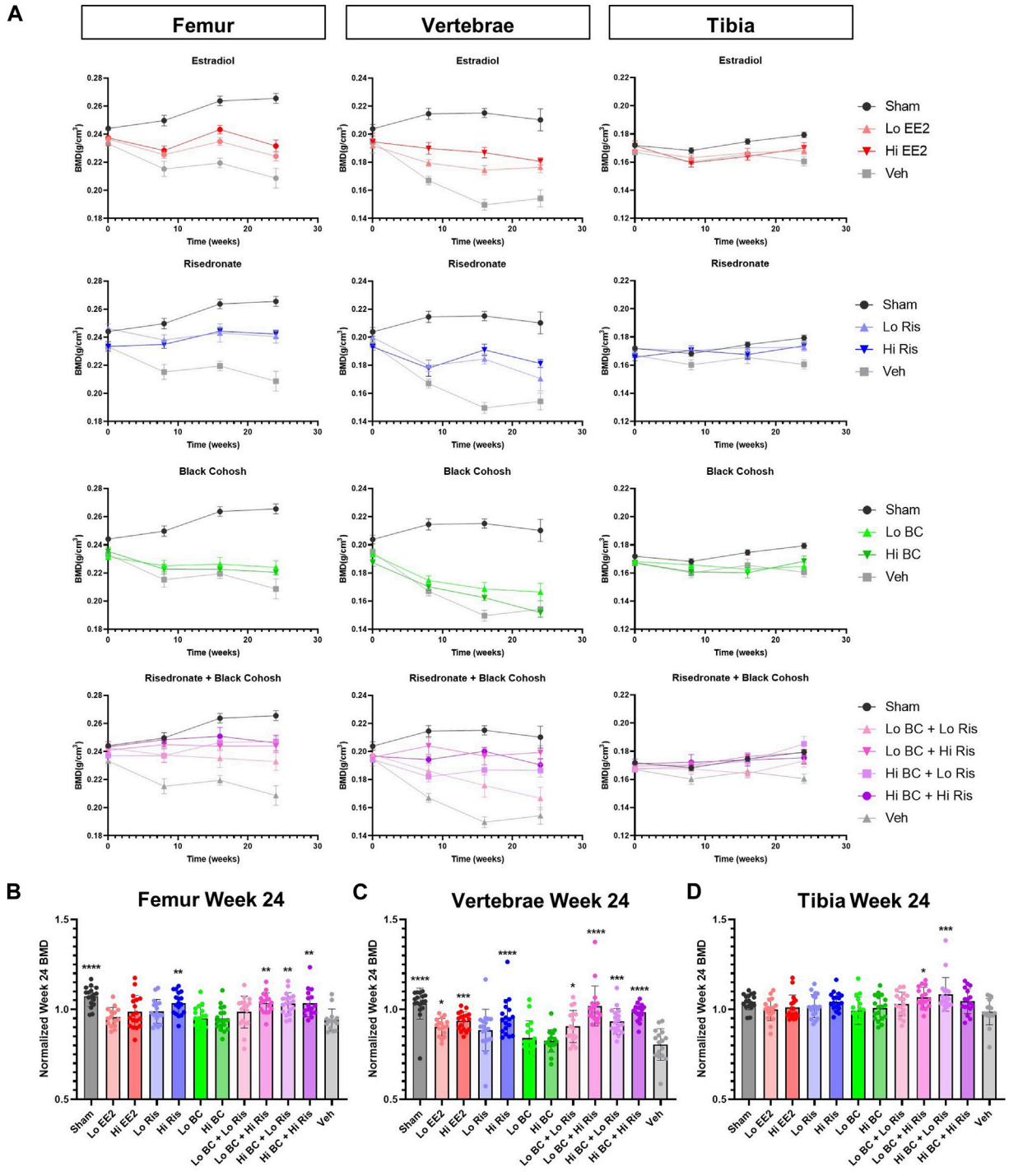

FIGURE 3
BMD of femur, vertebrae and tibia following treatment with black cohosh extract and/or risedronate. **(A)** Longitudinal measurement of BMD at 0, 8, 16, and 24 weeks of treatment is plotted to show the effects of EE2, risedronate, black cohosh extract and risedronate + black cohosh extract combination treatments, with sham and vehicle data shown on each graph. Data plotted as mean ± SEM; n = 9–10. **(B–D)** BMD at week 24 was normalized to week 0 for each animal. After normalization, significant differences in BMD were associated with Hi EE2, Hi Ris and combined BC + Ris treatments, as compared to vehicle control. No statistically significant differences were observed between Lo Ris vs. Lo/Hi BC + Lo Ris or between Hi Ris vs. Lo/Hi BC + Hi Ris groups. Data plotted as mean ± SD. Significance was evaluated by one-way ANOVA with Sidak's post-hoc for multiple comparisons. * Indicates difference vs. OVX-vehicle control; *$p < 0.05$, **$p < 0.01$, ***$p < 0.001$, ****$p < 0.0001$; n = 14–18. EE2 = ethinyl estradiol; BC = black cohosh extract; Ris = risedronate sodium; Veh = OVX-vehicle control.

BMDs at week 24 compared to the OVX-vehicle control. The vertebral BMD of the high-dose risedronate group was significantly larger (1.2-fold greater) than the OVX-vehicle control, whereas the low-dose risedronate treatment was statistically similar. There was no significant effect on vertebral BMD in the low or high-dose black cohosh extract groups. Low risedronate co-administered with either low or high doses of black cohosh extract led to statistically significant increases in vertebral BMD. Lastly, high-dose risedronate co-administered with low or high doses of black cohosh extract also showed significant increases in vertebral BMD, as compared to OVX-vehicle controls; however, the coadministration of black cohosh extract and risedronate did not significantly increase vertebral BMD compared to corresponding doses of risedronate alone (Lo BC + Lo Ris vs. Lo Ris, p = >0.9999; Hi BC + Lo Ris vs. Lo Ris, p = 0.7238; Lo BC + Hi Ris vs. Hi Ris, p = 0.2805; Hi BC + Hi Ris vs. Hi Ris, p = 0.9919).

Finally, normalized week 24 tibia BMD measurements showed very few statistically significant differences (Figure 3D). In the tibia, only low black cohosh extract/high risedronate and high black cohosh extract/low risedronate groups had statistically greater BMDs, as compared to OVX-vehicle control. Again, tibial BMD values in the coadministration groups were not statistically different from the corresponding doses of risedronate alone (Lo BC + Hi Ris vs. Hi Ris, p = 0.9945; Hi BC + Lo Ris vs. Lo Ris, p = 0.0588). Notably, the BMD in sham surgery tibias was not significantly different from OVX-vehicle controls (p = 0.2763), despite being the highest of all groups at week 24.

Changes in serum bone markers, osteocalcin, bone-specific alkaline phosphatase and C-terminal telopeptide, were also measured as markers for bone metabolism at week 24. Overall, there were no statistically significant differences between control and treatment groups (Supplementary Table S5, Figure S1).

4 Discussion

To ease the symptoms of menopause, many women turn to dietary supplements with little consideration of the possible unintended effects on the efficacy of their prescription medications. Here we investigated whether an extract of black cohosh had any pharmacodynamic interactions with risedronate effecting postmenopausal bone loss in the OVX rat model.

Ovariectomy decreased serum estradiol concentration, uterine weight (−81.8%), and BMD of the right femur (−6.1%), lumbar vertebrae (−19.5%) and right tibia (−1.4%) at 24 weeks, as expected. Ethinyl estradiol was included as a positive reference control to demonstrate suitability of the OVX rat model. Both low (2.5 μg/kg bw) and high doses (15 μg/kg bw) were tested; the low dose was expected to have minimal effects on bone loss and the higher dose was expected to normalize bone parameters. While the high dose did not completely normalize all biomarkers to the levels in sham animals, ethinyl estradiol treatment raised BMD levels over that of OVX-vehicle control animals in the femur, lumbar vertebrae, and tibia. Increases in the lumbar vertebrae were statistically significant. Together the data confirmed bone loss related to reductions in estrogen and appropriateness and sensitivity of the model for assessing interactions of black cohosh extract with risedronate.

Risedronate was selected for evaluation with black cohosh extract due to its prevalent use to treat osteoporosis in postmenopausal women and its demonstrated effectiveness in increasing BMD in OVX rats (Li et al., 1999; Yao et al., 2007; Cheng et al., 2009; Uyar et al., 2009; Shahnazari et al., 2010). Despite variations in dosing, previous studies were consistent in finding increased BMD, trabecular bone thickness, and volume of cortical bone area with risedronate treatment. In this study, both the low and high doses of risedronate had positive effects on BMD of the femur and the lumbar vertebrae when compared to OVX-vehicle control. As with ethinyl estradiol, BMD of the tibia was not significantly affected by risedronate treatment when compared to the OVX-vehicle group. Neither dose of risedronate influenced body weight or uterine weight, aside from the effects of ovariectomy, as expected (Erben et al., 2002).

In contrast to the positive effects observed on BMD in response to risedronate, black cohosh extract had no effect when given alone at high or low doses. After 24 weeks of treatment, BMD of the femur, lumbar vertebrae and tibia were statistically similar to OVX-vehicle control animals. Additionally, there were no differences in serum bone marker levels upon treatment with black cohosh extract. The lack of an impact on bone health upon treatment with black cohosh extract contrasts with others, which have previously reported positive associations with black cohosh extract on BMD, urine markers of bone turnover and bone morphometry (Seidlová-Wuttke et al., 2003b; Nisslein and Freudenstein, 2003; Kolios et al., 2010).

Chronic black cohosh extract administration in OVX rats also had no effect on body or uterine weights, which is consistent with previous reports demonstrating the lack of estrogenic effects of black cohosh extract. This finding was supportive of those in recent reports by Seidlová-Wuttke et al. and the National Toxicology Program, who also reported no effect of black cohosh extract on uterine weights or pubertal development in rats and mice (Seidlová-Wuttke et al., 2009; Mercado-Feliciano et al., 2012; Seidlová-Wuttke et al., 2013).

Importantly, when co-administered with risedronate, black cohosh extract did not counteract the BMD enhancing properties of risedronate. Increases in BMD were observed with certain dosage combinations but were dependent on the bone type measured. In the vertebrae, coadministration of black cohosh extract and risedronate, irrespective of the dose, had positive effects on BMD. Interestingly, the addition of a high dose of black cohosh extract with the low dose of risedronate produced a significant increase in BMD compared to vehicle in the femur and tibia, while BMD of animals administered a low dose of risedronate alone was not significantly different from vehicle. This modest increase may suggest that black cohosh extract enhances the bone-protective effects of low doses of risedronate. However, this difference was not statistically significant when comparing the coadministration groups with the same dose of risedronate treatment alone.

A consistent finding of this study was the varying patterns of BMD response across specific bones measured. Specifically, we found the greatest effect of OVX-induced bone loss and treatment-related recovery in the vertebrae, then the femur, and minimal changes in the tibia. It is known that postmenopausal bone loss in humans and in the OVX rat model, is primarily attributed to resorption of trabecular bone rather than cortical bone (Laib et al., 2001; Shin et al., 2012). Therefore, bones with higher composition of trabecular bone, such as the vertebrae, will exhibit increased rates of bone remodeling compared to those composed of more cortical

bone, such as the diaphysis of long bones (Thompson et al., 1995; Shin et al., 2012). In addition to composition, bone size and mechanical loading will influence rates of remodeling, which explains the larger changes observed in the femur versus tibial BMD.

While changes in bone strength (i.e., mass, stiffness) or quality cannot be ruled out, as they were not evaluated in this study, BMD is generally regarded as a good predictor of fracture risk and bone health (Uyar et al., 2009). Further, DEXA scanning and measurement of serum biomarkers are common, non-invasive and clinically relevant analyses for osteoporosis screening in postmenopausal women. It is important to note that, although the rat has been useful for predicting effects in humans, differences in human and rat bone physiology exist, which may limit the translation of the effects observed to postmenopausal women. For example, unlike humans, rats do not develop spontaneous bone fractures in response to declining estrogen levels. Additionally, the bones of rats do not stop growing and lack a well-developed Haversian-based remodeling system that occurs in human cortical bones (Lelovas et al., 2008).

Importantly, due to the lack of characterization and/or standardization for many preparations of black cohosh, the results and conclusions drawn from this study are limited to the specific water/ethanol extract of black cohosh used and the dose regimen described. The extraction method has been shown to play a critical role in the chemical profile and biological activity of black cohosh extract (Jiang et al., 2008). While our study utilized a water/ethanol extract, many of the previous studies in the OVX rat model used an iso-propanolic extract. Comparison of extraction methods have found that the ethanolic and iso-propanolic extracts are quantitatively different in their triterpene glycoside and polyphenolic composition (Jiang et al., 2008) and thus, may explain some of the differences observed in BMD between studies. The age of the animal at ovariectomy may also have affected the observed BMD response upon treatment with black cohosh extract. Ovariectomy in this study was performed when the animals were 6 months of age, opposed to 3 months of age in previous studies (Seidlová-Wuttke et al., 2003b; Nisslein and Freudenstein, 2003; Kolios et al., 2010). Yousefzadeh and others have suggested that for osteoporosis research the preferred age for ovariectomy in rats is 6–9 months old (Yousefzadeh et al., 2020). Animals in this age-range have fewer confounding effects of age-related changes in bone growth.

The present study demonstrates that alone the water/ethanol standardized extract of black cohosh tested did not affect BMD or serum bone biomarker levels in an OVX rat model for osteoporosis. When given in combination with risedronate, black cohosh extract did not negatively impact the positive BMD-enhancing properties of the oral bisphosphonate. While increases in BMD was observed in select combinations and bone regions, the increases were not significantly different than those of risedronate alone. Taken together, there does not appear to be any pharmacodynamic synergistic effects of the FDA-approved drug risedronate and the dietary supplement black cohosh.

Data availability statement

The original contributions presented in the study are included in the article/Supplementary Material, further inquiries can be directed to the corresponding author.

Ethics statement

The animal study was approved by the NCTR Institutional Animal Care and Use Committee. The study was conducted in accordance with the local legislation and institutional requirements.

Author contributions

AI: Conceptualization, Data curation, Formal Analysis, Supervision, Writing–original draft, Writing–review and editing. EM: Data curation, Formal Analysis, Writing–original draft, Writing–review and editing. JM: Formal Analysis, Writing–review and editing. RA: Conceptualization, Writing–review and editing. AG: Conceptualization, Writing–review and editing. GK: Conceptualization, Writing–review and editing. RB: Conceptualization, Writing–review and editing. KD: Conceptualization, Writing–review and editing. SS: Conceptualization, Writing–review and editing. LC: Conceptualization, Investigation, Writing–review and editing. MV: Investigation, Writing–review and editing. DS: Investigation, Writing–review and editing. NN: Investigation, Writing–review and editing. GG: Investigation, Writing–review and editing. KW: Investigation, Writing–review and editing. MB: Investigation, Writing–review and editing. RT: Investigation, Writing–review and editing. QW: Investigation, Writing–review and editing. FM: Investigation, Writing–review and editing. DC: Conceptualization, Writing–review and editing.

Funding

The author(s) declare financial support was received for the research, authorship, and/or publication of this article. This project was supported by the FDA's Chief Scientist Challenge Grants (OCS-challenge) under protocol NCTR E-0758301.

Acknowledgments

The authors would like to acknowledge Dr. Deborah K. Hansen, a retired employee of the NCTR, for her contributions to the study. Dr. Hansen was involved in study design, primary data analysis and drafting of the manuscript. The authors would also like to acknowledge Dr. Ikhlas Khan at the University of Mississippi for his assistance in obtaining the black cohosh test article. In addition, the authors recognize the tremendous support of the NCTR animal care staff, especially Florene Lewis. The authors also acknowledge Andy Matson with the NCTR Diet Preparation Group for his assistance in preparing the dose formulations, Patricia Porter-Gill in the Division of Biochemical Toxicology for her assistance in the DEXA data analysis, and Ralph Patton and Kristie Voris with TPA Inc. for their assistance with measuring estradiol levels. A special thank you to Tom Schmitt and Lisa Pence for their efforts to develop an LCMS assay to measure risedronate and to Robert Felton in the Office of Scientific Coordination for his advice on the statistical analysis.

Conflict of interest

The authors declare that the research was conducted in the absence of any commercial or financial relationships that could be construed as a potential conflict of interest.

Publisher's note

All claims expressed in this article are solely those of the authors and do not necessarily represent those of their affiliated organizations, or those of the publisher, the editors and the reviewers. Any product that may be evaluated in this article, or claim that may be made by its manufacturer, is not guaranteed or endorsed by the publisher.

Supplementary material

The Supplementary Material for this article can be found online at: https://www.frontiersin.org/articles/10.3389/fphar.2024.1365151/full#supplementary-material

References

Bai, W., Henneicke-von Zepelin, H. H., Wang, S., Zheng, S., Liu, J., Zhang, Z., et al. (2007). Efficacy and tolerability of a medicinal product containing an isopropanolic black cohosh extract in Chinese women with menopausal symptoms: a randomized, double blind, parallel-controlled study versus tibolone. *Maturitas* 58 (1), 31–41. doi:10.1016/j.maturitas.2007.04.009

Betz, J. M., Anderson, L., Avigan, M. I., Barnes, J., Farnsworth, N. R., Gerdén, B., et al. (2009). Black cohosh: considerations of safety and benefit. *Nutr. Today* 44 (4), 155–162. doi:10.1097/nt.0b013e3181af63f9

Cheng, Z., Yao, W., Zimmermann, E. A., Busse, C., Ritchie, R. O., and Lane, N. E. (2009). Prolonged treatments with antiresorptive agents and PTH have different effects on bone strength and the degree of mineralization in old estrogen-deficient osteoporotic rats. *J. Bone Min. Res.* 24 (2), 209–220. doi:10.1359/jbmr.81005

Coelingh Bennink, H. J. T., Heegaard, A. M., Visser, M., Holinka, C. F., and Christiansen, C. (2008). Oral bioavailability and bone-sparing effects of estetrol in an osteoporosis model. *Climacteric* 11 (Suppl. 1), 2–14. doi:10.1080/13697130701798692

Erben, R. G., Mosekilde, L., Thomsen, J. S., Weber, K., Stahr, K., Leyshon, A., et al. (2002). Prevention of bone loss in ovariectomized rats by combined treatment with risedronate and 1alpha,25-dihydroxyvitamin D3. *J. Bone Min. Res.* 17 (8), 1498–1511. doi:10.1359/jbmr.2002.17.8.1498

Foster, S. (1999). Black cohosh: a literature review. *HerbalGram* 45, 35–50.

Foster, S. (2013). Exploring the peripatetic maze of black cohosh adulteration: a review of the nomenclature, distribution, chemistry, market status, analytical methods, and safety. *HerbalGram* 98, 32–51.

Franco, O. H., Chowdhury, R., Troup, J., Voortman, T., Kunutsor, S., Kavousi, M., et al. (2016). Use of plant-based therapies and menopausal symptoms: a systematic review and meta-analysis. *JAMA* 315 (23), 2554–2563. doi:10.1001/jama.2016.8012

Geller, S. E., Shulman, L. P., van Breemen, R. B., Banuvar, S., Zhou, Y., Epstein, G., et al. (2009). Safety and efficacy of black cohosh and red clover for the management of vasomotor symptoms: a randomized controlled trial. *Menopause* 16 (6), 1156–1166. doi:10.1097/gme.0b013e3181ace49b

Jiang, B., Reynertson, K. A., Keller, A. C., Einbond, L. S., Bemis, D. L., Weinstein, I. B., et al. (2008). Extraction methods play a critical role in chemical profile and biological activities of black cohosh. *Nat. Prod. Commun.* 3 (9), 1934578X0800300. doi:10.1177/1934578X0800300925

Kalu, D. N. (1991). The ovariectomized rat model of postmenopausal bone loss. *Bone Min.* 15 (3), 175–191. doi:10.1016/0169-6009(91)90124-i

Kavanagh, K. L., Guo, K., Dunford, J. E., Wu, X., Knapp, S., Ebetino, F. H., et al. (2006). The molecular mechanism of nitrogen-containing bisphosphonates as antiosteoporosis drugs. *Proc. Natl. Acad. Sci. U. S. A.* 103 (20), 7829–7834. doi:10.1073/pnas.0601643103

Ke, H. Z., Chen, H. K., Simmons, H. A., Qi, H., Crawford, D. T., Pirie, C. M., et al. (1997). Comparative effects of droloxifene, tamoxifen, and estrogen on bone, serum cholesterol, and uterine histology in the ovariectomized rat model. *Bone* 20 (1), 31–39. doi:10.1016/s8756-3282(96)00313-4

Kolios, L., Schumann, J., Sehmisch, S., Rack, T., Tezval, M., Seidlová-Wuttke, D., et al. (2010). Effects of black cohosh (Cimicifuga racemosa) and estrogen on metaphyseal fracture healing in the early stage of osteoporosis in ovariectomized rats. *Planta Med.* 76 (09), 850–857. doi:10.1055/s-0029-1240798

Laib, A., Kumer, J. L., Majumdar, S., and Lane, N. E. (2001). The temporal changes of trabecular architecture in ovariectomized rats assessed by MicroCT. *Osteoporos. Int.* 12, 936–941. doi:10.1007/s001980170022

Leach, M. J., and Moore, V. (2012). Black cohosh (Cimicifuga spp.) for menopausal symptoms. *Cochrane Database Syst. Rev.* 2012 (9), CD007244. doi:10.1002/14651858.CD007244.pub2

Lelovas, P. P., Xanthos, T. T., Thoma, S. E., Lyritis, G. P., and Dontas, I. A. (2008). The laboratory rat as an animal model for osteoporosis research. *Comp. Med.* 58 (5), 424–430.

Li, Q. N., Liang, N. C., Huang, L. F., Wu, T., Hu, B., and Mo, L. E. (1999). Skeletal effects of constant and terminated use of risedronate on cortical bone in ovariectomized rats. *J. Bone Min. Metab.* 17 (1), 18–22. doi:10.1007/s007740050058

Mercado-Feliciano, M., Cora, M. C., Witt, K. L., Granville, C. A., Hejtmancik, M., Fomby, L., et al. (2012). An ethanolic extract of black cohosh causes hematological changes but not estrogenic effects in female rodents. *Toxicol. Appl. Pharmacol.* 263 (2), 138–147. doi:10.1016/j.taap.2012.05.022

Nappi, R. E., Malavasi, B., Brundu, B., and Facchinetti, F. (2005). Efficacy of Cimicifuga racemosa on climacteric complaints: a randomized study versus low-dose transdermal estradiol. *Gynecol. Endocrinol.* 20 (1), 30–35. doi:10.1080/09513590400020922

National Institues of Health (2023). Black cohosh - fact sheet for health professionals. Available at: https://ods.od.nih.gov/factsheets/BlackCohosh-HealthProfessional/#en7 (Accessed August 30, 2023).

National Research Council (2011). *Guide for the care and use of laboratory animals*. eighth edition. Washington D.C.: National Academies Press.

Newton, K. M., Reed, S. D., LaCroix, A. Z., Grothaus, L. C., Ehrlich, K., and Guiltinan, J. (2006). Treatment of vasomotor symptoms of menopause with black cohosh, multibotanicals, soy, hormone therapy, or placebo: a randomized trial. *Ann. Intern. Med.* 145 (12), 869–879. doi:10.7326/0003-4819-145-12-200612190-00003

Nisslein, T., and Freudenstein, J. (2003). Effects of an isopropanolic extract of Cimicifuga racemosa on urinary crosslinks and other parameters of bone quality in an ovariectomized rat model of osteoporosis. *J. Bone Min. Metab.* 21 (6), 370–376. doi:10.1007/s00774-003-0431-9

Osmers, R., Friede, M., Liske, E., Schnitker, J., Freudenstein, J., and Henneicke-von Zepelin, H. H. (2005). Efficacy and safety of isopropanolic black cohosh extract for climacteric symptoms. *Obstet. Gynecol.* 105 (5), 1074–1083. doi:10.1097/01.AOG.0000158865.98070.89

Picherit, C., Coxam, V., Bennetau-Pelissero, C., Kati-Coulibaly, S., Davicco, M. J., Lebecque, P., et al. (2000). Daidzein is more efficient than genistein in preventing ovariectomy-induced bone loss in rats. *J. Nutr.* 130 (7), 1675–1681. doi:10.1093/jn.130.7.1675

Qiu, S. X., Dan, C., Ding, L. S., Peng, S., Chen, S. N., Farnsworth, N. R., et al. (2007). A triterpene glycoside from black cohosh that inhibits osteoclastogenesis by modulating RANKL and TNFalpha signaling pathways. *Chem. Biol.* 14 (7), 860–869. doi:10.1016/j.chembiol.2007.06.010

Reagan-Shaw, S., Nihal, M., and Ahmad, N. (2008). Dose translation from animal to human studies revisited. *FASEB J.* 22 (3), 659–661. doi:10.1096/fj.07-9574LSF

Russell, R. G. G. (2011). Bisphosphonates: the first 40 years. *Bone* 49 (1), 2–19. doi:10.1016/j.bone.2011.04.022

Seidlová-Wuttke, D., Hesse, O., Jarry, H., Christoffel, V., Spengler, B., Becker, T., et al. (2003a). Evidence for selective estrogen receptor modulator activity in a black cohosh (Cimicifuga racemosa) extract: comparison with estradiol-17beta. *Eur. J. Endorinol.* 149 (4), 351–362. doi:10.1530/eje.0.1490351

Seidlová-Wuttke, D., Jarry, H., Becker, T., Christoffel, V., and Wuttke, W. (2003b). Pharmacology of Cimicifuga racemosa extract BNO 1055 in rats: bone, fat and uterus. *Maturitas* 44 (Suppl. 1), S39–S50. doi:10.1016/s0378-5122(02)00347-x

Seidlová-Wuttke, D., Jarry, H., and Wuttke, W. (2009). Effects of estradiol benzoate, raloxifen and an ethanolic extract of Cimicifuga racemosa in nonclassical estrogen regulated organs of ovariectomized rats. *Planta Med.* 75 (12), 1279–1285. doi:10.1055/s-0029-1185561

Seidlová-Wuttke, D., Jarry, H., and Wuttke, W. (2013). Plant derived alternatives for hormone replacement therapy (HRT). *Horm. Mol. Biol. Clin. Investig.* 16 (1), 35–45. doi:10.1515/hmbci-2013.0024

Seidlová-Wuttke, D., Stecher, G., Kammann, M., Haunschild, J., Eder, N., Stahnke, V., et al. (2012). Osteoprotective effects of Cimicifuga racemosa and its triterpene-saponins are responsible for reduction of bone marrow fat. *Phytomedicine* 19 (10), 855–860. doi:10.1016/j.phymed.2012.05.002

Shahnazari, M., Yao, W., Dai, W., Wang, B., Ionova-Martin, S. S., Ritchie, R. O., et al. (2010). Higher doses of bisphosphonates further improve bone mass, architecture, and strength but not the tissue material properties in aged rats. *Bone* 46 (5), 1267–1274. doi:10.1016/j.bone.2009.11.019

Shin, Y. H., Cho, D. C., Yu, S. H., Kim, K. T., Cho, H. J., and Sung, J. K. (2012). Histomorphometric analysis of the spine and femur in ovariectomized rats using micro-computed tomographic scan. *J. Korean Neurosurg. Soc.* 52 (1), 1–6. doi:10.3340/jkns.2012.52.1.1

Smith, T., Resetar, H., and Morton, C. (2022). US sales of herbal supplements increased by 9.7% in 2021. *HerbalGram* 136, 42–69.

Swanson, C. A. (2002). Suggested guidelines for articles about botanical dietary supplements. *Am. J. Clin. Nutr.* 75 (1), 8–10. doi:10.1093/ajcn/75.1.8

Thompson, D. D., Simmons, H. A., Pirie, C. M., and Ke, H. Z. (1995). FDA Guidelines and animal models for osteoporosis. *Bone* 17 (4), 125S–S133. doi:10.1016/8756-3282(95)00285-l

U.S. Securities and Exchange Commission (2012). Warner chilcott annual report. Available at: https://www.sec.gov/Archives/edgar/data/1323854/000119312513070525/d449969d10k.htm (Accessed December 18, 2023).

Uyar, Y., Baytur, Y., Inceboz, U., Demir, B. C., Gumuser, G., and Ozbilgin, K. (2009). Comparative effects of risedronate, atorvastatin, estrogen and SERMs on bone mass and strength in ovariectomized rats. *Maturitas* 63 (3), 261–267. doi:10.1016/j.maturitas.2009.03.018

Wuttke, W., Rauš, K., and Gorkow, C. (2006). Efficacy and tolerability of the Black cohosh (Actaea racemosa) ethanolic extract BNO 1055 on climacteric complaints: a double-blind, placebo-and conjugated estrogens-controlled study. *Maturitas* 55 (1), S83–S91. doi:10.1016/j.maturitas.2006.06.020

Yao, W., Cheng, Z., Koester, K. J., Ager, J. W., Balooch, M., Pham, A., et al. (2007). The degree of bone mineralization is maintained with single intravenous bisphosphonates in aged estrogen-deficient rats and is a strong predictor of bone strength. *Bone* 41 (5), 804–812. doi:10.1016/j.bone.2007.06.021

Yasuda, H., Shima, N., Nakagawa, N., Yamaguchi, K., Kinosaki, M., Mochizuki, S., et al. (1998). Osteoclast differentiation factor is a ligand for osteoprotegerin/osteoclastogenesis-inhibitory factor and is identical to TRANCE/RANKL. *Proc. Natl. Acad. Sci. U. S. A.* 95 (7), 3597–3602. doi:10.1073/pnas.95.7.3597

Yousefzadeh, N., Kashfi, K., Jeddi, S., and Ghasemi, A. (2020). Ovariectomized rat model of osteoporosis: a practical guide. *EXCLI J.* 19, 89–107. doi:10.17179/excli2019-1990

frontiers | Frontiers in Pharmacology

TYPE Review
PUBLISHED 15 May 2024
DOI 10.3389/fphar.2024.1396616

OPEN ACCESS

EDITED BY
Patricia Rijo,
Lusofona University, Portugal

REVIEWED BY
Ersilia Nigro,
University of Naples Federico II, Italy
Shih-Min Hsia,
Taipei Medical University, Taiwan

*CORRESPONDENCE
Bing-Bing Li,
lilucky0829@126.com

†These authors have contributed equally to this work and share first authorship

RECEIVED 06 March 2024
ACCEPTED 29 April 2024
PUBLISHED 15 May 2024

CITATION
Zhao Y-Q, Ren Y-F, Li B-B, Wei C and Yu B (2024), The mysterious association between adiponectin and endometriosis.
Front. Pharmacol. 15:1396616.
doi: 10.3389/fphar.2024.1396616

The mysterious association between adiponectin and endometriosis

Yong-Qing Zhao†, Yi-Fan Ren†, Bing-Bing Li*, Chao Wei and Bin Yu

College of Integrated Chinese and Western Medicine, Jining Medical University, Jining, Shandong Province, China

Adiponectin is a pleiotropic cytokine predominantly derived from adipose tissue. In addition to its role in regulating energy metabolism, adiponectin may also be related to estrogen-dependent diseases, and many studies have confirmed its involvement in mediating diverse biological processes, including apoptosis, autophagy, inflammation, angiogenesis, and fibrosis, all of which are related to the pathogenesis of endometriosis. Although many researchers have reported low levels of adiponectin in patients with endometriosis and suggested that it may serve as a protective factor against the development of the disease. Therefore, the purpose of this review was to provide an up-to-date summary of the roles of adiponectin and its downstream cytokines and signaling pathways in the aforementioned biological processes. Further systematic studies on the molecular and cellular mechanisms of action of adiponectin may provide novel insights into the pathophysiology of endometriosis as well as potential therapeutic targets.

KEYWORDS

adiponectin, endometriosis, apoptosis, angiogenesis, inflammation, fibrosis, metabolism, estrogen

1 Introduction

Endometriosis (EMs), which is considered to be a benign form of gynecological cancer, is a common gynecological disease caused by the invasive growth and development of active endometrial tissue at sites outside of the uterus (Taylor et al., 2021). EMs is often accompanied by chronic pelvic or sexual pain, dysuria, infertility, dysmenorrhea, constipation, anxiety, and depression, among other symptoms, all of which can seriously affect the quality of life and the physical and mental health of patients (Bulun et al., 2019; Zondervan et al., 2020; Lamceva et al., 2023). In recent years, the incidence of EMs has markedly increased, affecting approximately 10%–15% of women of childbearing age globally, with a prevalence of up to 50% of women with infertility and 50%–80% of women with pelvic pain (Mehedintu et al., 2014; Zondervan et al., 2018; Taylor et al., 2021). The "retrograde menstruation theory," which was first proposed by Sampson in 1927, is the classical doctrine describing the etiology of EMs (Sampson, 1927). While the incidence of retrograde menstruation is estimated to be approximately 90% in women of childbearing age, the much lower proportion of women affected by EMs suggests that other factors may be involved in its pathogenesis (Czyzyk et al., 2017). Inflammatory factors, immune dysregulation, angiogenesis, fluctuating hormone levels, genetic and epigenetic factors, environmental factors and other mechanisms, may contribute to the onset of the disease. In recent years, the study of EMs has become a hot spot of gynecological research, but its specific pathogenetic mechanisms are not yet fully understood.

Adiponectin is a pleiotropic cytokine that is predominantly secreted by adipose tissue and was initially considered to be an important insulin sensitizer and regulator of energy homeostasis (Wang and Scherer, 2016; Straub and Scherer, 2019). In recent years, an increasing number of studies have investigated the role of adiponectin in many diseases processes, and there is growing evidence of its involvement in the regulation of apoptosis, inflammation, angiogenesis, and fibrosis (Bråkenhielm et al., 2004; Fang and Judd, 2018), and adiponectin may be associated with estrogen-related diseases (Rizzo et al., 2020; Tsankof and Tziomalos, 2022), all of which contribute to the pathogenesis of EMs. Many studies have reported the presence of low adiponectin levels in those with EMs. The purpose of this review was to provide a detailed and up-to-date overview of the role of adiponectin in apoptosis, autophagy, inflammatory responses, angiogenesis, fibrosis, energy metabolism, and estrogen-related processes, and its potential correlation with the pathogenesis of EMs.

2 Obesity, adipose tissue, and EMs

The overall degree of obesity or the distribution of adipose tissue has been shown to be correlated with the development of EMs (Shah et al., 2013b; Backonja et al., 2016). For example, Goetz et al. demonstrated that the expression levels of four genes known to be associated with weight loss [cytochrome P450 2R1 (CYP2R1), fatty acid binding protein 4 (FABP4), mannose receptor C-Type I (MRC1), and Rho-associated coiled-coil containing protein kinase 2 (ROCK2)] were upregulated in the livers of mice in an animal model of EMS, whereas the expression levels of two genes associated with obesity [insulin-like growth factor binding protein 1 (IGFBP1) and monocyte to macrophage differentiation associated 2 (MMD2)] were downregulated; in addition, the presence of EMs was associated with a reduction in both the level of body fat and the degree of weight gain (Goetz et al., 2016). Another study reported a decrease in the proliferative ability of abdominal subcutaneous adipocytes in patients with EMs (Zolbin et al., 2019). The inflammatory response has also been shown to be intensified in the retroperitoneal adipose tissue adjacent to lesions in patients with pelvic EMs, and these changes were accompanied by a significant upregulation of the expression levels of angiogenic factors and inflammatory cytokines (Kubo et al., 2021). In addition, a reduction in the number of adipose stem cells and lipid dysfunction have been reported in a mouse model of EMs, which can affect the body mass index (BMI) by modulating adipocytes and lipid metabolism (Zolbin et al., 2019). There is a large body of evidence that suggests the risk of EMs is negatively correlated with the BMI (Vitonis et al., 2010; Backonja et al., 2016; Farland et al., 2017; Holdsworth-Carson and Rogers, 2018; Pantelis et al., 2021), with this negative correlation being intensified in women with infertility (Shah et al., 2013a).

It is important to acknowledge, however, that some studies have reported that the BMI had no effect on endometrial gene expression in patients with EMs (Holdsworth-Carson et al., 2020), and the negative correlation between EMs and BMI remains unexplained, as both have been shown to be associated with hyperestrogenemia and systemic inflammation, and obesity does not prevent the occurrence of EMs (Holdsworth-Carson and Rogers, 2018; Pantelis et al., 2021). Some studies have suggested that in addition to being a risk factor for the disease (Tang et al., 2020), obesity may also exacerbate the condition in clinical populations (Holdsworth-Carson et al., 2018). Collectively, these findings suggest that multiple factors affect the correlations between EMs, obesity, and the presence of adipose tissue (Figure 1).

3 Adiponectin

3.1 Overview, structure, and oligomers

Adipose tissue is a highly active endocrine organ that produces and expresses various factors such as leptin, adiponectin, and resistin, all of which participate in and coordinate a wide range of pathophysiological processes, including immune responses, inflammation, and energy metabolism (Kershaw and Flier, 2004). Adiponectin is an adipocytokine found in high abundance in peripheral blood, with a plasma concentration of 4–37 μg/mL, accounting for 0.01%–0.05% of total serum proteins, a concentration that is approximately a thousand times higher than that of other hormones, including insulin and leptin (Fang and Judd, 2018; Ye et al., 2020). Adiponectin has had many monikers over the years, including AdipoQ (Hu et al., 1996), apM1 (Maeda et al., 1996), Acrp30 (Scherer et al., 1995), and gelatin-binding protein 28 (GBP-28) (Díez and Iglesias, 2003). In humans, full-length adiponectin contains 244 amino acid residues and consists of an amino-terminal signaling peptide (amino acids 1–18), a variable region (amino acids 19–41), a collagen domain (amino acids 42–107), and a carboxy-terminal globular C1q head region (amino acids 108–244) (Achari and Jain, 2017). The isolated spherical C1q domain produced by protein hydrolysis, dubbed globular adiponectin, exhibits confirmed biological activity (Fruebis et al., 2001). As a monomer, adiponectin is difficult to detect in the blood (Waki et al., 2003), and three kinds of polymers can be found in the general circulation, including low-molecular weight (LMW) polymers (trimers of ~90 kDa in size), medium-molecular weight (MMW) polymers (hexamers of ~180 kDa), and high-molecular weight (HMW) polymers (chains of 12–18 monomers, with a size of ~360–540 kDa) (Fang and Judd, 2018) (Figure 2). The LMW form can cross the filtration barrier within the kidneys; therefore, adiponectin can be detected in the urine of healthy individuals with normal renal function (Kim and Park, 2019). However, in the general circulation, HMW and MMW adiponectin are predominant, whereas concentrations of LMW adiponectin tend to be much lower (Parker-Duffen et al., 2013). Among them, HMW adiponectin is considered to be the main bioactive complex of the various isoforms (Achari and Jain, 2017). Globular adiponectin can also be detected in the plasma at low levels in the general circulation (Fruebis et al., 2001). Three adiponectin monomers combine via the C-terminal globular and collagen-like structural domains to form a highly ordered LMW trimer, which can further polymerize to form MMW hexamers and HMW compounds (Magkos and Sidossis, 2007). Circulating adiponectin levels are not constant, and serum concentrations have been shown to be higher during the daytime than at night (Gavrila et al., 2003; Scheer et al., 2010). In addition to these diurnal fluctuations, sex differences also influence adiponectin levels, with concentrations being higher in women than in men (Ohman-Hanson et al., 2016; Christen et al.,

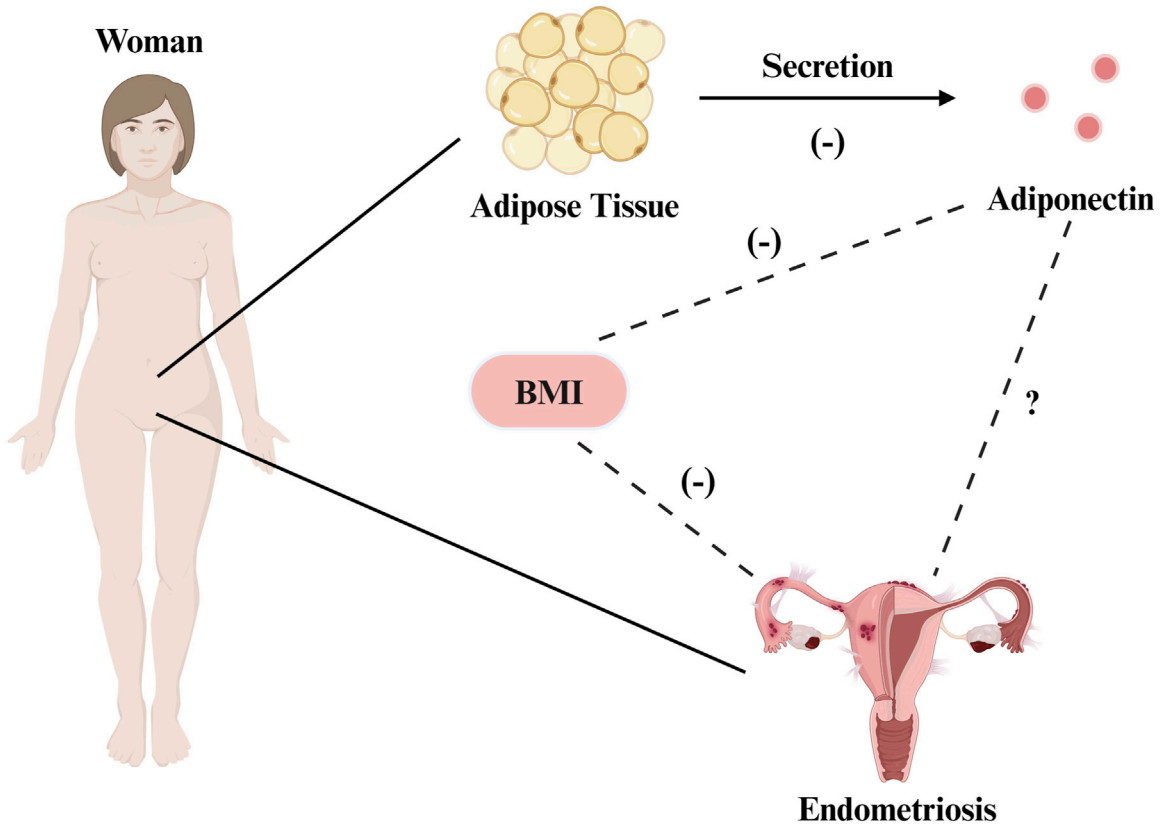

FIGURE 1
The correlation between EMs, obesity, and adipose tissue. There is a negative correlation between the risk of EMs and BMI. Adiponectin is produced by adipocytes, and its level is negatively corelated with BMI and fat accumulation. Evidence shows that adiponectin is underexpressed in endometriosis, and the two variables may exhibit a certain degree of correlation. Created with BioRender.com.

2018; Vučić Lovrenčić et al., 2020); this is particularly true in the case of HMW and MMW adiponectin, the levels of which are more than twice as high as in women (Peake et al., 2005). Higher circulating testosterone levels in males may explain the sex-specific difference in adiponectin concentrations after puberty (Handelsman et al., 2018), as testosterone lowers total adiponectin concentrations in serum (Nishizawa et al., 2002; Frederiksen et al., 2012; Yarrow et al., 2012). Although adiponectin is produced by adipocytes, significantly downregulated expression levels has been detected in the adipose tissue of fatty mice and overweight humans (Hu et al., 1996), with serum levels being negatively correlated with the BMI and fat accumulation (Brooks et al., 2007).

3.2 Adiponectin receptors and functions

Adiponectin was initially identified as an insulin-sensitive adipose factor related to the pathogenesis of metabolic syndrome; over time, however, many studies have confirmed its anti-inflammatory, anti-apoptotic, anti-fibrotic, and anti-angiogenic effects (Bråkenhielm et al., 2004; Fang and Judd, 2018). Adiponectin signal transduction mainly depends on receptor–ligand interactions, whereby adiponectin binds to its homologous receptor and initiates the activation of intracellular signaling cascades through the adenosine monophosphate-activated protein kinase (AMPK), peroxisome proliferator-activated receptor alpha (PPAR-α), phosphoinositide 3-kinase (PI3K)/protein kinase B (Akt), mammalian target or rapamycin (mTOR), mitogen-activated protein kinase (MAPK), signal transducer and nuclear factor kappa B (NF-κB) pathways and other pathways (Choi et al., 2020).

To date, three adiponectin receptors have been identified, including adiponectin receptor 1 (AdipoR1), adiponectin receptor 2 (AdipoR2), and T-cadherin (T-cad) (Yamauchi et al., 2003; Achari and Jain, 2017). AdipoR1 is predominantly expressed in skeletal muscle cells and acts as a high-affinity receptor for globular adiponectin and a low-affinity receptor for full-length adiponectin, whereas AdipoR2 is mainly expressed in hepatocytes and serves as a medium-affinity receptor for both full-length and globular adiponectin (Yamauchi et al., 2014). T-cad is mainly expressed in endothelial and smooth muscle cells, acting predominantly as a biologically active receptor that binds to adiponectin in diverse tissues and organs, such as in muscle, blood vessels, and the heart (Parker-Duffen et al., 2013; Clark et al., 2017). Adiponectin and its receptors are widely expressed in the hypothalamus, pituitary gland, and ovaries of humans, rats and pigs, as well as in the placenta and uterus of humans, mice and pigs, where they have been shown to functionally modulate the female reproductive system (Caminos et al., 2005; Kos et al., 2007; Rodriguez-Pacheco et al., 2007; Kim et al., 2011; Angelidis et al., 2013; Kiezun et al., 2013; Maleszka et al., 2014; Smolinska et al., 2014). As the characteristics of metabolic syndrome are associated

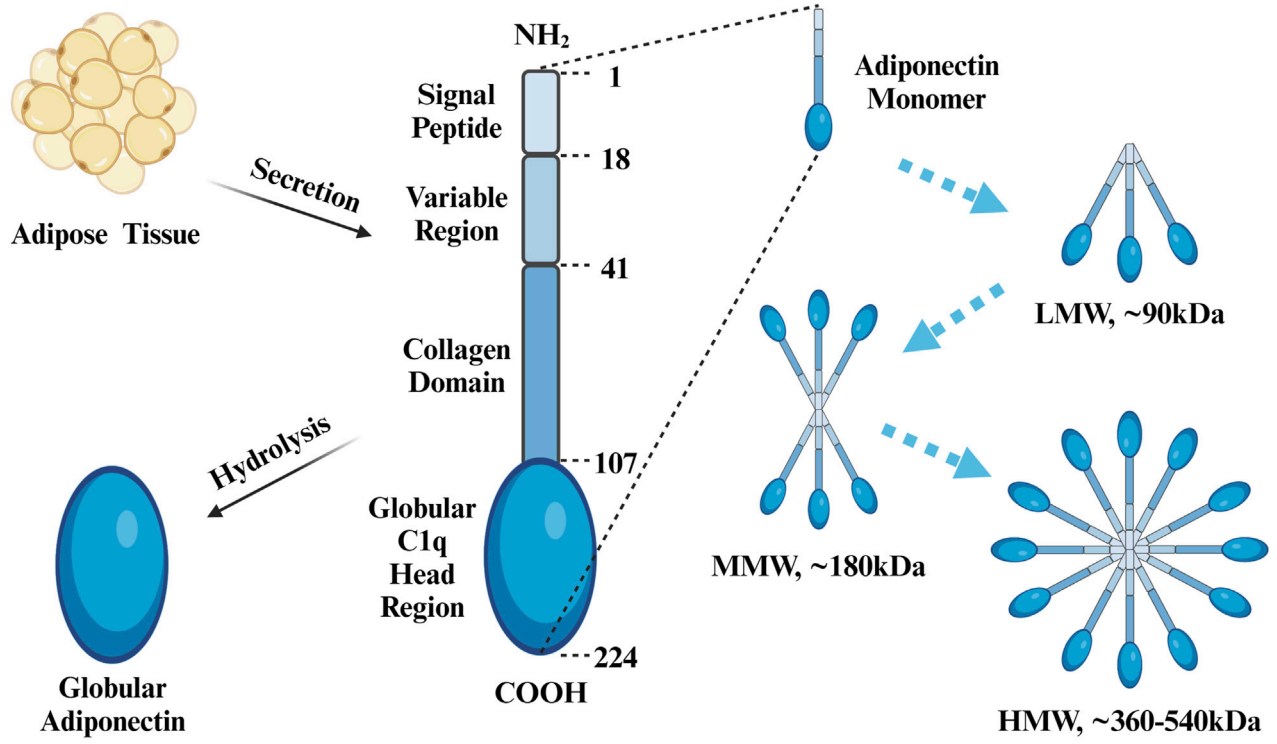

FIGURE 2
Protein Structure of APN. Adiponectin consists of an N-terminal signal peptide, variable region, collagen domain, and C-terminal globular c1q head region, with a total of 244 amino acids. Globular adiponectin is produced by proteolysis of full-length adiponectin. Three adiponectin monomers combine to form a trimer (LMW), two trimers combine to form a single hexamer (MMW), and four to six trimers combine to form a multimer (HMW). Created with BioRender.com.

with a number of reproductive disorders such as polycystic ovary syndrome (PCOS), gestational diabetes mellitus, preeclampsia, EMs, fetal growth restriction, and ovarian and endometrial cancers, their pathogenesis may be influenced by adiponectin (Barbe et al., 2019). AdipoR1 and AdipoR2 have been shown to be highly expressed in the normal human endometrium during the mid-secretory phase (i.e., during implantation), and adiponectin can induce the phosphorylation of AMPK, inhibit the expression of interleukin 1 beta (IL-1β), and promote the secretion of interleukin 6 (IL-6), interleukin 8 (IL-8), and monocyte chemoattractant protein 1 (MCP-1) in cultivated endometrial cells, suggesting that it may play both physiological and pathological roles within the endometrium (Takemura et al., 2006). In female mice, adiponectin may induce preimplantation embryo development and endometrial decidualization in an autocrine-, paracrine-, or endocrine-dependent manner (Kim et al., 2011). Furthermore, hypoadiponectinemia has been shown to be associated with an increased risk of hormone-dependent cancers, such as endometrial, ovarian, cervical, and breast cancers, as well as a poor prognosis (Zeng et al., 2015; Tsankof and Tziomalos, 2022).

4 Evidence for the association of adiponectin with EMs

Clinical studies, *in vitro* cell experiments, and animal experimental studies have provided evidence for the association between adiponectin and EMs. Clinical analysis has shown differences in adiponectin levels in patients with EMs. Moreover, studies have shown a decreased expression of adiponectin in patients with EMs; however, the findings are still controversial (Table 1). For example, Takemura et al. discovered a reduction in adiponectin levels in both the serum and peritoneal fluid (PF) of patients with EMs, with a particularly pronounced decrease in serum levels in those in the advanced stages of the disease (stage III/IV) (Takemura et al., 2005a,b). Similarly, another study reported lower serum levels of adiponectin in patients with EMs compared with that in healthy controls (Meng and Hao, 2020). However other researchers have observed no significant differences in the serum and PF levels of adiponectin between patients with infertility with and without concomitant pelvic EMs (Pandey et al., 2010). Others have reported no significant differential expression of adiponectin and AdipoRs in ectopic endometrial tissues of patients with ovarian EMs and patients with normal endometrial tissues who had undergone hysterectomy to treat cervical fibroids or carcinoma *in situ* (Choi et al., 2013). A meta-analysis published in 2021 that evaluated the results of 25 studies confirmed that although there was no significant association between the levels of adiponectin and disease severity, the patients with EMs did exhibit significantly lower levels of adiponectin and significantly higher levels of leptin compared to the concentrations in the control groups (Zhao Z. et al., 2021). Furthermore, a recent study that assessed adiponectin concentrations in the plasma, PF, and endometrioma fluids of 56 women with ovarian EMs reported that adiponectin levels

TABLE 1 Clinical studies on adiponectin levels in endometriosis.

References	Experiment	Control	Sample size (experiment vs control)	Location	Change (experiment vs control)
Takemura et al. (2005b)	Patients with endometriosis	Women of reproductive age without endometriosis	54:26	PF	↓
Takemura et al. (2005a)	Patients with endometriosis	Women of reproductive age without endometriosis	48:30	Serum	↓
Pandey et al. (2010)	Infertile patients with pelvic endometriosis	Infertile patients without pelvic endometriosis	15:35	PF	NS
				Serum	NS
Yi et al. (2010)	Patients with endometriosis	Patients without endometriosis who underwent surgical procedures for pelvic pain, infertility and / or other benign diseases	48:36	PF	NS
Huang et al. (2011)	Patients with endometriosis	Patients without endometriosis	57:30	PF	↓
	Patients with endometriosis (III~V)	Patients with endometriosis (I~II)	32:25		NS
Choi et al. (2013)	Patients with ovarian endometriosis	Age-matched patients who underwent hysterectomy because of myoma or carcinoma *in situ* of uterine cervix	44:42	Ectopic lesion	NS
Shah et al. (2013a)	Patients with endometriosis	Women of reproductive age without endometriosis	350:694	Blood	NS
Qin et al. (2014)	Patients with ovarian endometriosis	Healthy women	38:42	Serum	↓
Meng and Hao (2020)	Patients with endometriosis	Healthy women	30:30	Serum	↓
Wójtowicz et al. (2023)	Patients with ovarian endometriosis	Self-control	56	Plasma	9.8 μg/mL
					(7.3–13.1)
				PF	1.2 μg/mL
					(0.1–2.4)
				Endometrioma fluids	0.1 μg/mL
					(0.0–1.3)

were significantly lower in endometrioma fluids and PF than in serum, with a positive correlation between the concentrations in endometrioma fluids and PF (Wójtowicz et al., 2023). In addition, another group discovered that two polymorphisms in the adiponectin gene, rs2241766 and rs1501299, were associated with EMs susceptibility among women of childbearing age in Henan Province, China, and that the G mutation in the rs2241766 locus may affect splicing and modification of gene expression, resulting in the promotion of adiponectin secretion, which, in turn, induces AMPK phosphorylation and regulates its downstream pathway, thereby protecting against the development of EMs (Zhang et al., 2021). Both AdipoR1 and AdipoR2 are expressed in the endometrium, and their mRNA levels become significantly elevated in the mid-secretory phase (Takemura et al., 2006).

In addition, the relationship between adiponectin and EMs has been explored using animal models and *in vitro* experiments. In studies on animal models, the number of stem cells in adipose tissue in mouse models of EMs decreased, and EMs changed the expression of multiple adipocyte metabolic genes, including adiponectin and leptin (Zolbin et al., 2019). *In vitro* cell experiments, Adiponectin has been shown to inhibit the proliferation of ectopic endometrial cells in a dose- and time-dependent manner while simultaneously increasing the expression of both AdipoR1 and AdipoR2 to inhibit EMs development; these findings suggest that adiponectin may serve as a beneficial factor that limits the pathogenesis of EMs (Bohlouli et al., 2016). Despite the plethora of studies conducted to date, the detailed regulatory role of adiponectin in the pathogenesis of EMs has yet to be elucidated, and further research is needed to deepen the understanding of the complex biological mechanisms through which adiponectin protects against EMs pathogenesis.

5 Possible associations of adiponectin with the pathogenesis of EMs

The formation of ectopic endometriotic lesions involves a series of complex events, including the adhesion, invasion, and

angiogenesis of Endometrial cells to "take root, grow, and become sick." First, due to an imbalance in immune function, ectopic endometrial cells are able to evade immune clearance (Symons et al., 2018). In addition, there is an imbalance between the proliferation and apoptosis of ectopic endometrial cells, which contributes to their survival in ectopic sites (Reis et al., 2013; Azam et al., 2022). After the adhesion of ectopic endometrial cells to ectopic sites, an inflammatory response is initiated, leading to increased secretion of pro-inflammatory mediators, and more inflammatory mediators are recruited to invade surrounding tissues (Wei et al., 2020; Artemova et al., 2021; Kapoor et al., 2021). Periodic bleeding of ectopic lesions and chronic inflammation activate the deposition and adhesion of fibrin and scar formation, leading to fibrogenesis of the lesion (Eming et al., 2014; Garcia et al., 2023). Simultaneously, the production of angiogenesis-related factors increases, promoting neoangiogenesis, providing nutrients for the survival and growth of ectopic lesions (Wei et al., 2020). In addition, ectopic endometrial cells also have changes in mitochondrial morphology and function, which helps to increase the energy supply to ectopic lesions and meet the growth needs of lesions (Ye et al., 2023). EMs is an estrogen-dependent disease in which estrogen and estrogen receptor (ER) levels are elevated in ectopic lesions (Burney and Giudice, 2012; Chantalat et al., 2020). Dysregulation of estrogen signal transduction causes ectopic endometrial cells to appear abnormal in cell proliferation and apoptosis, migration, invasion, angiogenesis and immune function, accompanied by increased inflammation and enhanced mitochondrial biosynthesis, which further promote lesion progression (Monsivais et al., 2016; Wu L. et al., 2019; Xu Z. et al., 2019; Marquardt et al., 2019; Qi et al., 2020; Kobayashi et al., 2021a). Therefore, EMs is a complex disease that is simultaneously affected by multiple factors. In addition to estrogen dependence, its pathogenesis mainly involves apoptosis, autophagy, inflammation, angiogenesis, fibrogenesis, and energy metabolism. Current research on the pathogenesis of EMs and the function of adiponectin have shown that adiponectin may play a special regulatory role in multiple biological processes related to the pathogenesis of EMs, such as apoptosis, autophagy, inflammatory response, angiogenesis, fibrogenesis, energy metabolism, and estrogen regulation. This aspect is noteworthy; hence, we have summarized the following important biological processes to reveal the mysterious relationship between EMs and adiponectin.

5.1 Apoptosis and autophagy

EMs is characterized by the invasive growth of active endometrial tissue at sites other than the uterus, and these events may be related to a disequilibrium between proliferation and apoptosis in ectopic endometrial cells. During these processes, these cells are less sensitive to apoptotic signals (Reis et al., 2013; Azam et al., 2022), therefore, ectopic endometrial cells can easily escape clearance and invade the peritoneum. Moreover, their proliferative activity is markedly increased (Jiang and Wu, 2012), leading to neovascularization and the establishment of endometrial implants, which leads to the development of the disease and further malignant progression. Compared to that of healthy controls, the expression level of the anti-apoptotic gene B-cell lymphoma 2 (Bcl-2) is significantly elevated in the ectopic endometrium of patients with EMs (Agic et al., 2009; Jiang R. et al., 2020), whereas that of the pro-apoptotic genes p53 and caspase-3 is decreased (Sang et al., 2019; Duan R. et al., 2020; Zhang and Zhao, 2023). Cyclin D1 and cyclin E2 are key regulatory proteins that control the transition from the G1 phase into the S phase during the cell cycle (Zabihi et al., 2023), and the expression of cyclin D1 mRNA has been shown to be significantly elevated in ectopic endothelial tissues compared to that in normal and eutopic endothelium (Pellegrini et al., 2012). Knockdown of cyclin D1 in human ectopic endometrial cells has been shown to significantly reduce their rate of proliferation while significantly increasing the number of cells in the G1/G0 phase (Hirakawa et al., 2017). Akt is a major protein kinase that exists downstream of PI3K and regulates the expression of various proteins associated with both cellular proliferation and apoptosis (Cinar et al., 2009; Revathidevi and Munirajan, 2019), and a recent study demonstrated that PI3K expression increases and Akt phosphorylation levels become elevated in the eutopic and ectopic endometrium of patients with EMs compared to the levels in healthy controls, indicating that the PI3K/Akt signaling pathway may play an active role in facilitating the establishment of ectopic endometrial tissue (Madanes et al., 2020).

Another important factor downstream of the PI3K/Akt pathway is mTOR, an evolutionarily conserved serine/threonine protein kinase (Driva et al., 2023). Researchers have reported an upregulation in mTOR signaling in endometriotic foci (Choi et al., 2014), and the protein is involved in the modulation of key pathophysiological processes such as proliferation, differentiation, apoptosis, autophagy, and decidualization of endometrial cells (Guo and Yu, 2019; Driva et al., 2022). Administration of the mTOR inhibitor everolimus was shown to promote apoptosis and inhibit the formation of endometriotic foci, making it a potential therapeutic option for the treatment of EMs (Kacan et al., 2017). In addition, it has been demonstrated that the MAPK signaling pathway is involved in the survival and proliferation of ectopic endometrial cells as well as various other processes including but not limited to invasion and metastasis, inflammation, and angiogenesis (Bora and Yaba, 2021; Zhang et al., 2023). In the late proliferative and early secretory stages, the phosphorylation level of p38-MAPK becomes significantly elevated in both eutopic and ectopic endometriotic tissues in patients with EMs compared to that in the normal endometrium (Cakmak et al., 2018), and aberrant activation of the MAPK signaling pathway can aggravate the severity of EMs (Jiang Y. et al., 2020; Bora and Yaba, 2021). Extracellular signal-regulated kinase (ERK), a member of the classical MAPK family (Samson et al., 2022), transmits extracellular signals following its activation, thereby promoting MAPK phosphorylation and regulating the expression of downstream effectors; thus, it plays a significant role in cell proliferation, differentiation, and apoptosis (Zhu et al., 2019; Bora and Yaba, 2021).

In humans, adiponectin has been reported to inhibit the proliferation of both normal and ectopic endometrial cells in a dose- and time-dependent manner (Bohlouli et al., 2013,2016), thereby playing a potentially important role in the pathological processes that lead to EMs. Additionally, other studies have shown that adiponectin can inhibit the proliferation of focal cells and exert pro-apoptotic effects in various diseases, including uterine fibroids

as well as endometrial, ovarian, and breast cancers. The presence of both AdipoR1 and AdipoR2 has been confirmed in uterine leiomyoma cells, and adiponectin exerts a significant inhibitory effect on the proliferation of uterine Eker leiomyoma tumor 3(ELT-3) cells in rats (Wakabayashi et al., 2011; Strzałkowska et al., 2021). Adiponectin has been shown to decrease the expression of both cyclin D1 in the human endometrial adenocarcinoma cell lines HEC-1-A and KLE and cyclin E2 in the RL95-2 cell line by activating the AMPK signaling pathway, which led to the blockage of the cell cycle to inhibit the proliferation of cancer cells (Cong et al., 2007; Moon et al., 2011). In addition, adiponectin can mediate anti-proliferative and pro-apoptotic responses in endometrial cancer by inhibiting the activation of the Akt and ERK signaling pathways (Zhang et al., 2015). Administration of the AdipoR agonist AdipoRon has been shown to exert anti-tumor effects by inducing G1-phase cell cycle arrest and upregulating the expression of the pro-apoptotic gene caspase-3 via the activation of the AMPK and inhibition of mTOR signaling pathways, in human ovarian cancer cells (Ramzan et al., 2019). In the human breast cancer cell line MDA-MB-231, adiponectin was shown to inhibit cell growth by significantly reducing the expression of both cyclin D1 protein and the anti-apoptotic gene Bcl2, while simultaneously upregulating the expression of the pro-apoptotic genes p53 and Bax (Dos Santos et al., 2008; Delort et al., 2012). Furthermore, in MCF7 human breast cancer cells, adiponectin has been shown to induce anti-proliferative and pro-apoptotic responses by activating the AMPK signaling pathway and inhibiting the MAPK signaling pathways (Dieudonne et al., 2006).

While the pro-apoptotic effects of adiponectin can protect against the development of various diseases, some studies have also demonstrated its anti-apoptotic activity. For example, in a mouse model of sepsis, adiponectin has been shown to inhibit lipopolysaccharide (LPS)-induced cardiomyocyte apoptosis by downregulating connexin 43 (Cx43) expression and activating the PI3K/AKT signaling pathway to protect myocardial function (Liu et al., 2021). AdipoRon administration reduces high glucose-induced oxidative stress and apoptosis and ameliorates endothelial dysfunction via the activation of the AMPK/PPAR-α pathway, thereby exerting a nephroprotective effect in diabetic nephropathy (Kim Y. et al., 2018). In rheumatoid arthritis (RA), adiponectin has been shown to promote the proliferation and differentiation of B cells by inducing the activation of the PI3K/Akt and activator of transcription 3 (STAT3) signaling pathways, exacerbating RA development (Che et al., 2021). Additionally, in early pregnancy in pigs, adiponectin was shown to induce porcine uterine luminal epithelial cell proliferation while inhibiting apoptosis through the activation of the PI3K/Akt and MAPK signaling pathways, enhancing uterine tolerance to embryonic implantation (Lim et al., 2017). It is important to note, however, that some studies have also demonstrated no effect of adiponectin on apoptosis (Arditi et al., 2007; Pfeiler et al., 2008); thus, its role in such processes remains controversial, and its effects may be related to the disease, the source of adiponectin, as well as differences in conformations, concentrations, and treatment durations between studies (Sun and Chen, 2010).

Apoptosis is not the sole mechanism of endometrial cell death (Choi et al., 2015). Autophagy, another form of programmed cell death, involves a series of catabolic processes that depend on the lysosomal degradation of proteins and cytoplasmic organelles, which are closely related to cellular proliferation and apoptosis (Popli et al., 2022). The expression levels of autophagy-related genes such as microtubule-associated protein light chain 3 (LC3) and Beclin-1 have been shown to be reduced in the serum, PF, and eutopic endometrial tissue of patients with EMs compared with the levels in healthy controls (Sui et al., 2018), and the level of expression of autophagy-related genes (LC3B-II) was significantly reduced in ectopic endometrium compared with that in the eutopic endometrial tissues of patients with EMs (Li et al., 2018). Inhibition of autophagy can promote the expression of inflammatory cytokines, trigger inflammation and immune responses leading to autoimmune damage, enable endometrial cells to evade immune surveillance, and ultimately promote ectopic growth and implantation of ectopic endometrial cells in the peritoneal cavity (Ji et al., 2022). Autophagy and apoptosis are not two independent processes but two crosstalk mechanisms. Autophagy promotes the phagocytosis of apoptotic bodies and degradation of lysosomes (Mariño et al., 2014); therefore, decreased autophagic activity in ectopic and eutopic endometrial cells would lead to a decrease in apoptosis (Choi et al., 2014; Yu et al., 2016). As mTOR is a major negative regulator of autophagy, several studies have reported that cellular autophagy can be induced by inhibiting the mTOR signaling pathway in ectopic endometrial cells (Choi et al., 2015; Xu H. et al., 2019; Huang et al., 2023). In addition, in mouse models of EMs, in addition to inhibiting autophagy, the upregulation of mTOR in EMs tissues promoted the survival of ectopic endometrial cells (Yang et al., 2017). In terms of other signaling pathways, AMPK activation results in the downregulation of PI3K/Akt/mTOR signaling, leading to decreased phosphorylation of the protein autophagy-related 13 (ATG13) (Yang et al., 2017; Assaf et al., 2022; Ge et al., 2022) and an increase in the level of the unc-51-like autophagy activating kinase 1 (ULK1) complex formed by the interaction of ATG13 with ULK1, FAK family kinase-interacting protein of 200 kDa (FIP200), and autophagy-related 101 (ATG101); this complex is an important factor in the initiation of autophagy (Yang et al., 2017). Administration of AdipoRon can activate AMPK/mTOR signaling to promote autophagy (Duan Z. X. et al., 2020) and reduce the dysregulated expression of proteins involved in the autophagy-lysosomal pathway (He et al., 2021). Moreover, researchers have shown that adiponectin can induce autophagy in breast cancer cells by activating the AMPK-ULK1 axis mediated by serine/threonine kinase 11 (STK11)/liver kinase B1 (LKB1), which, in turn, promotes breast cancer cell apoptosis (Chung et al., 2017).

It must be acknowledged that the regulatory effect of adiponectin on autophagy is not unilateral, as others have shown that adiponectin inhibits autophagy and reduces angiogenesis in the choroidal retinal endothelial cell line RF/6A in monkeys through activation of the PI3K/AKT/mTOR pathway (Li et al., 2019). Adiponectin can protect against hypoxia/reperfusion injury-induced cardiomyocyte damage by inhibiting autophagy as well, an effect that may be related to the inhibition of the AMPK/mTOR/UKL1/Beclin-1 pathway (Guo et al., 2022).

Although the role of adiponectin in the regulation of apoptosis and autophagy may be bidirectional, many studies have provided ample evidence that it plays a role in protecting against the

development of various diseases and may serve as a potentially therapeutic strategy. Although relevant studies have confirmed the role of adiponectin in the inhibition of endometrial cells proliferation in EMs, whether the mechanism of action is related to the regulation of apoptotic genes and signal pathways such as AMPK, MAPK, PI3K/Akt/mTOR and so on, more research is needed to explain.

5.2 Angiogenesis

The shed endometrial cells undergo migration, adhesion, invasion and implantation with retrograde menstruation to form ectopic lesions, during which massive neovascularization occurs and a new blood supply is established to provide nourishment for the survival and growth of the lesions (Wei et al., 2020). Therefore, angiogenesis is considered a critical step in the establishment and persistence of endometriotic lesions. The results of studies involving animal models have suggested that anti-angiogenic therapies substantially reduce the size of ectopic lesions (Liu et al., 2016); in EMs, angiogenesis is regulated by a multitude of factors and pathways involved in those processes. For example, vascular growth factors may play an essential role in promoting the growth and differentiation of ectopic endometrial tissue, with vascular endothelial growth factor (VEGF) being the most critical. Members of the VEGF family, which includes VEGF-A, VEGF-B, VEGF-C, VEGF-D, and VEGF-E, as well as placental growth factors, have been shown to increase vascular permeability, accelerate vascular endothelial cell migration and proliferation, and promote angiogenesis (Ferrara and Adamis, 2016), and VEGF and its signaling pathway are considered the optimal targets for anti-angiogenic and anti-tumor therapies for a variety of cancers (Potente et al., 2011; Gao et al., 2020). VEGF expression was elevated in healthy controls, in the eutopic endometrium of patients with Ems, and in ectopic lesions sequentially (Di Carlo et al., 2009), and elevated VEGF expression in the serum and PF of patients with EMs may serve as a secondary diagnostic indicator of the disease (Bourlev et al., 2010; Li et al., 2020). VEGF expression in EMs is regulated by multiple factors and associated pathways, and it plays a pivotal regulatory role in neovascularization.

Adiponectin is an important regulator of angiogenesis, exerting its effect through the regulation of VEGF. In prostate cancer cells, adiponectin can prevent neovascularization by suppressing VEGF-A secretion (Gao et al., 2015), and adiponectin treatment has been shown to downregulate VEGF-B and VEGF-D mRNA expression while increasing the serum concentration of the anti-angiogenic factor IL-12 in mouse colon cancer cells (Moon et al., 2013). Other important factors to consider are the matrix metalloproteinases (MMPs), which are involved in the degradation of the extracellular matrix and the induction of vascular endothelial cell proliferation and angiogenesis (D'Amico et al., 2020). MMP-2 expression has been shown to be significantly elevated in the ectopic foci, PF, and serum of patients with EMs (Sui et al., 2018). And adiponectin inhibits angiogenesis by downregulating MMP expression. For example, in liver cancer tissues in mice, adiponectin has been shown to downregulate the mRNA expression of VEGF and MMP-9, thereby inhibiting tumor angiogenesis (Man et al., 2010). Furthermore, in human renal carcinoma cells, adiponectin can activate AMPK via binding to AdipoR1, inhibiting the mTOR signaling pathway and suppressing the production of VEGF, MMP-2, and MMP-9 (Kleinmann et al., 2014). There have also been reports that adiponectin can inhibit the proliferation and migration and angiogenesis of endothelial cells (Dubois et al., 2013; Li et al., 2019; Palanisamy et al., 2019). Such an inhibitory effect may indirectly hinder angiogenesis of ectopic lesions. Additionally, adiponectin can induce endothelial apoptosis, which occurs during angiogenesis (Watson et al., 2016), by activating caspase-8, thereby leading to the activation of caspase-3 or caspase-9 (Bråkenhielm et al., 2004).

The inhibitory role of adiponectin in angiogenesis has been demonstrated in multiple types of cancer, including fibrosarcoma (Bråkenhielm et al., 2004), hepatocellular carcinoma (Man et al., 2010), renal cell carcinoma (Kleinmann et al., 2014), basal cell breast cancer (Dubois et al., 2013), and prostate cancer (Gao et al., 2015). However, several other studies have shown that adiponectin can *enhance* angiogenesis by upregulating the expression of pro-angiogenic factors in human umbilical vein endothelial cells (HUVECs) and human microvascular endothelial cells (HMECs) (Adya et al., 2012; Nigro et al., 2021), and it has been shown to promote angiogenesis in chondrosarcoma (Lee et al., 2015), invasive colon cancer (Cai et al., 2016), and ovarian cancer (Ouh et al., 2019), possibly via the regulation of CXC motif chemokine ligand 1 (CXCL1), VEGF, and AMPK. Adiponectin enhances CXCL1 secretion, which, in turn, promotes VEGF secretion and angiogenesis (Kiefer and Siekmann, 2011) in various cancers, including colon (Cai et al., 2016) and ovarian cancer (Ouh et al., 2019). AMPK is a key molecule involved in the regulation of biological energy metabolism, and inhibition of its activity significantly attenuates VEGF secretion (Fisslthaler and Fleming, 2009). In HUVECs and HMEC-1 cells, adiponectin has been shown to induce angiogenesis by activating the AMPK/Akt pathway and phosphorylating endothelial nitric oxide synthase (eNOS) (Ouchi et al., 2004; Adya et al., 2012), which is various with the findings of another study that showed angiogenesis was inhibited by adiponectin (Dubois et al., 2013). In addition, adiponectin may play a pro-angiogenic protective role in ischemic tissue injury. For example, the overexpression of adiponectin was shown to induce the upregulation of VEGF mRNA expression within ischemic regions of the brains of mice, enhancing focal angiogenesis (Shen et al., 2013). Another study showed that recovery following ischemic reperfusion injury of a limb in mice was accelerated by giving adenovirus-mediated adiponectin and exogenous adiponectin administration stimulated angiogenesis in response to ischemic stress by activating the AMPK pathway (Shibata et al., 2004).

Collectively, angiogenesis in EMs has similar features to pathological angiogenesis in tumor growth and metastasis, being co-regulated by multiple factors. Existing studies have shown that adiponectin plays a role in the inhibition of angiogenesis in many oncological diseases; however, it is not clear whether adiponectin has a beneficial role in EMs by regulating signaling pathways such as AMPK and cytokines such as VEGF and MMPs to promote endothelial cell apoptosis, inhibit endothelial cell migration and thus inhibit angiogenesis. However, for this conjecture, we are currently inconclusive, because the regulation of adiponectin-mediated angiogenesis is bidirectional, especially in oncological diseases, with different modes of action. This paradoxical

phenomenon could be due to variability between studies in terms of the differences in cell types, *in vivo* and *in vitro* experimental methodologies, and the physiological and pathological conditions in which angiogenesis is observed.

5.3 Inflammatory processes

Chronic inflammation and immune dysregulation are essential microenvironment and pathophysiological features of EMs (Zhang et al., 2018; Encalada Soto et al., 2022). Due to the dysregulation of immune mechanisms, ectopic endometrial cells evade immune clearance to survive, adhere, and invade ectopic sites (Symons et al., 2018). Subsequently, during the formation of endometriotic lesions, the secretion of a large number of pro-inflammatory cytokines is increased. Inflammatory cells are recruited to the lesion site, which secrete a variety of inflammatory mediators to form an inflammatory microenvironment. These mediators counteract inflammatory cells and factors, leading to the recruitment of more inflammatory cells to the lesion site, forming a vicious circle in which these immune molecules not only promote cell proliferation and adhesion but also contribute to the cell evasion of immunosurveillance, further exacerbating the invasion of ectopic endometrial cells and promoting lesion formation and progression (Wei et al., 2020; Artemova et al., 2021; Kapoor et al., 2021). Numerous studies have shown that the lymphocytes present within the peritoneal cavity in EMs are predominantly macrophages (Bacci et al., 2009; Shao et al., 2016; Ramírez-Pavez et al., 2021), which are broadly classified into two main phenotypes, including the pro-inflammatory M1-type and the anti-inflammatory M2-type (Laskin et al., 2011). M1 macrophages predominantly secrete pro-inflammatory factors such as tumor necrosis factor alpha (TNF-α), IL-6, and IL-1β (Gordon, 2003,2007), all of which have been shown to be expressed at elevated levels in the PF, serum, and ectopic lesions of patients with EMs (Bergqvist et al., 2001; Richter et al., 2005; Cho et al., 2007; Wang F. et al., 2018; Wang X. M. et al., 2018; Jaeger-Lansky et al., 2018; Volpato et al., 2018). M2 macrophages mainly secrete transforming growth factor beta (TGF-β), interleukin-10 (IL-10), and other anti-inflammatory cytokines, while inhibiting the production of pro-inflammatory cytokines (Wang et al., 2019; Yao et al., 2019; Gao et al., 2022). In endometriotic lesions, M2-type macrophages are predominant (Bacci et al., 2009; Hogg et al., 2020); however, their numbers become significantly reduced throughout the menstrual cycle in patients with EMs compared with the changes observed in healthy controls in the same time period (Takebayashi et al., 2015). There have been reports suggesting that anti-inflammatory factors may play a dual role in the later stage of EMs, as they can promote the immune escape of ectopic endometrial cells and induce inflammation, while also inhibiting inflammatory responses and reducing disease activity; however, further studies are required to establish a better understanding of their roles in EMs (Zhou et al., 2019). What is known is that NF-κB, a major regulator of inflammation and immune responses, can stimulate LPS-induced pro-inflammatory cytokine expression in macrophages (Monaco and Paleolog, 2004). NF-κB is overactive in endometriotic lesions, enhancing the proliferation, adhesion, migration, and invasive ability of ectopic endometrial cells (Liu et al., 2022).

Reduced serum levels of adiponectin have been reported to be associated with chronic inflammation in various metabolic diseases, including type 2 diabetes, obesity, atherosclerosis, and non-alcoholic fatty liver disease, where the anti-inflammatory effects of adiponectin have been demonstrated (Fantuzzi, 2008; Achari and Jain, 2017; Choi et al., 2020). The anti-inflammatory effects of adiponectin are mainly mediated via the targeting of macrophages (Tsatsanis et al., 2005; Ohashi et al., 2014; Fang and Judd, 2018), which can suppress the growth of myelomonocytic progenitor cell as well as the function of mature macrophages, hindering their phagocytotic ability and lowering TNF-α production, as well as reducing the expression levels of class A scavenger receptors, as well as reducing the expression levels of class A scavenger receptors (Yokota et al., 2000; Ouchi et al., 2001). Adiponectin inhibits the progression of various metabolic and cardiovascular diseases by promoting the transition of macrophages from the pro-inflammatory M1 phenotype to the anti-inflammatory M2 phenotype (Ohashi et al., 2010). In humans, the adiponectin-induced differentiation of monocytes into anti-inflammatory M2-type macrophages is mediated via PPAR-α, and these M2 macrophages inhibit the secretion of pro-inflammatory molecules from M1 macrophages, which may contribute to the stability of atherosclerotic plaques (Lovren et al., 2010). Although adiponectin can affect macrophage function through multiple other signaling pathways as well, the main targets are the AdipoR1/Toll/NF-κB and AdipoR2/IL-4/STAT6 signaling pathways, which inhibit effects on macrophage activation to the M1 phenotype and promote macrophage polarization toward the M2 phenotype, respectively (Yamaguchi et al., 2005; Mandal et al., 2011; Wang N. et al., 2014). Other researchers have discovered that adiponectin can attenuate LPS-induced TNF-α and IL-6 production by macrophages while upregulating the expression of anti-inflammatory IL-10 (Wulster-Radcliffe et al., 2004). Several studies have demonstrated that adiponectin expression is also negatively regulated by pro-inflammatory TNF-α and IL-6, which may contribute to the presence of hypoadiponectinemia in inflammatory diseases (Tilg and Wolf, 2005; Brezovec et al., 2021). Furthermore, adiponectin effectively inhibits the activation of the NF-κB pathway by suppressing the expression of the NF-κB nuclear protein p65, which, in turn, reduces the expression of NF-κB-regulated pro-inflammatory factors and potently attenuates the inflammatory response to atherosclerosis (Wang et al., 2016). Within the endometrium, adiponectin plays a similar anti-inflammatory role by stimulating the phosphorylation of AMPK in Endometrial cells and inhibiting the IL-1β-induced secretion of the pro-inflammatory factors IL-6, IL-8, and MCP-1 (Takemura et al., 2006). These anti-inflammatory effects of adiponectin in Endometrial cells may be associated with endometrium-related events, such as endometrial implantation and the pathogenesis of EMs.

Although adiponectin is generally considered an anti-inflammatory adipokine, at high expression levels, it is positively correlated with the clinical progression of systemic autoimmune rheumatic diseases (SARDs), which are typically accompanied by high levels of inflammation; paradoxically, some studies have reported low expression levels of adiponectin in SARDs, with low levels of inflammation and a negative correlation with disease progression (Brezovec et al., 2021). Some recent studies have also

shown that adiponectin can act as an inducer of pro-inflammatory factors and that elevated levels of adiponectin may exacerbate the inflammatory response associated with various autoimmune diseases such as RA, osteoarthritis (OA), systemic lupus erythematosus, and inflammatory bowel diseases (Choi et al., 2020; Brezovec et al., 2021). Others have also found that HMW adiponectin promotes the secretion of TNF-α and IL-6 by fibroblasts from fibroblastic synoviocytes in patients with RA, aggravating the severity of inflammation (Kontny et al., 2015; Li et al., 2015; Liu et al., 2020). In OA, adiponectin has been shown to promote IL-8 secretion in osteoblasts, thereby affecting osteophyte development (Junker et al., 2017). In addition, others have reported than adiponectin can enhance the mRNA expression and protein secretion of IL-8 in human colonic epithelial and macrophage cell lines (Peng et al., 2018). Furthermore, globular adiponectin was shown to be capable of activating the NF-κB pathway and upregulating the expression of pro-inflammatory cytokines in human placenta and adipose tissue (Lappas et al., 2005), HUVECs (Hattori et al., 2006), and RAW264.7 murine macrophages (Lee et al., 2018).

Adiponectin can participate in the inflammatory response of many diseases by regulating macrophage polarization and proliferation and signaling pathways, such as NF-κB and AMPK, as well as the expression of related inflammatory mediators. However, depending on its isoforms and effector tissues, adiponectin may exert differential effects in various physiological processes (Choi et al., 2020), and its bidirectional regulatory function in inflammatory diseases may be related to the severity and stage of disease progression. Further studies is requires to determine whether adiponectin could inhibit the inflammatory response in EMs by regulating signaling pathways, such as NF-κB and AMPK, as well as the expression of related inflammatory mediators and macrophage polarization and proliferation. Moreover, whether adiponectin plays different roles, such as inhibiting or promoting inflammation depending on the severity and progression of EMs, needs to be established.

5.4 Fibrogenesis

Over time, ectopic endometrial cells gradually form ectopic lesions through migration, invasion, proliferation, and growth. The lesions undergo repeated bleeding and injury, triggering a recurrent cycle of inflammatory responses and tissue repair (Garcia et al., 2023). Dysregulated repair mechanisms result in excessive accumulation of extracellular matrix, leading to the formation of adhesions, permanent scarring, and the disruption of tissue structure, causing organ dysfunction and ultimately resulting in fibrosis of the endometriotic tissue. Immune cells migrate to the fibrotic region, releasing inflammatory factors, increasing local inflammatory response, and exacerbating the growth and invasion of endometrial cells (Izumi et al., 2018). Fibrosis is inherent in all forms of EMs, and it is associated with painful symptoms, altered tissue function, and impaired fertility in patients with EMs (Eming et al., 2014; Garcia et al., 2023). Fibrosis of ectopic lesions in EMs is an abnormally proliferative disorder that occurs with repeated rupture of the ectopic cyst wall and outflow of the cyst contents, which irritate the adjacent tissues, followed by a localized inflammatory response and fibrosis formation. The histopathological features of ectopic endometriotic lesions are dominated by a large amount of fibrotic tissue, in addition to the endothelial glands and mesenchymal stromal cells (Liu et al., 2018). Fibrogenesis is an important process in the development of EMs; therefore, probing the mechanism underlying fibrogenesis in EMs and finding specific and effective therapeutic targets to inhibit fibrogenesis may be a potential methodology for the treatment of EMs (Vigano et al., 2018). The process of fibrosis in EMs requires the involvement of a variety of cytokines and cells, including macrophages, myofibroblasts, platelets (Kendall and Feghali-Bostwick, 2014; Weiskirchen et al., 2019; Yang and Plotnikov, 2021). Of particular importance is TGF-β, a multipotent cytokine that regulates cell growth, development, differentiation, proliferation, immunomodulation, the maintenance of homeostasis, and fibrosis via its downstream signal transduction pathway (Morikawa et al., 2016). TGF-β1 is a major regulator of tissue repair as well as fibrosis, initiating the collagen accumulation program and mediating the fibrotic process through multiple signaling pathways (Kim K. K. et al., 2018; Hu et al., 2018; Lodyga and Hinz, 2020; Ye and Hu, 2021). Significantly elevated levels of TGF-β1 have been reported in the serum, PF, and ectopic endometrial tissue of patients with EMs (Chang et al., 2017; Gueuvoghlanian-Silva et al., 2018; Sikora et al., 2018). In ovarian EMs, these ectopic endometrial cells secrete TGF-β1 and activate the Smad signaling pathway to disrupt the extracellular matrix and promote fibrosis in the tissue surrounding the ectopic lesions (Shi et al., 2017). The degree of fibrosis in human ovarian EMs (Ding et al., 2020) and superficial peritoneal EMs (Ibrahim et al., 2019) was positively correlated with the expression levels of alpha-smooth muscle actin (α-SMA). Elevated α-SMA expression is a signifier of the transformation of fibroblasts into myofibroblasts, which is a key process of fibrosis (Malmström et al., 2004; Duan et al., 2018).

In recent years, many studies have demonstrated that adiponectin plays a role in preventing fibrosis in a wide range of organs and tissues and that it may represent a potential therapeutic target for the treatment of fibrosis. The anti-fibrotic effects are mediated through the altered signaling of various pathways such as AMPK, PPAR, and TGF-β1/Smad, inhibiting the differentiation of fibroblasts to myofibroblasts and reducing the production as well as the deposition of extracellular matrix. Numerous studies have investigated its mechanism of action in fibrotic diseases of the kidneys (Jing et al., 2020; Zhao D. et al., 2021), liver (Dong et al., 2015; Udomsinprasert et al., 2018), heart (Fujita et al., 2008; Qi et al., 2014), lungs (Kökény et al., 2021; Wang et al., 2022), and skin (Wang et al., 2023), among other organs and systems, confirming its protective effects. Adiponectin was found to be capable of ameliorating tubulointerstitial fibrosis and suppressing angiotensin II-induced secretion of TGF-β1 and fibronectin in human renal mesangial cells, thereby reducing extracellular matrix synthesis (Tan et al., 2015). Additionally, α-SMA expression was shown to be downregulated by adiponectin in the renal cortex of mice with progressive renal injury induced by the administration of deoxycorticosterone acetate and angiotensin II, as well as in the lung tissues of mice with bleomycin-induced idiopathic pulmonary fibrosis (Tian et al., 2018; Wang et al., 2022). Another showed that the administration of the AdipoR agonists JT002, JT003, and JT004 significantly reduced the protein expression

level of α-SMA in hepatic stellate cells and slowed the progression of hepatic fibrosis in mice (Xu et al., 2020).

While most studies to date have reported a protective effect of adiponectin, a few have shown the opposite effect, with adiponectin driving the pathogenesis of fibrosis. For example, one group showed that in mouse bone marrow-derived macrophages, adiponectin activated the AMPK signaling pathway in a time- and dose-dependent manner, induced α-SMA expression, enhanced the production and deposition of extracellular matrix, and promoted the cells' transformation into fibroblasts, which accelerated renal interstitial fibrosis (Yang et al., 2013). Several other researches have suggested an association between high serum levels of adiponectin and renal functional decline (Panduru et al., 2015; Zha et al., 2017).

Low levels of adiponectin are associated with fibrosis. Serum adiponectin levels in patients with non-alcoholic fatty liver disease are an independent predictor of advanced fibrosis and are negatively correlated with the stage of liver fibrosis (Savvidou et al., 2009). A study showed that serum adiponectin levels in patients with hypertension significantly correlated negatively with biomarkers of myocardial fibrosis (Balmaceda et al., 2020). However, some controversial views have been reported (Arvaniti et al., 2008; Korah et al., 2013; Yan et al., 2013). Adiponectin can inhibit fibrogenesis by regulating signaling pathways, such as TGF-β1/Smad, inhibiting α-SMA expression, and reducing the production and deposition of the extracellular matrix. Adiponectin acts as an important protective factor in fibrotic diseases of the liver, kidneys, heart, lungs, and skin, and low serum adiponectin levels may be an indicator of the progression of fibrogenesis. TGF-β1 is highly expressed in EMs, and activation of the Smad signaling pathway by TGF-β1 can promote fibrosis in tissues surrounding ectopic endometriotic lesions. EMs-associated fibrosis is a relatively new area of research, it is necessary to determine whether the low adiponectin levels in patients with EMs are related to the severity of fibrosis in EMs or whether adiponectin plays a protective role in fibrosis of EMs by modulating signaling pathways, such as TGF-β1/Smad.

5.5 Energy metabolism

The peritoneal microenvironment undergoes significant alterations in patients with EMs; these changes are characterized by imbalances in inflammation, hypoxic conditions, and increased oxidative stress (McKinnon et al., 2016; Ito et al., 2017; Lin et al., 2018; Wu M. H. et al., 2019), which can adversely affect mitochondrial respiration and dysfunctional activity in ectopic endometrial cells, leading to metabolic abnormalities (Atkins et al., 2019; Kobayashi et al., 2021b). In order to adapt to the complex environment and meet the energetic needs of proliferating lesions, ectopic endometrial cells regulate the morphology and function of mitochondria by transforming metabolic processes and activating various signaling pathways, such as that of AMPK, promoting mitochondrial energy production and increasing the supply of available energy to meet the growing requirements of diseased tissues; ultimately, these changes promote the migration, invasion and proliferation of ectopic endometrial cells and create an environment that is conducive to the progression of the lesions (Kasvandik et al., 2016; Kobayashi et al., 2021b; Assaf et al., 2022).

Mitochondria are the organelles that produce the energy required to sustain cellular activity by constantly undergoing repeated cycles of fusion and division (Ye et al., 2023). Mitochondrial dysfunction and reduced energy metabolism have been reported in granulosa and ectopic endometrial cells of patients with EMs (Hsu et al., 2015; Kobayashi et al., 2023), and the altered mitochondrial dynamics and morphology increase the survivability of ectopic endometrial cells in hypoxic and oxidative-stress-related environments, thereby facilitating EMS progression (Ye et al., 2023). Oxidative stress is defined as an imbalance between oxidants, such as reactive oxygen species (ROS), and antioxidants, such as the enzyme superoxide dismutase (SOD). ROS are chemically reactive substances that mediate redox signaling and regulate cellular functions; in patients with EMs, they are involved in maintaining the uterine proliferative phenotype of endometrial cells, increasing the likelihood of ectopic tissue invasion and implantation (Cacciottola et al., 2021). It has been shown that the production of endogenous ROS is increased above normal levels in ectopic endometrial cells of patients with EMs (Ngô et al., 2009); this is accompanied by elevated concentrations of oxidative stress markers in the PF, such as advanced oxidation protein products (Santulli et al., 2015). As a consequence of long-term exposure to oxidative stress, the mitochondria of ectopic endometrial cells promote ROS secretion through an elongation mechanism, further exacerbating oxidative stress and forming a vicious circle that promotes the progression of lesions in EMs (Assaf et al., 2022). Plasma SOD activity has been shown to be reduced in patients with EMs, which is an indicator that the antioxidant capacity has been compromised (Prieto et al., 2012).

Maintaining systemic energy homeostasis is an essential function of most adipocyte-derived hormones. Adiponectin is an adipocyte-derived hormone that improves insulin sensitivity in the liver and skeletal muscle. Studies have shown that in addition to insulin sensitization, adiponectin plays an important role in maintaining systemic energy homeostasis (Wang and Scherer, 2016; Fang and Judd, 2018); it can also promote mitochondrial biogenesis and oxidative metabolism in skeletal muscles of both animals and humans (Lee and Shao, 2014), protect the morphology and function of mitochondria, facilitate the restoration of mitochondrial antioxidant capacity, and protect against oxidative damage following traumatic brain injury (Zhang et al., 2022). Another study demonstrated that adiponectin can also prevent neuroinflammation associated with mitochondrial damage, thereby regulating senescence in the brain (He et al., 2023). Furthermore, adiponectin can inhibit oxidative stress by regulating the balance between ROS and SOD, counteracting obesity-related metabolic changes and cardiovascular diseases and protecting the vascular endothelium and myocardium from tissue damage (Matsuda and Shimomura, 2014). Mechanistically, adiponectin was shown to alleviate LPS-induced oxidative stress during the pre-differentiation of adipocytes through modulation of the peroxisome proliferator-activated receptor gamma (PPAR-γ)/Nnat/NF-κB axis, significantly reducing the concentration of ROS and increasing the level of SOD in cells (Yang et al., 2019). It was also shown to inhibit oxidative stress by enhancing SOD activity in the serum of homozygous apolipoprotein E-deficient (ApoE −/−) mice, thereby reducing the formation of atherosclerotic plaques (Wang X. et al., 2014). In mouse hepatocytes and podocytes, adiponectin was

shown to inhibit palmitic acid-induced ROS secretion and protect against liver and kidney injury (Dong et al., 2020; Xu et al., 2021).

However, a small number of studies have reported contradictory findings; for example, one group showed that adiponectin inhibits SOD activity and promotes ROS secretion in rat RINm insulinoma cells, but without reaching pathological concentrations (Chetboun et al., 2012), and others have reported that full-length adiponectin inhibits ROS production in human phagocytes, whereas globular adiponectin exerts the opposite effect (Chedid et al., 2012). The discrepant results of these studies suggest that adiponectin can modulate oxidate stress in a differential manner depending on the isoform.

Studies have shown that adiponectin can protect the morphology and function of the mitochondria, regulate the balance of ROS and SOD, and inhibit oxidative stress. Increased oxidative stress, mitochondrial dysfunction, and other abnormalities in energy metabolism in EMs increase the survival of ectopic endometrial cells; therefore, adiponectin may regulate energy metabolism in Endometrial cells in the microenvironment of the ectopic lesions to affect the ability of Endometrial cells to proliferate, migrate, and invade ectopic sites, and thus play a role in the pathogenesis of EMs; however, the specific mechanism requires further research.

5.6 Synthesis, metabolism, and effects of estrogen

EMs is an estrogen-dependent disease (Soares et al., 2012) and is characterized by estrogen-dependent growth of the ectopic endometrium and increased local estrogen secretion (Mori et al., 2019). Estrogen is mainly secreted by the ovarian granulosa and endothelial cells and includes three main types: estrone, estradiol (E2), and estriol, of which E2 has the highest expression and plays the greatest role (Mahboobifard et al., 2022). Aromatase P450, an important enzyme in the synthesis of estrogen, catalyzes the conversion of androstenedione and testosterone produced in ovarian follicular cells to estrone and E2 in ovarian granulosa cells, and its expression is increased in endometriotic lesions (Peitsidis et al., 2023). Aromatase inhibitors, such as anastrozole, letrozole, and exemestane, may be effective agents for the treatment of EMs, as they have the potential to control the symptoms associated with EMs in cases where no therapeutic response was achieved with an initial pharmacological intervention (Soares et al., 2012; Peitsidis et al., 2023). Estrogen plays a biological role by binding to ER. ERα expression is downregulated, and ERβ expression is abnormally high in ectopic endometrial cells compared with normal Endometrial cells. Moreover, ERβ can directly inhibit ERα expression (Monsivais et al., 2014; Yilmaz and Bulun, 2019). Localized high estrogenic environment and abnormally high ERβ levels promote ectopic endometrial cells proliferation, adhesion, and angiogenesis, as well as upregulated expression and release of pro-inflammatory factors, leading to immune dysfunction and enhancement of mitochondrial biosynthesis, which provides favorable conditions for lesion progression (Monsivais et al., 2016; Wu L. et al., 2019; Xu Z. et al., 2019; Marquardt et al., 2019; Qi et al., 2020; Kobayashi et al., 2021a).

Serum HMW adiponectin is negatively correlated with E2 concentrations in healthy premenopausal women (Merki-Feld et al., 2011), and this negative correlation may be related to the strong association between adiponectin and sex hormone-binding globulin (SHBG) (Tworoger et al., 2007). There is a significant positive correlation between serum adiponectin levels and SHBG levels (Tworoger et al., 2007; Wildman et al., 2013). SHBG can bind to estrogen in the plasma and directly regulate the bioavailability of estrogen and its access to target cells (Fortunati et al., 2010), whereas increased insulin resistance leads to inhibition of SHBG expression, which in turn leads to an increase in the concentration of biologically active estrogen (Hammond et al., 2008; Caselli, 2014; Winters et al., 2014). Adiponectin may counteract the inhibitory effect of SHBG by ameliorating insulin resistance. In addition, AdipoRon can activate the AMPK and PPAR-α pathways in human luteinized granulosa cells, down-regulating cyclic adenosine monophosphate production and aromatase protein expression, thereby reducing E2 production (Grandhaye et al., 2021). Similarly, Tao et al. found that in polycystic ovary syndrome disease, adiponectin downregulates P450 aromatase expression in human luteal granulosa cells and human chorionic gonadotropin-induced E2 synthesis, at least in part, through the activation of PPAR-α (Tao et al., 2019). A large number of studies have now demonstrated the correlation between low adiponectin levels and an increased risk of developing estrogen-dependent diseases (including cervical, endometrial, and breast cancers, as well as uterine fibroids) (Gelsomino et al., 2019; Strzałkowska et al., 2021). For example, Vivian et al. found that adiponectin inhibits the effects of estrogen on breast cancer cell proliferation by decreasing aromatase activity and ER mRNA levels (Morad et al., 2014). Low adiponectin levels are present in female patients with uterine fibroids, and adiponectin may inhibit smooth muscle tumor growth by lowering estrogen levels through the inhibition of the E2/ERα and insulin-like growth factor 1/insulin-like growth factor 1 receptor pathways (Strzałkowska et al., 2021).

The above studies revealed that adiponectin influences the synthesis, metabolism, and effects of estrogen by inhibiting aromatase expression and estrogen production through the regulation of AMPK and PPAR-α signaling pathways. Adiponectin may play a role in estrogen-dependent diseases by influencing insulin- and estrogen-dependent pathways. Studies have shown that there are high estrogen and low level of adiponectin expression in ectopic endometriotic lesions, and the regulatory effects of adiponectin on estrogen and estrogen receptor may be related to a series of pathogenetic processes, such as proliferation, adhesion, and invasion of ectopic endothelial cells.

6 Discussion

Most studies that have investigated the function of adiponectin have primarily been based on rodents and cellular modeling. Many of the effects of adiponectin appear to be paradoxicales with adiponectin, such as its proven ability to increase systemic insulin sensitivity, however, insulin resistance can also occur at high adiponectin levels (Kalkman, 2021). In some highly inflammatory diseases, serum adiponectin levels are high and are positively correlated with disease progression, while low adiponectin

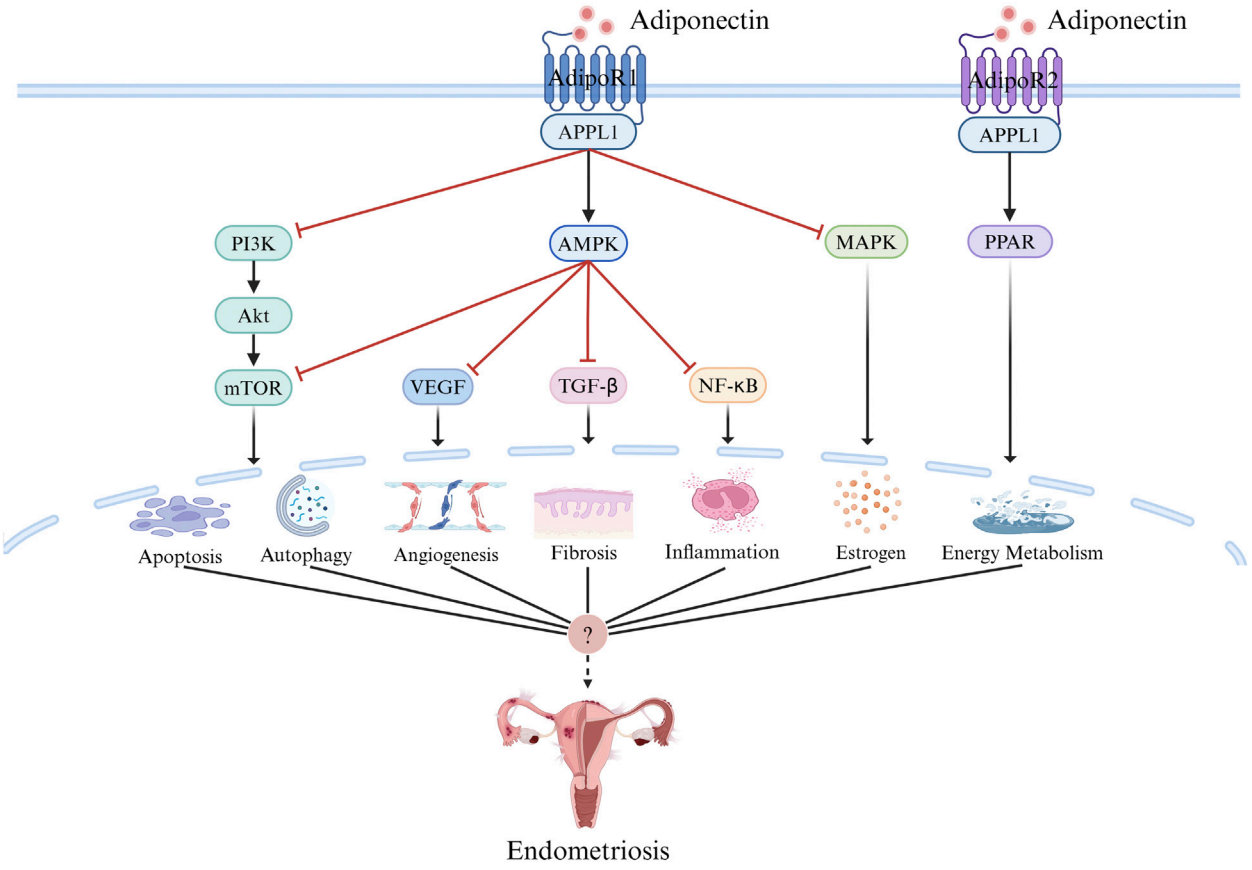

FIGURE 3
Adiponectin Signaling. Adiponectin signal transduction mainly depends on receptor ligand interaction, in which adiponectin binds to AdipoR1 and AdipoR2, and through AMPK,PPAR, PI3K/AKT, MTOR, MAPK, NF-κB, and other pathways initiate the activation of intracellular signal cascades and play a role in apoptosis, autophagy, inflammation, angiogenesis, fibrosis, energy metabolism, estrogen and other aspects, which may be related to the pathogenesis of endometriosis. Created with BioRender.com.

levels have been observed in some diseases in the absence of pronounced inflammation, with the expression levels being negatively correlated with disease severity (Brezovec et al., 2021). Furthermore, low levels of adiponectin have been shown to be associated with an increased prevalence of diseases such as cardiovascular disease and type 2 diabetes (Fantuzzi, 2008; Achari and Jain, 2017; Choi et al., 2020). However, in some cases, high levels of adiponectin may not be associated with any beneficial effects and may even be harmful (Francischetti et al., 2020). The paradoxes and controversies surrounding the actions of adiponectin must be further investigated.

There is evidence suggesting that low levels of adiponectin may be present in EMs and that they are associated with disease severity, a possibility that is supported by the findings of a recent meta-analysis. Therefore, adiponectin may be a beneficial factor that protects against EMs. However, there are many questions still to answer, including whether there is a clear, specific reduction in the expression level of adiponectin in EMs, whether its expression levels differ at various sites such as in ectopic lesions, PF, and serum, and whether these levels correlate with disease severity. In addition, EMs tends to be accompanied by a low BMI, which has been reported to be negatively correlated with adiponectin levels. However, this does not explain the low BMI and smaller than expected concentrations of adiponectin in many patients with EMs, as suggested by the current research evidence. These paradoxical observations could be related to the fact that the release of adiponectin depends on the quality rather than the quantity of adipose tissue, although this must be investigated further. Additionally, it will be necessary to determine whether there is an optimal window in which the adiponectin concentration protects against EMs, and it is currently unclear whether adiponectin could serve as a clinical and/or biochemical marker of EMs.

Relatively few studies have investigated the role of adiponectin in the pathogenesis of EMs at the clinical and cellular levels, although most have confirmed that adiponectin is an important participant in many biological processes, including apoptosis, autophagy, angiogenesis, inflammatory responses, fibrosis, energy metabolism, and estrogen-mediated effects, and an important correlation has been shown between many factors and their related pathways and the pathogenesis of EMs (Figure 3). However, many unexpected and interesting dual biological functions of adiponectin have been identified, including the bidirectional regulation of apoptosis, inflammation, and angiogenesis, in which there are still many questions that need to be answered. There is currently insufficient

data to definitively conclude whether adiponectin plays a protective role against EMs. The relationship between adiponectin and EMs has many mysteries to be explored, and elucidating its role in the pathogenesis of EMs may provide important insights into the pathogenesis and treatment of EMs.

Author contributions

Y-QZ: Writing–original draft, Writing–review and editing. Y-FR: Writing–original draft, Writing–review and editing. B-BL: Funding acquisition, Supervision, Writing–review and editing. CW: Funding acquisition, Writing–review and editing. BY: Writing–review and editing.

Funding

The author(s) declare that financial support was received for the research, authorship, and/or publication of this article. Supported by the National Natural Science Foundation of China (No. 82104920), the Natural Science Foundation of Shandong Province (No. ZR2021QH129), the Shandong Provincial Key Laboratory of Traditional Chinese Medicine [No. (2022)4].

Conflict of interest

The authors declare that the research was conducted in the absence of any commercial or financial relationships that could be construed as a potential conflict of interest.

Publisher's note

References

Achari, A. E., and Jain, S. K. (2017). Adiponectin, a therapeutic target for obesity, diabetes, and endothelial dysfunction. *Int. J. Mol. Sci.* 18 (6), 1321. doi:10.3390/ijms18061321

Adya, R., Tan, B. K., Chen, J., and Randeva, H. S. (2012). Protective actions of globular and full-length adiponectin on human endothelial cells: novel insights into adiponectin-induced angiogenesis. *J. Vasc. Res.* 49 (6), 534–543. doi:10.1159/000338279

Agic, A., Djalali, S., Diedrich, K., and Hornung, D. (2009). Apoptosis in endometriosis. *Gynecol. Obstet. Invest.* 68 (4), 217–223. doi:10.1159/000235871

Angelidis, G., Dafopoulos, K., Messini, C. I., Valotassiou, V., Tsikouras, P., Vrachnis, N., et al. (2013). The emerging roles of adiponectin in female reproductive system-associated disorders and pregnancy. *Reprod. Sci.* 20 (8), 872–881. doi:10.1177/1933719112468954

Arditi, J. D., Venihaki, M., Karalis, K. P., and Chrousos, G. P. (2007). Antiproliferative effect of adiponectin on MCF7 breast cancer cells: a potential hormonal link between obesity and cancer. *Horm. Metab. Res.* 39 (1), 9–13. doi:10.1055/s-2007-956518

Artemova, D., Vishnyakova, P., Khashchenko, E., Elchaninov, A., Sukhikh, G., and Fatkhudinov, T. (2021). Endometriosis and cancer: exploring the role of macrophages. *Int. J. Mol. Sci.* 22 (10), 5196. doi:10.3390/ijms22105196

Arvaniti, V. A., Thomopoulos, K. C., Tsamandas, A., Makri, M., Psyrogiannis, A., Vafiadis, G., et al. (2008). Serum adiponectin levels in different types of non alcoholic liver disease. Correlation with steatosis, necroinflammation and fibrosis. *Acta Gastroenterol. Belg* 71 (4), 355–360.

Assaf, L., Eid, A. A., and Nassif, J. (2022). Role of AMPK/mTOR, mitochondria, and ROS in the pathogenesis of endometriosis. *Life Sci.* 306, 120805. doi:10.1016/j.lfs.2022.120805

Atkins, H. M., Bharadwaj, M. S., O'Brien Cox, A., Furdui, C. M., Appt, S. E., and Caudell, D. L. (2019). Endometrium and endometriosis tissue mitochondrial energy metabolism in a nonhuman primate model. *Reprod. Biol. Endocrinol.* 17 (1), 70. doi:10.1186/s12958-019-0513-8

Azam, I. N. A., Wahab, N. A., Mokhtar, M. H., Shafiee, M. N., and Mokhtar, N. M. (2022). Roles of microRNAs in regulating apoptosis in the pathogenesis of endometriosis. *Life (Basel)* 12 (9), 1321. doi:10.3390/life12091321

Bacci, M., Capobianco, A., Monno, A., Cottone, L., Di Puppo, F., Camisa, B., et al. (2009). Macrophages are alternatively activated in patients with endometriosis and required for growth and vascularization of lesions in a mouse model of disease. *Am. J. Pathol.* 175 (2), 547–556. doi:10.2353/ajpath.2009.081011

Backonja, U., Buck Louis, G. M., and Lauver, D. R. (2016). Overall adiposity, adipose tissue distribution, and endometriosis: a systematic review. *Nurs. Res.* 65 (2), 151–166. doi:10.1097/nnr.0000000000000146

Balmaceda, J. B., Abd-Elmoniem, K. Z., Liu, C. Y., Purdy, J. B., Ouwerkerk, R., Matta, J. R., et al. (2020). Brief report: adiponectin levels linked to subclinical myocardial fibrosis in HIV. *J. Acquir Immune Defic. Syndr.* 85 (3), 316–319. doi:10.1097/qai.0000000000002440

Barbe, A., Bongrani, A., Mellouk, N., Estienne, A., Kurowska, P., Grandhaye, J., et al. (2019). Mechanisms of adiponectin action in fertility: an overview from gametogenesis to gestation in humans and animal models in normal and pathological conditions. *Int. J. Mol. Sci.* 20 (7), 1526. doi:10.3390/ijms20071526

Bergqvist, A., Bruse, C., Carlberg, M., and Carlström, K. (2001). Interleukin 1beta, interleukin-6, and tumor necrosis factor-alpha in endometriotic tissue and in endometrium. *Fertil. Steril.* 75 (3), 489–495. doi:10.1016/s0015-0282(00)01752-0

Bohlouli, S., Khazaei, M., Teshfam, M., and Hassanpour, H. (2013). Adiponectin effect on the viability of human endometrial stromal cells and mRNA expression of adiponectin receptors. *Int. J. Fertil. Steril.* 7 (1), 43–48.

Bohlouli, S., Rabzia, A., Sadeghi, E., Chobsaz, F., and Khazaei, M. (2016). *In vitro* anti-proliferative effect of adiponectin on human endometriotic stromal cells through AdipoR1 and AdipoR2 gene receptor expression. *Iran. Biomed. J.* 20 (1), 12–17. doi:10.7508/ibj.2016.01.002

Bora, G., and Yaba, A. (2021). The role of mitogen-activated protein kinase signaling pathway in endometriosis. *J. Obstet. Gynaecol. Res.* 47 (5), 1610–1623. doi:10.1111/jog.14710

Bourlev, V., Iljasova, N., Adamyan, L., Larsson, A., and Olovsson, M. (2010). Signs of reduced angiogenic activity after surgical removal of deeply infiltrating endometriosis. *Fertil. Steril.* 94 (1), 52–57. doi:10.1016/j.fertnstert.2009.02.019

Bråkenhielm, E., Veitonmäki, N., Cao, R., Kihara, S., Matsuzawa, Y., Zhivotovsky, B., et al. (2004). Adiponectin-induced antiangiogenesis and antitumor activity involve caspase-mediated endothelial cell apoptosis. *Proc. Natl. Acad. Sci. U. S. A.* 101 (8), 2476–2481. doi:10.1073/pnas.0308671100

Brezovec, N., Perdan-Pirkmajer, K., Čučnik, S., Sodin-Šemrl, S., Varga, J., and Lakota, K. (2021). Adiponectin deregulation in systemic autoimmune rheumatic diseases. *Int. J. Mol. Sci.* 22 (8), 4095. doi:10.3390/ijms22084095

Brooks, N. L., Moore, K. S., Clark, R. D., Perfetti, M. T., Trent, C. M., and Combs, T. P. (2007). Do low levels of circulating adiponectin represent a biomarker or just another risk factor for the metabolic syndrome? *Diabetes Obes. Metab.* 9 (3), 246–258. doi:10.1111/j.1463-1326.2006.00596.x

Bulun, S. E., Yilmaz, B. D., Sison, C., Miyazaki, K., Bernardi, L., Liu, S., et al. (2019). Endometriosis. *Endocr. Rev.* 40 (4), 1048–1079. doi:10.1210/er.2018-00242

Burney, R. O., and Giudice, L. C. (2012). Pathogenesis and pathophysiology of endometriosis. *Fertil. Steril.* 98 (3), 511–519. doi:10.1016/j.fertnstert.2012.06.029

Cacciottola, L., Donnez, J., and Dolmans, M. M. (2021). Can endometriosis-related oxidative stress pave the way for new treatment targets? *Int. J. Mol. Sci.* 22 (13), 7138. doi:10.3390/ijms22137138

Cai, L., Xu, S., Piao, C., Qiu, S., Li, H., and Du, J. (2016). Adiponectin induces CXCL1 secretion from cancer cells and promotes tumor angiogenesis by inducing stromal fibroblast senescence. *Mol. Carcinog.* 55 (11), 1796–1806. doi:10.1002/mc.22428

Cakmak, H., Seval-Celik, Y., Arlier, S., Guzeloglu-Kayisli, O., Schatz, F., Arici, A., et al. (2018). p38 mitogen-activated protein kinase is involved in the pathogenesis of endometriosis by modulating inflammation, but not cell survival. *Reprod. Sci.* 25 (4), 587–597. doi:10.1177/1933719117725828

Caminos, J. E., Nogueiras, R., Gallego, R., Bravo, S., Tovar, S., García-Caballero, T., et al. (2005). Expression and regulation of adiponectin and receptor in human and rat placenta. *J. Clin. Endocrinol. Metab.* 90 (7), 4276–4286. doi:10.1210/jc.2004-0930

Caselli, C. (2014). Role of adiponectin system in insulin resistance. *Mol. Genet. Metab.* 113 (3), 155–160. doi:10.1016/j.ymgme.2014.09.003

Chang, K. K., Liu, L. B., Jin, L. P., Zhang, B., Mei, J., Li, H., et al. (2017). IL-27 triggers IL-10 production in Th17 cells via a c-Maf/RORγt/Blimp-1 signal to promote the progression of endometriosis. *Cell Death Dis.* 8 (3), e2666. doi:10.1038/cddis.2017.95

Chantalat, E., Valera, M. C., Vaysse, C., Noirrit, E., Rusidze, M., Weyl, A., et al. (2020). Estrogen receptors and endometriosis. *Int. J. Mol. Sci.* 21 (8), 2815. doi:10.3390/ijms21082815

Che, N., Sun, X., Gu, L., Wang, X., Shi, J., Sun, Y., et al. (2021). Adiponectin enhances B-cell proliferation and differentiation via activation of akt1/STAT3 and exacerbates collagen-induced arthritis. *Front. Immunol.* 12, 626310. doi:10.3389/fimmu.2021.626310

Chedid, P., Hurtado-Nedelec, M., Marion-Gaber, B., Bournier, O., Hayem, G., Gougerot-Pocidalo, M. A., et al. (2012). Adiponectin and its globular fragment differentially modulate the oxidative burst of primary human phagocytes. *Am. J. Pathol.* 180 (2), 682–692. doi:10.1016/j.ajpath.2011.10.013

Chetboun, M., Abitbol, G., Rozenberg, K., Rozenfeld, H., Deutsch, A., Sampson, S. R., et al. (2012). Maintenance of redox state and pancreatic beta-cell function: role of leptin and adiponectin. *J. Cell Biochem.* 113 (6), 1966–1976. doi:10.1002/jcb.24065

Cho, S. H., Oh, Y. J., Nam, A., Kim, H. Y., Park, J. H., Kim, J. H., et al. (2007). Evaluation of serum and urinary angiogenic factors in patients with endometriosis. *Am. J. Reprod. Immunol.* 58 (6), 497–504. doi:10.1111/j.1600-0897.2007.00535.x

Choi, H. M., Doss, H. M., and Kim, K. S. (2020). Multifaceted physiological roles of adiponectin in inflammation and diseases. *Int. J. Mol. Sci.* 21 (4), 1219. doi:10.3390/ijms21041219

Choi, J., Jo, M., Lee, E., Kim, H. J., and Choi, D. (2014). Differential induction of autophagy by mTOR is associated with abnormal apoptosis in ovarian endometriotic cysts. *Mol. Hum. Reprod.* 20 (4), 309–317. doi:10.1093/molehr/gat091

Choi, J., Jo, M., Lee, E., Lee, D. Y., and Choi, D. (2015). Dienogest enhances autophagy induction in endometriotic cells by impairing activation of AKT, ERK1/2, and mTOR. *Fertil. Steril.* 104 (3), 655–664. doi:10.1016/j.fertnstert.2015.05.020

Choi, Y. S., Oh, H. K., and Choi, J. H. (2013). Expression of adiponectin, leptin, and their receptors in ovarian endometrioma. *Fertil. Steril.* 100 (1), 135–141. e1-2. doi:10.1016/j.fertnstert.2013.03.019

Christen, T., Trompet, S., Noordam, R., van Klinken, J. B., van Dijk, K. W., Lamb, H. J., et al. (2018). Sex differences in body fat distribution are related to sex differences in serum leptin and adiponectin. *Peptides* 107, 25–31. doi:10.1016/j.peptides.2018.07.008

Chung, S. J., Nagaraju, G. P., Nagalingam, A., Muniraj, N., Kuppusamy, P., Walker, A., et al. (2017). ADIPOQ/adiponectin induces cytotoxic autophagy in breast cancer cells through STK11/LKB1-mediated activation of the AMPK-ULK1 axis. *Autophagy* 13 (8), 1386–1403. doi:10.1080/15548627.2017.1332565

Cinar, O., Seval, Y., Uz, Y. H., Cakmak, H., Ulukus, M., Kayisli, U. A., et al. (2009). Differential regulation of Akt phosphorylation in endometriosis. *Reprod. Biomed. Online* 19 (6), 864–871. doi:10.1016/j.rbmo.2009.10.001

Clark, J. L., Taylor, C. G., and Zahradka, P. (2017). Exploring the cardio-metabolic relevance of T-cadherin: a pleiotropic adiponectin receptor. *Endocr. Metab. Immune Disord. Drug Targets* 17 (3), 200–206. doi:10.2174/1871530317666170818120224

Cong, L., Gasser, J., Zhao, J., Yang, B., Li, F., and Zhao, A. Z. (2007). Human adiponectin inhibits cell growth and induces apoptosis in human endometrial carcinoma cells, HEC-1-A and RL95 2. *Endocr. Relat. Cancer* 14 (3), 713–720. doi:10.1677/erc-07-0065

Czyzyk, A., Podfigurna, A., Szeliga, A., and Meczekalski, B. (2017). Update on endometriosis pathogenesis. *Minerva Ginecol.* 69 (5), 447–461. doi:10.23736/s0026-4784.17.04048-5

D'Amico, G., Muñoz-Félix, J. M., Pedrosa, A. R., and Hodivala-Dilke, K. M. (2020). Splitting the matrix": intussusceptive angiogenesis meets MT1-MMP. *EMBO Mol. Med.* 12 (2), e11663. doi:10.15252/emmm.201911663

Delort, L., Jardé, T., Dubois, V., Vasson, M. P., and Caldefie-Chézet, F. (2012). New insights into anticarcinogenic properties of adiponectin: a potential therapeutic approach in breast cancer? *Vitam. Horm.* 90, 397–417. doi:10.1016/b978-0-12-398313-8.00015-4

Di Carlo, C., Bonifacio, M., Tommaselli, G. A., Bifulco, G., Guerra, G., and Nappi, C. (2009). Metalloproteinases, vascular endothelial growth factor, and angiopoietin 1 and 2 in eutopic and ectopic endometrium. *Fertil. Steril.* 91 (6), 2315–2323. doi:10.1016/j.fertnstert.2008.03.079

Dieudonne, M. N., Bussiere, M., Dos Santos, E., Leneveu, M. C., Giudicelli, Y., and Pecquery, R. (2006). Adiponectin mediates antiproliferative and apoptotic responses in human MCF7 breast cancer cells. *Biochem. Biophys. Res. Commun.* 345 (1), 271–279. doi:10.1016/j.bbrc.2006.04.076

Díez, J. J., and Iglesias, P. (2003). The role of the novel adipocyte-derived hormone adiponectin in human disease. *Eur. J. Endocrinol.* 148 (3), 293–300. doi:10.1530/eje.0.1480293

Ding, D., Wang, X., Chen, Y., Benagiano, G., Liu, X., and Guo, S. W. (2020). Evidence in support for the progressive nature of ovarian endometriomas. *J. Clin. Endocrinol. Metab.* 105 (7), dgaa189. doi:10.1210/clinem/dgaa189

Dong, Z., Su, L., Esmaili, S., Iseli, T. J., Ramezani-Moghadam, M., Hu, L., et al. (2015). Adiponectin attenuates liver fibrosis by inducing nitric oxide production of hepatic stellate cells. *J. Mol. Med. Berl.* 93 (12), 1327–1339. doi:10.1007/s00109-015-1313-z

Dong, Z., Zhuang, Q., Ye, X., Ning, M., Wu, S., Lu, L., et al. (2020). Adiponectin inhibits NLRP3 inflammasome activation in nonalcoholic steatohepatitis via AMPK-JNK/ErK1/2-nfκb/ROS signaling pathways. *Front. Med. (Lausanne)* 7, 546445. doi:10.3389/fmed.2020.546445

Dos Santos, E., Benaitreau, D., Dieudonne, M. N., Leneveu, M. C., Serazin, V., Giudicelli, Y., et al. (2008). Adiponectin mediates an antiproliferative response in human MDA-MB 231 breast cancer cells. *Oncol. Rep.* 20 (4), 971–977. doi:10.3892/or_00000098

Driva, T. S., Schatz, C., and Haybaeck, J. (2023). Endometriosis-associated ovarian carcinomas: how PI3K/AKT/mTOR pathway affects their pathogenesis. *Biomolecules* 13 (8), 1253. doi:10.3390/biom13081253

Driva, T. S., Schatz, C., Sobočan, M., and Haybaeck, J. (2022). The role of mTOR and eIF signaling in benign endometrial diseases. *Int. J. Mol. Sci.* 23 (7), 3416. doi:10.3390/ijms23073416

Duan, J., Liu, X., Wang, H., and Guo, S. W. (2018). The M2a macrophage subset may be critically involved in the fibrogenesis of endometriosis in mice. *Reprod. Biomed. Online* 37 (3), 254–268. doi:10.1016/j.rbmo.2018.05.017

Duan, R., Wang, Y., Lin, A., Lian, L., Cao, H., Gu, W., et al. (2020a). Expression of nm23-H1, p53, and integrin β1 in endometriosis and their clinical significance. *Int. J. Clin. Exp. Pathol.* 13 (5), 1024–1029.

Duan, Z. X., Tu, C., Liu, Q., Li, S. Q., Li, Y. H., Xie, P., et al. (2020b). Adiponectin receptor agonist AdipoRon attenuates calcification of osteoarthritis chondrocytes by promoting autophagy. *J. Cell Biochem.* 121 (5-6), 3333–3344. doi:10.1002/jcb.29605

Dubois, V., Delort, L., Billard, H., Vasson, M. P., and Caldefie-Chezet, F. (2013). Breast cancer and obesity: *in vitro* interferences between adipokines and proangiogenic features and/or antitumor therapies? *PLoS One* 8 (3), e58541. doi:10.1371/journal.pone.0058541

Eming, S. A., Martin, P., and Tomic-Canic, M. (2014). Wound repair and regeneration: mechanisms, signaling, and translation. *Sci. Transl. Med.* 6 (265), 265sr6. doi:10.1126/scitranslmed.3009337

Encalada Soto, D., Rassier, S., Green, I. C., Burnett, T., Khan, Z., and Cope, A. (2022). Endometriosis biomarkers of the disease: an update. *Curr. Opin. Obstet. Gynecol.* 34 (4), 210–219. doi:10.1097/gco.0000000000000798

Fang, H., and Judd, R. L. (2018). Adiponectin regulation and function. *Compr. Physiol.* 8 (3), 1031–1063. doi:10.1002/cphy.c170046

Fantuzzi, G. (2008). Adiponectin and inflammation: consensus and controversy. *J. Allergy Clin. Immunol.* 121 (2), 326–330. doi:10.1016/j.jaci.2007.10.018

Farland, L. V., Missmer, S. A., Bijon, A., Gusto, G., Gelot, A., Clavel-Chapelon, F., et al. (2017). Associations among body size across the life course, adult height and endometriosis. *Hum. Reprod.* 32 (8), 1732–1742. doi:10.1093/humrep/dex207

Ferrara, N., and Adamis, A. P. (2016). Ten years of anti-vascular endothelial growth factor therapy. *Nat. Rev. Drug Discov.* 15 (6), 385–403. doi:10.1038/nrd.2015.17

Fisslthaler, B., and Fleming, I. (2009). Activation and signaling by the AMP-activated protein kinase in endothelial cells. *Circ. Res.* 105 (2), 114–127. doi:10.1161/circresaha.109.201590

Fortunati, N., Catalano, M. G., Boccuzzi, G., and Frairia, R. (2010). Sex Hormone-Binding Globulin (SHBG), estradiol and breast cancer. *Mol. Cell Endocrinol.* 316 (1), 86–92. doi:10.1016/j.mce.2009.09.012

Francischetti, E. A., Dezonne, R. S., Pereira, C. M., de Moraes Martins, C. J., Celoria, B. M. J., de Oliveira, P. A. C., et al. (2020). Insights into the controversial aspects of adiponectin in cardiometabolic disorders. *Horm. Metab. Res.* 52 (10), 695–707. doi:10.1055/a-1239-4349

Frederiksen, L., Højlund, K., Hougaard, D. M., Mosbech, T. H., Larsen, R., Flyvbjerg, A., et al. (2012). Testosterone therapy decreases subcutaneous fat and adiponectin in aging men. *Eur. J. Endocrinol.* 166 (3), 469–476. doi:10.1530/eje-11-0565

Fruebis, J., Tsao, T. S., Javorschi, S., Ebbets-Reed, D., Erickson, M. R., Yen, F. T., et al. (2001). Proteolytic cleavage product of 30-kDa adipocyte complement-related protein increases fatty acid oxidation in muscle and causes weight loss in mice. *Proc. Natl. Acad. Sci. U. S. A.* 98 (4), 2005–2010. doi:10.1073/pnas.041591798

Fujita, K., Maeda, N., Sonoda, M., Ohashi, K., Hibuse, T., Nishizawa, H., et al. (2008). Adiponectin protects against angiotensin II-induced cardiac fibrosis through activation of PPAR-alpha. *Arterioscler. Thromb. Vasc. Biol.* 28 (5), 863–870. doi:10.1161/atvbaha.107.156687

Gao, J., Liang, Y., and Wang, L. (2022). Shaping polarization of tumor-associated macrophages in cancer immunotherapy. *Front. Immunol.* 13, 888713. doi:10.3389/fimmu.2022.888713

Gao, Q., Zheng, J., Yao, X., and Peng, B. (2015). Adiponectin inhibits VEGF-A in prostate cancer cells. *Tumour Biol.* 36 (6), 4287–4292. doi:10.1007/s13277-015-3067-1

Gao, Y., Liu, P., and Shi, R. (2020). Anlotinib as a molecular targeted therapy for tumors. *Oncol. Lett.* 20 (2), 1001–1014. doi:10.3892/ol.2020.11685

Garcia, J. M., Vannuzzi, V., Donati, C., Bernacchioni, C., Bruni, P., and Petraglia, F. (2023). Endometriosis: cellular and molecular mechanisms leading to fibrosis. *Reprod. Sci.* 30 (5), 1453–1461. doi:10.1007/s43032-022-01083-x

Gavrila, A., Peng, C. K., Chan, J. L., Mietus, J. E., Goldberger, A. L., and Mantzoros, C. S. (2003). Diurnal and ultradian dynamics of serum adiponectin in healthy men: comparison with leptin, circulating soluble leptin receptor, and cortisol patterns. *J. Clin. Endocrinol. Metab.* 88 (6), 2838–2843. doi:10.1210/jc.2002-021721

Ge, Y., Zhou, M., Chen, C., Wu, X., and Wang, X. (2022). Role of AMPK mediated pathways in autophagy and aging. *Biochimie* 195, 100–113. doi:10.1016/j.biochi.2021.11.008

Gelsomino, L., Naimo, G. D., Catalano, S., Mauro, L., and Andò, S. (2019). The emerging role of adiponectin in female malignancies. *Int. J. Mol. Sci.* 20 (9), 2127. doi:10.3390/ijms20092127

Goetz, T. G., Mamillapalli, R., and Taylor, H. S. (2016). Low body mass index in endometriosis is promoted by hepatic metabolic gene dysregulation in mice. *Biol. Reprod.* 95 (6), 115. doi:10.1095/biolreprod.116.142877

Gordon, S. (2003). Alternative activation of macrophages. *Nat. Rev. Immunol.* 3 (1), 23–35. doi:10.1038/nri978

Gordon, S. (2007). The macrophage: past, present and future. *Eur. J. Immunol.* 37 (Suppl. 1), S9–S17. doi:10.1002/eji.200737638

Grandhaye, J., Hmadeh, S., Plotton, I., Levasseur, F., Estienne, A., LeGuevel, R., et al. (2021). The adiponectin agonist, AdipoRon, inhibits steroidogenesis and cell proliferation in human luteinized granulosa cells. *Mol. Cell Endocrinol.* 520, 111080. doi:10.1016/j.mce.2020.111080

Gueuvoghlanian-Silva, B. Y., Bellelis, P., Barbeiro, D. F., Hernandes, C., and Podgaec, S. (2018). Treg and NK cells related cytokines are associated with deep rectosigmoid endometriosis and clinical symptoms related to the disease. *J. Reprod. Immunol.* 126, 32–38. doi:10.1016/j.jri.2018.02.003

Guo, J., Zhu, K., Li, Z., and Xiao, C. (2022). Adiponectin protects hypoxia/reoxygenation-induced cardiomyocyte injury by suppressing autophagy. *J. Immunol. Res.* 2022, 8433464. doi:10.1155/2022/8433464

Guo, Z., and Yu, Q. (2019). Role of mTOR signaling in female reproduction. *Front. Endocrinol. (Lausanne)* 10, 692. doi:10.3389/fendo.2019.00692

Hammond, G. L., Hogeveen, K. N., Visser, M., and Coelingh Bennink, H. J. (2008). Estetrol does not bind sex hormone binding globulin or increase its production by human HepG2 cells. *Climacteric* 11 (Suppl. 1), 41–46. doi:10.1080/13697130701851814

Handelsman, D. J., Hirschberg, A. L., and Bermon, S. (2018). Circulating testosterone as the hormonal basis of sex differences in athletic performance. *Endocr. Rev.* 39 (5), 803–829. doi:10.1210/er.2018-00020

Hattori, Y., Hattori, S., and Kasai, K. (2006). Globular adiponectin activates nuclear factor-kappaB in vascular endothelial cells, which in turn induces expression of proinflammatory and adhesion molecule genes. *Diabetes Care* 29 (1), 139–141. doi:10.2337/diacare.29.1.139

He, K., Nie, L., Ali, T., Liu, Z., Li, W., Gao, R., et al. (2023). Adiponectin deficiency accelerates brain aging via mitochondria-associated neuroinflammation. *Immun. Ageing* 20 (1), 15. doi:10.1186/s12979-023-00339-7

He, K., Nie, L., Ali, T., Wang, S., Chen, X., Liu, Z., et al. (2021). Adiponectin alleviated Alzheimer-like pathologies via autophagy-lysosomal activation. *Aging Cell* 20 (12), e13514. doi:10.1111/acel.13514

Hirakawa, T., Nasu, K., Aoyagi, Y., Takebayashi, K., and Narahara, H. (2017). Arcyriaflavin a, a cyclin D1-cyclin-dependent kinase4 inhibitor, induces apoptosis and inhibits proliferation of human endometriotic stromal cells: a potential therapeutic agent in endometriosis. *Reprod. Biol. Endocrinol.* 15 (1), 53. doi:10.1186/s12958-017-0272-3

Hogg, C., Horne, A. W., and Greaves, E. (2020). Endometriosis-associated macrophages: origin, phenotype, and function. *Front. Endocrinol. (Lausanne)* 11, 7. doi:10.3389/fendo.2020.00007

Holdsworth-Carson, S. J., Chung, J., Sloggett, C., Mortlock, S., Fung, J. N., Montgomery, G. W., et al. (2020). Obesity does not alter endometrial gene expression in women with endometriosis. *Reprod. Biomed. Online* 41 (1), 113–118. doi:10.1016/j.rbmo.2020.03.015

Holdsworth-Carson, S. J., Dior, U. P., Colgrave, E. M., Healey, M., Montgomery, G. W., Rogers, P. A. W., et al. (2018). The association of body mass index with endometriosis and disease severity in women with pain. *J. Endometr. Pelvic Pain Disord.* 10 (2), 79–87. doi:10.1177/2284026518773939

Holdsworth-Carson, S. J., and Rogers, P. A. W. (2018). The complex relationship between body mass index and endometriosis. *J. Endometr. Pelvic Pain Disord.* 10 (4), 187–189. doi:10.1177/2284026518810586

Hsu, A. L., Townsend, P. M., Oehninger, S., and Castora, F. J. (2015). Endometriosis may be associated with mitochondrial dysfunction in cumulus cells from subjects undergoing *in vitro* fertilization-intracytoplasmic sperm injection, as reflected by decreased adenosine triphosphate production. *Fertil. Steril.* 103 (2), 347–352. doi:10.1016/j.fertnstert.2014.11.002

Hu, E., Liang, P., and Spiegelman, B. M. (1996). AdipoQ is a novel adipose-specific gene dysregulated in obesity. *J. Biol. Chem.* 271 (18), 10697–10703. doi:10.1074/jbc.271.18.10697

Hu, H. H., Chen, D. Q., Wang, Y. N., Feng, Y. L., Cao, G., Vaziri, N. D., et al. (2018). New insights into TGF-β/Smad signaling in tissue fibrosis. *Chem. Biol. Interact.* 292, 76–83. doi:10.1016/j.cbi.2018.07.008

Huang, H. Y., Zhang, F. L., Zhang, T. Y., Yan, Z. H., and Huang, H. (2011). Expression and significance of resistin and adiponectin in peritoneal fluid of patients with endometriosis. *Guangdong Med. J.* 32, 2007–2009. doi:10.13820/j.cnki.gdyx.2011.15.047

Huang, Z. X., He, X. R., Ding, X. Y., Chen, J. H., Lei, Y. H., Bai, J. B., et al. (2023). Lipoxin A4 depresses inflammation and promotes autophagy via AhR/mTOR/AKT pathway to suppress endometriosis. *Am. J. Reprod. Immunol.* 89 (3), e13659. doi:10.1111/aji.13659

Ibrahim, M. G., Sillem, M., Plendl, J., Taube, E. T., Schüring, A., Götte, M., et al. (2019). Arrangement of myofibroblastic and smooth muscle-like cells in superficial peritoneal endometriosis and a possible role of transforming growth factor beta 1 (TGFβ1) in myofibroblastic metaplasia. *Arch. Gynecol. Obstet.* 299 (2), 489–499. doi:10.1007/s00404-018-4995-y

Ito, F., Yamada, Y., Shigemitsu, A., Akinishi, M., Kaniwa, H., Miyake, R., et al. (2017). Role of oxidative stress in epigenetic modification in endometriosis. *Reprod. Sci.* 24 (11), 1493–1502. doi:10.1177/1933719117704909

Izumi, G., Koga, K., Takamura, M., Makabe, T., Satake, E., Takeuchi, A., et al. (2018). Involvement of immune cells in the pathogenesis of endometriosis. *J. Obstet. Gynaecol. Res.* 44 (2), 191–198. doi:10.1111/jog.13559

Jaeger-Lansky, A., Schmidthaler, K., Kuessel, L., Gstöttner, M., Waidhofer-Söllner, P., Zlabinger, G. J., et al. (2018). Local and systemic levels of cytokines and danger signals in endometriosis-affected women. *J. Reprod. Immunol.* 130, 7–10. doi:10.1016/j.jri.2018.07.006

Ji, X., Huang, C., Mao, H., Zhang, Z., Zhang, X., Yue, B., et al. (2022). Identification of immune- and autophagy-related genes and effective diagnostic biomarkers in endometriosis: a bioinformatics analysis. *Ann. Transl. Med.* 10 (24), 1397. doi:10.21037/atm-22-5979

Jiang, Q. Y., and Wu, R. J. (2012). Growth mechanisms of endometriotic cells in implanted places: a review. *Gynecol. Endocrinol.* 28 (7), 562–567. doi:10.3109/09513590.2011.650662

Jiang, R., Yang, Y., Huang, Q., Jin, Y., Feng, Y., Huang, X., et al. (2020a). Immunohistochemical expression of estrogen receptor α, Bcl-2 and NF-κB P65 in the polyps of patients with and without endometriosis. *J. Obstet. Gynaecol. Res.* 46 (9), 1819–1826. doi:10.1111/jog.14370

Jiang, Y., Li, R., Zhao, Y., Liu, J., Zhu, X., and Jin, L. (2020b). Mechanism of MAPK/ERK1/2 signaling pathway and related proteins on receptor activity of rats with endometriosis. *J. Biol. Regul. Homeost. Agents* 34 (4), 1519–1522. doi:10.23812/20-249-l

Jing, H., Tang, S., Lin, S., Liao, M., Chen, H., Fan, Y., et al. (2020). Adiponectin in renal fibrosis. *Aging (Albany NY)* 12 (5), 4660–4672. doi:10.18632/aging.102811

Junker, S., Frommer, K. W., Krumbholz, G., Tsiklauri, L., Gerstberger, R., Rehart, S., et al. (2017). Expression of adipokines in osteoarthritis osteophytes and their effect on osteoblasts. *Matrix Biol.* 62, 75–91. doi:10.1016/j.matbio.2016.11.005

Kacan, T., Yildiz, C., Baloglu Kacan, S., Seker, M., Ozer, H., and Cetin, A. (2017). Everolimus as an mTOR inhibitor suppresses endometriotic implants: an experimental rat study. *Geburtshilfe Frauenheilkd* 77 (1), 66–72. doi:10.1055/s-0042-115566

Kalkman, H. O. (2021). An explanation for the adiponectin paradox. *Pharm. (Basel)* 14 (12), 1266. doi:10.3390/ph14121266

Kapoor, R., Stratopoulou, C. A., and Dolmans, M. M. (2021). Pathogenesis of endometriosis: new insights into prospective therapies. *Int. J. Mol. Sci.* 22 (21), 11700. doi:10.3390/ijms222111700

Kasvandik, S., Samuel, K., Peters, M., Eimre, M., Peet, N., Roost, A. M., et al. (2016). Deep quantitative proteomics reveals extensive metabolic reprogramming and cancer-like changes of ectopic endometriotic stromal cells. *J. Proteome Res.* 15 (2), 572–584. doi:10.1021/acs.jproteome.5b00965

Kendall, R. T., and Feghali-Bostwick, C. A. (2014). Fibroblasts in fibrosis: novel roles and mediators. *Front. Pharmacol.* 5, 123. doi:10.3389/fphar.2014.00123

Kershaw, E. E., and Flier, J. S. (2004). Adipose tissue as an endocrine organ. *J. Clin. Endocrinol. Metab.* 89 (6), 2548–2556. doi:10.1210/jc.2004-0395

Kiefer, F., and Siekmann, A. F. (2011). The role of chemokines and their receptors in angiogenesis. *Cell Mol. Life Sci.* 68 (17), 2811–2830. doi:10.1007/s00018-011-0677-7

Kiezun, M., Maleszka, A., Smolinska, N., Nitkiewicz, A., and Kaminski, T. (2013). Expression of adiponectin receptors 1 (AdipoR1) and 2 (AdipoR2) in the porcine pituitary during the oestrous cycle. *Reprod. Biol. Endocrinol.* 11, 18. doi:10.1186/1477-7827-11-18

Kim, K. K., Sheppard, D., and Chapman, H. A. (2018a). TGF-β1 signaling and tissue fibrosis. *Cold Spring Harb. Perspect. Biol.* 10 (4), a022293. doi:10.1101/cshperspect.a022293

Kim, S. T., Marquard, K., Stephens, S., Louden, E., Allsworth, J., and Moley, K. H. (2011). Adiponectin and adiponectin receptors in the mouse preimplantation embryo and uterus. *Hum. Reprod.* 26 (1), 82–95. doi:10.1093/humrep/deq292

Kim, Y., Lim, J. H., Kim, M. Y., Kim, E. N., Yoon, H. E., Shin, S. J., et al. (2018b). The adiponectin receptor agonist AdipoRon ameliorates diabetic nephropathy in a model of type 2 diabetes. *J. Am. Soc. Nephrol.* 29 (4), 1108–1127. doi:10.1681/asn.2017060627

Kim, Y., and Park, C. W. (2019). Mechanisms of adiponectin action: implication of adiponectin receptor agonism in diabetic kidney disease. *Int. J. Mol. Sci.* 20 (7), 1782. doi:10.3390/ijms20071782

Kleinmann, N., Duivenvoorden, W. C., Hopmans, S. N., Beatty, L. K., Qiao, S., Gallino, D., et al. (2014). Underactivation of the adiponectin-adiponectin receptor 1 axis in clear cell renal cell carcinoma: implications for progression. *Clin. Exp. Metastasis* 31 (2), 169–183. doi:10.1007/s10585-013-9618-1

Kobayashi, H., Kimura, M., Maruyama, S., Nagayasu, M., and Imanaka, S. (2021a). Revisiting estrogen-dependent signaling pathways in endometriosis: potential targets for non-hormonal therapeutics. *Eur. J. Obstet. Gynecol. Reprod. Biol.* 258, 103–110. doi:10.1016/j.ejogrb.2020.12.044

Kobayashi, H., Matsubara, S., Yoshimoto, C., Shigetomi, H., and Imanaka, S. (2023). The role of mitochondrial dynamics in the pathophysiology of endometriosis. *J. Obstet. Gynaecol. Res.* 49 (12), 2783–2791. doi:10.1111/jog.15791

Kobayashi, H., Shigetomi, H., and Imanaka, S. (2021b). Nonhormonal therapy for endometriosis based on energy metabolism regulation. *Reprod. Fertil.* 2 (4), C42–c57. doi:10.1530/raf-21-0053

Kökény, G., Calvier, L., and Hansmann, G. (2021). PPARγ and tgfβ-major regulators of metabolism, inflammation, and fibrosis in the lungs and kidneys. *Int. J. Mol. Sci.* 22 (19), 10431. doi:10.3390/ijms221910431

Kontny, E., Janicka, I., Skalska, U., and Maśliński, W. (2015). The effect of multimeric adiponectin isoforms and leptin on the function of rheumatoid fibroblast-like synoviocytes. *Scand. J. Rheumatol.* 44 (5), 363–368. doi:10.3109/03009742.2015.1025833

Korah, T. E., El-Sayed, S., Elshafie, M. K., Hammoda, G. E., and Safan, M. A. (2013). Significance of serum leptin and adiponectin levels in Egyptian patients with chronic hepatitis C virus associated hepatic steatosis and fibrosis. *World J. Hepatol.* 5 (2), 74–81. doi:10.4254/wjh.v5.i2.74

Kos, K., Harte, A. L., da Silva, N. F., Tonchev, A., Chaldakov, G., James, S., et al. (2007). Adiponectin and resistin in human cerebrospinal fluid and expression of adiponectin receptors in the human hypothalamus. *J. Clin. Endocrinol. Metab.* 92 (3), 1129–1136. doi:10.1210/jc.2006-1841

Kubo, K., Kamada, Y., Hasegawa, T., Sakamoto, A., Nakatsuka, M., Matsumoto, T., et al. (2021). Inflammation of the adipose tissue in the retroperitoneal cavity adjacent to pelvic endometriosis. *J. Obstet. Gynaecol. Res.* 47 (10), 3598–3606. doi:10.1111/jog.14958

Lamceva, J., Uljanovs, R., and Strumfa, I. (2023). The main theories on the pathogenesis of endometriosis. *Int. J. Mol. Sci.* 24 (5), 4254. doi:10.3390/ijms24054254

Lappas, M., Permezel, M., and Rice, G. E. (2005). Leptin and adiponectin stimulate the release of proinflammatory cytokines and prostaglandins from human placenta and maternal adipose tissue via nuclear factor-kappaB, peroxisomal proliferator-activated receptor-gamma and extracellularly regulated kinase 1/2. *Endocrinology* 146 (8), 3334–3342. doi:10.1210/en.2005-0406

Laskin, D. L., Sunil, V. R., Gardner, C. R., and Laskin, J. D. (2011). Macrophages and tissue injury: agents of defense or destruction? *Annu. Rev. Pharmacol. Toxicol.* 51, 267–288. doi:10.1146/annurev.pharmtox.010909.105812

Lee, B., and Shao, J. (2014). Adiponectin and energy homeostasis. *Rev. Endocr. Metab. Disord.* 15 (2), 149–156. doi:10.1007/s11154-013-9283-3

Lee, H. P., Lin, C. Y., Shih, J. S., Fong, Y. C., Wang, S. W., Li, T. M., et al. (2015). Adiponectin promotes VEGF-A-dependent angiogenesis in human chondrosarcoma through PI3K, Akt, mTOR, and HIF-α pathway. *Oncotarget* 6 (34), 36746–36761. doi:10.18632/oncotarget.5479

Lee, K. H., Jeong, J., Woo, J., Lee, C. H., and Yoo, C. G. (2018). Globular adiponectin exerts a pro-inflammatory effect via IκB/NF-κB pathway activation and anti-inflammatory effect by IRAK-1 downregulation. *Mol. Cells* 41 (8), 762–770. doi:10.14348/molcells.2018.0005

Li, B. T., Zhang, F. Z., Xu, T. S., Ding, R., and Li, P. (2015). Increasing production of matrix metalloproteinases, tumor necrosis factor-α, vascular endothelial growth factor and prostaglandin E2 in rheumatoid arthritis synovial fibroblasts by different adiponectin isoforms in a concentration-dependent manner. *Cell Mol. Biol. (Noisy-le-grand)* 61 (7), 27–32.

Li, M., Lu, M. S., Liu, M. L., Deng, S., Tang, X. H., Han, C., et al. (2018). An observation of the role of autophagy in patients with endometriosis of different stages during secretory phase and proliferative phase. *Curr. Gene Ther.* 18 (5), 286–295. doi:10.2174/1566523218666181008155039

Li, R., Du, J., Yao, Y., Yao, G., and Wang, X. (2019). Adiponectin inhibits high glucose-induced angiogenesis via inhibiting autophagy in RF/6A cells. *J. Cell Physiol.* 234 (11), 20566–20576. doi:10.1002/jcp.28659

Li, W. N., Hsiao, K. Y., Wang, C. A., Chang, N., Hsu, P. L., Sun, C. H., et al. (2020). Extracellular vesicle-associated VEGF-C promotes lymphangiogenesis and immune cells infiltration in endometriosis. *Proc. Natl. Acad. Sci. U. S. A.* 117 (41), 25859–25868. doi:10.1073/pnas.1920037117

Lim, W., Choi, M. J., Bae, H., Bazer, F. W., and Song, G. (2017). A critical role for adiponectin-mediated development of endometrial luminal epithelial cells during the peri-implantation period of pregnancy. *J. Cell Physiol.* 232 (11), 3146–3157. doi:10.1002/jcp.25768

Lin, X., Dai, Y., Xu, W., Shi, L., Jin, X., Li, C., et al. (2018). Hypoxia promotes ectopic adhesion ability of endometrial stromal cells via TGF-β1/smad signaling in endometriosis. *Endocrinology* 159 (4), 1630–1641. doi:10.1210/en.2017-03227

Liu, L., Yan, M., Yang, R., Qin, X., Chen, L., Li, L., et al. (2021). Adiponectin attenuates lipopolysaccharide-induced apoptosis by regulating the Cx43/PI3K/AKT pathway. *Front. Pharmacol.* 12, 644225. doi:10.3389/fphar.2021.644225

Liu, R., Zhao, P., Zhang, Q., Che, N., Xu, L., Qian, J., et al. (2020). Adiponectin promotes fibroblast-like synoviocytes producing IL-6 to enhance T follicular helper cells response in rheumatoid arthritis. *Clin. Exp. Rheumatol.* 38 (1), 11–18.

Liu, S., Xin, X., Hua, T., Shi, R., Chi, S., Jin, Z., et al. (2016). Efficacy of anti-VEGF/VEGFR agents on animal models of endometriosis: a systematic review and meta-analysis. *PLoS One* 11 (11), e0166658. doi:10.1371/journal.pone.0166658

Liu, X., Zhang, Q., and Guo, S. W. (2018). Histological and immunohistochemical characterization of the similarity and difference between ovarian endometriomas and deep infiltrating endometriosis. *Reprod. Sci.* 25 (3), 329–340. doi:10.1177/1933719117718275

Liu, Y., Wang, J., and Zhang, X. (2022). An update on the multifaceted role of NF-kappaB in endometriosis. *Int. J. Biol. Sci.* 18 (11), 4400–4413. doi:10.7150/ijbs.72707

Lodyga, M., and Hinz, B. (2020). TGF-β1 - a truly transforming growth factor in fibrosis and immunity. *Semin. Cell Dev. Biol.* 101, 123–139. doi:10.1016/j.semcdb.2019.12.010

Lovren, F., Pan, Y., Quan, A., Szmitko, P. E., Singh, K. K., Shukla, P. C., et al. (2010). Adiponectin primes human monocytes into alternative anti-inflammatory M2 macrophages. *Am. J. Physiol. Heart Circ. Physiol.* 299 (3), H656–H663. doi:10.1152/ajpheart.00115.2010

Madanes, D., Bilotas, M. A., Bastón, J. I., Singla, J. J., Meresman, G. F., Barañao, R. I., et al. (2020). PI3K/AKT pathway is altered in the endometriosis patient's endometrium and presents differences according to severity stage. *Gynecol. Endocrinol.* 36 (5), 436–440. doi:10.1080/09513590.2019.1680627

Maeda, K., Okubo, K., Shimomura, I., Funahashi, T., Matsuzawa, Y., and Matsubara, K. (1996). cDNA cloning and expression of a novel adipose specific collagen-like factor, apM1 (AdiPose Most abundant Gene transcript 1). *Biochem. Biophys. Res. Commun.* 221 (2), 286–289. doi:10.1006/bbrc.1996.0587

Magkos, F., and Sidossis, L. S. (2007). Recent advances in the measurement of adiponectin isoform distribution. *Curr. Opin. Clin. Nutr. Metab. Care* 10 (5), 571–575. doi:10.1097/MCO.0b013e3282bf6ea8

Mahboobifard, F., Pourgholami, M. H., Jorjani, M., Dargahi, L., Amiri, M., Sadeghi, S., et al. (2022). Estrogen as a key regulator of energy homeostasis and metabolic health. *Biomed. Pharmacother.* 156, 113808. doi:10.1016/j.biopha.2022.113808

Maleszka, A., Smolinska, N., Nitkiewicz, A., Kiezun, M., Dobrzyn, K., Czerwinska, J., et al. (2014). Expression of adiponectin receptors 1 and 2 in the ovary and concentration of plasma adiponectin during the oestrous cycle of the pig. *Acta Vet. Hung* 62 (3), 386–396. doi:10.1556/AVet.2014.007

Malmström, J., Lindberg, H., Lindberg, C., Bratt, C., Wieslander, E., Delander, E. L., et al. (2004). Transforming growth factor-beta 1 specifically induce proteins involved in the myofibroblast contractile apparatus. *Mol. Cell Proteomics* 3 (5), 466–477. doi:10.1074/mcp.M300108-MCP200

Man, K., Ng, K. T., Xu, A., Cheng, Q., Lo, C. M., Xiao, J. W., et al. (2010). Suppression of liver tumor growth and metastasis by adiponectin in nude mice through inhibition of tumor angiogenesis and downregulation of Rho kinase/IFN-inducible protein 10/matrix metalloproteinase 9 signaling. *Clin. Cancer Res.* 16 (3), 967–977. doi:10.1158/1078-0432.Ccr-09-1487

Mandal, P., Pratt, B. T., Barnes, M., McMullen, M. R., and Nagy, L. E. (2011). Molecular mechanism for adiponectin-dependent M2 macrophage polarization: link between the metabolic and innate immune activity of full-length adiponectin. *J. Biol. Chem.* 286 (15), 13460–13469. doi:10.1074/jbc.M110.204644

Mariño, G., Niso-Santano, M., Baehrecke, E. H., and Kroemer, G. (2014). Self-consumption: the interplay of autophagy and apoptosis. *Nat. Rev. Mol. Cell Biol.* 15 (2), 81–94. doi:10.1038/nrm3735

Marquardt, R. M., Kim, T. H., Shin, J. H., and Jeong, J. W. (2019). Progesterone and estrogen signaling in the endometrium: what goes wrong in endometriosis? *Int. J. Mol. Sci.* 20 (15), 3822. doi:10.3390/ijms20153822

Matsuda, M., and Shimomura, I. (2014). Roles of adiponectin and oxidative stress in obesity-associated metabolic and cardiovascular diseases. *Rev. Endocr. Metab. Disord.* 15 (1), 1–10. doi:10.1007/s11154-013-9271-7

McKinnon, B. D., Kocbek, V., Nirgianakis, K., Bersinger, N. A., and Mueller, M. D. (2016). Kinase signalling pathways in endometriosis: potential targets for non-hormonal therapeutics. *Hum. Reprod. Update* 22 (3), 382–403. doi:10.1093/humupd/dmv060

Mehedintu, C., Plotogea, M. N., Ionescu, S., and Antonovici, M. (2014). Endometriosis still a challenge. *J. Med. Life* 7 (3), 349–357.

Meng, F. P., and Hao, P. (2020). Expression of adiponectin and inflammatory factors in estrogen - dependent uterine lesions. *Guangdong Med. J.* 41, 51–55. doi:10.13820/j.cnki.gdyx.20190636

Merki-Feld, G. S., Imthurn, B., Rosselli, M., and Spanaus, K. (2011). Serum concentrations of high-molecular weight adiponectin and their association with sex steroids in premenopausal women. *Metabolism* 60 (2), 180–185. doi:10.1016/j.metabol.2009.12.010

Monaco, C., and Paleolog, E (2004). Nuclear factor kappaB: a potential therapeutic target in atherosclerosis and thrombosis. *Cardiovasc Res.* 61 (4), 671–682. doi:10.1016/j.cardiores.2003.11.038

Monsivais, D., Dyson, M. T., Yin, P., Coon, J. S., Navarro, A., Feng, G., et al. (2014). ERβ- and prostaglandin E2-regulated pathways integrate cell proliferation via Ras-like and estrogen-regulated growth inhibitor in endometriosis. *Mol. Endocrinol.* 28 (8), 1304–1315. doi:10.1210/me.2013-1421

Monsivais, D., Dyson, M. T., Yin, P., Navarro, A., Coon, J. S. T., Pavone, M. E., et al. (2016). Estrogen receptor β regulates endometriotic cell survival through serum and glucocorticoid-regulated kinase activation. *Fertil. Steril.* 105 (5), 1266–1273. doi:10.1016/j.fertnstert.2016.01.012

Moon, H. S., Chamberland, J. P., Aronis, K., Tseleni-Balafouta, S., and Mantzoros, C. S. (2011). Direct role of adiponectin and adiponectin receptors in endometrial cancer: *in vitro* and *ex vivo* studies in humans. *Mol. Cancer Ther.* 10 (12), 2234–2243. doi:10.1158/1535-7163.Mct-11-0545

Moon, H. S., Liu, X., Nagel, J. M., Chamberland, J. P., Diakopoulos, K. N., Brinkoetter, M. T., et al. (2013). Salutary effects of adiponectin on colon cancer: *in vivo* and *in vitro* studies in mice. *Gut* 62 (4), 561–570. doi:10.1136/gutjnl-2012-302092

Morad, V., Abrahamsson, A., and Dabrosin, C. (2014). Estradiol affects extracellular leptin:adiponectin ratio in human breast tissue *in vivo*. *J. Clin. Endocrinol. Metab.* 99 (9), 3460–3467. doi:10.1210/jc.2014-1129

Mori, T., Ito, F., Koshiba, A., Kataoka, H., Takaoka, O., Okimura, H., et al. (2019). Local estrogen formation and its regulation in endometriosis. *Reprod. Med. Biol.* 18 (4), 305–311. doi:10.1002/rmb2.12285

Morikawa, M., Derynck, R., and Miyazono, K. (2016). TGF-B and the TGF-β family: context-dependent roles in cell and tissue physiology. *Cold Spring Harb. Perspect. Biol.* 8 (5), a021873. doi:10.1101/cshperspect.a021873

Ngô, C., Chéreau, C., Nicco, C., Weill, B., Chapron, C., and Batteux, F. (2009). Reactive oxygen species controls endometriosis progression. *Am. J. Pathol.* 175 (1), 225–234. doi:10.2353/ajpath.2009.080804

Nigro, E., Mallardo, M., Polito, R., Scialò, F., Bianco, A., and Daniele, A. (2021). Adiponectin and leptin exert antagonizing effects on HUVEC tube formation and migration modulating the expression of CXCL1, VEGF, MMP-2 and MMP-9. *Int. J. Mol. Sci.* 22 (14), 7516. doi:10.3390/ijms22147516

Nishizawa, H., Shimomura, I., Kishida, K., Maeda, N., Kuriyama, H., Nagaretani, H., et al. (2002). Androgens decrease plasma adiponectin, an insulin-sensitizing adipocyte-derived protein. *Diabetes* 51 (9), 2734–2741. doi:10.2337/diabetes.51.9.2734

Ohashi, K., Parker, J. L., Ouchi, N., Higuchi, A., Vita, J. A., Gokce, N., et al. (2010). Adiponectin promotes macrophage polarization toward an anti-inflammatory phenotype. *J. Biol. Chem.* 285 (9), 6153–6160. doi:10.1074/jbc.M109.088708

Ohashi, K., Shibata, R., Murohara, T., and Ouchi, N. (2014). Role of anti-inflammatory adipokines in obesity-related diseases. *Trends Endocrinol. Metab.* 25 (7), 348–355. doi:10.1016/j.tem.2014.03.009

Ohman-Hanson, R. A., Cree-Green, M., Kelsey, M. M., Bessesen, D. H., Sharp, T. A., Pyle, L., et al. (2016). Ethnic and sex differences in adiponectin: from childhood to adulthood. *J. Clin. Endocrinol. Metab.* 101 (12), 4808–4815. doi:10.1210/jc.2016-1137

Ouchi, N., Kihara, S., Arita, Y., Nishida, M., Matsuyama, A., Okamoto, Y., et al. (2001). Adipocyte-derived plasma protein, adiponectin, suppresses lipid accumulation and class A scavenger receptor expression in human monocyte-derived macrophages. *Circulation* 103 (8), 1057–1063. doi:10.1161/01.cir.103.8.1057

Ouchi, N., Kobayashi, H., Kihara, S., Kumada, M., Sato, K., Inoue, T., et al. (2004). Adiponectin stimulates angiogenesis by promoting cross-talk between AMP-activated protein kinase and Akt signaling in endothelial cells. *J. Biol. Chem.* 279 (2), 1304–1309. doi:10.1074/jbc.M310389200

Ouh, Y. T., Cho, H. W., Lee, J. K., Choi, S. H., Choi, H. J., and Hong, J. H. (2019). CXC chemokine ligand 1 mediates adiponectin-induced angiogenesis in ovarian cancer. *Tumour Biol.* 42 (4), 1010428319842699. doi:10.1177/1010428319842699

Palanisamy, K., Nareshkumar, R. N., Sivagurunathan, S., Raman, R., Sulochana, K. N., and Chidambaram, S. (2019). Anti-angiogenic effect of adiponectin in human primary microvascular and macrovascular endothelial cells. *Microvasc. Res.* 122, 136–145. doi:10.1016/j.mvr.2018.08.002

Pandey, N., Kriplani, A., Yadav, R. K., Lyngdoh, B. T., and Mahapatra, S. C. (2010). Peritoneal fluid leptin levels are increased but adiponectin levels are not changed in infertile patients with pelvic endometriosis. *Gynecol. Endocrinol.* 26 (11), 843–849. doi:10.3109/09513590.2010.487585

Panduru, N. M., Saraheimo, M., Forsblom, C., Thorn, L. M., Gordin, D., Wadén, J., et al. (2015). Urinary adiponectin is an independent predictor of progression to end-stage renal disease in patients with type 1 diabetes and diabetic nephropathy. *Diabetes Care* 38 (5), 883–890. doi:10.2337/dc14-2276

Pantelis, A., Machairiotis, N., and Lapatsanis, D. P. (2021). The formidable yet unresolved interplay between endometriosis and obesity. *ScientificWorldJournal* 2021, 6653677. doi:10.1155/2021/6653677

Parker-Duffen, J. L., Nakamura, K., Silver, M., Kikuchi, R., Tigges, U., Yoshida, S., et al. (2013). T-cadherin is essential for adiponectin-mediated revascularization. *J. Biol. Chem.* 288 (34), 24886–24897. doi:10.1074/jbc.M113.454835

Peake, P. W., Kriketos, A. D., Campbell, L. V., Shen, Y., and Charlesworth, J. A. (2005). The metabolism of isoforms of human adiponectin: studies in human subjects and in experimental animals. *Eur. J. Endocrinol.* 153 (3), 409–417. doi:10.1530/eje.1.01978

Peitsidis, P., Tsikouras, P., Laganà, A. S., Laios, A., Gkegkes, I. D., and Iavazzo, C. (2023). A systematic review of systematic reviews on the use of aromatase inhibitors for the treatment of endometriosis: the evidence to date. *Drug Des. Devel Ther.* 17, 1329–1346. doi:10.2147/dddt.S315726

Pellegrini, C., Gori, I., Achtari, C., Hornung, D., Chardonnens, E., Wunder, D., et al. (2012). The expression of estrogen receptors as well as GREB1, c-MYC, and cyclin D1, estrogen-regulated genes implicated in proliferation, is increased in peritoneal endometriosis. *Fertil. Steril.* 98 (5), 1200–1208. doi:10.1016/j.fertnstert.2012.06.056

Peng, Y. J., Shen, T. L., Chen, Y. S., Mersmann, H. J., Liu, B. H., and Ding, S. T. (2018). Adiponectin and adiponectin receptor 1 overexpression enhance inflammatory bowel disease. *J. Biomed. Sci.* 25 (1), 24. doi:10.1186/s12929-018-0419-3

Pfeiler, G. H., Buechler, C., Neumeier, M., Schäffler, A., Schmitz, G., Ortmann, O., et al. (2008). Adiponectin effects on human breast cancer cells are dependent on 17-β estradiol. *Oncol. Rep.* 19 (3), 787–793. doi:10.3892/or.19.3.787

Popli, P., Sun, A. J., and Kommagani, R. (2022). The multifaceted role of autophagy in endometrium homeostasis and disease. *Reprod. Sci.* 29 (4), 1054–1067. doi:10.1007/s43032-021-00587-2

Potente, M., Gerhardt, H., and Carmeliet, P. (2011). Basic and therapeutic aspects of angiogenesis. *Cell* 146 (6), 873–887. doi:10.1016/j.cell.2011.08.039

Prieto, L., Quesada, J. F., Cambero, O., Pacheco, A., Pellicer, A., Codoceo, R., et al. (2012). Analysis of follicular fluid and serum markers of oxidative stress in women with infertility related to endometriosis. *Fertil. Steril.* 98 (1), 126–130. doi:10.1016/j.fertnstert.2012.03.052

Qi, G. M., Jia, L. X., Li, Y. L., Li, H. H., and Du, J. (2014). Adiponectin suppresses angiotensin II-induced inflammation and cardiac fibrosis through activation of macrophage autophagy. *Endocrinology* 155 (6), 2254–2265. doi:10.1210/en.2013-2011

Qi, Q. R., Lechuga, T. J., Patel, B., Nguyen, N. A., Yang, Y. H., Li, Y., et al. (2020). Enhanced stromal cell CBS-H2S production promotes estrogen-stimulated human endometrial angiogenesis. *Endocrinology* 161 (11), bqaa176. doi:10.1210/endocr/bqaa176

Qin, Q. Q., Jia, C. Y., and Dai, Y. F. (2014). Clinical significance of serum high sensitivity C-reactive protein and adiponectin in patients with endometriosis. *J. Chin. Physician* 4, 533–534. doi:10.3760/cma.j.issn.1008-1372.2014.04.035

Ramírez-Pavez, T. N., Martínez-Esparza, M., Ruiz-Alcaraz, A. J., Marín-Sánchez, P., Machado-Linde, F., and García-Peñarrubia, P. (2021). The role of peritoneal macrophages in endometriosis. *Int. J. Mol. Sci.* 22 (19), 10792. doi:10.3390/ijms221910792

Ramzan, A. A., Bitler, B. G., Hicks, D., Barner, K., Qamar, L., Behbakht, K., et al. (2019). Adiponectin receptor agonist AdipoRon induces apoptotic cell death and suppresses proliferation in human ovarian cancer cells. *Mol. Cell Biochem.* 461 (1-2), 37–46. doi:10.1007/s11010-019-03586-9

Reis, F. M., Petraglia, F., and Taylor, R. N. (2013). Endometriosis: hormone regulation and clinical consequences of chemotaxis and apoptosis. *Hum. Reprod. Update* 19 (4), 406–418. doi:10.1093/humupd/dmt010

Revathidevi, S., and Munirajan, A. K. (2019). Akt in cancer: mediator and more. *Semin. Cancer Biol.* 59, 80–91. doi:10.1016/j.semcancer.2019.06.002

Richter, O. N., Dorn, C., Rösing, B., Flaskamp, C., and Ulrich, U. (2005). Tumor necrosis factor alpha secretion by peritoneal macrophages in patients with endometriosis. *Arch. Gynecol. Obstet.* 271 (2), 143–147. doi:10.1007/s00404-003-0591-9

Rizzo, M. R., Fasano, R., and Paolisso, G. (2020). Adiponectin and cognitive decline. *Int. J. Mol. Sci.* 21 (6), 2010. doi:10.3390/ijms21062010

Rodriguez-Pacheco, F., Martinez-Fuentes, A. J., Tovar, S., Pinilla, L., Tena-Sempere, M., Dieguez, C., et al. (2007). Regulation of pituitary cell function by adiponectin. *Endocrinology* 148 (1), 401–410. doi:10.1210/en.2006-1019

Sampson, J. (1927). Peritoneal endometriosis due to the menstrual dissemination of endometrial tissue into the peritoneal cavity. *Am. J. Obstet. Gynecol.* 14, 422–469. doi:10.1016/s0002-9378(15)30003-x

Samson, S. C., Khan, A. M., and Mendoza, M. C. (2022). ERK signaling for cell migration and invasion. *Front. Mol. Biosci.* 9, 998475. doi:10.3389/fmolb.2022.998475

Sang, L., Fang, Q. J., and Zhao, X. B. (2019). A research on the protein expression of p53, p16, and MDM2 in endometriosis. *Med. Baltim.* 98 (14), e14776. doi:10.1097/md.0000000000014776

Santulli, P., Chouzenoux, S., Fiorese, M., Marcellin, L., Lemarechal, H., Millischer, A. E., et al. (2015). Protein oxidative stress markers in peritoneal fluids of women with deep infiltrating endometriosis are increased. *Hum. Reprod.* 30 (1), 49–60. doi:10.1093/humrep/deu290

Savvidou, S., Hytiroglou, P., Orfanou-Koumerkeridou, H., Panderis, A., Frantzoulis, P., and Goulis, J. (2009). Low serum adiponectin levels are predictive of advanced hepatic fibrosis in patients with NAFLD. *J. Clin. Gastroenterol.* 43 (8), 765–772. doi:10.1097/MCG.0b013e31819e9048

Scheer, F. A., Chan, J. L., Fargnoli, J., Chamberland, J., Arampatzi, K., Shea, S. A., et al. (2010). Day/night variations of high-molecular-weight adiponectin and lipocalin-2 in healthy men studied under fed and fasted conditions. *Diabetologia* 53 (11), 2401–2405. doi:10.1007/s00125-010-1869-7

Scherer, P. E., Williams, S., Fogliano, M., Baldini, G., and Lodish, H. F. (1995). A novel serum protein similar to C1q, produced exclusively in adipocytes. *J. Biol. Chem.* 270 (45), 26746–26749. doi:10.1074/jbc.270.45.26746

Shah, D. K., Correia, K. F., Harris, H. R., and Missmer, S. A. (2013a). Plasma adipokines and endometriosis risk: a prospective nested case-control investigation from the Nurses' Health Study II. *Hum. Reprod.* 28 (2), 315–321. doi:10.1093/humrep/des411

Shah, D. K., Correia, K. F., Vitonis, A. F., and Missmer, S. A. (2013b). Body size and endometriosis: results from 20 years of follow-up within the Nurses' Health Study II prospective cohort. *Hum. Reprod.* 28 (7), 1783–1792. doi:10.1093/humrep/det120

Shao, J., Zhang, B., Yu, J. J., Wei, C. Y., Zhou, W. J., Chang, K. K., et al. (2016). Macrophages promote the growth and invasion of endometrial stromal cells by downregulating IL-24 in endometriosis. *Reproduction* 152 (6), 673–682. doi:10.1530/rep-16-0278

Shen, L., Miao, J., Yuan, F., Zhao, Y., Tang, Y., Wang, Y., et al. (2013). Overexpression of adiponectin promotes focal angiogenesis in the mouse brain following middle cerebral artery occlusion. *Gene Ther.* 20 (1), 93–101. doi:10.1038/gt.2012.7

Shi, L. B., Zhou, F., Zhu, H. Y., Huang, D., Jin, X. Y., Li, C., et al. (2017). Transforming growth factor beta1 from endometriomas promotes fibrosis in surrounding ovarian tissues via Smad2/3 signaling. *Biol. Reprod.* 97 (6), 873–882. doi:10.1093/biolre/iox140

Shibata, R., Ouchi, N., Kihara, S., Sato, K., Funahashi, T., and Walsh, K. (2004). Adiponectin stimulates angiogenesis in response to tissue ischemia through stimulation of amp-activated protein kinase signaling. *J. Biol. Chem.* 279 (27), 28670–28674. doi:10.1074/jbc.M402558200

Sikora, J., Smycz-Kubańska, M., Mielczarek-Palacz, A., Bednarek, I., and Kondera-Anasz, Z. (2018). The involvement of multifunctional TGF-β and related cytokines in pathogenesis of endometriosis. *Immunol. Lett.* 201, 31–37. doi:10.1016/j.imlet.2018.10.011

Smolinska, N., Maleszka, A., Dobrzyn, K., Kiezun, M., Szeszko, K., and Kaminski, T. (2014). Expression of adiponectin and adiponectin receptors 1 and 2 in the porcine uterus, conceptus, and trophoblast during early pregnancy. *Theriogenology* 82 (7), 951–965. doi:10.1016/j.theriogenology.2014.07.018

Soares, S. R., Martínez-Varea, A., Hidalgo-Mora, J. J., and Pellicer, A. (2012). Pharmacologic therapies in endometriosis: a systematic review. *Fertil. Steril.* 98 (3), 529–555. doi:10.1016/j.fertnstert.2012.07.1120

Straub, L. G., and Scherer, P. E. (2019). Metabolic messengers: adiponectin. *Nat. Metab.* 1 (3), 334–339. doi:10.1038/s42255-019-0041-z

Strzałkowska, B., Dawidowicz, M., Ochman, B., and Świętochowska, E. (2021). The role of adipokines in leiomyomas development. *Exp. Mol. Pathol.* 123, 104693. doi:10.1016/j.yexmp.2021.104693

Sui, X., Li, Y., Sun, Y., Li, C., Li, X., and Zhang, G. (2018). Expression and significance of autophagy genes LC3, Beclin1 and MMP-2 in endometriosis. *Exp. Ther. Med.* 16 (3), 1958–1962. doi:10.3892/etm.2018.6362

Sun, Y., and Chen, X. (2010). Effect of adiponectin on apoptosis: proapoptosis or antiapoptosis? *Biofactors* 36 (3), 179–186. doi:10.1002/biof.83

Symons, L. K., Miller, J. E., Kay, V. R., Marks, R. M., Liblik, K., Koti, M., et al. (2018). The immunopathophysiology of endometriosis. *Trends Mol. Med.* 24 (9), 748–762. doi:10.1016/j.molmed.2018.07.004

Takebayashi, A., Kimura, F., Kishi, Y., Ishida, M., Takahashi, A., Yamanaka, A., et al. (2015). Subpopulations of macrophages within eutopic endometrium of endometriosis patients. *Am. J. Reprod. Immunol.* 73 (3), 221–231. doi:10.1111/aji.12331

Takemura, Y., Osuga, Y., Harada, M., Hirata, T., Koga, K., Morimoto, C., et al. (2005a). Serum adiponectin concentrations are decreased in women with endometriosis. *Hum. Reprod.* 20 (12), 3510–3513. doi:10.1093/humrep/dei233

Takemura, Y., Osuga, Y., Harada, M., Hirata, T., Koga, K., Yoshino, O., et al. (2005b). Concentration of adiponectin in peritoneal fluid is decreased in women with endometriosis. *Am. J. Reprod. Immunol.* 54 (4), 217–221. doi:10.1111/j.1600-0897.2005.00300.x

Takemura, Y., Osuga, Y., Yamauchi, T., Kobayashi, M., Harada, M., Hirata, T., et al. (2006). Expression of adiponectin receptors and its possible implication in the human endometrium. *Endocrinology* 147 (7), 3203–3210. doi:10.1210/en.2005-1510

Tan, M., Tang, G., and Rui, H. (2015). Adiponectin attenuates Ang Ⅱ-induced TGFβ1 production in human mesangial cells via an AMPK-dependent pathway. *Biotechnol. Appl. Biochem.* 62 (6), 848–854. doi:10.1002/bab.1323

Tang, Y., Zhao, M., Lin, L., Gao, Y., Chen, G. Q., Chen, S., et al. (2020). Is body mass index associated with the incidence of endometriosis and the severity of dysmenorrhoea: a case-control study in China? *BMJ Open* 10 (9), e037095. doi:10.1136/bmjopen-2020-037095

Tao, T., Wang, Y., Xu, B., Mao, X., Sun, Y., and Liu, W. (2019). Role of adiponectin/peroxisome proliferator-activated receptor alpha signaling in human chorionic gonadotropin-induced estradiol synthesis in human luteinized granulosa cells. *Mol. Cell Endocrinol.* 493, 110450. doi:10.1016/j.mce.2019.110450

Taylor, H. S., Kotlyar, A. M., and Flores, V. A. (2021). Endometriosis is a chronic systemic disease: clinical challenges and novel innovations. *Lancet* 397 (10276), 839–852. doi:10.1016/S0140-6736(21)00389-5

Tian, M., Tang, L., Wu, Y., Beddhu, S., and Huang, Y. (2018). Adiponectin attenuates kidney injury and fibrosis in deoxycorticosterone acetate-salt and angiotensin II-induced CKD mice. *Am. J. Physiol. Ren. Physiol.* 315 (3), F558–F571. doi:10.1152/ajprenal.00137.2018

Tilg, H., and Wolf, A. M. (2005). Adiponectin: a key fat-derived molecule regulating inflammation. *Expert Opin. Ther. Targets* 9 (2), 245–251. doi:10.1517/14728222.9.2.245

Tsankof, A., and Tziomalos, K. (2022). Adiponectin: a player in the pathogenesis of hormone-dependent cancers. *Front. Endocrinol. (Lausanne)* 13, 1018515. doi:10.3389/fendo.2022.1018515

Tsatsanis, C., Zacharioudaki, V., Androulidaki, A., Dermitzaki, E., Charalampopoulos, I., Minas, V., et al. (2005). Adiponectin induces TNF-alpha and IL-6 in macrophages and promotes tolerance to itself and other pro-inflammatory stimuli. *Biochem. Biophys. Res. Commun.* 335 (4), 1254–1263. doi:10.1016/j.bbrc.2005.07.197

Tworoger, S. S., Mantzoros, C., and Hankinson, S. E. (2007). Relationship of plasma adiponectin with sex hormone and insulin-like growth factor levels. *Obes. (Silver Spring)* 15 (9), 2217–2224. doi:10.1038/oby.2007.263

Udomsinprasert, W., Honsawek, S., and Poovorawan, Y. (2018). Adiponectin as a novel biomarker for liver fibrosis. *World J. Hepatol.* 10 (10), 708–718. doi:10.4254/wjh.v10.i10.708

Vigano, P., Candiani, M., Monno, A., Giacomini, E., Vercellini, P., and Somigliana, E. (2018). Time to redefine endometriosis including its pro-fibrotic nature. *Hum. Reprod.* 33 (3), 347–352. doi:10.1093/humrep/dex354

Vitonis, A. F., Baer, H. J., Hankinson, S. E., Laufer, M. R., and Missmer, S. A. (2010). A prospective study of body size during childhood and early adulthood and the incidence of endometriosis. *Hum. Reprod.* 25 (5), 1325–1334. doi:10.1093/humrep/deq039

Volpato, L. K., Horewicz, V. V., Bobinski, F., Martins, D. F., and Piovezan, A. P. (2018). Annexin A1, FPR2/ALX, and inflammatory cytokine expression in peritoneal endometriosis. *J. Reprod. Immunol.* 129, 30–35. doi:10.1016/j.jri.2018.08.002

Vučić Lovrenčić, M., Gerić, M., Košuta, I., Dragičević, M., Garaj-Vrhovac, V., and Gajski, G. (2020). Sex-specific effects of vegetarian diet on adiponectin levels and insulin sensitivity in healthy non-obese individuals. *Nutrition* 79-80, 110862. doi:10.1016/j.nut.2020.110862

Wakabayashi, A., Takeda, T., Tsuiji, K., Li, B., Sakata, M., Morishige, K., et al. (2011). Antiproliferative effect of adiponectin on rat uterine leiomyoma ELT-3 cells. *Gynecol. Endocrinol.* 27 (1), 33–38. doi:10.3109/09513590.2010.487605

Waki, H., Yamauchi, T., Kamon, J., Ito, Y., Uchida, S., Kita, S., et al. (2003). Impaired multimerization of human adiponectin mutants associated with diabetes. Molecular structure and multimer formation of adiponectin. *J. Biol. Chem.* 278 (41), 40352–40363. doi:10.1074/jbc.M300365200

Wang, F., Wang, H., Jin, D., and Zhang, Y. (2018a). Serum miR-17, IL-4, and IL-6 levels for diagnosis of endometriosis. *Med. Baltim.* 97 (24), e10853. doi:10.1097/md.0000000000010853

Wang, L. X., Zhang, S. X., Wu, H. J., Rong, X. L., and Guo, J. (2019). M2b macrophage polarization and its roles in diseases. *J. Leukoc. Biol.* 106 (2), 345–358. doi:10.1002/jlb.3ru1018-378rr

Wang, N., Liang, H., and Zen, K. (2014a). Molecular mechanisms that influence the macrophage m1-m2 polarization balance. *Front. Immunol.* 5, 614. doi:10.3389/fimmu.2014.00614

Wang, X., Chen, Q., Pu, H., Wei, Q., Duan, M., Zhang, C., et al. (2016). Adiponectin improves NF-κB-mediated inflammation and abates atherosclerosis progression in apolipoprotein E-deficient mice. *Lipids Health Dis.* 15, 33. doi:10.1186/s12944-016-0202-y

Wang, X., Pu, H., Ma, C., Jiang, T., Wei, Q., Zhang, C., et al. (2014b). Adiponectin abates atherosclerosis by reducing oxidative stress. *Med. Sci. Monit.* 20, 1792–1800. doi:10.12659/msm.892299

Wang, X., Yan, X., Huang, F., and Wu, L. (2023). Adiponectin inhibits TGF-β1-induced skin fibroblast proliferation and phenotype transformation via the p38 MAPK signaling pathway. *Open Life Sci.* 18 (1), 20220679. doi:10.1515/biol-2022-0679

Wang, X., Yang, J., Wu, L., Tong, C., Zhu, Y., Cai, W., et al. (2022). Adiponectin inhibits the activation of lung fibroblasts and pulmonary fibrosis by regulating the nuclear factor kappa B (NF-κB) pathway. *Bioengineered* 13 (4), 10098–10110. doi:10.1080/21655979.2022.2063652

Wang, X. M., Ma, Z. Y., and Song, N. (2018b). Inflammatory cytokines IL-6, IL-10, IL-13, TNF-α and peritoneal fluid flora were associated with infertility in patients with endometriosis. *Eur. Rev. Med. Pharmacol. Sci.* 22 (9), 2513–2518. doi:10.26355/eurrev_201805_14899

Wang, Z. V., and Scherer, P. E. (2016). Adiponectin, the past two decades. *J. Mol. Cell Biol.* 8 (2), 93–100. doi:10.1093/jmcb/mjw011

Watson, E. C., Koenig, M. N., Grant, Z. L., Whitehead, L., Trounson, E., Dewson, G., et al. (2016). Apoptosis regulates endothelial cell number and capillary vessel diameter but not vessel regression during retinal angiogenesis. *Development* 143 (16), 2973–2982. doi:10.1242/dev.137513

Wei, Y., Liang, Y., Lin, H., Dai, Y., and Yao, S. (2020). Autonomic nervous system and inflammation interaction in endometriosis-associated pain. *J. Neuroinflammation* 17 (1), 80. doi:10.1186/s12974-020-01752-1

Weiskirchen, R., Weiskirchen, S., and Tacke, F. (2019). Organ and tissue fibrosis: molecular signals, cellular mechanisms and translational implications. *Mol. Asp. Med.* 65, 2–15. doi:10.1016/j.mam.2018.06.003

Wildman, R. P., Wang, D., Fernandez, I., Mancuso, P., Santoro, N., Scherer, P. E., et al. (2013). Associations of testosterone and sex hormone binding globulin with adipose tissue hormones in midlife women. *Obes. (Silver Spring)* 21 (3), 629–636. doi:10.1002/oby.20256

Winters, S. J., Gogineni, J., Karegar, M., Scoggins, C., Wunderlich, C. A., Baumgartner, R., et al. (2014). Sex hormone-binding globulin gene expression and insulin resistance. *J. Clin. Endocrinol. Metab.* 99 (12), E2780–E2788. doi:10.1210/jc.2014-2640

Wójtowicz, M., Zdun, D., Owczarek, A. J., Skrzypulec-Plinta, V., and Olszanecka-Glinianowicz, M. (2023). Evaluation of adipokines concentrations in plasma, peritoneal, and endometrioma fluids in women operated on for ovarian endometriosis. *Front. Endocrinol. (Lausanne)* 14, 1218980. doi:10.3389/fendo.2023.1218980

Wu, L., Lv, C., Su, Y., Li, C., Zhang, H., Zhao, X., et al. (2019a). Expression of programmed death-1 (PD-1) and its ligand PD-L1 is upregulated in endometriosis and promoted by 17beta-estradiol. *Gynecol. Endocrinol.* 35 (3), 251–256. doi:10.1080/09513590.2018.1519787

Wu, M. H., Hsiao, K. Y., and Tsai, S. J. (2019b). Hypoxia: the force of endometriosis. *J. Obstet. Gynaecol. Res.* 45 (3), 532–541. doi:10.1111/jog.13900

Wulster-Radcliffe, M. C., Ajuwon, K. M., Wang, J., Christian, J. A., and Spurlock, M. E. (2004). Adiponectin differentially regulates cytokines in porcine macrophages. *Biochem. Biophys. Res. Commun.* 316 (3), 924–929. doi:10.1016/j.bbrc.2004.02.130

Xu, H., Gao, Y., Shu, Y., Wang, Y., and Shi, Q. (2019a). EPHA3 enhances macrophage autophagy and apoptosis by disrupting the mTOR signaling pathway in mice with endometriosis. *Biosci. Rep.* 39 (7). doi:10.1042/bsr20182274

Xu, H., Zhao, Q., Song, N., Yan, Z., Lin, R., Wu, S., et al. (2020). AdipoR1/AdipoR2 dual agonist recovers nonalcoholic steatohepatitis and related fibrosis via endoplasmic reticulum-mitochondria axis. *Nat. Commun.* 11 (1), 5807. doi:10.1038/s41467-020-19668-y

Xu, X., Huang, X., Zhang, L., Huang, X., Qin, Z., and Hua, F. (2021). Adiponectin protects obesity-related glomerulopathy by inhibiting ROS/NF-κB/NLRP3 inflammation pathway. *BMC Nephrol.* 22 (1), 218. doi:10.1186/s12882-021-02391-1

Xu, Z., Zhang, L., Yu, Q., Zhang, Y., Yan, L., and Chen, Z. J. (2019b). The estrogen-regulated lncRNA H19/miR-216a-5p axis alters stromal cell invasion and migration via ACTA2 in endometriosis. *Mol. Hum. Reprod.* 25 (9), 550–561. doi:10.1093/molehr/gaz040

Yamaguchi, N., Argueta, J. G., Masuhiro, Y., Kagishita, M., Nonaka, K., Saito, T., et al. (2005). Adiponectin inhibits Toll-like receptor family-induced signaling. *FEBS Lett.* 579 (30), 6821–6826. doi:10.1016/j.febslet.2005.11.019

Yamauchi, T., Iwabu, M., Okada-Iwabu, M., and Kadowaki, T. (2014). Adiponectin receptors: a review of their structure, function and how they work. *Best. Pract. Res. Clin. Endocrinol. Metab.* 28 (1), 15–23. doi:10.1016/j.beem.2013.09.003

Yamauchi, T., Kamon, J., Ito, Y., Tsuchida, A., Yokomizo, T., Kita, S., et al. (2003). Cloning of adiponectin receptors that mediate antidiabetic metabolic effects. *Nature* 423 (6941), 762–769. doi:10.1038/nature01705

Yan, C. J., Li, S. M., Xiao, Q., Liu, Y., Hou, J., Chen, A. F., et al. (2013). Influence of serum adiponectin level and SNP +45 polymorphism of adiponectin gene on myocardial fibrosis. *J. Zhejiang Univ. Sci. B* 14 (8), 721–728. doi:10.1631/jzus.BQICC707

Yang, H. L., Mei, J., Chang, K. K., Zhou, W. J., Huang, L. Q., and Li, M. Q. (2017). Autophagy in endometriosis. *Am. J. Transl. Res.* 9 (11), 4707–4725.

Yang, J., Lin, S. C., Chen, G., He, L., Hu, Z., Chan, L., et al. (2013). Adiponectin promotes monocyte-to-fibroblast transition in renal fibrosis. *J. Am. Soc. Nephrol.* 24 (10), 1644–1659. doi:10.1681/asn.2013030217

Yang, S., and Plotnikov, S. V. (2021). Mechanosensitive regulation of fibrosis. *Cells* 10 (5), 994. doi:10.3390/cells10050994

Yang, W., Yuan, W., Peng, X., Wang, M., Xiao, J., Wu, C., et al. (2019). PPAR γ/nnat/NF-κB Axis involved in promoting effects of adiponectin on preadipocyte differentiation. *Mediat. Inflamm.* 2019, 5618023. doi:10.1155/2019/5618023

Yao, Y., Xu, X. H., and Jin, L. (2019). Macrophage polarization in physiological and pathological pregnancy. *Front. Immunol.* 10, 792. doi:10.3389/fimmu.2019.00792

Yarrow, J. F., Beggs, L. A., Conover, C. F., McCoy, S. C., Beck, D. T., and Borst, S. E. (2012). Influence of androgens on circulating adiponectin in male and female rodents. *PLoS One* 7 (10), e47315. doi:10.1371/journal.pone.0047315

Ye, C., Chen, P., Xu, B., Jin, Y., Pan, Y., Wu, T., et al. (2023). Abnormal expression of fission and fusion genes and the morphology of mitochondria in eutopic and ectopic endometrium. *Eur. J. Med. Res.* 28 (1), 209. doi:10.1186/s40001-023-01180-w

Ye, J. J., Bian, X., Lim, J., and Medzhitov, R. (2020). Adiponectin and related C1q/TNF-related proteins bind selectively to anionic phospholipids and sphingolipids. *Proc. Natl. Acad. Sci. U. S. A.* 117 (29), 17381–17388. doi:10.1073/pnas.1922270117

Ye, Z., and Hu, Y. (2021). TGF-β1: gentlemanly orchestrator in idiopathic pulmonary fibrosis (Review). *Int. J. Mol. Med.* 48 (1), 132. doi:10.3892/ijmm.2021.4965

Yi, K. W., Shin, J. H., Park, H. T., Kim, T., Kim, S. H., and Hur, J. Y. (2010). Resistin concentration is increased in the peritoneal fluid of women with endometriosis. *Am. J. Reprod. Immunol.* 64 (5), 318–323. doi:10.1111/j.1600-0897.2010.00840.x

Yilmaz, B. D., and Bulun, S. E. (2019). Endometriosis and nuclear receptors. *Hum. Reprod. Update* 25 (4), 473–485. doi:10.1093/humupd/dmz005

Yokota, T., Oritani, K., Takahashi, I., Ishikawa, J., Matsuyama, A., Ouchi, N., et al. (2000). Adiponectin, a new member of the family of soluble defense collagens, negatively regulates the growth of myelomonocytic progenitors and the functions of macrophages. *Blood* 96 (5), 1723–1732. doi:10.1182/blood.v96.5.1723

Yu, J. J., Sun, H. T., Zhang, Z. F., Shi, R. X., Liu, L. B., Shang, W. Q., et al. (2016). IL15 promotes growth and invasion of endometrial stromal cells and inhibits killing activity of NK cells in endometriosis. *Reproduction* 152 (2), 151–160. doi:10.1530/rep-16-0089

Zabihi, M., Lotfi, R., Yousefi, A. M., and Bashash, D. (2023). Cyclins and cyclin-dependent kinases: from biology to tumorigenesis and therapeutic opportunities. *J. Cancer Res. Clin. Oncol.* 149 (4), 1585–1606. doi:10.1007/s00432-022-04135-6

Zeng, F., Shi, J., Long, Y., Tian, H., Li, X., Zhao, A. Z., et al. (2015). Adiponectin and endometrial cancer: a systematic review and meta-analysis. *Cell Physiol. Biochem.* 36 (4), 1670–1678. doi:10.1159/000430327

Zha, D., Wu, X., and Gao, P. (2017). Adiponectin and its receptors in diabetic kidney disease: molecular mechanisms and clinical potential. *Endocrinology* 158 (7), 2022–2034. doi:10.1210/en.2016-1765

Zhang, H. W., Yang, L., Ren, C. C., Zhang, F., Li, F. Y., Lu, J., et al. (2021). Role of adiponectin gene polymorphisms in endometriosis. *Dep. Obstetrics Gynecol.* 30, 259–263. doi:10.13283/j.cnki.xdfckjz.2021.04.004

Zhang, L., Wen, K., Han, X., Liu, R., and Qu, Q. (2015). Adiponectin mediates antiproliferative and apoptotic responses in endometrial carcinoma by the AdipoRs/AMPK pathway. *Gynecol. Oncol.* 137 (2), 311–320. doi:10.1016/j.ygyno.2015.02.012

Zhang, M., Xu, T., Tong, D., Li, S., Yu, X., Liu, B., et al. (2023). Research advances in endometriosis-related signaling pathways: a review. *Biomed. Pharmacother.* 164, 114909. doi:10.1016/j.biopha.2023.114909

Zhang, S., Wu, X., Wang, J., Shi, Y., Hu, Q., Cui, W., et al. (2022). Adiponectin/AdiopR1 signaling prevents mitochondrial dysfunction and oxidative injury after traumatic brain injury in a SIRT3 dependent manner. *Redox Biol.* 54, 102390. doi:10.1016/j.redox.2022.102390

Zhang, T., De Carolis, C., Man, G. C. W., and Wang, C. C. (2018). The link between immunity, autoimmunity and endometriosis: a literature update. *Autoimmun. Rev.* 17 (10), 945–955. doi:10.1016/j.autrev.2018.03.017

Zhang, X., and Zhao, W. (2023). Expression and clinical significance of Capase3 and C-IAP1/2 in ectopic endometrium of patients with endometriosis. *Cell Mol. Biol. (Noisy-le-grand)* 69 (7), 127–130. doi:10.14715/cmb/2023.69.7.20

Zhao, D., Zhu, X., Jiang, L., Huang, X., Zhang, Y., Wei, X., et al. (2021a). Advances in understanding the role of adiponectin in renal fibrosis. *Nephrol. Carlt.* 26 (2), 197–203. doi:10.1111/nep.13808

Zhao, Z., Wu, Y., Zhang, H., Wang, X., Tian, X., Wang, Y., et al. (2021b). Association of leptin and adiponectin levels with endometriosis: a systematic review and meta-analysis. *Gynecol. Endocrinol.* 37 (7), 591–599. doi:10.1080/09513590.2021.1878139

Zhou, W. J., Yang, H. L., Shao, J., Mei, J., Chang, K. K., Zhu, R., et al. (2019). Anti-inflammatory cytokines in endometriosis. *Cell Mol. Life Sci.* 76 (11), 2111–2132. doi:10.1007/s00018-019-03056-x

Zhu, M. B., Chen, L. P., Hu, M., Shi, Z., and Liu, Y. N. (2019). Effects of lncRNA BANCR on endometriosis through ERK/MAPK pathway. *Eur. Rev. Med. Pharmacol. Sci.* 23 (16), 6806–6812. doi:10.26355/eurrev_201908_18719

Zolbin, M. M., Mamillapalli, R., Nematian, S. E., Goetz, T. G., and Taylor, H. S. (2019). Adipocyte alterations in endometriosis: reduced numbers of stem cells and microRNA induced alterations in adipocyte metabolic gene expression. *Reprod. Biol. Endocrinol.* 17 (1), 36. doi:10.1186/s12958-019-0480-0

Zondervan, K. T., Becker, C. M., Koga, K., Missmer, S. A., Taylor, R. N., and Viganò, P. (2018). Endometriosis. *Nat. Rev. Dis. Prim.* 4 (1), 9. doi:10.1038/s41572-018-0008-5

Zondervan, K. T., Becker, C. M., and Missmer, S. A. (2020). Endometriosis. *N. Engl. J. Med.* 382 (13), 1244–1256. doi:10.1056/NEJMra1810764

Glossary

AdipoR1	adiponectin receptor 1
AdipoR2	adiponectin receptor 2
Akt	protein kinase B
AMPK	adenosine monophosphate-activated protein kinase
α-SMA	alpha-smooth muscle actin
ATG13	autophagy-related 13
Bcl-2	B-cell lymphoma 2
BMI	body mass index
Cx43	connexin 43
CXCL1	CXC motif chemokine ligand 1
CYP2R1	cytochrome P450 2R1
ELT3	Eker leiomyoma tumor-3
EMs	endometriosis
eNOS	endothelial nitric oxide synthase
ERK	extracellular signal-regulated kinase
E2	estradiol
FABP4	fatty acid binding protein 4
FIP200	FAK family kinase-interacting protein of 200 kDa
GBP-28	gelatin-binding protein 28
HMEC-1	human microvascular endothelial cell 1
HMW	high-molecular weight
HUVECs	human umbilical vein endothelial cells
IGFBP1	insulin-like growth factor binding protein 1
IL-1β	interleukin 1 beta
IL-6	interleukin 6
IL-8	interleukin 8
IL-10	interleukin 10
LC3	microtubule-associated protein light chain 3
LKB1	liver kinase B1
LMW	low-molecular weight
LPS	lipopolysaccharide
MAPK	mitogen-activated protein kinase
MCP-1	monocyte chemoattractant protein 1
MMD2	monocyte to macrophage differentiation associated 2
MMPs	matrix metalloproteinases
MMW	medium-molecular weight
MRC-1	mannose receptor C-Type I
mTOR	mammalian target or rapamycin
NF-κB	nuclear factor kappa B
OA	osteoarthritis
PCOS	polycystic ovary syndrome
PF	peritoneal fluid
PI3K	phosphoinositide 3-kinase
PPAR-α	peroxisome proliferator-activated receptor alpha
PPAR-γ	peroxisome proliferator-activated receptor gamma
RA	rheumatoid arthritis
ROCK2	Rho-associated coiled-coil containing protein kinase 2
ROS	reactive oxygen species
SARDs	systemic autoimmune rheumatic diseases
SHBG	sex hormone-binding globulin
SOD	superoxide dismutase
STAT3	signal transducer and activator of transcription 3
STK11	serine/threonine kinase 11
T-cad	T-cadherin
TGF-β	transforming growth factor beta
TNF-α	tumor necrosis factor alpha
ULK1	unc-51-like autophagy activating kinase 1
VEGF	vascular endothelial growth factor

frontiers | Frontiers in Pharmacology

TYPE Review
PUBLISHED 04 June 2024
DOI 10.3389/fphar.2024.1394516

OPEN ACCESS

EDITED BY
Patricia Rijo,
Lusofona University, Portugal

REVIEWED BY
Aarti Sharma,
Mayo Clinic Arizona, United States
Marc López Cano,
University of Barcelona, Spain

*CORRESPONDENCE
Beki Kan,
beki.kan@acibadem.edu.tr

RECEIVED 01 March 2024
ACCEPTED 15 May 2024
PUBLISHED 04 June 2024

CITATION
Öz-Arslan D, Yavuz M and Kan B (2024), Exploring orphan GPCRs in neurodegenerative diseases.
Front. Pharmacol. 15:1394516.
doi: 10.3389/fphar.2024.1394516

Exploring orphan GPCRs in neurodegenerative diseases

Devrim Öz-Arslan [1,2], Melis Yavuz [2,3] and Beki Kan [1,2]*

[1]Department of Biophysics, Acibadem MAA University, School of Medicine, Istanbul, Türkiye,
[2]Department of Neurosciences, Acibadem MAA University, Institute of Health Sciences, İstanbul, Türkiye,
[3]Department of Pharmacology, Acibadem MAA University, School of Pharmacy, Istanbul, Türkiye

Neurodegenerative disorders represent a significant and growing health burden worldwide. Unfortunately, limited therapeutic options are currently available despite ongoing efforts. Over the past decades, research efforts have increasingly focused on understanding the molecular mechanisms underlying these devastating conditions. Orphan receptors, a class of receptors with no known endogenous ligands, emerge as promising druggable targets for diverse diseases. This review aims to direct attention to a subgroup of orphan GPCRs, in particular class A orphans that have roles in neurodegenerative disorders, including Alzheimer's disease, Parkinson's disease, Huntington's disease, and Multiple sclerosis. We highlight the diverse roles orphan receptors play in regulating critical cellular processes such as synaptic transmission, neuronal survival and neuro-inflammation. Moreover, we discuss the therapeutic potential of targeting orphan receptors for the treatment of neurodegenerative disorders, emphasizing recent advances in drug discovery and preclinical studies. Finally, we outline future directions and challenges in orphan receptor research.

KEYWORDS

GPCR, orphan GPCRs, Alzhemier's disease, Parkinson's disease, Neurodegenaration

Introduction

G protein-coupled receptors (GPCRs) also called seven transmembrane (7TM) receptors constitute the largest receptor family in the human protein atlas. GPCRs remain highly sought-after drug targets, owing to their ability to interact with numerous endogenous ligands. GPCRs are categorized into distinct classes based on sequence homology and functional similarities These are, Class A; rhodopsin-like receptors, Class B; secretin family, Class C; metabotropic glutamate receptors, Class D; fungal mating pheromone receptors, Class E; cAMP receptors, and Class F; frizzled (FZD) and smoothened (SMO) receptors (Lee et al., 2018). Among these families the largest is the Class A family, which also includes the class A orphan subgroup. GPCRs play a vital role in many physiological and pathological processes and mediate the signaling of nearly two-thirds of hormones and neurotransmitters (Spillantini et al., 1997). While GPCRs represent a vast array of potential therapeutic targets, there are still more than 140 GPCRs, notwithstanding the olfactory receptor family, for which the natural ligands are lacking. These so-called orphan receptors remain unexplored in terms of their endogenous ligands, molecular signaling pathways and functions (Sriram and Insel, 2018).

Despite their elusive nature, orphan GPCRs present an intriguing opportunity to unravel hidden molecular mechanisms and potential treatment avenues for many debilitating conditions. In this context, investigating the involvement of orphan receptors in the pathogenesis and progression of neurodegenerative diseases holds the

TABLE 1 Orphan GPCR expression and ligands.

Orphan Receptors	Other Names	Expressed in	Gene	Signaling	Hypothetical Endogenous Agonists	Agonist
GPR3	• GPCR21	Brain	1p36.11	Gi	S1P (Uhlenbrock et al., 2002)	**Inverse Agonists**
	• GPCR3	Hippocampus Habenula		Gs (Freudzon et al., 2005)	DHS1P and DPI (Capaldi et al., 2018)	AF64394 (Jensen et al., 2014)
	• ACCA orphan receptor adenylate cyclase constitutive activator G protein-coupled receptor R4	Cortex Amygdala		ERK1/2 and Akt (Morales et al., 2018b)		Diphenyleneiodonium chloride (Ye et al., 2014)
	• Gpcr20			β-arrestin2 (Laun et al., 2019; Isawi et al., 2020)		
GPR6	• Sphingosine 1-phosphate receptor	Basal Ganglia	6q21	G_s (Uhlenbrock et al., 2002)	S1P (Ignatov et al., 2003b)	
	• GPR6	Striatopallidal neurons frontal cortex, retrosplenial cortex, hippocampus, amygdala, and hypothalamus		Gi/o, affecting Ca2+ mobilization (Laun et al., 2019)		
				β-arrestin (Laun et al., 2019)		
GPR12	• Gpcr01/20/21/12	Brain	13q12.13	Gαs (Tanaka et al., 2007)	S1P (Ignatov et al., 2003a)	
	• R334	Cerebral cortex		Gαi (Laun et al., 2019)		
		Hippocampus Striatum				
GPR17	• P2Y-like receptor	Oligodendrocyte precursor cells	2q14.3	Gαi	LTC4, LTD4 (Benned-Jensen and Rosenkilde, 2010)	
	• UDP/CysLT receptorR12 Uracil nucleotide/cysteinyl leukotriene receptor	Frontal cortex Striatum		Gβγ (Liu et al., 2021)	UDP-glucose,	
		Brain stem Medulla		Gαs	UDP-galactose,	
				Gαq	UDP (Ciana et al., 2006; Benned-Jensen and Rosenkilde, 2010)	
				β-arrestins increased Ca2+ flux (Chen et al., 2009)		
				ERK1/2		
GPR18	- GPCRW		13q32.3	Gi/Go family, Gq/G11 family	N-arachidonoylglycine (Kohno et al., 2006)	**Agonists**
	- NAGly receptor			Gαi/o		N-arachidonoylglycine
	- N-arachidonoyol glycine receptor			PI3K/Akt-ERK1/2 (Matouk et al., 2017)		O-1602, abnormal cannabidiol
				MAPK (McHugh et al., 2010; McHugh et al., 2012) eNOS/NO (Fitzgerald et al., 2023)		Δ9-tetrahydrocannabinol
						Anandamide
						Arachidonylcyclopropylamide
						Cannabidiol
						AM251 (McHugh et al., 2012)
						PSB-KD107 (Schoeder et al., 2020)
GPR37	• EDNRBL/EDNRLB	Cerebellum Spleen	7q31.33	Gαi	The peptides prosaptide and prosaposin (Meyer et al., 2013)	**Agonists**
	• PAELR	Thymus Peripheral blood leukocytes		Gβγ	Regenerating islet-derived family member 4 (Reg4) (Rezgaoui et al., 2006; Meyer et al., 2013; Wang et al., 2016)	Neuropeptide head activator (Rezgaoui et al., 2006)
	• hET(B)R-LP	Lymph node		Gαs		
	• GPCR CNS1	Lung		Gαq		
	• Parkin-associated endothelin B-like receptor	Testis		β-arrestins increased Ca2+ flux		
	• Endothelin B receptor-like protein 1			MAPK		
				ERK1/2 (Yang et al., 2016)		

(Continued on following page)

TABLE 1 (*Continued*) Orphan GPCR expression and ligands.

Orphan Receptors	Other Names	Expressed in	Gene	Signaling	Hypothetical Endogenous Agonists	Agonist
GPR49	• Lgr5	Glioblastoma stem cells	12q21.1	Gα i/o		**Agonists**
	• GPR49	Spinal cord		PLC		R-spondin-1
	• FEX	Motor neurons of brain stem		PKC		R-spondin-2
	• GPR67	Layer 5a and 6 neurons in cortex		β-arrestin (Snow et al., 1998)		R-spondin-3
	• Orphan G protein-coupled receptor HG38			MAPK/ERK PI3K/Akt pathways (Watson et al., 2018)		R-spondin-4 (Carmon et al., 2011)
	• Leucine-rich repeat-containing G protein-coupled receptor 5			G 12/13		
				Rho kinase Pathway (Kwon et al., 2013)		
GPR50	• MTNRL	Cortex	Xq28	MT receptors		
	• H9	Midbrain		GPR50/MT1 heterodimer is without G protein coupling (Levoye et al., 2006)		
	• Mel1c	Pons		ADAM17-Notch (Saha et al., 2020)		
	• Melatonin-related receptor	Amygdala Hippocampus except glial cells				
		Inhibitory interneurons				
GPR52		Prefrontal cortex Basal ganglia Striatonig	1q25.1	Gαs (Lin et al., 2020) PKA CREB ERK1/2 β-arrestin-2-dependent (Wang et al., 2020a; Hatzipantelis et al., 2020b)		**Agonists** Derivative 17 (Nakahata et al., 2018) Compound 7a: 3-[2-(3-Chloro-5-fluorobenzyl)-1-benzothiophen-7-yl]-N-(2-ethoxyethyl)benzamide (Setoh et al., 2014)
GPR55		central nerve tissues and cells	2q37.1	MAPK/ERK (PI3K)/Akt RhoA-dependent Ca2+ signaling NFAT (Henstridge et al., 2008) Gα12/13-RhoA-ROCK and Gαq-PLC-PKC(88) Gq-G11, mitogen-activated protein kinase 1, and calcium signaling (Henstridge et al., 2008; Andradas et al., 2011)	anandamide 2-arachidonoylglycerol 2-arachidonoylglycerolphosphoinositol lysophosphatidylinositol N-palmitoylethanolamine (Ryberg et al., 2007)	2-arachidonoylglycerol N-palmitoylethanolamine JWH015 O-1602 (Ryberg et al., 2007)*
GPR78		Brain Frontal cortex Putamen Thalamus Hypothalamus Amygdala Hippocampus Pons Medulla Midbrain	4p16.1	Gαs Gαq-Rho GTPase (Dong et al., 2016)	Teratocarcinoma-derived growth factor I (Cripto) DnaJ-like protein MTJ-1 α2-macroglobulin Kringle 5 Par-4 (Arap et al., 2004; Gonzalez-Gronow et al., 2009; Araujo et al., 2018)	**Agonists** BC71 and two peptides
GPR83	• GIR	Hippocampus Amygdala	11q21	Gαi/o		**Agonists**
	• GPR72	Prefrontal cortex		Gαq (Lueptow et al., 2018)		PEN (Uhlenbrock et al., 2002)
	• Glucocorticoid induced receptor	Various hypothalamic nuclei		MAPK (Müller et al., 2013)		Zn2+ (Müller et al., 2013)
	• G protein-coupled receptor 72					
	• JP05					

(Continued on following page)

TABLE 1 (*Continued*) Orphan GPCR expression and ligands.

Orphan Receptors	Other Names	Expressed in	Gene	Signaling	Hypothetical Endogenous Agonists	Agonist
GPR84	• GPCR4	Microglial cells	12q13.13	Gαi/o (Suzuki et al., 2013b) MAPK/ERK (Wang et al., 2023)	Medium chain free fatty acids with carbon chain lengths of 9–14	**Agonists:** decanoic acid
	• Inflammation-related G-protein coupled receptor EX33				6-n-octylaminouracil (Suzuki et al., 2013a)	undecanoic acid
						lauric acid
						Embelin (orthosteric)
						PSB-16434 (orthosteric)
						ZQ-16 (orthosteric)
						6-nonylpyridine-2,4-diol (orthosteric)
						DL-175 (orthosteric)
						Allosteric modulator DIM (Agonist) (Wang et al., 2006; Suzuki et al., 2013a; Madar et al., 2021; Marsango et al., 2022)
GPR85	• Srep2	Hippocampal formation	7q31.1			New inverse agonists developed (Sakai et al., 2022)
	• SREB2/SREB	Olfactory bulb Cerebellum				
	• Super conserved receptor expressed in brain 2					
	• PKrCx1					
GPR88	• STRG	Striatum	1p21.2	Gαi/o (Ehrlich et al., 2017)		2-PCCA and RTI-13951–33 (Garisetti et al., 2023)
	• striatum-specific GPCR			β-arrestin (Laboute et al., 2020)		

*Those with multiple ligands have not been placed. Table has been updated from the https://www.guidetopharmacology.org/GRAC/FamilyDisplayForward?familyId=16#83
Genes: https://www.informatics.jax.org/marker/MGI:101908

promise of uncovering novel targets that could redefine the landscape of drug development and improve the lives of individuals affected by these disorders (Table 1). This exploration represents a dynamic and evolving area of research, poised to contribute significantly to the ongoing efforts to combat the complexities of neurodegenerative diseases.

The research on orphan receptors has emerged as a promising area in chasing for novel drug targets, particularly for neurodegenerative disorders such as Parkinson's disease (PD), Alzheimer's disease (AD), Huntington's disease (HD), and Multiple sclerosis (MS) (Figure 1). These disorders pose significant challenges, characterized by complex and multifaceted pathologies that currently lack comprehensive therapeutic solutions. Neurodegenerative disorders usually manifest as progressive decline in major functions such as cognition, motor functions and accompanying mood disorders depending on the anatomical region in the brain effected. For instance, PD is characterized by the gradual deterioration of dopaminergic neurons in the substantia nigra pars compacta, marked with the accumulation of intracellular protein inclusions known as Lewy bodies, composed of misfolded α-synuclein (α-syn) (Spillantini et al., 1997). The damage of PD is not restricted to the dopaminergic neurons in the substantia nigra but also expand to motor systems, the limbic system, medulla oblongata/pontine tegmentum and olfactory bulb and the autonomic centers, as inferred from the anticholinergic side effects of anti-Parkinson's medications (Braak et al., 2004). AD is another age related neurodegenerative disease in which mitochondrial dysfunction, tau pathology, Aβ plaques and neurofibrillary tangles are deposited and lead to neuronal damage and cell death, primarily affecting memory and cognitive functions (Tiraboschi et al., 2004). The genetic neurodegenerative Huntington's disease also causes a progressive breakdown of neurons, progressive tissue lost specifically in the caudate and cortical thinning related to distinct motor and cognitive phenotypes, affecting motor control, cognition, and behavior (Draganski and Bhatia, 2010). Another chronic inflammation-based pathology leads to MS, which targets the central nervous system (CNS). In MS the inflammation, demyelination, and neuronal damage (Korn, 2008) progresses into the axon injury/loss, which is followed by long-term physical and cognitive impairments (Springer, 2021).

Despite extensive research and progress in the de-orphanization of GPCRs, more than 1000 GPCRs are still classified as orphan receptors, without identified ligands and with unknown physiological functions. In this review, we draw attention to a subgroup of orphan GPCRs, in particular Class A orphans, including GPR3, GPR6, GPR12, GPR17, GPR18, GPR37, GPR49, GPR50, GPR52, GPR55, GPR78, GPR83, GPR84, GPR85, GPR88, that have links to neurodegenerative disorders.

We provide an overview of the proposed "hypothetical" endogenous ligands, and designed ligands according to the identified structures and signaling pathways linked to these receptors (Table 1). We seek to integrate this knowledge with insights into the pathophysiology of neurodegenerative disorders, while also considering the relevant anatomical brain locations

already associated and implicated in these neurodegenerative conditions.

GPR3, GPR6, and GPR12

GPR3, GPR6 and GPR12 comprise a family of closely related orphan receptors that belong to the class A family of GPCRs (Laun et al., 2019). These orphan receptors display high constitutive activity and are capable of signaling through G protein-mediated and non-G protein-mediated mechanisms (Morales et al., 2018a; Laun et al., 2019). Three independent groups reported the molecular cloning of GPR3, GPR6 and GPR12 (Saeki et al., 1993; Eggerickx et al., 1995; Song et al., 1995). The genes encoding these receptors were located in the human chromosomal regions 1p36.1, 6q21 and 13q12, respectively. GPR3, GPR6 and GPR12 share over 60% sequence identity and common conserved motifs and structural features among them. GPR3 and GPR6 share common chromosomal positions with cannabinoid receptors, suggesting that they have a common ancestor (Fredriksson et al., 2003). Molecules targeting GPR3, GPR6 and GPR12 are of interest for therapeutic applications since they are implicated in several neurodegenerative diseases, including AD, PD, HD and MS. In addition to neurodegenerative disorders, these orphan receptors may impact other brain-related processes such as neuropathic pain, cocaine reinforcement or cell survival and proliferation (Morales et al., 2018a). Their high presence in the central nervous system and also their proposed roles in neurite outgrowth renders them valuable for the basic understanding of physiological processes and the underlying mechanisms of orphan GPCRs and possibly all GPCRs.

GPR3: GPR3 is extensively expressed in the brain, primarily in the hippocampus, habenula, cortex and amygdala (Eggerickx et al., 1995). Activation of GPR3 leads to an increase in adenylyl cyclase, which in turn augments the level of intracellular cyclic adenosine monophosphate (cAMP). It is known that cAMP plays significant roles in neurons including neurite outgrowth, axonal regeneration and axonal guidance. Tanaka et al. have demonstrated that neuronal expression of the GPR3 receptor enhances neurite outgrowth, and regulates the proliferation of cerebellar granule cell precursors (Tanaka et al., 2007; Tanaka et al., 2009). The same group of investigators have shown that GPR3 protects neurons from apoptosis via activation of ERK and AKT signaling (Tanaka et al., 2014). Conversely, adverse effects of GPR3 are implicated in the amyloid pathology observed in AD.

One of the pathological hallmarks of AD is the progressive accumulation of aggregates of amyloid peptides in the brain. The amyloid beta (Aβ) peptides are generated from the sequential breakdown of amyloid precursor protein (APP) by two peptides, the β- and γ-secretases. The β-secretases and γ-secretases play a fundamental role in APP proteolysis and Aβ generation. GPR3 has been identified to play a role in regulating the breakdown of APP, thereby modulating the progression of AD. In both neuronal cultures and animal models, GPR3 was shown to upregulate the γ-secretase activity and Aβ accumulation (Thathiah et al., 2009). In a subsequent study, the same researchers demonstrated that GPR3 messenger RNA (mRNA) levels were elevated in 18 post-mortem brain tissue of AD patients (Thathiah et al., 2013). The physiological consequence of loss of the GPR3 gene was investigated in four AD-mouse models by Huang et al., 2015 (Huang et al., 2015). These investigators observed that genetic deletion of GPR3 reduced amyloid pathology in all of the AD mouse models they studied. These studies suggest that lowering GPR3 activity may be beneficial in reducing amyloid pathology in AD.

A Lysophospholipid sphingosine-1-phosphate (S1P) has been suggested as an endogenous ligand of GPR3 in rats (Uhlenbrock et al., 2002). DHS1P and DPI are also potential endogenous ligands for GPR3 mentioned in the literature (Uhlenbrock et al., 2002; Capaldi et al., 2018). Furthermore, an inverse agonist, AF64394, has been proposed for GPR3 (Jensen et al., 2014; Kaushik and Sahi, 2017).

GPR6: GPR6 was initially described as S1P receptor (Morales et al., 2018a; Atanes et al., 2021). It is co-localized to dopamine D1 and D2 receptors, as are GPR52 and GPR88 (Rahman et al., 2022). GPR6 which is extensively expressed in striatopallidal neurons in the basal ganglia (Lobo et al., 2007; Komatsu et al., 2014) has ubiquitous functions and it induces an increase in cAMP levels when it is linked to stimulatory Gs protein. It plays a significant role in human instrumental learning in which the dopaminergic system has a critical role. In rodent cerebellar granule neurons, overexpression of GPR6 boosts neurite outgrowth (Tanaka et al., 2007; Laun et al., 2019). On the other hand, studies carried out in GPR6-knock-out mouse models suggest that GPR6 inhibition may provide benefits for PD. In GPR6-knock out mice, phosphorylation of dopamine and cAMP-regulated phosphoprotein of 32 kDa (DARPP-32) at threonine 34 increased significantly, while production of DARPP-32 in the striatum did not (Oeckl et al., 2014; Nishi and Shuto, 2017).

GPR12: GPR12 is phylogenetically related to the Cannabidiol Receptors (CB-1 and CB-2) (Wong et al., 2023). GPR12 is also a constitutively active receptor expressed mainly in the central nervous system. S1P (Eggerickx et al., 1995; Uhlenbrock et al., 2002; Martin et al., 2015) and sphingosine-phosphorylcholine (SPC) (Ignatov et al., 2003a; Allende et al., 2020) are potential endogenous ligands for GPR12. GPR 12 is expressed mainly in the central nervous system, in structures related to cognitive processes such as the cerebral cortex, the hippocampus and the striatum (Saeki et al., 1993). In mice, GPR12 is expressed in the area controlling emotion and metabolism (Ignatov et al., 2003a). Other functions ascribed to GPR12 include pain control, neurite outgrowth and regeneration (Allende et al., 2020). A study in rat pheochromocytoma PC12 cells demonstrated that GPR12 overexpression promotes neurite outgrowth by inducing differentiation of PC12 into neuron-like cells. This effect was accompanied by activation of ERK1/2 signaling (Lu et al., 2012). A report based on SNP microarray-based genome-wide association suggests a link between GPR12 and antipsychotic response to schizophrenia treatment (Zhao et al., 2022).

GPR17

GPR17 is an orphan GPCR that is expressed in oligodendrocyte precursor cells (OPCs) and premature oligodendrocytes (Fumagalli et al., 2011). GPR17, a purinergic P2Y-like receptor, responds both to uracil nucleotides (UDP, UDP-glucose, UDP-galactose) and

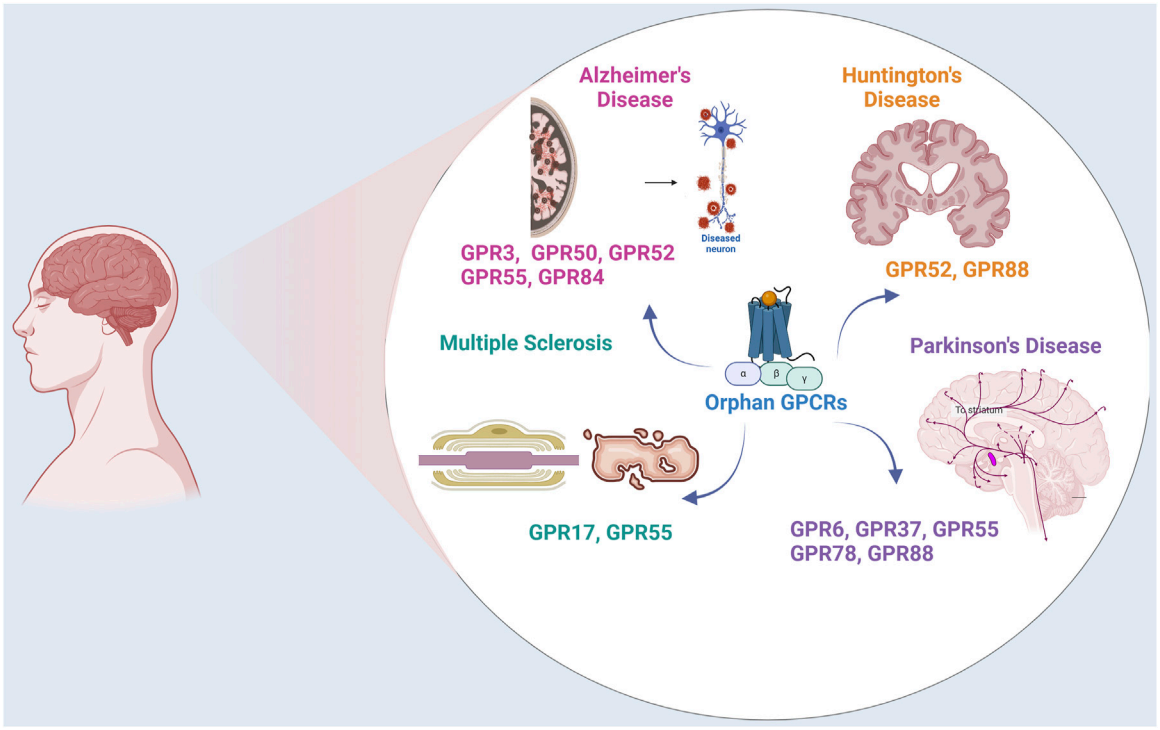

FIGURE 1
Orphan GPCRs in Neurodegenerative Disorders. The figure illustrates the expression and localization of orphan GPCRs in Parkinson's Disease, Alzheimer's Disease, Multiple Sclerosis, and Huntington Disease.

cysteinyl leukotrienes CysLTs, such as LTD4 and LTC4. These endogenous ligands are released extracellularly at sites of neuroinflammation, where GPR17 is elevated (Fumagalli et al., 2011). The expression of GPR17 increases during damage to nerve cells. Furthermore, it takes part both in the process of inducing damage and also in the local repair of the damaged myelin sheath. Thus, GPR17 is an attractive target for MS.

The GPR17 gene was first isolated in 1996 and characterized for the first time in 2006 (Raport et al., 1996; Ciana et al., 2006). Phylogenetically, GPR17 is closely related to the purine subfamily and cysteinyl leukotriene receptors CysLT1 and CysLT2 (Fumagalli et al., 2016). It has been classified into the rhodopsin-like family, together with the purinergic P2Y receptor. In humans, the gene for GPR17 is located on chromosome 2q21. GPR17 receptors are present in neurons and some parenchymal quiescent OPCs. GPR17 is one of the key proteins expressed in human adult neuroprogenitor cells and participates in neuronal repair. GPR17 receptors are found in abundance in the nervous system, including the frontal cortex, striatum, brain stem and medulla (Ceruti et al., 2011). In addition, it is expressed in organs that undergo ischemic injury, including the brain, kidney and heart (Ciana et al., 2006; Ceruti et al., 2011; Dziedzic et al., 2020).

The level of GPR17 receptors is increased in oligodendrocyte lineage cells during the differentiation of OPCs into premature oligodendrocytes (Alavi et al., 2018). Recent reports indicate that GPR17 receptors play a role in both demyelination and remyelination processes in the central nervous system (CNS) (Dziedzic et al., 2020). These receptors seem to contribute to the death of neurons in sites of inflammation and also cause nerve tissue repair. Myelin sheath destruction and axonal injury are among the hallmarks of MS. The presence of oligodendrocytes and intact myelin sheath are essential for the proper functioning of neurons. Thus, they can serve as a sensor for local damage to the myelin sheath and as a potential marker of the neurodegenerative process in MS. In an *in vivo* mouse model of MS that presents clinical and pathological similarities to human MS, a highly selective GPR17 agonist delayed the onset of encephalomyelitis (Parravicini et al., 2020).

GPR18

GPR18 was first cloned by Gantz et al., in 1997. In humans, GPR18 is abundantly expressed in the spleen, thymus, peripheral blood leukocytes, lymph node, cerebellum, lung and testis, among others (Gantz et al., 1997; Vassilatis et al., 2003). GPR18 is also expressed in several immune cell types where it is involved in different biological functions. It shares low sequence homology with the cannabinoid receptors CB-1R and CB-2R and displays moderate identity with the putative cannabinoid receptor GPR55 (Morales et al., 2020).

GPR18 regulates polymorphonuclear cell infiltration and protects organs from acute immune responses (Reyes-Resina et al., 2018). The interest in GPR18 lies in its ability to recognize cannabinoid ligands and its propensity to heteromize with CBRs. This suggests that GPR18 and its heteromers may be attractive targets for neurodegenerative disorders.

The therapeutic potential of GPR18 has been shown through *in vitro* and animal model studies. It has been shown that GPR18 can interact with the CB-2R in activating microglia of the AD model.

Two different compounds have been proposed as putative ligands for GPR18; however, due to insufficient *in vivo* data, GPR18 is still grouped under class A orphan GPCRs. (for an extensive review on GPR18, see Morales et al., 2020) (Morales et al., 2020).

GPR37

Among orphan receptors with therapeutic potential for the treatment of neurodegenerative diseases, GPR37 is of particular interest since it is extensively expressed in the brain and the central nervous system and because it is related to the dopaminergic system and brain myelination. GPR37 is recognized as the parkin-associated -endothelin receptor-like receptor (Pael receptor) since it was originally identified as a substrate of parkin (Imai et al., 2000; Imai et al., 2001). Parkin is an E3 ubiquitin ligase encoded by the PARK2 gene involved in ubiquitination and proteasome-mediated degradation of misfolded proteins (Imai et al., 2001). Mutations in the PARK2 gene are the most common cause of autosomal recessive juvenile parkinsonism (AR-JP) (Kitada et al., 1998). An insoluble form of GPR37 was reported to accumulate in the brains of AR-JP patients. It is worth mentioning that modulation of GPR37 signaling is implicated in other diseases such as bipolar and major depression disorders, autism and epilepsy.

The GPR37 gene was first discovered in humans and localized to chromosome 7 (7q3l) as encoding for 7TM 613 amino acid-protein (Marazziti et al., 1998). Immunohistochemical mapping of GPR37 protein levels in mouse brain showed that the receptor is widely expressed in oligodendrocytes, whereas neuronal expression is mainly limited to the nigrostriatal dopaminergic system and hippocampus (Imai et al., 2001).

Although its physiological relevance remains to be elucidated, GPR37 may be an attractive target for PD, since it interacts with the D2R, the 5-HT4R and also with the adenosine A_{2A} receptor, $A_{2A}R$. In PD, GPR37 acts as an $A_{2A}R$ inhibitor via receptor oligomerization. Recent studies suggest that GPR37 has a bidirectional role in PD pathogenesis. While its physiological role seems to be neuroprotective, it can misfold and aggregate intracellularly, ultimately leading to cell death (Leinartaité and Svenningsson, 2017).

Thus far, three different molecules, the head activator (HA), prosaposin (PSAP) and regenerating islet-derived family member 4 (Reg4) have been suggested to signal via GPR37, (Rezgaoui et al., 2006; Meyer et al., 2013; Wang et al., 2016), but currently GPR37 remains as a de-orphanized GPCR. Since GPR37 toxically accumulates in AR-JP, Morato et al. have explored the possibility of ecto-GPR37 as a potential biomarker for PD. Briefly, the presence of peptides from the N-terminus cleaved domain of GPR37 (i.e., ecto-GPR37) in human cerebrospinal fluid (CSF) samples of control subjects, PD patients and AD patients were identified by LC-MS analysis and quantified by an in-house ELISA method (Morató et al., 2021). The authors reported that significantly higher levels of ecto-GPR37 were detectable in the CSF of PD patients, but not in AD patients. Therefore, these authors suggest that ecto-GPR37 may be a promising potential biomarker for PD.

GPR49

GPR49, also known as Lgr5, that plays a critical role in various cancers, including basal cell carcinoma, head and neck squamous cell carcinoma, oral squamous cell carcinoma, and hepatocellular carcinoma (Yamamoto et al., 2003; Tanese et al., 2008; Major et al., 2013). Recent studies show that LCR5 is also expressed in neuronal stem cells such as glioblastoma stem cells and is associated with neuronal differentiation and maturation (Mao et al., 2013). In addition, LGR5 is abundantly expressed in spinal cord, motor neurons in brain stem, and neurons in Layer 5a and 6 in cortex, thereby LGR5 might be involved in the development of projection neuron in CNS (Song et al., 2015). Based on its expression in motor neurons and cortex, GPR49 may play a crucial role in the development of neurodegenerative diseases, although no studies have identified a link between this receptor and these disorders.

GPR50

GPR50 is widely distributed in many brain region such as cortex, midbrain, pons, amygdala and hippocampus except glial cells (Grunewald et al., 2012). In addition, it is also expressed in the inhibitory interneurons, These data suggest that GPR50 might modulate the excitability of neurons and regulate synaptic plasticity and cognitive function (Li et al., 2020). Furthermore, there is a growing evidence showing that GPR50 may be involved in the hypothalamus–pituitary–adrenal (HPA) axis and the glucocorticoid receptor (GR) signaling, leptin signaling, adaptive, thermogenesis, torpor and neuronal differentiation (Bechtold et al., 2012; Khan and He, 2017).

Although there is a potential link between GPR50 and psychiatric conditions and given the overlap between psychiatric and neurological disorders, recent findings have addressed the role of GPR50 in neurodegenerative diseases. Chen et al. (2019) have demonstrated a significant link between GPR50 hypomethylation and AD in males, suggesting a potential role for GPR50 in the development or progression of AD (Chen et al., 2019).

Moreover, GPR50, previously known as melatonin-related receptor, was cloned from the human pituitary and recognized as a member of the melatonin receptor subfamily and showed high amino acid similarities (45%) with MT1 and MT2 (Reppert et al., 1996). Zlotos et al. (2014) suggested the potential heterodimerization of melatonin receptor subtypes, including MT1 and MT2, with GPR50, which might affect melatonin receptor function (Zlotos et al., 2014). Changes in these receptors' expression patterns may contribute to the development and progression of the disease, pointing to a possible link between GPR50-related melatonin signaling pathways and neurodegenerative diseases like AD. Although the importance of GPR50 and ligand interactions has been established for neurodegenerative diseases, further research is needed to clarify downstream signaling pathways.

GPR52

GPR52 is predominantly expressed in the brain, particularly in regions associated with symptoms of neuropsychiatric disorders and Huntington's disease (Komatsu et al., 2014; Nishiyama et al., 2017; Hatzipantelis et al., 2020a; Wang P. et al., 2020; Ma et al., 2020). Along with GPR6 and GPR8, GPR52 shows promise as a therapeutic psychiatric receptor, especially due to its association with dopamine receptors in the basal ganglia (Rahman et al., 2023).

In light of its involvement in cAMP signaling pathways and potential effects on physiological functions, the expression and signaling cascade of the orphan receptor GPR52 has drawn attention in recent years. GPR52 has been found to co-localize with D1 receptors in the prefrontal cortex and with D2 receptors in the basal ganglia, indicating its involvement in dopaminergic transmission in these regions (Komatsu et al., 2014; Constantinof et al., 2019). In addition, the expression profiles in the prefrontal cortex overlap with D1 dopamine receptors, suggesting a potential influence on locomotor activity through the activation of DRD1 and NMDA receptors via cAMP accumulation (Hatzipantelis et al., 2020a). Moreover, it has been suggested that GPR52's activation of ERK1/2 signaling and the recruitment of β-arrestins in frontal cortical neurons are mechanisms that require further investigation (Woo et al., 2020).

GPR52 signaling via cAMP has been implicated in opposing D2 signaling in the striatum while stimulating D1/NMDA function in the frontal cortex (Russell et al., 2021). However, the effectiveness of GPR52 agonism in modulating D2/3 receptor signaling outside of the striatum may be limited by lower expression levels (Rahman et al., 2022). Moreover, GPR52-expressing neurons in the habenular nucleus have been suggested to provide negative compensatory signals to dopaminergic neurons in the midbrain. GPR52 has also been linked glutamatergic transmission in addition to the modulation of dopaminergic transmission, further emphasizing its role in cognitive and emotional processes (Komatsu et al., 2014).

Furthermore, the identification of GPR52 selective antagonists through high-throughput screening and studies of the structure-activity connection presents novel possibilities for therapeutic approaches for diseases such as Huntington's disease (Komatsu, 2021).

Reducing GPR52 or using antagonist can result in a decrease in soluble mutant Huntingtin (mHTT) protein levels, thereby improving HD-like phenotypes (Yao et al., 2015). This effect is linked to the modulation of mHTT levels through the inhibition of GPR52 function (Wu et al., 2023). Additionally, research has shown that GPR52 plays a role in rescuing behavioral phenotypes in HD mouse models, indicating its potential as a therapeutic target for the disease (Stott et al., 2021).

An understanding of the complex relationship between GPR52 and other receptors like dopamine D2 will help to develop novel treatment strategies that could address the complex pathophysiology of conditions like PD.

GPR55

G-protein coupled receptor 55 (GPR55) is widely expressed in the central nerve tissues and cells, and plays a role in controlling oxidative and inflammatory cell homeostasis (Apweiler et al., 2021). GPR55 interacts with two cannabinoid receptors (CB1/CB2). GPR55 forms heteromer structure with CB1 and CB2 receptors like other orphan receptors (GPR3/GPR6/GPR12/GPR18), or PPARγ, subsequently leading to complex interactions that can either inhibit or enhance GPR55-mediated signaling (Apweiler et al., 2021; Perez-Olives et al., 2021).

GPR55 plays a crucial role in various cellular processes such as cell proliferation, migration, survival, and tumorigenesis in various cancer cell lines (Hasenoehrl et al., 2019; Akimov et al., 2023). It triggers a cascade of signaling events by interacting with different receptors or ligands, leading to diverse outcomes in different cell types (Balenga et al., 2014; Shi et al., 2017; Hill et al., 2019). Additionally, GPR55 has been implicated in modulating neurotransmitter release at central synapses, further highlighting its diverse functions (Sylantyev et al., 2013).

Furthermore, it has been demonstrated that GPR55 stimulates the extracellular signal-regulated kinase (ERK) cascade, which in turn stimulates the growth of cancer cells (Andradas et al., 2011; Mangini et al., 2017). GPR55 has been shown to promote cancer cell proliferation via the extracellular signal-regulated kinase (ERK) cascade (Andradas et al., 2011; Mangini et al., 2017). The cell type-dependent RhoA activation reported upon activation of GPR55 in different studies indicate to cell type-specific downstream signaling cascade (Liu et al., 2016).

Numerous physiological processes and diseases, such as neuropathic pain, cancer, metabolic diseases, inflammatory pain, bone growth, and neurological disorders have been linked to GPR55 (Kotsikorou et al., 2013). While its role in diseases like obesity, diabetes, osteoporosis, and cancer has been studied, its involvement in CNS disorders such as depression, AD, and PD remains poorly understood (Apweiler et al., 2021). It has been implicated in various physiological processes and diseases, including neuroinflammation and neurodegenerative conditions like Multiple sclerosis (MS) (Saliba et al., 2018).

Very recent studies have delineated the association between GPR55 and cannabioid receptors and cannabidiol (CBD), a cannabinoid compound. CBD has been found to cause vasorelaxation through CB1 activation and has been implicated in modulating seizures through interactions with CB1, CB2, GPR18, GPR55, and other receptors (Stanley et al., 2015; Longoria et al., 2022). Additionally, CBD has been used in clinical practice for conditions like spasticity in MS and childhood epilepsy (Hind et al., 2016; Golub and Reddy, 2021). A number of studies demonstrate that the GPR55, PPARγ, and TRPV channels signaling pathways are linked to the anti-inflammatory effects of CBD (Lötsch et al., 2018). Since inflammation is one of the hallmarks of neurodegenerative diseases, targeting GPR55 might be a novel therapeutic approach for the treatment of neurodegenerative diseases like PD, AD, and MS (Saliba et al., 2018).

Recent evidence has pointed out that single nucleotide polymorphisms (SNPs) in GPR55 are linked to AD progression, suggesting a role in the disease (Mori-Fegan et al., 2023). In AD mouse models, activation of GPR55 has been shown to reduce synaptic dysfunction, oxidative stress, neuroinflammation, and cognitive impairment (Xiang et al., 2022). Furthermore, research indicates that endocannabinoid-related receptors, such as GPR55, are expressed more abundantly in mice models of AD, indicating that these receptors have a role in the disease (Medina-Vera et al., 2023). GPR55 is also expressed on microglia cells which are known to be essential for neuroinflammation. GPR55 antagonists have also been shown to have anti-neuroinflammatory properties in microglial cells, suggesting a possible treatment path for neurological disorders characterized by neuroinflammation (Saliba et al., 2018).

Activation of GPR55 has been observed to mitigate cognitive impairment, oxidative stress, neuroinflammation, and synaptic dysfunction in AD mouse models (Xiang et al., 2022). The GPR55 agonist, O-1602, has displayed a potential in ameliorating cognitive impairment, neuroinflammation, oxidative stress, and

apoptosis induced by lipopolysaccharide in mice, suggesting a neuroprotective role (Wang XS. et al., 2020).

In addition to AD, GPR55 has been implicated in PD. Recent studies have shown high expression of GPR55 in the striatum and in the external globus pallidus, indicating a potential link between GPR55 activity and motor dysfunction in PD (Patricio et al., 2022; Wong et al., 2023). GPR55 and CB1 heteromers have also shown significant neuroprotection against parkinsonism-inducing toxins, as in AD (Cooray et al., 2020). Additionally, the expression of heteromers consisting of GPR55 and CB1/CB2 receptors in the striatum has been evaluated in parkinsonian macaques, highlighting a correlation between Parkinsonism and altered expression of these heteromers (Basile and Mazzon, 2022). The use of GPR55 as a therapeutic target for managing motor deficits in PD has been proposed, with research focusing on the effects of GPR55 selective ligands in PD rat models (Fatemi et al., 2021; Sánchez-Zavaleta et al., 2023). The therapeutic potential of GPR55 has been also explored in PD, with studies indicating that GPR55 activation may reduce circuit dysfunction in PD-related afferent systems, making it a promising approach for treating disease-related motor dysfunction (Hewer et al., 2023).

In experimental autoimmune encephalomyelitis models of MS, the genetic background has been found to influence the effects of gene knockout, particularly of GPR55 and CB2 receptors, on disease severity (Nouh et al., 2023). Specifically, GPR55 has been associated with pro-inflammatory roles in mouse models of gastrointestinal inflammation and MS (Kurano et al., 2021; Nouh et al., 2023).

GPR78

GPR78 is closely analogous to the GPR26 gene and is exclusively identified in the placenta and pituitary glands of humans. There were no mRNA transcripts detected in other central nervous system regions, including the frontal cortex, putamen, thalamus, hypothalamus, amygdala, hippocampus, pons, medulla, and midbrain (Lee et al., 2001). GPR78 is generally expressed in endoplasmic reticulum and inactivates ER stress sensors ATF-6, PERK and IRE1 (Araujo et al., 2018). *In vitro*, GPR78 is shown to increase intracellular cAMP (Jones et al., 2007). Acting as a regulator within the phosphoinositide 3-kinase (PI3K)–protein kinase B (AKT) signaling network, it exerts varied downstream effects on the proliferation, survival, metastasis, and chemoresistance of cancer cells. BC71 and two peptides have been developed for the GPR78 receptors (Arap et al., 2004; Gonzalez-Gronow et al., 2009; Araujo et al., 2018). Since GPR78 is expressed in the basal ganglia, it may be also be involved in the pathophysiology of PD.

GPR83

GPR83, also known as JP05, GIR, and GPR72, is a GPCR initially identified in thymoma as a glucocorticoid-induced receptor. It is extensively present in $CD4^+CD25^+$ regulatory T (Treg) cells and the central nervous system, particularly in brain regions like the hippocampus, amygdala, prefrontal cortex, and various hypothalamic nuclei. GPR83 is implicated in stress-associated physiology and may play significant roles in learning and memory, reward, emotional behaviors, and stress regulation. GPR83-deficient mice showed delayed spatial learning acquisition and an increased preference for sucrose (Li DY. et al., 2013; Li J. et al., 2013). GPR83 and GPR171 signaling pathways in brain regions control feeding and reward behaviors. Recently, there has been discussion concerning the de-orphanization of GPR83, attributed to its discovery of binding with bigLEN or PEN, known to regulate feeding behavior (Gomes et al., 2016). FAM237A and FAM237B are the ligands which are shown to activate GPR83, and the latter activate GPR83 through the Gαq signaling pathway (Sallee et al., 2020). Although a direct correlation between GPR83 and neurodegenerative disorders has not been demonstrated yet, its involvement in learning and memory may have an impact for AD research.

GPR84

GPR84, a Gi-coupled GPCR, has been suggested to recognize endogenous medium-chain fatty acids (MCFAs) (Fredriksson et al., 2003; Foord et al., 2005). Similar to GPR83, GPR84 also takes part in immune defense through microglia, which are essential in immune defense of the CNS and its diseases (Simard et al., 2006). In addition to modulating the microglial cells, GPR84 modulates the production of interleukin-4 (IL-4) by T lymphocytes, as well (Wittenberger et al., 2001; Yousefi et al., 2001; Venkataraman and Kuo, 2005).

In an experimental study, the gene of GPR84 is upregulated in microglial cells within the brains of APP/PS1 transgenic mice, a model for AD. The increased GPR84 activity correlates with faster cognitive decline and a decrease in the number of microglia, particularly around areas with amyloid plaques. Interestingly, the absence of GPR84 does not impact the formation of plaques or the hippocampal neurogenesis, but leads to β-amyloid-induced microgliosis and therefore contributes to the β-amyloid-induced dendritic degeneration (Audoy-Rémus et al., 2015). A recent study of human data using machine learning methods, where human samples from the entorhinal cortex bearing neurofibrillary tangles or none were examined, showed that among the other genes, GPR84 gene is differentially expressed. This suggests GPR84 has a potential to be a marker for AD (Madar et al., 2021). 6-n-octylaminouracil and 9–14 carbon chain fatty acids have been proposed as endogenous ligands (Wang et al., 2006; Suzuki et al., 2013a). Decanoic acid, lauric acid, embelin, PSB-16434, ZQ-16, 6-nonylpyridine-2,4-diol, DL-175 are orthosteric and DIM is an allosteric agonist (Wang et al., 2006; Suzuki et al., 2013a; Southern et al., 2013; Marsango et al., 2022).

GPR85

GPR85 previously named as, Super conserved receptor expressed in brain-2, SREB2, has been associated with the brain, and has been linked to autism spectrum disorder and schizophrenia, so far. It has a neuroectodermal origin and is highly expressed in the mouse cerebral cortex and human adults. Its expression is increased with development and neuronal differentiation (Hellebrand et al., 2001). In rat, the expression of the gpr85 gene was found to be declined gradually after birth and became undetectable by postnatal day 18, but its weak expression was observed in the adult

hippocampal formation, olfactory bulb, and cerebellum (Jeon et al., 2002). mRNA profiling across the species of adult human, monkey, and rat forebrains, SREB2 mRNA were detected in the hippocampal dentate gyrus, hippocampal formation, olfactory system, and supraoptic and paraventricular nuclei (Matsumoto et al., 2005).

Few studies have explored the association of GPR85 with brain disorders. However, its expression holds potential as a target for conditions like schizophrenia or epilepsy. Overexpression in transgenic mice resulted in decreased social interaction, abnormal sensorimotor gating, and impaired memory. Additionally, GPR85 expression increased in the adult hippocampal formation, piriform cortex, and amygdaloid complex following treatment with kainic acid, which induces convulsive epilepsy (Jeon et al., 2002; Matsumoto et al., 2008).

Studies designing novel ligands for GPR85 continues and so far, a new inverse agonist has been identified (Sakai et al., 2022). The association of GPR85 with learning and memory suggests a potential link to AD. GPR85 continues to be investigated with specific ligands and antagonists.

GPR88

GPR88 exhibits widespread expression in the spleen, liver, and brain. It is conserved between humans and mice and is mapped to the 1p21.3 chromosomes in humans and 3G1 in mice. Initially characterized as a receptor specific to the striatum, GPR88 plays a role in various physiological processes within the central nervous system (Mizushima et al., 2000).

As it is connected to the striatum, it is no surprise that GPR88 has been extensively investigated with animal models of PD research. GPR88 is mainly expressed in the striatum of rodents, humans and is specifically associated with movement disorders (Ye et al., 2019). Knocking down Gpr88 negatively affected the expression of DARPP-32, a key protein in medium spiny neurons controlling dopamine reception. Gpr88 knockout mice showed increased spontaneous locomotion, drug-induced catalepsy sensitivity, and motor incoordination, suggesting GPR88's role in motor function. While direct links between Gpr88 mutations and human PD are lacking, sporadic chorea cases in humans have been associated with mutations in GPR88 (Ye et al., 2019).

One of the most problematic issue in the management of PD is L-DOPA mediated tardive dyskinesia due to the long term use of dopaminergic agents. GPR88 proteins seem to be promising targets for the mitigation of dyskinesia. For instance, Gpr88 knockdown seem to prevent the onset of dyskinesia (Mantas et al., 2020). In this study while Gpr88 knockout mice exhibited less involuntary movements, less serotonin displacement and reduced tacrine-induced PD-like tremor and spontaneous locomotion (Mantas et al., 2020). An association between HD, an autosomal dominant condition which emerges around midlife, and GPR88 has also been proposed. (Rocher et al., 2016). mHTT, that affects striatal medium spiny neurons (MSNs) sustain their functionality over several decades (Rocher et al., 2016). In an *in vivo* study with a mice model of HD, BACHD, in which there is high expression levels of neuropathogenic, full length mutant huntingtin (fl-mHTT) genes, lower expression of GPR88 has been found in the striatum, that is accompanied by hyperexcitability, increased amplitude of AMPA receptor-mediated synaptic and a decline in spine density (Rocher et al., 2016).

Similarly, in a Gpr88-inactivated lentiviral-mediated knock-down striatal 6-OHDA rat model, a specifically designated microRNA (miR) (KD-Gpr88) reduced acute amphetamine-induced turning behavior and normalized striatal Gad67 and proenkephalin expression, indicating to an association with the severity of L-DOPA induced dyskinesia (Ingallinesi et al., 2019). In a further study of the same group, using medial forebrain bundle injections in an early Parkinson (6-OHDA)_ model, lentiviral-delivery of the specific microRNA to knock down GPR88 seemed to mitigate mood, motivation, and cognition alterations by modulating the regulator of G-protein signaling 4 and the truncated splice variant of the FosB transcription factor (Galet et al., 2021). GPR88 primarily couples to Gi/o proteins (Jin et al., 2018) and its known agonists are 2-PCCA and RTI-13951-33 (Garisetti et al., 2023). In summary, GPR84 may be a promising target in PD and HD in the future.

Discussion

GPCRs are primary targets for drug development. Many drugs used today are the results of sustained research, stimulated by recent findings of additional signaling pathways. Orphan GPCRs hold the potential of being novel therapeutic targets for disorders that currently have no radical therapies. However, the allure of orphan GPCRs comes with a caveat. GPCRs, in general, are intricately linked to diverse signaling pathways, making them less than ideal drug targets. The association with multiple pathways raises concerns about potential side effects, already encountered with existing GPCR targets. Nevertheless, research on orphan GPCRs is expected to enhance our comprehension of their specific physiological and neuropathological functions in the years ahead. Orphan GPCRs have been associated with various physiological processes, including neuromodulation (Civelli, 2012), circadian behavior regulation (Doi et al., 2016), and immune response modulation that makes them this promising targets with the disorders that have these bases. Orphan GPCRs are also implicated in immune responses, with some receptors regulating key immune cells through metabolite signaling (Husted et al., 2017). Moreover, orphan GPCRs have shown a preference for associating with lipid and lipid-like molecules, suggesting a potential role in lipid metabolism and signaling pathways (Im, 2004; Wei et al., 2017; Jobe and Vijayan, 2024).

Sphingosine-1-phosphates (S1Ps) are signaling lipids which act on the S1PR family of cognate GPCRs and have been shown to modulate neuroinflammation, a process known to be involved in both neurodegenerative and cerebrovascular diseases (Chua et al., 2020). S1P, as an agonist on GPR3, GPR6, GPR12, may be a promising target in Alzheimer's Disease (Kunkel et al., 2013). Despite the promising roles of GPR3 (Huang et al., 2015; Capaldi et al., 2018), GPR6, and GPR12 in neurodegenerative diseases, including AD, further research is required to fully elucidate their mechanisms of action and validate them as viable therapeutic targets. Sphingosine 1-phosphate (S1P) also plays a crucial role in inflammation, particularly in the context of MS. For example, Fingolimod (FTY720), an S1P receptor modulator, has been approved as an oral treatment for relapsing forms of MS, highlighting the relevance of S1P in MS treatment (Choi et al.,

2010). Therefore, agonists on GPR3, GPR6, GPR12 can be considered as candidates for MS research.

Due to the heterogeneous expression of some orphan GPRCs such as; GPR3, GPR6, GPR18 and GPR55 with cannabinoid receptors of CB1 and CB2, the modulatory effects of CB receptors seem to be also intrinsically regulated by these specific orphan receptors. CB2 receptors, in particular, have been shown to have neuroprotective effects in conditions like HD by attenuating microglial activation and preventing neurodegeneration (Rajesh et al., 2007). CB1 receptors have been shown to provide neuroprotection through the inhibition of excitotoxicity and oxidative stress, as evidenced in animal models of some neurodegenerative diseases such as MS (Maresz et al., 2005; Gowran et al., 2010). The endocannabinoid system, involving CB1 and CB2 receptors, their ligands, and associated enzymes, acts as a key modulatory system influencing various pathological processes in neurodegenerative disorders (Jhaveri et al., 2007).

Furthermore, many orphan GPCRs, such as GPR83, GPR84 and GPR85 are expressed in various tissues, including immune system cells, Tregs, monocytes, macrophages, microglia and in the different brain regions (Wei et al., 2017). GPR83 has been linked to the regulation of stress, mood, reward-related behaviors, and immune function (Lueptow et al., 2018). GPR84 has been proposed to be involved in microglial motility after neuronal injury, suggesting a potential role in neuroprotection (Wei et al., 2017). Overall, these results indicate that orphan GPCRs are versatile receptors with implications in both immune responses and neuronal functions. Their involvement in inflammation and immune cell regulation, and along with their proposed neuroprotective roles make them promising targets for therapeutic interventions in conditions involving immune dysregulation and neuroinflammation.

Furthermore, current progress in GPCR structural biology, virtual libraries, molecular modelling and the use of cryo-EM for structure elucidation, has made a significant impact on overcoming different of obstacles in identifying orphan GPCRs ligands. These studies that emphasize the heterodimer or oligomeric structure of orphan GPCRs are critical for their function and signaling.

In conclusion, orphan GPCRs are widely expressed in the CNS and are involved in a wide range of physiological effects. Understanding the interactions of orphan receptors with other GPCRs such as cannabinoid receptors, dopamine receptors and melatonin receptors and their propensity to form heteromers will provide insights into the complex structural and functional mechanisms underlying neurodegenerative disease (Figure 1). Deciphering the ligands for orphan GPCRs and understanding their structure and signaling mechanism will facilitate identification of small molecules targeted for the therapy of neurodegenerative diseases.

Author contributions

DÖ-A: Visualization, Writing–review and editing, Writing–original draft, Conceptualization. MY: Writing–review and editing, Writing–original draft, Visualization, Conceptualization. BK: Supervision, Writing–review and editing, Writing–original draft, Conceptualization.

Funding

The author(s) declare that no financial support was received for the research, authorship, and/or publication of this article.

Conflict of interest

The authors declare that the research was conducted in the absence of any commercial or financial relationships that could be construed as a potential conflict of interest.

Publisher's note

All claims expressed in this article are solely those of the authors and do not necessarily represent those of their affiliated organizations, or those of the publisher, the editors and the reviewers. Any product that may be evaluated in this article, or claim that may be made by its manufacturer, is not guaranteed or endorsed by the publisher.

References

Akimov, M. G., Gretskaya, N. M., Dudina, P. V., Sherstyanykh, G. D., Zinchenko, G. N., Serova, O. V., et al. (2023). The mechanisms of GPR55 receptor functional selectivity during apoptosis and proliferation regulation in cancer cells. *Int. J. Mol. Sci.* 24 (6), 5524. doi:10.3390/ijms24065524

Alavi, M. S., Shamsizadeh, A., Azhdari-Zarmehri, H., and Roohbakhsh, A. (2018). Orphan G protein-coupled receptors: the role in CNS disorders. *Biomed. Pharmacother.* 98, 222–232. doi:10.1016/j.biopha.2017.12.056

Allende, G., Chavez-Reyes, J., Guerrero-Alba, R., Vazquez-Leon, P., and Marichal-Cancino, B. A. (2020). Advances in neurobiology and Pharmacology of GPR12. *Front. Pharmacol.* 11, 628. doi:10.3389/fphar.2020.00628

Andradas, C., Caffarel, M. M., Perez-Gomez, E., Salazar, M., Lorente, M., Velasco, G., et al. (2011). The orphan G protein-coupled receptor GPR55 promotes cancer cell proliferation via ERK. *Oncogene* 30 (2), 245–252. doi:10.1038/onc.2010.402

Apweiler, M., Saliba, S. W., Streyczek, J., Hurrle, T., Gräßle, S., Bräse, S., et al. (2021). Targeting oxidative stress: novel coumarin-based inverse agonists of GPR55. *Int. J. Mol. Sci.* 22 (21), 11665. doi:10.3390/ijms222111665

Arap, M. A., Lahdenranta, J., Mintz, P. J., Hajitou, A., Sarkis, Á. S., Arap, W., et al. (2004). Cell surface expression of the stress response chaperone GRP78 enables tumor targeting by circulating ligands. *Cancer Cell* 6 (3), 275–284. doi:10.1016/j.ccr.2004.08.018

Araujo, N., Hebbar, N., and Rangnekar, V. M. (2018). GRP78 is a targetable receptor on cancer and stromal cells. *EBioMedicine* 33, 2–3. doi:10.1016/j.ebiom.2018.06.030

Atanes, P., Ashik, T., and Persaud, S. J. (2021). Obesity-induced changes in human islet G protein-coupled receptor expression: implications for metabolic regulation. *Pharmacol. Ther.* 228, 107928. doi:10.1016/j.pharmthera.2021.107928

Audoy-Rémus, J., Bozoyan, L., Dumas, A., Filali, M., Lecours, C., Lacroix, S., et al. (2015). GPR84 deficiency reduces microgliosis, but accelerates dendritic degeneration and cognitive decline in a mouse model of Alzheimer's disease. *Brain, Behav. Immun.* 46, 112–120. doi:10.1016/j.bbi.2015.01.010

Balenga, N. A., Martínez-Pinilla, E., Kargl, J., Schröder, R., Peinhaupt, M., Platzer, W., et al. (2014). Heterogenization of GPR55 and cannabinoid CB2 receptors modulates signalling. *Br. J. Pharmacol.* 171 (23), 5387–5406. doi:10.1111/bph.12850

Basile, M. S., and Mazzon, E. (2022). The role of cannabinoid type 2 receptors in Parkinson's disease. *Biomedicines* 10 (11), 2986. doi:10.3390/biomedicines10112986

Bechtold, D. A., Sidibe, A., Saer, B. R., Li, J., Hand, L. E., Ivanova, E. A., et al. (2012). A role for the melatonin-related receptor GPR50 in leptin signaling, adaptive thermogenesis, and torpor. *Curr. Biol.* 22 (1), 70–77. doi:10.1016/j.cub.2011.11.043

Benned-Jensen, T., and Rosenkilde, M. M. (2010). Distinct expression and ligand-binding profiles of two constitutively active GPR17 splice variants. *Br. J. Pharmacol.* 159 (5), 1092–1105. doi:10.1111/j.1476-5381.2009.00633.x

Braak, H., Ghebremedhin, E., Rüb, U., Bratzke, H., and Del Tredici, K. (2004). Stages in the development of Parkinson's disease-related pathology. *Cell Tissue Res.* 318 (1), 121–134. doi:10.1007/s00441-004-0956-9

Capaldi, S., Suku, E., Antolini, M., Di Giacobbe, M., Giorgetti, A., and Buffelli, M. (2018). Allosteric sodium binding cavity in GPR3: a novel player in modulation of Aβ production. *Sci. Rep.* 8 (1), 11102. doi:10.1038/s41598-018-29475-7

Carmon, K. S., Gong, X., Lin, Q., Thomas, A., and Liu, Q. (2011). R-spondins function as ligands of the orphan receptors LGR4 and LGR5 to regulate Wnt/beta-catenin signaling. *Proc. Natl. Acad. Sci. U. S. A.* 108 (28), 11452–11457. doi:10.1073/pnas.1106083108

Ceruti, S., Viganò, F., Boda, E., Ferrario, S., Magni, G., Boccazzi, M., et al. (2011). Expression of the new P2Y-like receptor GPR17 during oligodendrocyte precursor cell maturation regulates sensitivity to ATP-induced death. *Glia* 59 (3), 363–378. doi:10.1002/glia.21107

Chen, W., Ji, H., Li, L., Xu, C., Zou, T., Cui, W., et al. (2019). Significant association between GPR50 hypomethylation and AD in males. *Mol. Med. Rep.* 20 (2), 1085–1092. doi:10.3892/mmr.2019.10366

Chen, Y., Wu, H., Shu-zong, W., Koito, H., Li, J., Ye, F., et al. (2009). The oligodendrocyte-specific G protein–coupled receptor GPR17 is a cell-intrinsic timer of myelination. *Nat. Neurosci.* 12, 1398–1406. doi:10.1038/nn.2410

Choi, J. W., Gardell, S. E., Herr, D. R., Rivera, R., Lee, C.-W., Noguchi, K., et al. (2010). FTY720 (Fingolimod) efficacy in an animal model of multiple sclerosis requires astrocyte sphingosine 1-phosphate receptor 1 (S1P 1) modulation. *Proc. Natl. Acad. Sci.* 108, 751–756. doi:10.1073/pnas.1014154108

Chua, X. Y., Chai, Y. L., Chew, W., Chong, J., Ang, H. L., Xiang, P., et al. (2020). Immunomodulatory sphingosine-1-phosphates as plasma biomarkers of Alzheimer's disease and vascular cognitive impairment. *Alzheimer S Res. Ther.* 12, 122. doi:10.1186/s13195-020-00694-3

Ciana, P., Fumagalli, M., Trincavelli, M. L., Verderio, C., Rosa, P., Lecca, D., et al. (2006). The orphan receptor GPR17 identified as a new dual uracil nucleotides/cysteinyl-leukotrienes receptor. *Embo J.* 25 (19), 4615–4627. doi:10.1038/sj.emboj.7601341

Civelli, O. (2012). Orphan GPCRs and neuromodulation. *Neuron* 76 (1), 12–21. doi:10.1016/j.neuron.2012.09.009

Constantinof, A., Moisiadis, V. G., Kostaki, A., Szyf, M., and Matthews, S. G. (2019). Antenatal glucocorticoid exposure results in sex-specific and transgenerational changes in prefrontal cortex gene transcription that relate to behavioural outcomes. *Sci. Rep.* 9 (1), 764. doi:10.1038/s41598-018-37088-3

Cooray, R., Gupta, V., and Suphioglu, C. (2020). Current aspects of the endocannabinoid system and targeted THC and CBD phytocannabinoids as potential therapeutics for Parkinson's and Alzheimer's diseases: a review. *Mol. Neurobiol.* 57 (11), 4878–4890. doi:10.1007/s12035-020-02054-6

Doi, M., Murai, I., Kunisue, S., Setsu, G., Uchio, N., Tanaka, R., et al. (2016). Gpr176 is a gz-linked orphan G-protein-coupled receptor that sets the pace of circadian behaviour. *Nat. Commun.* 7, 10583. doi:10.1038/ncomms10583

Dong, D., Zhou, H., and Gao, L. (2016). GPR78 promotes lung cancer cell migration and metastasis by activation of gαq-rho GTPase pathway. *BMB Rep.* 49, 623–628. doi:10.5483/bmbrep.2016.49.11.133

Draganski, B., and Bhatia, K. P. (2010). Brain structure in movement disorders: a neuroimaging perspective. *Curr. Opin. neurology* 23 (4), 413–419. doi:10.1097/WCO.0b013e32833bc59c

Dziedzic, A., Miller, E., Saluk-Bijak, J., and Bijak, M. (2020). The GPR17 receptor-A promising goal for therapy and a potential marker of the neurodegenerative process in multiple sclerosis. *Int. J. Mol. Sci.* 21 (5), 1852. doi:10.3390/ijms21051852

Eggerickx, D., Denef, J. F., Labbe, O., Hayashi, Y., Refetoff, S., Vassart, G., et al. (1995). Molecular cloning of an orphan G-protein-coupled receptor that constitutively activates adenylate cyclase. *Biochem. J.* 309 (Pt 3), 837–843. doi:10.1042/bj3090837

Ehrlich, A. T., Semache, M., Bailly, J., Wojcik, S., Arefin, T. M., Colley, C., et al. (2017). Mapping GPR88-venus illuminates a novel role for GPR88 in sensory processing. *Brain Struct. Funct.* 223, 1275–1296. doi:10.1007/s00429-017-1547-3

Fatemi, I., Abdollahi, A., Shamsizadeh, A., Allahtavakoli, M., and Roohbakhsh, A. (2021). The effect of intra-striatal administration of GPR55 agonist (LPI) and antagonist (ML193) on sensorimotor and motor functions in a Parkinson's disease rat model. *Acta Neuropsychiatr.* 33 (1), 15–21. doi:10.1017/neu.2020.30

Fitzgerald, H. K., Bonin, J. L., Sadhu, S., Lipscomb, M., Biswas, N., Decker, C., et al. (2023). The resolvin D2-gpr18 Axis enhances bone marrow function and limits hepatic fibrosis in. *Aging*. doi:10.1101/2023.01.05.522881

Foord, S. M., Bonner, T. I., Neubig, R. R., Rosser, E. M., Pin, J. P., Davenport, A. P., et al. (2005). International Union of Pharmacology. XLVI. G protein-coupled receptor list. *Pharmacol. Rev.* 57 (2), 279–288. doi:10.1124/pr.57.2.5

Fredriksson, R., Lagerström, M. C., Lundin, L. G., and Schiöth, H. B. (2003). The G-protein-coupled receptors in the human genome form five main families. Phylogenetic analysis, paralogon groups, and fingerprints. *Mol. Pharmacol.* 63 (6), 1256–1272. doi:10.1124/mol.63.6.1256

Freudzon, L., Norris, R. P., Hand, A. R., Tanaka, S., Saeki, Y., Jones, T. L. Z., et al. (2005). Regulation of meiotic prophase arrest in mouse oocytes by GPR3, a constitutive activator of the gs G protein. *J. Cell Biol.* 171, 255–265. doi:10.1083/jcb.200506194

Fumagalli, M., Daniele, S., Lecca, D., Lee, P. R., Parravicini, C., Fields, R. D., et al. (2011). Phenotypic changes, signaling pathway, and functional correlates of GPR17-expressing neural precursor cells during oligodendrocyte differentiation. *J. Biol. Chem.* 286 (12), 10593–10604. doi:10.1074/jbc.M110.162867

Fumagalli, M., Lecca, D., and Abbracchio, M. P. (2016). CNS remyelination as a novel reparative approach to neurodegenerative diseases: the roles of purinergic signaling and the P2Y-like receptor GPR17. *Neuropharmacology* 104, 82–93. doi:10.1016/j.neuropharm.2015.10.005

Galet, B., Ingallinesi, M., Pegon, J., Do Thi, A., Ravassard, P., Faucon Biguet, N., et al. (2021). G-protein coupled receptor 88 knockdown in the associative striatum reduces psychiatric symptoms in a translational male rat model of Parkinson disease. *J. psychiatry & Neurosci. JPN* 46 (1), E44–e55. doi:10.1503/jpn.190171

Gantz, I., Muraoka, A., Yang, Y. K., Samuelson, L. C., Zimmerman, E. M., Cook, H., et al. (1997). Cloning and chromosomal localization of a gene (GPR18) encoding a novel seven transmembrane receptor highly expressed in spleen and testis. *Genomics* 42 (3), 462–466. doi:10.1006/geno.1997.4752

Garisetti, V., Dhanabalan, A. K., and Dasararaju, G. (2023). Orphan receptor GPR88 as a potential therapeutic target for CNS disorders - an *in silico* approach. *J. Biomol. Struct. Dyn.* 42, 4745–4758. doi:10.1080/07391102.2023.2222820

Golub, V., and Reddy, D. S. (2021). Cannabidiol therapy for refractory epilepsy and seizure disorders. *Adv. Exp. Med. Biol.* 1264, 93–110. doi:10.1007/978-3-030-57369-0_7

Gomes, I., Bobeck, E. N., Margolis, E. B., Gupta, A., Sierra, S., Fakira, A. K., et al. (2016). Identification of GPR83 as the receptor for the neuroendocrine peptide PEN. *Sci. Signal.* 9 (425), ra43–ra. doi:10.1126/scisignal.aad0694

Gonzalez-Gronow, M., Selim, M. A., Papalas, J., and Pizzo, S. V. (2009). GRP78: a multifunctional receptor on the cell surface. *Antioxidants redox Signal.* 11 (9), 2299–2306. doi:10.1089/ARS.2009.2568

Gowran, A., Noonan, J., and Campbell, V. A. (2010). The multiplicity of action of cannabinoids: implications for treating neurodegeneration. *CNS Neurosci. Ther.* 17, 637–644. doi:10.1111/j.1755-5949.2010.00195.x

Grunewald, E., Tew, K. D., Porteous, D. J., and Thomson, P. A. (2012). Developmental expression of orphan G protein-coupled receptor 50 in the mouse brain. *ACS Chem. Neurosci.* 3 (6), 459–472. doi:10.1021/cn300008p

Hasenoehrl, C., Feuersinger, D., Kienzl, M., and Schicho, R. (2019). GPR55-Mediated effects in colon cancer cell lines. *Med. Cannabis Cannabinoids* 2 (1), 22–28. doi:10.1159/000496356

Hatzipantelis, C. J., Langiu, M., Vandekolk, T. H., Pierce, T. L., Nithianantharajah, J., Stewart, G. D., et al. (2020a). Translation-focused approaches to GPCR drug discovery for cognitive impairments associated with schizophrenia. *ACS Pharmacol. Transl. Sci.* 3 (6), 1042–1062. doi:10.1021/acsptsci.0c00117

Hatzipantelis, C. J., Lu, Y., Spark, D. L., Langmead, C. J., and Stewart, G. D. (2020b). β-Arrestin-2-Dependent mechanism of GPR52 signaling in frontal cortical neurons. *ACS Chem. Neurosci.* 11 (14), 2077–2084. doi:10.1021/acschemneuro.0c00199

Hellebrand, S., Wittenberger, T., Schaller, H. C., and Hermans-Borgmeyer, I. (2001). Gpr85, a novel member of the G-protein coupled receptor family, prominently expressed in the developing mouse cerebral cortex. *Brain Res. Gene Expr. patterns* 1 (1), 13–16. doi:10.1016/s1567-133x(01)00002-3

Henstridge, C. M., Balenga, N., Ford, L., Ross, R. A., Waldhoer, M., and Irving, A. J. (2008). The GPR55 ligand L-α-lysophosphatidylinositol promotes RhoA-dependent Ca2+signaling and NFAT activation. *Faseb J.* 23, 183–193. doi:10.1096/fj.08-108670

Hewer, R. C., Christie, L. A., Doyle, K. J., Xu, X., Roberts, M. J., Dickson, L., et al. (2023). Discovery and characterization of novel CNS-penetrant GPR55 agonists. *J. Med. Chem.* 66 (18), 12858–12876. doi:10.1021/acs.jmedchem.3c00784

Hill, J. D., Zuluaga-Ramirez, V., Gajghate, S., Winfield, M., Sriram, U., Rom, S., et al. (2019). Activation of GPR55 induces neuroprotection of hippocampal neurogenesis and immune responses of neural stem cells following chronic, systemic inflammation. *Brain Behav. Immun.* 76, 165–181. doi:10.1016/j.bbi.2018.11.017

Hind, W. H., England, T. J., and O'Sullivan, S. E. (2016). Cannabidiol protects an *in vitro* model of the blood-brain barrier from oxygen-glucose deprivation via PPARγ and 5-HT1A receptors. *Br. J. Pharmacol.* 173 (5), 815–825. doi:10.1111/bph.13368

Huang, Y., Skwarek-Maruszewska, A., Horre, K., Vandewyer, E., Wolfs, L., Snellinx, A., et al. (2015). Loss of GPR3 reduces the amyloid plaque burden and improves memory in Alzheimer's disease mouse models. *Sci. Transl. Med.* 7 (309), 309ra164. doi:10.1126/scitranslmed.aab3492

Husted, A. S., Trauelsen, M., Rudenko, O., Hjorth, S. A., and Schwartz, T. W. (2017). GPCR-mediated signaling of metabolites. *Cell Metab.* 25 (4), 777–796. doi:10.1016/j.cmet.2017.03.008

Ignatov, A., Lintzel, J., Hermans-Borgmeyer, I., Kreienkamp, H. J., Joost, P., Thomsen, S., et al. (2003a). Role of the G-protein-coupled receptor GPR12 as high-affinity receptor for sphingosylphosphorylcholine and its expression and function in brain development. *J. Neurosci.* 23 (3), 907–914. doi:10.1523/JNEUROSCI.23-03-00907.2003

Ignatov, A., Lintzel, J., Kreienkamp, H. J., and Schaller, H. C. (2003b). Sphingosine-1-phosphate is a high-affinity ligand for the G protein-coupled receptor GPR6 from mouse and induces intracellular Ca2+ release by activating the sphingosine-kinase pathway. *Biochem. Biophys. Res. Commun.* 311 (2), 329–336. doi:10.1016/j.bbrc.2003.10.006

Im, D. S. (2004). Discovery of new G protein-coupled receptors for lipid mediators. *J. Lipid Res.* 45 (3), 410–418. doi:10.1194/jlr.R300006-JLR200

Imai, Y., Soda, M., Inoue, H., Hattori, N., Mizuno, Y., and Takahashi, R. (2001). An unfolded putative transmembrane polypeptide, which can lead to endoplasmic reticulum stress, is a substrate of parkin. *Cell* 105 (7), 891–902. doi:10.1016/s0092-8674(01)00407-x

Imai, Y., Soda, M., and Takahashi, R. (2000). Parkin suppresses unfolded protein stress-induced cell death through its E3 ubiquitin-protein ligase activity. *J. Biol. Chem.* 275 (46), 35661–35664. doi:10.1074/jbc.C000447200

Ingallinesi, M., Galet, B., Pegon, J., Faucon Biguet, N., Do Thi, A., Millan, M. J., et al. (2019). Knock-down of GPR88 in the dorsal striatum alters the response of medium spiny neurons to the loss of dopamine input and L-3-4-dyhydroxyphenylalanine. *Front. Pharmacol.* 10, 1233. doi:10.3389/fphar.2019.01233

Isawi, I. H., Morales, P., Sotudeh, N., Hurst, D. P., Lynch, D. L., and Reggio, P. H. (2020). GPR6 structural insights: homology model construction and docking studies. *Molecules* 25, 725. doi:10.3390/molecules25030725

Jensen, T., Elster, L., Nielsen, S. M., Poda, S. B., Loechel, F., Volbracht, C., et al. (2014). The identification of GPR3 inverse agonist AF64394; the first small molecule inhibitor of GPR3 receptor function. *Bioorg Med. Chem. Lett.* 24 (22), 5195–5198. doi:10.1016/j.bmcl.2014.09.077

Jeon, J., Kim, C., Sun, W., Chung, H., Park, S.-H., and Kim, H. (2002). Cloning and localization of rgpr85 encoding rat G-protein-coupled receptor. *Biochem. Biophysical Res. Commun.* 298 (4), 613–618. doi:10.1016/s0006-291x(02)02515-9

Jhaveri, M. D., Sagar, D. R., Elmes, S. J. R., Kendall, D. A., and Chapman, V. (2007). Cannabinoid CB2 receptor-mediated anti-nociception in models of acute and chronic pain. *Mol. Neurobiol.* 36, 26–35. doi:10.1007/s12035-007-8007-7

Jin, C., Decker, A. M., Makhijani, V. H., Besheer, J., Darcq, E., Kieffer, B. L., et al. (2018). Discovery of a potent, selective, and brain-penetrant small molecule that activates the orphan receptor GPR88 and reduces alcohol intake. *J. Med. Chem.* 61 (15), 6748–6758. doi:10.1021/acs.jmedchem.8b00566

Jobe, A., and Vijayan, R. (2024). Orphan G protein-coupled receptors: the ongoing search for a home. *Front. Pharmacol.* 15, 1349097. doi:10.3389/fphar.2024.1349097

Jones, P. G., Nawoschik, S. P., Sreekumar, K., Uveges, A. J., Tseng, E., Zhang, L., et al. (2007). Tissue distribution and functional analyses of the constitutively active orphan G protein coupled receptors, GPR26 and GPR78. *Biochimica Biophysica Acta (BBA) - General Subj.* 1770 (6), 890–901. doi:10.1016/j.bbagen.2007.01.013

Kaushik, A. C., and Sahi, S. (2017). Molecular modeling and molecular dynamics simulation-based structural analysis of GPR3. *Netw. Model. Analysis Health Inf. Bioinforma.* 6 (1), 9. doi:10.1007/s13721-017-0150-0

Khan, M. Z., and He, L. (2017). Neuro-psychopharmacological perspective of Orphan receptors of Rhodopsin (class A) family of G protein-coupled receptors. *Psychopharmacol. Berl.* 234 (8), 1181–1207. doi:10.1007/s00213-017-4586-9

Kitada, T., Asakawa, S., Hattori, N., Matsumine, H., Yamamura, Y., Minoshima, S., et al. (1998). Mutations in the parkin gene cause autosomal recessive juvenile parkinsonism. *Nature* 392 (6676), 605–608. doi:10.1038/33416

Kohno, M., Hasegawa, H., Inoue, A., Muraoka, M., Miyazaki, T., Oka, K., et al. (2006). Identification of N-arachidonylglycine as the endogenous ligand for orphan G-protein-coupled receptor GPR18. *Biochem. Biophysical Res. Commun.* 347 (3), 827–832. doi:10.1016/j.bbrc.2006.06.175

Komatsu, H. (2021). Discovery of the first druggable GPR52 antagonist to treat Huntington's disease. *J. Med. Chem.* 64 (2), 938–940. doi:10.1021/acs.jmedchem.0c02235

Komatsu, H., Maruyama, M., Yao, S., Shinohara, T., Sakuma, K., Imaichi, S., et al. (2014). Anatomical transcriptome of G protein-coupled receptors leads to the identification of a novel therapeutic candidate GPR52 for psychiatric disorders. *PLoS One* 9 (2), e90134. doi:10.1371/journal.pone.0090134

Korn, T. (2008). Pathophysiology of multiple sclerosis. *J. neurology* 255 (Suppl. 6), 2–6. doi:10.1007/s00415-008-6001-2

Kotsikorou, E., Sharir, H., Shore, D. M., Hurst, D. P., Lynch, D. L., Madrigal, K. E., et al. (2013). Identification of the GPR55 antagonist binding site using a novel set of high-potency GPR55 selective ligands. *Biochemistry* 52 (52), 9456–9469. doi:10.1021/bi4008885

Kunkel, G. T., Maceyka, M., Milstien, S., and Spiegel, S. (2013). Targeting the sphingosine-1-phosphate Axis in cancer, inflammation and beyond. *Nat. Rev. Cancer* 12, 688–702. doi:10.1038/nrd4099

Kurano, M., Kobayashi, T., Sakai, E., Tsukamoto, K., and Yatomi, Y. (2021). Lysophosphatidylinositol, especially albumin-bound form, induces inflammatory cytokines in macrophages. *Faseb J.* 35 (6), e21673. doi:10.1096/fj.202100245R

Kwon, M. S., Park, B.-O., Kim, H. M., and Kim, S. (2013). Leucine-rich repeat-containing G-protein coupled receptor 5/gpr49 activates G12/13-rho GTPase pathway. *Mol. Cells* 36, 267–272. doi:10.1007/s10059-013-0173-z

Laboute, T., Gandía, J., Pellissier, L. P., Corde, Y., Rebeillard, F., Gallo, M., et al. (2020). The orphan receptor GPR88 blunts the signaling of opioid receptors and multiple striatal GPCRs. *Elife* 9, e50519. doi:10.7554/eLife.50519

Laun, A. S., Shrader, S. H., Brown, K. J., and Song, Z. H. (2019). GPR3, GPR6, and GPR12 as novel molecular targets: their biological functions and interaction with cannabidiol. *Acta Pharmacol. Sin.* 40 (3), 300–308. doi:10.1038/s41401-018-0031-9

Lee, D. K., Nguyen, T., Lynch, K. R., Cheng, R., Vanti, W. B., Arkhitko, O., et al. (2001). Discovery and mapping of ten novel G protein-coupled receptor genes. *Gene* 275 (1), 83–91. doi:10.1016/s0378-1119(01)00651-5

Lee, Y., Basith, S., and Choi, S. (2018). Recent advances in structure-based drug design targeting class A G protein-coupled receptors utilizing crystal structures and computational simulations. *J. Med. Chem.* 61 (1), 1–46. doi:10.1021/acs.jmedchem.6b01453

Leinartaité, L., and Svenningsson, P. (2017). Folding underlies bidirectional role of GPR37/pael-R in Parkinson disease. *Trends Pharmacol. Sci.* 38 (8), 749–760. doi:10.1016/j.tips.2017.05.006

Levoye, A., Dam, J., Ayoub, M. A., Guillaume, J. L., Couturier, C., Delagrange, P., et al. (2006). The orphan GPR50 receptor specifically inhibits MT1 melatonin receptor function through heterodimerization. *Embo J.* 25, 3012–3023. doi:10.1038/sj.emboj.7601193

Li, D. Y., Smith, D. G., Hardeland, R., Yang, M. Y., Xu, H. L., Zhang, L., et al. (2013a). Melatonin receptor genes in vertebrates. *Int. J. Mol. Sci.* 14 (6), 11208–11223. doi:10.3390/ijms140611208

Li, J., Guo, B., Wang, J., Cheng, X., Xu, Y., and Sang, J. (2013b). Ovarian cancer G protein coupled receptor 1 suppresses cell migration of MCF7 breast cancer cells via a Gα 12/13-Rho-Rac1 pathway. *J. Mol. Signal.* 8 (1), 6–8. doi:10.1186/1750-2187-8-6

Li, Q., Zhang, Y., Ge, B. Y., Li, N., Sun, H. L., Ntim, M., et al. (2020). GPR50 distribution in the mouse cortex and Hippocampus. *Neurochem. Res.* 45 (10), 2312–2323. doi:10.1007/s11064-020-03089-w

Lin, X., Li, M., Wang, N., Wu, Y., Luo, Z., Guo, S., et al. (2020). Structural basis of ligand recognition and self-activation of orphan GPR52. *Nature* 579 (7797), 152–157. doi:10.1038/s41586-020-2019-0

Liu, B., Song, S., Ruz-Maldonado, I., Pingitore, A., Huang, G. C., Baker, D., et al. (2016). GPR55-dependent stimulation of insulin secretion from isolated mouse and human islets of Langerhans. *Diabetes, Obes. metabolism* 18 (12), 1263–1273. doi:10.1111/dom.12780

Liu, H., Xing, R., Ou, Z., Zhao, J., Hong, G., Zhao, T. J., et al. (2021). G-Protein-Coupled receptor GPR17 inhibits glioma development by increasing polycomb repressive complex 1-mediated ROS production. *Cell Death Dis.* 12, 610. doi:10.1038/s41419-021-03897-0

Lobo, M. K., Cui, Y., Ostlund, S. B., Balleine, B. W., and Yang, X. W. (2007). Genetic control of instrumental conditioning by striatopallidal neuron-specific S1P receptor Gpr6. *Nat. Neurosci.* 10 (11), 1395–1397. doi:10.1038/nn1987

Longoria, V., Parcel, H., Toma, B., Minhas, A., and Zeine, R. (2022). Neurological benefits, clinical challenges, and neuropathologic promise of medical marijuana: a systematic review of cannabinoid effects in multiple sclerosis and experimental models of demyelination. *Biomedicines* 10 (3), 539. doi:10.3390/biomedicines10030539

Lötsch, J., Weyer-Menkhoff, I., and Tegeder, I. (2018). Current evidence of cannabinoid-based analgesia obtained in preclinical and human experimental settings. *Eur. J. Pain* 22 (3), 471–484. doi:10.1002/ejp.1148

Lu, X., Zhang, N., Meng, B., Dong, S., and Hu, Y. (2012). Involvement of GPR12 in the regulation of cell proliferation and survival. *Mol. Cell Biochem.* 366 (1-2), 101–110. doi:10.1007/s11010-012-1287-x

Lueptow, L. M., Devi, L. A., and Fakira, A. K. (2018). Targeting the recently deorphanized receptor GPR83 for the treatment of immunological. *Neuroendocrine Neuropsychiatric Disord.* doi:10.1016/bs.pmbts.2018.07.002

Ma, M., Guo, S., Lin, X., Li, S., Wu, Y., Zeng, Y., et al. (2020). Targeted proteomics combined with affinity mass spectrometry analysis reveals antagonist E7 acts as an intracellular covalent ligand of orphan receptor GPR52. *ACS Chem. Biol.* 15 (12), 3275–3284. doi:10.1021/acschembio.0c00867

Madar, I. H., Sultan, G., Tayubi, I. A., Hasan, A. N., Pahi, B., Rai, A., et al. (2021). Identification of marker genes in Alzheimer's disease using a machine-learning model. *Bioinformation* 17 (2), 348–355. doi:10.6026/97320630017348

Major, A. G., Pitty, L. P., and Farah, C. S. (2013). Cancer stem cell markers in head and neck squamous cell carcinoma. *Stem Cells Int.* 2013, 319489. doi:10.1155/2013/319489

Mangini, M., Iaccino, E., Mosca, M. G., Mimmi, S., D'Angelo, R., Quinto, I., et al. (2017). Peptide-guided targeting of GPR55 for anti-cancer therapy. *Oncotarget* 8 (3), 5179–5195. doi:10.18632/oncotarget.14121

Mantas, I., Yang, Y., Mannoury-la-Cour, C., Millan, M. J., Zhang, X., and Svenningsson, P. (2020). Genetic deletion of GPR88 enhances the locomotor response to L-DOPA in experimental parkinsonism while counteracting the induction of dyskinesia. *Neuropharmacology* 162, 107829. doi:10.1016/j.neuropharm.2019.107829

Mao, X. G., Song, S. J., Xue, X. Y., Yan, M., Wang, L., Lin, W., et al. (2013). LGR5 is a proneural factor and is regulated by OLIG2 in glioma stem-like cells. *Cell Mol. Neurobiol.* 33 (6), 851–865. doi:10.1007/s10571-013-9951-6

Marazziti, D., Gallo, A., Golini, E., Matteoni, R., and Tocchini-Valentini, G. P. (1998). Molecular cloning and chromosomal localization of the mouse Gpr37 gene encoding an orphan G-protein-coupled peptide receptor expressed in brain and testis. *Genomics* 53 (3), 315–324. doi:10.1006/geno.1998.5433

Maresz, K., Carrier, E. J., Ponomarev, E. D., Hillard, C. J., and Dittel, B. N. (2005). Modulation of the cannabinoid CB2 receptor in microglial cells in response to inflammatory stimuli. *J. Neurochem.* 95, 437–445. doi:10.1111/j.1471-4159.2005.03380.x

Marsango, S., Barki, N., Jenkins, L., Tobin, A. B., and Milligan, G. (2022). Therapeutic validation of an orphan G protein-coupled receptor: the case of GPR84. *Br. J. Pharmacol.* 179 (14), 3529–3541. doi:10.1111/bph.15248

Martin, A. L., Steurer, M. A., and Aronstam, R. S. (2015). Constitutive activity among orphan class-A G protein coupled receptors. *PLoS One* 10 (9), e0138463. doi:10.1371/journal.pone.0138463

Matouk, A. I., Taye, A., El-Moselhy, M. A., Heeba, G. H., and Abdel-Rahman, A. A. (2017). The effect of chronic activation of the novel endocannabinoid receptor GPR18 on myocardial function and blood pressure in conscious rats. *J. Cardiovasc. Pharmacol.* 69, 23–33. doi:10.1097/FJC.0000000000000438

Matsumoto, M., Beltaifa, S., Weickert, C. S., Herman, M. M., Hyde, T. M., Saunders, R. C., et al. (2005). A conserved mRNA expression profile of SREB2 (GPR85) in adult human, monkey, and rat forebrain. *Mol. Brain Res.* 138 (1), 58–69. doi:10.1016/j.molbrainres.2005.04.002

Matsumoto, M., Straub, R. E., Marenco, S., Nicodemus, K. K., Matsumoto, S., Fujikawa, A., et al. (2008). The evolutionarily conserved G protein-coupled receptor SREB2/GPR85 influences brain size, behavior, and vulnerability to schizophrenia. *Proc. Natl. Acad. Sci. U. S. A.* 105 (16), 6133–6138. doi:10.1073/pnas.0710717105

McHugh, D., Hu, S. S. J., Rimmerman, N., Juknat, A., Vogel, Z., Walker, J. M., et al. (2010). N-arachidonoyl Glycine, an abundant endogenous lipid, potently drives directed cellular migration through GPR18, the putative abnormal cannabidiol receptor. *BMC Neurosci.* 11, 44. doi:10.1186/1471-2202-11-44

McHugh, D., Page, J., Dunn, E., and Bradshaw, H. B. (2012). Δ(9) -Tetrahydrocannabinol and N-arachidonyl glycine are full agonists at GPR18 receptors and induce migration in human endometrial HEC-1B cells. *Br. J. Pharmacol.* 165 (8), 2414–2424. doi:10.1111/j.1476-5381.2011.01497.x

Medina-Vera, D., Zhao, H., Bereczki, E., Rosell-Valle, C., Shimozawa, M., Chen, G., et al. (2023). The expression of the endocannabinoid receptors CB2 and GPR55 is highly increased during the progression of Alzheimer's disease in *App^{NL-G-F}* knock-in mice. *Biol. (Basel).* 12 (6), 805. doi:10.3390/biology12060805

Meyer, R. C., Giddens, M. M., Schaefer, S. A., and Hall, R. A. (2013). GPR37 and GPR37L1 are receptors for the neuroprotective and glioprotective factors prosaptide and prosaposin. *Proc. Natl. Acad. Sci. U. S. A.* 110 (23), 9529–9534. doi:10.1073/pnas.1219004110

Mizushima, K., Miyamoto, Y., Tsukahara, F., Hirai, M., Sakaki, Y., and Ito, T. (2000). A novel G-protein-coupled receptor gene expressed in striatum. *Genomics* 69 (3), 314–321. doi:10.1006/geno.2000.6340

Morales, P., Isawi, I., and Reggio, P. H. (2018a). Towards a better understanding of the cannabinoid-related orphan receptors GPR3, GPR6, and GPR12. *Drug Metab. Rev.* 50 (1), 74–93. doi:10.1080/03602532.2018.1428616

Morales, P., Isawi, I. H., and Reggio, P. H. (2018b). Towards a better understanding of the cannabinoid-related orphan receptors GPR3, GPR6, and GPR12. *Drug Metab. Rev.* 50, 74–93. doi:10.1080/03602532.2018.1428616

Morales, P., Lago-Fernandez, A., Hurst, D. P., Sotudeh, N., Brailoiu, E., Reggio, P. H., et al. (2020). Therapeutic exploitation of GPR18: beyond the cannabinoids? *J. Med. Chem.* 63 (23), 14216–14227. doi:10.1021/acs.jmedchem.0c00926

Morató, X., Garcia-Esparcia, P., Argerich, J., Llorens, F., Zerr, I., Paslawski, W., et al. (2021). Ecto-GPR37: a potential biomarker for Parkinson's disease. *Transl. Neurodegener.* 10 (1), 8. doi:10.1186/s40035-021-00232-7

Mori-Fegan, D. K., Noor, S., Wong, Y. Y., Wu, C. Y., Black, S. E., Ross, R. A., et al. (2023). Association between G-protein coupled receptor 55 (GPR55) single nucleotide polymorphisms and Alzheimer's disease. *Alzheimer's Dementia* 19 (S15). doi:10.1002/alz.073447

Müller, A., Kleinau, G., Piechowski, C. L., Müller, T. D., Finan, B., Pratzka, J., et al. (2013). G-protein coupled receptor 83 (GPR83) signaling determined by constitutive and zinc(II)-induced activity. *PLoS One* 8 (1), e53347. doi:10.1371/journal.pone.0053347

Nakahata, T., Tokumaru, K., Ito, Y., Ishii, N., Setoh, M., Shimizu, Y., et al. (2018). Design and synthesis of 1-(1-benzothiophen-7-yl)-1H-pyrazole, a novel series of G protein-coupled receptor 52 (GPR52) agonists. *Bioorg. Med. Chem.* 26 (8), 1598–1608. doi:10.1016/j.bmc.2018.02.005

Nishi, A., and Shuto, T. (2017). Potential for targeting dopamine/DARPP-32 signaling in neuropsychiatric and neurodegenerative disorders. *Expert Opin. Ther. targets* 21 (3), 259–272. doi:10.1080/14728222.2017.1279149

Nishiyama, K., Suzuki, H., Harasawa, T., Suzuki, N., Kurimoto, E., Kawai, T., et al. (2017). FTBMT, a novel and selective GPR52 agonist, demonstrates antipsychotic-like and procognitive effects in rodents, revealing a potential therapeutic agent for schizophrenia. *J. Pharmacol. Exp. Ther.* 363 (2), 253–264. doi:10.1124/jpet.117.242925

Nouh, R. A., Kamal, A., and Abdelnaser, A. (2023). Cannabinoids and multiple sclerosis: a critical analysis of therapeutic potentials and safety concerns. *Pharmaceutics* 15 (4), 1151. doi:10.3390/pharmaceutics15041151

Oeckl, P., Hengerer, B., and Ferger, B. (2014). G-protein coupled receptor 6 deficiency alters striatal dopamine and cAMP concentrations and reduces dyskinesia in a mouse model of Parkinson's disease. *Exp. Neurol.* 257, 1–9. doi:10.1016/j.expneurol.2014.04.010

Parravicini, C., Lecca, D., Marangon, D., Coppolino, G. T., Daniele, S., Bonfanti, E., et al. (2020). Development of the first *in vivo* GPR17 ligand through an iterative drug discovery pipeline: a novel disease-modifying strategy for multiple sclerosis. *PLoS One* 15 (4), e0231483. doi:10.1371/journal.pone.0231483

Patricio, F., Morales Davila, E., Patricio-Martinez, A., Arana Del Carmen, N., Martinez, I., Aguilera, J., et al. (2022). Intrapallidal injection of cannabidiol or a selective GPR55 antagonist decreases motor asymmetry and improves fine motor skills in hemiparkinsonian rats. *Front. Pharmacol.* 13, 945836. doi:10.3389/fphar.2022.945836

Perez-Olives, C., Rivas-Santisteban, R., Lillo, J., Navarro, G., and Franco, R. (2021). Recent advances in the potential of cannabinoids for neuroprotection in Alzheimer's, Parkinson's, and Huntington's diseases. *Adv. Exp. Med. Biol.* 1264, 81–92. doi:10.1007/978-3-030-57369-0_6

Rahman, M. M., Islam, M. R., Mim, S. A., Sultana, N., Chellappan, D. K., Dua, K., et al. (2022). Insights into the promising prospect of G protein and GPCR-mediated signaling in neuropathophysiology and its therapeutic regulation. *Oxid. Med. Cell Longev.* 2022, 8425640. doi:10.1155/2022/8425640

Rahman, M. M., Mim, S. A., Islam, M. R., Sultana, N., Ahmed, M., and Kamal, M. A. (2023). Role of G-proteins and GPCR-mediated signalling in neuropathophysiology. *CNS Neurol. Disord. Drug Targets* 22 (1), 2–5. doi:10.2174/1871527321666220430142722

Rajesh, M., Pān, H., Mukhopadhyay, P., Bátkai, S., Osei-Hyiaman, D., Haskó, G., et al. (2007). Pivotal advance: cannabinoid-2 receptor agonist HU-308 protects against hepatic ischemia/reperfusion injury by attenuating oxidative stress, inflammatory response, and apoptosis. *J. Leukoc. Biol.* 82, 1382–1389. doi:10.1189/jlb.0307180

Raport, C. J., Schweickart, V. L., Chantry, D., Eddy, R. L., Jr., Shows, T. B., Godiska, R., et al. (1996). New members of the chemokine receptor gene family. *J. Leukoc. Biol.* 59 (1), 18–23. doi:10.1002/jlb.59.1.18

Reppert, S. M., Weaver, D. R., Ebisawa, T., Mahle, C. D., and Kolakowski, L. F., Jr (1996). Cloning of a melatonin-related receptor from human pituitary. *FEBS Lett.* 386 (2-3), 219–224. doi:10.1016/0014-5793(96)00437-1

Reyes-Resina, I., Navarro, G., Aguinaga, D., Canela, E. I., Schoeder, C. T., Załuski, M., et al. (2018). Molecular and functional interaction between GPR18 and cannabinoid CB(2) G-protein-coupled receptors. Relevance in neurodegenerative diseases. *Biochem. Pharmacol.* 157, 169–179. doi:10.1016/j.bcp.2018.06.001

Rezgaoui, M., Süsens, U., Ignatov, A., Gelderblom, M., Glassmeier, G., Franke, I., et al. (2006). The neuropeptide head activator is a high-affinity ligand for the orphan G-protein-coupled receptor GPR37. *J. Cell Sci.* 119 (Pt 3), 542–549. doi:10.1242/jcs.02766

Rocher, A. B., Gubellini, P., Merienne, N., Boussicault, L., Petit, F., Gipchtein, P., et al. (2016). Synaptic scaling up in medium spiny neurons of aged BACHD mice: a slow-progression model of Huntington's disease. *Neurobiol. Dis.* 86, 131–139. doi:10.1016/j.nbd.2015.10.016

Russell, B., Barrus, M. M., Tremblay, M., Ma, L., Hrelja, K., Wong, C., et al. (2021). GPR52 agonists attenuate ropinirole-induced preference for uncertain outcomes. *Behav. Neurosci.* 135 (1), 8–23. doi:10.1037/bne0000391

Ryberg, E., Larsson, N., Sjögren, S., Hjorth, S., Hermansson, N. O., Leonova, J., et al. (2007). The orphan receptor GPR55 is a novel cannabinoid receptor. *Br. J. Pharmacol.* 152 (7), 1092–1101. doi:10.1038/sj.bjp.0707460

Saeki, Y., Ueno, S., Mizuno, R., Nishimura, T., Fujimura, H., Nagai, Y., et al. (1993). Molecular cloning of a novel putative G protein-coupled receptor (GPCR21) which is expressed predominantly in mouse central nervous system. *FEBS Lett.* 336 (2), 317–322. doi:10.1016/0014-5793(93)80828-i

Saha, S. K., Choi, H. Y., Yang, G. M., Biswas, P. K., Kim, K., Kang, G. H., et al. (2020). GPR50 promotes hepatocellular carcinoma progression via the notch signaling pathway through direct interaction with ADAM17. *Mol. Ther. oncolytics* 17, 332–349. doi:10.1016/j.omto.2020.04.002

Sakai, A., Yasui, T., Watanave, M., Tatsumi, R., Yamamoto, Y., Takano, W., et al. (2022). Development of novel potent ligands for GPR85, an orphan G protein-coupled receptor expressed in the brain. *Genes Cells* 27 (5), 345–355. doi:10.1111/gtc.12931

Saliba, S. W., Jauch, H., Gargouri, B., Keil, A., Hurrle, T., Volz, N., et al. (2018). Anti-neuroinflammatory effects of GPR55 antagonists in LPS-activated primary microglial cells. *J. Neuroinflammation* 15 (1), 322. doi:10.1186/s12974-018-1362-7

Sallee, N. A., Lee, E., Leffert, A., Ramirez, S., Brace, A. D., Halenbeck, R., et al. (2020). A pilot screen of a novel peptide hormone library identified candidate GPR83 ligands. *SLAS Discov.* 25 (9), 1047–1063. doi:10.1177/2472555220934807

Sánchez-Zavaleta, R., Segovia, J., Ruiz-Contreras, A. E., Herrera-Solís, A., Méndez-Díaz, M., de la Mora, M. P., et al. (2023). GPR55 activation prevents amphetamine-induced conditioned place preference and decrease the amphetamine-stimulated inflammatory response in the ventral hippocampus in male rats. *Prog. Neuropsychopharmacol. Biol. Psychiatry* 120, 110636. doi:10.1016/j.pnpbp.2022.110636

Schoeder, C. T., Mahardhika, A. B., Drabczyńska, A., Kieć-Kononowicz, K., and Müller, C. E. (2020). Discovery of tricyclic xanthines as agonists of the cannabinoid-activated orphan G-protein-coupled receptor GPR18. *ACS Med. Chem. Lett.* 11 (10), 2024–2031. doi:10.1021/acsmedchemlett.0c00208

Setoh, M., Ishii, N., Kono, M., Miyanohana, Y., Shiraishi, E., Harasawa, T., et al. (2014). Discovery of the first potent and orally available agonist of the orphan G-protein-coupled receptor 52. *J. Med. Chem.* 57 (12), 5226–5237. doi:10.1021/jm5002919

Shi, Q. X., Yang, L. K., Shi, W. L., Wang, L., Zhou, S. M., Guan, S. Y., et al. (2017). The novel cannabinoid receptor GPR55 mediates anxiolytic-like effects in the medial orbital cortex of mice with acute stress. *Mol. Brain* 10 (1), 38. doi:10.1186/s13041-017-0318-7

Simard, A. R., Soulet, D., Gowing, G., Julien, J. P., and Rivest, S. (2006). Bone marrow-derived microglia play a critical role in restricting senile plaque formation in Alzheimer's disease. *Neuron* 49 (4), 489–502. doi:10.1016/j.neuron.2006.01.022

Snow, B. E., Krumins, A. M., Brothers, G. M., Lee, S.-F., Wall, M. A., Chung, S., et al. (1998). A G protein Γ subunit-like domain shared between RGS11 and other RGS proteins specifies binding to G β5 subunits. *Proc. Natl. Acad. Sci.* 95, 13307–13312. doi:10.1073/pnas.95.22.13307

Song, S. J., Mao, X. G., Wang, C., Han, A. G., Yan, M., and Xue, X. Y. (2015). LGR5/GPR49 is implicated in motor neuron specification in nervous system. *Neurosci. Lett.* 584, 135–140. doi:10.1016/j.neulet.2014.09.056

Song, Z. H., Modi, W., and Bonner, T. I. (1995). Molecular cloning and chromosomal localization of human genes encoding three closely related G protein-coupled receptors. *Genomics* 28 (2), 347–349. doi:10.1006/geno.1995.1154

Southern, C., Cook, J. M., Neetoo-Isseljee, Z., Taylor, D. L., Kettleborough, C. A., Merritt, A., et al. (2013). Screening β-arrestin recruitment for the identification of natural ligands for orphan G-protein-coupled receptors. *J. Biomol. Screen.* 18 (5), 599–609. doi:10.1177/1087057113475480

Spillantini, M. G., Schmidt, M. L., Lee, V. M.-Y., Trojanowski, J. Q., Jakes, R., and Goedert, M. (1997). Alpha-synuclein in Lewy bodies. *Nature* 388 (6645), 839–840. doi:10.1038/42166

Springer (2021) *Translational methods for multiple sclerosis research*. Berlin, Germany: Springer.

Sriram, K., and Insel, P. A. (2018). G protein-coupled receptors as targets for approved drugs: how many targets and how many drugs? *Mol. Pharmacol.* 93 (4), 251–258. doi:10.1124/mol.117.111062

Stanley, C. P., Hind, W. H., Tufarelli, C., and O'Sullivan, S. E. (2015). Cannabidiol causes endothelium-dependent vasorelaxation of human mesenteric arteries via CB1 activation. *Cardiovasc Res.* 107 (4), 568–578. doi:10.1093/cvr/cvv179

Stott, L. A., Brighton, C. A., Brown, J., Mould, R., Bennett, K. A., Newman, R., et al. (2021). Characterisation of inverse agonism of the orphan-G protein-coupled receptor GPR52 by cannabinoid ligands Cannabidiol and O-1918. *Heliyon* 7 (6), e07201. doi:10.1016/j.heliyon.2021.e07201

Suzuki, M., Takaishi, S., Nagasaki, M., Onozawa, Y., Iino, I., Maeda, H., et al. (2013a). Medium-chain fatty acid-sensing receptor, GPR84, is a proinflammatory receptor. *J. Biol. Chem.* 288 (15), 10684–10691. doi:10.1074/jbc.M112.420042

Suzuki, M., Takaishi, S., Nagasaki, M., Onozawa, Y., Iino, I., Maeda, H., et al. (2013b). Medium-chain fatty acid-sensing receptor, GPR84, is a proinflammatory receptor. *J. Biol. Chem.* 288, 10684–10691. doi:10.1074/jbc.M112.420042

Sylantyev, S., Jensen, T. P., Ross, R. A., and Rusakov, D. A. (2013). Cannabinoid- and lysophosphatidylinositol-sensitive receptor GPR55 boosts neurotransmitter release at central synapses. *Proc. Natl. Acad. Sci. U. S. A.* 110 (13), 5193–5198. doi:10.1073/pnas.1211204110

Tanaka, S., Ishii, K., Kasai, K., Yoon, S. O., and Saeki, Y. (2007). Neural expression of G protein-coupled receptors GPR3, GPR6, and GPR12 up-regulates cyclic AMP levels and promotes neurite outgrowth. *J. Biol. Chem.* 282 (14), 10506–10515. doi:10.1074/jbc.M700911200

Tanaka, S., Miyagi, T., Dohi, E., Seki, T., Hide, I., Sotomaru, Y., et al. (2014). Developmental expression of GPR3 in rodent cerebellar granule neurons is associated with cell survival and protects neurons from various apoptotic stimuli. *Neurobiol. Dis.* 68, 215–227. doi:10.1016/j.nbd.2014.04.007

Tanaka, S., Shaikh, I. M., Chiocca, E. A., and Saeki, Y. (2009). The Gs-linked receptor GPR3 inhibits the proliferation of cerebellar granule cells during postnatal development. *PLoS One* 4 (6), e5922. doi:10.1371/journal.pone.0005922

Tanese, K., Fukuma, M., Yamada, T., Mori, T., Yoshikawa, T., Watanabe, W., et al. (2008). G-protein-coupled receptor GPR49 is up-regulated in basal cell carcinoma and promotes cell proliferation and tumor formation. *Am. J. Pathol.* 173 (3), 835–843. doi:10.2353/ajpath.2008.071091

Thathiah, A., Horre, K., Snellinx, A., Vandewyer, E., Huang, Y., Ciesielska, M., et al. (2013). β-arrestin 2 regulates Aβ generation and γ-secretase activity in Alzheimer's disease. *Nat. Med.* 19 (1), 43–49. doi:10.1038/nm.3023

Thathiah, A., Spittaels, K., Hoffmann, M., Staes, M., Cohen, A., Horre, K., et al. (2009). The orphan G protein-coupled receptor 3 modulates amyloid-beta peptide generation in neurons. *Science* 323 (5916), 946–951. doi:10.1126/science.1160649

Tiraboschi, P., Hansen, L. A., Thal, L. J., and Corey-Bloom, J. (2004). The importance of neuritic plaques and tangles to the development and evolution of AD. *Neurology* 62 (11), 1984–1989. doi:10.1212/01.wnl.0000129697.01779.0a

Uhlenbrock, K., Gassenhuber, H., and Kostenis, E. (2002). Sphingosine 1-phosphate is a ligand of the human gpr3, gpr6 and gpr12 family of constitutively active G protein-coupled receptors. *Cell Signal* 14 (11), 941–953. doi:10.1016/s0898-6568(02)00041-4

Vassilatis, D. K., Hohmann, J. G., Zeng, H., Li, F., Ranchalis, J. E., Mortrud, M. T., et al. (2003). The G protein-coupled receptor repertoires of human and mouse. *Proc. Natl. Acad. Sci. U. S. A.* 100 (8), 4903–4908. doi:10.1073/pnas.0230374100

Venkataraman, C., and Kuo, F. (2005). The G-protein coupled receptor, GPR84 regulates IL-4 production by T lymphocytes in response to CD3 crosslinking. *Immunol. Lett.* 101 (2), 144–153. doi:10.1016/j.imlet.2005.05.010

Wang, H., Hu, L., Zang, M., Zhang, B., Duan, Y., Fan, Z., et al. (2016). REG4 promotes peritoneal metastasis of gastric cancer through GPR37. *Oncotarget* 7 (19), 27874–27888. doi:10.18632/oncotarget.8442

Wang, J., Wu, X., Simonavicius, N., Tian, H., and Ling, L. (2006). Medium-chain fatty acids as ligands for orphan G protein-coupled receptor GPR84. *J. Biol. Chem.* 281 (45), 34457–34464. doi:10.1074/jbc.M608019200

Wang, P., Felsing, D. E., Chen, H., Stutz, S. J., Murphy, R. E., Cunningham, K. A., et al. (2020a). Discovery of potent and brain-penetrant GPR52 agonist that suppresses psychostimulant behavior. *J. Med. Chem.* 63 (22), 13951–13972. doi:10.1021/acs.jmedchem.0c01498

Wang, S., Zhang, Q., Lu, D., Fang, Y. C., Yan, X.-C., Chen, J., et al. (2023). GPR84 regulates pulmonary inflammation by modulating neutrophil functions. *Acta Pharmacol. Sin.* 44, 1665–1675. doi:10.1038/s41401-023-01080-z

Wang, X. S., Yue, J., Hu, L. N., Tian, Z., Zhang, K., Yang, L., et al. (2020b). Activation of G protein-coupled receptor 30 protects neurons by regulating autophagy in astrocytes. *Glia* 68 (1), 27–43. doi:10.1002/glia.23697

Watson, U., Jain, R., Asthana, S., and Saini, D. K. (2018). "Chapter four - spatiotemporal modulation of ERK activation by GPCRs," in *International review of cell and molecular biology*. Editor A. K. Shukla (Cambridge, Massachusetts, United States: Academic Press), 111–140.

Wei, L., Tokizane, K., Konishi, H., Yu, H., and Kiyama, H. (2017). Agonists for G-protein-coupled receptor 84 (GPR84) alter cellular morphology and motility but do not induce pro-inflammatory responses in microglia. *J. Neuroinflammation* 14, 198. doi:10.1186/s12974-017-0970-y

Wittenberger, T., Schaller, H. C., and Hellebrand, S. (2001). An expressed sequence tag (EST) data mining strategy succeeding in the discovery of new G-protein coupled receptors. *J. Mol. Biol.* 307 (3), 799–813. doi:10.1006/jmbi.2001.4520

Wong, T.-S., Gao, W., Chen, G., Qiu, C., He, G., Ye, F., et al. (2023). Cryo-EM structure of orphan G protein-coupled receptor GPR21. *MedComm* 4 (1), e205. doi:10.1002/mco2.205

Woo, J. A. A., Liu, T., Fang, C. C., Castaño, M. A., Kee, T., Yrigoin, K., et al. (2020). β-Arrestin2 oligomers impair the clearance of pathological tau and increase tau aggregates. *Proc. Natl. Acad. Sci. U. S. A.* 117 (9), 5006–5015. doi:10.1073/pnas.1917194117

Wu, Z., Han, Z., Tao, L., Sun, X., Su, J., Hu, J., et al. (2023). Dynamic insights into the self-activation pathway and allosteric regulation of the orphan G-protein-coupled receptor GPR52. *J. Chem. Inf. Model* 63 (18), 5847–5862. doi:10.1021/acs.jcim.3c00672

Xiang, X., Wang, X., Wu, Y., Hu, J., Li, Y., Jin, S., et al. (2022). Activation of GPR55 attenuates cognitive impairment, oxidative stress, neuroinflammation, and synaptic dysfunction in a streptozotocin-induced Alzheimer's mouse model. *Pharmacol. Biochem. Behav.* 214, 173340. doi:10.1016/j.pbb.2022.173340

Yamamoto, Y., Sakamoto, M., Fujii, G., Tsuiji, H., Kenetaka, K., Asaka, M., et al. (2003). Overexpression of orphan G-protein-coupled receptor, Gpr49, in human hepatocellular carcinomas with beta-catenin mutations. *Hepatol. Baltim. Md* 37 (3), 528–533. doi:10.1053/jhep.2003.50029

Yang, H.-J., Vainshtein, A., Maik-Rachline, G., and Peles, E. (2016). G protein-coupled receptor 37 is a negative regulator of oligodendrocyte differentiation and myelination. *Nat. Commun.* 7 (1), 10884. doi:10.1038/ncomms10884

Yao, Y., Cui, X., Al-Ramahi, I., Sun, X., Li, B., Hou, J., et al. (2015). A striatal-enriched intronic GPCR modulates huntingtin levels and toxicity. *Elife* 4, e05449. doi:10.7554/eLife.05449

Ye, C., Zhang, Z., Wang, Z., Hua, Q., Zhang, R., and Xie, X. (2014). Identification of a novel small-molecule agonist for human G protein-coupled receptor 3. *J. Pharmacol. Exp. Ther.* 349 (3), 437–443. doi:10.1124/jpet.114.213082

Ye, N., Li, B., Mao, Q., Wold, E. A., Tian, S., Allen, J. A., et al. (2019). Orphan receptor GPR88 as an emerging neurotherapeutic target. *ACS Chem. Neurosci.* 10 (1), 190–200. doi:10.1021/acschemneuro.8b00572

Yousefi, S., Cooper, P. R., Potter, S. L., Mueck, B., and Jarai, G. (2001). Cloning and expression analysis of a novel G-protein-coupled receptor selectively expressed on granulocytes. *J. Leukoc. Biol.* 69 (6), 1045–1052. doi:10.1189/jlb.69.6.1045

Zhao, M., Ma, J., Li, M., Zhu, W., Zhou, W., Shen, L., et al. (2022). Different responses to risperidone treatment in Schizophrenia: a multicenter genome-wide association and whole exome sequencing joint study. *Transl. Psychiatry* 12 (1), 173. doi:10.1038/s41398-022-01942-w

Zlotos, D. P., Jockers, R., Cecon, E., Rivara, S., and Witt-Enderby, P. A. (2014). MT1 and MT2 melatonin receptors: ligands, models, oligomers, and therapeutic potential. *J. Med. Chem.* 57 (8), 3161–3185. doi:10.1021/jm401343c

Frontiers in Pharmacology

Explores the interactions between chemicals and living beings

The most cited journal in its field, which advances access to pharmacological discoveries to prevent and treat human disease.

Discover the latest Research Topics

See more →

Frontiers

Avenue du Tribunal-Fédéral 34
1005 Lausanne, Switzerland
frontiersin.org

Contact us

+41 (0)21 510 17 00
frontiersin.org/about/contact